Cancer Imaging with Radiolabeled Antibodies

Cancer Treatment and Research

WILLIAM L. MCGUIRE, *series editor*

Livingston, R.B. (ed): Lung Cancer 1. 1981. ISBN 90-247-2394-9.
Humphrey G.B., Dehner L.P., Grindey G.B., Acton, R.T. (eds): Pediatric Oncology 1. ISBN 90-274-2408-2.
Decosse J.J., Sherlock P. (eds): Gastrointestinal Cancer 1. 1981. ISBN 90-247-2461-9.
Bennett J.M. (ed): Lymphomas 1, including Hodgkin's Disease. 1981. ISBN 90-247-2479-1
Bloomfield C.D. (ed): Adult Leukemias 1. 1982. ISBN 90-247-2478-3.
Paulson D.F. (ed): Genitourinary Cancer 1. 1982. ISBN 90-247-2480-5.
Muggia F.M. (ed): Cancer Chemotherapy 1. 1983. ISBN 90-247-2713-8.
Humphrey G.B., Grindey G.B. (eds): Pancreatic Tumors in Children. 1982. ISBN 90-247-2702-2.
Costanzi J.J. (ed): Malignant Melanoma 1. 1983. ISBN 90-247-2706-5.
Griffiths C.T., Fuller A.F. (eds): Gynecologic Oncology. 1983. ISBN 0-89838-555-5.
Greco A.F. (ed): Biology and Management of Lung Cancer. 1983. ISBN 0-89838-554-7.
Walker M.D. (ed): Oncology of the Nervous System. 1983. ISBN 0-89838-567-9.
Higby D.J. (ed): Supportive Care in Cancer Therapy. 1983. ISBN 0-89838-569-5.
Herberman R.B. (ed): Basic and Clinical Tumor Immunology. 1983. ISBN 0-89838-579-2.
Baker L.H. (ed): Soft Tissue Sarcomas. 1983. ISBN 0-89838-584-9.
Bennett J.M. (ed): Controversies in the Management of Lymphomas. 1983. ISBN 0-89838-586-5.
Humphrey G.B., Grindey G.B. (eds): Adrenal and Endocrine Tumors in Children. 1983. ISBN 0-89838-590-3.
DeCosse J.J., Sherlock P. (eds): Clinical Management of Gastrointestinal Cancer. 1984. ISBN 0-89838-601-2.
Catalona W.J., Ratliff, T.L. (eds): Urologic Oncology. 1984. ISBN 0-89838-628-4.
Santen R.J., Manni A. (eds): Diagnosis and Management of Endocrine-related Tumors. 1984. ISBN 0-89838-636-5.
Costanzi J.J. (ed): Clinical Management of Malignant Melanoma. 1984. ISBN 0-89838-656-X.
Wolf G.T. (ed): Head and Neck Oncology. 1984. ISBN 0-89838-657-8.
Alberts D.S., Surwit E.A. (eds): Ovarian Cancer. 1985. ISBN 0-89838-676-4.
Muggia, F.M. (ed): Experimental and Clinical Progress in Cancer Chemotherapy. 1985. ISBN 0-89838-679-9.
Higby D.J. (ed): Issues in Supportive Care of Cancer Patients. 1986. ISBN 0-89838-816-3.
Surwit E.A., Alberts D.S. (eds): Cervix Cancer. 1987. ISBN 0-89838-822-8.
Jacobs C. (ed): Cancers of the Head and Neck. 1987. ISBN 0-89838-825-2.
MacDonald J.S. (ed): Gastrointestinal Oncology. 1987. ISBN 0-89838-829-5.
Ratliff T.L., Catalona W.J. (eds): Genitourinary Cancer. 1987. ISBN 0-89838-830-9.
Nathanson L. (ed): Basic and Clinical Aspects of Malignant Melanoma. 1987. ISBN 0-89838-856-2.
Muggia F.M. (ed): Concepts, Clinical Developments, and Therapeutic Advances in Cancer Chemotherapy. 1987. ISBN 0-89838-879-5.
Frankel A.E. (ed): Immunotoxins. 1988. ISBN 0-89838-984-4.
Bennett J.M., Foon K.A. (eds): Immunologic Approaches to the Classification and Management of Lymphomas and Leukemias. 1988. ISBN 0-89838-355-2.
Osborne C.K. (ed): Endocrine Therapies in Breast and Prostate Cancer. 1988. ISBN 0-89838-365-X.
Lippman M.E., Dickson R. (eds): Breast Cancer: Cellular and Molecular Biology. 1988. ISBN 0-89838-368-4.
Kamps W.A., Humphrey G.B., Poppema S. (eds): Hodgkin's Disease in Children: Controversies and Current Practice. 1988. ISBN 0-89838-372-2.
Muggia F.M. (ed): Cancer Chemotherapy: Concepts, Clinical Investigations and Therapeutic Advances. 1988. ISBN 0-89838-381-1.
Nathanson L. (ed): Malignant Melanoma: Biology, Diagnosis, and Therapy. 1988. ISBN 0-89838-384-6.
Pinedo H.M., Verweij J. (eds): Treatment of Soft Tissue Sarcomas. 1989. ISBN 0-89838-391-9.
Hansen H.H. (ed): Basic and Clinical Concepts of Lung Cancer. 1989. ISBN 0-7923-0153-6.
Lepor H., Ratliff T.L. (eds): Urologic Oncology. 1989. ISBN 0-7923-0161-7.
Benz C., Liu E. (eds): Oncogenes. 1989. ISBN 0-7923-0237-0.
Ozols R.F. (ed): Drug Resistance in Cancer Therapy. 1989. ISBN 0-7923-0244-3.
Surwit E.A., Alberts D.S. (eds): Endometrial Cancer. 1989. ISBN 0-7923-0286-9.
Champlin R., (ed): Bone Marrow Transplantation. 1990. ISBN 0-7923-0612-0.

Cancer Imaging with Radiolabeled Antibodies

Edited by

DAVID M. GOLDENBERG, Sc.D., M.D.

Center for Molecular Medicine and Immunology,
at the University of Medicine and Dentistry of New Jersey
Newark, New Jersey, USA

1990 **KLUWER ACADEMIC PUBLISHERS**
BOSTON / DORDRECHT / LONDON

Distributors for North America:
Kluwer Academic Publishers
101 Philip Drive
Assinippi Park
Norwell, Massachusetts 02061 USA

Distributors for all other countries:
Kluwer Academic Publishers Group
Distribution Centre
Post Office Box 322
3300 AH Dordrecht, THE NETHERLANDS

Library of Congress Cataloging-in-Publication Data
Cancer imaging with radiolabeled antibodies/edited by David M. Goldenberg.
p. cm. — (Cancer treatment and research)
Includes bibliographical references.

ISBN-13: 978-1-4612-8805-3 e-ISBN-13: 978-1-4613-1497-4
DOI: 10.1007/978-1-4613-1497-4

1. Cancer — Radioimmunoimaging. I. Goldberg, David M., 1938– II. Series.
[DNLM: 1. Antibodies, Monoclonal — diagnostic use. 2. Antibodies, Neoplasm. 3. Isotope Labeling. 4. Neoplasms — radionuclide imaging. W1 CA693/QZ241 C2145]
RC270.3.R33C36 1990
616.99'407575 — dc20
DNLM/DLC
for Library of Congress 89-71628
CIP

Cancer Treatment and Research

Foreword

Where do you begin to look for a recent, authoritative article on the diagnosis or management of a particular malignancy? The few general oncology textbooks are generally out of date. Single papers in specialized journals are informative but seldom comprehensive; these are more often preliminary reports on a very limited number of patients. Certain general journals frequently publish good in-depth reviews of cancer topics, and published symposium lectures are often the best overviews available. Unfortunately, these reviews and supplements appear sporadically, and the reader can never be sure when a topic of special interest will be covered.

Cancer Treatment and Research is a series of authoritative volumes that aim to meet this need. It is an attempt to establish a critical mass of oncology literature covering virtually all oncology topics, revised frequently to keep the coverage up to date, and easily available on a single library shelf or by a single personal subscription.

We have approached the problem in the following fashion: first, by dividing the oncology literature into specific subdivisions such as lung cancer, genitourinary cancer, pediatric oncology, etc.; and second, by asking eminent authorities in each of these areas to edit a volume on the specific topic on an annual or biannual basis. Each topic and tumor type is covered in a volume appearing frequently and predictably, discussing current diagnosis, staging, markers, all forms of treatment modalities, basic biology, and more.

In *Cancer Treatment and Research*, we have an outstanding group of editors, each having made a major commitment to bring to this new series the very best literature in his or her field. Kluwer Academic Publishers has made an equally major commitment to the rapid publication of high-quality books and to worldwide distribution.

Where can you go to find quickly a recent authoritative article on any major oncology problem? We hope that *Cancer Treatment and Research* provides an answer.

WILLIAM L. MCGUIRE
Series Editor

Table of Contents

Preface

Cancer remains the most formidable challenge of our generation, afflicting several million people in the United States and killing about half a million annually. Despite considerable efforts in past years, we do not yet have a clear insight into how cancer originates, what it is at a very basic level, and how we can prevent or cure it. This is to be expected, given the complexity of the problem and the magnitude and diversity of cancer types that occur, and that cancer as a group of diseases is being studied at many different levels and from many different perspectives. Patients do not lend themselves to careful and accurate study, since varied and rigorous experimental protocols are not feasible nor often ethically defensible in individuals with different, poorly defined diseases. Because of these limitations, we are restricted to improving our methods of diagnosis, detection, and treatment; prevention must await more progress in etiology and pathogenesis. Of the three modalities — diagnosis, detection and therapy — the last has received the most attention and has been almost exclusively surgery, radiotherapy, and chemotherapy. However, a fourth dimension is now evolving, biologic therapy, which itself encompasses a number of different and sometimes complementary approaches. This new technology requires that the oncologic specialist and general practitioner become acquainted with a new language and science derived from the principles and foundations of cell biology, biochemistry, and immunology in order to understand and employ the new molecules of our day, such as interferons, cytokines, growth factors, monoclonal antibodies, and the like.

This book is intended to present a current perspective of the use of one set of molecules, antibodies, to target diagnostic isotopes to tumors. Antibodies with reasonable specificity can be developed against almost any substance. Obviously, if selective targeting to cancer cells can be achieved, the prospects for a selective therapy are equally intriguing. But the development of cancer detection, or imaging, with radiolabeled antibodies has depended upon advances in a number of different areas, including cancer immunology and immunochemistry for identifying suitable antigen targets and antibodies to these targets, tumor biology for model systems, radiochemistry for the attachment of radionuclides to antibodies, molecular biology for reengineer-

ing the antibodies for safer and more effective use in humans, and nuclear medicine for providing the best imaging protocols and instrumentation to detect minute amounts of elevated radioactivity against a background of considerable noise. Accordingly, this book has been organized to address the advances that are being made in many of these areas, and I am grateful that I have been able to secure the contributions of many of the leaders in their respective fields.

Organizing and editing a multiauthor volume brings a number of challenges to the editor and publisher. I have few complaints, since the contributing authors were very responsive and cooperative. But I must proclaim publicly my own embarrassment to the series editor, Dr. William L. McGuire, and to the publisher, Mr. Jeffrey K. Smith of Kluwer, for my being less responsible than the others.

David M. Goldenberg

List of contributors

Dr. Rosalyn D. Blumenthal
Center for Molecular Medicine and Immunology,
at the University of Medicine and Dentistry of New Jersey
1 Bruce St.
Newark, NJ 07103

Dr. A.R. Bradwell
Director, Immunodiagnostic Research Laboratory
The Medical School, Vincent Drive
Birmingham B15 2TJ
England

Dr. Martin W. Brechbeil
National Institutes of Health
Bldg. 10, Rm. B3 B69
9000 Rockville Pike
Bethesda, MD 20892

Dr. G. Bryant
Dept. of Pathology
National Cancer Institute
Bethesda, MD 20892

Dr. G.L. Buraggi
Instituto Nazionale Tumori
Via Venezian, 1
Milan 20143
Italy

Dr. Jorge Carrasquillo
Dept. of Nuclear Medicine
Clinical Center
National Institutes of Health
Bethesda, MD 20892

Dr. Catherine Chapman
Registrar
Dept. of Immunology
The Medical School
Birmingham University
Birmingham B15 2TJ
England

Dr. David Colcher
Laboratory of Tumor Immunology and Biology
NCI — Bldg. 10
National Institutes of Health
9000 Rockville Pike
Bethesda, MD 20892

Dr. Nigel Courtenay-Luck
Dept. of Clinical Oncology
Royal Postgraduate Medical School
Hammersmith Hospital
London W12 0HS
England

Dr. Peter Dykes
Consultant Physician
General Hospital
Steel House Lane
Birmingham B4
England

Dr. A.A. Epenetos
Hammersmith Oncology Group
Hammersmith Hospital
London W12 0HS
England

Dr. Paul B. Fisher
Dept. of Cell Biology and Urology
Columbia University College of Physicians and Surgeons
New York, NY 10032

Dr. Otto Gansow
National Institutes of Health
Bldg. 10, Rm. B3 B69
9000 Rockville Pike
Bethesda, MD 20892

Dr. David M. Goldenberg
Center for Molecular Medicine and Immunology,
at the University of Medicine and Dentistry of New Jersey
1 Bruce St.
Newark, NJ 07103

Dr. Hildegard Goldenberg
Center for Molecular Medicine and Immunology,
at the University of Medicine and Dentistry of New Jersey
1 Bruce St.
Newark, NJ 07103

Dr. Ruth Grebenau
Immunomedics, Inc.
5 Bruce St.
Newark, NJ 07103

Dr. Hildegard Goldenberg
Center for Molecular Medicine and Immunology
University of Medicine and Dentistry of New Jersey
1 Bruce St.
Newark, NJ 07103

Dr. John W. Greiner
Laboratory of Tumor Immunology and Biology
NCI — National Institutes of Health
Bldg. 10, Rm. 8B07
9000 Rockville Pike
Bethesda, MD 20892

Dr. Fiorella Guadagni
Laboratory of Tumor Immunology and Biology
NCI — National Institutes of Health
Bldg. 10, Rm. 8B07
9000 Rockville Pike
Bethesda, MD 20892

Dr. Thomas C. Hall
Center for Molecular Medicine and Immunology,
at the University of Medicine and Dentistry of New Jersey
1 Bruce St.
Newark, NJ 07103

Dr. Patricia Horan Hand
Laboratory of Tumor Immunology and Biology
NCI — National Institutes of Health
Bldg. 10, Rm. 8B07
9000 Rockville Pike
Bethesda, MD 20892

Dr. Hans J. Hansen
Immunomedics, Inc.
5 Bruce St.
Newark, NJ 07103

Mr. George Hinkle
Dept. of Nuclear Medicine
The Ohio State University
410 W. 10th Ave.
Columbus, OH 43210

Dr. Donald J. Hnatowich
Associate Professor
Department of Nuclear Medicine
University of Massachusetts Medical Center
55 Lake Avenue, N.
Worcester, MA 01605

Dr. Won-Pyo Hong
Radiopharmaceutic Chemistry
Dept. of Nuclear Medicine
George Washington University Medical Center
2300 I St.
Washington, DC 20037

Dr. Jo Ann Horowitz
Center for Molecular Medicine and Immunology,
at the University of Medicine and Dentistry of New Jersey
1 Bruce St.
Newark, NJ 07103

Dr. W.W. Johnston
Dept. of Pathology
Duke University Medical Center
Durham, NC 27710

Ms. Anastasia L. Jones
Immunomedics, Inc.
5 Bruce St.
Newark, NJ 07103

Dr. Peter L. Jones
E.I. DuPont de Nemours & Co.
Medical Products Dept.
331 Treble Cove Rd.
No. Billerica, MA 01862

Dr. A.M. Keenan
Dept. of Nuclear Medicine
University of Pennsylvania
Philadelphia, PA 19104

Mr. Arthur Kunz
Immunomedics, Inc.
5 Bruce St.
Newark, NJ 07103

Dr. Lamk M. Lamki
Dept. of Nuclear Medicine
M.D. Anderson Hospital
6723 Bertner Ave.
Houston, TX 77030

Dr. Steven Larson
Chief, Nuclear Medicine
Memorial Sloan-Kettering Cancer Center
1275 York Ave.
New York, NY 10021

Mr. Robert E. Lee
Center for Molecular Medicine and Immunology,
at the University of Medicine and Dentistry of New Jersey
1 Bruce St.
Newark, NJ 07103

Dr. Edward W. Martin, Jr.
Dept. of Surgery
Ohio State University
N-908 Doan Hall
410 W. 10th Ave.
Columbus, OH 43210–1228

Dr. Claude F. Meares
Dept. of Chemistry
University of California, Davis
Davis, CA 95616

Dr. Saed Mirzadeh
National Institutes of Health
Bldg. 10, Rm. B3 B69
9000 Rockville Pike
Bethesda, MD 20892

Cathy Mojzisik, R.N., M.S.
Dept. of Surgical Oncology
Ohio State University
410 W. 10th Ave.
Columbus, OH 43210–1228

Dr. James L. Murray
Dept. of Clinical Immunology and Biological Therapy
M.D. Anderson Hospital
6723 Bertner Ave.
Houston, TX 77030

Dr. Philip Noguchi
National Center for Drugs and Biologics
FDA
Bethesda, MD 20892

Dr. Chang H. Paik
Radiopharmacy
Ross Hall, Rm. 656
George Washington University
2300 I St.
Washington, DC 20037

Dr. Yehuda Patt
M.D. Anderson Hospital
Dept. of Oncology
1515 Holcombe Blvd.
Houston, TX 77030

Dr. Sidney Pestka
Dept. of Molecular Genetics and Microbiology
UMDNJ — Robert Wood Johnson Medical School
Piscataway, NJ 08854

Dr. Syed M. Quadri
Radiopharmaceutical Chemistry
Dept. of Nuclear Medicine
George Washington University Medical Center
2300 I St.
Washington, DC 20037

Dr. Richard C. Reba
Dept. of Nuclear Medicine
George Washington University Medical Center
2300 I St.
Washington, DC 20037

Dr. J.C. Reynolds
Dept. of Nuclear Medicine
Clinical Center
National Institutes of Health
Bethesda, MD 20892

Dr. Mario Roselli
National Institutes of Health
Bldg. 10, Rm. B3 B69
9000 Rockville Pike
Bethesda, MD 20892

Dr. Howard Sands
New Technology Research
E.I. DuPont
331 Treble Cove Rd.
No. Billerica, MA 01862

Dr. Jeffrey Schlom
National Cancer Institute
Bldg. 10, Rm. 8B07
9000 Rockville Pike
Bethesda, MD 20892

Dr. Sudhir A. Shah
Director, Pre-Clinical Animal Studies,
ImmunoGen, Inc.
148 Sidney Street
Cambridge, MA 02139

Dr. Robert M. Sharkey
Center for Molecular Medicine and Immunology,
at the University of Medicine and Dentistry of New Jersey
1 Bruce St.
Newark, NJ 07103

Dr. K. Siler
Laboratory of Tumor Immunology and Biology
NCI — Bldg. 10
National Institutes of Health
9000 Rockville Pike
Bethesda, MD 20892

Dr. Ramaswamy Subramanian
Bionetics Research
1330-A Piccard Dr.
Rockville, MD 20850–4373

Dr. P. Sugarbaker
Dept. of Surgical Oncology
Emory Clinic
Emory University
Atlanta, GA 30322

Dr. C.A. Szpak
Dept. of Pathology
Duke University Medical Center
Durham, NC 27710

Dr. Gillian Thomas
Research Fellow, Dept. of Immunology
Medical School, Birmingham University
Birmingham B15 2TJ
England

Dr. A. Thor
Laboratory of Tumor Immunology and Biology
NCI — Bldg. 10
National Institutes of Health
9000 Rockville Pike
Bethesda, MD 20892

Dr. Marlin Thurston
Dept. of Surgery
Ohio State University
410 W. 10th Ave.
Columbus, OH 43210–1228

Dr. Richard Wahl
Dept. of Nuclear Medicine
University of Michigan Medical Center
1500 E. Medical Center Dr.
Ann Arbor, MI 48109–0228

Dr. John N. Weinstein
Mathematical Biology
Division of Cancer Biology and Diagnosis
National Cancer Institute
Bethesda, MD 20892

Dr. Robert Sundoro Wu
Immunomedics, Inc.
5 Bruce St.
Newark, NJ 07103
New address:
Hoffmann-La Roche, Inc.
Kingsland Rd.
Nutley, NJ 07110

I

Historical and Theoretical Perspectives

1. Clinical radioimmunodetection: The second decade

David M. Goldenberg

The history of cancer radioimmunodetection (RAID) has been reviewed in previous articles [1–4]. Its beginning can be traced to the work of Pressman and his colleagues and their labeling of antibodies against normal rat organs in 1948 [5] and then rat tumors in 1953 [6] for localization after intravenous injection. This tumor targeting in rodent models with radiolabeled polyclonal antibodies was confirmed by Bale et al. [7]. Later reports indicated that when the antibodies localized within the tumor, they were actually sequestered to fibrin or fibrinogen [8]. Based upon these findings, radiolabeled antibodies to fibrin or fibrinogen were evaluated for tumor targeting [9,10], but these antibodies did not show localization in all tumors studied in animals or humans [10–13]. When large doses of radioiodinated antibodies to human fibrinogen were administered to selected cancer patients, short-term remissions were obtained in a few patients [12–14]. In 1965, Mahaley and Day reported on the localization of antibodies in gliomas in patients by means of autoradiography on excised specimens [15]. Finally, using radiolabeled antibodies to an undefined renal cancer antigen, Belitsky et al. [16] reported tumor imaging. An important development in this first phase, spanning almost 20 years (Table 1), was the use of paired radioiodine labeling of different immunoglobulin preparations in order to show specific localization of the antibody of interest [17]. This first phase of antibody targeting in experimental cancer models and in limited clinical trials has been reviewed by Presmann [18], as well as the more general reviews already cited [1–4].

The second phase (Table 2) of RAID is characterized by two major accomplishments, 1) the development of specific antibodies against defined cancer-associated antigens, or markers, such as human chorionic gonadotropin (hCG) or carcinoembryonic antigen (CEA), and 2) the use of human tumor xenograft models for evaluating the targeting of these antibodies [19–22]. Improved targeting was then accomplished by affinity purification of the polyclonal antibodies in order to increase their immunoreactivity [23]. Finally, anti-CEA antibodies were shown to localize in a human colonic carcinoma xenograft in short-term passage in immunosuppressed monkeys [24]. The first two phases of RAID were characterized by the almost exclusive use of I-125 and I-131 for antibody labeling.

Goldenberg, D.M., (ed.), Cancer Imaging with Radiolabeled Antibodies.

Table 1. Phase I: Early experimental and clinical studies with diverse, undefined, radioiodinated antibodies

Investigators	Publication Year	Accomplishments
Pressman and Keighley	1949	First radiolabeling of antibody
Pressman and Korngold	1953	Localization of sarcomas in rats
Pressman et al.	1957	Developed paired radioiodine labeling method showing specific localization
Dewey et al.	1963	Fibrin antibodies imaged tumors in patients
Mahaley and Day	1965	Antiglioma antibodies accreted in human gliomas
Belitsky et al.	1978	Anti-renal antibody imaged renal tumors in patients

Table 2. Phase II: First animal model experiments demonstrating localization with defined, radioiodinate anti-tumor antibodies

Investigators	Publication Year	Accomplishments
Quinones et al.	1971	Choriocarcinoma in hamsters imaged with anti-HCG antibodies
Primus et al.	1973	Anti-CEA antibodies localized human colon cancer xenografts in hamsters
Goldenberg et al.	1974	Anti-CEA antibodies imaged human colon cancer xenografts in hamsters
Mach et al.	1974	Anti-CEA antibodies imaged human colon cancer xenografts in nude mice
Primus et al.	1977	Affinity-purified anti-CEA antibodies showed improved tumor localization in hamsters
Goldenberg et al.	1979	Anit-CEA antibodies imaged human colon cancer xenografts in immunosuppressed monkeys

The clinical demonstration of RAID became the focus in the third phase of RAID (Table 3), where anti-cancer-marker antibodies labeled with I-131 were shown to image tumors producing these cancer markers, such as CEA, HCG, and alpha fetoprotein, or AFP [25–28]. These studies showed that these antibodies could target radioactivity to the tumors, despite the presence of circulating antigen that could and did complex to the foreign antibodies; target/nnontarget radioactivity ratios could be enhanced by dual-isotope subtraction methods, thus permitting imaging of the lesions within 48 hours; tumor accretion of the I-131 antibody label was found to be about 2.5-fold that of adjacent normal tissue; tumors as small as 2 cm could be disclosed; occult tumors were detected; and non-antigen-containing neoplasms were not imaged [25,29,30]. During this period, it was also shown that radiolabeled anti-CEA antibodies could be used to detect tumors by lymphoscintigraphy [31]. Although there was some dispute with regard to the actual levels of

Table 3. Phase III: First successful clinical trials with defined, radioiodinated anti-tumor antibodies

Investigators	Publication Year	Accomplishments
Goldenberg et al.	1978	Purified anti-CEA antibodies imaged tumors in patients; circulating CEA did not block RAID; Tc-99m HSA and pertechnetate used for subtracting background radioactivity, resulting in target enhancement; resolution found to be 2-cm diameter tumor lesions; tumor uptake of I-131 found to be 2.5-fold over adjacent normal tissue; occult tumors disclosed
DeLand et al.	1979	Antibody lymphoscintigraphy performed in breast cancer patients with anti-CEA antibodies
Primus et al.	1980	Circulating immune complexes shown in patients given anti-CEA antibodies
Goldenberg et al.	1980	Antibodies to AFP and HCG imaged tumors in patients having high circulating levels of these markers

Table 4. Phase IV: Introduction of monoclonal antibodies, antibody fragments, antibody combinations, emission tomography, and use of metallic radionuclides for cancer imaging

Investigators	Publication Year	Accomplishments
Krejcarek and Tucker	1977	Described basic method of chelating radiometals to proteins
Ballou et al.	1979	Animal experiments showing tumor imaging with monoclonal antibodies
Pettit et al.	1980	Described improved antibody labeling with Tc-99m
Mach et al.	1980	Use of anti-CEA antibody fragments for imaging in patients
Mach et al.	1981	Tumor imaging with anti-CEA monoclonal antibodies in patients
Gaffar et al.	1981	Improved tumor localization using antibody mixtures in humans bearing human colon cancers
Scheinberg et al.	1982	Tumor imaging with In-111 monoclonal antibodies in mice
Epenetos et al.	1982	Tumor imaging in patients with I-123 monoclonal antibodies
Fairweather et al.	1983	Tumor imaging with In-111 antibodies in patients
Buraggi et al.	1984	Tumor imaging with Tc-99m antibodies in melanoma patients
Schwarz and Steinsträsser	1987	Kit for direct labeling of Tc-99m to whole IgG
Hansen et al.	1989	Kit for direct labeling of Tc-99m to antibody Fab′ fragment

sensitivity for tumor detection [32], it was not doubted that radiolabeled anti-cancer antibodies, even when the antigen targets were not truly specific for cancer, could reveal tumors by external scintigraphy, and so the stage was set for improvements to be made.

Major improvements were made in the fourth phase of the development of RAID and involved the introduction of monoclonal antibodies experimentally [33] and then clinically [34] and, finally, the clinical demonstration of the advantages of using antibody fragments [35,36] and the demonstration of improved imaging with other isotopes, particularly I-123, In-111, and Tc-99m [37–40] (Table 4). Antibody mixtures were also found to be useful for improved targeting in an animal model [41]. Radiolabeling with metallic radionuclides was based upon the earlier work of Krejcarek and Tucker with chelates [42] and some intitial experiences of direct antibody labeling with Tc-99m by Pettit et al. [43] and by Rhodes et al. [44]. The use of antibody fragments, which targeted to tumors and cleared from background tissues more rapidly than intact IgG, obviated the need for dual-isotope subtraction, while the use of lower energy radionuclides permitted the exploitation of emission tomographic techniques. The outcome has been earlier, more sensitive imaging of lesions, even those below 1 cm in diameter [40]. A final refinement has come with the development of very rapid kits for direct linking of Tc-99m, the most suitable radionuclide for imaging, to antibodies [45,46], particularly antibody Fab′ fragments [46,47], which are very rapid in targeting and less immunogenic than the intact IgG molecule (Table 4).

What will the next, or second, decade in clinical RAID offer? Prospective trials of RAID with the various agents available will determine which agents (Mab, isotope and labeling kit, and imaging method) are best, in comparison with other detection modalities, in terms of each tumor and indication, so that the proper role for RAID agents, and their relative values, will be better known. Current acquisition times are quite long, which is in part due to the low tumor uptake of Mabs [48]. Therefore, both for RAID and radioimmunotherapy, methods to achieve higher tumor doses of radioactivity should, hopefully, become available. Finally, the next decade should witness a flurry in the evaluation of human and humanized Mabs and their fragments. Indeed, initial studies by Bischof-Delaloye et al. [49] indicate the usefulness of radiolabeled chimeric mouse-human anti-CEA antibodies for tumor imaging. However, as discussed elsewhere [50], perhaps the greatest advances in the use of radiolabeled antibodies in the near future will be in cancer radioimmunotherapy (RAIT), especially when the limiting human anti-mouse antibody responses due to the injection of murine antibodies is mitigated or avoided with human or humanized antibodies.

Acknowledgment

My research has been supported in part by USPHS grant CA39841.

References

1. DeLand, F.H., and Goldenberg, D.M. (1986) Radiolabeled antibodies: Radiochemistry and clinical applications. In: Freeman, L.M. (ed.), *Freeman and Johnson's Clinical Radionuclide Imaging*. Philadelphia: Grune & Stratton, pp. 1915–1992.
2. Goldenberg, D.M., and DeLand, F.H. (1982) History and status of tumor imaging with radiolabeled antibodies. J. Biol. Response Modif. 1:121–136.
3. Goldenberg, D.M. (1987) Current status of cancer imaging with radiolabeled antibodies. J. Cancer Res. Clin. Oncol. 113:203–208.
4. Murray, J.L., and Unger, M.W. (1988) Radioimmunodetection of cancer with monoclonal antibodies: Current status, problems, and future directions. CRC Crit. Rev. Oncol./Hemat. 8:227–253.
5. Pressman, D., and Keighley, G. (1948) The zone of activity of antibodies as determined by the use of radioactive tracers; the zone of activity of nephrotoxic anti-kidney serum. J. Immunol. 59:141–146.
6. Pressman, D., and Korngold, L. (1953) The in vivo localization of anti-Wagner osteogenic sarcoma antibodies. Cancer 6:619–623.
7. Bale, W.F., Spar, I.L., Goodland, R.L., et al. (1955) In vivo and in vitro studies of labeled antibodies against rat kidney and Walker carcinoma. Proc. Soc. Exp. Biol. Med. 89:564–568.
8. Day, E.D., Planinsek, J.A., and Pressman, D. (1959) Localization in vivo of radioiodinated anti-rat-fribin antibodies and radioiodinated rat fibrinogen in the Murphy rat lymphosarcoma and in other transplantable rat tumors. J. Natl. Cancer Inst. 22:413–426.
9. Bale, W.F., and Spar, I.L. (1957) Studies directed toward the use of antibodies as carriers of radioactivity for therapy. Adv. Biol. Med. Physics 5:285–356.
10. Dewey, W.C., Bale, W.F., Rose, R.G., et al. (1963) Localization of antifibrin antibodies in human tumors. Acta Unio. Int. Contra Cancer. 19:185–196.
11. Bale, W.F., Spar, I.L., Casarett, G.W., et al. (1960) Distribution of injected I^{131}-labeled antibody to dog fibrin in tumor-bearing dogs. Cancer Res. 20:1501–1504.
12. McCardle, R.J., Harper, P.V., Spar, I.L., et al. (1966) Studies with iodine-131-labeled antibody to human fibrinogen for diagnosis and therapy of tumors. J. Nucl. Med. 7:837–847.
13. Bale, W.F., Spar, I.L., and Goodland, R.L. (1960) Experimental radiation therapy of tumors with I^{131} carrying antibodies to fibrin. Cancer Res. 20:1488–1494.
14. Spar, I.L., Bale, W.F., Marrack, D., et al. (1967) ^{131}I-labeled antibodies to human fibrinogen. Diagnostic studies and therapeutic trials. Cancer 20:865–870.
15. Mahaley, M.S., Jr., and Day, E.D. (1965) Immunological studies of human gliomas. Neurosurgery 23:363–370.
16. Belitsky, P., Ghose, T., Aquino, J., et al. (1978) Radionuclide imaging of metastasis in renal cell carcinoma patients by ^{131}I-labeled antitumor antibody. Radiology 126:515–517.
17. Pressman, D., Day, E.D., and Blau, M. (1957) The use of paired labeling in the determination of tumor-localizing antibodies. Cancer Res. 17:845–850.
18. Pressman, D. (1980) The development and use of radiolabeled antitumor antibodies. Cancer Res. 40:2960–2964.
19. Quiniones, J., Mizejewski, G., and Beierwaltes, W.H. (1971) Choriocarcinoma scanning using radiolabeled antibody to chorionic gonadotropin. J. Nucl. Med. 12:69–75.
20. Primus, F.J., Wang, R.H., Goldenberg, D.M., and Hansen, H.J. (1973) Localization of human GW-39 tumors in hamsters by radiolabeled heterospecific antibody to carcinoembryonic antigen. Cancer Res. 33:2977–2982.
21. Goldenberg, D.M., Preston, D.F., Primus, F.J., and Hansen, H.J. (1974) Photoscan localization of GW-39 tumors in hamsters using radiolabeled anticarcinoembryonic antigen immunoglobulin G. Cancer Res. 34:1–9.
22. Mach, J.P., Carrel, S. Merenda, et al. (1974) In vivo localization of radiolabeled antibodies to carcinoembryonic antigen in human colon carcinoma grafted into nude mice. Nature 248:704–706.

23. Primus, F.J., MacDonald, R., Goldenberg, D.M., and Hansen, H.J. (1977) Tumor detection and localization with purified antibodies to carcinoembryonic antigen. Cancer Res. 37:1544–1547.
24. Goldenberg, D.M., Primus, F.J., and DeLand, F. (1979) Tumor detection and localization with purified antibodies to carcinoembryonic antigen. In: Herberman, R.B., and McIntire, K.R. (eds.), *Immunodiagnosis of Cancer*, Part 1. New York: Marcel Dekker, pp. 265–304.
25. Goldenberg, D.M., DeLand, F., Kim, E., et al. (1978) Use of radiolabeled antibodies to carcinoembryonic antigen for the detection and localization of diverse cancers by photoscanning. N. Engl. J. Med. 298:1384–1388.
26. Dykes, P.W., Hine, K.R., Bradwell, A.R., et al. (1980) Localization of tumour deposits by external scanning after injection of radiolabelled anti-carcinoembryonic antigen. Br. Med. J. 280:220–222.
27. Goldenberg, D.M., Kim, E.E., DeLand, F., et al. (1980) Clinical studies on the radioimmunodetection of tumors containing alpha-fetoprotein. Cancer 45:4500–4505.
28. Goldenberg, D.M., Kim, E.E., DeLand, F., et al. (1980) Clinical radioimmunodetection of cancer with radioactive antibodies to human chorionic gonadotropin. Science 208:1284–1286.
29. Goldenberg, D.M., Kim, E.E., DeLand, F.H., et al. (1980) Radioimmunodetection of cancer with radioactive antibodies to carcinoembryonic antigen. Cancer Res. 40:2984–2992.
30. Primus, F.J., Bennett, S.J., Kim, E.E., et al. (1980) Circulating immune complexes in cancer patients receiving goat radiolocalizing antibodies to carcinoembryonic antigen. Cancer Res. 40:497–501.
31. DeLand, F.H., Kim, E., Corgan, R., et al. (1979) Axillary lymphoscintigraphy in radioimmunodetection of carcinoembryonic antigen in breast cancer. J. Nucl. Med. 20:1243–1250.
32. Mach, J.P., Carrel, S., Forni, M., et al. (1980) Tumor localization of radiolabeled antibodies against carcinoembryonic antigen in patients with carcinoma: A critical evaluation. N. Engl. J. Med. 303:5–10.
33. Ballou, B., Leving, G., Hakala, R.R., and Solter, D. (1979) Tumor location with radioactivity labeled monoclonal antibody and external scintigraphy. Science 206:844–847.
34. Mach, J.P., Buchegger, R., Forni, M., et al. (1981) Use of radiolabeled monoclonal anti-CEA antibodies for the detection of human carcinomas by external photoscanning and tomoscintigraphy. Immunol. Today 2:239–249.
35. Mach, J.P., Forni, M., Ritschard, J., et al. (1980) Use and limitations of radiolabeled anti-CEA antibodies and their fragments for photoscanning detection of human colorectal carcinomas. Oncodevel. Biol. Med. 1:49–69.
36. Larson, S.M., Carrasquillo, J.A., Krohn, K.A., et al. (1983) Localization of ^{131}I-labeled p97-specific Fab fragments in human melanoma as a basis for radiotherapy. J. Clin. Invest. 72:2101–2114.
37. Scheinberg, D.A., Strand, M., and Gansow, O. (1982) Tumor imaging with radiometal chelate conjugated monoclonal antibodies. Science 215:1511–1513.
38. Epenetos, A., Britton, K.E., Mather, S., et al. (1983) Targeting of I-123 tumor-associated antibodies to ovarian, breast and gastrointestinal tumors. Lancet 2:999–1005.
39. Fairweather, D., Bradwell, A., Dykes, P., et al. (1983) Improved tumor localization using In-111 labeled antibodies. Br. Med. J. 287:167–170.
40. Buraggi, G.L., Callegaro, L., Turrin, A., et al. (1984) Immunoscintigraphy with I-123, Tc-99m and In-111-labeled $F(ab')_2$ fragments of monoclonal antibodies to human high molecular weight melanoma-associated antigen (HMW-MAA). J. Nucl. Med. Allied Sci. 28:283–295.
41. Gaffar, S.A., Pant, K.D., Shochat, D., et al. (1981) Experimental studies of tumor radioimmunodetection using antibody mixtures against carcinoembryonic antigen (CEA) and colon-specific antigen-p (CSAp). Int. J. Cancer 27:101–105.

42. Krejcarek, G.E., and Tucker, K.L. (1977) Covalent attachment of chelating groups to macromolecules. Biochem. Biophys. Res. Commun. 77:581–585.
43. Pettit, W.A., DeLand, F.H., Bennett, S.J., and Goldenberg, D.M. (1980) Radiolabeling of affinity-purified goat anti-carcinoembryonic antigen immunoglobulin G with technetium-99m. Cancer Res. 40:3043–3045.
44. Rhodes, B.A., Torvestad, D.A., Breslow, K., et al. (1982) ^{99m}Tc-labeling and acceptance testing of radiolabeled antibodies and antibody fragments. In: Burchiel, S.W., and Rhodes, B.S. (eds.), *Tumor Imaging. The Radioimmunochemical Detection of Cancer*, New York: Masson Publishing, pp. 111–123.
45. Schwarz, A., and Steinstrasser, A. (1987) A novel approach to Tc99m-labeled monoclonal antibodies (abstract). J. Nucl. Med. 28:721.
46. Hansen, H.J., Jones, A.L., Grebenau, R., et al. (1990) Labeling of anti-tumor antibodies and antibody fragments with ^{99m}Tc. In: Goldenberg, D.M. (ed.), *Cancer Imaging with Radiolabeled Antibodies*, Norwell, MA: Kluwer, pp. 233–244.
47. Goldenberg, D.M., Goldenberg, H., Sharkey, R.M., et al. (1989) Imaging of colorectal carcinoma with radiolabeled antibodies. Semin. Nucl. Med. 19:262–281.
48. Epenetos, A.A., Snook, D., Durbin, H., et al. (1986) Limitations of radiolabeled monoclonal antibodies for localization of human neoplasms. Cancer Res. 46:3183–3191.
49. Bischof-Delaloye, A., Delaloye, B., Buchegger, F., et al. (1989) Chimeric mouse-human anti-CEA antibody of IgG4 isotype used in a pilot immunoscintigraphy study of patients with colorectal carcinomas (abstract). J. Nucl. Med. 30:809.
50. Goldenberg, D.M. (1989) Future role of radiolabeled monoclonal antibodies in oncological diagnosis and therapy. Semin. Nucl. Med. 19:332–339.

2. Antibody targeting: Theoretical considerations

Arthur Bradwell, Peter Dykes, and Gillian Thomas

The detection of tumors using radiolabeled antibodies has been usefully applied to many tumor types [1]. Many important factors can be defined and thereby developed into mathematical models to assess the potential and limitations of the technique. This allows a clear understanding of the physical and biologic problems that need to be solved. At present fairly superficial lesions, between ½ and 1 cm in diameter, are likely to be detected with an optimal combination of attainable factors. Theoretically, for the majority of tumors, the technique is not significantly more sensitive than several other imaging methods.

Model of radioimmunodetection

Many parameters are involved in the production of successful scans and, whilst some have an obvious relationship to the outcome, others may have a more subtle influence. With this in mind, Rockoff [2] defined the major parameters involved and used a computed model to show the likely limitations. We have used this model and adapted it to our own requirements and assessed a variety of situations.

Methods

The derivation of the mathematical model is based on that of Rockoff [2] with the addition of a subtracting isotope. Eleven parameters were used (Figure 1).

The model is one of subtractive processing scanning of a spherical tumor, cross-sectional area As, at depth d, in an otherwise uniform box of radioactive solution. The two isotopes used are referred to as the *subtracting isotope* and the *scanning isotope*, the parameters being subscripted tc and i, respectively. These are assumed to exist in a fixed ratio (hence the usefulness of a subtracting isotope), except in the tumor, where the imaging isotope concentration is increased by the antibody uptake ratio, U. Thus, when the

Goldenberg, D.M., (ed.), Cancer Imaging with Radiolabeled Antibodies.

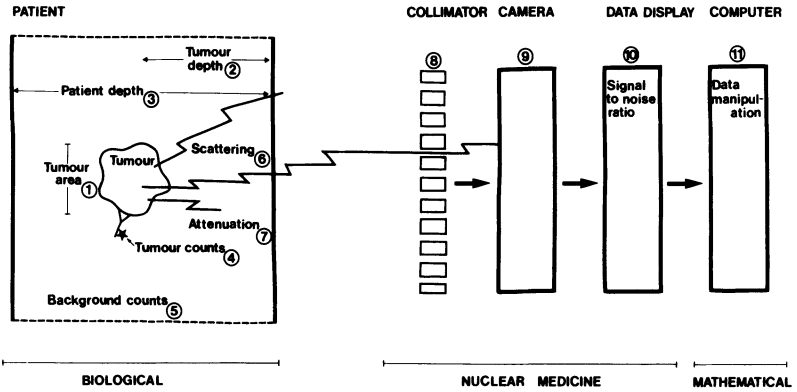

Figure 1. Parameters, symbols, and units. 1) As, cm^2; 2) d, cm^2; 3) L, cm^2; 4) SNR; 5) U; 6) C_i, counts/cm^2; 7) C_{tc}, counts/cm^2; 8) mu, per cm; 9) R_i, FWHM in mm; 10) hole diameter x, mm; 11) col. depth, t, mm.

count density, C_i, from the scanning isotope is uniformly distributed in a patient of depth L, and z = atomic number of material, O_i = system sensitivity (efficiency) for imaging isotope, P_i = scanning isotope radioactivity concentration, and mu = x-ray attenuation coefficient for imaging isotope in patient,

$$C_i = O_i.P_i \int_0^L e^{-\mathrm{mu}.z.}\, dz$$
$$= \frac{O_i.P_i(1 - e^{-\mathrm{mu}.L})}{\mathrm{mu}}. \qquad [1]$$

The tumor detection criterion is the increase in the scanning isotope count density (due to tumor) observable above the statistical fluctuation (noise) of the signal count density, compared with that of an equivalent area of normal background.

If it is assumed that the effective tumor area, A_{eff}, (i.e., that in the final picture) is large enough, then the net integrated tumor signal strength is determined primarily by: O_i, P_i, mu, and V (the tumor volume). Thus the total extra counts, in area A_{eff} due to the lesion C_L is given by

$$C_L = O_i(U - 1)P_i.V.e^{-\mathrm{mu}.d}. \qquad [2]$$

The substraction processing involves scaling one isotope count density such that it matches that of the other isotope over a chosen normalizing area and then obtaining the difference. In this case it is supposed that the subtraction isotope is to be scaled by a factor f, given by

$$f = \frac{C_i}{C_{tc}}. \qquad [3]$$

Through such scaling, the noise in the subtracting signal will be increased by the same factor, and convolution of the random noise on the signals from both isotopes gives a total noise N of

$$\begin{aligned} N &= \sqrt{C_i.A_{eff} + f^2.C_{tc}.A_{eff}} \\ &= \sqrt{C_i.A_{eff} + f.Ci.A_{eff}} \qquad \text{(by [3])} \\ &= \sqrt{C_i.A_{eff}^{(1+f)}}, \end{aligned}$$

where the subtracting isotope must add to the noise.

Hence the signal-to-noise ratio, SNR, is given by

$$\begin{aligned} \text{SNR} &= \frac{C-L}{N} = \frac{O_i.(U-1)P_i.V.e^{-\text{mu}.d}}{\sqrt{C_i.A_{eff}^{(1+f)}}} \\ &= \frac{O_iP_i.}{C_i} \frac{C_i.(U-1)V.e^{-\text{mu}.d}}{\sqrt{A_{eff}(1+f)}}. \end{aligned}$$

Substituting from [1] gives

$$\text{SNR} = \frac{\text{mu}.\sqrt{C_i}.(U-1)V.e^{-\text{mu}.d}}{(1-e^{-\text{mu}.L})\sqrt{A_{eff}(1+f)}}. \qquad [4]$$

Assuming a Gaussian spread function for the camera, this yields the following expression for A_{eff}:

$$\begin{aligned} A_{eff} &= 4\pi\sigma^2 \\ &= 4\pi(\sigma i^2 + \sigma g^2 + R_i^2), \end{aligned} \qquad [5]$$

where

$$\begin{aligned} &\sigma i = \text{camera intrinsic resolution}, \\ &\sigma g = \text{camera geometric resolution} = x(d+t)/t, \end{aligned} \qquad [6]$$

with x = collimator hole diameter and t = collimator thickness. R_i (standard deviation of the tumor signal) may then be determined y

$$As = 4\pi R_i^2, \qquad [7]$$

and hence the volume, V, of the spherical tumor:

$$V = \tfrac{4}{3}[\pi(2R_i)^3]. \qquad [8]$$

Thus, by employing equations 3, 5, and 6–8, equation 4 may be solved to give a relationship between the 11 parameters of the model (Figure 1).

We used the following data for the model: imaging isotope attenuation coefficients (mu) in water for iodine-131 [0.11 (364 keV)] and indium-111 [0.127 (247 keV). The Searle gamma camera has an intrinsic resolution of 4.0 for I-131 and 4.8 for In-111. The hole diameter and thickness of the medium-energy collimator is 4.3 mm and 5.0 mm, respectively (used for In-111) and 6.0 mm and 6.0 mm for the high-energy collimator (used for I-131).

Results

Figure 2 indicates that for In-111-labeled antibodies at a reasonable count density, lesions less than 1 cm in diameter are unlikely to be detected with reported uptake ratios (Table 1) unless situated superficially. Figure 3 indicates that there is a useful gain in detecting deeper lesions, as both scanning and subtracting isotope count densities increase, but beyond 500 counts/cm^2 the improvement rate is reduced. Figure 4 indicates that relatively small uptake ratios can detect small, superficial lesions such as those in the parathyroid gland or on the external surface of the liver.

Implications of the model results

Several of the parameters are patient dependent and clearly cannot be altered. These are: 1) the tumor area (as seen by the camera), 2) the tumor depth, and 3) the patient's body thickness at the site of the tumor. 4) The signal-to-noise ratio seen in the final picture is also fixed, and it is generally considered that the minimum value that can be reliably visualized is 3. 5) the uptake ratio of the localizing antibody onto the tumor compared with the surrounding normal tissue is the most important single determinant of scan sensitivity. Unfortunately there are a host of factors that reduce antibody uptake in vivo, some of which are discussed below. Reported values in patients average less than 5 and are usually nearer 1 (Table 1), although animal results have been considerably better [3,4].

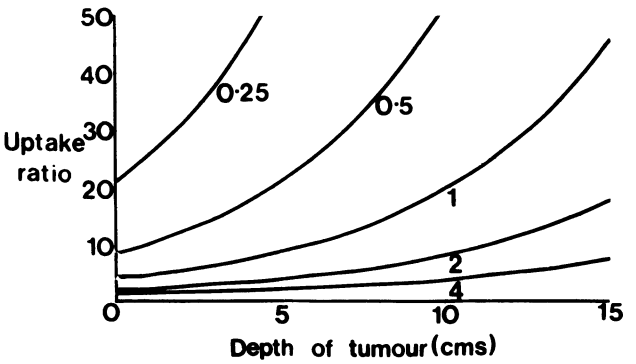

Figure 2. Tumor detection model. Relationship between uptake ratio, U, and tumor depth, d, with contours on tumor area, As. Other parameters: L = 20, SNR = 3, C_i = 300, C_{tc} = 300, mu = 0.127 (111-ind), R_i = 4.8, X = 4.3, and t = 50).

Table 1. Clinical studies with radiolabeled antibodies

Antibody Type	Tumor Type	Uptake Ratio (U)	% Injected Activity Per Gm Tumor	Reference
AP	Mixed	2.5	—	Goldenberg 1978 [5]
Pab	Germ cell	40[a]	—	Goldenberg 1980 [6]
Mab	Kidney	2.3	—	Ghose 1980 [7]
Pab	Colon	2.5	—	Dykes 1980 [8]
Ap	Colon	3.6	0.0033	Mach 1980 [9]
Mab	Mixed	4	0.0026	Mach 1981 [10]
Mab	Colon	2.3	0.005	Farrands 1982 [11]
AP	Hepatoma	5	—	Ishii 1983 [12]
Mab	Colon	2–5	—	Mach 1983 [13]
Mab	Melanoma	4.3	0.0057–0.01	Larson 1983 [14]
Mab	Breast	4	—	Rainsbury 1983 [15]
Mab	Colon	2.5	—	Armitage 1984 [16]
Mab	Colon	3	—	Chatal 1984 [17]
Mab	Breast	> 2	—	Thompson 1984 [18]
Mab	Melanoma	2.3	0.0036	Buraggi 1985 [19]
Fab_2	Melanoma	2.4	0.0017	Buraggi 1985 [19]
Mab	Ovary	2.2	—	Epenetos 1986 [20]
Mab	Various	1.22–35.8[b]	0.015	Epenetos 1986 [21]
Mab	Bone	2.8[a]	—	Armitage 1986 [22]

Pab = polyclonal antibody; AP = affinity purified polyclonal; Mab = monoclonal; U = tumor-to-normal tissue ratio in surgically resected samples.
[a] = one sample only; [b] = sample taken 12 days post injection.

The influence of the uptake ratio in detecting different-sized lesions at various depths as determined by the model is shown in Figure 2.

The model indicates that, next to uptake ratios, the most important factors that can be improved is the absolute count rate of the tumor locating isotope. 6) When using I-131, count rates are usually low, compared with other isotopic scanning methods, and in our hands are often 100/cm^2 in the image. Trebling of this rate would improve the clarity of the image and be equivalent

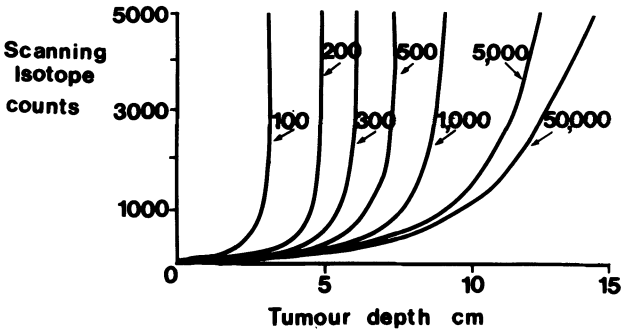

Figure 3. Relationship between the scanning isotope count density, C_i; depth of tumor, d; with contours on subtraction isotope count density, C_{tc}. Other parameters: $As = 1$, $L = 20$, SNR = 3, $U = 8$, mu = 0.127 (111-ind), $R_i = 4.8$, $x = 4.3$, $t = 50$).

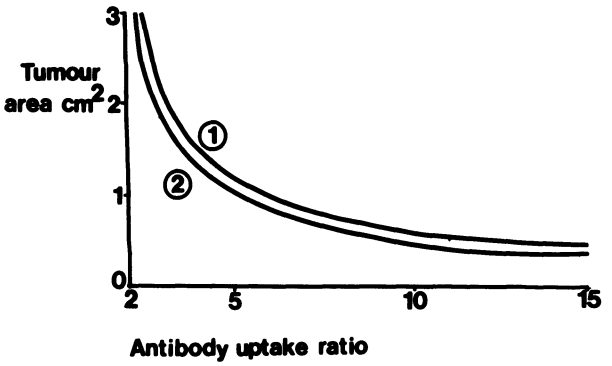

Figure 4. Antibody uptake ratios required to detect parathyroid tumors of different sizes with contours on scanning isotope count density, C_i, Other parameters: $d = 3$, $L = 10$, SNR = 3, $C_{tc} = 300$, mu = 0.127, $R_i = 4.8$, $X = 4.3$, $t = 50$.

to doubling the uptake ratio. A tenfold increase would be equivalent to a threefold rise in the uptake ratio.

Technetium-99 (Tc-99m) has frequently been used as the subtracting isotope (Figure 1; factor 7) to mask the variation in vascular supply to different tissues. This assists the detection of small tumors with low uptake ratios (see below). Indeed, it was the use of this procedure that enabled Goldenberg [5] to obtain the first convincing results in patients. However, this has caused considerable controversy and attempts have been made to avoid its use [23]. The calculation indicates that such a process must add noise.

Biologic considerations

It is apparent from the clinical studies that only a small amount of the injected antibody binds to tumor (Table 1). There are many reasons for this, which need to be understood before improvements can be made.

Antibody characteristics

Antibodies have a variety of characteristics, each of which can affect the outcome.

Specificity. Most of the reported studies have used polyclonal antibodies (Pabs), but these may react with more than the target antigen. Careful testing and adsorption is required. Monoclonal antibodies (Mabs) also require careful evaluation for specificity. Any antibody may bind to Fc receptor sites in the host, rendering it nonspecific (see below).

Affinity. It is assumed that high-affinity antibodies are preferable, and Mach et al. [13] suggested the affinity characteristics of antibodies used for tumor imaging were important, with the highest affinity being preferable, but experimental data are lacking.

Titre. In the case of Pabs, those with the least nonspecific immunoglobulin should be used. Affinity purification is generally used and this improves the specificity and titre, but at the expense of losing the highest affinity antibody.

Fragments. Several studies have reported the use of immunoglobulin fragments of Pabs and Mabs for tumor imaging. Advantages include reduced Fc interaction and more rapid tumor penetration than the intact molecule. Results were little better in an imaging study in which $F(ab)_2$ fragments were compared with intact Mab [24]. Although the antibody uptake by the tumor is more rapid, there is faster excretion into the urine, which reduces the tumor dose. Fab monomer fragments should penetrate the tumor more quickly but will be cleared faster than $F(ab)_2$ fragments. This is found in practice [24] and improvements in the relative tumor dose have not yet been demonstrated.

Species. Pab from a variety of animals, including sheep, goat, rabbit, and mouse, have been used in clinical studies. Every species has antibodies of several classes and subclasses, each with different characteristics. For sheep and goat reagents, use has been of the IgG1 class, which is robust and has little human Fc receptor cross-reactivity [25].

The advent of Mabs seemed the ideal answer to many difficulties. They could be prepared to tumor-specific antigens, there would be no cross-reacting antibodies, and there would be no need for affinity purification. Indeed, there is overall in-vitro and animal work to show that some have superior tumor uptake in comparison with polyclonal antisera, but this has not been transformed into important clinical benefit. There are several reasons for this.

No human tumor-specific antigen has been discovered, and indeed CEA is as specifically tumor related as many of the more recently described antigens. An apparently specific Mab may bind unexpectedly to similar determinants on other antigens. The affinity, as well as the titre of the antiserum, may have to be high, which has not been easy to achieve. They also have idiosyncratic properties, which create difficulties in purification, labeling, and in-vivo stability [26]. Mouse immunoglobulins, and hence mouse Mabs, may interact with human Fc receptors and produce false-positive localization unless fragments are prepared; again this has posed problems [13]. Possibly, some mouse or rat immunoglobulin isotypes are more suitable than others [25], but reports have indicated the use of IgM and IgG antibody classes, IgG_1, IgG_2, and IgG_{2b} subclasses [1]. Each type varies in its stability to purification, labeling, and storage, and reactions with human Fc receptors differ [25]. Careful selection of Mabs is, therefore, essential. Alternatively, the Fc

interaction may be reduced by inhibiting synthesis of the carbohydrate side chains of the antibodies [27]. Theoretically the extreme specificity of Mabs could reduce tumor accumulation if the quantity of antigen was limited. In contrast, several polyclonal antibody molecules attach to each antigen. In practice, antigenic sites are probably not saturated, so this is not a limitation. Atttempts to mix Mabs have given no improvement [17], probably because the more effective antibodies are merely diluted out by the less effective ones.

Labeling ratios. Every antibody molecule should be radiolabeled, but damage increases with the number of atoms added, both at the time of labeling and subsequently during storage. It has been shown that for iodine labeling more than one atom per protein molecule causes progressive damage [28]. Since I-131 has, at best, an abundance of less than 20% when supplied, only 1 in 5 molecules will be labeled with an active atom. There is no need to label to higher specific activities unless the amount of target antigen is limited.

There has been considerable discussion about labeling carbohydrate side chains, which would limit damage to the antibody binding site. This is particularly relevant when conjugating with chelates prior to metal labeling. However, since little damage to the antibody molecule is demonstrable [29], novel methods can have little advantage over the cyclic anhydride technique of Hnatowich [30,31].

Second antibodies. Alternatively the administration of a clearing second antibody directed against the first might be useful [32]. The resultant immune complex is absorbed by the reticuloendothelial system and then degraded with elimination of the label. The second antibody technique is most effective at removing circulating antibody, but extravascular sites are poorly cleared. More biologic data is required before a useful evaluation can be made, for example, radiation may be transferred to the marrow or bladder, making these organs the dose-limiting factor. The probable mechanism of second antibody clearance is combination with the first antibody followed by reticuloendothelial uptake (liver, spleen, and bone marrow) via Fc receptors. The second antibody must have a strong cross-reaction with human Fc receptors, and rabbit IgG seems ideal. It should preferably be affinity purified and needs to be given in a dose of at least five-fold that of the first antibody. The optimal time of injection appears to be at 24 hours, but repeated doses may be preferable; however, there is little available data on the best regimen. The second antibody removes little unbound first antibody from the extravascular space, and since this contains at least 50% of the injected dose, the effect is inevitably limited. For example, if all the circulating antibody were to be removed, this would approximately halve the whole body dose but will redistribute the activity to other organs. The likely benefit is unclear.

Host factors

Blood supply. There are several explanations for why antibody uptake by tumors is so low. A small lesion receives only a minute proportion of the cardiac output, so tumor binding is slow. Another restriction is the slow rate of immunoglobulin diffusion out of the intravascular compartment: 50% in approximately 18 hours. Inevitably, the majority of the antibody will never gain access to the tumor and will be catabolized elsewhere. The detection of differentiated thyroid carcinoma with I-131 provides a useful analogy, where a very high dose may have to be given to disclose small lesions, despite more rapid diffusion and a specific and high-affinity uptake mechanism.

Circulating antigen. Antibody access may also be limited by circulating antigen. Nadler and colleagues [33] demonstrated that serum taken from a patient with circulating tumor antigen inhibited antibody binding in vitro to tumor cells expressing the antigen, and Meeker [34] showed that circulating tumor antigen increased the requirement for mouse antibody to achieve tumor penetration. Surprisingly, imaging studies have not confirmed this. One study showed that even when the concentration of circulating antigen was extremely high (many times that required to combine with the injected antibody), it still had no obvious effect on the positivity of the scan [12]. Perhaps the circulating antigen provided only a temporary barrier and the antibody eventually bound to the site of greatest antigen concentration, i.e., the tumor.

Expression of target antigen. Antigen expression by tumors is often heterogeneous and, in addition, the pattern of antigen expression of a metastatic deposit may differ from that of the primary tumor. Furthermore, tumor antigen is often expressed in nontumor sites. CEA, for example, is widespread on many epithelial surfaces and is bound to compete with the tumor-bound CEA for antibody. The amount of tumor antigen available for targeting is generally unknown, but the quantity is probably not limiting. Increasing the antigen expression may increase the amount of antibody bound to the tumor, but this has yet to be demonstrated.

Clearance rates. This has already been discussed under theoretical limitations and second antibodies.

Immune reactions. Many different types of allergic response could occur, but immune complex activation of complement is that most frequently reported. Occasionally steroid therapy is necessary but reactions are usually self-limiting. Human anti-mouse antibodies have been encountered in most therapeutic and diagnostic studies involving repeated injection of monoclonal antibodies. High levels of anti-mouse antibodies prevent continued treatment

by accelerating clearance of the injected antibody, thereby reducing its efficacy. Clinical problems may result, such as acute tubular necrosis [34].

It is not clear which of the above factors are the most important in limiting antibody uptake, but poor capillary permeability and inadequate antibody affinity are important. This can be shown by calculation based upon:

1. The injected antibody dose — a maximum of 100 μg, with a ratio of 1:1 with radiolabel, is permissible for imaging. The resultant antibody concentration in the capillaries is approximately 25 ng/ml (or 10^{11} molecules per 1000 cubic μm, this being the approximate volume of a tumor cell).
2. Effective molecular radius of antibody — 8.5 nm (MW, 150,000). This is an important determinant of molecular movement into the extravascular compartment.
3. Capillary permeability coefficient for antibody in tumor tissue is 56×10^{-8} cm of vessel surface area/sec. For normal connective tissues this is eight times less [35]. By calculation, about one antibody molecule would extravasate and pass each tumor cell every 10 minutes.
4. A representative dissociation constant (k_d) for antibody of 10^{-3} would allow binding with a half time of 12 minutes.
5. Typical antibody association constants k_a (e.g., 10^5) do not affect the result, since the forward reaction is so fast. Even antibodies with very low association constants would bind in less than 1 second.
6. Antigen density of 10,000 molecules per tumor cell (e.g., carcinoembryonic antigen). This does not limit antibody accumulation, in view of the poor capillary permeability of antibody and its fast dissociation.

The modest success to date could be attributable to the increased permeability of tumor compared with normal tissue capillaries. Antibody molecules one tenth the size with a k_d of 10^{-4} would enter the tumor faster and adhere longer to give 100-fold greater tumor accumulation, thereby permitting superb tumor imaging — assuming, incorrectly of course, that no other factors are involved.

Radioisotope limitations

Initially, only iodine isotopes were suitable for simple attachment to proteins and were appropriate for external scanning with gamma cameras. The chloramine-T or Iodogen methods are usually employed for iodination, since they cause little or no detectable change in the biologic behavior of immunoglobulin molecules. Unfortunately, iodine isotopes are not ideal for radioimmunodetection. I-131, for instance, has a high-energy photon (364 keV), which is poorly detected by present gamma cameras and requires the use of a high-energy collimator, which reduces the sensitivity still further. Second, the beta emission contributes a high radiation dose to the patient and this limits the activity that can be injected. A dose of 74 MBq of I-131-labeled antibody gives a similar absorbed radiation dose to x-ray CT (1 rem), and a

scanning time of 5–10 minutes per view is comparable with other nuclear medicine techniques. These factors limit the injected dose and the resultant picture counts.

I-123 has a more suitable photon energy for detection and delivers a radiation dose that is only one-tenth that from I-131. Unfortunately, the short half-life (13 hours) is not ideal, so the count rate at 48 hours is low. Also it cannot be used with Tc-99m for background subtraction due to overlapping photon energies. I-123-labeled antibodies have been used successfully [36] but, as with I-131-labeled antibodies, only tumors larger than 2 cm were visualized. I-124 has been used for position tomography but is unlikely to find wide application (see below).

In-111 has been suggested as a useful alternative to I-131 for several reasons: first, its lower energy (241 and 171 keV), higher abundance photons, are more readily detected by the camera and less obstructed by the medium-energy collimator; second, the lack of high-radiation beta particles gives more favorable dosimetry; third, the half-life (2.83 days) is ideal for antibody scanning. The cyclic anhydride method of labeling [30] is simple, reliable, and 'gentle' on the antibody. The results indicate greater sensitivity than comparable I-131-labeled antibodies [29].

Unfortunately, the long biologic half-life of In-111 contributes to an absorbed dose equal to that of I-131 (which has a shorter biological half-life). Its biologic disadvantage is that it accumulates in the liver and other organs containing reticuloendothelial cells, such as the bone marrow, and these are important organs for accurate imaging. In-111 is therefore only preferable for scanning certain organs.

The most useful isotope for nuclear medicine is unquestionably Tc-99m, but for antibody localization work it has serious disadvantages. It is chemically very impure, being contaminated with at least 99.9% aluminium ions, and the half-life of 6 hours is too short unless fragments are used. One study claimed to use it successfully, but once again only large tumors were detected [37].

An additional way of increasing count rates is to redesign the collimator. They are usually manufactured for images with high count rates and give good resolution. This is inappropriate for radioimmunodetection, which involves low count rates. If the collimator hole diameters are doubled, it would quadruple the count rates and could increase the sensitivity. The resolution would be decreased, but the wider signal can be reconstructed if the characteristics of the camera are known.

Computer subtraction of background counts

Only a small percentage of the injected dose of labeled antibody binds to the tumor, so it is common practice to simultaneously inject a second isotope. This mimics the distribution of the tumor-seeking antibody, apart from the

specific tumor uptake, but has a different photon emission energy. The two images are then subtracted. Although this technique improves contrast, there are several problems.

Attenuation characteristics

The localizing isotope usually has more energetic gamma rays than the subtracting isotope and their greater penetration results in artifacts.

The in-vivo biologic characteristics of the two isotopes are dissimilar, causing differential organ accumulation. This leads to false hot and cold areas. For example, the bladder always contains an excess of free iodine or technetium, which leads to hot or cold areas. Inequalities may also occur around the heart or stomach, although the latter can usually be blocked with a combination of potassium iodide and potassium perchlorate.

The process of subtraction, whilst improving contrast, introduces additional statistical fluctuations without increasing the signal, i.e., the signal-to-noise ratio is reduced.

There is no ideal subtracting isotope although some combinations such as gallium-67 with In-111, may be better than others. It seems that intelligent assessment of the scans will always be required.

Improved imaging systems

Improvements to the Anger camera are unlikely to provide strikingly better results. Greater improvements may come from tomographic methods, such as SPET (single photon emission tomography) and PET (positron emission tomography). SPET can be implemented with a conventional rotating gamma camera and established isotopes but is subject to the limitations inherent in collimated systems. Berche et al. [38] have applied SPET and I-123-labeled monoclonal antibodies to patients with apparent success. Unfortunately tomographic reconstruction is heavily dependent upon good count rates, which is perhaps reflected in their need for scans up to 40 minutes, and has frequent artifacts and relatively poor resolution. In-111 requires assessment in SPET because of its higher count rate and better accumulation in tumors.

PET utilizes the paired 511 keV gamma rays produced from the annihilation of positrons with electrons in the body. These rays are emitted at 180° to each other and their source can be accurately located by two opposed detectors without the need for a collimator. PET has minimal attenuation with depth because the photons are so energetic, and, potentially, it has better sensitivity because collimation is not required. The present PET cameras are not sensitive enough, nor do they have sufficient resolution to detect small tumors reliably.

Data manipulation remains a major area of development in camera systems and includes filtration and deconvolution techniques, in addition to

tomographic algorithms. The contribution of these methods to radioimmunodetection remains to be determined.

Conclusion

Many aspects of radioimmunodetection lend themselves to calculation and modeling. The resulting insight into this complex area of clinical science should allow rational strategies for future research. Much of the work undertaken to date would have benefitted from a more logical approach based upon clearer understanding of physical and biologic limitiations.

Acknowledgments

This work is supported by a grant from the Cancer Research Campaign. The figures have been reproduced with the kind permission of *Immunology Today*.

References

1. Bradwell, A.R., Fairweather, D.S., Dykes, P.W., Keeling, A., Vaughan, A.T.M., and Taylor, J. (1985) Limiting factors in the localization of tumors with radiolabeled antibodies. Immunol. Today 6:163–170.
2. Rockoff, S.D., Goodenough, D., and McIntire, K.R. (1980) Theoretical limitations in the immunodiagnostic imaging of cancer with computed tomography and nuclear scanning. Cancer Res. 40:3054–3058.
3. Hedin, A., Wahren, B., and Hammerstrom, S. (1982) Tumor localization of CEA-containing human tumors in nude mice by means of monoclonal anti-CEA antibodies. Int. J. Cancer. 30:547–552.
4. Moshakis, V., Bailey, M.J., Ormerod, M.G., Westwood, J.H., and Neville. A.M. (1981) Localization of human breast-carcinoma xenografts using antibodies to carcinoembryonic antigen. Br. J. Cancer 43:575–581.
5. Goldenberg, D.M., DeLand, F.H., Kim, E., Bennett, S., Primus, F.J., van Nagell, J.R., Estes, N., DeSimone, P., and Rayburn, P. (1978) Use of radiolabeled antibodies to carcinoembryonic antigen for the detection and localization of diverse cancers by external photoscanning. N. Engl. J. Med. 298:1384–1388.
6. Goldenberg, D.M., Kim, E.E., DeLand, F.H., Van Nagell, J.R., and Javadpour, N. (1980) Clinical radioimmunodetection of cancer with radioactive antibodies to human chorionic gonadotrophin. Science 208:1284–1286.
7. Ghose, T., Norvell, S.T., Aquino, J., Belitsky, P., Tai, J., Guclu, A., and Blair, A.H. (1980) Localization of 131-I-labeled antibodies in human renal cell carcinomas and in a mouse hepatoma and correlation with tumor detection by photoscanning. Cancer Res. 40:3018–3031.
8. Dykes, P.W., Hine, K.R., Bradwell, A.R., Blackburn, J.C., Reeder, T.A., Drolc, Z., and Booth, S.N. (1980) Localization of tumor deposits by external scanning after injection of radiolabeled anti-carcinoembryonic antigen. Br. Med. J. 280:220–222.
9. Mach, J-P., Carrel, S., Forni, M., Ritschard, J., Donath, A., and Alberto, P. (1980) Tumor

localization of radiolabeled antibodies against carcinoembryonic antigen in patients with carcinoma. N. Engl. J. Med. 303:5–10.

10. Mach, J-P., Buchegger, F., Forni, M., Ritschard, J., Berche, C., Lumbroso, J.D., Schreyer, M. Giardet, C., Accolla, R.D. and Carrel, S. (1981) Use of radiolabeled monoclonal anti-CEA antibodies for the detection of human carcinomas by external photoscanning and tomoscintigraphy. Immunol. Today 2:239–249.
11. Farrands, P.A., Perkins. A.C., Pimm, M.V., Hardy, J.D., Embleton, M.J., Baldwin, R.W., and Hardcastle, J.D. (1982) Radioimmunodetection of human colorectal cancers by an anti-tumor monoclonal antibody. Lancet 2:398–400.
12. Ishii, N., Nakata, K., Munehisa, T., Koji, T., Nishi, S., and Hirai, H. (1983) Radioimmunodetection of cancer using radiolabeled antibodies to alphafetoprotein. Prot. Biol. Fluids. 31:305–308.
13. Mach, J-P., Chatal, J.F., Lumbroso, J.D., Buchegger, F., Forni, M., Ritschard, J., Berche, C., Douillard, J-Y., Carrel, S., Herlyn, M., Steplewski, Z., and Koprowski, H. (1983) Tumor localization in patients by radiolabeled monoclonal antibodies against colon carcinoma. Cancer Res. 43:5593–5600.
14. Larson, S.M., Brown, J.P., Wright, P.W., Carrasquillo, J.A., Hellstrom, I, and Hellstrom, K.E. (1983) Imaging of melanoma with I-131-labeled monoclonal antibodies. J. Nucl. Med. 24:123–129.
15. Rainsbury, R.M., Ott, R.J., Westwood, J.H., Kalirai, T.S., Coombes, R.C., McCready, V.R., Neville, A.M., and Gazet, J-C. (1983) Location of metastatic breast carcinoma by a monoclonal antibody chelate labelled with indium-III. Lancet 2:934–938.
16. Armitage, N.C., Perkins, A.C., Pimm, M.V., Farrands, P.A., Baldwin, R.W., and Hardcastle, J.D. (1984) The localization of an anti-tumor monoclonal antibody (791T/36) in gastrointestinal tumors. Br. J. Surg. 71:407–412.
17. Chatal, J.F., Saccavini, J.C., Fumoleau, P., Douillard, J-Y., Curtet, C., Kremer, M., LeMevel, B.Q., and Koprowski, H. (1984) Immunoscintigraphy of colon carcinoma. J. Nucl. Med. 25:307–314.
18. Thompson, C.H., Lichtenstein, M., Stacker, S.A., Leyden, M.J., Salehi, N., Andrews, J.T., and McKenzie, I.F.C. (1984) Immunoscintigraphy for detection of lymph node metastases from breast cancer. Lancet 2:1245–1247.
19. Buraggi, G.L., Callegaro, L., Mariani, G., Turrin, A., Cascinelli, N., Attili, A., Bombardieri, E., Terno, G., Plassio, G., Dovis, M., Mazzuca, N., Natali, P.G., Scassallati, G.A., Rosa, U., and Ferrone, S. (1985) Imaging with I-131 labeled monoclonal antibodies to a high-molecular-weight melanoma-associated antigen in patients with melanoma: Efficacy of whole immunoglobulin and its $F(ab')_2$ fragments. Cancer Res. 45:3378–3387.
20. Epenetos, A.A., Carr, D., Johnson, P.M., Bodmer, W.F., and Lavender, J.P. (1986) Antibody guided radiolocalization of tumors in patients with testicular or ovarian cancer using two radioiodinated monoclonal antibodies to placental alkaline phosphatase. Br. J. Radiol. 59:117–125.
21. Epenetos, A.A., Snook, D., Durban, H., Johnson, P.M., and Taylor-Papadimitriou, J. (1986) Limitations of radiolabeled monoclonal antibodies for localization of human neoplasms. Cancer Res. 46:3183–3191.
22. Armitage, N.C., Perkins, A.C., Pimm, M.V., Wastie, M., Hopkins, J.S., Dowling, F., Baldwin, R.W., and Hardcastle, J.D. (1986) Imaging of bone tumors using a monoclonal antibody raised against human osteosarcoma. Cancer 58:37–42.
23. Begent, R.H.J., Keep, P.A., Green, A.J., Searle, F., Bagshawe, K.D., Jewkes, R.F., Jones, B.E., Barratt, G.M. and Ryman, B.E. (1982) Liposomally entrapped second antibody improves tumor imaging with radiolabeled (first) anti-tumor antibody. Lancet 2:739–742.
24. Mach, J-P., Forni, M., Ritschard, J., Buchegger, F., Carrel, S., Widgren, S., Donath, A., and Alberto, P. (1980) Use and limitations of radiolabeled anti-CEA antibodies and their fragments for photoscanning detection of human colorectal carcinomas. Oncol. Dev. Biol. Med. 1:49–69.

25. Keeling, A.A., Bradwell, A.R., Fairweather, D.S., Dykes, P.W., and Vaughan, A. (1984) Characteristics of first and second antibodies for tumor imaging. Prot. Biol. Fluids. 32: 455–457.
26. Haskell, C.M., Buchegger, F., Schreyer, M., Carrel, S., and Mach, J.P. (1983) Monoclonal antibodies to carcinoembryonic antigen: Ionic strength as a factor in the selection of antibodies for immunoscintigraphy. Cancer Res. 43:3857–3864.
27. Nose, M., and Wigzell, H. (1983) Biological significance of carbohydrate chains on monoclonal antibodies. Proc. Natl. Acad. Sci. USA 80:6632–6636.
28. Greenwood, F.C., Hunter, W.M., and Glover, J.S. (1963) The preparation of 131-I-labeled human growth hormone of high specific radioactivity. Biochem. J. 89:114–123.
29. Fairweather, D.S., Bradwell, A.R., Dykes, P.W., Vaughan, A.T., Watson-James, S.F., and Chandler, S. (1983) Improved tumor localization using indium-111 labeled antibodies. Br. Med. J. 287:167–170.
30. Hnatowich, D.J., Layne, W.W., Childs, R.L., Lanteigne, D., Davis, M.A., Griffin, T.W., and Doherty, P.W. (1983) Radioactive labelling of antibody: A simple and efficient method. Science 220:613–615.
31. Hnatowich, D.J., Layne, W.W., and Childs, R.L. (1982) The preparation and labelling of DTDA-coupled albumin. Int. J. Appl. Radiat. Isot. 33:327–332.
32. Goodwin, D., Meares, C., Diamanti, C., McCall, M., Lai, X., Torti, F., McTigue, M., and Martin, B. (1984). Use of specific antibody for rapid clearance of circulating blood background from radiolabeled tumor imaging proteins. Eur. J. Nucl. Med. 9:209–215.
33. Nadler, L.M., Stashenko, P., Hardy, R., Kaplan, W.D., Button, L.N., Kufe, D.W., Antman, K.H., and Schlossman, S.F. (1980) Serotherapy of a patient with a monoclonal antibody directed against a human lymphoma-associated antigen. Cancer Res. 40:3147–3154.
34. Meeker, T.C., Lowder, J., Maloney, D.G., Miller, R.A., Thielemans, K., Warnke, R., and Levy, R. (1985) A clinical trial of anti-idiotype therapy for B cell malignancy. Blood 65:1349–1363.
35. Gerlowski, L.E., and Jain, R.K. (1986) Microvascular permeability of normal and neoplastic tissues. Microvasc. Res. 31:288–305.
36. Epenetos, A.A., Britton, K.E., Mather, S., Shepherd, J., Granowska, M., Taylor-Papadimitriou, J., Nimmon, C.C., Durbin, H., Hawkins, L.R., Malpas, J., and Bodmer, W.F. (1982) Targeting of iodine-123-labelled tumor-associated monoclonal antibodies to ovarian, breast, and gastrointestinal tumors. Lancet 2:999–1005.
37. Morrison, R.T., Lyster, D.M., Alcorn, L., Rhodes, B.A., Breslow, K., and Burchiel, S.W. (1984) Radioimmunoimaging with ^{99m}Tc monoclonal antibodies: Clinical studies. Int. J. Nucl. Med. Biol. 11:184–188.
38. Berche, C., Mach, J-P., Lumbroso, J.D., Langlais, C., Aubrey, F., Buchegger, F., Carrel, S., Rougier, P., Parmentier, C., and Tubiana, M. (1982) Tomoscintigraphy for detecting gastrointestinal and medullary thyroid cancers: First clinical results using carcinoembryonic antigen. Br. Med. J. 285:1447–1451.

II

Model Systems

3. Experimental model systems for antibody targeting and radioimmunodetection

Rosalyn D. Blumenthal, Robert M. Sharkey, and David M. Goldenberg

The development of radiolabeled antibodies for clinical imaging and therapy has relied extensively on a variety of animal models. The design and use of animal models in radiotracer studies, including radiolabled antibodies, has been reviewed [1]. The first animal studies in the field of radioimmunodetection (RAID) were performed in the late 1940s and early 1950s. In a study to determine if anti-organ antibodies could localize specifically to the target organ, Pressman and Keighly [2] were the first to show localization of kidney following intravenous injection of I-131-labeled rabbit antibody against rat kidney. Subsequent studies confirmed that antibodies could be prepared with specificities against other organs, such as adrenals, ovary, lung, and small intestine [3]. Encouraged by these findings that organ-specific antibodies could be developed, investigations began to determine if tumor-specific antibodies could be generated. Pressman and Korngold [4] demonstrated selective tumor targeting in mice bearing the Wagner-osteogenic mouse sarcoma cell line. One of the earliest antigens used to localize humans tumors was fibrin [5], and I-131-labeled antibodies to fibrin were used in two patients for therapy [6]. However, it was recognized that more extensive investigations were needed to make this method useful for the early detection of tumors in humans.

The delay in the further development of RAID through the 1960s and into the early 1970s was as much due to the inability to identify a suitable animal model for studying the localization of human tumors as it was due to problems in developing an antibody against a suitable target antigen associated with human tumors. The discovery that a human tumor xenograft originally adapted for growth in the cheek pouch of the hamster, GW-39 [7], had maintained the production of a newly defined, human tumor-associated antigen (TAA) found in colorectal cancer, namely, carcinoembryonic antigen (CEA) [8], marked a turning point in the further development of RAID. Using this model, the feasibility of targeting human tumors with an antibody directed against human TAAs was realized [9–11], and within 5 years after the initial publication of tumor targeting in this animal model, successful clinical trials were reported [12]. The studies with this human tumor xenograft model and anti-CEA antibodies confirmed the findings of the animal studies

Goldenberg, D.M., (ed.), Cancer Imaging with Radiolabeled Antibodies.

in the 1950s and the 1960s that 1) a specific antibody targeted tumors better than a nonspecific antibody, 2) selective purification of the specific anti-tumor antibodies from irrelevant antibodies in the antiserum improved tumor targeting, and 3) tumors could not be imaged until excessive amounts of background radioactivity in the body were reduced. Thus, the animal studies helped result in a better understanding of some of the difficulties with RAID and assisted in developing some solutions.

The GW-39 tumor has been transplanted in the cheek pouch or hind leg of hamsters without immunosuppression for more than 20 years, and it has been serially propagated in hamsters for hundreds of generations without losing its histologic charcteristics or ability to synthesize CEA. It has served as an integral part of our preclinical RAID and radioimmunotherapy (RAIT) investigations. In this chapter, we will summarize some of our experiences with the GW-39 hamster host model and its importance in evaluating the localization of radiolabeled polyclonal and monoclonal antibodies directed against CEA and other colorectal TAAs, and we will compare it to GW-39 tumors that are serially propagated in nude mice.

Tumor host and site of implantation

Although the hamster was the first model used to test RAID with human tumor xenografts [10,13], Mach et al. [14] turned to the athymic nude mouse for RAID studies once it was shown that this was available to support foreign tumor growth [15]. Using nude mice bearing a human colonic tumor xenograft, Mach et al. reported a higher percent uptake per gram tumor than that reported by Primus et al. [11] using the GW-39 human colonic tumor xenograft in hamsters. Both groups used affinity-purified, goat anti-CEA antibodies for their studies, and questions were raised regarding differences between the two experimental models and the antibody preparations. Explaining some of the differences in radioantibody localization seen between two very closely related animal species may help in an understanding of how to correlate animal with human studies. The obvious difference between the models is the size of the animals (15–20 g for nude mice vs. 100–150 g for hamsters) and the location of tumor transplants (usually subcutaneous in the nude mouse vs. cheek pouch or hind leg muscle of the hamster) has been considered. In addition, standardization of the tumor xenograft and the antibody was also required. In this regard, we have studied tumor targeting using a murine monoclonal antibody against CEA in GW-39 tumors grown subcutaneously in both the hamster and the nude mouse. We have summarized below some of the similarities and differences in these models with regard to their impact on tumor targeting. Figure 1A compares the tumor uptake of an anti-CEA murine monoclonal antibody (Mab) in nude mice bearing GW-39 tumors in the conventional subcutaneous (SC) site with hamsters bearing SC GW-39 tumors. It is apparent that differences exist in both the magnitude and kinetics of radioantibody uptake in GW-39 tumors

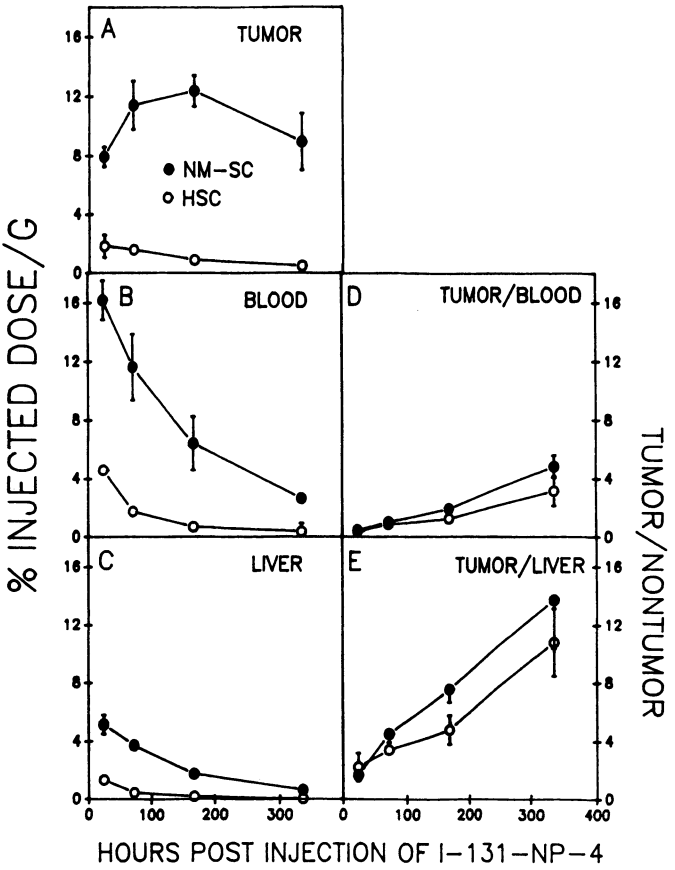

Figure 1. Biodistribution of I-131 NP-4 in hamsters or nude mice bearing subcutaneous GW-39 tumors from day 1–14, recorded as the percent injected dose per gram tumor (A), blood (B), and liver (C). Tumor/liver ratios and tumor/blood are given in panels D and E, respectively. Results are expressed as the mean of 15–30 tumors and 8–15 samples of blood and liver ± SE.

grown subcutaneously in the two species. Further evaluation of the magnitude of radioantibody uptake in blood (Figure 1B) and liver (Figure 1C) reveals similar differences in the percentage uptake in normal tissues and in the clearance kinetics between the two host species, which is easily appreciated by assessing the tumor/blood (Figure 1D) and the tumor/liver (Figure 1E) ratios. To determine whether the difference in animal size might affect radioantibody uptake, we calculated the relative concentration (RC) of antibody in the tumor, a measure that corrects the percent injected dose per gram (%ID/g) for animal body weight [4]. Table 1 illustrates how this measurement helps reduce, but not eliminate, ($p < 0.001$) the differences in the magnitude of radioantibody uptake in tumor between the two species. Differences in the kinetics of uptake still remain.

To explain the difference in antibody uptake between the two species, we evaluated the role that varying protein dose has on radioantibody accretion,

Table 1. Comparison of radioiodinated anti-CEA NP-4 Mab uptake in two experimental animal models

	Hamster SC Tumor			Nude Mouse SC Tumor		
	Time Postinjection					
	24 hr	72 hr	168 hr	24 hr	72 hr	168 hr
% ID/g	1.82 ±0.78	1.58 ±0.40	0.90 ±0.41	7.92 ±0.68	11.40 ± 1.65	12.37 ± 1.06
RC	2.08 ±0.30	1.73 ±0.16	1.01 ±0.17	1.26 ±0.14	2.67 ± 0.29	2.04 ± 0.22

since doses of injectables are usually adjusted to account for differences in body weight or surface area of the host animal, and concentration of antibody is critical for the optimization of antigen-antibody interactions. The hamsters used in many of our studies varied in weight from 80 to 150 g, and the nude mice weighed between 12 and 18 g. Body weight differences may have been as much as 12.5-fold, and differences in body surface area may be as much as 14.4-fold (21.6 cm^2 for a 12 g mouse and 312 cm^2 for a 150 g hamster). In Figure 1, nude mice were injected with 2.0 μg of protein, whereas hamsters were given 5–10 μg of protein. The higher protein dose given to the hamsters somewhat compensates for the differences in body weight of these animals, but not completely. We have shown previously that hamsters given anti-CEA antibody at doses of 10–1000 μg of antibody protein showed no change in the percent uptake of the antibody in tumor or in normal tissues [16]. Saturation of antigenic sites in the tumor was also not apparent in this dose range. We have extended these studies to doses as low as 0.1 μg of antibody protein with no evidence of a protein dose effect. Although we have not studied the same extensive dose range in nude mice, doses from 1 to 50 μg of protein have not altered the biodistribution of radioiodinated anti-CEA Mab [unpublished observation]. Other investigators similarly have shown no significant changes in the biodistribution of radiolabeled antibody in other animal models unless very high protein doses are used [17–19]. Rogers et al. [18] showed saturation of antigen binding sites using a protein dose in excess of 500 μg (20 mg/kg), but only with an 18 mg tumor (0.09% of the animal's body weight). Rostock et al. [17] used an anti-ferritin antibody, which reacted with a transplanted hepatoma line and with ferritin in normal tissue to show that the ratio of the anti-ferritin antibody to an irrelevant IgG increased as protein doses increased from 1 to 200 μg (up to 0.8 mg/kg) and then decreased at protein doses of 2000 μg. Their studies suggested that tumor targeting could be optimized by adjusting the amount of protein injected. This study may have more relevance to some of the observations made in humans than in the case of anti-CEA antibodies, because of the cross-reactivity of their anti-tumor antibody with normal tissues of the animal host. Higher protein doses may be required in these cases to allow for a higher proportion of the antibody to

reach the tumor due to the competition presented by normal tissues for available antibody. The fact that preclinical animal models do not have human tissue antigens complicates our ability to extrapolate tumor targeting in animals to humans. Perhaps this is the major difficulty in using animal models for predicting RAID in humans, and it is the principal reason why limited human trials must be considered as part of the standard methods used in selecting a Mab for more extensive clinical study.

The radionuclide used to tag the antibody may also play a role in determining whether protein dose influences the distribution of radioactivity in the tissues. Otsuka and Welch [20] showed that liver uptake of an In-111-labeled antibody was reduced as the amount of labeled antibody was increased, but no dose effect was seen for radioiodinated antibody. In patients, higher protein doses of several antibodies labeled with In-111 have led to changes in blood clearance rates and improved tumor targeting [21–24]. We are unaware of a similar finding with radiodinated antibodies. Thus, the radionuclide used for labeling may need to be included in the list of factors governing protein dose effects. Since the protein dose for our comparisons of tumor targeting in the hamster and nude mouse was not a likely source of the differences we noted, other factors were explored.

Along with differences in radioantibody uptake between two species with one tumor site, differences also exist between the tumor uptake of radioantibody when matched-sized tumors are grown in one of three different sites in the hamster. Figure 2 shows that GW-39 grown in the cheek pouch (CP) accretes four times more antibody than the same tumor grown either in the

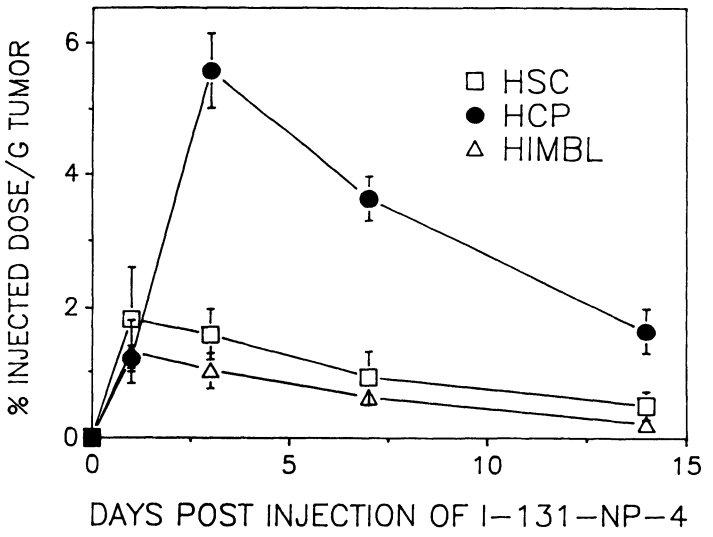

Figure 2. Biodistribution of I-131 NP-4 recorded as the percent injected dose per gram for GW-39 grown in the hamster cheek pouch (HCP) ○--○, back leg muscle (HIMBL) △--△, or subcutaneously (HSC) □--□. Results are expressed as the mean ± SE for 12–20 tumor samples.

back leg muscle (IMBL) or subcutaneously (SC). However, the tumor site does not affect radioantibody uptake in normal tissues (results not shown). It is necessary to explain why tumor localization is influenced by anatomic site and by the animal host. Organ and tumor physiology factors have been evaluated and are discussed.

Tumor vascular activity

Changes in blood flow rate in and around tumor masses [25] and in vascular permeability [26,27] can alter the uptake of Mab-radionuclide conjugates. Sands et al. [26] demonstrated a definitive relationship between monoclonal antibody uptake in tumor xenografts and vascular permeability and blood flow. In one key study, tumor oxygenation, a measure of underlying tumor blood flow, correlated closely with antibody delivery, i.e., when the mean PO_2 fell below 16 mm Hg, tumors could not be imaged, even when the presence of antigen was confirmed [28]. We have quantified the blood flow rate (BF), vascular volume (VV), and vascular permeability (VP) to intact IgG in the GW-39 tumor grown in three sites in the hamster (SC, CP, IMBL) and SC in the nude mouse (Figure 3). Of the three sites in the hamster, the CP, which accretes the most radioantibody, has the highest BF and VV and the second highest VP. The SC and IMBL tumor sites take up an equal amount of radioantibody, but only 25% of the amount in the CP site. The SC tumor has a 1.5-fold higher BF and VV than the IMBL tumor and 65% of the activity in the cheek pouch, but the IMBL tumor has a 3.5-fold higher VP than the SC tumor. The same tumor grown subcutaneously in the nude mouse takes up 8–10 times more radioantibody than the SC tumor in the hamster and two times more than the CP tumor. The BF and VV of the nude mouse tumor are comparable with those in the SC tumor; however, the VP in the nude mouse is six times higher than in the SC tumor and almost two times higher than the CP model. It is quite apparent from these studies, and from the work of Sands et al. and of O'Conner and Bale [26,29], that accessibility of circulating immunoglobulin, as measured by vascular function, is critical for antibody localization. We are currently using the nude mouse SC xenograft model to evaluate the effect of varying one or more of these vascular parameters on radioantibody uptake, using such physical methods as ionizing radiation [30,31], hyperthermia [32], or pharmacologic methods involving vasoactive agents [33,34].

Tumor size and viability

Several investigators have demonstrated an inverse relationship between Mab uptake and tumor mass [35–38]. Our results show this for tumor size and antibody accretion in the GW-39 tumor grown in the hamster cheek pouch, as

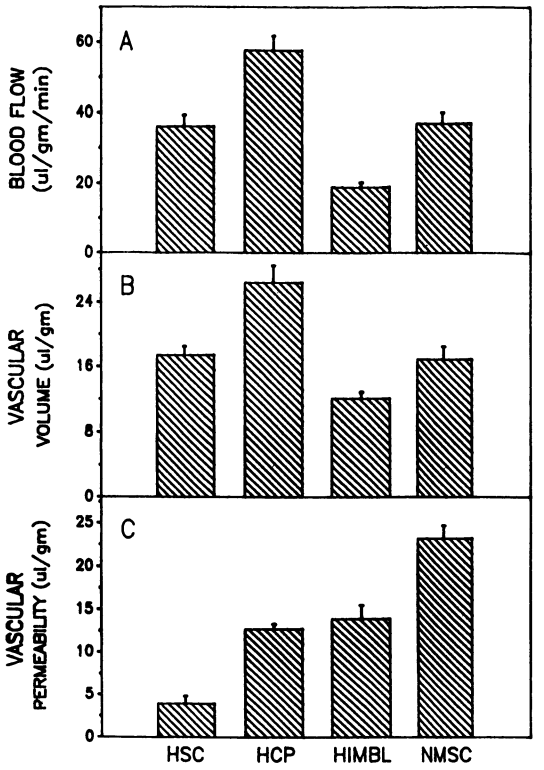

Figure 3. Radiotracer results of blood flow rate (A), vascular volume (B), and vascular permeability (C) of GW-39 tumors grown in the hamster subcutaneously (HSC), in the cheek pouch (HCP), and in the back leg (HIMBL) or in the nude mouse subcutaneously (NMSC). Results are expressed as the mean ± SE for 18–32 samples.

depicted in Figure 4. Tumors between 0.1 and 0.5 g in size localized 3.8% of the injected dose per gram (ID/g), while 2.3% ID/g was found in tumors that exceeded 1.5 g. A similar relationship between tumor size and percent uptake was observed with the nude mouse model (results not shown). These results are consistent with the decrease in blood flow and vascular space that occurs with tumor enlargement [39,40] and the elevation in tumor interstitial fluid pressure associated with increasing tumor size [41]. The internal region of large masses would not be expected to be accessible to any blood-borne agent.

Several studies have established a differential viability associated with solid tumors that are greater than several centimeters in diameter; the core region is characterized by central necrosis [42] and reduced vascularity [39,43]. Double-tracer, whole-body autoradiography studies using simultaneous localization kinetics of anti-tumor radioantibodies with ^{3}H-thymidine to map corresponding regional topographic viability for the same tumor specimen have demonstrated the selectivity of radioantibodies for viable cells [44].

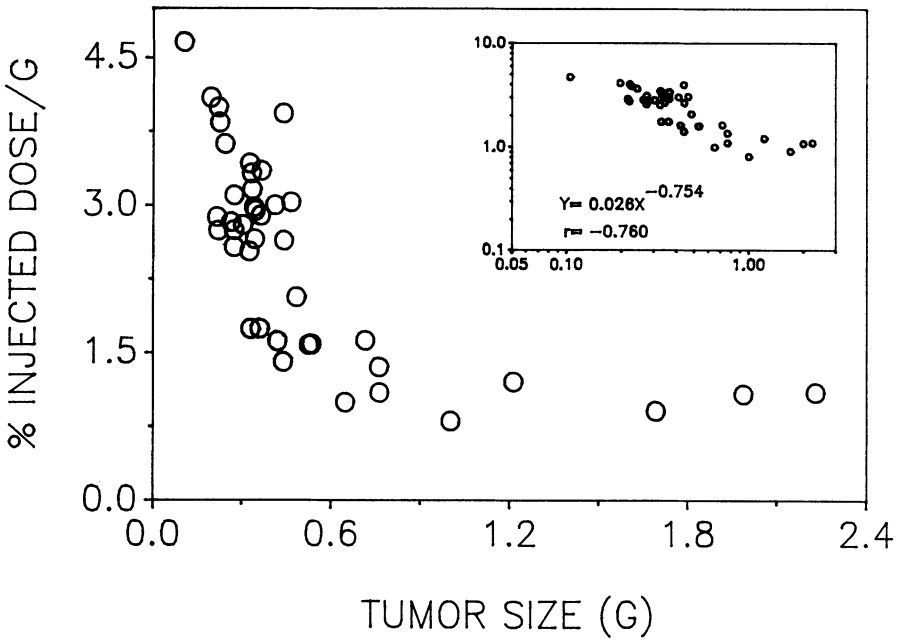

Figure 4. Biodistribution of I-131 NP-4 in GW-39 tumors grown in the hamster cheek pouch recorded as the percent injected dose per gram versus the size of the tumor (0.1–2.4 g). Inset represents the log-log transformation of the data.

Fand et al. showed a correlation between local accretion of radioantibody in tumor perimeters and rapid cell division. These results confirmed earlier studies linking radioantibody uptake with tumor viability [35,45]. Similar observations of perimeter localization of radioantibody have been reported with other xenografted tumors, including an osteosarcoma [46] and a malignant teratoma [47]. These results assist in explaining the high percent uptake of radioantibody in smaller tumors compared with larger ones.

The observation that relates antibody uptake to mass has several implications. First, to compare various radioantibody/tumor combinations in vivo, tumor uptake should be considered in terms of tumor mass. Ideally, the same-size tumor should be used to evaluate 1) uptake of a radioantibody in different tumors, 2) uptake of different radioantibodies in the same tumor, and 3) uptake of a radioantibody in the same tumor grown in different anatomic locations. Second, to understand the relationship between animal results and human data, one must appreciate that a given tumor mass in humans would demonstrate a lower uptake than the same-sized mass in a smaller animal. The uptake would be expected to be related to the total blood volume directed to the tumor i.e., uptake should be proportional to m/M, where m = tumor mass and M = the organism's total mass. Since humans weigh approximately three orders of magnitude more than murine models, human tumor uptake would be scaled accordingly. This relationship can

explain in part the difference in radioantibody uptake in the hamster tumor model and in the nude mouse tumor model.

Antigen concentration in tumor tissue and serum

Using ^{131}I-labeled anti-CEA monoclonal antibodies, Hedin et al. [48] found a positive correlation between the CEA content of xenografted tumors and imaging. This observation was further supported by Philben et al. [37] using ^{111}In-labeled anti-CEA antibodies and evaluating both biodistribution and scintiscan results. In our studies, differences in the CEA content of GW-39 tumors grown in the two different hosts or in the three anatomic sites were observed (Figure 5). GW-39 in the hamster SC site had 13.49 ± 2.28 μg CEA/g tumor, while the same tumor grown SC in the nude mouse had 29.79 ± 2.32 μg CEA/g tumor ($p < 0.001$). When the tumor was grown in the IMBL region, it contained 20.14 ± 2.3 μg/g CEA (not significantly different from the hamster SC tumor). GW-39 tumor grown in the CP contained 25.13 ± 2.46 μg/g CEA ($p < 0.001$ when compared with the tumor in the SC region). Thus, the higher uptake of radiolabeled antibody in a particular tumor may be explained partially by the higher amount of CEA in the tumor. However, similar to Philben et al.'s [37] observation in nude mice, as the tumor CEA content increases above 29 μg/g, the relationship between CEA levels and radioantibody uptake is not perfect.

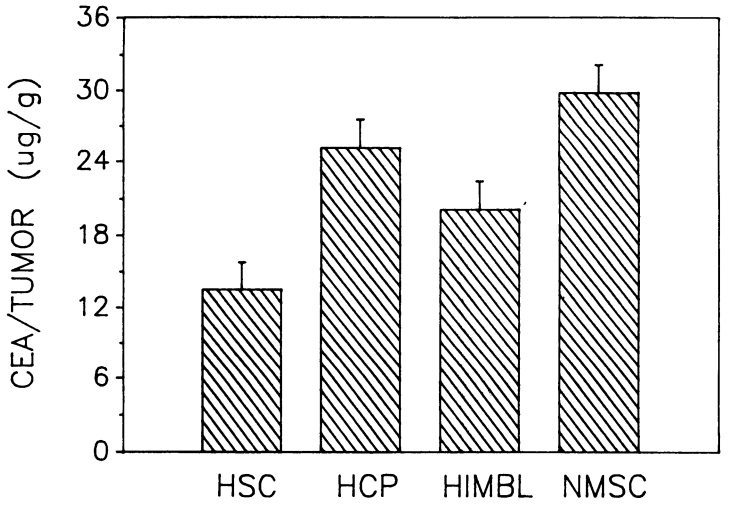

Figure 5. Enzyme immunoassay measurements of CEA in tumors (μg/g) for GW-39 tumors. Results are expressed as the mean ± SE for 16–24 samples. HSC = hamster subcutaneously; HCP = hamster cheek pouch; HIMBL = hamster intramuscular back leg; NMSC = nude mouse subcutaneously.

If the antibody used for RAID interacts with shed antigen in the serum, then the concentration of serum antigen may affect the amount of free antibody available to the tumor, as well as the kinetics of clearance of the antibody from the blood. In our two tumor-bearing models, the amount of CEA in the serum does vary: 0.9 ± 0.3 ng/ml in hamster serum and 10.6 ± 1.9 ng/ml in nude mouse serum ($p < 0.001$). Although the anti-CEA Mab used in these studies (NP-4) does not complex readily with circulating CEA [49], serum CEA is a factor to be considered when evaluating RAID in a particular model with very high serum CEA or when using other anti-CEA antibodies that do interact readily with serum CEA. The effect that immune complex formation with serum CEA has on radioimaging is further complicated by the finding that a variety of CEA species are produced and secreted with unique pharmacokinetics [50]. The CEA content in serum also depends on the tumor size, another reason for standardizing tumor size in RAID studies and evaluating tumor xenografts for antigen content, liberation of antigen into the circulation, and complexation of radioantibody in the blood.

The almost undetectable CEA in hamster serum contrasts with the findings in patients with colorectal cancer who have elevated plasma CEA. Higher amounts of CEA in the plasma correlate well with the extent of metastatic spread, suggesting that antigen shed from the tumor gains greater access to the circulation once the tumor breaks through the serosal barrier of the colon. Since human tumors grown in animals are generally encapsulated and do not usually metastasize, liberation of antigen into the blood of animals may be limited in many instances. Furthermore, in normal adult hamsters, CEA is a foreign substance, and hamsters bearing IMBL GW-39 tumors develop a weak immune response to CEA, primarily IgM, when the tumor burden in the animal is greater than 5–10 g per leg [51]. Thus, the lack of circulating CEA makes the GW-39 hamster tumor model different from most colorectal cancers found in humans. However, CEA can be detected in the plasma of nude mice, and the amount in plasma increases as the tumor grows. The reason why CEA detection is possible in nude mouse sera but not in hamster sera may be because 1) of a higher CEA content in the tumor of nude mice than hamsters, 2) the same size tumor in both animals results in a greater tumor burden in the mouse relative to the overall size of the animal, or 3) of the inability of the nude mouse to build an immune response to the antigen. Thus, by growing the tumor in a different animal we have added to the versatility of the model so that localization studies may be conducted with the added variable of antigen in the blood.

Histopathology and accessibility of antigen

The GW-39 tumor model has played an important part in our investigations, but it is a signet-ring carcinoma, and therefore may not be representive of well to poorly differentiated adenocarcinomas of the colon. Therefore, we have established several additional human colorectal tumors in nude mice.

One such xenograft, called GS-2, is a well to moderately differentiated adenocarcinoma. GS-2 grown in nude mice has 130 μg CEA/g tumor by extraction, fourfold higher than the GW-39 tumor grown in the same animal host. Although GS-2 has more antigen present than GW-39, GS-2 tumor targeting with radiolabeled NP-4 anti-CEA Mab is not as effective as that seen with GW-39 (Figure 6A). One explanation for this observation is the more rapid blood clearance of antibody from animals with GS-2 tumors (Figure 6B). Sera from mice with GS-2 tumors contain 113 ng CEA/ml, ten times more than sera from animals bearing GW-39 tumors. Some complexing (< 20% at 1 hour after injection) of the radiolabeled antibody has been detected in animals bearing the GS-2 tumor, while no complexing is found in animals bearing even larger GW-39 tumors. Use of another anti-CEA Mab that does not complex with CEA in the plasma [49], as well as a Mab directed against colon-specific antigen-p (CSAp) that recognizes an epitope not found in the plasma but that is in the tumor [52], have shown a similar reduction in tumor targeting when comparing GS-2 with GW-39 [unpublished data]. Thus, complexation with circulating antigen does not explain the poor tumor targeting against GS-2. The presentation of antigen (membrane-associated vs. intracellular), the amount of tumor compared with interstitial tissue, and the permeability of tumor endothelium may all contribute to the observed differences in tumor targeting between GS-2 and GW-39.

Additional localization studies have been performed with yet another human colorectal xenograft, the LS174T line [53], a moderately to poorly differentiated adenocarcinoma containing 22 μg CEA/g tumor and releas-

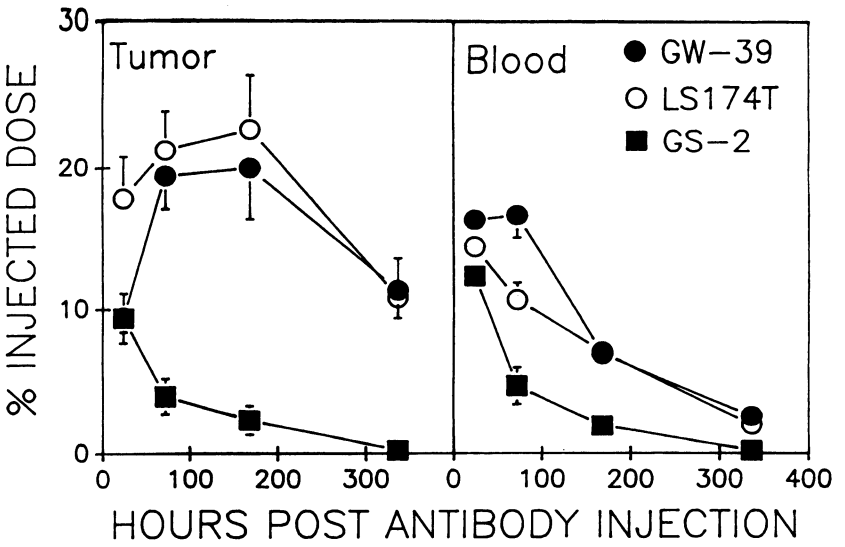

Figure 6. Biodistribution of I-131 NP-4 in GW-39, LS174T, and GS-2 human colorectal tumors grown subcutaneously in the nude mouse. Percent injected dose per gram in tumors (left panel) and in blood (right panel).

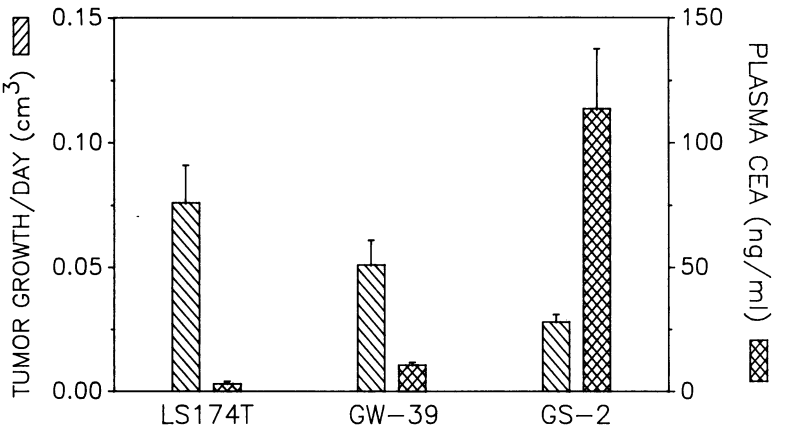

Figure 7. Tumor growth rate and plasma CEA from three colorectal tumors grown subcutaneously in the nude mouse.

ing very small amounts of CEA into the blood (~3 ng/ml). These amounts are comparable with the GW-39 xenograft, but this tumor has a different histopathology. Radioantibody uptake in tumor and blood clearance are similar to that observed in mice with GW-39 xenografts (Figures 6A and 6B). These results suggest that tumor histopathology by itself may not be critical for antibody localization but that accessibility of antigen is a more important factor.

Variability in the growth rate of tumor transplants is another parameter that needs to be considered when evaluating a particular tumor model. Growth kinetic studies of each tumor model should be done and related to the tumor antigen content, plasma antigen content, and vascular activity. Figure 7 illustrates differences in the tumor growth rate and plasma CEA for our three colorectal lines grown in nude mice. LS-174T is the fastest growing of the three xenografts, followed by GW-39 and then GS-2. Plasma CEA is indirectly correlated with the growth rate of all three lines. These differences in tumor biology may be important in assessing the potential for radioantibody targeting in a particular model and in evaluating how representative a model is of the human colon cancer population.

Antibody form and antibody mixtures

Thus far, we have shown that the choice of the animal host and the site of implantation of a tumor xenograft are critical factors in developing an animal model for RAID studies and in evaluating the magnitude and kinetics of radioantibody uptake in a tumor model. However, for any one experimental model, several other lessons on antibody form (whole IgG vs. fragments) and

single versus multiple antibodies can be learned that are applicable to the clinical situation.

The pharmacokinetics of intact immunoglobulin and its $F(ab')_2$ and Fab' fragments are significantly different. Analysis of each antibody form has demonstrated that the more rapid clearance of antibody fragments results in less radioactivity in the blood and normal tissues [54–56], and therefore, the ability to produce better images at an earlier time after administration. The reason for the more rapid clearance of fragments from the blood may be related to the removal of the Fc portion of the antibody, thereby reducing recognition of an intact IgG by reticuloendothelial tissues. This may account for less tissue uptake, but the faster clearance from the blood is related principally to the smaller size of the protein. A detailed analysis of volume of distribution, permeability surface area product, organ clearance, organ extraction, mean residence time, and number of cycles through various body regions for each antibody form has been presented by Covell et al. [57]. Figure 8 illustrates the marked difference in tumor/blood and tumor/liver ratios that we have observed using either intact NP-4 IgG, NP-4 $F(ab')_2$, or NP-4 Fab' in the GW-39 nude mouse xenograft. The $F(ab')_2$ form yields the highest ratios 7 days after injection. The Fab' produces the second highest tumor/nontumor ratios, which occur 48 hours after injection and thereafter decline. Ratios from whole antibody treatments are far lower than either form of fragment and are not achieve for 2 weeks. These results, demonstrating that $F(ab')_2$ is superior to the less well-localized Fab' and the slowly cleared intact antibody, are consistant with scintiscan data presented by Wahl et al. [54]. The advantage of improved tumor targeting with antibody

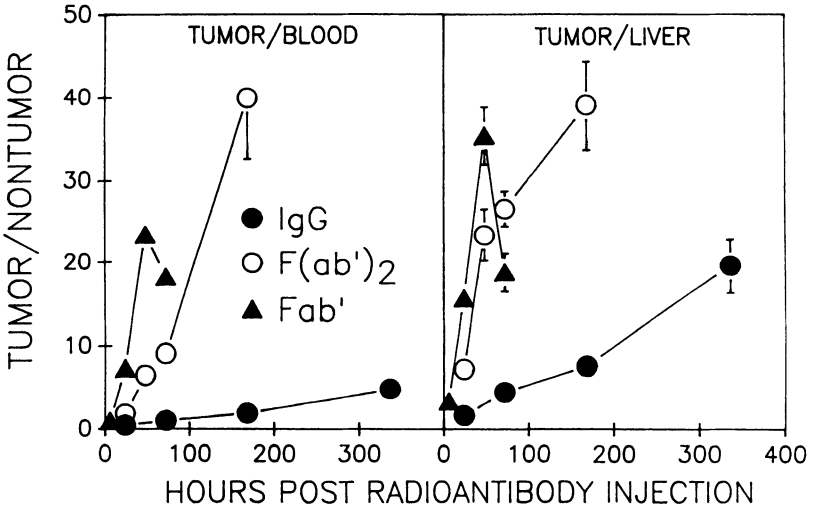

Figure 8. Tumor/blood (left panel) and tumor/liver (right panel) for I-131 NP-4 intact IgG, NP-4 $F(ab')_2$, and NP-4 Fab' in GW-39 tumors grown subcutaneously in the nude mouse.

fragments is opposed by the lower amount of antibody accretion in the tumor. Thus, the highest amount of antibody uptake in the tumor occurs with intact IgG and decreases as the size of the fragments decreases. Maximum accretion of IgG occurs within 3 days, and then, depending on the antibody, is bound to the tumor for longer periods than the fragments. $F(ab')_2$ reaches its highest levels within 1 day and then decreases after 2 days. Maximum tumor accretion of Fab′ occurs before 24 hours and decreases thereafter at a more rapid rate than the intact IgG or $F(ab')_2$.

Several clinical reports have also found better imaging results with fragments than with whole antibody [57–60]. These observations are quite consistent for imaging with radioiodinated antibodies. However, in one study using nude mice with mammary tumors, indium-111-labeled intact antibody provided a better tumor image than In-111-fragments because of the high liver and kidney uptake of indium-labeled fragments [61]. These results have been confirmed in cancer patients [62]. Thus, the animal models have accurately predicted the general relationship between IgG and fragments in humans for both radioiodinated and radiometal-labeled antibodies, but, obviously, differences in the percent injected dose in the tumors and the optimal accretion times exist between rodents and humans [63,64].

Another concept to improve tumor targeting with Mabs has been the engineering of Mab mixtures that will identify different antigens in tumors. The major difference between this approach and polyclonal antibodies is that Mabs that identify the most, as well as the least, prevalent antigens can be combined to what may be considered an ideal mixture of antibodies. Such selection criteria are difficult with polyclonal antisera. Surprisingly, there have been relatively few reports of improved tumor targeting with Mab mixtures [65]. Our group initially reported combinations of polyclonal antibodies against CEA and another colonic-cancer-associated antigen, first identified from extracts of GW-39 tumors and named colon-specific antigen-*p* (CSAp) [66,67], showed improved tumor/nontumor ratios in comparison with the combination of anti-CEA and normal goat IgG [68]. More recently, we have developed Mabs against colorectal cancer cell lines, including GW-39 [69], and one of the antibodies identifies an epitope similar to that initially described for CSAp [52]. Combination of this Mab, called Mu-9, with the anti-CEA NP-4 Mab has shown an improvement in tumor targeting only on day 1 post-injection when compared with each Mab alone [unpublished results]. In addition, combinations of Mabs recognizing distinct epitopes on CEA [70] have not shown improved tumor targeting [71]. In this latter case, the percent uptake in the tumor was reduced to an amount near the average percent uptake of the highest and lowest Mab used in the mixture.

Tables 2 and 3 show the consequences of injecting individual or combinations of two Mabs in a theorectical tumor model containing two antigens (Ags). Several assumptions have been made based on actual experimental observations. We have defined the model with two Ags that are expressed in different concentrations in the tumor and the two Mabs have

Table 2. Theoretical considerations for the use of monoclonal antibody mixtures: Comparison of the percent injected dose per gram (%ID/g) and saturation of antigen bidning sites for two monoclonal antibodies used alone or in combination

Mab	Total Units Mab Injected	%ID/g Tumor	Total Tumor-Bound Mab	Units Ag 1 Total	Units Ag 1 Total Bound	Units Ag 2 Total	Units Ag 2 Total Bound	% Total Ag Bound
A. 1	100	5%	**5**	1000	5	5000	0	**0.08**
2	100	10%	**10**	1000	0	5000	10	**0.16**
1 + 2	100 + 100	7.5%	**15**	1000	5	5000	10	**0.25**
1 + 2	100 + 500	9.2%	**55**	1000	5	5000	50	**0.92**
B. 1	20,000	5%	**1000**	1000	1000	5000	0	**16.6**
2	50,000	10%	**5000**	1000	0	5000	5000	**83.3**
1 + 2	20,000+ 50,000	8.5%	**6000**	1000	1000	5000	5000	**100.0**
C. 1	20,000	5%	**1000**	1000	1000	5000	0	**16.6**
2	100,000	5%	**5000**	1000	0	5000	5000	**83.3**
1 + 2	20,000+ 100,000	5%	**6000**	1000	1000	5000	5000	**100.0**
1 + 2	40,000+ 100,000	4.3%	**6000**	1000	1000	5000	5000	**100.0**

Table 3. Theoretical considerations for the use of monoclonal antibody mixtures: Comparison of tumor/blood ratios for two monoclonal antibodies used alone or in combination

Mab	Total Units Mab Injected	%ID/g Blood	Units of Mab per g Blood	Total Tumor Bound Mab	Tumor/Blood
A. 1	100	20%	20	5	**0.25**
2	100	20%	20	10	**0.50**
1 + 2	100 + 100	20%	40	15	**0.38**
1 + 2	100 + 500	20%	120	55	**0.46**
B. 1	20,000	20%	4,000	1,000	**0.25**
2	50,000	20%	10,000	5,000	**0.50**
1 + 2	70,000	20%	14,000	6,000	**0.43**
C. 1	20,000	20%	4,000	1,000	**0.25**
2	50,000	10%	5,000	5,000	**1.00**
1 + 2	70,000	15%	10,500	6,000	**0.57**
1 + 2	70,000	10%	7,000	6,000	**0.86**
1 + 2	70,000	5%	3,500	6,000	**1.71**

different percent injected doses per gram of tumor. We have assumed that the percent injected dose per gram of tissue does not change with an increasing protein dose. The amount of Mab has been varied to account for conditions of nonsaturation and saturation of Ag sites in the tumor. In Table 2A, 100 molecules of Mab 1 and 2 were injected separately. As expected, a higher percentage of total Ag sites (1000 of #1 and 5000 of #2 = 6000 total Ag sites) were bound when Mab 2 was used instead of Mab 1. Mixing an equal amount

of the Mabs increases the percentage of total Ag bound, but the percent injected dose per gram of tumor of the Mabs is reduced to the average of the two Mabs when used alone. If the amount of Mab 2 is increased in relation to Mab 1, the percent injected dose per gram of tumor will increase but will never exceed the highest percent of Mab. The total percentage of Ag bound in the tumor will also increase. In situation B, an Ag saturating dose of Mab 1 and 2 is injected, resulting in 100% binding of each individual Ag, but collectively there are more sites to be bound when Mab 1 and 2 are used individually. Combining the 2 Mabs achieves 100% saturation of all Ag sites (1 + 2), but the percent injected dose per gram is no higher than the percentage observed for Mab 2 alone. Under these conditions, there is a higher percent injected dose per gram of tumor with the Mab than seen with an equal, but nonsaturating dose of Mab 1 and 2 injected together, because more of Mab 2 was injected than Mab 1. Increasing the protein dose of either Mab would reduce the percent injected dose per gram of tumor for that Mab (Table 2C), and combinations of excessive amounts of each Mab would further reduce the observed percent injected dose per gram of tumor.

The impact of combinations of Mabs on tumor/blood ratios is shown in Table 3. In situations A and B, we have assumed a similar percent injected dose per gram of blood for Mab 1 and 2, and that this percentage is not influenced by the protein dose. Tumor/blood ratios are the highest for Mab 2, which binds more sites in the tumor. Combining Mab 1 and 2 at equal protein doses would reduce the tumor/blood ratios. Increasing the proportion of Mab 2 in the mixture would increase the tumor/blood ratios, but they would not exceed the tumor/blood ratios of Mab 2 alone. Similar results would occur at saturating doses of Mab (Table 3B). In Table 3C, we assumed that the blood clearance properties of the Mabs were different, with Mab 2 having the fastest clearance rate, such that only 10% per gram remained in the blood. Under this condition, tumor/blood ratios are the highest with Mab 2 alone. If by combining Mab 1 and 2 the blood clearance properties change so that the percent injected dose in the blood is more than Mab 2 alone, then the tumor/blood ratios decline. However, if the blood clearance is similar to or faster than for Mab 2, the tumor/blood ratios will improve.

From these examples, it is not surprising that more reports of improved tumor targeting with combinations of Mabs have not been published. Since these models may be an oversimplification of the dynamics of Mabs in tumors and normal tissues, it is possible that some combinations of Mabs could work synergistically and tumor targeting could improve, but to combine Mabs without first testing each Mab separately could decrease the sensitivity of RAID. Although RAID may be compromised, RAIT may benefit by some of these procedures. Combinations of Mabs recognizing distinctly different cells in a tumor based on the presence of uniques epitopes would allow for targeting of a greater number of cells, thereby increasing the tumoricidal ability of the procedure. These issues require further testing in animals to

determine if this added effort is warranted. Indeed, the examples presented in Tables 2 and 3 suggest that any advantage afforded to combinations of Mabs may be difficult to measure, especially if the data derived in vivo have a high degree of variability. Although tumor cell populations in xenografts may be heterogeneous, the degree of heterogeneity may not be large enough for experiments to show a definite advantage for antibody combinations. The artificial creation of a mixed tumor cell population may be one way to improve our ability to appreciate the value of Mab combinations.

New tumor models

Before the availability of nude mice, the cheek pouch of the hamster was one of the principal sites used in attempts to establish human tumors in an animal model, because it was considered to be an immunologically privileged site [72]. Nevertheless, hamsters were given immunosuppressive agents, such as cortisone, to aid in the establishment of xenografted tissues. With the development of nude mice, the subcutaneous site was the most practical for tumor transplantation. Althogh many human tumors can grow in nude mice without immunosuppression, some tumor types require special treatment to support their growth, e.g., some breast tumors require estrogen [73], whereas immunosuppression by total-body irradiation or anti-lymphocyte serum has been used to encourage the growth of other human tumors [15].

Since the most lethal characteristic of human tumors is their metastasis to visceral organs, it is important to determine whether tumors can be established in more clinically relevant sites. For colorectal cancer, the liver is the principal organ for metastatic spread, in addition to seeding in the peritoneal cavity. We have shown that GW-39 could be established in the liver of adult hamsters without immunosuppression by directly injecting the tumor into the liver [74]. Tumors could also be established in the liver by splenic injection, but direct injection into the liver is more reliable. In almost 80% of the animals receiving a hepatic injection, foci of tumor also developed in the lungs. In some instances, lung involvement was very extensive. Radiolocalization studies confirmed tumor targeting in the liver, but we could not demonstrate tumor targeting in the lung by either external imaging or by direct tissue counting [74]. However, the higher sensitivity of autoradiography showed discrete localization of tumor foci in the lungs with the anti-CEA antibody, but not with an irrelevant antibody. Further studies with this model showed that the tumors were rejected eventually (within 4–8 weeks) by most of the hamsters. Tumor progression could be encouraged with immunosuppression, but we found that the tumor would grow easily in nude mice without additional manipulation [unpublished data]. We have explored the establish-

ment of GW-39 in the nude mouse liver by direct injection into the liver or by splenic innoculation. We found that splenic injection leads to disseminated foci in the liver, whereas direct injection in the liver lobe generally leads to only a single focus of tumor. This represents two distinct varieties of hepatic metastasis and may be useful for further studies.

Tumors in the lung can be established by intravenous injection of tumor suspensions, and tumors can also grow in the peritoneal cavity as multiple foci with progression to a cell-rich ascites form. The effects of host environmental factors on antigen expression and vascular activity in these various tumor sites will be important to determine. Figure 9 illustrates several of these models

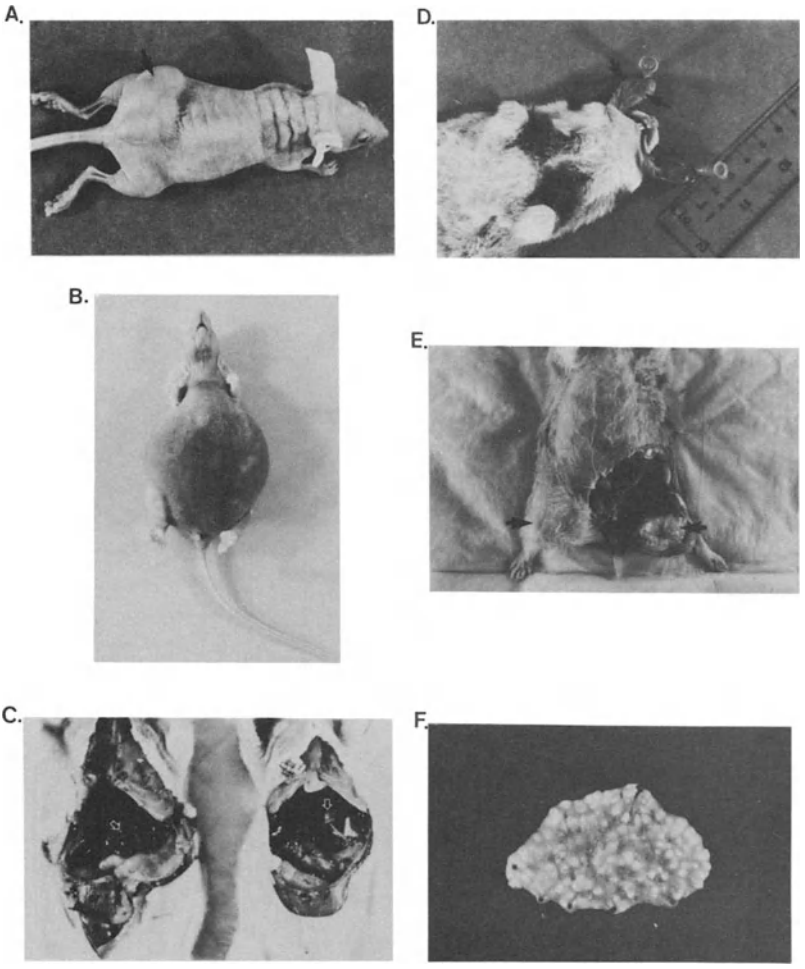

Figure 9. Animal models in use: A: nude mouse subcutaneous tumor; B: nude mouse ascites model; C: nude rat liver tumor; D: hamster cheek pouch tumor; E: hamster intramuscular back leg tumor; and F: nude mouse lung tumors.

(A, nude mouse SC; B, nude mouse ascites; C, nude rat liver implant; D, hamster cheek pouch; E, hamster back leg; and F, lung metastasis). Other investigators have shown that human tumors can be implanted in various sites of clinical relevance [75–77], and these models now serve as the focus for the future evaluation of RAID and RAIT.

We have also investigated the use of nude rats for RAID and RAIT studies [78]. Like their smaller counterpart, the nude mouse, human tumors can be implanted in athymic rats. We initially attempted external imaging studies in these animals given intrahepatic transplants to determine if the greater spatial resolution provided by the larger animal would improve our ability to visualize tumors in the lungs. We have only been able to visualize these lung tumors by the use of a second antibody method [79] that removes excessive background activity from the blood, thereby improving tumor targeting. Because of the expense and limited availability of these animals, routine tumor localization studies are not practical. However, in instances where the

Table 4. Comparison of RAID results in preclinical and clinical situations

Observation	Preclinical	Clinical
1. Antitumor antibodies target better than irrelevant antibodies	Yes	Yes
2. Tumor imaging requires reduction of background activity accomplished by time, fragments, or second antibody	Yes	Yes
3. Iodinated fragments clear faster than intact IgG and as a result provide an earlier tumor image	Yes	Yes
4. Presence of protein dose effect	No apparent effect with I-131; possible effect with In-111	May be important but may depend on circulating antigen levels, tumor burden, nonspecific interaction with normal tissue, or isotope
5. Circulating antigen does not influence tumor targeting but may alter the tissue uptake pattern of radioantibody	Yes	Yes
6. Percent injected dose per gram tumor during first 7 days	Hamster: 1–5% Mouse: 7–30%	< 0.001%
7. Tumor/nontumor ratios during first 7 days	Hamster: 2–12 Mouse: 3–40	1.5–30
8. Resolution (ratio to total body size)	Hamster: 2–5 Mouse: 2–6	At 0.01%/g in 70 kg patient RC = 7.0; at 0.001%/g in 70 kg patient RC = 0.7
9. Minimum-size tumor detectable	0.5 cm	Planar: 1–2 cm Spect: 0.4–0.5

larger nude rat would provide easier access for certain surgical manipulations that are easy to perform in nude mice, utilization of the nude rat model for RAID and RAIT may increase.

Conclusions

The field of RAID and the developing area of RAIT have witnessed a rapid expansion over the past ten years. There is now abundent evidence that RAID is a safe and useful procedure, and may provide greater specificity and sensitivity for tumor imaging than other conventional radiologic procedures [80]. Despite the need to test antibodies clinically, animals provide a useful and expeditious preclinical screen for assessing tumor targeting of monoclonal antibodies in vivo. However, one must appreciate that animal models do not give the definitive answer in the selection of the most clinically useful antibody, but are one category of information that can be added to other in-vitro selection criteria. Table 4 compares RAID results in preclinical and clinical settings. Undoubtedly, many issues concerning how to further improve RAID and RAIT have need of further investigation. A better appreciation of the role of animal tumor models in predicting clinical applications of Mab targeting should help advance the clinical prospects of this technology.

Acknowledgments

This work was supported in part by USPHS grant CA 39841 and BRSG grant SO7 RR05903-04 from the National Institutes of Health.

References

1. Gallagher, B.M. (1983) Monoclonal antibodies: The design of appropriate carrier and evaluation systems. In: Lambrecht, R.M., and EcKelman, W.C. (eds.), *Animal models in Radiotracer Design*. New York: Springer-Verlag, pp. 61–105.
2. Pressman, D., and Keighly, G. (1948) The zone of activity of antibodies as determined by the use of radioactive tracers; the zone of activity of nephrotoxic anti-kidney serum. J. Immunol. 59:141–146.
3. Pressman, D. and Korngold, L. (1953) The in vivo localization of anti-Wagner-osteogenic-sarcoma antibodies. Cancer 6:619–623.
4. Bale, W.F., and Spar, I.L. (1957) Studies directed toward the use of antibodies as carriers of radioactivity for therapy. Adv. Biol. Med. Phys. 5:285–356.
5. Spar, I.L., Bale, W.F., Goodland, R.L., and DiChiro, G. (1963) Preparation of purified I-131-labeled antisera to human fibrinogen. Preliminary studies in human patients. Acta Univ. Int. Contre le Cancer 19:197–200.
6. McCardle, R.J., Harper, P.V., Spar, I.L., Bale, W.F., Andros, G., and Jiminez, F. (1966) Studies with iodine-131-labeled antibody to human fibrinogen for diagnosis and therapy of tumors. J. Nucl. Med. 7:837–847.

7. Goldenberg D.M., Witte, S., and Elster, K. (1966) A new human tumor serially transplantable in the golden hamster. Transplantation 4:760–763.
8. Goldenberg, D.M., and Hansen, H.J. (1972) Carcinoembryonic antigen present in human colonic neoplasms serially propagated in hamsters. Science 175:1117–1118.
9. Primus, F.J., Wang, R.H., Goldenberg, D.M., and Hansen, H.J. (1973) Localization of human GW-39 tumors in hamsters by radiolabeled heterospecific antibody to carcinoembryonic antigen. Cancer Res. 33:2977–2982.
10. Goldenberg, D.M., Preston, D.F., Primus, F.J., and Hansen, H.J. (1974) Photoscan localization of GW-39 tumors in hamsters using radiolabeled anticarcinoembryonic antigen G. Cancer Res. 34:1–9.
11. Primus, F.J., McDonald, R., Goldenberg, D.M., and Hansen, H.J. (1977) Localization of GW-39 human tumors in hamsters by affinity purified antibody to CEA. Cancer Res. 37: 1544–1547.
12. Goldenberg, D.M., Deland, F.H., Kim, E., Bennet, S., Primus, F.J. Van Nagell, J.R., Jr., Estes, N., DeSimone, P., and Rayburn, P. (1978) Use of radiolabeled antibodies to carcinoembryonic antigen for the detection and localization of diverse cancers by photoscanning. N. Engl. J. Med. 298:1384–1388.
13. Quinones, J., Mizejewski, G., and Beirwaltes, W.H. (1975) Choriocarcinoma scanning using radiolabeled antibody to chorionic gonadotropin. J. Nucl. Med. 12:69–75.
14. Mach, J.P., Carrel, S., Merenda, C., Heumana, D., and Roenspie, U. (1978) In vivo localization of anti-CEA antibody in colon carcinoma. Can the results obtained in the nude mouse model be extrapolated to the patient? Eur. J. Cancer 1(Suppl):113–120.
15. Giovanella, B.C., and Fogh, J. (1985) The nude mouse in cancer rsearch. Adv. Cancer Res. 44:69–120.
16. Sharkey, R.M., Primus, F.J., and Goldenberg, D.M. (1987) Antibody protein dose and radioimmunodetection of GW-39 human colon tumor xenografts. Int. J. Cancer 39:611–617.
17. Rostock, R.A., Klein, J.L., Kopher, K.A., and Order, S.E. (1984) Variables affecting the tumor localization of I-131-antiferritin in experimental hepatoma. Am. J. Clin. Oncol. 6:9–18.
18. Rogers, G.T., Pedley, R.B., Boden, J., Harwood P.J., and Bagshawe, K.D. (1986) Effect of dose escalation of a monoclonal anti-CEA IgG on tumor localization and tissue distribution in nude mice xenografted with human colon carcinoma. Cancer Immunol. Immunother. 23:107–112.
19. Wahl, R.L., Liebert, M., and Wilson, B.S. (1986) The influence of monoclonal antibody dose on tumor uptake of radiolabeled antibody. Cancer Drug Deliv. 3:243–249.
20. Otsuka, F.L., and Welch M.J. (1985) Evidence for a saturable clearance mechanism for In-111-labeled monoclonal antibodies. Int. J. Nucl. Med. Biol. 12:331–332.
21. Halpern, S.E., Dillman, R.O., Witzmtum, K.F., Shega, I.F., Hagan, P.L., Burrows, W.M., Dillman, J.B., Clutter, M.L., Sobol, R.E., Frincke, J.M., Bartholmew, R.M., David, G.S., and Carlo, D.J. (1985) Radioimmunodetection of melanoma utilizing In-111 96.5 monoclonal antibody: A preliminary report. Radiology 155:493–499.
22. Murray, J.L., Lamki, L.M., Shanken, L.J., Blade, M.E., Plager, C.E., Benjamin, R.S., Schweighardt, S., Unger, M.W., and Rosenblum, M.G. (1988) Immunospecific saturable clearance mechanisms for In-111-labeled anti-melanoma monoclonal antibody 96.5 in humans. Cancer Res. 48:4417–4422.
23. Carrasquillo, J.A., Abrams, P.G., Schroff, R.W., Reynolds, J.C., Woodhouse, C.S., Morgan, A.C., Keenan, A.M., Foon, K.A. Parentesis, P., Marshall, S., Horowitz, M., Szymendea, J., Englert, J., Oldham, R.K., and Larson, S.M. (1988) Effect of antibody dose on imaging and biodistribution of indium-111 9.2.27 anti-melanoma monoclonal antibody. J. Nucl. Med. 29:39–47.
24. Patt, Y.Z., Lamki, L.M., Haynie, T.P., Unger, M.W., Rosenblum M.G., Shirkhoda, A., and Murray, J.L. (1988) Improved tumor localization with increasing dose of indium-111-labeled anti-carcinoembryonic antigen monoclonal antibody ZCE-025 in metastatic colorectal cancer. J. Clin. Oncol. 6:1220–1230.

25. Bomber, P., McCreedy, R., and Hamersley, P. (1986) Propranolol hydrochloride enhancement of tumor perfusion and uptake following gallium 67 in a mouse sarcoma. J. Nucl. Med. 27: 243–245.
26. Sands, H., Jones, P.L., and Shah, L. (1988) Correlation of vascular permeability and blood flow with monoclonal antibody uptake by human Clousner and renal cell xenografts. Cancer Res. 48:188–193.
27. Stickney, D.R., Gridley, D.S., Kirk, G.A., and Slater, J.M. (1987) Enhancement of monoclonal antibody binding to melanoma with single dose radiation or hyperthermia. NCI Monographs 3:47–52.
28. Gatenby, R.A., Moldofsky, P.J., Weiner, L.M. (1988) Metastatic colon cancer: Correlation of oxygen levels with I-131 $F(ab')_2$ uptake. Radiology 166:757–759.
29. O'Conner S.W., and Bale W.F. (1984) Accessibility of circulating immunoglobulin G to the extravascular compartment of solid rat tumors. Cancer Res. 44:3719–3723.
30. Law, M.P., Thomilson, R.H., and Chin, B. (1978) Vascular permeability in the ears of rats after x-irradiation. Br. J. Radiology 51: 895–904.
31. Mounts, P., and Bruce, W.N. (1969) Local plasma volume and vascular permeability of rabbit skin after irradiation. Radiation Res. 23:430–445.
32. Song, C.W. Kang, M.S., Rhea, J.G., and Levitt, S.H. (1980) The effect of hyperthermia on vascular function, pH and cell survival. Radiology 137:795–803.
33. Suzuki, M., Hori, K., and Ane, I. (1984) A new approach to cancer chemotherapy: Selective enhancement of tumor blood flow with Ang II. J. Natl. Cancer Inst. 61:663–669.
34. Smyth, M.J., Pietesz, G.A., and McKenzie I.F.C. (1987) Use of vasoactive agents to increase tumor perfusion and the antitumor efficacy of drug-monoclonal antibody conjugates. J. Natl. Cancer Inst. 79:1367–1373.
35. Moshakis, V., McIhinney, R.A.J., and Raghaven, D. (1981) Localization of human tumor xenografts after iv administration of radiolabeled MAbs. Br. J. Cancer 44:91–99.
36. Menard, S., Miotti, S., and Taghaboe, E. (1983) Tumor radioimmunolocalization in the murine system using monoclonal antibodies. Tumori 69:185–190.
37. Philben, V.J., Jakowitz, J.G., Beatty B.G., Vlahos, W.G. (1986) The effect of tumor CEA content and tumor size on tissue uptake of indium-111-labeled anti-CEA monoclonal antibody. Cancer 57:571–576.
38. Hagan, P.L., Halpern, S.E., and Dillman, R. (1986) Tumor size: Effect of monoclonal antibody uptake in a tumor model. J. Nucl. Med. 27:1421–1427.
39. Cataland, S., Cohen, C., and Sapirstein, L.A. (1962) Relationship between size and perfusion of transplantation. J. Natl. Cancer Inst. 29:389–391.
40. Gullino, P.M., and Gratham, F.H. (1964) The vascular space of growing tumors. Cancer Res. 24:1727–1732.
41. Hori, K., Suzuki, M., and Saito, S. (1986) Increased tumor tissue pressure in association with the growth of tumors. Jpn. J. Cancer Res. 77:65–73.
42. Weiss, L. (1977) Tumor regions and cell detachment. Int. J. Cancer 20:87–92.
43. Rogers, W., Edlich, R., and Aust, B. (1969) Tumor blood flow II. Distribution of blood flow in experimental tumors. Angiology 20:374–387.
44. Fand, I., Sharkey, R.M., Primus, F.J., Cohen, S.A., and Goldenberg, D.M. (1987) Relationship of radioantibody localization and cell viability in a xenografted human cancer model as measured by whole-body autoradiography. Cancer Res. 47:2179–2183.
45. Goldenberg, D.M., Preston, D.F., Primus, F.J., and Hansen, H.J. (1974) Photoscan localization of GW-39 tumors in hamsters using radiolabeled anticarcinoembryonic antigen immunoglobulin G. Cancer Res. 34:1–9.
46. Pimm, M.V., Embleton, M.J., and Perkins, A.C. (1982) In vivo localization of anti-osteogeneic sarcoma xenografts. Int. J. Cancer 30:75–85.
47. Moshakis, V., McIlhinney, R.A.J., Roghaven, D., and Nevile, A.M. (1981) Monoclonal antibodies to detect human tumors: An experimental approach. J. Clin. Pathol. 34:314–319.
48. Hedin, A., Wahren, B., and Hammerstein, S. (1982) Tumor localization of CEA containing human tumors in nude mice by means of monoclonal anti-CEA antibodies. Int. J. Cancer

30:547–552.
49. Sharkey, R.M., Goldenberg, D.M., Goldenberg, H., Lee, R.E., Ballance, C., Pawlyk, D., Varga, D., and Hansen, H.J. (1990) Murine monoclonal antibodies against carcinoembryonic antigen: Immunological, pharmacokinetic and targeting properties in humans. Cancer Res., in press.
50. Martin, K.W., and Halpern, S.E. (1984) Carcinoembryonic antigen production, secretion and kinetics in BALB/c mice and a nude mouse-human tumor model. Cancer Res. 44:5475–5481.
51. Primus, F.J., Wang, R.H., Cohen, H.J., and Goldenberg, D.M. (1976) Antibody to CEA in hamsters bearing GW-39 human tumors. Cancer Res. 36:2176–2181.
52. Gold, D., Nocera, M., Shochat, D., Primus, F.J., Stevens, R., and Goldenberg, D.M. (1989) Generation of monoclonal antibody Mu9 to colon specific antigen-p (CSAp). Submitted.
53. Tom, B.H., Rutsky, L.P., Jakstys, M.M., Oyasu, R., Kaye, C.I., and Kahan, B.D. (1976) Human colonic adenocarcinoma cells: I. Establishment and description of a new line. In Vitro 12:180–191.
54. Wahl, R.L., Parker, C.W., and Philpott, G.W. (1983) Improved tumor imaging and tumor localization with monoclonal $F(ab')_2$. J. Nucl. Med. 24:316–325.
55. Harwood, P.J., Boder, J., Pedley, R.B., Rauling, G., Rogers, G.T., and Bagshawe, K.D. (1985) Comparative tumor localization of antibody fragments and intact IgG in nude mice bearing CEA producing human colon carcinoma xenografts. Eur. J. Cancer Clin. Oncol. 21:1515–1522.
56. Buchegger, F., Mach, J.P., Leonnard, P., and Carrel, S. (1986) Selective tumor localization of radiolabeled anti-human melanoma monoclonal antibody fragment demonstrated in the nude mouse model. Cancer 58:655–662.
57. Covell, D.G., Barbet, J., Holton, O.D., Black, C.D.V., Parker, R.J., and Weinstein, J.N. (1986) Pharmacokinetics of monoclonal immunoglobulin G_1 $F(ab')_2$ and Fab′ in mice. Cancer Res. 46:3969–3978.
58. Siccardi, J.F., Buraggi, G.L., and Callegaro, L. (1986) Multicenter study of immunoscintigraphy with radiolabeled monoclonal antibodies in patients with melanoma. Cancer Res. 46:4817–4822.
59. Chatal, J.F., Saccavini, J.L., and Fumoleau, P. (1984) Immunoscintigraphy of colon carcinom. J. Nucl. Med. 25:307–314.
60. Carrasquillo, J.A., Krohn, K.A., Beaumier, P., McGuffin, R.W., Brown, J.P., Hellstrom, K.E., Hellstrom I., and Larson, S.M. (1984) Diagnosis and therapy for solid tumors with radiolabeled antibodies and immune fragments. Cancer Treat. Rep. 68:317–328.
61. Khaw, B.A., Strauss, H.W., and Cahill, S.L. (1984) Sequential imaging of indium-111-labeled monoclonal antibody in human mammary tumors hosted in nude mice. J. Nucl. Med. 25:592–603.
62. Hnatowich, D.J., Griffin T.W., and Kosiuczyk, Z. (1985) Pharmacokinetics of indium-111-labeled monoclonal antibody in cancer patients. J. Nucl. Med. 26:849–858.
63. Larson, S.M., Brown, J.P., Wright, P.W., Carrasquilo, J.A., Hellstrom, I., and Hellstrom, K.E. (1983) Imaging of melanoma with I-131-labeled monoclonal antibodies. J. Nucl. Med. 24:123–129.
64. Mach, J.P., Cahatal, J.F., and Lumbroso, J.D. (1983) Tumor localization in patients by radiolabeled monoclonal antibodies against colon carcinoma. Cancer Res. 43:5593–5600.
65. Munz, D.L., Alavi, A., Koprowski, H., and Herlyn D. (1986) Improved radioimaging of human tumor xenografts by a mixture of monoclonal antibody $F(ab')_2$ fragments. J. Nucl. Med. 27:1739–1745.
66. Goldenberg, D.M., Pant, K.D., and Dahlman, H. (1976) A new oncofetal antigen associated with gastrointestinal cancer. Proc. Am. Assoc. Cancer Res. 17:155.
67. Pant, K.D., Dahlman, H.L., and Goldenberg, D.M. (1978) Further characterization of CSAp, an antigen associated with gastrointestinal and ovarian tumors. Cancer 42:230–238.
68. Gaffar, S.A., Pant, K.D., Shochat, D., Bennett, S.J., and Goldenberg, D.M. (1981)

Experimental studies of tumor radioimmunodetection using antibody mixtures against carcinoembryonic antigen (CEA) and colon-specific antigen-p (CSAp). Int. J. Cancer 27:101–105.

69. Nocera, M., Jesperson, D.L., Krupey, J., Shochat, D., Primus F.J., and Goldenberg, D.M. (1986) Representation of epitopes on a gastrointestinal specific antigen defined by monoclonal antibodies. Proc. Am. Assoc. Cancer Res. 27:236.
70. Primus, F.J., Kuhns, W.J., and Goldenberg, D.M. (1983) Immunological heterogeneity of carcinoembryonic antigen: Immunohistochemical detection of carcinoembryonic antigen determinants in colonic tumors with monoclonal antibodies. Cancer Res. 43:693–701.
71. Sharkey, R.M., Primus, F.J., Shochat, D., and Goldenberg, D.M. (1988) Comparison of tumor targeting of mouse monoclonal and goat polyclonal antibodies to carcinoembryonic antigen in the GW-39 human tumor-hamster host model. Cancer Res. 48:1823–1828.
72. Goldenberg, D.M., and Steinborn W. (1970) Reduced lymphatic drainage from hamster cheek pouch. Proc. Soc. Exp. Biol. Med. 135:724–726.
73. Ozello, L., and Sordat, M. (1980) Behavior of tumors produced by transplantation of human mammary cell lines in athymic nude mice. Eur. J. Cancer 16:553–560.
74. Sharkey, R.M., Filion, D., Fand, I., Primus, F.J., and Goldenberg, D.M. (1986) A human colon cancer metastasis model for radioimmunodetection. Cancer Res. 46:3677–3683.
75. Aamdal, S., Fodstod, O., Nesland, J.M., and Pihl, L. (1985) Characteristics of human tumor xenografts transplanted under the renal capsule of immunocomperent mice. Br. J. Cancer 51:347–356.
76. Givazzi, R., Campbell, D.E., Jessup, J.M., Cleary, K., and Fidler, I.J. (1986) Metastatic behavior of tumor cells isolated from primary and metastatic human colorectal carcinoma implanted in different sites in nude mice. Cancer Res. 46:1928–1933.
77. Bressalier, R.S., Raper, S.E., Hujanen, E.S., and Kim, Y.S. (1987) A new animal model for human colon cancer metastasis. Int. J. Cancer 39:625–630.
78. Sharkey, R.M., Mabus, J., Rubin, E., Aninipot, R., Blumenthal, R.D., and Goldenberg, D.M. (1988) Radiolocalization of a human colonic tumor transplanted in the liver of nude rats. Proc. Am. Assoc. Cancer Res. 29:386.
79. Sharkey, R.M., Primus, F.J., and Goldenberg, D.M. (1984) Second antibody clearance of radiolabeled antibody in cancer detection. Proc. Natl. Acad. Sci. USA 81:2843–2846.
80. Goldenberg, D.M. (1988) Targeting of cancer with radiolabeled antibodies. Arch. Path. Lab. Med. 112:580–587.

4. Preclinical models and methods for the study of radiolabeled monoclonal antibodies in cancer diagnosis and therapy

Sudhir A. Shah and Howard Sands

Since the first report of Kohler and Milstein [1] on the somatic cell hybridization techique for establishing continuous cultures of specific antibody forming cells, numerous monoclonal antibodies have been generated against human and animal cancer cell surface markers for their potential use in cancer diagnosis and therapy [2–4]. To better understand the clinical utility of these antibodies, various animal models have been utilized.

An animal model for evaluating the clinical potential of radiolabeled monoclonal antibodies as therapuetic or diagnostic agents needs to closely mimic the disease in the patient. The concept of using either animal tumor systems or human tumor xenografts in animals, although a convenient one, implies a similarity with the clinical situation that may not necessarily exist. The tumor-host relationship may be important in antibody localization. Therefore, syngeneic (genetically identical) animal tumor models may give more reproducible results than allogeneic or xenogeneic (graft from a donor of dissimilar species) tumor models.

The human tumor xenograft model in immunocompromised athymic (absence of a thymus gland and 'T' lymphocytes) mice is widely used for evaluating radiolabeled antibodies. It is attractive because of the clinical origins of the tumor. It should be noted that the vasculature and connective tissue of a human tumor xenograft grown in an immunosuppressed animal is xenogeneic. Therefore, some properties of xenograft tumor models that depend on the stroma may deviate considerably from the clinical situation [5–6]. Furthermore, since human tumors do not readily metastasize in athymic mice [7–9], metastatic models that mimic this important clinical problem have been rarely used for evaluating antibodies [10].

Most of the published literature on models of tumor diagnosis with radiolabeled monoclonal antibodies has used large, subcutaneous, superficial tumors. Detection of small tumors in the visceral organs such as kidney, liver, and spleen would better mimic the clinical situation [11], i.e., the need to detect in patients small metastatic lesions located in or near critical organs. Several models are now available.

Monoclonal antibodies carrying therapeutic radionuclides offer a unique possibility for the specific killing of tumor cells. Following classic oncologic

Goldenberg, D.M., (ed.), Cancer Imaging with Radiolabeled Antibodies.

treatment (surgery, radiotherapy, and chemotherapy), antibodies carrying therapeutic radionuclides may be useful to eradicate the residual tumor burden. The ultimate efficacy of a radiolabeled antibody will be determined in the clinic by its ability to reduce tumor size and to prolong the survival time of the patient. Similar criteria need to be applied to the preclinical evaluation of radiolabeled antibodies. These evaluation protocols should include tumor measurement models in which the effects of therapy on tumor size can be accurately assessed, and the determination of the survival times of tumor-bearing animals can be made.

No matter how attractive the tumor model, experimental animals are not people, and great caution must be exercised in extrapolating results obtained in the laboratory to the clinical situation. Animal models should be regarded as useful only for providing guidance for the selection of agents that are to be evaluated in the clinic.

This review will discuss various animal models currently in use for evaluating radiolabeled monoclonal antibodies. For convenience, the discussion of these animal models has been presented according to the site of tumor location in the host animal. We also discuss some of our own recent relevant data where appropriate.

DIAGNOSIS

The terms *radioimmunodetection* and *radioimmunodiagnosis* refer to the detection of a tumor by gamma camera imaging using a 'tumor-specific' radiolabeled antibody. Radioimmunodetection is based on the premise that the antibody (polyclonal or monoclonal) raised against tumor cell-surface antigen(s) will target to tumors to a greater extent than to the normal tissue. A variety of animal models have been described for the evaluation of radiolabeled monoclonal antibodies.

Subcutaneous tumor models

General considerations

Description. The tumor is usually located either on the flank or thigh of an animal. Cell suspensions containing a known number of viable tumor cells obtained from tissue culture growth are injected in genetically similar (homografts) or genetically dissimilar (xenografts) animals. This protocol can give rise to tumors of similar size in a number of mice [12]. Since all tumors cannot be adapted to growth in tissue culture, some have to be passaged as solid tumors from animal to animal [13]. In this case, tumors are prepared for passage by surgically excising them from the host animals. These tumors are minced to separate the host tissue and necrotic tumor from the viable tumor

and then injected into a new host. Inevitably cells are damaged during this process and the actual number of viable tumor cells present in the tumor inoculum may vary considerably.

Advantages. The subcutaneous tumor model has attracted much attention for several reasons: 1) induction of subcutaneous tumors in animals involves simple tumor implantation procedures; 2) tumors of approximately equal size can be generated in a large number of animals, which can be readily employed for extensive pharmacokinetic studies; 3) the size of tumors can be fairly accurately determined by calliper measurement. Since the measured tumor size and actual tumor weight have shown good correlation [14], tumors of similar weight can be used in interrelated experiments.

Disadvantage. The major drawback of the subcutaneous tumor model is the site of tumor growth. It does not resemble the visceral location of many metastases observed in cancer patients. Nevertheless, subcutaneous tumor models have been widely used for understanding the mechanisms of antibody localization in tumors.

Utility. Subcutaneous models of a variety of human and animal tumor types have been utilized to study the radioimmunodetection of tumors by monoclonal antibodies and antibody fragments labeled with a variety of radionuclides. Since it is not the authors' intention to summarize all published results using this model, Table 1 gives references and details on types of tumors, cell lines, and antibodies of representative examples, and will be useful to the reader interested in obtaining further details on such studies. Most of these studies have employed human tumor xenografts in immunocompromised animals, though a few studies have utilized homograft models. The use of subcutaneous tumor models has provided insight into the role of physiologic and immunologic factors that affect tumor uptake of monoclonal antibodies.

Homograft models

Tumor types. Some of the homologous tumor types used for evaluating monoclonal antibodies as imaging agents are heptocarcinoma grown in guinea pigs [15], mouse adenocarcinoma [16], teratocarcinoma [17], lymphoma [18,19], and rat mammary carcinoma [20].

Advantage. Since the cancer patient is isogeneic with respect to tumor, homograft models may be considered to be better models than the xenograft models. Unlike the xenograft models, where the vasculature originates from the heterologous host rather than the tumor, the tumor and host vasculatures in homograft models are both isologous.

Table 1. Subcutaneous tumor models proposed for evaluating monoclonal antibodies in cancer diagnosis

Human Tumor, Unless Specified (Cell Lines)	Host	Class of Antibody	Form of Antibody	Radionuclide	Investigator(s)
Melanoma	Athymic mice	IgG_1	Intact	^{111}In, ^{67}Ga	Engelstad et al. [100]
Thyroid carcinoma (surgical specimens)	Athymic mice	IgG_1	Intact	^{111}In	Fischer et al. [101]
Colon carcinoma (WiDr, SW403, LS174T)	Athymic mice	IgG(?)	Intact	^{111}In	Philben et al. [102]
Colon carcinoma (CO-112)	Athymic mice	IgG_1	Intact	^{131}I	Duewell et al. [103]
Osteogenic sarcoma (788T)	Athymic mice	IgG(?)	Intact	^{111}In	Pimm & Baldwin [20]
Melanoma (M20), lung carcinoma (P3)	Athymic mice	IgG_1	Intact	^{131}I, ^{125}I	Mann et al. [104]
Colon carcinoma (LS174T)	Athymic mice	IgG_1	Intact	^{111}In	Jakowatz et al. [105]
Colon carcinoma (LS174T)	Athmic mice	IgG_1	Intact	^{125}I, ^{131}I	Keenan et al. [106]
Breast carcinoma (MDA-MB-157)	Athymic mice	IgG_1	Intact	^{111}In	Haisma et al. [107]
Colon carcinoma (T-84, T-157, T-379)	Athymic mice	IgG_1	Intact	^{111}In, ^{125}I	Hagan et al. [32]
Osteogenic sarcoma (788T & 791T)	Athymic mice	IgG_1	Intact	^{111}In	Perkins et al. [108]
Testicular carcinoma	Athymic mice	$IgG_{1(?)}$	Intact	^{111}In, ^{131}I	Sakahara et al. [109]
Breast carcinoma (BT-20)	Athymic mice	IgG_1	Intact	^{111}In, ^{125}I	Khaw et al. [110]
Melanoma (RM)	Athymic mice	IgG_1	Intact	^{131}I	Stuhlmiller et al. [111]
Melanoma (M1)	Athymic mice	IgG_1	Intact	^{131}I	Ghose et al. [112]
Colon carcinoma (T-380)	Athymic mice	IgG_1	Intact	^{111}In, ^{75}Se	Halpern et al. [113]

Table 1 (continued)

Human Tumor, Unless Specified (Cell Lines)	Host	Class of Antibody	Form of Antibody	Radionuclide	Investigator(s)
Hepato-carcinoma (L10)	Guinea pigs	IgG_1	Intact	^{125}I, ^{111}In	Bernhard et al. [15]
Colon (HT29), gastric (MKN45) carcinomas	Athymic mice	IgG_1	Intact	^{131}I	Macdonald et al. [114]
Mammary carcinoma (Sp4)	WAB rats	IgG_1	Intact	^{131}I	Pimm et al. [22]
Mammary carcinoma (Clouser), renal cell carcinoma (TK177G)	Athymic mice	IgG_1	Intact	^{131}I	Sands et al. [28]
Colon carcinoma (CO-112)	Athymic mice	IgG	Intact	^{131}I	Haskell et al. [115]
Colon carcinoma (LS174T), lung adenocarcinoma (A549)	Athymic mice	IgG_1	Intact	^{131}I, ^{125}I	Shah & Sands [76]
Colon carcinoma (GW-39)	Hamster	IgG (polyclonal)	Intact	^{125}I	Fand et al. [116]
		IgG	Intact	^{131}I	Fand et al. [117]
Colon carcinoma (LS174T), melanoma (A375)	Athymic mice	IgG_1	Intact	^{125}I	Colcher et al. [118]
Mammary carcinoma (Clouser), melanoma (A375)	Athymic mice	IgG_1	Intact	^{125}I	Shah et al. [27]
Murine adenocarcinoma (KHJJ)	BALB/c mice	IgG	Intact	^{111}In	Goodwin et al. [16]
Colon carcinoma (HCT-8, HRT-18, HT-29, LS174T), rectal carcinoma (HRVB), osteosarcoma (791T)	CBA mice	IgG_1	Intact	^{125}I	Pimm et al. [119]
Mouse lymphoma (THY 1.1 +)	AKR mice	IgG_1	Intact	^{125}I, ^{131}I	Sands et al. [19]
HeLa, Hep2 colon carcinoma (LS174T), rhabdomyosarcoma (RD)	Athymic mice	IgG_1	Intact, Fab	^{125}I	Jeppsson et al. [120,121]
Breast carcinoma (BT-20, HS-578T)	Athymic mice	IgG_1	Intact, $F(ab')_2$ Fab	^{111}In	Khaw et al. [122]

Table 1 (continued)

Human Tumor, Unless Specified (Cell Lines)	Host	Class of Antibody	Form of Antibody	Radionuclide	Investigator(s)
Breast carcinoma (Clouser)	Athymic mice	IgG_1	Intact, $F(ab')_2$ Fab	^{125}I	Zalutsky et al. [123]
Colon carcinoma (CO-112)	Athymic mice	IgG_1	Intact, $F(ab')_2$	^{131}I	Buchegger et al. [124]
Colon carcinoma (T-380)	Athymic mice	IgG	Intact $F(ab')_2$, Fab	^{125}I, ^{111}In	Buchegger et al. [125]
Colon carcinoma (LS174T) and osteogenic sarcoma (791T)	Athymic mice	IgG_1	Intact $F(ab')_2$, Fab	^{125}I, ^{131}I	Andrew et al. [34]
Colon carcinoma (LS174T)	Athymic mice	IgG_1	Intact $F(ab')_2$, Fab	^{125}I, ^{111}In	Brown et al. [12]
Colon carcinoma (LS174T)	Athymic mice	IgG_1	Intact $F(ab')_2$	^{99m}Tc, ^{131}I	Hadjian et al. [126]
Colon carcinoma (T-380), melanoma T-cell lymphoma (MOLT-4)	Athymic mice	IgG_1 IgG_{2a}	Intact	^{111}In, ^{125}I ^{75}Se	Hagan et al. [25]
Glioma	Athymic mice	IgG_{2a}	$F(ab')_2$	^{131}I	Takahashi et al. [127]
Colon carcinoma (SW-948)	Athymic mice	IgG_1 IgG_{2a}	$F(ab')_2$	^{131}I	Munz et al. [128]
Melanoma (FMX-Met SESX, LOX-L	Athymic mice	IgG_{2a}	Intact	^{125}I	Hwang et al. [129]
Squamous cell carcinoma (UMSCC-2, UM-SCC-11B)	Athymic mice	IgG_{2a}	Intact	^{131}I	Wahl et al. [98]
Colon carcinoma (SW948, SW1116, SW1222)	CBA mice	$IgG2_a$	Intact $F(ab')_2$	^{125}I, ^{131}I	Heryln et al. [130]
Teratoma (HX39/7)	CBA mice	IgG_{2a}	Intact	^{125}I	Moshakis et al. [24]
Colon carcinoma (SW948) and melanoma (WM9)	Athymic mice	IgG_{2a}	Intact $F(ab')_2$	^{111}In, ^{131}I	Powe et al. [131]

Table 1 (continued)

Human Tumor, Unless Specified (Cell Lines)	Host	Class of Antibody	Form of Antibody	Radionuclide	Investigator(s)
Melanoma (Me 67)	Athymic mice	IgG_{2a}	Intact $F(ab')_2$ Fab	^{131}I, ^{125}I	Buchegger et al. [132]
Melanoma (MeWo)	Athymic mice	IgG_{2a}	Intact	^{67}Ga, ^{131}I	Matzku et al. [133]
Colon carcinoma (COLO205), murine thymoma (ITT(1)75NS)	Athymic mice c57BL/6 B6cF1	IgG_1 IgG_{2a} IgG_{2b}	Intact	^{99m}Tc	Kanellos et al. [134]
Osteosarcoma (79IT)	CBA mice	IgG_{2b}	Intact	^{125}I	Baldwin & Pimm [135]
Osteosarcoma (79IT)	Athymic mice	IgG_{2b}	Intact	^{131}I	Pimm & Baldwin [136]
Glioma (D-54MG)	Athymic mice	IgG_{2b}	Intact	^{131}I, ^{125}I	Lee et al. [99]
Lymphoma (BN)	Athymic mice	IgG_{2c}	Intact	^{111}In, ^{125}I	Rodwell et al. [137]
Bladder carcinoma (T24)	Athymic mice	IgG_1 IgG_3	Intact	^{131}I	Bubenik et al. [138]
Choriocarcinoma (BeWo), mouse teratocarcinoma (MH-15)	Athymic mice	IgMk	Intact	^{125}I, ^{131}I	Ballou et al. [139]
Small-cell lung carcinoma (NCI-H69)	Athymic mice	IgM	Intact	^{131}I	Zimmer et al. [140]
Colon carcinoma (HCT-8, HRT-18)	Athymic mice	IgM	Intact	^{125}I	Pimm & Baldwin [141]
Mouse teratocarcinoma (MH-15)	Athymic mice	IgM $F(ab')_{2\mu}$	Intact	^{131}I	Ballou et al. [17]
Melanoma (UCLA-SO-M14)	Athymic mice	IgM	Intact	^{131}I	Gomibuchi et al. [142]
Choriocarcinoma (SCH)	Athymic mice	IgM	Intact	^{125}I, ^{131}I	Mano et al. [29]
Mouse lymphoma (B6EL4, BALBUr2, B6Ur24)	C57/BL mice	IgM IgG	Intact	^{131}I	Menard et al. [18]

Disadvantage. A disadvantage in using a homograft model in animals is that animal tumors may not mimic human tumors with regard to their vasculature, blood flow, and transport of macromolecules. For example, accumulation of a nonspecific IgG was found to be significantly greater in a human tumor than in a mouse tumor, both tumors being grown in mice. This may have been due to a greater vascular permeability to macromolecules in the human tumor than in the mouse tumor [21].

Examples of use. Studies using the murine lymphoma homograft model in a mouse strain that lacks the antigen and specific monoclonal antibody showed three times greater accumulation of the specific antibody in the antigen-bearing tumor than in the control tumor [19]. The antigen-positive tumor grown subcutaneously accumulated only one-fourth the amount of radiolabeled specific antibody when compared with that of the same tumor grown in the subrenal capsule (for details see Subrenal Tumor Models).

Using a rat homograft mammary tumor model, Pimm et al. [22] confirmed the antibody dose-dependent pharmacokinetics observed previously in melanoma cancer patients by Halpern and Hagan [23]. It was believed that the observed difference resulted from the saturation of minute amounts of antigen in normal tissues, and consequently this phenomenon could not be studied in the xenograft model. Virtually identical dose-dependent distribution was seen in normal rats. Moreover, since this effect was not seen with control mouse IgG_1, it almost certainly reflected reaction of the putatively 'tumor-specific' antibody with antigen expressed in normal rat tissues [22].

Conclusions. Homograft models have not gained wide acceptance because they cannot be used for evaluating antibodies raised against human tumor antigens that are not found in animal tumors or tissue. On the other hand, the homograft models may be more analogous to the situation in the cancer patient, since the tumor and the host are both genetically similar, and thus one can study certain phenomenon that cannot be studied in the xenograft models.

Xenograft models

Tumor types. In the xenograft model a human tumor is grown in a pharmacologically or genetically immunocompromised animal. The subcutaneous xenograft model that has been most extensively used is a human tumor growing in athymic mice.

Advantages. 1) The major advantage of this model is that it allows the investigator to study the uptake of anti-human tumor antibody by a human tumor; 2) due to the superficial nature of the tumor growth, tumor size can be fairly accurately controlled. Most studies have used relatively large tumors. Tumors greater than 1 g are so large in proportion to a mouse that the tumor-

host relationship is not representative of tumors generally found in cancer patients. Therefore, animals bearing small tumors (< 0.1 g) could be and should be used. It should be pointed out that a 0.2–0.3 g tumor in a 20–25 g mouse is roughly equivalent to a 600 g tumor in a 60–75 kg patient.

Disadvantages. 1) In the xenograft, the tumor vasculature is derived from the host rather than from the tumor. One must ask how antibody localization in tumors is affected by the host vascular bed and the genetic and immunologic relationships between the tumor and the host. As mentioned above, this may be important, since blood flow and permeability of the tumor could influence the accumulation of antibody. 2) This tumor model may not allow the study of the antibody dose-dependent pharmacokinetics observed in cancer patients. Halpern and Hagen [23] found that monoclonal antibodies directed against melanoma that showed dose-dependent pharmacokinetics in patients failed to show this effect in the xenograft model in the mouse. 3) Due to the needs of an imaging experiment, the amount of radionuclide injected into a mouse is about 70 times the dose used in a patient in terms of μCi/kg body weight. The use of a larger animal, e.g., the athymic rat, should be encouraged, since the size of this host is an order of a magnitude greater than the athymic mouse.

Examples of use. The subcutaneous xenograft model has been used in many experimental studies. The following will summarize some of the results.

Using the subcutaneous tumor models, several investigators have shown that a critical factor in antibody localization in tumors may be the tumor size. Simultaneous injection of radioiodinated tumor-specific and nonspecific antibody in mice bearing a human germ-cell tumor showed decreased uptake of only the tumor-specific but not the control antibody with increasing tumor mass (Figure 1) [24]. Hagan et al. [25] observed similar effects with a variety of tumors (colon, melanoma, and lymphoma). This finding was independent of the radionuclide (^{111}In, ^{125}I, or ^{131}I) and was demonstrable when the mouse bore two tumors of differing size. In our laboratory we could demonstrate this relationship for a human colon-tumor xenograft but not for a human mammary-tumor xenograft [26]. The decreased antibody uptake by larger tumors may be attributed, in part, to increased tumor necrosis, decreased blood perfusion, and decreased vascular permeability in necrotic areas of the tumor.

Using subcutaneous tumor models we have shown that both tumor blood flow and vascular permeability may affect antibody localization. Blood perfusion, as measured by the ^{86}Rb method, was similar for antigen-positive Clouser tumor and antigen-negative A375 melanoma grown subcutaneously in athymic mice (Figure 2). However, accumulation of specific antibody (B6.2) was observed only in the antigen-positive xenograft, but not in the antigen-negative xenograft, suggesting that immunospecificity was a major factor in specific antibody localization [27]. In comparison with the B6.2/Clouser tumor system, the specific uptake of both radioiodinated tumor (A6H) and

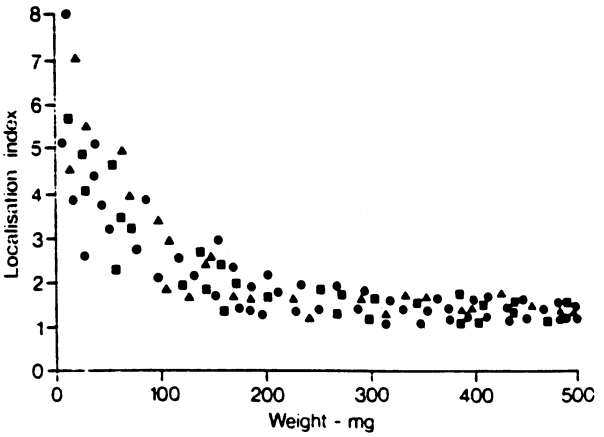

Figure 1. The localization index (specific/nonspecific antibody accumulation in the tumor divided by the same ratio in the blood) of LICR-LON/HT13 monoclonal antibody in three different experiments (●, ■, and ▲) with tumors (H×39) of varying weights, dissected and counted 48 hours after injection. From Moshakis et al. [24].

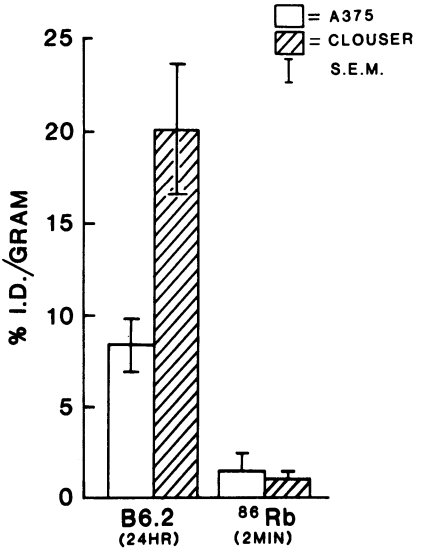

Figure 2. ^{125}I-B6.2 monoclonal antibody accumulation at 24 hours and blood perfusion as assessed by ^{86}RbCl in antibody-'specific' human mammary tumor Clouser and -'nonspecific' human melanoma A375 growing subcutaneously in athymic mice. The mean ± SEM values were obtained from seven to ten tumors of 200–300 mg size.

anti-human (anti-HLA) antibody accumulation in a human renal cell carcinoma (RCC) xenograft was considerably higher. This difference was attributed to a greater blood flow and greater vascular permeability to IgGs; both parameters were significantly greater in the RCC tumor xenografts than in the Clouser tumors [28]. It is known that the vasculature of a xenograft is derived from the host. These data suggest that a xenograft can have a profound an influence on its host's local vascular permeability. Therefore, broad generalizations cannot be made from the study of a single xenograft.

Studies using the subcutaneous model have shown that a key factor that affected antibody localization in tumor was the antigen content of the tumor. Mano et al. [29] examined the effect of placental alkaline phosphatase (PLAP) content with respect to an anti-PLAP IgM's ability to image the tumor. Radioiodinated monoclonal antibody was administered intraperitoneally in athymic mice bearing subcutaneous choriocarcinomas of various sizes and various PLAP contents. The ability to image tumors correlated fairly well with the PLAP content of the tumor (Figure 3). Antigenic heterogeneity in tumors would influence antibody localization [30]. In one study antigenic expression was significantly enhanced by treatment with alpha interferon. Enhanced antigen expression was shown also to correlate with greater localization of ^{125}I-F(ab')$_2$ B6.2 antibody [31].

By using three different subcutaneous human colon tumors, each secreting a different amount of CEA, Hagan et al. [32] showed the effects of circulating CEA on antibody accumulation in tumors in athymic mice. The anti-CEA antibody was radiolabeled with either ^{111}In or ^{125}I. Circulating CEA led to the removal of both ^{111}In- and ^{125}I-labeled antibody from blood. Liver concentrations of ^{111}In increased and those of ^{125}I decreased as the secretory rate of the tumor rose. ^{111}In was retained by the liver, whereas the radioiodinated antibody-antigen complexes were dehalogenated. This resulted in decreased uptake of both ^{111}In- and ^{125}I-labeled antibodies by the tumor. These studies suggests that circulating tumor antigen would potentially interfere with antibody accumulation in tumor. It is interesting to note that these observations in animal models do not agree with the findings of Goldenberg and coworkers [33], who have frequently found that circulating antigen levels do not alter the pharmacokinetics of the anti-CEA antibody or radioimmunodetection of tumor in cancer patients. The reasons for this disparity are not readily apparent.

The subcutaneous tumor model has provided valuable information pertaining to differences in the pharmacokinetics of radiolabeled monoclonal antibody, either intact, F(ab')$_2$, or Fab. Results from a number of studies comparing the pharmacokinetics of intact antibody with antibody fragment in the same subcutaneous model indicated that tumors could be imaged earlier with antibody fragments than with the intact antibody. This was presumably due to faster blood clearance of the antibody fragments, which resulted in a higher target to background ratio. The absolute amount of antibody accumulation in the tumor was, however, much lower with the antibody fragments

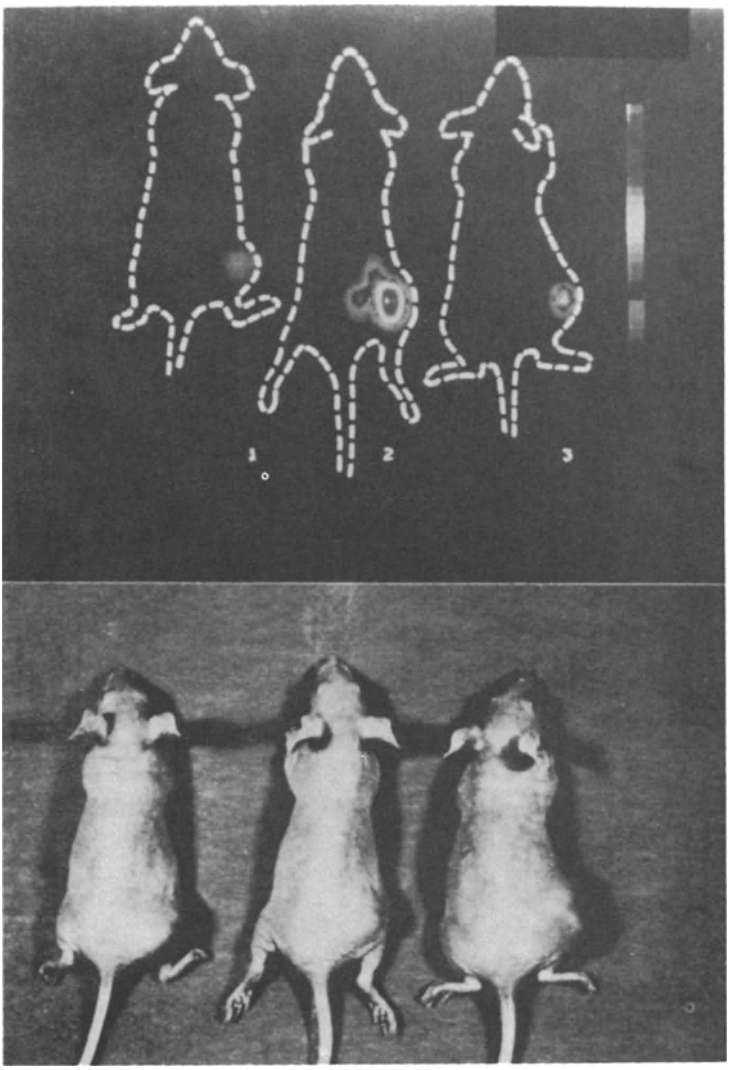

Figure 3. Gamma scintigraphy with ^{131}I-labeled Mab 11-D-10 of athymic mice bearing BeWo, NaUCC-3, NaUCC-1 choriocarcinoma having different PLAP contents. Tumor-bearing athymic mice, in which tumors had developed to 1 cm in diameter, were given IP 50 μCi of ^{131}I-labeled Mab 11-D-10 (10 μCi/μg). The mice were imaged 3 days after the administration with a middle-energy, parallel-hole collimator. 1, NaUCC-1; 2, BeWo; 3, NaUCC-3. The relative amounts of radioactivity in the tumor image were BeWo:NaUCC-3:NaUCC-1 = 30:14:10. In agreement with the PLAP content, the strength of the radioimage was thus in the order of BeWo, NaUCC-3, NaUCC-1. From Mano et al. [29].

than with the intact antibody. There was no universal agreement as to which of the two antibody fragments, $F(ab')_2$ or Fab, would give better localization. For example, Andrew et al. [34] found that Fab gave earlier and superior images of CEA-producing tumors in athymic mice than did the $F(ab')_2$ fragment of the same monoclonal antibody. On the other hand, Brown et al. [12] observed that the Fab fragment labeled with either ^{111}In or ^{125}I failed to image colon tumor xenografts. In this study, tumors could be imaged at earlier times with $F(ab')_2$ than with intact antibody. These differences may be attributed to the reduction of valency from two to one as one goes from the $F(ab')_2$ to the Fab fragment. Thus, the use of an Fab may require starting with very much higher affinity antibodies in order to achieve sufficient affinity for localization.

The above studies suggest that the subcutaneous xenograft models would be useful for selecting the most suitable form and type of antibodies that should be used in the clinical trials.

Conclusions. The widely used subcutaneous tumor model has provided important information on the interplay of various physiologic and immunologic factors that may potentially influence antibody accumulation into tumors in the clinic. Some of the factors examined are tumor and normal tissue blood flow; vascular permeability of tumor; tumor size; antigenic heterogeneity in tumor; antibody and its fragments; and form of radiolabel used on the antibody. These studies have shown that immunospecificity of the antibody and antigen content of tumor are the two most important parameters that could ultimately determine the localization of antibody in tumor.

It should be emphasized that the superficial location of the tumor in the above models does not truly mimic small, deep-seated metastases found in many cancer patients. Small tumors located within or around major visceral organs, such as the liver and kidneys, with a much greater perfusion rate than the tumor could potentially influence specific tumor imaging by radiolabeled antibodies. This must be considered a major limitation of the subcutaneous model. Therefore, imaging results in the subcutaneous tumor model should be interpreted with great caution.

Intramuscular tumor models

General considerations

Description. Tumors can be readily grown in the thigh muscle of an animal by injecting either tumor cells obtained from tissue culture or by injecting tumor pieces (see above for details). The tumor is grown within the muscle, either in the upper thigh [35,36] or in the foot [37] of the animal.

Advantage. The intramuscular tumor model may be considered more physiologic since the tumor is located deep within the muscle. The greater

blood flow in the muscle surrounding the tumor may lead to a high background of the radiolabeled antibody, which could potentially interfere with specific tumor imaging.

Disadvantage. A tumor growing within the muscle cannot be measured accurately with callipers, as can a tumor growing in a subcutaneous site. This is a disadvantage from the point of view of standardizing tumor size for interrelated experiments.

Examples of use. An intramuscular CEA-secreting tumor model was used by Sharkey et al. [38] to demonstrate increased tumor uptake of a radiolabeled anti-CEA antibody following administration of a unlabeled antibody directed against the anti-tumor antibody. Enhanced clearance of the unbound radiolabeled anti-tumor antibody by the cold antibody increased the tumor to normal tissue ratio by 3- to 12-fold as compared with those in animals not given the second antibody. Despite much greater blood flow in muscle, tumor to muscle and tumor to blood ratios of 150:1 and 15:1, respectively, have been reported at 5 days following antibody injection in a teratocarcinoma model [39]. A more recent study by Ballou et al. [36], using the intramuscular teratocarcinoma model, have claimed to localize tumors as small as 10 mg.

In experiments using a rat glioma grown in the thigh muscle of athymic mice, the detection of radioiodine in the thyroids 30 minutes after antibody injection suggested to Stavrou et al. [35] that radioiodinated tumor-specific, but not a nonspecific, antibody was rapidly dehalogenated. This was most likely due to dehalogenation of antibody following its deposition in tumor. It is not known if the rapid dehalogenation of the antibody observed in this study was related to the site of tumor location, since sites other than muscle for tumor growth were not compared.

^{111}In-labeled anti-melanoma monoclonal antibody was used in a intramuscular melanoma xenograft model to monitor the therapeutic effects of cytotoxic chemotherapeutic agents [40]. After injection of the ^{111}In-labeled antibody, human melanoma cells inoculated in untreated mice could be distinguished from cells killed after cytotoxic treatment. In order to allow sufficient time for drug effects to take place and to allow dead tumor cells to be cleared by the host mice, the ^{111}In-labeled antibody was injected IP several days after drug administration. Relatively lower ^{111}In uptake in the area of tumor correlated well with prevention or delay of tumor growth.

Conclusions. The intramuscular tumor model has not been used widely. Unrealistically large tumors have been used in some studies [39,41]. The major limitations of this tumor model are the difficulty of measuring small tumors accurately and the peripheral growth of tumor. The ability to image tumors located in limbs well away from the major visceral organs by radiolabeled antibodies may have little significance as compared with tumors located near major visceral organs.

Subrenal tumor models

General considerations

Description. The subrenal capsule model [42] initially developed for testing chemotherapeutic agents [43], has been recently used for the evaluation of radiolabeled monoclonal antibodies directed to relatively small tumor burdens (20–60 mg) growing in this deep-seated site. For inducing tumors, a 1 mm^3 piece of experimentally grown tumor or a clinical sample is implanted under the subrenal capsule of mice. The size of the implant and subsequent tumor growth is measured with a stereoscopic microscope fitted with an ocular micrometer [11]. This model has also been recently adapted to growing cryopreserved human tumor cell lines, including leukemia cells [44,45].

Advantages. 1) The major advantage of this tumor model is the site of tumor growth. Imaging of tumors growing under the renal capsule could be affected by nonspecific accumulation of the antibody in normal surrounding kidneys, liver, spleen, and other tissues within the abdominal cavity. Thus the ability to show specific tumor imaging of a renal tumor may be predictive of clinical utility. 2) Relatively small tumors of between 20 and 60 mg can be grown confined within the subrenal capsule.

Disadvantages. This tumor model was originally developed in immunocompetent mice using a 6-day time frame [46] to evade the complications of the immunoresponsiveness of the normal lost, which takes 12–14 days to reject such a graft. Abrams and coworkers [47] found no viable tumor growth on day 6 after subrenal capsule implants of human non-small-cell lung cancers and ovarian cancers in immunocompetent animals. Bogden et al. [48,49] have reduced the assay time to only 3 days for evaluating surgical explants, most likely due to the tumor rejection problems. Since the tumor vasculature through which the drug or antibody must diffuse to all parts of the tumor does not develop before 5–6 days after tumor implantation, the use of a 3-day assay time therefore has severe delivery limitations. These limitations are a greater disadvantage to the evaluation of macromolecular agents than to classic chemotherapeutic drugs.

Examples of use. The subrenal model was used for evaluating radiolabeled antibodies against a murine tumor lymphoma, and human breast and colon tumors [19,27,50]. With the *homograft models*, antibody specifically localized in the antigen-positive 20 to 60 mg tumors by 24 hours following antibody injection. Although the perfusion rate of normal kidneys surrounding the tumors was about five to six times greater than that of the tumors, the antibody accumulation in the kidney was similar to that in the antigen-negative lymphoma. The antigen-positive lymphoma showed four times

better accumulation of antibody than the control tumor. Despite the fact that the visceral location of the subrenal tumors presents a higher background, specific gamma camera images of subrenal tumors were obtained with ^{125}I-labeled monoclonal antibody [19].

Subrenal models of *xenograft tumors* in athymic mice were utilized by Hnatowich et al. [51] and Lundy et al. [52] for evaluating anti-CEA antibody and B72.3 antibody, respectively. Hnatowich et al. [51] found that the ratio of accumulation of ^{111}In-labeled or ^{125}I-labeled antibody to that of a control non-specific antibody in the CEA-producing colon tumor was between 4 and 5 at 24 hours following antibody injection. Localization of ^{125}I-B72.3 antibody in the antigen-positive subrenal colon tumor was about four to five times greater than that in the antigen-negative melanoma at 3 days after antibody injection [52].

Conclusions. The above results clearly showed that radiolabeled monoclonal antibodies can specifically image small tumors grown in a highly perfused organ such as the kidney of athymic mice. Nonviable human tumor undergoing rejection by the immune system of the immunocompetent mouse may interfere with antibody localization [Shah and Sands, unpublished observations]. Further utilization of this visceral tumor model, in immunocompromised animals, should continue, since this model is biologically more relevant in the human setting for imaging and therapy protocols.

Intrasplenic tumor models

General considerations

Description. Murine erythroleukemia can be initiated in mouse spleen by injecting the inducing virus [53]. Splenic human tumors in athymic mice can be induced by either implanting tumor pieces [26] or by injecting suspensions of tumor cells [52]. In our laboratory, intrasplenic human tumors were initiated in mice by implanting a 1 mm^3 tumor piece (obtained from a subcutaneous tumor) into the splenic bed. Tumors of up to 100 mg grew entirely within the spleen, whereas tumors larger than 100 mg grew partly in the spleen and partly in the abdominal cavity [26]. Lundy and coworkers [52] induced tumors in spleen by injecting one million tumor cells directly into the splenic bed.

Advantages. 1) The ability to detect deep-seated tumors in the spleen, which is located near the highly perfused liver and kidneys and which could potentially interfere with tumor imaging, may have greater predictive value. 2) The spleen bed should support the growth of all human tumors that would grow as xenografts. 3) Relatively small tumors (20–60 mg) can be grown confined within the splenic bed.

Disadvantage. The major disadvantage of using the intrasplenic tumor model is that the tumor size cannot be measured prior to tumor imaging in each animal and that tumor growth cannot always be confined to the spleen.

Examples of use. The spleen model was first used by Scheinberg et al. [53] to localize a virus-induced murine erythroleukemia with ^{111}In-labeled monoclonal antibodies. Tumors could be imaged 5–6 hours following intravenous injection of the tumor-specific monoclonal antibody but not by a nonspecific antibody. This erythroleukemic spleen model was subsequently used by Scheinberg and Strand [54] to explore parameters that affect antibody localization. Specific targeting of an antibody was reflected by 20-fold shorter half-lives of antibody in the blood of tumor-bearing mice. Bound antibody was rapidly catabolized and the radiolabel was cleared from the target (within hours) and appeared in organs metabolizing or excreting the radioisotope. Changing the immunoglobulin isotype class or the use of fragments had large effects on the half-life of the antibody, but did not improve cell targeting uptake ratios or image contrast, or alleviate the problem of specific antibody catabolism.

We have described the development and use of splenic models in athymic mice for human breast, colon, and melanoma tumors [26]. Pharmacokinetic and imaging studies showed specific localization of radioiodinated monoclonal antibodies in antigen-positive tumors. Images of small (about 20 mg) tumors were seen by 48 hours following antibody injection (Figure 4). The control antibody did not image target tumors. Also, the control tumor was not imaged with any of the three antibodies tested (Figure 5). These results showed that radiolabeled monoclonal antibodies can specifically localize in small, deeply seated human tumor xenografts in sufficient quantity to produce excellent gamma camera images [26].

Conclusions. The splenic models described above have provided additional information in evaluating antibodies for their abilities to detect deep-seated tumors. Induction of splenic tumors is relatively easy, and this site supports the growth of a variety of tumors. The biodistribution and imaging results obtained with the intrasplenic tumors described above are similar to those obtained previously with these tumors grown subcutaneously or in the subrenal site [55]. The major limitation of this model is that tumor size cannot be assessed or controlled in the individual animal prior to tumor imaging.

Lymphatic tumor models

General considerations

Description. Assessment of tumor metastases in lymph nodes may be important in the staging of disease in cancer patients. Therefore, preclinical models of lymph node metastases of human tumors are needed for evaluating

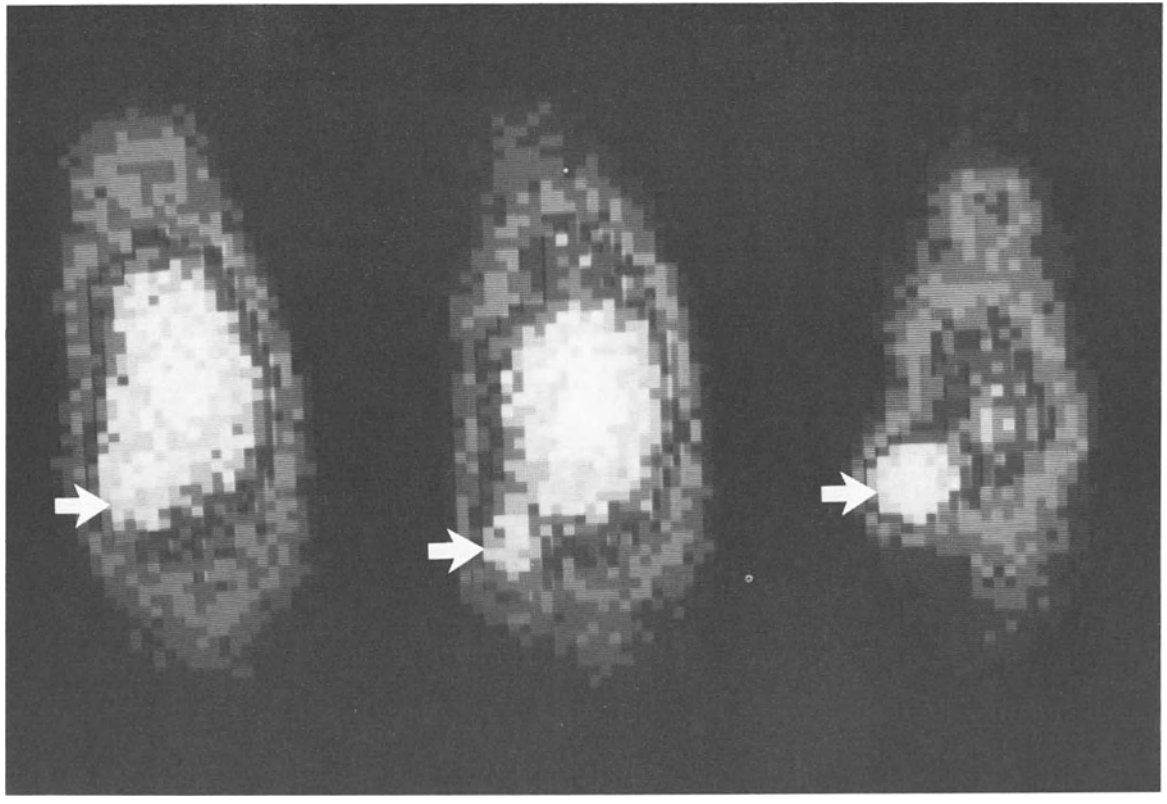

Figure 4. Images of 22 mg intrasplenic LS174T tumor at 24 (left), 48 (middle), and 120 (right) hours after intravenous injection of ^{131}I-B72.3. Images were obtained using a Pho/Gamma HP Camera. *Arrows*, location of the tumors. Nembutal anesthetized mice were positioned with the dorsal surface facing the camera. Each image was formed by the accumulation of 100,000 counts. No background subtraction techniques were used to generate these images. From Shah et al. [26].

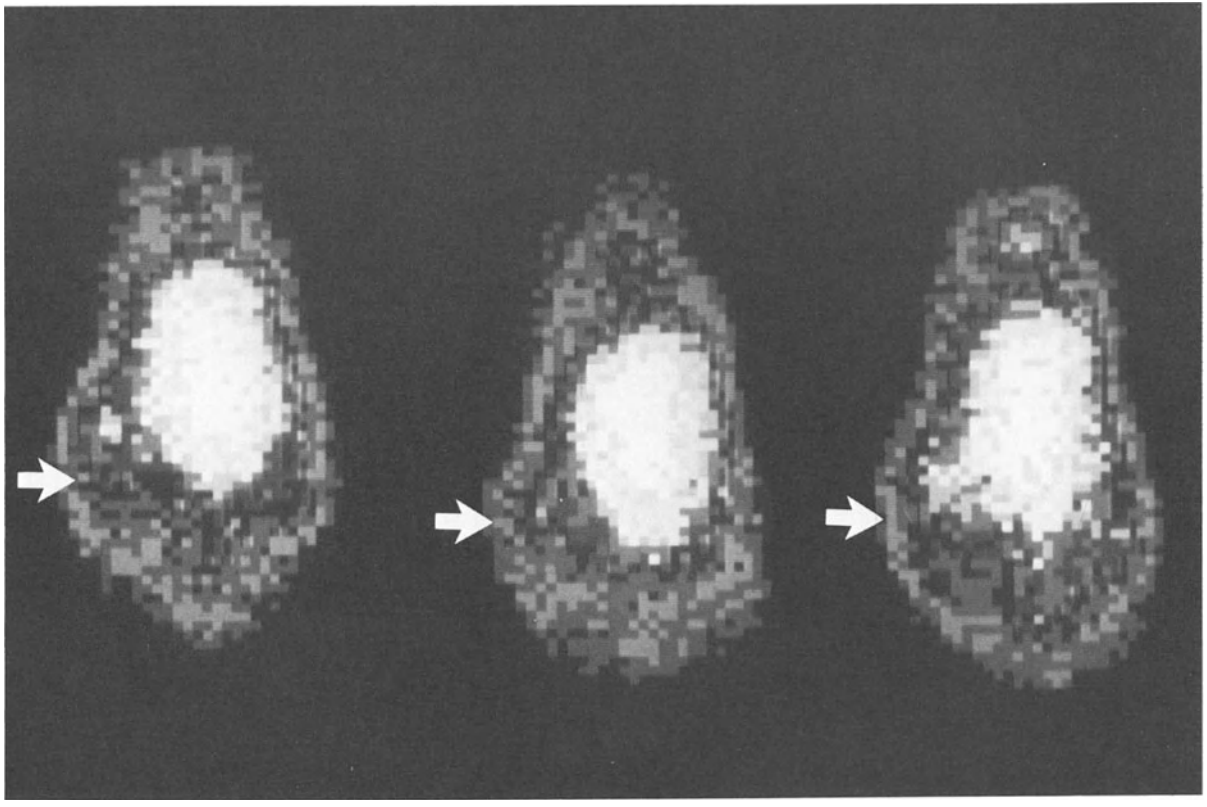

Figure 5. Images of an 80 mg intrasplenic control A375 human melanoma at 24 (left), 48 (middle), and 72 (right) hours after intravenous injection of ^{131}I-B72.3. The faint tumor image at 72 hours was due to blood-pool activity. Other details were as for Figure 4. From Shah et al. [26].

the utility of antibodies for the detection of nodal involvement. One of the original studies on animal nodal tumor detection by monoclonal antibodies was that of Weinstein and coworkers [56]. In this tumor model, hepatocarcinoma metastases in guinea pigs were imaged following subcutaneous injection of a monoclonal antibody directed against the tumor. Studies using human tumor xenografts have been difficult, because while many human tumors grow in the athymic mouse, metastases to lymph nodes from the primary tumor xenografts have been rarely demonstrated. We have developed axillary and popliteal lymph-node metastases models for a human colorectal carcinoma in athymic mice and used them for tumor localization by lymphoscintigraphy (i.e., the subcutaneous injection of a radiolabeled antibody and its delivery and accumulation via the lymphatic system) using radiolabeled monoclonal antibody. Tumors in axillary nodes of athymic mice were obtained from intravenous injection of human colon cells, whereas tumor metastases in popliteal nodes were induced following surgical excision of primary tumor from the hindfoot pad [10].

Advantages. The advantages of using this model are twofold. 1) The location of the tumor is visceral and may mimic nodal metastases observed in patients. 2) This model can be used to assess the ability of a radiolabeled antibody to detect tumors residing in the lymph nodes via the lymphatic delivery of the antibody.

Disadvantages. The major problems with this model are that tumor size cannot be assessed or controlled and that lymph nodal growth cannot be easily achieved with most human xenografts. Control of nodal tumor growth is critical if the animal model is to be used for the development of lymphoscintigraphic agents. If the lymphatics are blocked, the antibody cannot be delivered to the tumor via the lymphatics.

Examples of use. Lymph-node tumor models have been extensively used because of the possible importance of staging cancer patients using lymphoscintigraphy. The lymph-node tumor models and lymphatic delivery of antibody were originally described by Weinstein et al. [56]. These investigators reported imaging 2–7 mg hepatocarcinoma metastases in lymph node in guinea pigs 2.5 hours after the subcutaneous injection of ^{125}I-labeled antibody. The specificity of this early accumulation in relation to a nonspecific control antibody was, however, not determined. Tumor-specific localization of specific antibody over a control antibody in tumor metastases was reported only 24 hours after antibody injection.

The axillary and popliteal lymph-node metastases in athymic mice were used by us to assess ^{125}I-labeled antibody (and a nonspecific antibody) by lymphoscintigraphy [10]. Both normal and tumor-bearing axillary and popliteal lymph nodes imaged up to 6 hours after the subcutaneous injection of either antibody into either the forefoot or hindfoot pads. At 6 hours

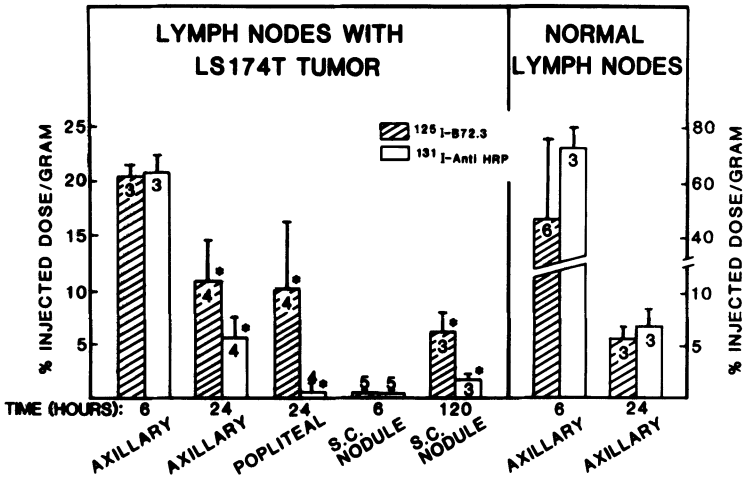

Figure 6. Accumulation of radioiodinated antibodies in tumor-positive or tumor-negative normal lymph nodes and in subcutaneous tumor on the backs of mice inoculated with LS174T tumor cells. The tumor-specific (B72.3) and -nonspecific (anti-HRP) antibodies were mixed together and injected subcutaneously into the forepaws or into the hindfoot pads to localize tumors in the axillary lymph nodes or in the popliteal lymph nodes, respectively. Animals were sacrificed at the indicated times for evaluation. Data are presented as means ± SD obtained from different numbers of animals shown within the histograms.* = $p \leq .03$, when distribution of the two antibodies was compared for the same group of normal or tumor tissue. From Shah et al. [10].

normal nodes showed two to four times greater accumulation of the two antibodies (Figure 6), compared with tumor-bearing nodes. Twenty-four hours and later after subcutaneous injection, images of nodal metastases (14–477 mg) and specific antibody accumulations were observed. Tumor-negative nodes did not image at 24 hours after injection of ^{125}I-labeled antibody. The antibody accumulation in nodal tumor at 24 hours observed in this study was similar to that obtained 24 hours after intravenous administration of antibodies in mice bearing subcutaneous, subrenal, or intrasplenic tumors [26,27,57].

Conclusions. To date only a limited number of lymph-node metastasis models for the study of monoclonal antibodies have been described. Development of this model for the evaluation of monoclonal antibodies directed against human tumors has been even more restricted, since human tumors do not readily metastasize to lymph nodes of immunosuppressed animals such as athymic mice. The major limitation of this tumor model in relation to the evaluation lymphatic delivery of the antibody is the tumor size. Successful lymphoscintigraphy depends on a balance between two competing parameters. Antibodies need to localize in nodes of a lymphoid chain via the unrestricted flow of lymph, while the amount of tumor in the lymph node must be sufficient to bind enough antibody for detection or therapy. Therefore, failure of lymphoscintigraphy can occur because either the

lymphatic delivery to the node is blocked or there is too little tumor to be detected.

Other sites

A number of other models have been described with respect to the site of tumor growth. Some of these models may provide useful information if utilized in the study of radiolabeled antibodies.

Hamster cheek pouch. Tumor in the cheek pouch is induced by implanting 1 mm^3 tumor pieces. The advantages of using this model are twofold: 1) The cheek pouch of hamster is a relatively immunoprivileged site and hence supports the growth of a foreign graft such as a human tumor. 2) Tumor growing in the cheek pouches can be measured in three dimensions with a small calliper. The major disadvantage of using this tumor model is that the tumor cannot be grown beyond 12–14 days due to rejection of the tumor by the host immune system.

One of the original reports on radiolocalization of an IgG used a CEA-producing human colonic carcinoma grown in the hamster cheek pouch [58]. ^{125}I-goat anti-CEA IgG specifically localized in tumors less than 200 mg in size. This initial study showed that tumor to blood ratios of about five could be attained 6 days post antibody injection. More recently, human choriocarcinoma grown in the hamster's cheek pouch has been used to study antibody localization [59]. These investigators found tumor to blood ratios of up to about six, 5 days following antibody injection.

The hamster cheek pouch model has not gained wide acceptance due to problems associated with tumor rejection by the host.

Liver model. Several models are available for the growth of tumors in the liver. Tumor metastasis in liver induced from a primary human colon carcinoma in the spleen of athymic mice [60] may provide valuable information on imaging and therapy. The rat model of Saini et al. [61], which used direct implantation of a 1 mm^3 fragment of a rat mammary adenocarcinoma into the liver parenchyma, may be useful for evaluating antibodies. This tumor model had tissue characteristics and morphologic features similar to human liver metastases, as demonstrated by sonography, CT, in-vitro magnetic resonance spectroscopy, and in-vivo magnetic resonance imaging [61]. While no reports on radioimmunodiagnosis using this model are known, imaging by magnetic resonance identified this tumor in liver as early as 1 week following implantation.

Brain tumor models

Description. Detection of brain tumors by radiolabeled tracer compounds have proved difficult due to the blood-brain barrier (BBB). A vascular barrier

between circulating blood and the brain tissue prevents many substances, including immunoglobulins, from reaching brain tissue. Brain tumors in athymic rats have been utilized for imaging studies with radiolabeled antibodies by Bullard and coworkers [62,63]. Intracranial tumors were grown in female athymic rats after injecting tumor homogenate into the right cerebral hemisphere. The intracranially growing tumor doubling time compared well with the subcutaneous tumor doubling time. Other investigators [64] have also grown intracranial tumors in athymic mice by injecting a tumor cell suspension into the right frontal hemisphere.

Advantage. If in a brain tumor model the tumor resides on the brain side of the BBB, the intracranial model could provide a unique opportunity to investigate the role of the osmotic blood-brain barrier in diagnosis and treatment using monoclonal antibodies.

Disadvantage. A drawback in using a brain tumor model is that the tumor size cannot be measured prior to imaging. It is important that an experimental tumor and its clinical counterpart reside on the same side of the BBB.

Examples of use. Bullard and coworkers found that antiglioma monoclonal antibody 4 days after antibody injection specifically imaged 20 mg brain tumors in athymic rats. A nonspecific control monoclonal antibody imaged these tumors only when the tumor was greater than 300 mg in size [62,63]. It has been shown that there is considerable variability in the permeability of tumor blood vessels to immunoglobulin [65], and therefore the role of vascular permeability of the BBB must be considered. For example, Blasberg et al. [64] showed that, due to the long plasma half-life of this immunoglobulin, accumulation of a tumor-specific monoclonal antibody was not significantly limited by the permeability of blood vessels or blood flow. This long plasma half-life of the antibody resulted in high levels of antibody for at least 3–5 days [64].

Intraabdominal tumor models. Intraperitoneal metastasis is a common problem in ovarian, pancreatic, and colorectal cancer. Intraperitoneal tumor models in athymic mice have been described for human breast and ovarian cancer [66,67], and for human malignant mesothelioma [68,69]. Tumors are grown by either injecting a cell suspension or by implanting tumor pieces.

The major advantage of this model is that the efficacy of intracavitary administration of antibodies for the diagnosis and treatment of tumors located in the peritoneal cavity can be assessed. Injection in the peritoneal cavity bathes peritoneal ovarian tumors in antibody and this gives higher tumor to normal tissue ratios for anti-tumor antibody, as compared with intravenous injection of the same antibody [67]. These results in mice agree with those obtained in patients bearing intraperitoneal implants from colorectal carcinoma [70]. In the case of ovarian cancer patients, however, better antibody localization was observed for the peritoneal ascites tumor

cells but not for solid tumors [71]. Further clinical studies are needed in this area to see if intraperitoneal administration for targeting intraperitoneal tumors in patients is advantageous over the intravenous administration of the same antibody. Treatment of intraabdominal tumors in mice was more effective following intraperitoneal administration of the antibody than after intravenous injection of the antibody (see below). Local antibody injection may thus reduce systemic exposure of other organs and limit toxicity.

A major drawback of this model may be the difference in the absorption of macromolecules from the peritoneum found in humans and mice. In mice, large molecular weight proteins are more rapidly transferred from this cavity to the vascular compartment. In ovarian-tumor-bearing mice, plasma levels of an intraperitoneally administered antibody approach those following an intravenous injection by about 24–48 hours [67,72]. In cancer patients antibody diffuses out of the cavity at a much slower rate, and the plasma levels are similar by about 96 hours for the intravenously and intraperitoneally administered antibody [70]. These differences in basic physiology between humans and mice should be considered when conclusions and predictions are made using the mouse tumor model.

Ear tumor models

Description. The ear tumor models have been employed for both imaging purposes and for evaluating the transport of macromolecules in tumor microcirculation. For imaging studies, tumors are grown by implanting a 2 mm^3 tumor fragment in the pinna of an anesthetized athymic mouse. Implantation is accomplished by guiding a trocar along the pinnal ridge from an insertion site in the vicinity of the opposite shoulder. In studies related to the transport of macromolecules in tumor, transparent plastic ring chambers are surgically implanted into the ears of the rabbits. After 40 days, when granulation tissue growth reaches maturity, the cover glass of the chamber is removed and then replaced with a sterile cover-glass coated with carcinoma cells.

Advantages and disadvantages. An advantage of the ear tumor model is the ability to accurately measure tumor size due to tumor accessibility. The rabbit ear model has been adapted for growth in a transparent chamber, which can be used to study tumor microcirculation at the cell level in vivo. A drawback of the ear chamber model is that rabbit does not support the growth of human tumors. The superficial nature of tumor growth in the ear does not make it an attractive model for tumor imaging purposes.

Examples of use. Hnatowich et al. [51] used ^{111}In-labeled monoclonal antibodies to CEA and to prostatic acid phosphatase (PAP) for imaging human colon tumor in mouse ear. Anti-CEA, but not an anti-PAP control

antibody, imaged the tumor at 24 hours post antibody injection. The tumor was not visualized in the animals that received ^{67}Ga-labeled citrate, an additional control. Jain and coworkers [73,74] developed and studied the neovascularization and transport of FITC-conjugated proteins (BSA, M_W = 67,000) and dextrans (MW = 19,400–150,000) in VX2 carcinoma grown in the rabbit ear chamber. Using quantitative fluorescent microscopy, these investigators showed that microvascular and interstitial resistances to the transport of the above macromolecules in the VX2 tumor were considerably less than those in a non-tumorous (mature granulation) tissue. These results suggests that transport of antibodies would be greater in tumor than in normal tissues.

The rabbit-ear chamber model could provide valuable information on extravasation rates of intact IgG, $F(ab')_2$, and Fab fragments in tumors and in normal tissues. However, the peripheral location of tumor growth does not make it an attractive model for antibody imaging studies.

'Artificial tumors'

Description. In the rare case in which it is necessary to study either the targeting potential or pharmacokinetics of an antibody for which a natural antigen is not available, it is possible to use an artificial tumor. For example, when we wanted to study the targeting ability and pharmacokinetics of mutant antibodies lacking different genetic domains, it was necessary to develop artificial tumors. The only antibodies available for this study were to the ARS (p-azophenylarsonate) antigen [75]. Micropore diffusion chambers containing immobilized ARS antigen on Sepharose beads were implanted subcutaneously in CD1 mice to serve as 'tumors.'

Advantages and disadvantages. There are several advantages of this model. 1) The chamber method can be readily modified for evaluating antibodies against different chemical-defined and synthesized antigens. 2) The amount of antigen placed in the chamber can be precisely controlled. 3) Interstitial fluid present in the chamber can be sampled and analyzed for the functional antibody present in the microenvironment of the 'tumor.' Since there is no blood flow within the chamber, a disadvantage of this model is that accretion into the 'artificial tumor' depends on diffusion of the antibody through the pores of the millipore filters attached to the ring chamber. The above model can be modified by the growth of human tumor around the micropore chamber. Tumor imaging by radiolabeled anti-tumor antibody can be assessed in relation to the levels of catabolic products of the antibody and shed tumor antigens by sampling the tumor interstitial fluid contained within the chamber [76].

Example of use. Using the 'ARS-tumor' model we found that the blood clearance of a monoclonal antibody and several of its deletion mutants was

biphasic, i.e., an initial rapid decrease was followed by a slower rate of disappearance [75]. At 13 days following antibody injection, the ratios of antibody accumulation in 'ARS tumors' over blood were 1680, 80, and 65 for ArM1 (CH_3-), ArM16 (CH_2-), and Ar13.4 (parent molecule), respectively. All three antibodies gave excellent gamma camera images of the 'ARS tumors' in mice; images with ArM1 antibody were superior than images obtained with ArM16 or Ar13.4 at 5 days after antibody injection (Figure 7).

Conclusion. The micropore chamber method used for evaluating monoclonal antibodies against chemical antigens or for collecting catabolic products of antibodies within the tumor milieu is novel and of interest. Such methods would allow studies of tumor-related factors that could potentially influence tumor diagnosis by radiolabeled antibodies.

THERAPY

Monoclonal antibodies carrying radionuclides with high beta energies could deliver lethal dose of radiation to the tumor, sparing other tissues. Cell damage is produced by the emitted particles and thus internalization of labeled antibody is not required. Radiolabeled antibody bound to a cell could deliver radiation to neighboring cells that lack the appropriate target antigen. The average distance traveled by an emitted beta particle is in the order of several millimeters. For example, a ^{186}Re emission will travel 4 mm, while the higher energy emission from ^{90}Y will travel 10 mm. Because the dose/survival curve for cells is exponential, i.e., for a given dose the probability of cell survival is related to the volume of tumor cells; the response is greater for smaller tumors than for larger ones [77].

The first clinical demonstration of the efficacy of a classical anti-cancer agent is in protocols designed to determine if the agent causes shrinkage or regression of a large measurable tumor burden. If the agent produces positive results, it will then be evaluated in patients with disseminated disease. In the latter case, the agent is assessed for its ability to increase patient survival time. The development of radioimmunotherapeutic agents will probably follow a similar pattern in both preclinical and clinical studies.

A key factor that determines the tumor response to a radioimmunotherapeutic agent is the radiation dose (in rads) delivered to the tumor. In experimental tumor models, the radiation dose is computed indirectly by estimating the absorbed dose rate and the cumulative doses for tumor and other organs using the mean specific activities (in μCi/g) as determined from biodistribution experiments. These data are then used to calculate organ doses using the medical internal radiation dose (MIRD) formulation [78]. The MIRD dosimetry calculations make several assumption regarding geometric and radiation attenuation factors. Wessels and coworkers [79] compared MIRD calculations with the direct measurement of the absorbed

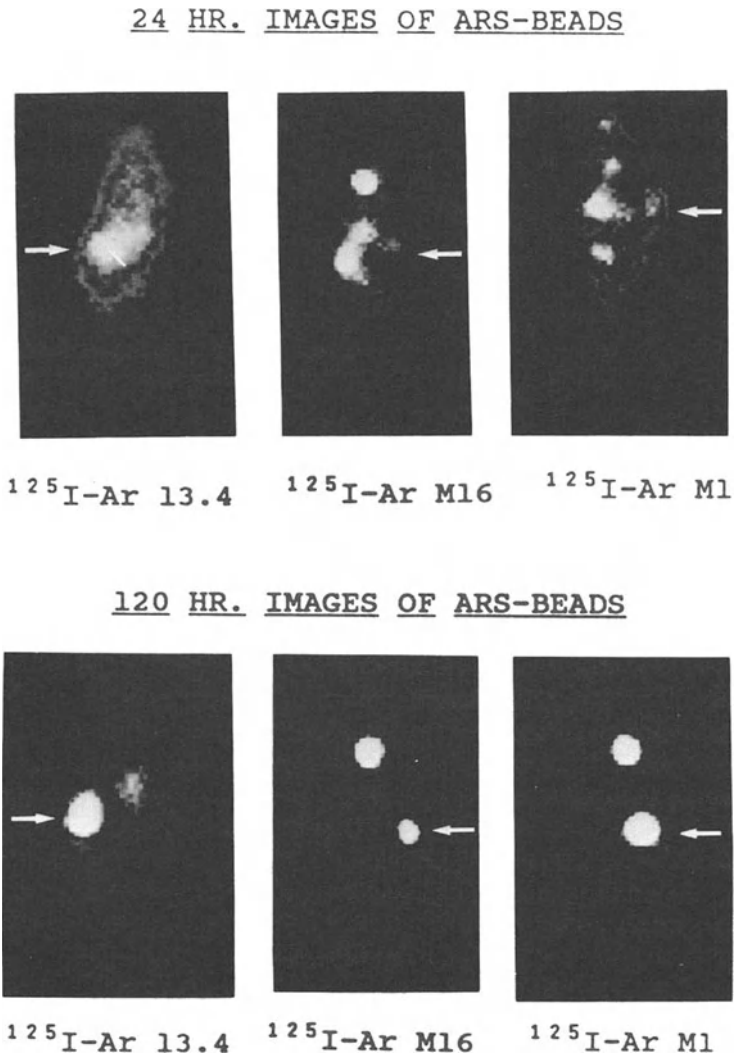

Figure 7. Images of micropore chambers containing between 50 and 75 mg of ARS-Sepharose beads at 24 and 120 hours after IV injection of 60 μCi of ^{125}I-Ar13.4, ^{125}I-ArM16, or ^{125}I-ArM1 antibodies. The images were obtained using a Picker gamma camera. Arrows indicate location of the ARS chambers in the CD1 mice. Nembutal-anesthetized mice were positioned with the dosal surface facing the camera. Each image was formed by the accumulation of 50,000 counts. No background subtraction techniques were used to generate these images.

radiation dose through the use of thermoluminescent dosimeters (TLD) implanted in various organs and tumors in mice. The MIRD calculations and TLD dose data indicated reasonable agreement between the two methods.

There have been many reports proposing the destruction of tumors by radiolabeled monoclonal antibodies [2,3]. The results suggest that consider-

able progress needs to be made to improve target to background levels [80]. Boven and Pinedo [3] have outlined a number of problems associated with the conjugation of antibodies with therapeutic radionuclides, as well as factors that would affect antibody localization in tumors. Hopefully, further advances will be made after we fully understand tumor cell biology and overcome the problems of tumor antigenic heterogeneity [31,81,82]. Suitable preclinical models are needed to fully evaluate the potential of radioimmunotherapeutic agents before they are administered to the patient.

Murine tumor models are commonly employed for evaluating the efficacy of anti-cancer drugs. These animal tumor models cannot be used for evaluating antibodies that are raised against human tumor antigens. Animals bearing human tumors, therefore, have to be used. Since radioimmunotherapy is likely to be more effective in eradicating disseminated disease or a small number of tumor cells [78], metastatic models of human tumors should be also used. Most human tumors do not, however, metastasize in athymic mice [7–9], and hence the effects of radioimmunotherapy on distant metastases and on survival times of the host animal cannot be readily assessed.

In the past few years, a number of animal models have been described for assessing radioimmunotherapy using antibodies. Essentially two types of animal models have been used. These are measurement models and survival models.

Measurement models

There are two types of measurement models used in the assessment of radioimmunotherapy. In the first the effect of radiolabeled antibody on the growth of a tumor is assessed. In the second type the ability of a radiolabeled antibody to produce shrinkage of a tumor is followed.

In the tumor growth model, tumors are grown either subcutaneously or in a deep-seated site such as under the renal capsule. Small tumors of known size are treated. The percent change in tumor size, as determined by calliper measurement, is related to the dose of the drug or radiation used. The measured tumor size and actual tumor weight have shown good correlation ($r = 0.985$) [14]. However, this type of measurement cannot give an accurate assessment of the actual mass of viable tumor present, since the regressing tumor contains nonmalignant fibrotic and necrotic tissue. A disadvantage of using the growth measurement model is that a minimal-detectable-size tumor must be used at the beginning of an experiment. The effects of radioimmunotherapy on a small number of established tumor foci, which may be analogous to the metastatic disease, cannot be assessed with the measurement model. Nevertheless, this model has provided valuable information on tumor regression, regrowth, and doubling times following radioimmunotherapy.

In the tumor shrinkage model, tumors are usually grown subcutaneously. Large tumors (about 1–2 g in size) are treated, and a change in tumor size is related to the dose of the drug or antibody used [14]. This model is used to

determine if the radiolabeled antibody causes shrinkage of a large measurable tumor burden.

Homografts

Description. Subcutaneous tumors are induced by implanting tumor cells or tumor pieces (see Diagnosis).

Advantage. The homograft models may mimic the situation in cancer patients in that the tumor and the host are isogeneic. Efficacy can be easily followed through repeated determinations of tumor over a long period of time.

Disadvantages. 1) Animal tumors differ from human tumors in radiosensitivity and tumor-cell doubling times. These parameters would have a strong influence on the success of radioimmunotherapy. 2) Due to the lack of antigen, the homograft tumor models cannot be used for the evaluation of monoclonal antibodies raised against human tumor-associated antigens.

Examples of use. Using a murine lymphoma model, Badger and co-workers [83] observed better therapeutic effects with ^{131}I-labeled tumor-specific antibody than with a nonspecific antibody. High doses (1500 μCi), however, of both specific and nonspecific antibodies proved toxic to the bone marrow, and all animals died of marrow aplasia. In a previous study with this tumor model, both tumor regression and prolongation of animal survival time (for details see below, Survival Models) were observed with a antibody dose of 500 μCi [84]. Up to 1000 μCi of ^{131}I-labeled nonspecific antibody showed no effect on tumor growth.

In a murine thymoma model, Zalcberg et al. [85] failed to demonstrate therapeutic effects of a ^{131}I-labeled anti-tumor antibody (1100 μCi). This was attributed to the rapid growth of the thymoma, with a doubling time of less than 2 days.

Conclusion. These studies showed that rapidly growing homograft tumors do not respond as well to radioimmunotherapy as would slow-growing tumors. Also, radiolabeled antibodies used against differentiation antigens may be useful for therapy, in spite of binding to normal lymphocytes, but curative therapy would require infusion of unirradiated bone marrow.

Hamster cheek pouch

Description. Cheek pouches of hamsters will support the growth of human tumors. The GW-39 human colon carcinoma is not very responsive to a

number of anticancer drugs or external x-irradiation [86], thus resembling the behavior of human colon cancer. The hamster cheek pouch model has been used for the evaluation of radioimmunotherapy by Goldenberg et al. [87].

Advantages. 1) The cheek pouches can be everted to permit measurement with a small calliper of tumor size in three dimensions. 2) Human tumors can be grown in relatively inexpensive hamsters (athymic animals are more costly to buy and require greater care to house).

Disadvantage. The major disadvantage of this model is that long-term studies are not possible due to immune rejection of the tumor by the host.

Example of use. Antitumor effects of ^{131}I-labeled goat antibody to CEA, which GW-39 tumor growing in the cheek pouch secrete, have been evaluated by Goldenberg et al. [87]. In this study tumor-specific antibody produced better tumor regression than a nonspecific antibody (1000 μCi dose). However, 2000 μCi of either tumor specific or nonspecific antibody showed similar inhibition of tumor growth.

Conclusion. While the efficacy of radioimmunotherapy has been shown in the hamster cheek-pouch tumor model, this model has not gained wide acceptance, because long-term studies involving tumor regression and regrowth are not possible due to the immune rejection of the tumor.

Athymic mice. Most of the studies described in which radiolabeled antibodies as therapeutic agents were evaluated have utilized the measurement model in athymic mice. For convenience, these tumor models have been assessed from the point of view of the site of tumor growth.

Subcutaneous

Description. Radioimmunotherapy of a variety of subcutaneous human tumor xenografts have been described. These include colon tumors [85,88,89], glioma [90], neuroblastoma [14,91], renal cell carcinoma [92], and pancreatic carcinoma [93].

Advantages. 1) This animal model allows the study of human tumors. 2) Tumor size can be accurately monitored, thus both the affects on well-established tumors (shrinkage) and on tumor development (growth) can be followed.

Disadvantage. Tumors from the subcutaneous site rarely metastasize to distant organs of vital importance. Therefore, the effects of radioimmunotherapy on micrometastases and on survival times cannot be studied using this model. Other disadvantages related to the xenografts can be found in Diagnosis.

Examples of use. A colon tumor xenograft model was used by Zalcberg et al. [85] to demonstrate the therapeutic efficacy of ^{131}I-labeled tumor-specific antibody. In contrast, a ^{131}I-labeled nonspecific antibody produced no significant effect on tumor growth. This study further showed that the effects of radioimmunotherapy could be improved by reducing dehalogenation of the antibody by pretreating mice with the antithyroid drug propylthiouracil.

Using a colorectal subcutaneous xenografts in athymic mice, Neacy et al. [88] compared the effects of 4 MV x-ray external beam radiotherapy with radioimmunotherapy using ^{131}I-labeled antibody. The dose delivered to the tumor by either irradiation modality was measured directly by implanted miniature thermoluminescent dosimeters. The tumor-volume doubling time was used as a determinate of therapeutic response. The results showed a greater response to ^{131}I-antibody therapy than to external beam therapy on a per rad basis. Mornex [89] showed a dose/response effect of ^{131}I-antibody using this xenograft model. Although 500 μCi and 600 μCi of ^{131}I-B72.3 resulted in complete inhibition of tumor growth, it produced lethal side effects (aplasia or bone-marrow toxicity).

Regression of relatively large (0.5–2 cm^3 size) human neuroblastoma xenografts in athymic mice was observed by Cheung et al. [14] with an IgG_3 monoclonal antibody labeled with ^{131}I. Dose-dependent shrinkage was demonstrated (Figure 8). Radioiodinated nonspecific antibody or unlabeled tumor-specific antibody did not induce tumor regression. Only those tumors that received more than 4200 rads (as calculated by MIRD) completely disappeared. Whole-body doses ranged between 110 and 380 rads. The recurrent tumors were not antigen negative or radioresistant, since they could be effectively treated with a subsequent ^{131}I-antibody injection. Toxicity from ^{131}I antibody at therapeutic doses greater than 500 μCi per mouse was manifested mainly in weight loss. There were no gross abnormalities or microscopic evidence of radiation damage in the major organs at a follow-up of 1 month or more after treatment.

A renal-cell carcinoma xenograft model was employed by Vessella et al. [92] to demonstrate the therapeutic effects of ^{131}I tumor-specific antibody. Following treatment with a relatively moderate dose (100 μCi) of ^{131}I antibody, prolonged (> 90 days) regression of the RCC tumors was observed.

Intratumor versus intravenous injection of ^{131}I antibody in human pancreatic carcinoma xenografts was compared by Klapdor et al. [93]. ^{131}I antibody content of tumor at 24 hours following intratumor injection was about 20 times greater than that after intravenous injection of the antibody. Despite the fact that a much higher radiation dose to the tumor was delivered by the intratumor injection as compared with the intravenous injection, similar or better antitumor effects were observed in animals given intravenous injection of the antibody. The authors attributed this to factors (which they did not specify) rather than to a direct toxic effects of tumor irradiation [93].

Conclusions. The above studies suggest that regression of subcutaneously grown human tumors can be obtained by radiolabeled anti-tumor monoclonal

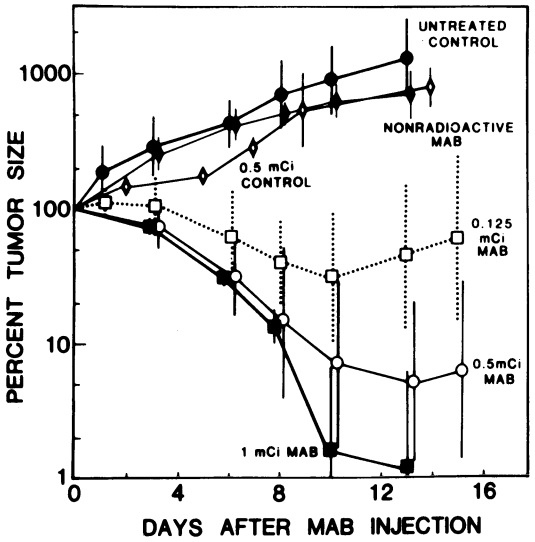

Figure 8. In-vivo treatment of human neuroblastoma (NB) xenografts. Established NBs were treated intravenously with varying doses: 1 (■), 0.5 (○), and 0.125 mCi (□) ^{131}I-labeled 3F8 (100 μg 3F8). Tumor response over time (in days) was expressed as percent of original tumor volume at the beginning of the experiment. Groups of three to seven mice were used. The geometric means ± SD of the percent tumor sizes are depicted. The control group (●) mice did not receive any treatment. The nonradioactive Mab (MAB) group (⧫) received 100 μg unlabeled 3F8 intravenously. The 0.5 mCi group (◊) received 0.5 mCi of ^{131}I-radiolabeled anti-sheep red blood cell Mab intravenously. From Cheung et al. [14].

antibodies. In some cases, radioimmunotherapy may give better results than external beam irradiation. Before general conclusions can be drawn from these studies, they must be confirmed and expanded using a variety of tumor types.

Subrenal

Description. Details on tumor induction under the renal capsule can be found in Diagnosis.

Advantages and disadvantages. The location of tumor under the renal capsule near other visceral organs make this an attractive model for evaluation of radioimmunotherapy. Some disadvantages of this model are: 1) The effect of radioimmunotherapy is assessed by determination of tumor size only on the day of tumor implant and the day of analysis. Therefore, one cannot make sequential tumor measurements to assess tumor regression or regrowth following radioimmunotherapy. 2) Implanted tumor lacks vasculature and receives its oxygen, nutrients, and antibody by diffusion for at least 5–6 days after tumor implantation.

Example of use. The subrenal tumor model has not been extensively used for assessing effects of radioimmunotherapy. In our laboratory, we have evaluated the affects of ^{131}I-labeled monoclonal antibodies on a human colon tumor grown in the subrenal capsule [57]. In these experiments, 1 day after tumor implantation, 160 μCi of either the ^{131}I-specific antibody or a nonspecific antibody was injected intravenously. ^{131}I-specific antibody produced marked inhibition of tumor growth when measured 12 days following therapy. ^{131}I-nonspecific antibody also produced significant therapeutic response due to nonspecific uptake of this antibody by the tumor.

Conclusion. Although widely used for the assessment of chemotherapeutic agents, the subrenal model has not been utilized by many investigators for evaluating the efficacy of radioimmunotherapy. This is most likely due to the fact that: 1) large number of animals cannot be readily used since the tumor implantation procedure is rather cumbersome, and 2) repeated tumor measurements cannot be made to follow tumor regression or regrowth following antibody therapy.

Spleen. Radioimmunotherapy of erythroleukemia-virus-infected mice using ^{90}Y-labeled monoclonal antibody was studied recently by Anderson-Berg et al. [94]. This virus infection results in primary splenic disease, which, when untreated, leads to systemic viremia and erythroleukemia, with metastases in liver and bone marrow. Specific monoclonal antibody was two- to threefold more potent than bovine immunoglobulin in therapy, as assessed by a reduction of splenomegaly (dose required for half-maximal effect, 9 μCi vs. 16–27 μCi). Mice trated with 50 μCi ^{90}Y-labeled control immunoglobulin had spleens that were twice the normal size and showed extensive areas of erythropoiesis indicative of the presence of tumor foci; in contrast, doses as low as 27 μCi of ^{90}Y-labeled specific antibody resulted in complete remission, with no microscopic evidence of tumor foci in either the spleen or liver. Although reversible marrow toxicity was observed, it was not dose limiting.

To our knowledge the splenic tumor xenograft models [26,52] have not been yet used for evaluating radiolabeled antibodies as therapeutic agents. The size of tumor can be controlled well, since the tumor growth is initially (up to 100 mg size) confined to the spleen bed. However, as with the subrenal tumor model, intrasplenic tumors cannot be sequentially measured due to their visceral location.

Survival models

Description. Survival models are models of malignant disease that, if untreated, would be lethal to the host. Thus these models may mimic the clinical situation, since most cancer patients die of disseminated disease.

Experimental metastases are produced in animals by implanting tumor cells subcutaneously [84], intraperitoneally [68,69,95,96], or in the brain [90,97].

Advantages. Advantages of this model are: 1) It quantitates the full effect of a classical anti-cancer agent because it is relatable to the host toxicity and therefore to the therapeutic efficacy (because of the geometry dependence of radiation, this is not of advantage when used for studying radiotherapy). 2) The tumor is highly metastatic and rapidly lethal to the animal, giving a reproducible mortality rate in untreated animals. 3) The survival models allow the study of the effects of therapy on minimal residual tumor burden.

Disadvantages. Disadvantages of this model are: 1) Human tumors do not readily metastasize in immunosuppressed animals such as athymic mice. 2) Since a monoclonal antibody will bind to only a limited number of human tumor lines, it becomes necessary to develop survival models for each antibody/tumor system. 3) As with any visceral tumor model, in survival models tumor size cannot be measured following antibody therapy. 4) Its most important disadvantage is the small size of an experimental animal in comparison with a human. Radiotherapy is extremely geometry dependent. The small size of a mouse, for example, in relation to the distances a beta particle travels, make the estimations of efficacy and radiotoxicity very difficult.

Examples of use. The following summary will discuss a few models that have been utilized to evaluate the effects of radiolabeled monoclonal antibodies on survival times of animals. Some recently developed survival models that have the potential for assessing radioimmunotherapy are also discussed.

Homografts. Homograft models are isologous (tumor and host genetically similar) with respect to the cancer patient. It should be noted that the radiosensitivities of human tumors differ greatly from the rodent tumors. Therefore, the data obtained from the homograft models should be interpreted with caution.

Using a murine lymphoma model, Badger et al. [84] demonstrated a dose/response effect of ^{131}I-tumor specific antibody. Fifty percent survival for mice treated with a single dose of 500 μCi, 1000 μCi, or 1500 μCi of ^{131}I antibody were 35, 25, or 20 days, respectively. In contrast, up to 1000 μCi of ^{131}I-labeled nonspecific antibody had no effect on tumor growth, in spite of slower clearance of the control antibody from the blood. No long-term survivors were observed. Death in animals treated with 500 μCi of labeled antibody was a result of progressive metastatic lymphoma. In animals treated with 1000 μCi, death was a result of a combination of tumor growth and radiation toxicity to the bone marrow.

Athymic mouse

Intraperitoneal models. These models are analogous to some clinical situations with respect to tumor location. Multiple tumor seedings in the abdominal cavity of ovarian cancer patients are observed. Tumor to normal tissue ratios may be improved by administering radiolabeled antibody by the local intraperitoneal route as opposed to the commonly employed intravenous route for intraabdominal metastases [67]. A drawback of this model may be the inability to assess tumor burden at different times after radioimmunotherapy and the vast differences in pharmacokinetics seen in mice and humans after an intraperitoneal injection.

Survival models of human ovarian [98] and colon [96] carcinoma grown in the abdominal cavity of athymic mice were used to evaluate the effects of ^{131}I-labeled monoclonal antibodies. In these studies, either ovarian cancer cells or colon tumor cells were injected intraperitoneally and 1–2 hours later 450 μCi of tumor-specific antibody was injected either intraperitoneally or intravenously. In the ovarian model, the ^{131}I antibody treatment prolonged the survival times to 139 days after intraperitoneal injection, and 147 days after intravenous injection. The saline-treated mice showed a mean survival times of only 84 days [96]. Using the colon tumor model, the mean survival in the saline group was shown to be 37 days. After intravenous injection of ^{131}I-labeled antibody, survival time increased to 44 days, and after intraperitoneal injection to 67 days. Radioimmunotherapy produced statistically significant improvements in survival regardless of the antibody injection site. The data with the colon tumor model (but not with the ovarian model) further showed that intraperitoneal delivery of radiolabeled antibody produced better survival in mice than did antibody administered by the intravenous route.

Intraabdominal models of human malignant mesothelioma [68,69] and a variety of ovarian breast and colon carcinoma cell lines [66] have been described. These models have yet to be utilized for evaluating radiolabeled monoclonal antibodies. The mesothelioma model has, however, been used to test the effects of ricin-A chain conjugated to murine monoclonal antibody against human transferrin receptor [69].

It remains to be demonstrated with a variety of intraabdominal human tumor models if local antibody injection is advantageous over the intravenous route of antibody administration. The effects of radioimmunotherapy on established tumors should be evaluated, rather than antibody treatment, within a few hours after tumor cell implantation.

Athymic rat. The size of the host in relationship to the effects of radiation is most important. Therefore, the use of a rat, which is ten times larger than a mouse, may offer some predictive advantage. Survival studies using athymic rats bearing intracranial human glioma [90] have been used for evaluating radioimmunotherapy. Lee and coworkers [99] showed significant prolonga-

tion in survival times of animals bearing small tumors after treatment with a 1250 μCi dose of ^{131}I tumor-specific antibody. The control groups of mice treated with either ^{131}I-labeled nonspecific antibody or the unlabeled tumor-specific antibody showed no significant prolongation in survival times, as compared with the untreated animals.

In the intracranial model of human lung tumor developed by Neuwelt et al. [97] the medium survival time was 13 days and all animals died by day 26. This tumor was impermeable to Evan's blue: albumin (MW, 68,500). This model may be useful in evaluating the role of the osmotic blood-brain barrier opening in the monoclonal antibody delivery and treatment of brain tumor.

Conclusion. Further systematic studies are needed for evaluating the efficacy of monoclonal antibodies carrying therapeutic radionuclides of varying energies. These studies should include radiolabeled tumor-specific and nonspecific antibodies; measurement models to evaluate the effects on tumor regression, regrowth, and doubling times; and survival models with minimal tumor burden, as well as established tumors, to study the effects on prolongation of life.

Conclusions

Advantages and disadvantages of an animal model should be carefully considered prior to its selection for use in the evaluation of radiolabeled monoclonal antibodies as diagnostic and therapeutic agents. The model selected should mimic the clinical situation as closely as possible. All conclusions drawn from data obtained from experimental models must reflect the biases and limitations of that particular model. The localization of radiolabeled antibodies in true metastatic models is an almost totally unexplored area for animal investigation and represents perhaps the most clinically relevant evaluation system. Great caution should be exercised, however, in extrapolating animal data to humans. Animal models should be regarded as useful only for understanding mechanisms of antibody localization in tumors (which cannot be readily studied in the clinic) and for providing guidance in the selection of agents that are to be evaluated in the clinic.

Acknowledgments

The authors thank Dr. Stephen B. Haber for his critical review and Mrs. Amy L. Ilovici for typing this manuscript.

References

1. Kohler, G., and Milstein, C. (1975) Continuous cultures of fused cells secreting antibody of predefined specificity. Nature 256:495–497.

2. Chu, T.M. (1985) Potential applications of monoclonal antibodies in cancer diagnosis and therapy. Cancer Invest. 3:565–584.
3. Boven, E., and Pinedo, H.M. (1986) Monoclonal antibodies in cancer treatment. Where do we stand after 10 years? Radiother Oncol 5:109–117.
4. Halpern, S.E., and Dillman, R.O. (1987) Problems associated with radioimmunodetection and possibilities for future solutions. J. Biol. Response Modifiers 6:235–262.
5. Kallman, R.F. ed. (1987). *Rodent Tumor Models In Experimental Cancer Therapy*. New York: Pergamon Press.
6. Kallman, R.F., Brown, J.M., Denekamp, J., Hill, R.P., Kummermehr, Jr., and Trott, K.-R. (1985) The use of rodent tumors in experimental cancer therapy. Cancer Res. 45:6541–6545.
7. Hanna, N., Pollack, V.A., and Fidler, I.J. (1983) The use of young nude mice to study metastasis of human neoplasms. In: Humphrey, G., Grindey, G.B., and Dehner, L., et al. (eds.), *Adrenal and Endocrine Tumors in Children*. Boston: Martinus Nijhoff, pp. 1–18.
8. Sharkey, F.E., and Fogh, J. (1984) Considerations in the use of nude mouse for cancer research. Cancer Metastasis Rev. 3:341–360.
9. Fidler, I.J. (1986) Rationale and methods for the use of nude mice to study the biology and therapy of human cancer metastasis. Cancer Metast. Rev. 5:29–49.
10. Shah, S.A., Gallagher, B.M., and Sands, H. (1987) Lymphoscintigraphy of human colorectal carcinoma metastases in athymic mice by use of radioiodinated B72.3 monoclonal antibody. J. Natl. Cancer Inst. 78:1069–1077.
11. Gallagher, B.M. (1983) Monoclonal antibodies: The design of the appropriate carrier and evaluation systems. In: Lambrecht, R.M., and Eckelman, W.C. (eds.), *Animal Models in Radiotracer Design*. New York: Springer-Verlag, pp. 62–105.
12. Brown, B.A., Comeau, R.D., Jones, P.L., Liberatore, F.A., Neacy, W.P., and Sands, H. (1987) Pharmacokinetics of the monoclonal antibody B72.3 and its fragments labeled with either ^{125}I or ^{111}In. Cancer Res. 47:1149–1154.
13. Fogh, J., Fogh, J.M., Sharkey, F.E., Hajdu, S.I., and Fitzgerald, P.J. (1977) Forty-eight serially transplanted human tumors in nude mice. Proc. Am. Assoc. Cancer Res. 18:183.
14. Cheung, N.-K.V., Landmeier, B., Neely, J., Nelson, A.D., and Abramowsky, C. (1986) Complete tumor ablation with iodine ^{131}I-radiolabeled disialoganglioside GD2-specific monoclonal antibody against human neuroblastoma xenografted in nude mice. J. Natl. Cancer Inst. 77:739–745.
15. Bernhard, M.I., Hwang, K.M., Foon, K.A., Keenan, A.M., Kessler, R.M., Frincke, J.M., Tallam, D.J., Hanna, M.G., Peters, L., and Oldham, R.K. (1983) Localization of ^{111}In- and ^{125}I-labeled monoclonal antibody in guinea pigs bearing line 10 hepatocarcinoma tumors. Cancer Res. 43:4429–4433.
16. Goodwin, D., Meares, C., Diamanti, C., McCall, M., Lai, C., and Torti, F. (1984) Use of specific antibody for rapid clearance of circulating blood background from radiolabeled tumor imaging proteins. Eur. J. Nucl. Med. 9:209–215.
17. Ballou, B., Reiland, J., Levine, G., Knowles, B., and Hakala, T.R. (1985) Tumor location using $F(ab')_{2m}$ from a monoclonal IgM antibody: Pharmacokinetics. J. Nucl. Med. 26:283–292.
18. Menard, S., Miotti, S., Tagliabue, E., Parmi, L., Buraggi, G.L., and Colnaghi, M.I. (1983) Tumor radioimmunolocalization in a murine system using monoclonal antibodies. Tumori 69:185–190.
19. Sands, H., Jones, P.L., Neacy, W.P., Shah, S.A., and Gallagher, B.M. (1986) Site-related differences in the localization of the monoclonal antibody OX7 in SL2 and SL1 lymphomas. Cancer Immunol. Immunother. 22:169–175.
20. Pimm, M.V., and Baldwin, R.W. (1986) Effect of tumor size on monoclonal antibody uptake in tumor models. J. Nucl. Med. 27:1788–1789.
21. Shah, S.A., Sands, H., and Gallagher, B.M. (1985) Rapid simultaneous determination of vascular volume (vv) and vascular permeability (vp) of human and murine tumors grown in athymic mice. Proc. Am. Assoc. Cancer Res. 26:1142.

22. Pimm, M.V., Pascoe, W., Robins, A.R., Price, M.R., and Baldwin, R.W. (1986) Effect of protein mass on the pharmacokinetics and tumor discrimination of a murine monoclonal antibody in a rat mammary tumor model. IRCS Med. Sci. 14:876–877.
23. Halpern, S., and Hagan, P. (1985) Effect of protein mass on the pharmacokinetics of murine monoclonal antibodies. J. Nucl. Med. 26:818–819.
24. Moshakis, V., McIlhinney, R.A.J., Raghavan, D., and Neville, A.M. (1981) Localization of human tumor xenografts after iv administration of radiolabeled monoclonal antibodies. Br. J. Cancer. 44:91–99.
25. Hagan, P.L., Halpern, S.E., Dillman, R.O., Shawler, D.L., Johnson, D.E., Chen, A., Krishnan, L., Frincke, J., Bartholomew, R.M., David, G.S., and Carlo, D. (1986) Tumor size: Effect on monoclonal antibody uptake in tumor models. J. Nucl. Med. 27:422–427.
26. Shah, S.A., Gallagher, B.M., and Sands, H. (1985) Radioimmunodetection of small human tumor xenografts in spleen of athymic mice by monoclonal antibodies. Cancer Res. 45:5824–5829.
27. Shah, S.A., Sands, H., Jones, P.L., Neacy, W., and Gallagher, B.M. (1984) Relationship between blood flow and the localization of monoclonal antibodies in human tumors in nude mice. Proc. Am. Assoc. Cancer Res. 25:260.
28. Sands, H., Jones, P.L., Shah, S.A., Palme, D., Vessella, R.L., and Gallagher, B.M. (1988) Correlation of vascular permeability and blood flow with monoclonal antibody uptake by Clouser and renal cell xenografts. Cancer Res. 48:188–193.
29. Mano, H., Furuhashi, Y., Hattori, S., Goto, S., Tomoda, Y., and Ichikatai, T. (1986) Radioimmunodetection of human choriocarcinoma xenografts by monoclonal antibody to placental alkaline phosphate. Jpn. J. Cancer Res. (Gann) 77:160–167.
30. Jones, P.L., Gallagher, B.M., and Sands, H. (1986) Autoradiographic analysis of monoclonal antibody distribution in human colon and breast tumor xenografts. Cancer Immunol. Immunother. 22:139–143.
31.. Greiner, J.W., Guadagni, F., Noguchi, P., Pestka, S., Colcher, D., Fisher, P.B., and Schlom, J. (1987) Recombinant interferon enhances monoclonal antibody-targeting of carcinoma lesions in vivo. Science 235:895–898.
32. Hagan, P.L., Halpern, S.E., Chen, A., Krishnan, L., Frincke, J., Bartholomew, M., David, G.S., and Carlo, D. (1985) In vivo kinetics of radiolabeled monoclonal anti-CEA antibodies in animal models. J. Nucl. Med. 26:1418–1423.
33. Goldenberg, D.M., DeLand, F., Kim, E., Bennett, S., Primus, F.J., Nagell, J.R., Estes, N., DeSimone, P., and Rayburn, P. (1978) Use of radiolabeled antibodies to carcino-embryonic antigen for the detection and localization of diverse cancers by external photoscanning. N. Engl. J. Med. 298:1384–1388.
34. Andrew, S.M., Pimm, M.V., Perkins, A.C., and Baldwin, R.W. (1986) Comparative imaging and biodistribution studies with anti-CEA monoclonal antibody and its $F(ab')_2$ and F(ab′) fragments in mice with colon carcinoma xenografts. Eur. J. Nucl. Med. 12:168–175.
35. Stavrou, D., Mellert, W., Bilzer, T., Senekowitsch, R., Keiditsch, E., and Mehraein, P. (1985) Radioimmunodetection of gliomas by administration of radiolabeled monoclonal antibodies. Anticancer Res. 5:147–156.
36. Ballou, B., Reiland, J.M., Levine, G., Taylor, R.J., Shen, W-C, Ryser, H. J.-P., Solter, D., and Hakala, T.R. (1986) Tumor location and drug targeting using a monoclonal antibody (anti-SSEA-1) and antigen-binding fragments. J. Surg. Oncol. 31:1–12.
37. Shah, S.A. (1986) Metastases and hyperthermia. In: Anghileri, L.J., and Roberts, J. (eds.), *Hyperthermia in Cancer Treatment*. Boston: G.K. Hall, pp. 191–227.
38. Sharkey, R.M., Primus, F.J., and Goldenberg, D.M. (1984) Second antibody clearance of radiolabeled antibody in cancer radioimmunodetection. Proc. Natl. Acad. Sci. USA. 81:2843–2846.
39. Levine, G., Ballou, B., Reiland, J., Solter, D., Gumerman, L., and Hakala, T. (1980) Localization of I-131-labeled tumor-specific monoclonal antibody in the tumor-bearing BALB/c mouse. J. Nucl. Med. 21:570–573.
40. Lockshin, A., Kozielski, T., and Stehlin, J.S. (1986) Prediction of anticancer activity by

tumor uptake of radiolabeled monoclonal antibody. Cancer Lett. 30:1–9.
41. Wahl, R.L., Parker, C.W., and Philpott, G.W. (1983) Improved radioimaging and tumor localization with monoclonal $F(ab')_2$. J. Nucl. Med. 24:316–325.
42. Bogden, A.E., Kelton, D.E., Cobb, W.R., and Esber, H.J. (1978) A rapid screening method for testing chemotherapeutic agents against human tumor xenografts. In: Houchens, D.P., and Ovejera, A.A. (eds.), *Symposium on the Use of Athymic Mice in Cancer Research*. New York: Fisher, pp. 231–250.
43. Griffin, T.W., Bogden, A.E., Reich, S.D., Antonelli, D., Hunter, R.E., Ward, A., Yu, D.J., Greene, H.L., and Costanza, M.E. (1983) Initial clinical trials of the subrenal capsule assay as a predictor of tumor response to chemotherapy. Cancer 52:2185–2192.
44. Cobb, W.R., Bogden, A.E., Shoemaker, R.H., and LePage, D.J. (1987) In vivo testing of cryopreserved human tumor cell lines: Subrenal capsule/fibrin clot assay. Proc. Am. Assoc. Cancer Res. 28:429.
45. Fingert, H.J., Chen, Z., Mizrahi, N., Gajewski, W.H., Bamberg, M.P., and Kradin, R.L. (1987) Rapid growth of human cancer cells in a mouse model with fibrin clot subrenal capsule assay. Cancer Res. 47:3824–3829.
46. Bogden, A.E., Haskell, P.H., LePage, D.J., Kelton, D.E., Cobb, W.R., and Esber, H.J. (1979) Growth of human tumor xenografts implanted under the renal capsule of normal immunocompetent mice. Exp. Cell Biol. 47:281–293.
47. Abrams, J., Jacobovitz, D., Dumont, P., Semal, P., Mommen, P., Klastersky, and Atassi, G. (1986) Subrenal capsule assay of fresh human tumors: Problems and pitfalls. Eur. J. Cancer Clin. Oncol. 22:1387–1394.
48. Bogden, A.E., Hnatowick, D.J., Doherty, P.W., and Griffin, T.W. (1983) In vivo localization of monoclonal antibody in fresh surgical explants of human tumors: 3-day subrenal capsule (SRC) assay. Proc. Am. Assoc. Cancer Res. 24:218.
49. Bogden, A.E., Griffin, T.W., LePage, D.J., and Cobb, W.R. (1987) Testing biological response modifiers against human tumors in the subrenal capsule assay. Proc. Am. Assoc. Cancer Res. 28:429.
50. Sands, H., Jones, P.L., Neacy, W., Shah, S.A., and Gallagher, B.M. (1984) The imaging of small experimental murine tumors grown in the subrenal capsule using monoclonal antibodies. Cancer Lett. 24:65–72.
51. Hnatowich, D.J., Layne, W.W., Childs, R.L., Lanteigne, D., Davis, M.A., Griffin, T.W., and Doherty, P.W. (1983) Radioactive labeling of antibody: A simple and efficient method. Science 220:613–615.
52. Lundy, J., Mornex, F., Keenan, A.M., Greiner, J.W., and Colcher, D. (1986) Radioimmunodetection of human colon carcinoma xenografts in visceral organs of congenitally athymic mice. Cancer 57:503–509.
53. Scheinberg, D.A., Strand, M., and Gansow, O.A. (1982) Tumor imaging with radioactive metal chelators conjugated to monoclonal antibodies. Science 215:1511–1513.
54. Scheinberg, D.A., and Strand, M. (1983) Kinetic and catabolic considerations of monoclonal antibody targeting in erythroleukemic mice. Cancer Res. 43:265–272.
55. Gallagher, B.M., Sands, H., Neacy, W., Jones, P.L., and Shah, S.A. (1984) Monoclonal antibody localization and imaging of human mammary carcinoma grown at various sites in the nude mouse. J. Nucl. Med. 25:112.
56. Weinstein, J.N., Steller, M.A., Keenan, A.M., Covell, D.G., Key, M.E., Sieber, S.M., Oldham, R.K., Hwang, K.M., and Parker, R.J. (1983) Monoclonal antibodies in the lymphatics: Selective delivery to lymph node metastases of a solid tumor. Science 222:423–426.
57. Sands, H., Shah, S.A., Jones, P.L., Neacy, W.P., and Gallagher, B.M. (1985) Non-immunological factors affecting the localization of monoclonal antibodies in xenografts of human breast and colon tumors. In: Ceriani, R.L. (ed.), *Monoclonal Antibodies and Breast Cancer*. Boston: Martinus Nijhoff, pp. 303–314.
58. Goldenberg, D.M., Preston, D.F., Primus, F.J., and Hansen, H.J. (1974) Photoscan localization of GW-39 tumors in hamsters using radiolabeled anticarcinoembryonic antigen

immunoglobulin G. Cancer Res. 34:1–9.
59. Khazaeli, M.B., Brown, L.E., Kabza, G.A., Sargent, E.W., and Beierwalters, W.H. (1984) Selection of monoclonal antibody to hCG which localizes in human choriocarcinoma growing in the Syrian hamster cheek pouch. Hybridoma 3:41–47.
60. Giavazzi, R., Jessup, J.M., Campbell, D.E., Walker, S.M., and Fidler, I.J. (1986) Experimental nude mouse model of human colorectal cancer liver metastases. J. Natl. Cancer Inst. 77:1303–1308.
61. Saini, S., Stark, D.D., Wittenberg, J., Vici, L.-G., Brown, A.S., and Ferrucci, J.T. (1987) A rat model of liver cancer for imaging research. Invest. Radiol. 22:149–152.
62. Bullard, D.E., Adams, C.J., Coleman, R.E., and Bigner, D.D. (1986) In vivo imaging of intracranial human glioma xenografts comparing specific with nonspecific radiolabeled monoclonal antibodies. J. Neurosurg. 64:257–262.
63. Bullard, D.E., Wikstrand, C.J., Humphrey, P.A., Lee, Y.S., Coleman, R.E., Zalutsky, M., and Bigner, D.D. (1986) Specific imaging of human brain tumor xenografts utilizing radiolabeled monoclonal antibodies. Nucl. Med. 25:210–215.
64. Blasberg, R.G., Nakagawa, H., Bourdon, M.A., Groothuis, D.R., Patlak, C.S., and Bigner, D.D. (1987) Regional localization of a glioma-associated antigen defined by monoclonal antibody 81C6 in vivo: Kinetics and implications for diagnosis and therapy. Cancer Res. 47:4432–4443.
65. Groothuis, D.R., Fisher, J.M., Lapin, G., Bigner, D.D., and Vick, N.A. (1982) Permeability of different brain tumor models to horseradish peroxidase. J. Neuropathol. Exp. Neurol. 41:164–185.
66. Ripamonti, M., Canevari, S., Menard, S., Mezzanzanica, D., Miotti, S., Orlandi, R., and Rilke, F. (1987) Human carcinoma cell lines xenografted in athymic mice: Biological and antigenic characteristics of an intraabdominal model. Cancer Immunol. Immunother. 24:13–18.
67. Ward, B.G., and Wallace, K. (1987) Localization of the monoclonal antibody $HMFG_2$ after intravenous and intraperitoneal injection into nude mice bearing subcutaneous and intraperitoneal human ovarian cancer xenografts. Cancer Res. 47:4714–4718.
68. Reale, F.R., Griffin, T.W., Compton, J.M., Graham, S., Townes, P.L., and Bogden, A. (1987) Characterization of a human malignant mesothelioma cell line (H-MESO-1): A biphasic solid and ascitic tumor model. Cancer Res. 47:3199–3205.
69. Griffin, T.W., Richardson, C., LePage, D., Bogden, A., and Raso, V. (1987) Antitumor activity of intraperitoneal immunotoxins in a nude mouse model of human malignant mesothelioma. Cancer Res. 47:4266–4270.
70. Colcher, D., Estaban, J., Carrasquillo, J.A., Sugarbaker, P., Renolds, J.C., and Bryant, G. (1987) Complementation of intracavity and intravenous administration of a monoclonal antibody (B72.3) in patients with carcinoma. Cancer Res. 47:4218–4224.
71. Ward, B.G., Mather, S.J., Hawkins, L.R., Crowther, M.E., Stepherd, J.H., Granowska, M., Britton, K.E., and Slevin, M.L. (1987) Localization of radioiodine conjugated to the monoclonal antibody $HMFG_2$ in human ovarian carcinoma: Assessment of intravenous and intraperitoneal routes of administration. Cancer Res. 47:4719–4723.
72. Rowlinson, G., Snook, D., Busza, A., and Epenetos, A.A. (1986) Antibody guided localization of intraperitoneal tumors following I.P. or I.V. antibody administration. Br. J. Cancer 54:553.
73. Jain, R.K. (1985) Transport of macromolecules in tumor microcirculation. Biotech. Progess. 1:81–94.
74. Gerlowski, L.E., and Jain, R.K. (1986) Microvascular permeability of normal and neoplastic tissues. Microvasculature Res. 31:288–305.
75. Shah, S.A., Pollock, R.R., Brown, B.A., Gallagher, B.M., Scharff, M.D., and Sands, H. (1986) Pharmacokinetics and imaging using mutant monoclonal anti-ARS antibodies. Proc. Am. Assoc. Cancer Res. 27:335.
76. Shah, S.A., and Sands, H. (1988) Influence of antibody catabolism and shed antigen on uptake of B72.3 and B6.2 monoclonal antibodies by human tumor xenografts in athymic

mice. Proc. Am. Assoc. Cancer Res. 29:823.
77. Marks, M.A., and Adelstein, S.J. (1986) Radiation doses from radionuclides administered for therapy. Clin. Oncol. 5:271–286.
78. Sharkey, R.M., Pykett, M.J., Siegel, J.A., Alger, E.A., Primus, F.J., and Goldenberg, D.M. (1987) Radioimmunotherapy of GW-39 human colonic tumor xenograft with ^{131}I-labeled murine monoclonal antibody to carcinoembryonic antigen. Cancer Res. 47:5672–5677.
79. Wessels, B.W., Bacha, P., and Quadri, S.M. (1984) Microdosimetry TLD measurements for tumor associated antibody therapy. J. Nucl. Med. 25:39.
80. DeNardo, G.L., Raventos, A., Hines, H.H., Scheibe, P.O., Macey, D.J., Hays, M.T., and Denardo, S.J. (1985) Requirements for a treatment planning system for radioimmunotherapy. Int. J. Radiat. Oncol. Biol. Phys. 11:335–348.
81. Greiner, J.W., Horan Hand, P., Noguchi, P., Fisher, P.B., Pestka, S., and Schlom, J. (1984) Enhanced expression of surface tumor-associated antigens on human breast and colon tumor cells after recombinant human leukocyte α-interferon treatment. Cancer Res. 44:3208–3214.
82. Rowlinson, G., Balkwill, F., Snook, D., Hooker, G., and Epenetos, A.A. (1986) Enhancement of gamma-interferon of in vivo tumor radiolocalization by a monoclonal antibody against HLA-DR antigen. Cancer Res. 46:6413–6417.
83. Badger, C.C., Krohn, K.A., Shulman, H., Flournoy, N. and Bernstein, I.D. (1986) Experimental radioimmunotherapy of murine lymphoma with ^{131}I-labeled anti-T-cell antibodies. Cancer Res. 46:6223–6228.
84. Badger, C.C., Krohn, K.A., Peterson, A.V., Shulman, H., and Bernstein, I.D. (1985) Experimental radiotherapy of murine lymphoma with ^{131}I-labeled anti-Thy 1.1 monoclonal antibody. Cancer Res. 45:1536–1544.
85. Zalcberg, J.R., Thompson, C.H., Lichtenstein, M., and McKenzie, F.C. (1984) Tumor immunotherapy in the mouse with the use of ^{131}I-labeled monoclonal antibodies. J. Natl. Cancer Inst. 72:697–704.
86. Goldenberg, D.M., and Ammersdorfer, E. (1970) Synergistic effects of x-rays and drugs on a human tumor xenograft, GW-39. Eur. J. Cancer 6:73–80.
87. Goldenberg, D.M., Gaffar, S.A., Bennett, S.J., and Beach, J.L. (1981) Experimental radioimmunotherapy of a xenografted human colonic tumor (GW-39) producing carcinoembryonic antigen. Cancer Res. 41:4354–4360.
88. Neacy, W.P., Wessels, B.W., Bradley, E., Kovandi, S., Justice, T., Danskin, S., and Sands, H. (1986) Comparison of radioimmunotherapy (RIT) and 4MV external beam radiotherapy of human tumor xenografts in athymic mice. J. Nucl. Med. 27:902–903.
89. Mornex, F. (1987) Radioimmunotherapy of colon carcinoma: Use of ^{131}I-B72.3 monoclonal antibody in athymic mice bearing human colon carcinoma xenografts In: *International Conference on Covalently Modified Antigens and Antibodies in Diagnosis and Therapy*. June 3–5. Abstracts. Lyon, France, p. 46.
90. Lee, Y.S., Bullard, D.E., Friedman, H.S., Wikstrand, C.J., Coleman, R.E., Zalutsky, M., Muhlbaier, L.H., and Bigner, D.D. (1987) Experimental radioimmunotherapy of subcutaneous and intracranial human glioma xenografts in rodents with ^{131}I-monoclonal antibody 81C6. Proc. Am. Assoc. Cancer Res. 28:392.
91. Jones, D.H., Goldman, A., Gordon,, I., Pritchard, J., Gregory, B.J., and Kemshead, J.T. (1985) Therapeutic application of a radiolabeled monoclonal antibody in nude mice xenografted with human neuroblastoma: Tumoricidal effects and distribution studies. Int. J. Cancer. 35:715–720.
92. Vessella, R.L., Alvarez, V., Chiou, R.-K., Rodwell, J., Elson, M., Palme, D., Shafter, R., and Lange, P. (1987) Radioimmunoscintigraphy and radioimmunotherapy of renal cell carcinoma xenografts. NCI Monogr. 3:159–167.
93. Klapdor, R., Lander, S., Bahlo, M., and Montz, R. (1986) Radioimmunotherapy of xenografts of human pancreatic carcinomas — intravenous and intratumoral application of ^{131}I-labeled monoclonal antibodies. Nucl. Med. 25:235–238.

94. Anderson-Berg, W.T., Squire, R.A., and Strand, M. (1987) Specific radioimmunotherapy using 90Y-labeled monoclonal antibody in erythroleukemic mice. Cancer Res. 47:1905–1912.
95. Wahl, R.L., Liebert, M., Fisher, S., and Boland, R. (1987) Enhanced radioimmunotherapy of intraperitoneal human colon cancer xenografts by intraperitoneal monoclonal antibody delivery. Proc. Am. Assoc. Cancer Res. 28:438.
96. Wahl, R.L., Liebert, M., Fisher, S., Sherman, P., Jackson, G., Laino, L., and Wissing, J. (1987) Radioimmunotherapy of human ovarian carcinoma xenografts: Preliminary evaluation. Proc. Am. Assoc. Cancer Res. 28:384.
97. Neuwelt, E.A., Frenkel, E.P., D'Agostino, A.N., Carney, D.N., Minna, J.D., Barnett, P.A., and McCormick, C.I. (1985) Growth of human lung tumor in the brain of the nude rat as a model to evaluate antitumor agent delivery across the blood-brain barrier. Cancer Res. 45:2827–2833.
98. Wahl, R.L., Kimmel, K.A., Beierwalters, W.H., and Carey, T.E. (1987) Radioimmunodiagnosis of human-derived squamous cell carcinoma. Hybridoma 6:111–117.
99. Lee, Y., Bullard, D.E., Wikstrand, C.J., Zalutsky, M.R., Muhlbaier, L.H., and Bigner, D.D. (1987) Comparison of monoclonal antibody delivery to intracranial glioma xenografts by intravenous and intracarotid administration. Cancer Res. 47:1941–1946.
100. Engelstad, B.L., Ramos, E.C., Stoudemire, J., O'Connell, J.W., Villanueva, J., Faulkner, D.E., Hattner, R.S., Spitler, L.E., and Scannon, P. (1986) Improved immune-specificity in monoclonal radioimmunoimaging using dual radionuclide color functional maps. Invest. Radiol. 21:917–921.
101. Fischer, M., Hoffman, V.J., Kohnlein, W., and Skutta, D. (1986) Radioimmunoscintigraphy with antithryoglobulin monoclonal antibodies. Nucl. Med. 25:232–234.
102. Philben, V.J., Jakowatz, J.G., Beatty, B.G., Vlahos, W.G., Paxton, R.J., Williams, L.E., Shively, J.E., and Beatty, J.D. (1986) The effect of tumor CEA content and tumor size on tissue uptake of indium 111-labeled anti-CEA monoclonal antibody. Cancer 57:571–576.
103. Duewell, S., Horst, W., and Westera, G. (1986) Uptake of a monoclonal antibody against CEA (Tumak 431/31) in a human colon tumor (Co-112) xenografted in the nude mouse: Dependence on tumor size and injected dose. Cancer Immunol. Immunother. 23:101–106.
104. Mann, B.D., Cohen, M.B., Saxton, R.E., Morton, D.L., Benedict, W.F., Korn, E.L., Spolter, L., Graham, L.S., Chang, C.C., and Burk, M.W. (1984) Imaging of human tumor xenografts in nude mice with radiolabeled monoclonal antibodies. Cancer 54:1318–1327.
105. Jakowatz, J.G., Beatty, B.G., Vlahos, W.G., Porudominsky, D., Philben, V.J., Williams, L.E., Paxton, R.J., Shively, J.E., and Beatty, D.J. (1985) High-specific-activity ^{111}In-labeled anticarcinoembryonic antigen monoclonal antibody: Biodistribution and imaging in nude mice bearing human colon cancer xenografts. Cancer Res. 45:5700–5706.
106. Keenan, A.M., Colcher, D., Larson, S.M., Schlom, J. (1984) Radioimmunoscintigraphy of human colon cancer xenografts in mice with radioiodinated monoclonal antibody B72.3. J. Nucl. Med. 25:1197–1203.
107. Haisma, H., Goedemans, W., de Jong, M., Hilkens, J., Hilgers, J., Dullens, H., and Otter, W.D. (1984) Specific localization of In-111-labeled monoclonal antibody versus 67-GA-labeled immunoglobulin in mice bearing human breast carcinoma xenografts. Cancer Immunol. Immunother. 17:62–65.
108. Perkins, A.C., Pimm, M.V., and Birch, M.K. (1985) The preparation and characterization of ^{111}In-labeled 791T/36 monoclonal antibody for tumor immunoscintigraphy. Eur. J. Nucl. Med. 10:296–301.
109. Sakahara, J., Endo, K., Nakashima, T., Koizumi, M., Ohta, H., Torizuka, K., Furukawa, T., Ohmomo, Y., Yokoyama, A., Okada, K., Yoshida, O., and Nishi, S. (1985) Effect of DTPA conjugation on the antigen binding activity and biodistribution of monoclonal antibodies against α-fetoprotein. J. Nucl. Med. 26:750–755.
110. Khaw, B.A., Cooney, J., Edgington, T., and Strauss, H.W. (1986) Differences in experimental tumor localization of dual-labeled monoclonal antibody. J. Nucl. Med. 27:1293–1299.

111. Stuhlmiller, G.M., Sullivan, D.C., Vervaert, C.E., Croker, B.P., Harris, C.C., and Seigler, H.F. (1981) In vivo tumor localization using tumor-specific monkey xenoantibody, alloantibody, and murine monoclonal xenoantibody. Ann. Surg. 194:592–601.
112. Ghose, T., Ferrone, S., Imai, K., Norvell, S.T., Luner, S.J., Martin, R.H., and Blair, A.H. (1982) Imaging of human melanoma xenografts in nude mice with a radiolabeled monoclonal antibody. J. Natl. Cancer Inst. 69:823–826.
113. Halpern, S.E., Hagan, P.L., Garver, P.R., Koziol, J.A., Chen, A.W., Frincke, J.M., Bartholomew, R.M., David, G.S., and Adams, T.H. (1983) Stability, characterization, and kinetics of ^{111}In-labeled monoclonal antitumor antibodies in normal animals and nude mouse-human tumor models.
114. Macdonald, F., Crowson, M.C., Allum, W.H., Life, P., and Fielding, J.W.L. (1986) In vivo studies on the uptake of radiolabeled antibodies by colorectal and gastric carcinoma xenografts. Cancer Immunol. Immunother. 23:119–124.
115. Haskell, C.M., Buchegger, F., Schreyer, M., Carrel, S., and Mach, J.-P. (1983) Monoclonal antibodies to carcinoembryonic antigen: Ionic strength as a factor in the selection of antibodies for immunoscintigraphy. Cancer Res. 43:3857–3864.
116. Fand, I., Sharkey, R.M., McNally, W.P., Brill, A.B., Som, P., Yamamoto, K., Primus, F.J., and Goldenberg, D.M. (1986) Quantitative whole-body autoradiography of radiolabeled antibody distribution in a xenografted human cancer model. Cancer Res. 46:271–277.
117. Fand, I., Sharkey, R.M., Primus, F.J., Cohen, S.A., Goldenberg, D.M. (1987) Relationship of radioantibody localization and cell viability in a xenografted human cancer model as measured by whole-body autoradiography. Cancer Res. 47:2177–2183.
118. Colcher, D., Keenan, A.M., Larson, S.M., and Schlom, J. (1984) Prolonged binding of a radiolabeled monoclonal antibody (B72.3) used for the in situ radioimmunodetection of human colon carcinoma xenografts. Cancer Res. 44:5744–5751.
119. Pimm, M.V., Armitage, N.C., Perkins, A.C., Smith, W., and Baldwin, R.W. (1985) Localization of an anti-CEA monoclonal antibody in colorectal carcinoma xenografts. Cancer Immunol. Immunother. 19:8–17.
120. Jeppsson, A., Wahren, B., Millan, J.L., and Stigbrand, T. (1984) Tumor and cellular localization by use of monoclonal and polyclonal antibodies to placental alkaline phosphatase. Br. J. Cancer, 49:123–128.
121. Jeppsson, A., Wahren, B., Millan, J.L., and Stigbrand, T. (1984) Localization of human tumor xenografts by ^{125}I-labeled monoclonal and polyclonal antibodies to placental alkaline phosphatase. In: *Human Alkaline Phosphatases*. New York: Alan R. Liss, pp. 257–264.
122. Khaw, B.A., Strauss, H.W., Cahill, S.L., Soule, H.R., Edgington, T., and Cooney, J. (1984) Sequential imaging of indium-111-labeled monoclonal antibody in human mammary tumors hosted in nude mice. J. Nucl. Med. 25:592–603.
123. Zalutsky, M.R., Colcher, D., Kaplan, W.D., and Kufe, D.W. (1985) Radioiodinated B6.2 monoclonal antibody: Further characterization of a potential radiopharmaceutical for the identification of breast tumors. Int. J. Nucl. Med. Biol. 12:227–233.
124. Buchegger, F., Haskell, C.M., Schreyer, M., Scazziga, B.R., Randin, S., Carrel, S., and Mach, J.-P. (1983) Radiolabeled fragments of monoclonal antibodies against carcinoembryonic antigen for localization of human colon carcinoma grafted into nude mice. J. Exp. Med. 158:413–427.
125. Buchegger, F., Halpern, S.E., Sutherland, R.M., Schreyer, M., and Mach, J.-P. (1986) In vitro and in vivo tumor models for studies of distribution of radiolabeled monoclonal antibodies and fragments. Nucl. Med. 25:207–209.
126. Hadjian, R.A., Tolman, G.L., Drozynski, C.A., Malone, M.E., Shah, S.A., and Sands, H. (1986) In vivo tumor localization, biodistribution, and pharmacokinetic analysis of Tc-99m-metallothionein conjugated mouse monoclonal antibody B72.3. J. Nucl. Med. 27:1015.
127. Takahashi, H., Herlyn, D., Atkinson, B., Powe, J., Rodeck, V., Alavi, A., and Bruce, D.A. (1987) Radioimmunodetection of human glioma xenografts by monoclonal antibody

to epidermal growth factor receptor. Cancer Res. 47:3847–3850.
128. Munz, D.L., Alavi, A., Koprowski, H., and Herlyn, D. (1986) Enhancement of tumor contrast on radioimmunoscans by using mixtures of monoclonal antibody $F(ab')_2$ fragments. Nucl. Med. 25:216–219.
129. Hwang, K.M., Fodstad, O., Oldham, R.K., and Morgan, A.C. (1985) Radiolocalization of xenografted human maligant melanoma by a monoclonal antibody (9.2.27) to a melanoma-associated antigen in nude mice. Cancer Res. 45:4150–4155.
130. Herlyn, D., Powe, J., Alavi, A., Mattis, J.A., Herlyn, M., Ernst, C., and Vaum, R. (1983) Radioimmunodetection of human tumor xenografts by monoclonal antibodies. Cancer Res. 43:2731–2735.
131. Powe, J., Pak, K.Y., Paik, C.H., Steplewski, Z., Ebbert, M.A., Herlyn, D., et al. (1984) Labeling monoclonal antibodies and $F(ab')_2$ fragments with (^{111}In) indium using cyclic DTPA anhydride and their in vivo behavior in mice bearing human tumor xenografts. Cancer Drug Deliv. 1:125–135.
132. Buchegger, F., Mach, J.-P., Leonnard, P., and Carrel, S. (1986) Selective tumor localization of radiolabeled anti-human melanoma monoclonal antibody fragment demonstrated in the nude mouse model. Cancer 58:655–662.
133. Matzku, S., Schuhmacher, J., Kirchgebner, H., and Bruggen, J. (1986) Labeling of monoclonal antibodies with a ^{67}Ga-phenolic aminocarboxylic acid chelate. Part II, Comparison of immunoreactivity and biodistribution of monoclonal antibodies labeled with the ^{67}Ga-chelate or with ^{131}I. Eur. J. Nucl. Med. 12:405–412.
134. Kanellos, J., Pietersz, G.A., McKenzie, I.F., Bonnyman, J., and Baldas, J. (1986) Coupling of the ^{99m}technetium-nitrido group to monoclonal antibody and use of the complexes for the detection of tumors in mice. J. Natl. Cancer Inst. 77:431–439.
135. Baldwin, R.W., and Pimm, M.V. (1983) Antitumor monoclonal antibodies for radioimmunodetection of tumors and drug targeting. Cancer Metastasis Rev. 2:89–106.
136. Pimm, M.V., and Baldwin, R.W. (1986) Accelerated catabolism of an anti-tumor monoclonal antibody in nude mice bearing human tumor xenografts. IRCS Med. Sci. 14:790–791.
137. Rodwell, J.D., Alvarez, V.L., Lee, C., Lopes, A.D., Goers, J.W., King, H.D., Powsner, H.J., and McKearn, T.J. (1986) Site-specific covalent modification of monoclonal antibodies: In vitro and in vivo evaluations. Proc. Natl. Acad. Sci. USA 83:2632–2636.
138. Bubenik, J., Kieler, J., Perlmann, P., Paulie, S., Koho, H., Christensen, B., et al. (1985) Monoclonal antibodies against human urinary bladder carcinoma: Selectivity and utilization for gamma scintigraphy. Eur. J. Cancer Clin. Oncol. 21:701–710.
139. Ballou, B., Jaffe, R., Taylor, R.J., Solter, D., and Hakala, T.R. (1984) Tumor radioimmunolocation: Differential antibody retention by antigenic normal tissue and tumor. J. Immunol. 132:2111–2116.
140. Zimmer, A.M., Rosen, S.T., Spies, S.M., Polovina, M.R., Minna, J.D., Spies, W.C., and Silverstein, E.A. (1985) Radioimmunoimaging of human small cell lung carcinoma with I-131 tumor specific monoclonal antibody. Hybridoma 4:1–11.
141. Pimm, M.V., and Baldwin, R.W. (1985) Distribution of IgM monoclonal antibodies in mice with human tumor xenografts: Lack of tumor localization. Eur. J. Cancer Clin. Oncol. 21:765–768.
142. Gomibuchi, M., Saxton, R.E., Lake, R.R., Katano, M., and Irie, R.F. (1986) Radioimmunodetection of human melanoma tumor xenografts with human monoclonal antibodies. Nucl. Med. Biol. 13:13–19.

5. Physiology of monoclonal antibody accretion by tumors

Howard Sands and Peter L. Jones

The method for the production of monoclonal antibodies that was introduced by Kohler and Milstein in 1976 gave the promise of generating reagents with exquisite specificity and great utility for the diagnosis and treatment of cancer and other diseases [1]. Over the past 11 years numerous monoclonal antibodies have been generated using human tumor cell lines [2,3] and tumor homogenates [3,4] as the source of immunogen. Many of these antibodies when 'tagged' with radionuclides have produced radioimmunodiagnostic and radioimmunotherapeutic agents for use in either animal experiments or in the clinic [5–19].

The results from clinical evaluations have emphasized that antibodies are subjected to the same physiologic and metabolic processes as any drug and hormone. The net result of these processes may markedly reduce the accretion of these agents. Clinical results have indeed not lived up to the earlier expectations. In general, uptake of the radionuclide into the tumor of patients has been found to be in the range of 0.001–0.01% of the injected dose (%ID) per gram of tumor [6,13–14,17,19]. This is considerably lower than one would expect based on animal studies in which considerably more antibody was found to accumulate in tumors.

One factor that could account for the low accretion of radiolabeled monoclonal antibodies in patients may be dilution. A man weighing 70 kg is 2800 times larger (by weight) than a mouse weighing 0.025 kg. One would expect, on the basis of dilution alone, that human tumor accretion of radiolabeled antibody would be only 1/2800 of the amount of antibody that is taken up by a similar tumor growing as a xenograft in an athymic mouse. A typical accretion value for a monoclonal antibody by a human xenograft is 20%ID per gram of tumor [15,16]. This extrapolates to 0.007%ID per gram of tumor,a value within the range reported in clinical trials.

Other mechanisms based on physiologic and metabolic processes may be more subtle than dilution. The route of antibody administration, the amount of nonspecific organ uptake, the rate at which the radionuclide is removed from the antibody, the barriers that the antibody has to overcome, the degree of blood flow, and the location of capillaries within the tumor all affect the total amount of radiolabeled antibody that can be delivered to and bind in a

Goldenberg, D.M., (ed.), Cancer Imaging with Radiolabeled Antibodies.

tumor. This review will discuss the basic physiologic mechanisms that can account for the preclinical and clinical results that have been reported using radiolabeled monoclonal antibodies. In these cases, it must be remembered that the accumulation and pharmacokinetics of radiolabeled monoclonal antibodies are determined by following the distribution of the attached radionuclide. It is the distribution of the radionuclide that is being traced and not necessarily the antibody. The various approaches being taken to overcome these physiologic barriers in order to improve the diagnostic and therapeutic utility of radiolabeled monoclonal antibodies will also be reviewed. It is not the authors intention to cite all relevant references on a given topic and, therefore, for the sake of brevity and timeliness, only a limited number of recent references are given as examples.

Physiology of antibody delivery

Site of injection

Radiolabeled monoclonal antibodies and their proteolytic fragments are macromolecules that range from 40,000 to 150,000 daltons. The route these proteins travel, the barriers that need to be crossed, and the organs of nonspecific antibody uptake and radionuclide accretion, as well as the degree of excretion, will differ with the site of antibody injection. The product of these factors will be the amount of antibody available for delivery to the tumor, as well as the amount of antibody specifically taken up by the tumor.

Intravenous administration. To date most preclinical and clinical trials for the evaluation of radiolabeled antibodies as agents for the detection and therapy of cancer have been performed using the IV route of administration. When administered by this route, the antibody has to successfully cross several barriers and avoid nonspecific uptake by several organ systems before it can bind specifically at the site of the tumor. Injection into the blood stream results in the rapid dilution of the antibody in the fluid of this compartment. In most cases, the circulating antibody is passed through the organs of metabolism (liver and spleen) and of excretion (kidneys) before it has a chance of reaching its target. To reach its cellular targets it must pass out of the vascular compartment into the tumor. It must traverse the vascular endothelium, a process whose rate is inversely proportional to the molecular weight of the agent. Thus, one would expect that an $F(ab')_2$ would permeate into a tumor at a faster rate then would an intact IgG. An additional factor of importance is the permeability of the vasculature. While the vasculature of tumors appears to be more permeable to macromolecules then does that of normal tissues [20–26], it remains a major barrier to be crossed. These factors will be discussed in detail later in this chapter.

Preclinical data. Most preclinical modeling with radiolabeled antibodies has utilized xenografts of human tumors growing in either the athymic or immunodeprived mouse [27–32]. Other studies have used homografts such as murine lymphomas growing in AKR mice [33]. While the athymic mouse-human xenograft system is very convenient for the study of anti-human tumor antibodies, one must remember that it differs from the clinical situation in some important aspects. These lead to the four major drawbacks of the xenograft model: 1) The host is severely immunocompromised; 2) the human xenograft is being sustained via a murine vasculature; 3) a murine antibody is being evaluated in a mouse; and 4) doses (both on a microgram and microcurie basis) of antibody used are larger, in proportion to body weight, then those used in the clinic.

The results from pharmacokinetic studies of several different radiolabeled murine monoclonal antibodies were quite similar [15,32,34]. Radiolabeled intact IgGs have a relatively long half-life in the blood compared with either their $F(ab')_2$ or Fab fragments [15,35,36]. Blood values 24 hours after injection were usually 15–20%ID/g for the intact antibody, 2–4%ID/g for the $F(ab')_2$, and less than 1%ID/g for the Fab [15]. Radionuclide uptake by the liver and kidney differs with the nature of the radionuclide, as well as with the antibody form to which they were attached. For all antibody forms the radioiodine (^{123}I, ^{125}I, and ^{131}I) content of the liver peaked very quickly and then decreased over 48 [15,35]. The level of radionuclide in the liver, when ^{111}In-DTPA antibody was injected, remained relatively constant. The amount of ^{111}In found in the liver 24 hours postinjection was greater than that of radioiodine after injection of radioiodinated antibody [15,35]. Kidney uptake of antibody fragments was greater than that of the intact IgG [15]. Radioiodine from antibody fragments cleared from the kidney with time. The rate of kidney clearance was similar to the clearance from the liver. In the kidney, which accumulated indium after antibody fragment injection, the ^{111}In content increased with time, reaching values of several hundred %ID/g [15]. The differences in the uptake values and clearance rates of the two radionuclides (radioiodine and ^{111}In) by the liver and kidney most likely can be explained by differences in the processing of each radionuclide. At early times antibodies labeled with either radionuclide were found in approximately equal amounts in the liver, suggesting that liver uptake was a function of the antibody and not of the radionuclide (Figure 1). With time the process(es) of dehalogenation resulted in the removal of the radioiodine from the protein. Since the liver does not accumulate free iodine, it was expelled from the liver and eventually was either taken up by the thyroid or excreted. ^{111}In was trapped in the liver by one or more unknown mechanisms [37]. An analogous explanation can be offered for the kidney values obtained after IV injection of radiolabeled antibody fragments.

One recent and promising attempt at overcoming these limitations to the DTPA chelation of ^{111}In has been to replace the DTPA with a metabolizable

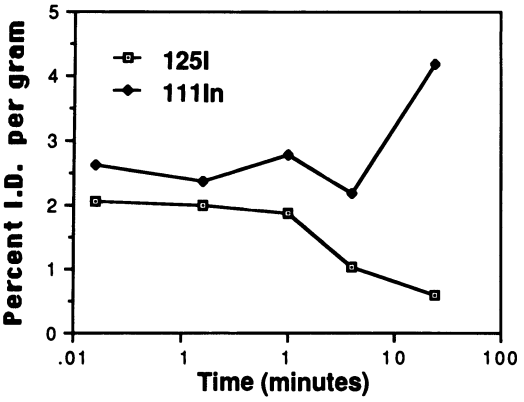

Figure 1. Liver accumulation of the radionuclide from radiolabeled murine monoclonal antibody (B6.2) by the rat liver after intravenous (IV) and interperitoneal (IP) injection.

bifunctional chelator [38]. Preliminary data suggested that the use of metabolizable chelators resulted in lower blood and liver background, shorter initial biologic half-life, and higher tumor to blood ratios. A slight decrease in tumor uptake of ^{111}In was seen. Another promising approach is to replace DTPA with a stable chelator such as benzyl DTPA [39].

Other factors that are of importance in determining the degree of tumor accretion of radiolabeled antibodies after IV injection include the amount of antigen shed into the blood and the size of the tumor. Antigen shed by the tumor into the vascular space is accessible to injected antibody. The fate of the antibody-antigen complex has not been extensively studied. In one study [40] three tumors that secrete carcinoembryonic antigen (CEA) were implanted into athymic mice, and the pharmacokinetics of either ^{125}I or ^{111}In labeled anti-CEA were studied. The higher the level of circulating CEA, the more rapid was the removal of the antibody from the vascular compartment by the liver and spleen. In the case of ^{111}In, the accumulation in the liver increased with increased amounts of circulating CEA. No liver accumulation was observed with ^{125}I-labeled anti-CEA, probably due to rapid liver dehalogenation of radioiodinated proteins. Additional studies showed that the uptake of radiolabeled antibody by the liver and spleen of normal mice could be enhanced by preincubating the anti-CEA with CEA [40]. These data suggested that the antibody-antigen complex was rapidly taken up by both of these organs.

Attempts to reduce nonspecific uptake of antibody by liver and other organs in the murine xenograft model, including the use of high doses of unlabeled nonspecific antibody, have been unsuccessful [41]. When athymic mice bearing melanoma xenografts were pretreated (IV) with large doses of nonradiolabeled, isotype-matched nonspecific antibody (up to 3.5 mg) 1 hour before the IV injection of the ^{131}I-specific antibody (0.004 mg), no significant increase in the tumor to liver, or tumor to blood, ratios was reported [41].

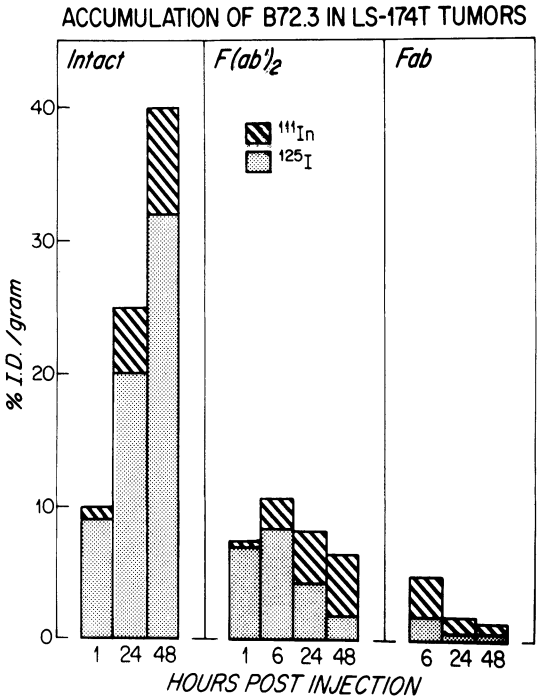

Figure 2. Accumulation of radionuclide by human xenografts (LS174T) after the injection of radiolabeled murine monoclonal antibody (B72.3). Figure taken from Brown et al. [15].

The extratumoral factors described above impact radioimmunodiagnostics and radioimmunotherapeutics in several ways. Rapid accumulation and lack of clearance in either the liver or kidney may result in the toxic accumulation of radionuclides. The nonspecific accumulation of radionuclide compromises the utility of the radiolabeled monoclonal antibody for the localization of tumors in or near the liver and kidneys. Lastly, the rapid blood clearance of the $F(ab')_2$ and Fab, while helping to reduce the background for imaging [15,30], resulted in an even greater reduction of the absolute accumulation of radionuclide by tumor, as illustrated in Figure 2 [15]. The greater accumulation of ^{111}In than ^{125}I in the liver was also seen for tumor accretion, with 30–100% more ^{111}In usually found in tumors than radioiodine [15,35]. Mechanisms of tumor retention of ^{111}In are probably similar to those in the liver, described above.

The last area to be dealt with in regard to IV injection is tumor size. Two studies have demonstrated an inverse relationship between the size of subcutaneous [42] and intrasplenic [43] xenografts in athymic mice and the uptake of certain radiolabeled antibodies. The exact reasons for these findings were not known but could have involved such factors as antigenic heterogeneity, necrotic areas of the tumor, and patterns of antibody delivery. These factors are discussed later in this chapter.

Clinical data. Most clinical studies of radiolabeled monoclonal antibodies have been directed at the determination of the utility of these agents for the detection of metastatic disease. In the vast majority of cases, either the intact antibody or its fragments were administered via an intravenous injection. In addition to radionuclide-related properties (e.g., energy and half-life) and mode of data acquisition (e.g., planar or single photon emission computerized tomography), tumor detection can be considered as the summation of two additional critical factors: 1) the absolute amount of radiolabel that accumulates in the tumor and 2) the tumor to background ratio. For radioimmunodetection to become a viable technique it must provide information that is not readily available from other diagnostic modalities and that will change patient management. Therefore, radiolabeled monoclonal antibodies need to accumulate in tumors that are small and that are not detectable by existing means. Only in a few cases have the results met these criteria [44,45].

In general, the number of known tumors or metastases detected by the IV injection of radiolabeled intact IgG has been in the range of 60–90%, regardless of the radionuclide. Several representative examples from the literature are: 1) gastrointestinal tumors using ^{131}I-791/T36 — 72% [46]; 2) melanoma using ^{131}I-anti-p97 — 88% [47]; 3) melanoma using ^{111}In-ZME-018 — 60% [48]; 4) metastatic prostatic cancer using ^{111}In-Pay-276 — 29 to 53% [49]; and 5) gastrointestinal cancers using ^{131}I anti-CEA — 54% and 66% [50]. The nature of the results were not dependent on the subclass of the antibody. IgG_1s [51] and IgG_{2a}s [50] or IgG_{2b}s [46] gave similar results. In clinical studies in which the size of the lesions was determined, the limits of detection appear to be tumors of approximately 1.0–1.5 cm [7,47,48]. This level of detection limits the widespread utility of radioimmunodetection, since lesions of this size can generally be detected by other diagnostic imaging modalities.

One major determinant of diagnostic sensitivity is the absolute amount of radionuclide accumulated by the tumor, generally reported as the percent of the injected dose per gram of tumor (%ID/g). Reported tumor accretion following IV administration have been extremely low (in the range of 0.0006–0.015%ID/g [13,17–19] for antibodies labeled with radioiodine). Since the reported accretion of ^{111}In was in the range of 0.006%ID/g [14], there did not appear to be a greater uptake of ^{111}In than ^{131}I by tumors, as was seen in the data derived from animal models. In contrast was the rapid and large accumulation of ^{111}In in the liver of patients [14], which was similar to that observed in the animal studies.

Of importance, in addition to the absolute amount of radionuclide, is the tumor to background ratio. This is determined by two factors: 1) nonspecific antibody accumulation and clearance from normal tissue, and 2) clearance of the radionuclide from the blood. A general rule of thumb suggests that these ratios must be at least between 5 and 10 to have successful imaging. Ratios of 2–20 have been reported in clinical studies by Epenetos et al. [6] and of 3–30

Table 1. Typical blood clearance data obtained after the IV injection of radiolabeled antibodies and fragments into patients

Antibody		Radionuclide	Dose	Initial		Ref
				Late	$t_{1/2}$ (hours)	
791/T36	IgG	^{131}I	1 mg	14.8	44.4	8
		^{111}In	1 mg	10.1	33.6	8
B6.2	IgG	^{131}I	0.05–1.5 mg	6.2	20	10
UJ13A	IgG	^{131}I	?	1.8	53	11
$NDOGL_2$	IgG	^{123}I	?		20.8	12
9.2.27	IgG	^{111}In	1 mg	2.1	27	5
			50 mg	9.0	60	5
			100 mg	8.9	78	5
T101	IgG		2.3–17.5 mg	0.9	20	53
			643–1707 mg	1.2	18	53
(Polyclonal human)	IgG	^{125}I			20 days	52
19-9	$F(ab')_2$	^{111}In	1 mg	2	19	9
17-1A	$F(ab')_2$	^{131}I	0.15–0.4 mg	3.5	27.6	54
48.7	Fab	^{131}I	2–10 mg		0.9–3.2	55

in studies by Esteban et al. [19] and Colcher et al. [7]. These studies followed the accumulation of radioiodinated antibodies, and the ratios were calculated from excised tissues.

The amount of radiolabeled monoclonal antibody found in the blood is also a determinant of the absolute amount of antibody to be taken up by the tumor and the level of background counts. Clearance of radionuclide from the blood is the summation of the amount of uptake (both specific and nonspecific by tumors and other organs) and the clearance from the blood by liver, spleen, and kidney. The latter elements were dependent on the class of the antibody [52], the nature of the radionuclide, and the size of the antibody or antibody fragment. Typical data from clinical trials involving the intact antibody are summarized in Table 1. Most clinical studies describe the blood clearance as being a biphasic curve, with the initial clearance having $t_{1/2}$s ranging from 2 to 15 hours. The $t_{1/2}$s of the late component of the clearance curve ranges from 20 to 78 hours. This variability did not seem dependent on the nature of the radionuclide, but may have been due to such factors as tumor burden, amount of circulating antigen, and patient-to-patient differences. It is of interest that the clearance data reported for the radioiodinated B6.2 fits well with the other values reported, despite the fact that B6.2 is bound to circulating granulocytes and showed a large amount of marrow accumulation [10]. These clearance rates are considerably faster than the clearance of human antibodies in the human reported in the classic work of Waldmann and Strober [52], in which the half-life of human polyclonal IgG was 20 *days*.

Even though the murine antibodies clear from the blood at a rapid rate, attempts have been made at improving the tumor to background ratio by

increasing the rate of blood clearance of antibodies through the use of antibody fragments. As shown in Table 1, the initial clearance rates of the smaller (approximately 100,000 daltons) radiolabeled $F(ab')_2$ fragments were approximately the same as or faster than that of the larger (150,000 daltons), intact IgG. Late clearance rates were at the lower end of the range reported for intact IgGs. In general, the clearance rate of radiolabeled $F(ab')_2$'s was more rapid than that of the intact IgG. For diagnostic purposes this would be expected to result in an increase in the tumor to background ratio if tumor uptake remains similar to that reported for the intact IgG. Limited data on the absolute amount of tumor uptake of the $F(ab')_2$ could be found but appear to be in the range of 0.005%ID/g [54], a value similar to that found when the intact IgG was used. Therefore, it is surprising that the use of radiolabeled $F(ab')_2$'s did not increase the number of known lesions detected. Several reports indicated a detection rate of approximately 60% [9,55–57]. In some studies a number of occult lesions were also detected [57]. The limits of detection were similar to that reported for the IgG, i.e, lesions had to be 1.5 cm or greater [54,55]. Assuming a spherical shape, the tumor would weigh approximately 1.7 g. Radiolabeling the $F(ab')_2$ of an anti-CEA with ^{123}I allowed the use of SPECT rather than the customary planar imaging. By using SPECT a significant improvement in the detection rate (86%) was reported by Delaloye et al. [58]. The smallest tumors visualized were reported to be 3–5 g in size. Clearance appeared to be through the kidney and urine, as would be expected of the smaller protein [9,54]. When the radiolabel used was ^{111}In, rapid uptake and persistent liver accumulation, similar to that seen with ^{111}In label IgGs, was seen [9]. Very few clinical trials used the Fab fragment of antibodies. One reason may be the marked reduction in avidity that occurs with the reduction of valance from two to one that occurs with the separation of the two Fab binding sites found on the $F(ab')_2$ and the intact IgG. Absolute accumulation data in tumors for Fabs are, however, not available. Unless the intact IgG had an extremely high affinity, this reduction in avidity would be expected to drastically lower the amount of radiolabeled antibody bound in the tumor. Using the ^{131}I-Fab of the anti-melanoma antibody 48.7, Larson et al. found that 40% of the total radioactivity cleared from the blood in the first 5 minutes. $T_{1/2}$s were reported to range from 0.9 to 3.2 hours [55]. Despite this extremely rapid clearance, the Fab of this anti-melanoma was able to detect 74% of known lesions. The use of a ^{123}I-Fab anti-CEA with SPECT imaging produced a detection rate of 94% and was able to detect tumors in the 3–5 g range. Despite the very rapid blood clearance, the tumor to blood ratio improved with the use of the Fab fragment [58].

To summarize, the clinical findings are suggestive of a role for radiolabeled monoclonal antibodies in the diagnosis of cancer. These studies clearly point out the limitations of this technique, i.e., the low detection rate of known lesions and 1.0–1.5 cm lesions being the smallest that can be visualized. These limitations are due to both a low absolute uptake of antibody by the tumor and low tumor to background ratios.

Intracavitary administration. The limitations of intravenously administered monoclonal antibodies described above have led to attempts to enhance the absolute amount of antibody that localizes in the tumor and to reduce the background by means of local administration. By limiting the dilution of the radiolabeled antibody and increasing the time the antibody is in contact with the tumor, extratumorial factors that might limit antibody delivery to tumor binding sites may be reduced. Injection of antibody into a discrete anatomic compartment such as the cranial, peritoneal, pericardial, or pleural cavities may result in a greater antibody uptake by the tumor. Since both the rate of radiolabeled antibody uptake and the amount of antibody in the vascular compartment is reduced, one would expect lower uptake by normal organs. Intracavitary administration, in addition, may reduce uptake in organs that catabolize immunoglobulin, such as the liver and kidney.

Preclinical data. In several preclinical experiments, delivery of antibody via intracavitary administration has been studied [57–62]. Few studies, however, have fully evaluated factors such as blood clearance and tumor uptake to determine whether intracavitary administration would be more appropriate than intravenous administration. Of the intracavitary routes of administration, the most fully evaluated has been the IP route. In a study designed to measure the kinetics of blood clearance of intact and $F(ab')_2$ in non-tumor-bearing athymic mice, the $t_{1/2}$s for ^{90}Y-labeled intact antibody and $F(ab')_2$ were 39 and 14 hours, respectively [5,63]. These values are not strikingly different from those seen for antibodies injected by the IV route (see Table 1). In athymic mice bearing xenografts of a colon carcinoma growing in the peritoneal cavity, the tumor to background ratio was 50 times that observed in mice injected with the same antibody via the IV route [59]. The absolute values obtained in this study were not reported. The IP/IV ratio fell to approximately 1 during the next 23 hours, thus indicating a more rapid tumor uptake and clearance after IP administration. The uptake of ^{131}I-labeled antibody into colon carcinoma xenografts grown in a subcutaneous site in athymic mice was also shown to be similar for both IV and IP routes at 24 hours after injection [W.P. Neacy, personal communication]. Ward et al. have measured the uptake of radiolabeled andtibody that localizes in tumors in both subcutaneous and intraperitoneal sites after antibody injection by either the IV or IP routes. [62]. Blood values were higher following IV. injection up to 96 hours after administration; thereafter clearance rates from the blood were similar for both routes (Figure 3). Antibody uptake in tumors at both sites was less after injection by the IP route (Figure 3). The authors concluded that IP-injected antibody is taken up by tumor following absorption into the vascular compartment. A further study has reported the uptake of radiolabeled monoclonal antibody in intracranial human glioma xenografts grown in immunosuppressed rats [60]. The tumor uptake of antibody during the 5 days following intracarotid injection was only 20% higher than that seen in rats where the antibody was injected intravenously.

It remains to be demonstrated that localized administration of radiolabeled

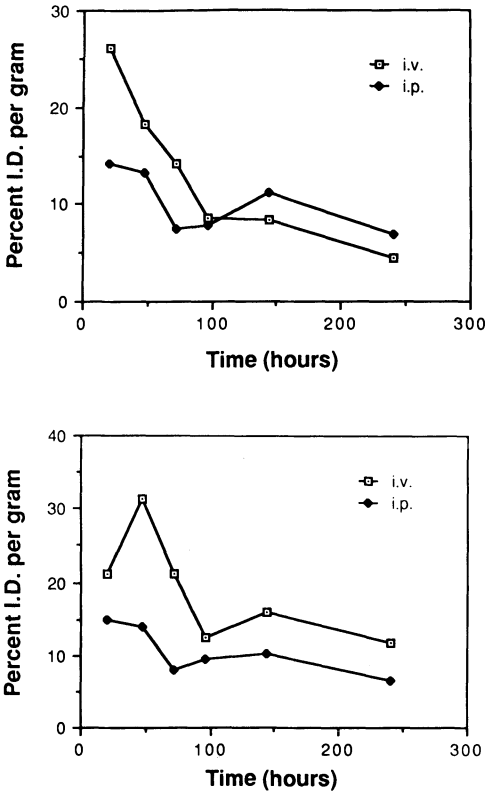

Figure 3. *A*: Blood clearance of radioiodinated murine monoclonal antibody after either IV or IP injection into athymic mice. Data taken from Ward and Wallace [62]. *B*: Tumor accretion of radioiodinated murine monoclonal antibody after either IV or IP injection into athymic mice. Data taken from Ward and Wallace [62].

antibody, in all cases, confers any advantage over IV administration. In specific instances, localized adminstration may confer an advantage. For example, in a model of human intraperitoneal carcinomatosis in athymic mice, IP delivery of ^{131}I-radiolabeled antibody appeared to increase survival times to a greater extent than did antibody administered by the IV route [61]. The mean survival times were 67.3 ± 7.9 days following IP administration and 43.8 ± 3.9 days for a group of mice injected IV with the same dose of radiolabeled antibody. Thus IP radioimmunotherapy may be a viable clinical approach to the treatment of intraperitoneal neoplasia.

Clinical data. Clinical studies that compared IP and IV routes of labeled antibody administration failed to conclusively demonstrate that IP administration resulted in improved antibody localization. Colcher et al. have studied two types of colorectal metastases in patients [64]. Metastatic lesions that were implanted via direct migration in the peritonium accumulated more

radiolabeled antibody after an IP injection than after an IV injection. In contrast, lesions that seeded in the peritonium via the vasculature (as well as those found in lymph nodes) accumulated more antibody after IV than after IP administration. The results from this study suggest that only when peritoneal lesions are derived via intraperitoneal seeding would IP administration be advantageous for use in either the detection or treatment of peritoneal metastases. Ward et al. measured antibody localization following either IP or IV injection in patients with peritoneal deposits from ovarian cancer [65]. They have reported that the localization of ^{131}I in solid tumors of patients with ovarian carcinoma tumors was *less* when the ^{131}I-labeled monoclonal antibody, HMFG2, was administered by the IP route than that following administration of the same antibody IV. The %ID per gram of ^{131}I-HMFG2 18 hours after IP administration was 0.0005 ± 0.0001 as compared with 0.0029 ± 0.0005 after IV administration. Tumor accretion after IV injection was also greater than IP injection at 4 and 36 hours. Based on these data, the authors predicted that the IP administration of this radioiodinated antibody would be ineffective in treating solid tumors in patients with ovarian carcinoma. Other workers, however, have reported some success in the treatment of metastases of ovarian [66,67] and colorectal [64] carcinoma by administration of ^{131}I-labeled monoclonal antibodies by the IP route. For example, patients with small volume, stage III ovarian cancer injected IP with doses in excess of 140 mCi of ^{131}I-monoclonal antibody responded favorably with minimal toxicity [67].

Intracavitary administration of radiolabeled monoclonal antibodies has also had some success as an effective treatment for the relief of fluid accumulation, a frequent problem accompanying various forms of cancer. In an 11-patient study, ^{131}I-antibodies raised against delipidated milk fat globule were administered either intrapleurally or intrapericardially, depending on the disease [68]. Seventy-seven percent of the pleural effusions responded completely, as defined by the lack of fluid reaccumulation for 3 and 18 months, respectively.

The data for the use of intracavitary administration of radiolabeled monoclonal antibodies indicates that this method may have the potential for increasing the specific tumor uptake under certain circumstances. Though promising, intracavitary administration will probably not be a means to increase tumor accretion in most clinical situations.

Immunolymphoscintigraphy

Assessment of the metastatic involvement of the lymph nodes is important in the staging of many malignancies. Radioimmunoolymphoscinigraphy (i.e., the subcutaneous injection of a radiolabeled antibody and its delivery and accumulation via the lymphatic system) has considerable appeal, since traditional techniques for the detection of nodal involvement in malignant disease are both relatively insensitive and nonspecific. A sensitive, nonsurgi-

cal means of assessing lymph node status could be useful in the staging of many malignancies, including lymphoma, Hodgkin's disease, melanoma, and carcinoma of the breast, colon, lung, testis, prostate, and cervix. The advantages of lymphatic delivery of radiolabeled monoclonal are threefold. Firstly, antibody uptake by tumors residing in the lymph nodes is via the lymphatics and may result in a greater uptake then after IV administration. This may allow the detection of smaller metastases using a lower dose of radioactivity. Secondly, the lymphatic route of antibody administration may be preferable to the IV route, since antibody localization is potentially more rapid. Finally, the signal-to-noise ratio may be higher than that following systemic administration, partly because less radiolabeled monoclonal antibody would be available to bind to circulating antigen and also because more antibody would be delivered to the tumor. The major limitation of immunolymphoscintigraphy is that localization is limited to regional draining nodes. Though less of both antibody and radionuclide are injected, and therefore the risk of systemic toxicity is not as great as that following IV administration, the possibility of local toxicity at the injection site is a concern. This may be especially important when therapeutic isotopes are administered. Finally, subcutaneous injection of any protein heightens the possibility of an immunogenic response. Since the subcutaneous route is the typical route of administration for lymphoscintigraphy, the likelihood of human anti-murine antibodies being produced is greater than that following IV administration. It is possible that such a response could pose a risk of hypersensitivity or reduced efficacy on subsequent administration.

Preclinical data. Early studies have measured the accumulation of radiolabeled monoclonal antibody directed against murine Class I major histocompatability antigens in the regional nodes in non-tumor-bearing Kk-positive mice [69,70]. Two hours after injection of the antibody into the footpads, the ratio of uptake into popliteal nodes in non-tumor-bearing Kk-positive versus Kk-negative mice was 50:1 [69]. At lower doses of anti-K antibody, the binding of the antibody approached saturation only in the nodes nearest to the injection site [70]. The fact that distant nodes did not accumulate radioactivity suggested that the radiolabeled antibody was removed from the lymph by binding at the lymph nodes proximal to the injection site, and thus less antibody was available for binding to distant nodes. This phenomenon was also seen in normal dogs injected with ^{131}I-monoclonal antibody through the mucosa of the lungs using a fiberoptic bronchoscope [71]. The uptake of antibody, which was directed against determinants found on normal lymphocytes, was as much as 100-fold greater in some of the regional draining nodes as compared with nondraining nodes at sites more distant from the injection site. Weinstein et al. imaged guinea pigs bearing nodal metastases from a L10 hepatocarcinoma following SC injection with ^{125}I-labeled antibody and detected foci estimated to be between 2 and 7 mg [72]. The contralateral nodes, which had no tumor foci, did not image.

Lymphoscintigraphy would be expected to localize antibody in nodes of a lymphoid chain only when the flow of lymph has not been restricted due to the presence of a large tumor mass. This was shown to be the case using a murine model of 'experimental metastasis,' where athymic mice bore LS174T colon adenocarcinoma xenografts in their axillary lymph nodes. ^{131}I-B72.3 failed to specifically localize in the involved tumors 2 hours after subcutaneous injections into the animals' footpads. Twenty-four hours after subcutaneous injection, specific accretion of the radiolabeled antibody by the tumor was seen. At this relatively late time post-subcutaneous injection, it was presumed that the antibody was delivered to the tumor via the vascular circulation rather than by the lymphatics [73]. Consequently, it appears that the success of lymphoscintigraphy may be dependent on two competing criteria. The amount of tumor in the lymph node must be sufficient to bind enough antibody for detection or therapy.On the other hand, the amount of tumor in the node must not be so great as to block lymphatic drainage through the node.

Clinical data. More than half of the known metastatic lesions of human melanoma are located in skin and superficial lymph nodes. Since melanoma lesions are often accessible for analysis following antibody administration, a number of studies on melanoma patients have been performed to test the diagnostic value of immunoscintigraphy. Several clinical studies have been performed using intact anti-melanoma antibodies [74,75] or their fragments [74,76,78]. The results have been disappointing. In several reported cases neither intact antibody nor fragments have been shown to adequately differentiate between normal nodes and nodes bearing metastatic foci. The reason for the lack of specificity may simply be because there is insufficient antigen in the positive nodes. False positives may result from either partial or complete disruption of lymph flow to these nodes or as the result of binding of shed antigen accumulated in tumor-negative nodes. Since tumor-negative lymph nodes may concentrate sufficient radiolabeled antibody to be visualized, gamma camera imaging may not be predictive of the presence of metastases in regional lymph nodes. For example, in a Phase I study using ^{111}In-labeled monoclonal antibody, all patients exhibited uptake of the radiopharmaceutical in draining lymph nodes, even though in 3 out of the 6 patients studied nodal tissue was histologically negative for tumor [74]. Similarly, in a study where both ^{111}In-labeled intact and Fab fragments directed against melanoma were administered to patients subcutaneously, some nodal uptake was seen in tumor-negative nodes [75]. Paganelli et al. however, have reported that in melanoma patients injected with ^{99m}Tc-labeled F(ab')$_2$ into the draining nodes, normal and pathologic nodes could be distinguished due to the greater uptake and persistence of ^{99m}Tc in the involved nodes [76].

Other clinical trials of radioimmunolymphoscintigraphy have produced mixed results. In a report from a multicenter study designed to evaluate the

clinical utility of subcutaneous injection of ^{99m}Tc-F(ab')$_2$ and ^{111}In-F(ab')$_2$ for the detection of melanoma lesions, the importance of the clinical stage of the disease was demonstrated [57]. The frequency of false-negative results was significantly higher in patients with Stage IV disease than in those with earlier stages of disease. Two immunolymphoscintigraphic studies have been performed that have detected tumor foci in patients with T-cell lymphoma [78] and axillary lymph node metastasis in breast carcinoma patients [79]. In the first, gamma camera images clearly demonstrated the efficiency of antibody delivery to and antibody uptake in the inguinal-femoral and iliac lymph nodes following injection into the web spaces between the toes of the patient [78]. Antibody localization, however, could not be correlated with the degree of nodal involvement, since the antigen against which the antibody was directed was expressed on normal T lymphocytes [78]. In the second study, by Mandeville and coworkers, there was a close correlation between the affected lymph nodes and nodal uptake of the antibody; gamma camera images taken at 4 and 8 hours after ^{123}I-antibody injection showed that out of seven patients with positive scans, six showed positive tumor involvement [79]. In the same study two patients' axillary nodes, which were subsequently found to be disease free, were negative by gamma camera imaging.

Thus, in limited cases it has been demonstrated that the subcutaneous administration of radiolabeled antibody may overcome some of the limitations of IV administration, i.e., high background radioactivity, nonspecific accumulation of radiolabel in the liver, spleen, and kidneys, and 'modest' tumor/background ratio. The large-scale clinical utility of lymphoscintigraphy is has yet to be demonstrated.

Barriers to antibody accretion

Tumor vasculature. Tumors derive their vasculature system from the host organism. It is within this system that radiolabeled antibodies are delivered to the tumor via the blood flow, and it is through this system that the antibodies must pass to be bound by tumor cells. It is thought that either the capillaries grow into the tumor from the host as outgrowths of a preexisting capillary bed [80] or the tumor acquires its vasculature by growing around pre-existing capillaries [81]. Regardless of the mechanism by which tumors develop their vasculature, the system that develops within tumors has been shown to lack uniformity [82,83]. The vascular density of rodent tumors was shown to be greater at the tumor's periphery an growing edge, and greatly reduced at the tumor core [82,83]. A necrotic center developed in larger tumors despite the occurrence of intact blood vessels within the core [84]. In experimental tumors only 1.5% of the tumor's volume was found to be vascular tissue [81]. Blood flow through these vessels was shown to be less than through normal tissues [84]. For example, when comparing the blood flow in a transplanted hepatoma with that of the liver, Gullino and Grantham found that the liver had a blood flow approximately 20 times greater than that of a hepatoma

growing at a subcutaneous site [84]. This decreased blood flow results in reduced delivery of radiolabeled antibody to the tumor.

In the authors' laboratory the importance of blood flow and delivery of antibody within the tumor was studied (Figure 4) [85]. ^{125}I-labeled antibodies to different tumor associated antigens were injected into athymic mice bearing either the Clouser (mammary carcinoma) or TK-177G (renal cell carcinoma) human xenografts. Twenty-four hours after injection the tumors were removed, sectioned, and prepared for autoradiographic analysis. The in-vivo binding pattern of the anti-renal cell carcinoma antibody ^{125}I-A6H to TK177G is shown in Figure 4A. The binding was in a streaking pattern, predominantly at the tumor periphery. Figure 4B shows the in-vivo binding pattern in the same xenograft of an antibody to a major human histocompatability marker (anti-HLA). Since this antibody will bind to most human cells, binding would be expected to be equal throughout the human xenografts if delivery was uniform. The binding pattern, however, was very similar to that of the tumor-associated antibody. Similar results were seen when the in-vivo binding pattern in the Clouser tumor of the 'tumor-associated' antibody B6.2 (Figure 4C) was compared with the pattern obtained using the anti-HLA (Figure 4D). In this example, both antibodies localized in discrete 'nests' scattered throughout the tumor. The fact that the same antibody, anti-HLA, had binding patterns tht were different in both tumors, yet similar to the 'tumor-associated' antibody, strongly suggest that the delivery of the antibody by the blood is a major determinant of where within a tumor the antibody will accumulate.

Tumor uptake of radiolabeled monoclonal antibody is limited by the rate at which these macromolecules enter the interstital fluid. Figure 5 is a stylized diagram representing various mechanisms by which an antibody can exit from the vascular compartment into the interstitial fluid. Migration out of the vascular compartment may be via passive diffusion through either intracellular clefts, pores in the fenestrae, or via lipid solubilization. Alternatively, passage could be by active pinocytosis. Large molecular weight substances such as antibodies most probably pass through intracellular clefts and pores in the fenestrae. Circular pores as large as 500 Å have been reported in the fenestrae of some tumors [86]. These data support the generally accepted concept that the vasculature of tumors is more 'leaky' or more permeable to drugs and macromolecules than is the vasculature of normal tissue [20–26]. This increased permeability of the tumor vasculature results in an increase in the nonspecific accretion of macromolecules. A thorough review of the mechanisms of transport of macromolecules through the vasculature of tumors can be found in the review by Jain [20].

The size of a macromolecule is a major determinant of its rate of movement. Size and shape determine which molecules will pass through cellular pores and intracellular clefts. Size, and to a lesser degree shape, also determine the diffusion rate of macromolecules in the interstitial space. Halpern et al. designed experiments to determine the role of antibody size on

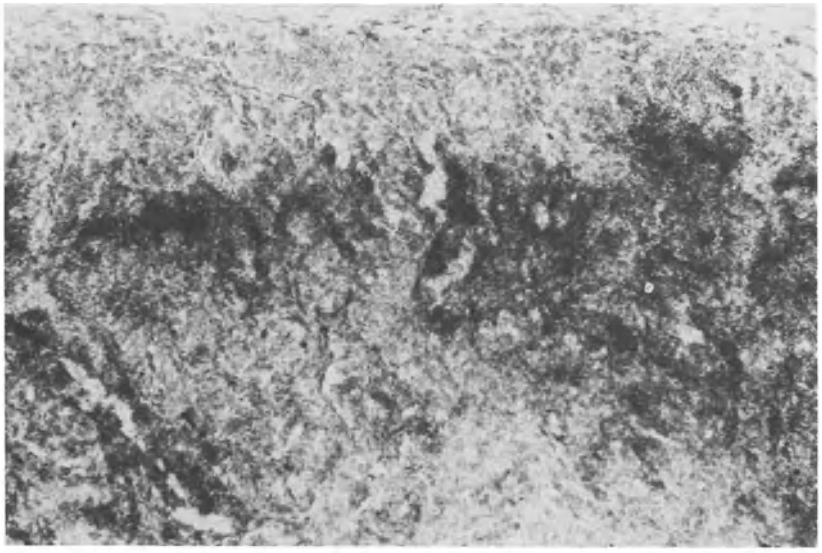

A

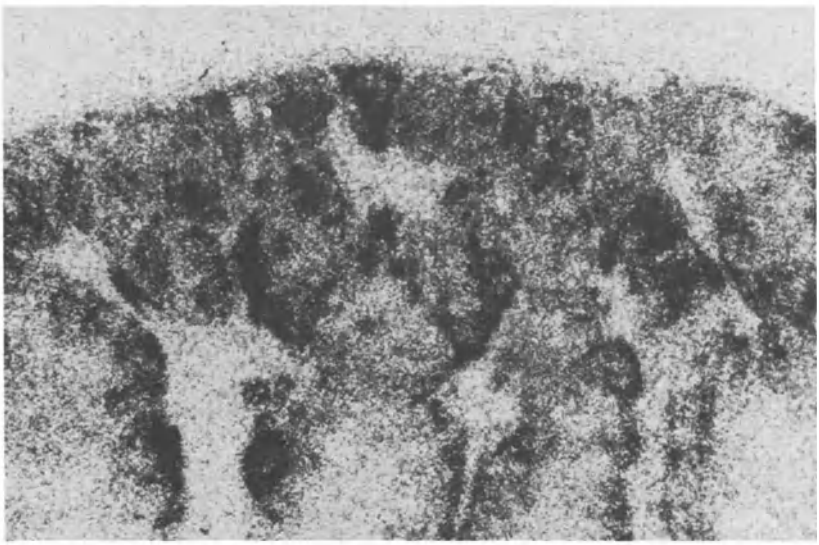

B

Figure 4. Autoradiographic analysis of tumor-associated antibody binding 24 hours after IV injection into tumor-bearing athymic mice. *A*: Binding of the tumor-specific antibody ^{125}I-A6H to the renal-cell carcinoma xenograft, TK 177G, magnification 233x. *B*: Binding of the anti-human histocompatibility antibody ^{125}I-anti-HLA to the renal-cell carcinoma xenograft, TK 177G, magnification 233x. *C*: Binding of the tumor-specific antibody ^{125}I-B6.2 to the Clouser mammary carcinoma xenograft, magnification 233x. *D*: Binding of the anti-human histocompatibility antibody ^{125}I-anti-HLA to the Clouser mammary carcinoma xenograft, magnification 233x.

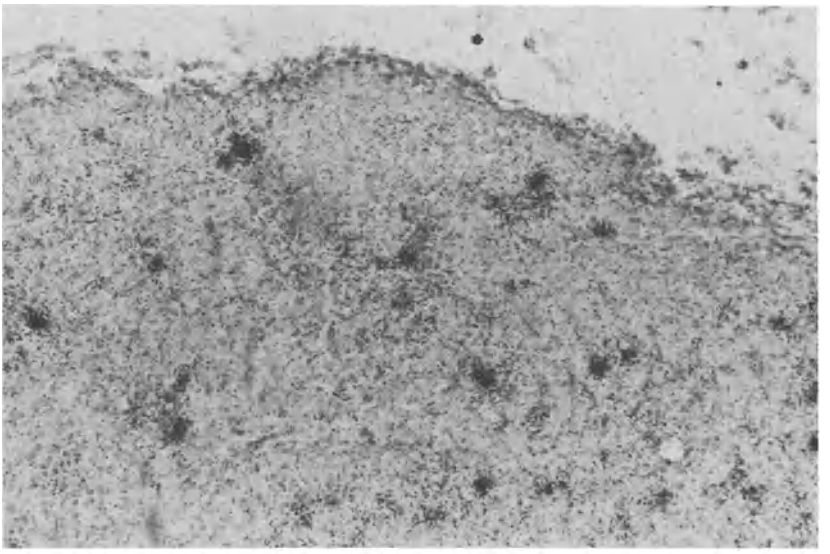

C

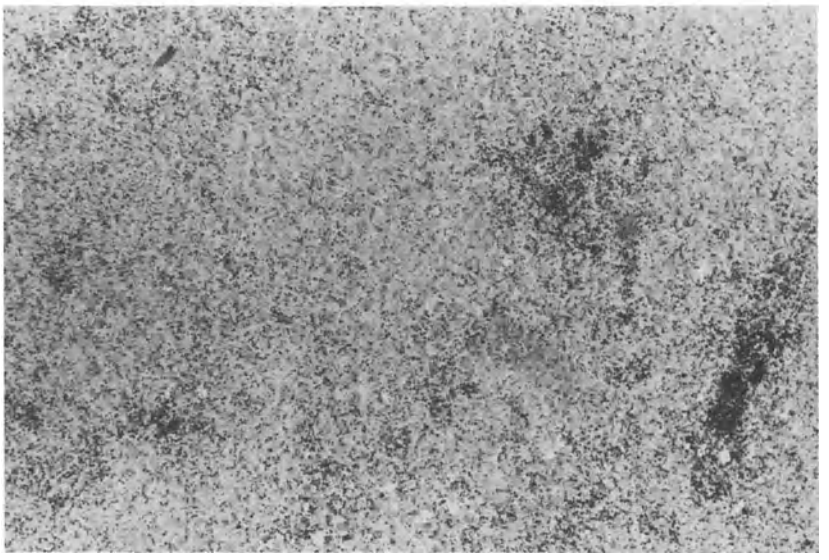

D

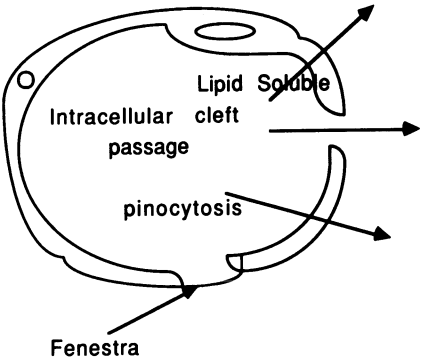

Figure 5. Schematic representation of the various mechanisms of vascular permeability.

the uptake by tumor [87]. As mentioned above, antibody fragments rapidly clear the blood via excretion through the kidneys. To eliminate clearance as a factor, the experiment was conducted in nephrectomized mice. They found that the tumor accretion of antibody (MW, 150,000 daltons), its $F(ab')_2$ (MW, 100,000 daltons), and its Fab fragment (MW, 50,000 daltons) were in the ratio of 1:1.25:1.86. This is a pattern predicted from the findings outlined above. In a similar study by Sands et al. [88] using non-nephrectomized mice, the rate of extravascularization of proteins within a tumor were determined. The rate for bovine serum albumin (MW, 68,000 daltons) was found to be 77% greater than that of a nonspecific intact IgG (MW, 150,000 daltons). Thus antibody size will affect the rate at which an antibody transverses the capillary wall and enters the interstitial space. This rate may be a major determinant of the amount of antibody that ultimately accumulates within the tumor.

Vascular permeability, blood flow, and tumor accretion of radiolabeled antibodies. Both the permeability of the tumor vasculature to radiolabeled monoclonal antibodies and the blood flow to the tumor may be critical factors that contribute to the uptake of antibody by the tumor. In the author's laboratory, a study was carried out to correlate the accretion of radiolabeled antibodies with the degree of vascular permeability of the tumor [85]. The uptake of two ^{125}I specific antibodies by their target xenografts was studied. Tumor accretion of A6H by the renal cell carcinoma (RCC) was considerably greater than that seen for B6.2 by the mammary carcinoma (Clouser) (Table 2) [85]. Blood flow and vascular permeability were found to be significantly greater in the RCC tumor xenografts than in Clouser tumors. Differences in vascular permeability were especially dramatic, showing that the vasculature of the RCC xenograft was twice as permeable as that of the Clouser tumor (Table 2). In order to determine if this increase in accretion could be extended to other antibodies, animals bearing either RCC or Clouser xenografts were injected with an anti-human antibody (anti-HLA). Accretion

Table 2. Antibody accretion and physiologic factors for two human xenografts

	RCC	CLOUSER
Vascular volumes (μl/g tissue)	42.1 ± 5.0	36.4 ± 3.0[a]
Vascular permeability — IgG (μl/g/hr)	172.1 ± 5.0	128.0 ± 9.0[a]
Vascular permeability — BSA (μl/g/hr)	139.1 ± 6.0	76.1 ± 5.0[a]
Relative blood flow (%ID/g)	1.9 ± 0.7	1.1 ± .05[a]
Tumor accretion — 24 hours (%ID/g) — A6H	55.97 ± 6.31	na
Tumor accretion — 24 hours (%ID/g) — B6.2	na	21.08 ± 3.84[b]
Tumor accretion — 24 hours (%ID/g) — anti-HLA	45.74 ± 6.29	8.47 ± 0.59[a]

Data are mean ± SEM.
[a] Clouser vs. RCC — $p < 0.05$.
[b] A6H vs. B6.2 — $p < 0.05$.
na = not applicable.

of this antibody was found to be five times greater in RCC than in Clouser xenografts (Table 2). These results suggest that the differences seen in these physiologic factors could account for some of the greater specific uptake of the tumor-specific antibody by the RCC tumor than the Clouser xenograft.

Pharmacological manipulations to increase tumor uptake of radiolabeled antibodies

Researchers in the field of monoclonal antibodies are just becoming aware that the low tumor uptake of radiolabeled monoclonal antibodies is the net result of the many independent and interrelated factors described above. In only a few studies have attempts been made to manipulate these factors to increase tumor accretion of radiolabeled monoclonal antibodies. Increasing blood flow by pretreatment with either external beam irradiation [89] or hyperthermia [90] resulted in only a small increase in tumor uptake by xenografts in athymic mice. Attempts at increasing relative blood flow through pharmacologic intervention in patients has also been tried [91]. Increasing tumor blood flow by the injection of alpha-adrenergic stimulants failed to change either tumor uptake or blood levels of radiolabeled monoclonal antibodies. Injections of beta-adrenergic blockers were used to decrease blood flow to other organs relative to the tumor. This procedure did produce a increase in the tumor to blood ratio. The ratio changed because the level of antibody in the blood decreased and not because the amount of

radionuclide found in the tumor increased. Treatment of patients with mannitol increased the penetration of radiolabeled Fab into melanoma metastic to the central nervous system (osmotic blood-brain barrier modification) but failed to produce consistent large increases in radionuclide accretion [92]. One possible explanation is the rather short duration (3–5 hours) of mannitol's action. Based on the data presented, classical pharmacologic intervention would not be expected to alter the accretion of radiolabeled monoclonal antibodies by tumors.

To date there have been no reports of the successful use of pharmacologic manipulations to increase the uptake of radiolabeled monoclonal antibody by tumors in either the laboratory or the clinic. If this approach is successful, it may vastly increase the ultimate utility of these molecules as both diagnostic and therapeutic agents.

An alternative approach to the problem of low tumor uptake might be to increase the number of antigenic sites available for binding the radiolabeled monoclonal antibody. This would be especially appealing in the antibody binding sites were saturated with bound antibody, a situation yet to be shown, either in the laboratory or the clinic. Greiner et al. have shown that alpha interferon was capable of enhancing the expression of human tumor-associated antigens in experimental tumors and that it and increased the accretion of its specific antibody by experimental tumors [93,94]. Pretreatment of athymic mice bearing antigen-positive xenografts with recombinant human interferon resulted in an increase in tumor accretion of radiolabeled monoclonal antibody [95,96]. This approach, i.e., increasing the number of antigenic sites of a tumor, has yet to be tried in the clinic.

Summary

During the past 8 years numerous patients have been injected with radiolabeled monoclonal antibodies for both the diagnosis and treatment of cancer. In general the results, while somewhat promising, have failed to fulfill initial expectations. It is now clear that there are many physiologic barriers that antibodies face in their trek toward their tumor-binding site. Use of terms such as *antibody-guided delivery* or *antibody-guided targeting* do not take into account the fact that the antibodies are subject to the same physiologic rules as drugs and hormones. Antibodies are no more 'guided' than any drug or hormone. They reach their binding site via the same delivery mechanisms and accumulate in proportion to their 'receptor's' (antigen's) density.

Our knowledge and understanding of the physiologic barriers to the uptake of tumor-associated monoclonal antibodies is limited. To date very few studies have been reported that shed light on this problem. For radiolabeled monoclonal antibodies to fulfill their promise, a greater understanding of these physiologic barriers is needed in order to devise ways in which they may be overcome.

Acknowledgments

The authors thank Drs. B.M. Gallagher, T. Griffin, and S.B. Haber for their critical review and Mrs. Nancy Silva for typing this manuscript.

References

1. Kohler, G., and Milstein, C. (1975) Continuous cultures of fused cells secreting antibodies of predefined specificity. Nature (London) 256:495–497.
2. Embleton, M.J., Gunn, B., Byers, V.S., and Baldwin, R.W. (1981) Antitumour reactions of monoclonal antibody against a human osteogenic-sarcoma cell line. Br. J. Cancer 43:582–587.
3. Vessella, R.L., Moon, T.D., Chiou, R.-K., Nowak, J.A., Arfman, E.W., Palme, D.F., Peterson, G.A., and Lange, P.H. (1985) Monoclonal antibodies to human renal cell carcinoma: Recognition of shared and restricted tissue antigens. Cancer Res. 45:6131–6139.
4. Colcher, D., Hand, P.H., Nuti, M., and Schlom, J. (1981) A spectrum of monoclonal antibodies reactive with human mammary tumor cells. Proc. Natl. Acad. Sci. USA 78:3199–3203.
5. Eger, R.R., Covell, D.G., Carrasquillo, J.A., Abrams, P.G., Foon, K.A., Reynolds, J.C., Schroff, R.W., Morgan, A.C., Larson, S.M., and Weinstein, J.N. (1987) Kinetic model for the biodistribution of an ^{111}In-labeled monoclonal antibody in humans. Cancer Res. 47:3328–3336.
6. Epenetos, A.A., Snook, D., Durbin, H., Johnson, P.M., and Taylor-Papadimitriou, J. (1986) Limitations of radiolabeled monoclonal antibodies for localization of human neoplasms. Cancer Res. 46:3183–3191.
7. Colcher, D., Esteban, J.M., Carrasquillo, J.A., Sugerbaker, P., Reynolds, J.C., Bryant, G., Larson, S.M., and Schlom, J. (1987) Quantitative analyses of selective radiolabeled monoclonal antibody localization in metastatic lesions of colorectal cancer patients. Cancer Res. 47:1185–1189.
8. Pimm, M.V., Perkins, A.C., Armitage, N.C., and Baldwin, R.W. (1985) The characteristics of blood-borne radiolabels and the effect of anti-mouse IgG antibodies on localization of radiolabeled monoclonal antibody in cancer patients. J. Nucl. Med. 26:1011–1023.
9. Hnatowich, D.F., Griffin, T.W., Kosciuczyk, C., Rusckowski, M.,Childs, R.L., Mattis, J.A., Shealy, D., and Doherty, P.W. (1985) Pharmacokinetics of an indium-111-labeled monoclonal antibody in cancer patients. J. Nucl. Med. 26:849–858.
10. Hayes, D.F., Zalutsky, M.R., Kaplan, W., Noska, M., Thor, A., Colcher, D., and Kufe, D.W. (1986) Pharmacokinetics of radiolabeled monoclonal antibody B6.2 in patients with metastatic breast cancer. Cancer Res. 46:3157–3163.
11. Richardson, R.B., Davies, A.G., Bourne, S.P., Staddon, G.E., Jones, D.H., Kemshead, J.T., and Coakham, H.B. (1986) Radioimmunolocalisation of human brain tumors: Biodistribution of radiolabelled monoclonal antibody UJ13A. Eur. J. Nucl. Med. 12:313–320.
12. Jackson, P.C., Pitcher, E.M., Davies, J.O., Davies, E.R., Sadowski, C.S., Staddon, G.E., Stirrat, G.M., and Sunderland, C.A. (1985) Radionuclide imaging of ovarian tumors with a radiolabelled (^{123}I) monoclonal antibody (NDOG2). Eur. J. Nucl. Med. 11:22–28.
13. Esteban, J.M., Colcher, D., Sugerbaker, P., Carrasquillo, J.A., Bryant, G., Thor, A., Reynolds, J.C., Larson, S.M., and Schlom, J. (1987) Quantitative and qualitative aspects of radiolocalization in colon cancer patients of intravenously administered MAb B72.3. Int. J. Cancer 39:50–59.
14. Beatty, J.D., Duda, R.B., Williams, L.E., Sheibani, K., Paxton, R.J., Beatty, B.G., Philben, V.J., Werner, J.L., Shively, J.E., Vlahos, W.G., Kokal, W.A., Riihimaki, D.U., Terz, J.J., and Wagman, L.D. (1986) Preoperative imaging of colorectal carcinoma with

^{111}In-labeled anticarcinoembryonic antigen monoclonal antibody. Cancer Res. 46:6494–6502.

15. Brown, B.A., Comeau, R.D., Jones, P.L., Liberatore, F.A., Neacy, W.P., Sands, H., and Gallagher, B.M. (1987) Pharmacokinetics of the monoclonal antibody B72.3 and its fragments labeled with either ^{125}I or ^{111}-In. Cancer Res. 47:1149–1154.
16. Andrew, S.M., Pimm, M.V., Perkins, A.C., and Baldwin, R.W. (1986) Comparative imaging and biodistribution studies with an anti-CEA monoclonal antibody and its $F(ab)_2$ and Fab fragments in mice with colon carcinoma xenografts. Eur. J. Nucl. Med. 12:168–175.
17. Greager, J.A., Brown, J.M., Pavel, D.G., Garcia, J.L., Blend, M., and Das Gupta, T.K. (1986) Localization of human sarcoma with radiolabeled monoclonal antibody. Cancer Immunol. Immunother. 23:148–154.
18. Douillard, J.Y., Lehur, P.A., Aillet, G., Kremer, M., Bianco-Arco, A., Peltier, P., and Chatal, J.F. (1986) Immunohistochemical antigenic expression and in vivo tumor uptake of monoclonal antibodies with specificity for tumors of the gastrointestinal tract. Cancer Res. 46:4221–4224.
19. Price, M.R., Pimm, M.V., Page, C.M., Armitage, N.C., Hardcastle, J.D., and Baldwin, R.W. (1984) Immunolocalization of the murine monoclonal antibody, 791T/36 within primary human colorectal carcinomas and identification of the target antigen. Br. J. Cancer 49:809–812.
20. Jain, R.K. (1985) Transport of macromolecules in tumor microcirculation. Biotech. Prog. 1:81–93.
21. Underwood, J.C.E., and Carr, I. (1971) The ultrastructure and permeability characteristics of the blood vessels of a transplantable rat sarcoma. J. Path. 107:157–166.
22. Ackerman, N.B., and Hechmer, P.A. (1978) Studies of the capillary permeability of experimental liver metastases. Surg. Gynecol. Obstet. 146:884–888.
23. Peterson, H-I., and Appelgren, L. (1977) Tumor vessel permeability and transcapillary exchange of large molecules of different size. Bibl. Anat. 15:262–265.
24. Ackerman, N.B., and Hechmer, P.A. (1977) Comparisons of vascular permeability of tumors and liver host tissue. Bibl. Anat. 15:304–306.
25. Peterson, H-I., Appelgren, L., and Kjartansson, I. (1977) Tumor blood flow and tumor vessel permeability. Bibl. Anat. 15:277–280.
26. Waggener, J.D., and Beggs, J.L. (1976) Vasculature of neural neoplasms. Adv. Neurol. 25:27–49.
27. Pimm, M.V., Perkins, A.C., and Baldwin, R.W. (1987) Diverse characteristics of ^{111}In labelled anti-CEA monoclonal antibodies for tumor immunoscrintigraphy: Radiolabeling, biodistribution and imaging studies in mice with human tumor xenografts. Eur. J. Nucl. Med. 12:515–521.
28. Stya, M., Wahl, R.L., Natale, R.B., and Beierwaltes, W.H. (1987) Radioimmunoimaging of human small cell lung carcinoma xenografts in nude mice receiving several monoclonal antibodies. NCI Monogr. 3:19–23.
29. Stavrou, D., Glassner, H., Bilzer, T., Senekowitsch, R., Keiditsch, E., and Mehraein, P. (1986) Radioimaging of experimental glioma grafts using $F(ab')_2$-fragments of monoclonal antibodies. Anticancer Res. 6:897–904.
30. Munz, D.L., Alavi, A., Koprowski, H., and Herlyn, D. (1986) Improved radioimmunoimaging of human tumor xenografts by a mixture of monoclonal antibody $F(ab')_2$ fragments. J. Nucl. Med. 27:1739–1745.
31. Pimm, M.V., Perkins, A.C., Armitage, N.C., and Baldwin, R.W. (1985) Localization of anti-osteogenic sarcoma monoclonal antibody 791T/36 in a primary human osteogenic sarcoma and its subsequent xenograft in immunodeprived mice. Cancer Immunol. Immunother. 19:18–21.
32. Pimm, M.V., Armitage, N.C., Perkins, A.C., Smith, W., and Baldwin, R.W. (1985) Localization of an anti-CEA monoclonal antibody in colorectal carcinoma xenografts. Cancer Immunol. Immunother. 19:8–17.
33. Sands, H., Jones, P.L., Neacy, W.P., Shah, S.A., and Gallagher, B.M. (1986) Site-related

differences in the localization of the monoclonal antibody OX7 in SL2 and SL1 lymphomas. Cancer Immunol. Immunother. 22:169–175.
34. Pimm, M.V., and Baldwin, R.W. (1984) Quantitative evaluation of the localization of a monoclonal antibody (791T/36) in human osteogenic sarcoma xenografts. Eur. J. Cancer Clin. Oncol. 20:515–524.
35. Thedrez, Ph., Blottiere, H., Chatal, J.F., Grzyb, J., and Bouillard, J.Y., (1986) Comparison between 131-I and 111-In as radiolabels for monoclonal antibodies in immunoscintigraphy of tumor bearing nude mice. Tumor Biol. 7:137–145.
36. Herlyn, D., Powe, J., Munz, D.L., Alavi, A., Herlyn, M., Meinken, G.E., Srivastava, S.C., and Koprowski, H. (1986) Radioimmunodetection of human tumor xenografts by monoclonal antibody F(ab′)2 fragments, Nucl. Med. Biol. 13:401–405.
37. Sands, H., and Jones, P.L. (1987) Methods for the study of the metabolism of radiolabeled monoclonal antibodies by liver and tumor. J. Nucl. Med. 28:390–398.
38. Haseman, M.K., Goodwin, D.A., Meares, C.F., Kaminski, M.S., Wensel, T.G., McCall, M.J., and Levy, R. (1986) Metabolizable ^{111}In chelate conjugated anti-iodiotype monoclonal antibody for radioimmunodetection of lymphoma in mice. Eur. J. Nucl. Med. 12:455–460.
39. Esteban, J.M., Schlom, J., Gansow, O.A., Atcher, R.W., Brechbiel, M.W., Simpson, D.E., and Colcher, D. (1987) New method for the chelation of indium-111 to monoclonal antibodies: Biodistribution and imaging of athymic mice bearing human colon carcinoma xenografts. J. Nucl. Med. 28:861–870.
40. Hagan, P.L., Halpern, S.E., Chen, A., Krishnan, L., Frincke, J., Bartholomew, R.M., David, G.S., and Carlo, D. (1985) In vivo kinetics of radiolabeled monoclonal anti-CEA antibodies in animal models. J. Nucl. Med. 26:1418–1423.
41. Wahl, R.L., Wilson, B.S., Liebert, M., and Beierwaltes, W.H. (1987) High-dose, unlabeled, nonspecific antibody pretreatment: Influence on specific antibody localization to human melanoma xenografts. Cancer Immunol. Immunother. 24:221–224.
42. Hagan, P.L., Halpern, S.E., Dillman, R.O., Shawler, D.L., Johnson, D.E., Chen, A., Krishnan, L., Frincke, J., Bartholomew, R.M. David, G.S., and Carlo, D. (1986) Tumor size: Effect on monoclonal antibody uptake in tumor models. J. Nucl. Med. 27:422–427.
43. Shah, S.A., Gallagher, B.M., and Sands, H. (1985) Radioimmunodetection of small human tumor xenografts in spleen of athymic mice by monoclonal antibodies. Cancer Res. 45:5824–5829.
44. Abdel-Nabi, H.H., Schwartz, A.N., Higano, C.S., Wechter, D.G., and Unger, M.W. (1987) Colorectal carcinoma: Detection with indium-111 anticarcinoembryonic-antigen monoclonal antibody ZCE-025. Radiology 164:617–621.
45. Moldofsky, P.J., Sears, H.F., Mulhern, C.B., Hammond, N.D., Powe, J., Gatenby, R.A., Steplewski, Z., and Koprowski, H. (1984) Detection of metastatic tumor in normal-sized retroperitoneal lymph nodes by monoclonal-antibody imaging. N. Engl. J. Med. 311:106–107.
46. Armitage, N.C., Perkins, A.C., Pimm, M.V., Farrands, P.A., Baldwin, R.W., and Hardcastle, J.D. (1984) The localization of an anti-tumor monoclonal antibody (791T/36) in gastrointestinal tumors, Br. J. Surg. 71:407–412.
47. Larson, S.M., Brown, J.P., Wright, P.W., Carrasquillo, J.A., Hellstrom, I., and Hellstrom, K.E. (1983) Imaging of melanoma with I-131-labeled monoclonal antibodies. J. Nucl. Med. 24:123–129.
48. Murray, J.L., Rosenblum, M.G., Lamki, L., Glenn, H.J., Krizan, Z., Hersh, E.M., Plager, C.E., Bartholomew, R.M., Unger, M.W., and Carlo, D.J. (1987) Clinical parameters related to optimal tumor localization of indium-111-labeled mouse antimelanoma monoclonal antibody ZME-018. J. Nucl. Med. 28:25–33.
49. Lamki, L.M., Babian, R.J., Murray, J.L., Haynie, T.P., Glenn, H.J., and Hersh, E.M. (1986) Detection of metastatic prostatic cancer using indium-111 labeled monoclonal antibody PAY-276. J. Nucl. Med. 27:316.
50. Mach, J.-P., Chatal, J.-F., Lumbroso, J.-D., Buchegger, F., Forni, M., Ritschard, J., Berche, C., Douillard, J.-Y., Carrel, S., Herlyn, M., Steplewski, Z., and Koprowski, H.

(1983) Tumor localization in patients by radiolabeled monoclonal antibodies against colon carcinoma. Cancer Res. 43:5593–5600.

51. Allum, W.H., MacDonald, F., Anderson, P., and Fielding, J.W.L. (1986) Localization of gastrointestinal cancer with a ^{131}I labeled monoclonal antibody to CEA. Br. J. Cancer 53:203–210.
52. Waldmann, T.A., and Strober, W. (1969) Metabolism of immunoglobulins. Progr. Allergy 13:1–110.
53. Rosen, S.T., Zimmer, A.M., Goldman-Leikin, R., Gordon, L.I., Kazikiewicz, J.M., Kaplan, E.H., Variakojis, D., Marder, R.J., Dykewicz, M.S., Piergies, A., Silverstein, E.A., Roenigk, H.H., Jr., and Spies, S.M. (1987) Radioimmunodetection and radioimmunotherapy of cutaneous T cell lymphomas using an ^{131}I-labeled monoclonal antibody: An Illinois Cancer Council Study. J. Clin. Oncol. 5:562–573.
54. Moldofsky, P.J., Powe, J., Mulhern, C.B., Jr., Hammond, N., Sears, H.F., Gatenby, R.A., Steplewski, Z., and Koprowski, H. (1983) Metastatic colon carcinoma detected with radiolabeled F(ab')2 monoclonal antibody fragments. Radiology 149:549–555.
55. Larson, S.M., Carrasquillo, J.A., McGuffin, R.W., Krohn, K.A., Ferens, J.M., Hill, L.D., Beaumier, P.L., Reynolds, J.C., Hellstrom, K.E., and Hellstrom, I. (1985) Use of I-131 labeled, murine Fab against a high molecular weight antigen of human melanoma: Preliminary experience. Radiology 155:487–492.
56. W. Buraggi, G.L., Callegaro, L., Turrin, A., Cascinelli, N., Attili, A., Emanuelli, H., Gasparini, M., Deleide, G., Plassio, G., Dovis, M., Mariani, G., Natali, P.G., Scassellati, G.A., Rosa, U., and Ferrone, S. (1984) Immunoscintigraphy with ^{123}I, ^{99m}Tc and ^{111}In-labelled $F(ab')_2$ fragments of monoclonal antibodies to a human high molecular weight-melanoma associated antigen. J. Nucl. Med. All. Sci. 28:283–295.
57. Siccardi, A.G., Buraggi, G.L., Callegaro, L., Mariani, G., Natali, P.G., Abbati, A., Bestagno, M., Caputo, V., Mansi, L., Masi, R., Paganelli, G., Riva, P., Salvatore, M., Sanguineti, M., Troncone, L., Turco, G.L., Scassellati, G.A., and Ferrone, S. (1986) Multicenter study of immunoscintigraphy with radiolabeled monoclonal antibodies in patients with melanoma. Cancer Res. 46:4817–4822.
58. Delaloye, B., Bischof-Delaloye, A., Buchegger, F., von Fliedner, V., Grob, J.-P., Volant, J.-C., Pettavel, and Mach, J.-P. (1986) Detection of colorectal carcinoma by emission-computerized tomography after injection of ^{123}I-labeled Fab or $F(ab')_2$ fragments from monoclonal anti-carcinoembryonic antigen antibodies. J. Clin. Invest. 77:301–311.
59. Rowlinson, G., Snook, D., Busza, A., and Epenetos, A.A. (1986) Antibody guided localization of intraperitoneal tumors following IP or IV antibody administration. Br. J. Cancer 54:553.
60. Lee, Y., Bullard, D.E., Wikstrand, C.J., Zalutsky, M.R., Muhlbaier, L.H., and Bigner, D.D. (1987) Comparison of monoclonal antibody delivery to intracranial glioma xenografts by intravenous and intracarotid administration. Cancer Res. 47:1941–1946.
61. Wahl, R.L., Liebert, M., Fisher, S., and Boland, R. (1987) Enhanced radioimmunotherapy of intraperitoneal human colon cancer xenografts by intraperitoneal monoclonal antibody delivery. Proc. Am. Assoc. Cancer Res. 28:438.
62. Ward, B.G., and Wallace, K. (1987) Localization of the monoclonal antibody HMFG2 after intravenous and intraperitoneal injection into nude mice bearing subcutaneous and intraperitoneal human ovarian cancer xenografts. Cancer Res. 47:4714–4718.
63. Snook, D., Rowlinson, G., and Epenetos, A.A. (1987) Preparation and in vivo study of yttrium-90 labelled immunoconjugates. Nuclear Med. Commun. 8:257.
64. Colcher, D., Esteban, J., Carrasquillo, J.A., Sugarbaker, P., Reynolds, J.C., Bryant, G., Larson, S.M., and Schlom, J. (1987) Complementation of intracavitary and intravenous administration of a monoclonal antibody (B72.3) in patients with carcinoma. Cancer Res. 47:4218–4224.
65. Ward, B.G., Mather, S.J., Hawkins, L.R., Crowther, M.E., Shepherd, J.H., Granowski, M., Britton, K.E., and Slevin, M.L. (1987) Localization of radioiodine conjugated to the monoclonal antibody HMFG2 in human ovarian carcinoma: Assessment of intravenous and

intraperitoneal routes of administration. Cancer Res. 47:4719–4723.
66. Epenetos, A.A. (1984) Antibody-guided irradiation of malignant lesions: Three cases illustrating a new method of treatment. Lancet 2:1441–1443.
67. Hooker, G., Snook, D., Courtenay-Luck, N., Rowlinson, G., Stewart, S., and Epenetos, A.A. (1987) Radiolabelled monoclonal antibodies for intracavitary treatment of ovarian cancer. Nucl. Med. Commun. 8:256–257.
68. Pectasides, D., Stewart, S., Courtenay-Luck, N., Rampling, R., Munro, A.J., Krausz, T., Dhokia, B., Snook, D., Hooker, G., Durbin, H., Taylor-Papadimitriou, J., Bodmer, W.F., and Epenetos, A.A. (1986) Antibody-guided irradiation of malignant pleural and pericardial effusions. Br. J. Cancer 53:727–732.
69. Weinstein, J.N., Steller, M.A., Covell, D.G., Holton, O.D., Keenan, A.M., Sieber, S.M., and Parker, R.J. (1984) Monoclonal antitumor antibodies in the lymphatics. Cancer Treat. Rep. 68:257–264.
70. Parker, R.J., Keenan, A.M., Dower, S.K., Steller, M.A., Holton, O.D., Sieber, S.M., and Weinstein, J.N. (1987) Targeting of murine radiolabeled monoclonal antibodies in the lymphatics. Cancer Res. 47:2073–2076.
71. Mulshine, J.L., Keenan, A.M., Carrasquillo, J.A., Walsh, T., Linnoila, R.I., Holton, O.D., Harwell, J., Larson, S.M., Bunn, P.A., and Weinstein, J.N. (1987) Immunolymphoscintigraphy of pulmonary and mediastinal lymph nodes in dogs: A new approach to lung cancer imaging. Cancer Res. 47:3572–3576.
72. Weinstein, J.N., Steller, M.A., Keenan, A.M., Covell, D.G., Key, M.E., Sieber, S.M., Oldham, R.K., Hwang, K.M., and Parker, R.J. (1983) Monoclonal antibodies in the lymphatics: Selective delivery to lymph node metastases of a solid tumor, Science 222:423–426.
73. Shah, S.A., Gallagher, B.M., and Sands, H. (1987) Lymphoscintigraphy of human colorectal carcinoma metastases in athymic mice by use of radioiodinated B72.3 monoclonal antibody. J. Natl. Cancer Inst. 78:1069–1077.
74. Lotze, M.T., Carrasquillo, J.A., Weinstein, J.N., Bryant, G.J., Perentesis, P., Reynolds, J.C., Matis, L.A., Eger, R.R., Keenan, A.M., Hellstrom, I., Hellstrom, K.-E., and Larson, S.M. (1986) Monoclonal antibody imaging of human melanoma. Ann. Surg. 204:22–235.
75. Engelstad, B.L., Spitler, L.E., Del Rio, M.J., Ramos, E.C., Rosendorf, L.L., Reinhold, C.E., Khentigan, A., Huberty, J.P., Corpuz, S.W., Lee, H.M., Okerlund, M.D., Hattner, R.S., and Scannon, P.J. (1986) Phase 1 immunolymphoscintigraphy with an In-111-labeled antimelanoma monoclonal antibody. Radiology 161:419–422.
76. Paganelli, G., Riva, P., Moscatelli, G., Stacchiotti, A., Agostini, M., Landi, G., Tison, V., Pancea, P., and Siccardi, A.G. (1986) Improved immunoscintigraphy by subcutaneous injection of ^{99m}Tc or ^{111}In labeled F(ab')$_2$ fragments of an anti-melanoma monoclonal antibody. Nucl. Med. Biol. 13:423–428.
77. Nelp, W.B., Eary, J.F., Jones, R.F., Hellstrom, K.E., Hellstrom, I., Beaumier, P.L., and Krohn, K.A. (1987) Preliminary studies of monoclonal antibody lymphoscintigraphy in malignant melanoma. J. Nucl. Med. 28:34–41.
78. Keenan, A.M., Weinstein, J.N., Mulshine, J.L., Carrasquillo, J.A., Bunn, P.A., Jr., Reynolds, J.C., and Larson, S.M. (1987) Immunolymphoscintigraphy in patients with lymphoma after subcutaneous injection of indium-111-labeled T101 monoclonal antibody. J. Nucl. Med. 28:42–46.
79. Mandeville, R., Pateisky, N., Philipp, K., Kubista, E., Dumas, F., and Grouix, B. (1986) Immunolymphscintigraphy of axillary lymph node metastases in breast cancer patients using monoclonal antibodies: First clinical findings. Anticancer Res. 6:1257–1264.
80. Warren, B.A. (1970) The ultrastructure of the microcirculation at the advancing edge of Walker 256 carcinoma. Microvasc. Res. 2:443–453.
81. Thompson, W.D., Shiach, K.J., Fraser, R.A., McIntosh, L.C., and Simpson, J.G. (1987) Tumors acquire their vasculature by vessel incorporation, not vessel ingrowth. J. Pathol. 151:323–332.
82. Tannock, I.F., and Steel, G.G. (1969) Quantitative techniques for study of the anatomy and

function of small blood vessels in tumors. J. Natl. Cancer Inst. 42:771–782.
83. Vaupel, P. (1975) Interrelationship between mean arterial blood pressure, blood flow, and vascular resistance in solid tumor tissue of DS-carcinosarcoma. Experimentia 31:587–589.
84. Gullino, P.M., and Grantham, F.H. (1961) Studies on the exchange of fluids between host and tumor. II. The blood flow of hepatomas and other tumors in rats and mice. J. Natl. Cancer Inst. 27:1465–1491.
85. Sands, H., Jones, P.L., Shah, S., Palme, D., Vassela, R.L., and Gallagher, B.M. (1988) Correlation of vascular permeability and blood flow with monoclonal antibody uptake by Clouser and renal cell xenografts. Cancer Res. 48:188–195.
86. Hirano, A., and Matsui, T. (1975) Vascular structures in brain tumors. Human Pathol. 6:611–621.
87. Halpern, S.E., Buchegger, F., Schreyer, M., and Mach, J.-P. (1986) Effect of size of radiolabeled antibody and fragments on tumor uptake and distribution in nephrectomized mice. J. Nucl. Med. 25:112–113.
88. Sands, H., Shah, S.A., and Gallagher, B.M. (1985) Vascular volume and permeability of human and murine tumors grown in athymic mice. Cancer Lett. 27:15–21.
89. Stickney, D.R., Gridley, D.S., Kirk, G.A., and Slater, J.M. (1987) Enhanced binding of ^{111}In monoclonal antibody to melanoma by single-dose radiation. Abstracts, Second International Conference on Monoclonal Antibodies, San Diego, CA, p. 96.
90. Stickney, G.R., Gridley, D.S., Kirk, G.A., and Slater, J.M. (1985) Enhancement of monoclonal antibody binding with a single dose radiation or hyperthermia. Cancer Drug Deliv. 2:225.
91. McKenzie, I.F.C., Smyth, M.J., Kanellos, J., Sacks, N.P.M., Thompson, C.H., and Pietersz, G.A. (1987) Preclinical studies with a variety of immunoconjugates. Abstracts, Second International Conference on Monoclonal Antibodies, San Diego, Cal. p. 21.
92. Neuwelt, E.A., Sprecht, H.D., Barnett, R.A., Dahlborg, S.A., Miley, A., Larson, S.M., Brown, P., Eckerman, K.F., Hellstrom, K.E., and Hellstrom, I. (1987) Increased delivery of tumor specific monoclonal antibodies to brain after osmotic blood-brain barrier modification in patients with melanoma metastic to central nervous system. Neurosurgery 20:885–895.
93. Greiner, J.W., Hand, P.H., Noguchi, P., Fisher, P.B., Pestka, S., and Schlom, J. (1984) Enhanced expression of surface tumor-associated antigens on human breast and colon tumor cells after recombinant human leukocyte a-interferon treatment. Cancer Res. 44:3208–3214.
94. Greiner, J.W., Tobi, M., Fisher, P.B., Langer, J.A., and Pestka, S. (1985) Differential responsiveness of cloned mammary carcinoma cell populations to the human recombinant leukocyte interferon enhancement of tumor antigen expression. Int. J. Cancer 36:159–166.
95. Rowlinson, G., Balkwill, F., Snook, D., Hooker, G., and Epenetos, A.A. (1986) Enhancement of g-interferon of in vivo tumor radiolocalization by a monoclonal antibody against HLA-DR antigen. Cancer Res. 46:6413–6417.
96. Greiner, J.W., Guadagni, F., Noguchi, P., Pestka, S., Colcher, D., Fisher, P.B., and Schlom, J. (1987) Recombinant interferon enhances monoclonal antibody-targeting of carcinoma lesions in vivo. Science 235:895–898.

6. Intraperitoneal delivery of monoclonal antibodies

Richard L. Wahl

The use of intact radiolabeled antibodies, administered intravenously, in experimental animals and in humans has been complicated by the relatively low tumor/background ratios and the low absolute tumor uptakes achieved [1]. While antibody fragments enhance the tumor/background ratios (at the cost of lower absolute tumor uptake), as does the systemic administration of polyclonal anti-mouse antibodies, these tumor/nontumor ratios often remain relatively low, as do absolute tumor uptakes [2–6]. While these facts have not prevented radioimmunodetection from being a viable clinical undertaking, particularly as radiolabeling methods with a higher photon flux are becoming available and with the use of background subtraction, a method of delivering more antibody to tumors and less to normal tissues would be most valuable [7–10].

Dilution of antibodies given IV in the body's plasma and extracellular fluid coupled with limited blood flow to tumors and possibly the limited degree of vascular permeability of tumors, means that antibody presentation to tumors may be a limiting factor, even with an ideal antibody/antigen system [1]. In experimental systems, available antigen saturation following IV delivery is rarely a limiting factor [11]. Binding kinetic considerations indicate that higher absolute tumor uptakes would be achieved if higher concentrations of antibody could reach the tumor [12]. Such should be the case when antibodies are delivered at a high concentration to a region of the body containing tumor, sparing dilution in the blood stream. Two examples of such regional delivery approaches are intraperitoneal delivery to tumors involving the peritoneal cavity or subcutaneous delivery of antibody to lymph nodes via the lymphatics [13–16] (Intralymphatic delivery is discussed elsewhere in this text.) While intraperitoneal delivery of antibodies is still under intensive investigation, this chaper attempts to provide a status report on this regional delivery approach.

Anatomy of the peritoneal cavity

The peritoneal cavity is a complex anatomic space, which generally represents a potential space, as only a few milliliters of peritoneal fluid are generally

Goldenberg, D.M., (ed.), Cancer Imaging with Radiolabeled Antibodies.

present within it. The space can accomodate far more fluid or tumor than this, however , being able to hold 3 l or more of fluid without a significant problem [17]. The peritoneal cavity's embryologic development is a complex process, as in the development of the midgut several surfaces fold about one another, while others fuse with one another [18]. An example of the complex embryology of this region is the fusion of the transverse mesocolon and parietal peritoneum with the dorsal mesogastrium or greater omentum. The embryology of the region is beyond the scope of this chapter but is reviewed in several publications [19]. Briefly stated, the complex embryology leads to a somewhat complex potential space.

The peritoneal cavity is closed to the outside in males, but has the potential of communication externally in females through the fallopian tubes. While the peritoneal membrane is essentially continuous, it is common to divide the membrane into the visceral and the parietal peritoneum. The visceral peritoneum directly overlies the major organs, and the parietal peritoneum is in contact with the outer fascia and the musculature of abdominal cavity. Much of the liver, spleen, stomach, and nearly all of the bowel is covered with peritoneum. The pancreas, aorta, vena cava, and kidneys lie behind the parietal pertioneum and are considered retroperitoneal structures. The ovaries and uterus are largely covered with peritoneum, invaginating into the peritoneal space from below [19].

The two major compartments of the peritoneal cavity are the greater and lesser sacs. The greater sac is by far the larger of these compartments and stretches from the anatomic pelvis to the hemidiaphragms. The far smaller lesser sac lies anterior to the pancreas but behind the stomach. These two potential spaces communicate via the foramen of Winslow (epiploic foramen), situated just to the right of the midline and slightly posterior and inferior to the liver. Since the foramen of Winslow can become obstructed, inflammatory processes originating near the pancreas can become confined in the lesser sac. This also means that the lesser sac may be harder to reach with radiolabeled antibodies than other areas of the greater sac. The complex folding of the peritoneal cavity reults in a large surface area of approximately 5 m^2 [19].

Patterns of fluid flow in the peritoneal cavity have been extensively studied, and it is clear that while the anatomic pelvis and the regions of the posterior hemidiaphragms are the most dependent areas (when an individual patient is supine), there is a normal pattern of flow of fluid from the lower abdomen to the right upper abdomen [20]. This is in part due to differentials in intraabdominal fluid pressure with respiration and in part due to the presence of the splenocolic ligament, which limits fluid flow to the left upper abdomen. Meyer's text on the subject of intraperitoneal fluid distribution is a source of extensive additional information on this subject [20].

Normal peritoneal anatomy, displayed scintigraphically by the distribution of Tc-99m sulfur colloid administered intraperitoneally to a patient without known residual tumor, is shown clearly in Figures 1A to 1C. Activity

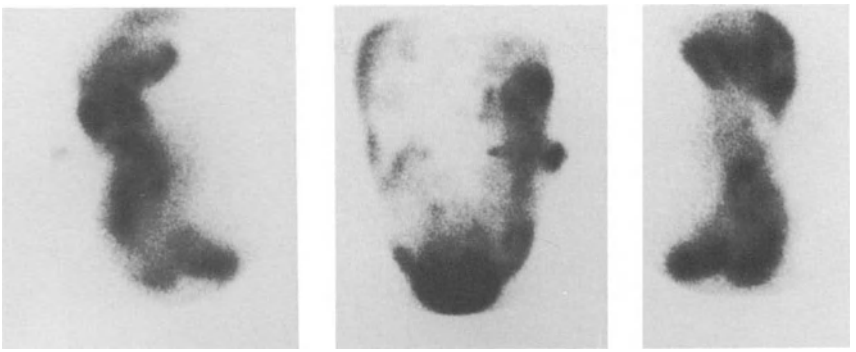

Figure 1. A–C: Normal, complete peritoneal tracer distribution. Views shown are left lateral (left), anterior (center), and right lateral (right).

is clearly seen in the anatomic pelvis, left and right paracolic gutters, and over the right to a greater extent than the left hemidiaphragm [21]. This anatomy can also be seen following the injection of P-32, using Brehmsstrahlung scanning, although the resolution is inferior to that of gamma scanning [22]. We and others have recently used single photon emission computed tomography (SPECT) as an imaging tool to better define the complicated peritoneal anatomy [23,24]. An example of a SPECT, as compared with a planar scan is shown in Figure 2. In our experience, SPECT is the only method that has reliably let us see radioactivity entering the lesser sac of the peritoneal cavity and that allows us to define the extent of radioactivity distribution about the liver, particularly in the region of the bare area.

SPECT can also be used to quantitate the distribution of fluid in the

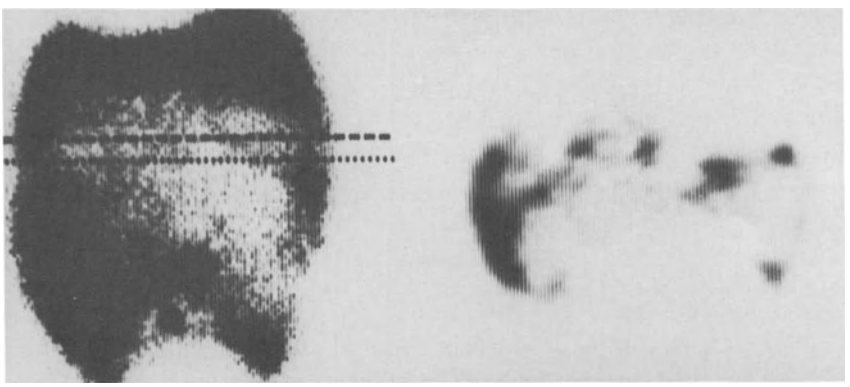

Figure 2. Planar and transverse SPECT scan of intraperitoneal Tc-99m sulfur colloid activity. A normal distribution is seen.

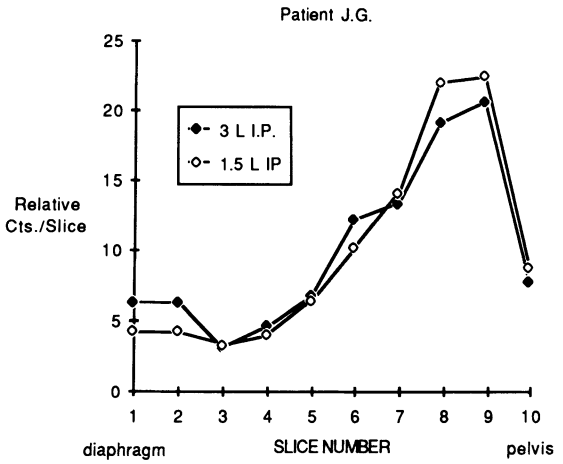

Figure 3. Quantitative SPECT profile of intraperitoneal fluid distribution of Tc-99m sulfur colloid at two infusion volumes. Note the lack of change between the 1.5 l and 3.0 l volumes.

peritoneal cavity. Since the surface area of the peritoneal cavity is large, it is apparent that a moderately large amount of fluid would need to be instilled to guarantee good contact between the IP fluid and the peritoneal surface. We have reported that 1.5 l and 3.0 l instilled give comparable IP distributions by quantitative SPECT. An example of a quantitative SPECT histogram is shown in Figure 3, at both 1.5 l and 3.0 l. As will be discussed, a nonuniform distribution of the radiolabeled compound IP would predict that therapeutic results would be unsuccessful, as areas not bathed by the radiolabeled compound will not be reached by gamma rays or particles from the injected radioactivity. In addition, one would predict that pain due to local overdosage might occur if radioactivity was loculated following injection [22]. Thus, we feel a knowledge of IP fluid distribution is critical prior to the installation of therapeutic antibodies. A knowledge of normal intraperitoneal anatomy is essential for such an undertaking.

We have studied the distribution of Tc-99m sulfur colloid administered intraperitoneally to colon cancer patients being considered for adjuvant chemotherapy intraperitoneally. Our results are summarized in Table 1 [21].

Table 1. IP scan patterns versus CT and surgical findings in 26 patients

Scan Pattern	No. of Patients*	CT or Surgical Findings
Normal	9	No tumor masses
Decreased right lower quadrant	3	Three right-lower-quadrant masses
Decreased pelvis	6	Four pelvic masses
Decreased right upper quadrant	10	Seven with liver metastasis
Decreased left upper quadrant	8	One left-upper-quadrant mass
Loculation	1	Peritoneal fibrosis

* Several patients had more than one abnormality on scan, thus the patient total is larger than 26.

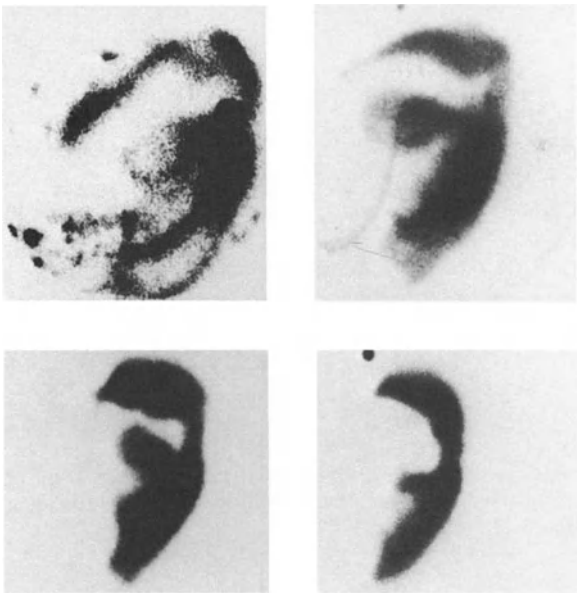

Figure 4. Diminished tracer activity in right lower quadrant. In this example, the decrease was progressive over 16 months and eventually involved the entire right abdomen. Tumor in the right lower abdomen was responsible.

It is apparent that decreased activity in the lower abdomen commonly indicates the presence of bulky tumor (Figure 4). Decreased activity in the right upper abdomen can often be due to the presence of hepatic metastases (Figure 5), decreased pelvic activity is commonly associated with pelvic masses, while decreased left upper quadrant activity can be a normal variant. It is also apparent, from our experience with these nonantibody studies, that patient motion following intraperitoneal fluid administration is important in assuring a uniform distribution of radiolabeled compound, as a nonuniform distribution can be seen if a little motion is undertaken prior to imaging (Figure 6). Thus, a working knowledge of the normal fluid distribution in the peritoneal cavity is essential to a full understanding of the abnormal fluid distribution.

Intraperitoneal radionuclide therapy (nonantibody)

Before discussing the use of radiolabeled antibodies administered intraperitoneally, it is important to review the history of intraperitoneal delivery of radiolabeled compounds to treat cancers involving the peritoneal cavity. This application dates to the work of Muller in 1945 in which ^{63}Zn colloid was used for the treatment of ovarian cancer metastases [26]. Hahn used colloidal gold

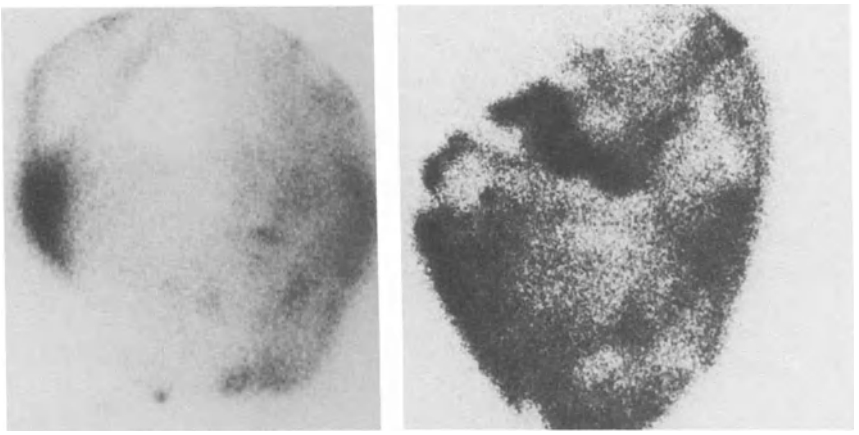

Figure 5. Decreased pelvic activity (left) and diminished activity in right upper quadrant (right). No tracer is present over dome of liver. These patterns are often seen when tumor involves the liver or pelvis, respectively.

(Au-198) in the late 1940s for similar purposes [27]. Considerable complications were observed with doses of 100–200 mCi of Au-198 colloid IP, with bowel obstruction and bowel damage relatively common [28]. With the use of P-32 colloid, which lacks a gamma emission, in doses of 10–20 mCi, considerably less complications have been seen [29–30]. This technique, and the use of P-32 intraperitoneally, have been relatively common adjuvants to the treatment of ovarian carcinoma [28].

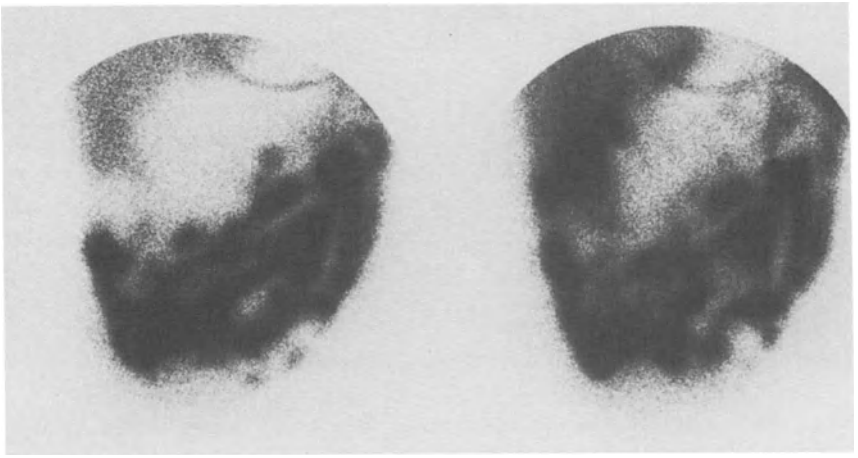

Figure 6. Decreased right-upper-quadrant activity is seen (left). With patient motion, activity increases in the right upper abdomen (right).

P-32 colloid given IP takes advantage of the fact that much of the injected dose of the colloid given intraperitoneally is retained in the peritoneal cavity, with only a small portion leaving via the lymphatics. Certainly, some colloid will leave and become trapped in the lymphatics, but relatively little will escape to the blood stream [31]. Thus, tumor exposures of 6000+ rads are seen, with little systemic exposure [32]. Much of the systemic exposure may in fact be due to metabolism and breakdown of the P-32 colloid, with subsequent catabolism. Probably about 90% of the injected dose remains intraperitoneal in humans [28]. A major quantity of P-32 does accumulate in lymph nodes draining the peritoneal cavity, though the data of Currie suggests that these doses are subtherapeutic [32].

There is certainly a strong suggestion that P-32 adds survival time to patients with stage I ovarian cancer, as suggested by Clark's work in which 5-year survival with P-32 treatment was 93% and without P-32 or with external beam therapy was 60–70% [33]. Creasman has also reported improved survival in patients with stage I endometrial carcinoma and positive cytologies, showing an 80+% survival in those treated with P-32 IP and only an approximately 50% survival in the untreated patients [34]. Also reported by Creasman was a lack of intraperitoneal recurrences in those treated with P-32 (though recurrences could occur elsewhere), indicating the efficacy of P-32 for peritoneal disease [34]. Complications regarding the bowel are infrequent with P-32, in contrast to the gamma-emitting Au-198 or external beam irradiation.

There is no question that P-32 can diminish the accumulation of ascites in patients with ovarian cancer, though the effect may take several months to become apparent. A 50–85% response rate to this mode of treatment has been quoted, though the higher figure excludes those patients who expired prior to 3 months of treatment [35–36]. The procedure for palliation of ascites is well tolerated if care is taken to avoid injecting into a loculated peritoneal cavity. P-32 would generally be used after the failure of systemic chemotherapy to control ascites.

The mechanism of decreasing malignant ascites is probably at least twofold with intraperitoneal radiocolloid treatment. Animal studies have clearly shown that the malignant potential of sarcoma cells in an animal model of intraperitoneal carcinoma following treatment with ^{198}Au is abrogated as the sarcoma cells die or beocme greatly altered morphologically [27]. In addition, since colloids seem to 'plate out' on the peritoneal surfaces, apparently following ingestion by macrophages, the peritoneal surface is morphologically altered with fibrosis and fibrous thickening of the peritoneum and diaphragm [22,38]. It is theorized that this fibrosis may diminish leakiness of the serosa of the viscera. While strictly randomized studies may not be available, it is clear that the intracavitary treatment experience with radiocolloids lays a framework of safety and a strong suggestion of efficacy for radiolabeled antibodies administered intraperitoneally.

Intraperitoneal chemotherapy

While an comprehensive review of intraperitoneal chemotherapy lies outside the scope of this chapter, it is apparent that this approach has had considerable acceptance in the oncologic community for the treatment of intraperitoneal malignancies, such as ovarian cancer or the rarer peritoneal mesothelioma [38]. The concept of the regional delivery advantage to the peritoneal cavity (AUC agent given IP/AUC; systemic given IP) originated from this literature [39], in which it was observed that certain drugs were cleared more rapidly from the blood stream than they were from the peritoneal cavity. This meant that the peritoneal cavity would be exposed to higher levels of the chemotherapeutic agent than the blood (and the rest of the body) and that for small tumors IP should be a considerable delivery advantage. For example, cisplatinum has an AUC IP of 11 times more than blood levels, while adriamycin has an even larger advantage [40]. A recent review suggested that the IP chemotherapeutic approach was best suited to patients with tumors under 2 cm in size (low bulk disease) and indicated that reported results in ovarian cancer following IP antibody delivery are considerably better than following IV delivery, though no strictly randomized results were yet available [41]. These data again support the rationale for the intraperitoneal delivery of therapeutic agents.

Intraperitoneal antibody delivery

Intraperitoneal delivery of unlabeled antibodies for the therapy of intraperitoneal neoplasia was reported in 1962 by Order and his colleagues [41]. In this instance, the successful therapy was of intraperitoneal murine ovarian cancers. In this manuscript he and his coauthors observed that 'clinical ovarian carcinoma has the unique feature of allowing intraperitoneal administration of immune antiserum directly into the tumor-bearing volume. If nonspecific binding of species or histocompatibility antibodies occurs it will be with tumor cells and peritoneal cells first because of the intraperitoneal route of administration thereby avoiding absorption in other organs' [41]. Using polyclonal rabbit unlabeled antibodies reactive with the murine cancer, Order was able to show prolonged survival with treatment by the IP route, though no comparisons with IV delivery were made.

While considerable progress occurred using intravenous and subcutaneously administered antibodies in humans from 1978 to 1983, intraperitoneal antibody delivery in humans was not reported until Epenetos' results on the use of monoclonal antibodies given IP for human ovarian cancer therapy in 1983 [15]. More recently, several other investigators have begun to evaluate this delivery route [42–45].

Kinetics of antibody clearance from the peritoneal cavity

Against this background, relatively little has been reported specifically regarding the kinetics of clearance of antibody from the peritoneal cavity, though many other molecules of a wide range of sizes have been studied. Major textbooks of oncology state that larger, less lipophilic molecules leave the peritoneal cavity more slowly than do smaller molecules [46]. 'The slower the peritoneal clearance of a drug, the greater the potential pharmacologic advantage' is stated in DeVita's text [46]. In fact, the 'peritoneal membrane' is crossed by small molecules in a molecular-weight-related fashion, at least in the ranges of molecular weight from < 100 to approximately 6000, with the slowest clearance for the larger molecules [38]. There is some data to suggest that this size/weight relationship also holds for larger molecules up to 2 million in molecular weight [47]. Recent data on liposome resorption suggests that there is not a major relationship between liposome size and absorption rates [48]. Thus, this is an area of some controversy.

It is known that very large molecules, such as colloidal P-32 or gold, do not rapidly clear from the peritoneal cavity in humans (though in some animals they clear from the peritoneal cavity quite extensively, emphasizing the occasional difficulty in extrapolation from animal to human data). In fact, these colloids have been extensively used for the treatment of intraperitoneal ovarian cancer, as discussed earlier. These agents are reported to clear the peritoneal cavity via the lymphatics [49–51]. It is known that days to weeks after such an intraperitoneal administration, a small amount of this activity can be seen in lymph nodes [52]. The route of clearance is largely via the diaphragmatic lymphatics $R > L$, with spread to the lymph nodes of the anterior mediastinum. Little colloid escapes systemically, however, and local toxicity predominates. It is well known that even larger molecules such as red blood cells can escape the peritoneal cavity, reaching the circulation in animals reasonably rapidly [51].

An understanding of the kinetics of antibody clearance from the peritoneal cavity is fundamental to rationally applying the intraperitoneal antibody-delivery methodology. Obviously, if antibodies are rapidly transferred from the peritoneal cavity to the blood stream and are then retained in the blood for the same time period as are antibodies given IV, there will be little advantage to IP delivery. If they are cleared from the peritoneal cavity more slowly, enhanced regional delivery to the peritoneal cavity will result. The clearance of radiolabeled albumin from the peritoneal cavity has been studied in humans, and it is clear that, while much albumin does eventually escape to the circulation, a considerable quantity is retained in the peritoneal cavity out to 12 or more hours post i.p. injection [53].

To evaluate the rate of clearance of antibodies from the peritoneal cavity, we studied the clearance rate of an intact IgG_{2a} murine antibody from the peritoneal cavity of normal rats to the blood, using sequential sampling

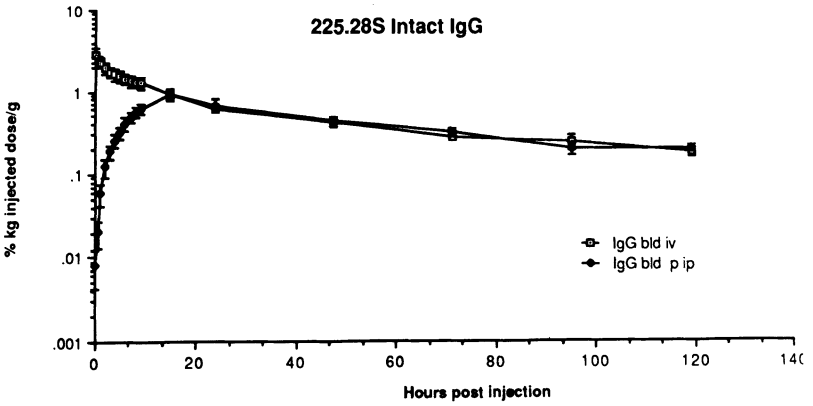

Figure 7. Clearance of intact IgG following IV or IP delivery.

techniques from the peritoneal fluid and blood [42]. These studies indicated that in this system much higher IP fluid levels were achieved by the IP delivery route than by the IV route (Figure 7), at least in the first hours following IP injection in a 20 cc volume (corresponding to over 3 l in humans). These studies also showed that the IP fluid was relatively rapidly absorbed, with little residual fluid apparent at 15–24 hours after IP injection. Noteworthy is that at sacrifice the levels of radioantibody in normal tissues were comparable between the IP and IV routes (Table 2) [54].

The regional delivery advantage to the peritoneal cavity can be expressed

Table 2. Mean tissue levels of antibodies or fragments at sacrifice

	IgG		$F(ab')_2$		Fab		IgM[a] (FT166)	
	IP	IV	IP	IV	IP	IV	IP	IV
Liver	.0456 ± .0026	.0390 ± .0028	.0066 ± .0030	.0068 ± .0054	.0062 ± .00090	.0155 ± .0036	.0394 ± .0208	.0196 ± .0164
Kidney	.1167 ± .0073	.1011 ± .0091	.0078 ± .0012	.0054 ± .0025	.1158 ± .0275	.1637 ± .0272	.1462 ± .0784	.0454 ± .0034
Heart	ND	ND	ND	ND	.0010 ± .0001	.0014 ± .0002	.0017 ± .0005	ND
Lung	.2470 ± .0069	.2580 ± .025	.0100 ± .0027	.0089 ± .0041	.0021 ± .00025	.0025 ± .0003	.0032 ± .0010	.0010 ± .0004
Diaphragmatic muscle[b]	.0689 ± .0078	.0276 ± .0029	.0047 ± .0030	.0009 ± .0004	.0113 ± .0016	.0010 ± .0001	.0711 ± .0350	.0013 ± .0001
Skeletal muscle	.0177 ± .0020	.0158 ± .0018	.0009 ± .0002	.0007 ± .0004	.0006 ± .0002	.0008 ± .0003	BKG	.0052 ± .0053

Data shown are means of three to five animals and represent time-corrected % kg/dose/g at 5 days postinjections.

[a] 7 days postinjection.

[b] Diaphragmatic muscle radioantibody levels are significantly greater following intraperitoneal delivery ($p < .001$) than IV delivery for all antibodies.

in two ways: Rd_1 is the area under the curve (AUC) for the peritoneal fluid/area under the curve for the blood (following IP antibody delivery). Rd_1 reflects the safety advantage IP delivery would have over IV delivery (i.e., assuming toxicity is due to a systemic effect, how much toxicity would be spared the whole body). Rd_2 is Rd_1/AUC IP (post IV delivery)/AUC blood (post IV delivery) and, in contrast, reflects how much more radioactivity the peritoneal cavity receives for a given dose of antibody given IP as compared with IV [54].

The true values of Rd_1 and Rd_2 are quite difficult to determine to infinity, as the peritoneal fluid (cavity) can be hard to sample at times many hours post IP antibody injection, particularly if small injection volumes are used. Our preliminary studies of an IgG_{2a} antibody in rats indicated an Rd_1 to 9 hours of 7.85, to 15 hours of 4.21, and an Rd_2 to 10 hours of about 10 [42,54]. Tissue levels of intact antibody at 5 days post IV or IP injection are virtually identical, however, indicating that antibody has escaped from the peritoneal cavity and reached systemic structures. The blood levels of the IgG_{2a} following IP and IV delivery are shown in Figure 8) and indicate the merging of these values at all times post 24 hours of injection in these normal rats. Our preliminary data indicate that the regional delivery advantage for Fab fragments is considerably superior to that of IgGs [Rd 0–9 hours for Fab 13.6 vs. IgG 7.85; ($p < .005$) (Figure 9)]. It also appeas that some, but not all, IgMs have a comparable delivery advantage over Fab [54].

Recently Ward et al. have reported a similar study on the clearance of monoclonal antibody from the peritoneal cavity and blood of normal mice [55]. They studied the clearance of radiolabeled UJ13A and HMFG2 IgG_1s following IV or IP injection. The IP injection volume used was 3 cc (extrapolating to 10.5 l by weight in humans). They reported that for both antibodies the blood levels reached following IP administration were less than those following IV administration at essentially all times. In these normal animals peak blood levels following IP administration occurred 3 days

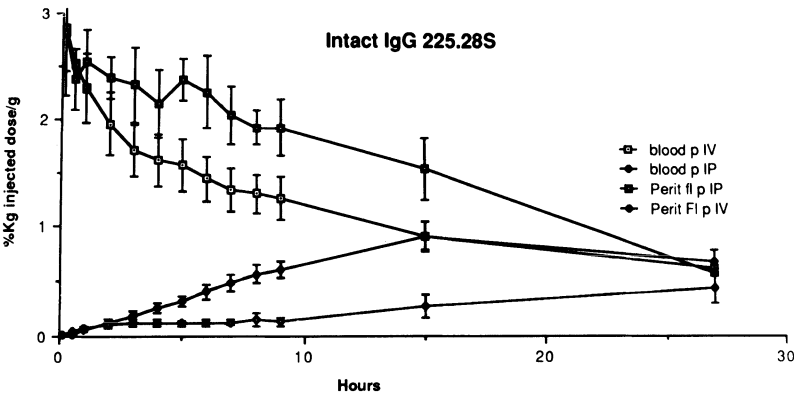

Figure 8. Blood levels of IgG following IP or IV delivery. Note similarity of levels post 15 hours.

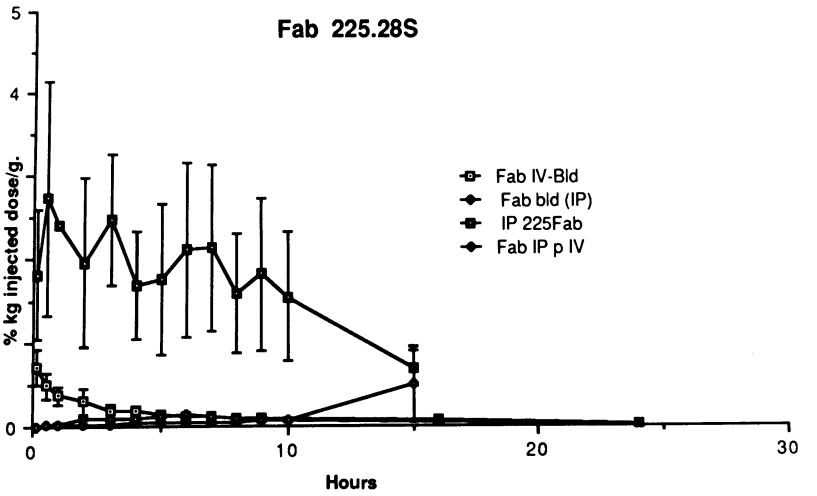

Figure 9. IP and IV injections of Fab demonstrate very low levels of Fab in blood following IP administration.

following injection. In other studies in the same manuscript, peak blood levels of antibody following IP injection to tumor-bearing animals occurred variably from 20 to 48 hours. It is clear from our data and theirs that peak levels in the blood stream occur later following IP than IV injection, though our peak blood levels in rats following IP injection were earlier than those reported by Ward.

In the normal mice studied by Ward et al., apparently lower levels of iodinated antibody (though this was not treated statistically) were found in the blood stream of animals following IP injection than following IV injection, at late as well as at early time points. This observation is at variance with our experience in normal rats and mice with a variety of antibodies and fragments, where while initial blood levels are far lower for IP-injected antibody than for IV, at later times the blood levels are nearly identical [54]. The reason for this discrepancy is unclear. It is conceivable that the antibodies they used deiodinate more by IP delivery than by IV or that the intra-

Table 3. Absorption rate constants from the peritoneal cavity in normal rats

Antibody	Absorption Rate Constant ± SEM (hr^{-1})
Intact 225.28S	.098 ± .027
$F(ab')_2$ 225.28S	.118 ± .017
Fab 225.28S	.153 ± .022
IgM FT166	.157 ± .055
IgM BA-1	.141 ± .028

There is no satistically significant difference among the mean absorption rate constant for the above reagents.

peritoneal injections were not completely IP; however, the explanation for this variance in normal animals is unclear and warrants additional study. It is also conceivable that the later peak blood values seen by Ward were due to the large amount of fluid the antibodies were administered IP, relative to the animals' size, though this also needs additional study.

Extensive studies have recently been reported by us regarding the pharmacokinetics of antibody and fragment clearance from the peritoneal cavity in normal rats and mice, and indicate that the Fab fragment has a somewhat higher regional delivery advantage than intact IgG. Somewhat surprising was the observation that the small Fab and very large IgMs had similar rates of egress from the peritoneal cavity (Table 3). This indicates that the rate of systemic clearance, and not the rate of peritoneal cavity clearance, will be the more important determinant of the regional delivery advantage to the peritoneal cavity. These pharmacokinetic data will need additional study in animal models of intraperitoneal carcinomatosis.

These data (the similar uptake rates for a variety of antibodies of different molecular weights) suggest that a significant route of antibody clearance from the peritoneal cavity is via a somewhat size-independent pathway. This clearly needs additional study, but the lymphatic system, particularly that of the diaphragm, would seem to be a reasonable possibility. The importance of lymphatic drainage of the peritoneal cavity, even for small molecules, has been underscored by the work of Rubin, who showed that in eviscerated animals the rate of clearance of small molecules was only slowed slightly compared with those animals with most of their viscera remaining [56]. This suggests that the lymphatics and the abdominal wall are very important to the absorption of protein-containing fluid and probably antibody molecules from the peritoneal cavity. The quantitative autoradiographic studies of Flessner et al. indicate that there is considerable transdiaphragmatic flux of I-125 albumin, but also that there is considerable entry of that substance into the anterior abdominal wall. In their study, the depth of penetration of I-125 albumin into the anterior abdominal wall was at least 2.5 mm, which is far greater than that into the gut [57]. One would predict similar behavior for radioantibodies.

Animal tumor-bearing systems

In animals, the IP route of antibody delivery to IP tumors has shown superiority over IV in several studies. We have demonstrated in an intraperitoneal model of human ovarian cancer that higher absolute and relative tumor uptake of specific antibody is seen in IP tumor foci following IP versus IV delivery at 4 hours post antibody injection (Figure 10) [54,58]. The absolute and relative uptake of the tumor foci by the two routes becomes comparable by 24 hours postinjection and at subsequent time points, indicating that the bulk of the IP delivery advantage is within the first 24 hours

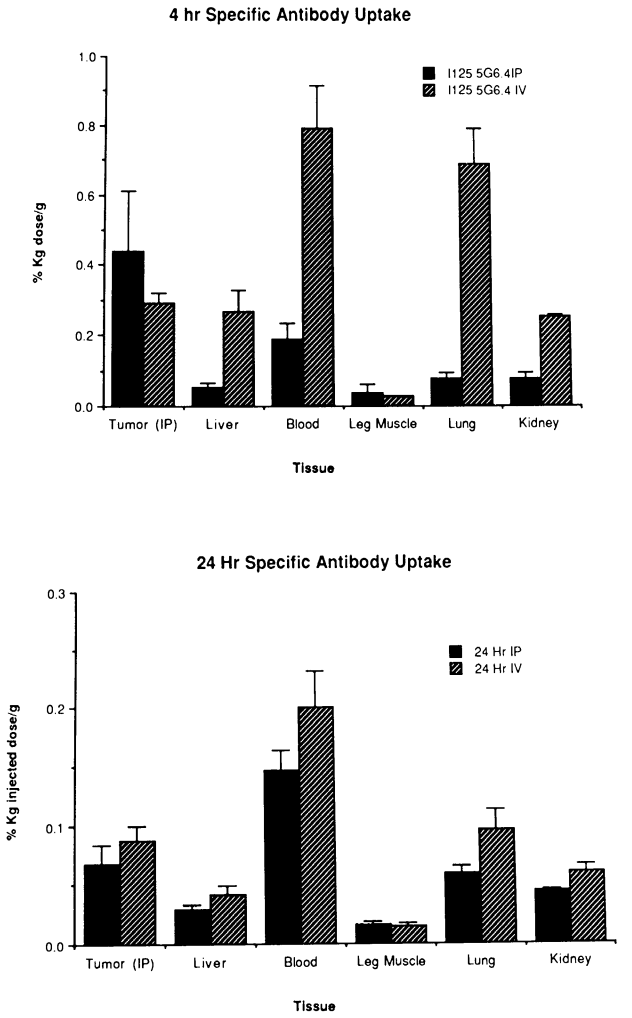

Figure 10. A, B: Tumor and nontumor uptakes following IP or IV delivery. Note that IP tumor uptakes are higher and nontarget tissue uptakes lower following IP delivery (A). By 24 hours (B), the levels in all tissues are comparable by IP or IV delivery.

of antibody injection Tumor/nontumor ratios are higher at earlier time points as well. These studies were done in animals with moderate bulk ovarian carcinoma. While our observation achieves statistical significance, the absolute antibody uptake in the tumor foci following IP injection at 4 hours is only slightly greater than that following IV administration. More dramatic is how much superior the tumor/blood ratio is at this time. With time, there is considerable absorption of the antibody systemically, and at 24 hours and beyond no major difference is seen between the two delivery routes [54,58].

Prior to our establishing the HTB77IP3 tumor line, we evaluated the delivery of another anti-ovarian cancer antibody to large IP or EP ovarian tumor xenografts at 7 days postinjection [59]. In this pilot study, there was no advantage to the IP delivery route for the large IP tumor as compared with the extraperitoneal tumor at the injection site.

Ward has recently reported somewhat similar experiments in several xenograft systems of ovarian cancer at early passage [55]. In one series of experiments, they compared IP and IV delivery to IP xenografts of ovarian cancer. They found no clear advantage to the IP or IV route in this study, even when examining the 2-hour postinjection time point. This series was somewhat different from other experiments they had reported, in that peak blood levels following IP injection were seen at 24 hours after injection, not at 48–72 hours, as seen in other studies, and in that the blood levels in the animals following IV injection were virtually constant over a 4-day period (not dropping as rapidly as expected). In these studies, they used the HMFG2-specific antibody. These results, though not statistically compared directly, appear to indicate that the IP and IV delivery routes were quite comparable in this xenograft system and that much of the antibody reaches the tumors via the blood stream, and not via direct binding to the peritoneal cavity. The size of the tumors is not stated in this study.

In the same article, in an ascites tumor system expressing the HMFG2 antibody, a clear delivery advantage is seen in IP ascites tumors with the IP as compared with the IV delivery routes [55]. At 2 hours post-injection, there was a tumor/blood ratio of 10:1 following IP delivery, as compared with one of .106:1 following IV delivery, a nearly 100-fold improvement, with over 10 times more absolute binding to the IP tumor cells with IP delivery than with IV. This delivery advantage decreased with time, however, so that it was only about twice that of IV delivery by 2–4 days. There also appeared to be less clearance of the HMFG2 antibody to the circulation following IP delivery, though this is somewhat hard to assess, as the nonspecific antibody blood levels were also quite low following IP injection in this tumor-bearing system. These latter data clearly support the superiority of IP over IV delivery for suspension tumors [55].

Human studies of IP antibody delivery for diagnostic purposes

Colon cancer

Paganelli et al. have briefly reported on their experience in colon cancer using the IP and IV routes, as has Colcher et al. [43] and Paganelli et al. [44]. Paganelli found, in 60 patients with colorectal cancer, that following IV injection with I-131 anti-CEA $F(ab')_2$ a detection rate of about 80% could be seen in documented lesions of colorectal cancer. Results were improved

by the use, in 20 of these patients, of I-131 anti-CEA antibody fragments IP. In patients given anti-CEA, IP lesions in several locations were better visualized following IP delivery: liver metastases (9/11 visualized IP) versus (5/11 IV), abdominal recurrences (17/17 visualized IP vs. 14/17 IV) and nodal recurrences (9/9 visualized IP vs. 7/9 IV). Tumor/background ratios, apparently determined by gamma counting, were significantly better by IP than IV administration (mean of 4.7 vs. 2.1) ($p < .001$). They also found that tumor could be seen in the liver without the use of background subtraction. The reason for the superior liver lesion visualization is somewhat unclear, as when dual isotope studies were conducted in patients with primary colon tumors that were removed and counted, it was seen that there was no difference in tumor/background uptake ratios between the two delivery routes. This, albeit limited, data supports the concept that tumor must be accessible to the peritoneal fluid to achieve a superior tumor/nontumor ratio following IP delivery, but suggests that such tumors do benefit from IP antibody delivery.

Colcher et al. recently reported their experience in humans with the B72.3 antibody given IP to 10 patients with colon cancer [43]. In this series, they found that in certain instances more uptake was present in IP tumor foci following IP delivery than in IP tumor foci following IV delivery. In this series, 3 of 10 patients were found to have tumor by external scintigraphy following IP antibody delivery that were not detected by standard CAT scans or x-ray. In patients with larger tumor burdens, a significant fraction of the injected dose was found to reach the tumor (up to 40%). In four of the patients, a dual-label approach was used, so that I-131 B72.3 was given IP and I-125 B72.3 was given IV at equal milligram doses. Surgery was performed at 4–7 days post antibody injection. In these patients, it was found that IP delivery was two times better than IV in 35 of 55 carcinoma lesions, equivalent in seven, and two times less than IV in 13 lessions. On pathologic examination, it was found that "peritoneal implant lesions" were much more commonly associated with high antibody uptake following IP administration of antibody than were nonimplant lesions. While the number of patients involved was small, and in only one of the patients were there both peritoneal implant and non-peritoneal-implant lesions, these data strongly support the concept that IP delivery is rational for accessible peritoneal implant lesions, but that it may not be a good method of delivery for nonaccessible lesions (such as hematogenously borne metastases, lymph node metastases, or subserosal local recurrences, which in many cases had more antibody delivered following IV than IP delivery. This latter point regarding blood-borne delivery is supported by the fact that blood levels in patients given B72.3 antibody IP peak at 2–3 days postinjection at levels one-third those seen at the maximum following IV administration. There also appears to be a faster clearance from the high-antigen-expressing patients, suggesting that the formation of immune complexes, possibly in the peritoneal cavity, may have a major impact on the amount of radioantibody that reaches the blood stream [43].

Ovarian cancer

While ovarian cancer has been treated by IP radioimmunotherapy (as will be discussed shortly), recently quantitative studies of the distribution in vivo following IP injection of imaging doses of radiolabeled monoclonal antibody reactive with human milk fat globule have become available. Ward and his coinvestigators reported on the IP administration of the HMFG2 antibody in 18 patients with a past history of ovarian cancer [60]. A variety of time points for sampling, ranging from 4 hours to 168 hours from injection to surgery, were studied. The majority (13 of 17 with tumors at surgery) had bulky disease at operation. In ten of these patients dual-label studies with specific and nonspecific antibody were performed, and it was clearly shown that specific antibody uptake at the tumor was due to antibody specificity. In eight of the patients studied, dual-label studies with the specific antibody HMFG2 labeled with I-131 (apparently given IP) and I-125 (apparently given IV), showed that consistently more activity reached the solid tumor foci by the IV as compaed with the IP route (Table 4).

Of note was the rapid drop in tumor uptake from the IP tumors at 4–18 and 36 hours. Tumor/blood ratios were considerably superior (estimated 4:1 IP vs. .3:1 following IV delivery) at 4 hours for the IP route as compared with the IV route, though the advantage in tumor/blood ratios eventually disappeared by 36 hours postinjection. The high early tumor/blood ratios are due to the fact that little radioantibody had yet reached the blood stream. Eventually, blood levels of antibody peak at about 60 hours following IP antibody injection. These investigators also found that markedly less absolute uptake of the HMFG2 antibody was achieved in ovarian tumors following IP delivery than IV. There data also did not show a clear relationship in antibody uptake to tumor size. From their data it does not appear that the HMFG2 antibody given IP is well retained at solid IP tumor foci in these patients, who generally had bulky disease (though three patients had very small disease foci). Not stated is whether immune complexes were formed in the peritoneal cavity that may have diverted antibody from reaching its target cells. This is a potential problem, though the explanation for the poor uptake at the tumor site could be due to multiple etiologies, with the most probable being only a limited amount of antigen-bearing tumor being exposed to the radioantibody in the peritoneal fluid. Alternatively, the affinity of this antibody on the stability of the antigen-antibody interaction could be responsible.

The results Ward reports in the patients with ascites were considerably more encouraging, however, in that the IP route of delivery provided a regional delivery advantage of 4 to 71-fold over the IP route, with ascites/blood ratios of up to 448:1. These latter numbers indicate the likelihood for successful therapeutic administration. Our initial clinical work with human ovarian cancer using the 5G6.4 antibody given IP or IV suggests that the IP route of delivery is preferable to the IV, at least pharmacokinetically. Additional study is clearly indicated [67].

Table 4. Comparison of HMFG2 localization after IV and IP injection

Time Studied (h)	No. Patients	Normal tissue			Blood (% Injected Activity/g)		Solid Tumor			Ascites		
		No. Samples	% Injected Activity/g				No. Samples	% Injected Activity/g		No. Samples	% Injected Activity/g	
			IVI[a]	IPI	IVI	IPI		IVI	IPI		IVI	IPI
4	4	9	0.0024 ± 0.0007	0.0012 ± 0.0003	0.0102 ± 0.0051	0.0004 ± 0.0001	20	0.0029 ± 0.0004	0.0016 ± 0.0005	6	0.0121 ± 0.0072	0.1792 ± 0.0032
18	2	10	0.0026 ± 0.0006	0.0005 ± 0.0001	0.0150	0.0014	11	0.0029 ± 0.0005	0.0005 ± 0.0001	8	0.0036 ± 0.0005	0.2560 ± 0.1428
36	2	2	0.0010	0.0001	0.0045	0.0003	8	0.0014 ± 0.0003	0.0001 ± 0.0001	4	0.0095 ± 0.0035	0.0363 ± 0.0132

[a] IVI, IV; IPI, IP. From [60].

Radioimmunotherapy

Therapy of malignancies by the IP route has been undertaken by several investigators. These studies in humans have been encouraging, yet do not clearly define whether the IP route of delivery is superior to the IV route. To evaluate this issue, we have studied, in a preliminary fashion, radioimmunotherapy by the IP or the IV route in a nude mouse model of intraperitoneal human colon cancer, in which 1 million LS174T colon cancer cells are innoculated IP in .5 cc of media. These studies have shown significantly ($p < .005$) prolonged survival for animals treated with 450 μCi of I-131 5G6.4 antibody given IP versus the same reagent IV (67.3 ± 7.9 days vs. 43.8 ± 3.9 days). Saline treatment alone resulted in survival of just 37.5 ± 1.9 days. Both of the survivals are superior to those with the same dose of nonspecific antibody by the two routes. These animal studies support the concept that intraperitoneal antibody delivery is superior to IV delivery in the treatment of IP ascites colon cancer. In these studies, the treatments were conducted 1 hour after the cells were given. Whether this effect would persist with treatment administered later is under further study. [61]

Human therapeutic studies by the IP route were first reported by Epenetos et al. [15]. In their first therapeutic study, they reported treating one patient by the IP route for ovarian cancer, one by administration of antibody intrapericardially, and one by intrapleural antibody injection. In all three cases, a normalization of fluid cytology or a shrinkage of tumor mass on CT was seen. Estimated radiation doses of 5000–7000 cGy to the malignant sites and of only 20–2000 cGy to the whole body were reported. More recently, this group has reported on the treatment of 24 patients with persistent epithelial ovarian cancer after chemotherapy and/or radiotherapy. They used four different antibodies, in nine different combinations, reactive with ovarian-tumor-associated antigens. Eight of the patients had large volume disease (> 2 cm diameter) and did not respond to treatment. Sixteen patients had small volume (< 2 cm) disease at the time of treatment with radioantibody. Seven of the patients had no response, but of the nine initial responders, four patients remain alive 6 months to 3 years after treatment. Three of the four had doses of over 140 mCi, while the fourth had a dose of only 20 mCi. Thus, there is a suggestion that higher doses are superior to low doses [62].

The 'gross estimates' of tumor dosimetry provided in patients with small-volume disease < 2 cm in size has suggested that 150 mCi of antibody could deliver > 8000 cGy to tumor cells and only 600 cGy to the bladder [62]. Clearly, this dosimetry would appear to be an area of some controversy, as the data of Ward would suggest this to be an optimistic estimate of tumor dose, at least for the HMFG2 antibody [60].

Epenetos et al. have also recently reported on the treatment of a patient with malignant ascites whose cells reacted with the AUA1 and HMFG2

antibodies [62]. Initially treatment with 48.6 mCi of I-131 AUA1 showed a reduction in ascites, but the cytology was still positive for cells reactive with HMFG2 (though not AUA1). Retreatment with 39.0 mCi of HMFG2 resulted in a lack of recurrence of the ascites. This report emphasized the need for using antibodies reactive with antigens on all cells and suggests the specificity of the radioimmunotherapeutic approach. The data from the 24 patients does not definitively support the use of the antibody cocktail, however [62]. Why good therapeutic results have been seen in some patients treated with the HMFG2 antibody, given the poor absolute tumor uptakes seen by Ward, is uncertain. Certainly, IP antibody treatment would appear to be most rational in the treatment of ascites. Other investigators are beginning to use this method as a therapeutic approach in ovarian cancer [63]. It is impossible to meaningfully assess the response data until controlled studies are done, however, relatively little toxicity has been seen with this therapeutic approach.

A major caveat in the use of intraperitoneally administered radioantibodies for diagnosis or treatment is that the radioantibody must distribute evenly throughout the peritoneal cavity, or at least to all tumor foci. In addition, it is probable that the technique will be most useful only for thin tumors, though the exact depth of penetration of radioantibodies into IP tumors is unclear at present. The work of Epenetos and Ward certainly suggest that high bulk tumor will not benefit from I-131 treatment with IP monoclonal antibodies. What is clear is that with bulky tumors, the uniformity of distribution of radionuclide given IP can be severely compromised by prior surgery or by bulk tumor [21]. A knowledge of the normal patterns of intraperitoneal fluid distribution in patients with tumor will be essential, particularly for treatment. Certainly, it would seem logical to expect that if a tumor has grown extensively in the peritoneal cavity, the access of peritoneal fluid to the tumor would be limited. This problem of nonuniformity of fluid distribution may be a major one for this route of treatment. Our experience with intraperitoneal antibody delivery suggests that nonuniform distribution is particularly problematic and common in patients who have had multiple surgical procedures, the very patients we are seeing for potential treatment. It has been clearly shown that for P-32 treatment, a loculation of the injection dose may result in local toxicity [28].

New approaches to enhance IP delivery of antibodies to tumors

While IP delivery seems rational for small IP tumor foci and ascites, this delivery method does not totally spare the rest of the body from toxicity. While tumors may slow the egress of antibody from the peritoneal cavity, antibody given IP eventually reaches the circulation. This systemic antibody can cause toxicity, and in normal nude mice the toxicities for similar doses of antibodies given by the IP or IV routes are quite comparable [64].

If it were possible to deliver antibody intraperitoneally, and then rapidly clear any antibody from the blood stream once it appears there, it would probably be possible to limit systemic toxicity (and potentially allow for an increase in dose to the peritoneal cavity and tumor). We have described a method to accelerate the systemic clearance of intact antibodies following intraperitoneal delivery in which polyclonal anti-mouse antibody is given systemically. This results in the formation of immune complexes that are cleared from the blood stream more rapidly than intact antibody [65]. We have evaluated a modification of this approach in normal rats. In these studies, I-125 UPC-10, a murine IgG2a, was given intraperitoneally to two groups of rats. In one group, saline was administered IV 6 hours later. In the other group, a dose of polyclonal anti-mouse antibody was given. Blood levels of the radioantibody were far lower in the animals given the polyclonal anti-mouse antibody systemically than in the animals given saline IV. The level of radioactivity in normal tissues was also considerably lower for the animals given the polyclonal anti-mouse antibody. No difference in IP fluid levels of radioantibody were seen, and the net result was a considerable

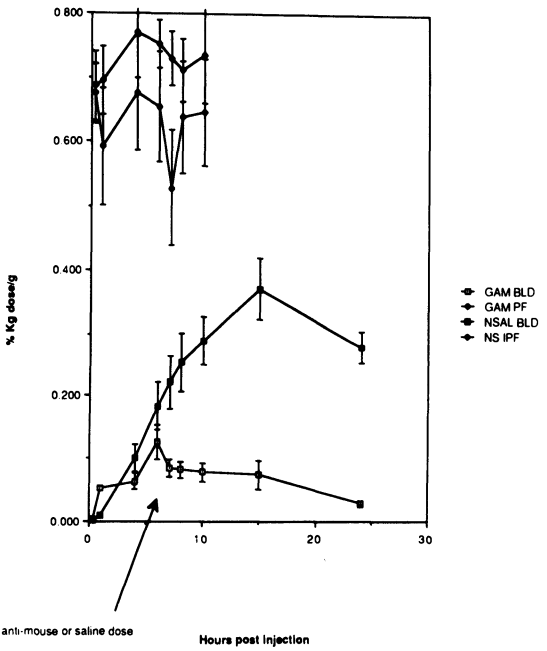

Figure 11. Time-activity curve of blood or peritoneal fluid radio-activity levels (% kg-dose/g) with or without unlabeled IV anti-mouse antibody treatment at 6 hours post intraperitoneal I-125 UPC-10 delivery. Note the sharp and persistent decline in UPC-10 blood levels following IV polyclonal anti-mouse antibody administration. This is in contrast to the lack of change in peritoneal fluid radioantibody levels. Thus there is a significant enhancement of Rd for the unlabeled goat anti-mouse antibody-treated group ($p < 0.025$). Plots reflect mean of seven animals/group ± SEM.

improvement in the regional delivery advantage to the peritoneal cavity. This is clearly shown in Figures 11 and 12. The technique should be equally useful in tumor-bearing animals, but this will need additional study.

Another technique that appears promising is the use of peritoneal lavage following intraperitoneal antibody administration. This method, which we have recently evaluated in a preliminary fashion in an animal model of human ovarian carcinomatosis, attempts to cause antibody to reach and bind to the intraperitoneal tumor rapidly, but then removes the unbound antibody from the peritoneal cavity, thus limiting systemic exposure. In brief, specific antibody is injected intraperitoneally, then after a dwell of 2–6 hours is exhaustively washed from the peritoneal cavity. In our studies, sacrifice was at 24 hours post antibody injection IP. Using this technique in nude mice with ovarian cancer, several-fold increases in IP tumor/background ratios have been achieved, which are far better than if no lavage was used. The phenomenon is due to antibody specificity, as nonspecific antibody will simply be washed away from tumors using such a manipulation. This simple technique will almost certainly undergo more extensive evaluation in humans in the next several years. An example of the improvements in tumor/background ratios following lavage versus no lavage is shown in Figure 13. Note that the improvement in tumor/background ratios appears more marked with lavage at 2 rather than at 6 hours postinjection [66,67].

While the major isotope used for IP delivery studies of antibodies has been

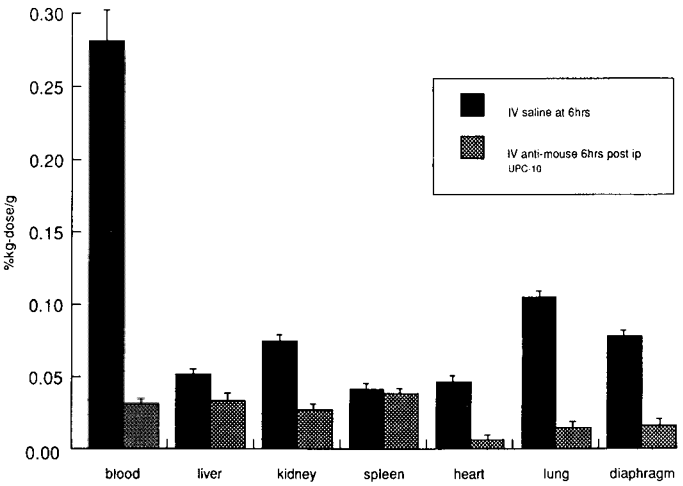

Figure 12. Tissue uptakes of radiolabeled UPC-10 (mean ± SEM of seven animals/group) 24 hours post I-125 UPC-10 injection IP, and 18 hours post IV polyclonal goat anti-mouse or normal saline injection. Note the significantly lower ($p < 0.005$) tissue levels in the anti-body-treated group (except for the spleen, where there is no statistically significant difference between saline- and anti-mouse-treated groups). The thyroids in the saline groups (not shown) had less radioactivity per gram than did those of the animals treated with polyclonal goat anti-mouse antibody.

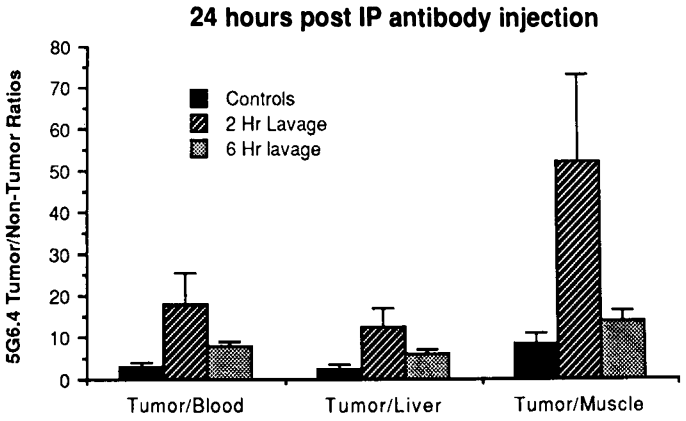

Figure 13. Peritoneal lavage is shown to considerably enhance tumor/nontumor levels (see text). The effect is more pronounced at 2 hours than at 6 hours postinjection.

iodine, it is certainly possible that other isotopes, such as alpha or pure beta emitters, will be of utility in intraperitoneal delivery. Candidate isotopes include Y-90, P-32, and certain alpha emitters such as ^{212}Bi or ^{211}At. This area needs considerable study, as betas emitters, though desirable for tumor treatment, will be potentially more dangerous to the bowel. The availability of generator systems for these isotopes will certainly make their evaluation in vivo a realistic expectation in the coming years [68,69].

Conclusions

Intraperitoneal delivery of radiolabeled antibodies to the peritoneal space is a pharmacokinetically rational technique, particularly for antibody fragments. The technique delivers more antibody to IP ascites tumors than IV delivery. In our animal study, somewhat more absolute and considerably more relative delivery of antibody to solid tumors has been seen in the first hours following IP antibody injection. In human studies, higher relative delivery of radioantibody to IP tumor foci has been seen in the first hours following IP administration, though results in patients with colon and ovarian cancers are somewhat at variance in terms of the benefit of the IP delivery route. It seems clear, however, that large IP tumors, or those not accessible by peritoneal fluid, will not be benefitted by intraperitoneal antibody delivery, and in fact will receive the bulk of the tumor-bound antibody via the blood stream.

Radioimmunotherapeutic studies in experimental colon cancer show the IP route to be superior to the IV route, though the cells being treated are in suspension. Clinical therapeutic studies suggest the IP route will be quite useful, particularly for low bulk disease and ascites, though controlled studies are needed to allow comparisons with other therapeutic methods. Enhance-

ments in the relative delivery of radiolabeled antibody to the peritoneal cavity have been achieved through the use of polyclonal anti-mouse antibodies and via peritoneal lavage. While considerable study is needed, it is certain that the IP route of antibody delivery will assume increasing importance in the diagnosis and treatment of a variety of intraperitoneal cancers in the coming years.

Acknowledgments

This work was supported in part by NIH grants CA41531 and CA33802. The valuable contributions of O. Geatti, J. Barrett, J. Wagner, M. Liebert, S. Fisher, P. Sherman, G. Jackson, M. Strnat, C. Piko, J. Wissing, S. Kronberg, L. Laino, J. Roberts, K. Hopkins, R. Schmidt, and M. Curro to this work are greatly appreciated.

References

1. Goodwin, D.A. (1987) Pharmacokinetics and antibodies. J. Nucl. Med. 28:1358–1362.
2. Wahl, R.L., Parker, C.W., and Philpott, G.W. (1983) Improved radioimaging and tumor localization with monoclonal $F(ab')_2$. J. Nucl. Med. 24:316–325.
3. Colcher, D., Zalutsky, M., Kaplan, W., Kufe, D., Austin, F., and Schlom, J. (1983) Radiolocalization of human mammary tumors in athymic mice by a monoclonal antibody. Cancer Res. 43:736–742.
4. Buchegger, F., Haskell, C.M., Schreyer, M., Scazziga, B.R., Randin, S., Carrel, S., and Mach, J. (1983) Radiolabeled fragments of monoclonal antibodies against carcinoembryonic antigen for localization of human colon carcinoma grafted into mice. J. Exp. Med. 158: 413–427.
5. Begent, R.H., Keep, P.A., Green, A.F., et al. (1982) Liposomally entrapped second antibody improved tumor imaging with radiolabeled (first) anti-tumor antibody. Lancet 1:1047–1048.
6. Sharkey, R.M., Primus, F.J., and Goldenberg, D.M. (1985) Second antibody clearance of radiolabeled antibody in cancer radioimmunodetection. Proc. Natl. Acad. Sci. USA 81: 2843–2846.
7. Goldenberg, D.M., DeLand, F., Kim, E., Bennett, S., Primus, F.J., van-Nagel, J.R., Estes, N., DeSimone, P., and Rayburn, P. (1978) Use of radiolabeled antibodies to carcinoembryonic antigen for the detection and localization of diverse cancer by external photoscanning. N. Engl. J. Med. 298:1384–1386.
8. Wahl, R.L., Tuscan, M.J., and Botti, J.M. (1986) Dynamic variable background subtraction: A simple means of displaying radiolabeled monoclonal antibody scintigraphy. J. Nucl. Med. 27:454–548.
9. Early, J., Schroff, R., Abrams, P., Kasina, S., Srinivasan, A., Reno, J., Woodhouse, C., and Nelp, W. (1987) Imaging of known and occult metastatic melanoma with Tc-99m monoclonal antibody. J. Nucl. Med. 28:573.
10. Epenetos, A.A., Snook, D., Durbin, H., Johnson, P.M., and Taylor-Papadimitriou, J. (1986) Limitations of radiolabeled monoclonal antibodies for localization of human neoplasms. Cancer Res. 46:3183–3191.
11. Wahl, R.L., Liebert, M., and Wilson, B.S. (1986) The influence of radiolabeled monoclonal antibody dose on tumor uptake of radiolabeled antibody. Cancer Drug Deliv. 3:243–249.

12. Meyers, M.A. (1976) In: *Dynamic Radiology of the Abdomen: Normal and Pathologic Anatomy*. New York: Springer-Verlag, pp. 1–110.
13. DeLand, F.H., Kim, E.E., and Goldenberg, D.M. (1980) Lymphoscintigraphy with radionuclide-labeled antibodies to carcinoembryonic antigen. Cancer Res. 40:2997–3000.
14. Weinstein, J.N., Steller, M.A., Keenan, A.M., Covell, D.G., Key, M.E., Sieber, S.M., Oldham, R.K., Hwang, K.M., and Parker, R.J. (1983) Monoclonal antibodies in the lymphatics: Selective delivery to lymph node metastases of a solid tumor. Science 222: 423–426.
15. Hammersmith Oncology Group and the Imperial Cancer Reseearch Fund. (1984) Antibody-guided irradiation of malignant lesions: Three cases illustrating a new method of treatment. Lance 1:1441–1443.
16. Wahl, R.L., Geatti, O., and Fisher, S. (1985) Intraperitoneal delivery of monoclonal antibodies: Influence of class and fragmentation on kinetics and intraperitoneal dosing advantage. J. Nucl. Med. 26:114.
17. Dunnick, N.R., Jones, R.B., Doppman, J.L., Speyer, J., and Myers, C.E. (1979) Intraperitoneal contrast infusion for assessment of intraperitoneal fluid dynamics. Am. J. Radiat. 133:221–223.
18. Netter, F.H. (1962) Lower digestive tract — Part II. In: Oppenheimer, E. (ed.), *Digestive System*. CIBA, pp. 23–29.
19. Hollinshead, W.H. (1967) Thorax and abdomen. In: *Textbook of Anatomy*, 2nd ed. New York: Harper & Row, pp. 590–597.
20. Scatchard, G. (1949) The attractions of proteins for small molecules and ions. Ann. N.Y. Acad. Sci. 51:660–672.
21. Arnstein, N.B., Wahl, R.L., Cochran, M., and Gyves, J. (1987) Adenocarcinoma of the alimentary tract: Peritoneal distribution scintigraphy. Radiology 162:439–441.
22. Kaplan, W.D., Zimmermann, R.E., Bloomer, W.D., Knapp, R.C., and Adelstein, S.J. (1981) Therapeutic intraperitoneal P-32: A clinical assessment of the dynamics of distribution. Radiology 138:683–688.
23. Slosman, D., Forni, M., Townsend, D., Brioschi, P.A., Krauer, F., and Conath, A. (1985) SPECT study of the fluid distribution in the intraabdominal space during intraperitoneal treatment of ovarian cancer. Nucl. Med. Commun. 6:91–96.
24. Arnstein, N.B., Wahl, R.L., Cochran, M., and Gyves, J. (1987) Adenocarcinoma of the alimentary tract: Peritoneal distribution scintigraphy. Radiology 162:439–441.
25. Wahl, R.L., Gyves, J., Gross, B.H., Cochran, M., Juni, J.E., Arnstein, N.B., Lahti, D., and Ackermann, R.J. (1989) SPECT of the peritoneal cavity: Method for delineating intraperitoneal fluid distribution. Am. J. Roent. 152:1205–1210.
26. Muller, J.H. (1945) Uber die verwendung von kunstlichen radioaktiven isotopen zur erzielung von lokalisierten biologischen strahlenwirkungen. Experientia 1:199.
27. Goldie, H., and Hahn, P.F. (1950) Distribution and effect of colloidal radioactive gold in peritoneal fluid containing free sarcoma 37 cells. Proc. Soc. Exp. Biol. Med. 74:638.
28. Harbert, J.C. (1987) Adjunct therapy of peritoneal metastases using intraperitoneal radiocolloids. In: *Nuclear Medicine Therapy*. New York: Thieme Medical, pp. 109–127.
29. Hester, L.L., and White, L. (1969) Radioactive colloidal chromic phosphate in the treatment of ovarian malignancies. Am. J. Obstet. Gynecol. 103:911.
30. Hilaris, B.S., and Clark, D.G. (1971) The value of post-operative intraperitoneal injection of radiocolloids in early cancer of the ovary. Am. J. Roentgenology 112:749.
31. Boye, E., Lindegaard, M.W., Paus, E., et al. (1984) Whole body distribution of radioactivity after intraperitoneal administration of P-32 colloids. Br. J. Radiol. 57:395.
32. Currie, J.L., Bagne, F., Harris, C., et al. (1981) Radioactive chromic phosphate suspension: Studies on distribution, dose absorption, and effective therapeutic radiation in phantoms, dogs and patients. Oncology 12:193.
33. Clark, D.G., Hilaris, B., Rosussis, E., et al. (1973) The role of radiation therapy (including isotopes) in the treatment of cancer of the ovary: Results of 614 patients treated at Memorial

Hospital, New York, NY. Prog. Clin. Cancer 5:227.
34. Creasman, W.T., Disaia, P.J., Belssing, J., et al. (1981) Prognostic significance of peritoneal cytology in patients with endometrial cancer and preliminary data concerning therapy with intraperitoneal radiopharmaceuticals. Am. J. Obstet. Gynecol. 141:921.
35. Card, R.Y., Cole, D.R., and Henschke, U.K. (1960) Summary of ten years of the use of radioactive colloids in intracavitary therapy. J. Nucl. Med. 1:195.
36. Jackson, G.L., and Blosser, N.M. (1981) Intracavitary chromic phosphate (P-32) colloidal suspension therapy. Cancer 48:2596.
37. Kniseley, R.M., and Andrews, G.A. (1953) Pathological changes following intracavitary therapy with colloidal Au-198. Cancer 6:303.
38. Myers, C. (1984) The use of intraperitoneal chemotherapy in the treatment of ovarian cancer. Semin. Oncol. 11:275–284.
39. Dedrick, R., Myers, C., Bungay, P., et al. (1978) Pharmacokinetic rationale for peritoneal drug administration in the treatment of ovarian cancer. Cancer Treat. Rep. 62:1–11.
40. Casper, E.S., Kelsen, D.P., Alcock, N.W., and Lewis, J.L. (1983) IP cisplatin in patients with malignant ascites: Pharmacokinetic evaluation and comparison with the IV route. Cancer Treat. Rep. 67:235–238.
41. Order, S.E., Donahue, V., and Knapp, R. (1973) Immunotherapy of ovarian carcinoma: An experimental model. Cancer 32:573–579.
42. Wahl, R.L., Geatti, O., and Fisher, S. (1985) Intraperitoneal delivery of monoclonal antibodies: Influence of class and fragmentation on kinetics and intraperitoneal dosing advantage. J. Nucl. Med. 26:114.
43. Colcher, D., Esteban, J., Carrasquillo, J.A., Sugerbaker, P., Reynolds, J.C., Bryant, G., Larson, S.M., and Scholom, J. (1987) Complementation of intracavitary and intravenous administration of a monoclonal antibody (B72.3) in patients with carcinoma. Cancer Res. 47:4218–4224.
44. Paganelli, G., Riva, P., Sarti, G., Tison, V., Cacciaguerra, G., Fiorentini, G., Moscatelli, G., Benini, S., and Agostini, M. (1984) Intraperitoneal versus intravenous injection of radiolabeled monoclonal antibodies in patient with colorectal carcinoma. Br. J. Cancer 54:542.
45. Ward, B.G., Mather, S.J., Hawkins, L.R., Crowther, M.E., Shepherd, J.H., Granowska, M., Britton, K.E., and Slevin, M.L. (1987) Localization of radioiodine conjugated to the monoclonal antibody NMFG2 in human ovarian carcinoma: Assessment of intravenous and intraperitoneal routes of administration. Cancer Res. 47:4719–4723.
46. Young, R.C., Fuks, Z., Knapp, R.C., and DiSaia, P.J. (1985) Cancer of the ovary. In: DeVita, V.T., Hellman, S., and Rosenberg, S.A., (eds.), *Cancer: Principles & Practice of Oncology*, 2nd ed. Philadelphia: J.B. Lippincott, pp. 1083–1117.
47. Torres, I.J., Litterst, C.L., and Guarino, A.M. (1978) Transport of model compounds across the peritoneal membrane in the rat. Pharmacology 17:330–340.
48. Kirano, K., and Hunt C.A. (1985) Lymphatic transport of liposome-encapsulated agents: Effects of liposome size following intraperitoneal administration. J. Pharmaceut. Sci. 74: 915–921.
49. French, J.E., Florey, H.W., and Morris, B. (1960) The absorption of particles by the lymphatics of the diaphragm. Q. J. Exp. Biol. 45:88–103.
50. Feldman, G.B., and Knapp, R.C. (1974) Lymphatic drainage of the peritoneal cavity and its significance in ovarian cancer. Am. J. Obstet. Gynecol. 119:991–994.
51. Feldman, G.B., Knapp, R.C., Order, S.E., and Hellman, S. (1972) The role of lymphatic obstruction in the formation of ascites in murine ovarian carcinoma. Cancer Res. 32: 1663–1666.
52. Coates, G., Bush, R.S., and Aspin, N. (1973) A study of ascites using lymphoscintigraphy with Tc-99m sulfur colliod. Radiology 107:577–583.
53. Daugirdas, J.T., Ing, T.S., Gandhi, V.C., Hano, J.E., Chen, W.T., and Yaun, L. (1980) Kinetics of peritoneal fluid absorption in patients with chronic renal failure. J. Lab. Clin. Med. 95:351–361.

54. Wahl, R.L., Barrett, J., Geatti, O., Liebert, M., Wilson, B.S., Fisher, S., and Wagner, J.G. (1988) Intraperitoneal delivery of radiolabeled monoclonal antibodies: Studies on the regional delivery advantage. Cancer Immunol. Immunother. 26(3):187–201.
55. Ward, B.G., and Wallace K. (1987) Localization of the monoclonal antibody HMFG after intravenous and intraperitoneal injection into nude mice bearing subcutaneous and intraperitoneal human ovarian cancer xenografts. Cancer Res. 47:4714–4718.
56. Rubin, J., Jones, Q., Planch, A., Rushton, F., and Bower, J. (1986) The importance of the abdominal viscera to peritoneal transport during peritoneal dialysis in the dog. Am. J. Med. Sci. 292:203–208.
57. Flessner, M.F., Fenstermacher, J.D., Blasberg, R.G., and Dedrick, R.L. (1985) Peritoneal absorption of macromolecules studies by quantitative autoradiography. Am. J. Physiol. 248:H26–H32.
58. Wahl, R.L., Liebert, M., Laino, L., and Fisher, S. (1987) Intraperitoneal ovarian carcinoma: IP delivery of specific monoclonal antibodies is superior to IV delivery. J. Nucl. Med. 28:651–652.
59. Wahl, R.L., and Piko, C. (1985) Intraperitoneal (IP) delivery of radiolabeled monoclonal antibody to IP-induced xenografts of human ovarian cancer. Proceedings Am. Assoc. Cancer Res. 26:298.
60. Ward, B.G., Mather, S.J., Hawkins, L.R., Crowther, M.E., Shepherd, J.H., Granowska, M., Britton, K.E., and Slevin M.L. (1987) Localization of radioiodine conjugated to the monoclonal antibody HMFG2 in human ovarian carcinoma: Assessment of intravenous and intraperitoneal routes of administration. Cancer Res. 47:4719–4723.
61. Wahl, R.L., Liebert, M., Fisher, S., and Boland, R. (1987) Enhanced radioimmunotherapy of intraperitoneal human colon cancer xenografts by intraperitoneal monoclonal antibody delivery. Proc. Am. Assoc. Cancer Res. 28:438.
62. Epenetos, A.A., Munro, A.J., Stewart, S., Rampling, R., Lambert, H.E., McKenzie, C.G., Soutter, P., Rahemtulla, A., Hooker, G., Sivolapenko, G.B., Snook, D., Courtenay-Luck, N., Dhokia, B., Krausz, T., Taylor-Papadimitriou, J., Durbin, H., and Bodmer, W.F. (1987) Antibody-guided irradiation of advanced ovarian cancer with intraperitoneally administered radiolabeled monoclonal antibodies. J. Clin. Oncol. 5:1890–1899.
63. Ashorn, R., Ashorn, P., Punnonen, R., Poyhonen, L., Turjanmaa, V., Koskinen, M., Helle, M., Uusitalo, A., Pystynen, P., and Krohn, K. (1985) The use of radiolabeled monoclonal antibodies to human milk fat globule membrane antigens in antibody-guided tumour imaging, and administration of therapeutic dose of labeled antibody in wide-spread ovarian carcinoma. Ann. Chir. Gynaecol. 74(Suppl. 197):5–10.
64. Wahl, R.L., Liebert, M., Fisher, S., and Laino, L. (1987) The toxicity of radiolabeled antibodies. J. Nucl. Med. 28:684.
65. Wahl, R.L., and Fisher, S. (1987) Intraperitoneal delivery of monoclonal antibodies: Enhanced regional delivery advantage using intravenous unlabeled anti-mouse antibody. Nucl. Med. Biol. 14:611–615.
66. Wahl, R.L., and Liebert, M. (1989) Improved radiolabeled monoclonal antibody uptake by lavage of intraperitoneal carcinomatosis in mice. J. Nucl. Med. 30(1):60–65.
67. Wahl, R.L., Roberts, J., Liebert, M., Hopkins, M.P., Shulkin, B., Johnson, J.W., and Mallette, S. (1988) Comparison of intraperitoneal and intravenous delivery routes of radiolabeled monoclonal antibody 5G6.4 in patients with ovarian carcinoma. Radiology 169(P):75.
68. Chinol, M., and Hnatowich, D.J. (1987) Generator produced yttrium-90 for radioimmunotherapy. J. Nucl. Med. 28:1465–1470.
69. Gansow, O.A., Atcher, R.W., Link, D.C., Friedman, A.M., Seevers, R.H., Anderson, W., Scheinberg, D.A., and Strand M. (1984) Generator-produced Bi-212 chelated to chemically modified monoclonal antibody for use in radiotherapy. Am. Chem. Soc. 241:215–227.

III

Radiochemistry

7. Chelates and antibodies: Current methods and new directions

Otto A. Gansow, Martin W. Brechbiel, Saed Mirzadeh, David Colcher, and Mario Roselli

The first labeling of antibodies with radioactive isotopes was reported by Pressman [1] in 1948. A radioiodine was employed. Over the next two decades, extensive development of the chemistry of iodination methods and the general utility of iodine-based radioimmunoassays resulted in radioiodination becoming a familiar tool in most biochemistry laboratories. Thus, shortly after the development of monoclonal antibodies by Kohler and Milstein [2], these exquisitely specific immunoproteins were soon being explored as vehicles for targeting of iodine radionuclides to tumors for gamma camera imaging or for therapy [3,4].

Unfortunately, none of the iodine isotopes are optimal for either scanning of tumors or for therapy. Iodine-123 has an emission energy of 159 keV, well within the photopeak of the sodium iodide crystals so useful for gamma-ray detection, but it has a short half-life, 13.3 hours. The technetium x-ray from iodine-125 at 35 keV is too weak to penetrate tissues efficiently. Iodine-131, whose beta decay is accompanied by x-rays from 80 to 723 keV, has often been employed for use with antibodies, but it is undesirable for imaging, not only because of its long half-life (8.05 days) and cytotoxic beta radiations, but also because of image background associated with the higher energy gammas. Numerous therapy studies in animals and humans have been initiated with iodine-131-labeled immunoproteins [5–9], but it can fairly be said that little success has been reported, likely due to the low dose and dose rates delivered by the relatively weakly energetic beta emission. Additionally, the deiodination of tumor-bound antibodies may lead to uptake in the thyroid and gut, thus obscuring images and delivering misplaced doses of radiation [10].

The labeling of immunoproteins with metallic radioisotopes by the use of chemically modified organic molecules called *chelating agents* would seem to be a more versatile method. The selection of radionuclides that might successfully be chelated spans the periodic table and is really limited only by the skill of the synthetic chemist in designing suitable ligands.

Interestingly, at the time Pressman was performing his early radioiodination studies, Schwartzenbach, Sillen, and Martell were first exploring the chemistry by which complex organic molecules called *ligands* could effectively bind and sequester metal ions from aqueous solution [11,12]. Most ligands attach

Goldenberg, D.M., (ed.), Cancer Imaging with Radiolabeled Antibodies.

to cations at more than one binding site and are referred to as being *multidentate*, since they take several 'bites' out of the spherical space immediately surrounding the surface of the electron shell of the ion. That space is commonly referred to as the *first coordination sphere* of the metal ion, and the number of atoms bound directly to the metal within that sphere is called the coordination number (C.N.) of the cation. The actual C.N. of a cation varies usually not more than ±1 from that found to be most characteristic of its coordination chemistry. The terms *chelate* or *chelating agent* are often given to a ligand that is multidentate in its coordination of metals to form complex ions (or more generally, metal complexes) [13].

The production of a monoclonal antibody linked to a radiometal is a difficult and lengthy process, as illustrated in Figure 1 below, in which we summarize a protocol we use for preparation of indium-111-labeled Mab B72.3 for clinical studies.

In formulating such a protocol, many choices must be made. Primarily, of course, the Mab must be obtained and the metal chosen. Inasmuch as this

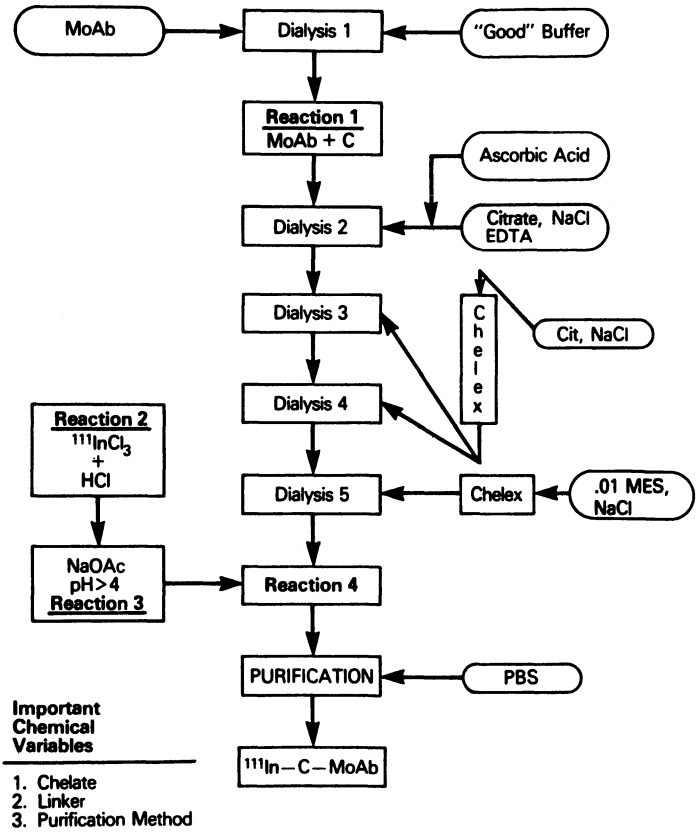

Figure 1. ^{111}IN labeling protocol.

review is directed to a discussion of the metal chelate-related aspects of the process, no discussion of Mab issues will be presented. Usually, preliminary experiments are performed with radioiodine to ensure that the immunoprotein is of sufficient purity and that it has the desired binding characteristics and tumor specificity.

The radiometal is selected according to the purpose to which the radioimmunoconjugate is directed. Gamma-ray emitting radiometals have often been used for tumor imaging with Mabs, that is, radioimmunoimaging, while alpha and beta particle emitters seem suitable for use in antibody-directed therapy, that is, radioimmunotherapy [14,15]. Recently, it has been suggested that positron emitters could be useful for both tomography and therapy, but no investigations have been reported to date [16].

Choice of the radionuclide also determines which chelating agent may be employed. It may be anticipated, for example, that radiometals with high coordination numbers, 7–9, will require chelates of greater denticity than those with C.N = 6.

Chelating agents must be chemically modified with a reactive functional group that can react with amino acid residues or oxidized carbohydrates to form secure, covalent linkages of ligand to antibody. Linkage reaction conditions must be mild so as not to alter either the specificity or activity of the Mab. After linkage, complexation of the radiometal ion is usually accomplished in water at pH 4–6.5, with care again being given to not compromise the immunoprotein.

Finally, ideally immediately before use, the radioimmunoconjugate must be purified of adventitiously bonded radiometal ions. The degree of binding of the metal to the amino acid structures of the protein determines the difficulty of the purification required. As an example, indium^{+3} is inherently a relatively unreactive ion, is easily hydrolyzed, and may precipitate on the protein surface. Tight linkage to the protein backbone is expected. In this case, very efficient methods of purification, such as HPLC size-exclusion chromatography, may be required, whereas labile divalent metal ions such as lead^{+2} or copper^{+2} could in most cases be removed effectively by simple addition of strong chelating agents. More detailed consideration will now be given to each of the chemical variables identified above.

Selection and availability of radiometals

Nuclear chemistry has provided a wide selection of radionuclides suitable for linkage to Mab. In practice, though, cations in the trivalent oxidation state have been most frequently used, since they form stable and inert metal complexes with the EDTA [17–20] and DTTA [21,22] or DTPA [23] polyaminocarboxylates, although more recently diamine disulfide ligands have been shown useful for technetium-99m and rhenium-186,188 [24,25].

Selection of the radiometal principally depends on the decay characteristics

of the radionuclide. Half-lives within the range of 5–96 hours are long enough to allow for localization of Mab or Mab fragment. Photon emitters (gamma or x-rays) are chosen for radioimmunoimaging; beta- or alpha-particle emitters are of use in therapy. Little use has been made of positron emitters to date.

One wishes the radioimmunoconjugate to be readily applicable in the clinic, and conventional scintillation cameras are optimized to detect photons with energies in the range 80–280 keV. Fortunately, there are a reasonable number of gamma emitters with appropriate energies and for which suitable bifunctional ligands exist. In Table 1 we summarize the more useful radionuclides and comment on the availability of each.

Technetium-99m is now employed in all radiopharmacies but its short half-life renders it suboptimal for use with antibodies. Nevertheless, substantial effort has been expended in producing chelates useful for linkage to antibody fragments [26]. The direct labeling of sulfhydryl residues on antibody by technetium has also been extensively explored [27].

Most radiometal immunoimaging studies have employed indium-111, a pure gamma emitter. The applicability of technetium-99m will be limited by its short half-life to Mab fragment labeling. Gallium-67, with its complex

Table 1. Radionuclides suitable for imaging and/or therapy

Isotope	Half-life (h)	Particle	Maximum Energy[a] (MeV)	Source[b]
Imaging				
Indium (^{111}In)	67.9	γ	0.173, 0.245	@/+
Technetium (^{99m}Tc)	6.0	γ	0.140	#/+
Gallium (^{67}Ga)	78.3	γ	0.093, 0.184, 0.296	@/+
Rhenium (^{186}Re)	90.6	γ	0.137	*/−
		β	1.072	
Iodine (^{132}I)	13.0	γ	0.159	@/+
Therapy				
Iodine (^{131}I)	192.0	γ	0.364	*/+
		β	0.810	
Rhenium (^{188}Re)	17.0	γ	0.155	# or */−
		β	2.116	
Copper (^{67}Cu)	62.0	γ	0.185	@/−
		β	0.577	
Palladium (^{109}Pd)	13.5	γ	0.088	@ or */−
		β	1.028	
Scandium (^{47}Sc)	81.6	γ	0.159	*/−
		β	0.600	
Yttrium (^{90}Y)	64.1	β	2.288	#/+
Astatine (^{211}At)	7.2	α	5.866	@/−
Lead (^{212}Pb)	10.6	β	0.569	#/+
		γ	0.239	
Bismuth (^{212}Bi)	1.0	α	6.090, 8.78	#/+
		β	2.251	
		γ	0.727	

[a] Average energies are usually approximately one third of the maximum energy values.
[b] Source of nuclide: generator (#), accelerator (@), or nuclear, reactor (*). Availability whether more (+) or less (−) obtainable for general use.

x-ray spectrum, does not give the clearest of images. Rhodium-105 and rhenium-186 provide a beta dose along with the imagable gamma emisson. Particle-emitting radionuclides would seem to be required for radioimmunotherapy. The concentration of antibodies is usually less than 100,000 on a cell surface, so the dose from the more disperse gamma radiation could not be effectively cytotoxic. Alpha emitters appear to be most useful because of the very high linear energy transfer (LET) associated with the short ion track of the particle. The utility of the most available alpha-emitting radionuclide, bismuth-212, is limited by its 1-hour half-life. Except for blood-borne diseases, access of intact IgG to tumor cells usually takes 5–10 hours. A recent report has demonstrated the exquisite and specific cytotoxicity of antibody conjugates of bismuth-212 [14].

Several beta-particle emitters have been suggested for use in situations where tumors of a few centimeters or more are to be treated. The average range of the beta particle varies from a few millimeters to a centimeter, depending on the energy of the decay. Thus, in modest-size tumors, one could expect most of the decay energy to be absorbed in the tissues. In such a circumstance, the highest energy would be delivered to the tumor by the radionuclide with the greatest decay energy. Thus a number of workers have focused their efforts on the chelation of Y-90 [28–30]. Another beta emitter that has received substantial attention is the moderately energetic copper-67 [31–34]. A modified TETA chelate has been synthesized and is said to be suitable for use in vivo [35].

The group of Srivastava [36] has been active in working with palladium-109, but difficulties with the nuclear preparation of the radioisotope have resulted in the availability of only low-specific-activity material, which is not optimal for antibody labeling.

Several groups are now exploring the use of rhenium-186 and rhenium-188 for immunotherapy [25]. The former radionuclide has an appropriate half-life but a low energy beta emission, while the latter has a relatively short half-life but a high energy beta particle.

Chelates and linkers

Most methodologies for labeling antibody with radiometal require the use of chelating agents whose chemical structure has been modified by introduction of a reactive functional group, a linker, which couples readily to amino acid residues of the immunoprotein.

Chemically modified derivatives of the polyaminecarboxylate ligands diethylenetriaminepentaacetic acid (DTPA) and ethylenediaminetetraacetic acid (EDTA) have most often been employed. Covalent linkage to proteins was accomplished by acylation with activated carbonyls, aromatic diazonium coupling, bromoacetyl alkylation, or an isothiocyanate alkylamino-addition reaction. All the above coupling methods were inefficient; extensive purifi-

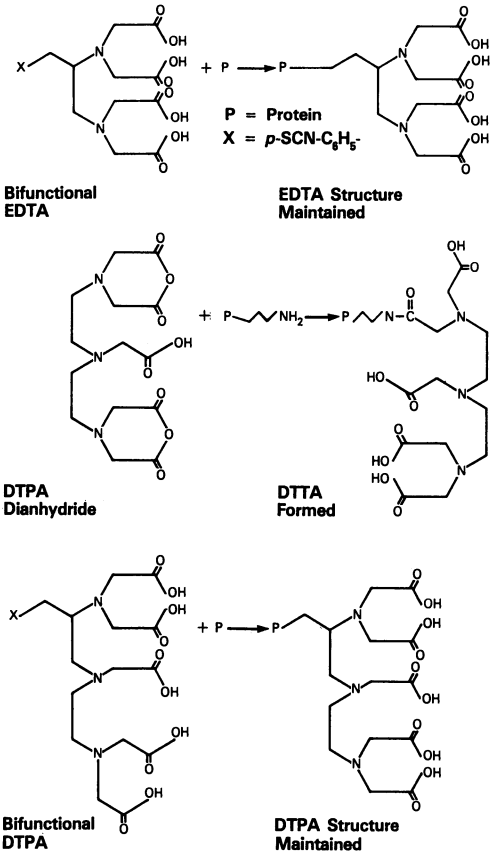

Figure 2. Chelate conjugation.

cation of ligand protein conjugates from unreacted chelate was required prior to radiometal labeling.

Anhydride linkage of the isobutylcarboxycarbonic anhydride of DTPA (MA-DTPA) and the dicyclic anhydride of DTPA (CA-DTPA) has probably been the most used method for chelate conjugation because of the simplicity of preparation of the former and the commercial availability of CA-DTPA. As shown in Figure 2, when linked to antibody, one carboxylate metal-binding site is used to form an acid amide bond, thus the available ligand is actually a diethylenetriamine*tetra*acetic acid (DTTA). Chemically modified EDTA derivatives have been extensively studies by Meares and coworkers [17–20]. Therein, substitution of a functionalized phenyl or benzyl group at a carbon on the ethylenediamine backbone provides a point for linkage to antibody while still retaining the integrity of the EDTA chelating moiety. Brechbiel, Gansow et al. reported the synthesis of the analogous DTPA series of the benzyl-substituted compounds shown in Figure 3, and Johnson and coworkers have described a novel carboxymethylene-substituted benzyl DTPA [37].

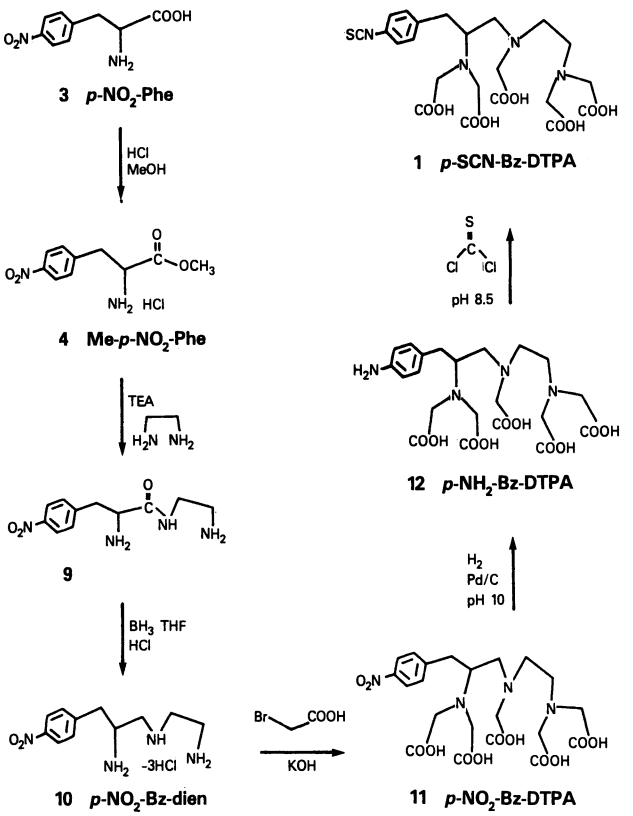

Figure 3. Benzyl-substituted compounds.

The principal difference among the ligands of Figure 2 is their denticity. EDTA has a maximum coordination number of six, DTTA has seven, and DTPA has eight. Not surprisingly, the larger the metal ion, the more necessary it becomes to employ a ligand of higher denticity.

Synthesis of backbone-substituted ligands has depended upon preparation of an amino acid amide such as 9 of Figure 3 by reaction of an amino acid ester with an amine. The peptide methods reported by Brechbiel, Gansow, et al. [10] are considerably more versatile in that they may be employed to prepare the more highly substituted DTPA derivatives shown in Table 2. As anticipated from the early work of Margerum [46], strategic substitution on the carbon backbone results in more stable metal complexes. Substitution, particularly in the backbone carbons alpha to the dicarboxymethylene-substituted amine nitrogens, sterically hinders the opening of the chelate ring required for metal complex dissociation.

Two examples of synthetic methods are presented in Figures 4 and 5. To prepare the 1-methyl-3-(p-NO_2-benzyl)DTPA of Figure 5, an amine-blocked amino acid is condensed with an alpha amino acid to give the resulting amide,

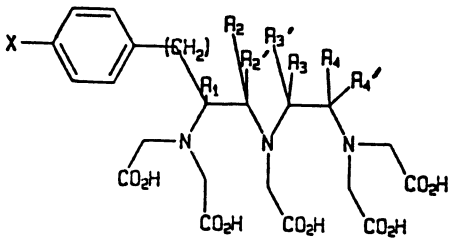

FORMULA 3

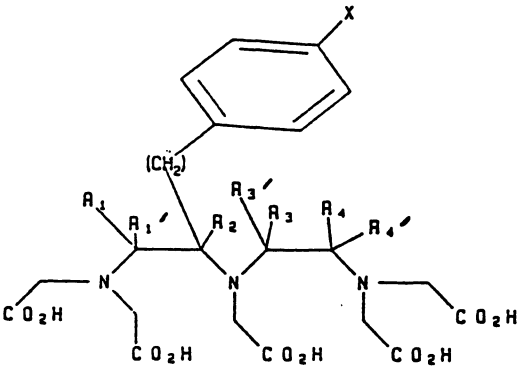

FORMULA 4

Figure 4. The polysubstituted DTPA chelating agent of claim 15, having the following formula 3 or 4.

which after deblocking is reduced to the parent diethylenetriamine and subsequently alkylated with bromoacetic acid to give the desired product.

In Figure 6 an amino acid amide is coupled with BOC-alanine via a carbodiimide to form a ketoamine, which after deprotection is reduced to the parent diethylenetriamine followed by the usual alkylation to form the chelate.

The polyazamacrocyclic polymethylenecarboxylate chelating agents of the DOTA, NOTA, TETA type [38–41] represent the future of the development of ligands for use with antibodies, since they exhibit among the highest known thermodynamic stability constants for the radionuclides Y-90, Pb-203,212, and Bi-212. Although the copper-67 complex of the ligand TETA has been reported to be stable in serum [35], the known complexes of DOTA with divalent and trivalent metal ions are invariably more stable than those of TETA [41]. In Figure 7 we report a 'brute force' method by which we prepared small amounts of a bifunctional DOTA. We are currently evaluating the several approaches to the ligand in order to optimize yields.

The isothiocyanate linker has proven to be useful for the above-listed ligands. Reaction with primary amines to form thiourea at protein amino acid residues is easily accomplished at mildly basic solution pH values easily tolerated by Mabs. Chelates may be prepared from parent amine in almost a

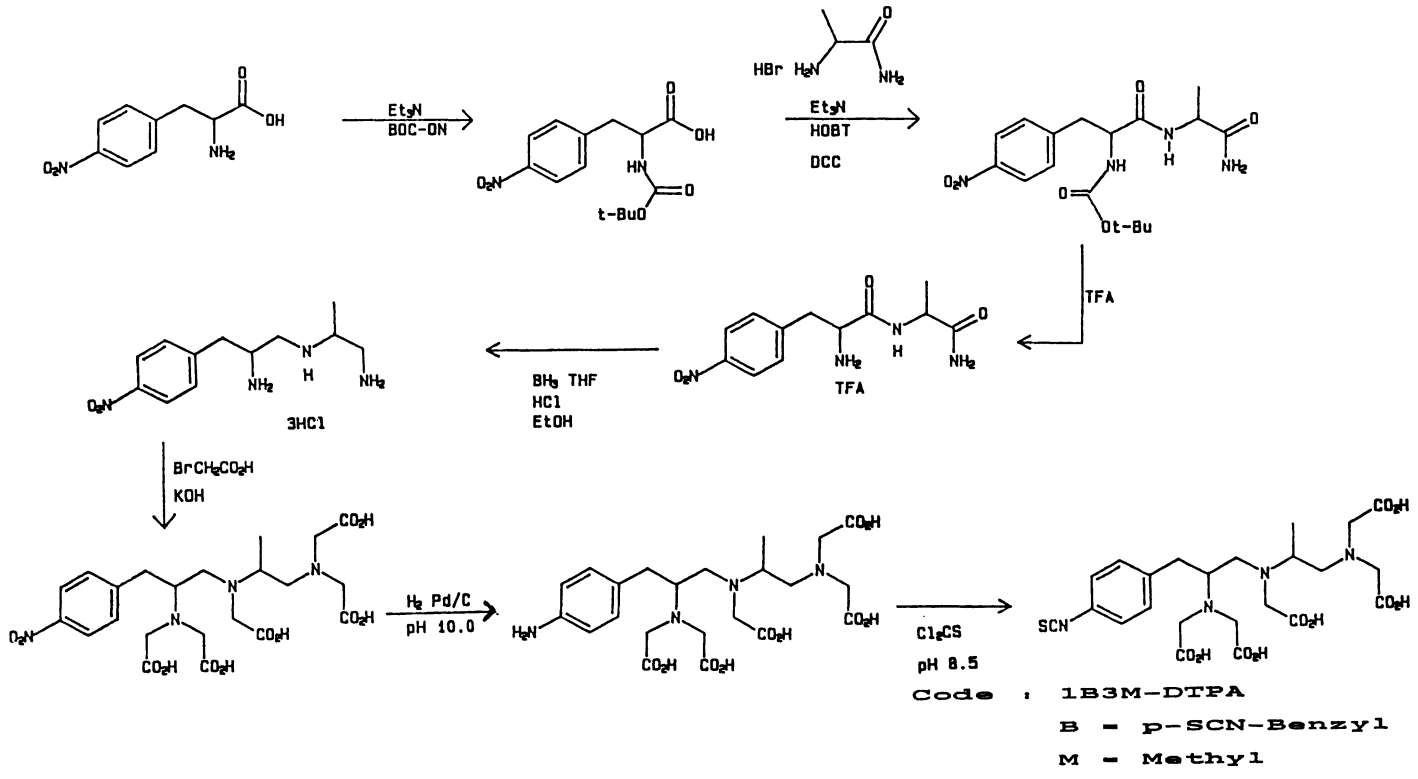

Figure 5. 1-methyl-3-(p-NO_2-benzyl) DTPA synthetic method.

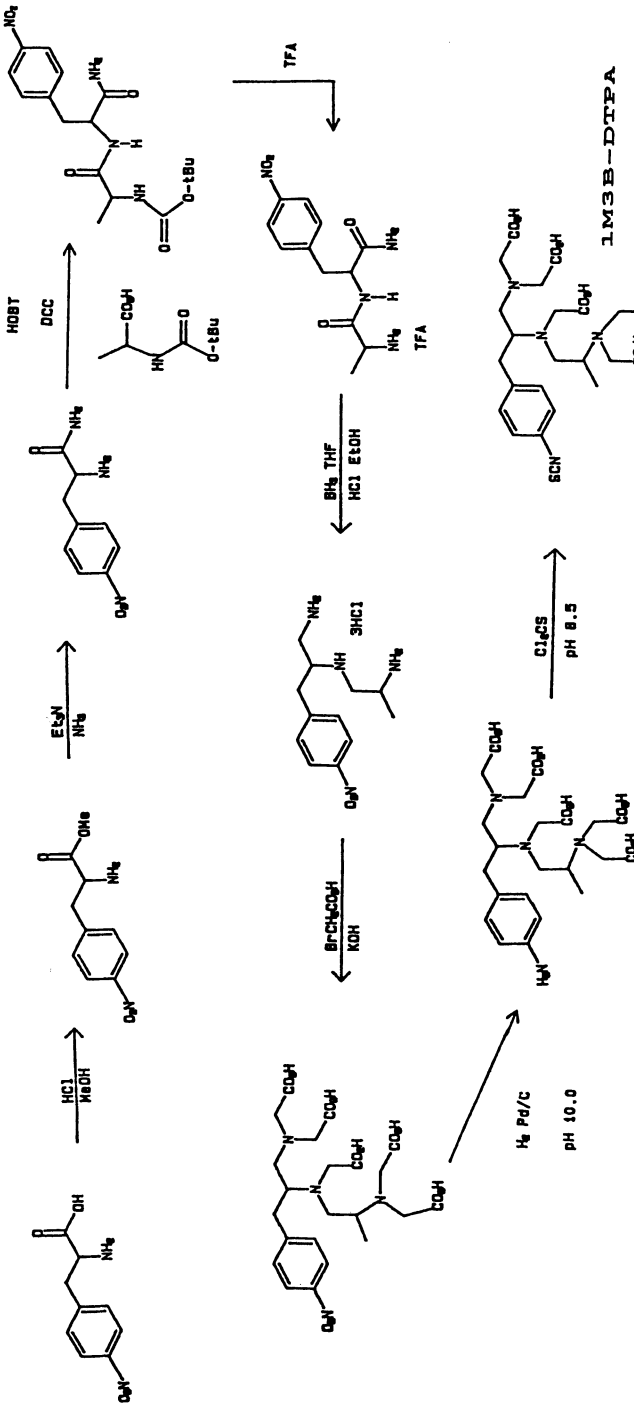

Figure 6. Amino acid amide coupled with BOC-alanine via carbodiimide forms a ketoamine, which after deprotection is reduced to the parent diethylenetriamine followed by the usual alkylation to form the chelate.

quantitative yield and as analytically pure compounds. The Meares group has made extensive use of bromoacetamido derivatives of amines [20], but in our hands the reported preparative methods provide mixtures of N-alkylated and N-acetylated compounds. Linkages to antibodies to form secondary amines is reported, with no measurable damage to the immunoprotein. Alternatively, use of benzimidates or aromatic diazonium salts would seem to be contra-indicated because of the harshly basic reaction conditions required for protein linkage. Clearly much remains to be done in the development of linker technology.

Radiometal ion complexation

Upon having successfully formed an antibody-ligand conjugate, one must devise mild protocols for labeling with the radiometal. While most divalent metals would form complexes rapidly with protein-linked aminocarboxylate ligands at pH 4–7 by simply mixing with the metal salts, trivalent cation salts will undergo hydrolysis to unreactive polymers. This is especially evident for bismuth(III). Labeling of DTTA ligands attached to antibody anti-Tac could only be accomplished by preparing the tetraiodobismuthate^{-1} ion in acidic medium in the absence of chloride, neutralizing the solution with a phosphate buffer and immediately reacting the solution with the DTTA antibody [14]. Therein, the stable iodo complex served as a carrier ligand by preventing hydrolysis of Bi(III).

For labeling with indium(III), citrate and acetate have proven to form useful carrier complexes for antibody labeling [18]. Radiometal chelates formed by those ligands with the metal ion are relatively weak compared with those of the ligands of Figure 2, so the transchelation required for protein labeling readily occurs at pH 4–6, with hydrolysis prevented by the carrier chelate. Similar protocols were used for labeling antibody ligand conjugates with yttrium-88,90 [29].

However, unless large amounts of protein conjugate are used, or if each protein molecule is linked to several ligands, uptake of the radiometal is not complete. Purification of the labeled immunoprotein from unreacted metal ion is complicated by the adventitious binding of radiometal to natural metal chelation sites on the protein backbone. Several purification methods have been suggested. Extensive dialysis in the presence of free chelating ligands is adequate but time consuming. Use of small gel-filtration columns was employed but proved to be inadequate. When ion-exchange resins were stacked on top of the sizing columns, improved results were noted [43]. Simple addition of EDTA to labeled protein solutions prior to injection [42] as a 'chase' method of purification depended upon rapid clearance of metal chelates by the RES system. Chase methods were recently shown to be suboptimal as compared with high-pressure liquid chromatography (HPLC) [23]. In practice, in clinical trials at our institution, addition of a chase chelate followed by HPLC is the purification method of choice.

It seems entirely possible that many of the problems associated with the undesirable behavior of labeled antibodies might be associated with the difficult chelate linkage and labeling chemistry and subsequent purifications. Logically it would appear to be more desirable to form the chelate complex first, with the linker at the ready for antibody linkage. This we call a *direct-coupling* protocol, as opposed to the *indirect labeling* described above.

Our attempts to use the isothiocyanate chelates of Figure 2 for direct coupling of indium-111 resulted in several observations. Formation of the metal chelate went well in acetate buffer at pH 4–6 with no loss of isothiocyanate. A ligand to protein ratio of 0.2 sufficed to complex 5 mCi for coupling to 1 mg of antibody B72.3. When this was reacted with antibody at pH 8.6–8.8, labeling was effected within a few hours. However, it was apparent that in this time the radioindium complexes of these ligands underwent about 50% base hydrolysis to the metal hydroxo species, as clearly evidenced in HPLC traces. The hydrolysis occurs only in the presence of protein. Thus the experiment worked, but complex purification procedures were still required to produce pure, labeled antibody solutions. Efforts to refine direct coupling protocols are underway.

Status of in-vivo studies

That rapid and specific tumor imaging without subtraction or computer enhancement was possible with radioactive metal chelates linked to monoclonal antibodies was conclusively demonstrated by Scheinberg, Strand, and Gansow in 1981 [43]. Mice spleens invaded with the Rauscher leukemia virus were easily detected by gamma camera imaging, as shown in Figure 8. However, when the techniques used in this study were employed in attempts to obtain images of solid colorectal tumors grown in athymic mice, very substantial background was observed due to appreciable uptake of radiolabel, principally in the liver. A recent study by Brechbiel et al. showed that substantial improvement of solid tumor images may be obtained (Figure 9) by using the strongest chelating agent now available, 1-p-isothiocyanatobenzyl(DTPA), and by being quite careful to adequately purify the labeled immunoprotein conjugate [23]. A comparison of purification methods was also conducted. Results revealed that size-exclusion HPLC provided by far the most efficient purification. In clinical trials with radiolabeled antibodies at the NIH, HPLC techniques are routinely used.

Relatively few studies of tumor therapy have been conducted with chelate-linked Mab. Most workers who have tried to use yttrium-90 chose to use the DTTA chelate formed by the cyclic anhydride of DTPA and have discovered that much of the metal ion is released from the chelate in vivo within a day or two [29,30].

We have recently investigated the differences in the biodistribution of indium- and yttrium-labeled monoclonal B72.3 antibody in athymic mice

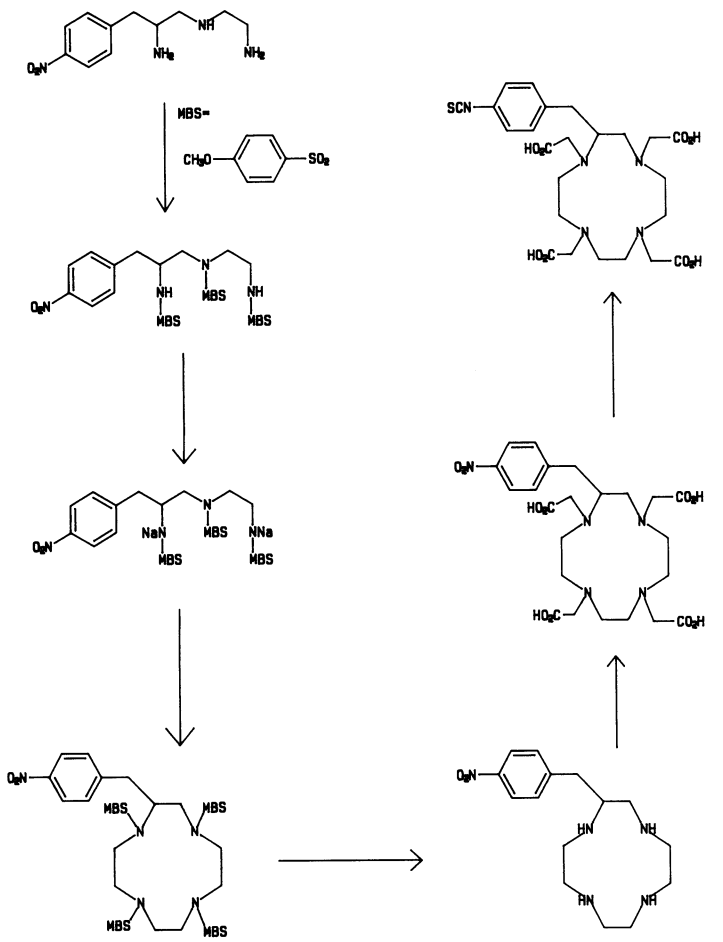

Figure 7. Small amounts of a bifunctional DOTA are prepared by a 'brute-force' method.

bearing the human carcinoma LS-174T. The chelates of Figure 2 were linked to antibody and purified by an EDTA chase followed by HPLC.

Despite the major differences in indium-111 and yttrium-90 chelate chemistry, the use of yttrium-90 has often been suggested in conjunction with indium-111 Mab (using the identical chelate) to be used as a tracer for in-vivo biodistribution and dosimetry studies. Indium complexes are inherently inert, while yttrium complexes are reactive, mostly due to the coordination number of yttrium being 8 or 9, versus 6 for indium. We determined the biodistribution of indium- and yttrium-labeled Mab B72.3 using three different chelates (SCN-Bz-EDTA, CA-DTPA, SCN-Bz-DTPA) with maximum coordination number of 6, 7, and 8, respectively.

For biodistribution studies of radioactive yttrium, yttrium-90 (a pure beta emitter with no gamma rays) is not suitable due to absorption of beta particles by organs. Yttrium-88 (half-life = 106.6 days), which emits intense, high-

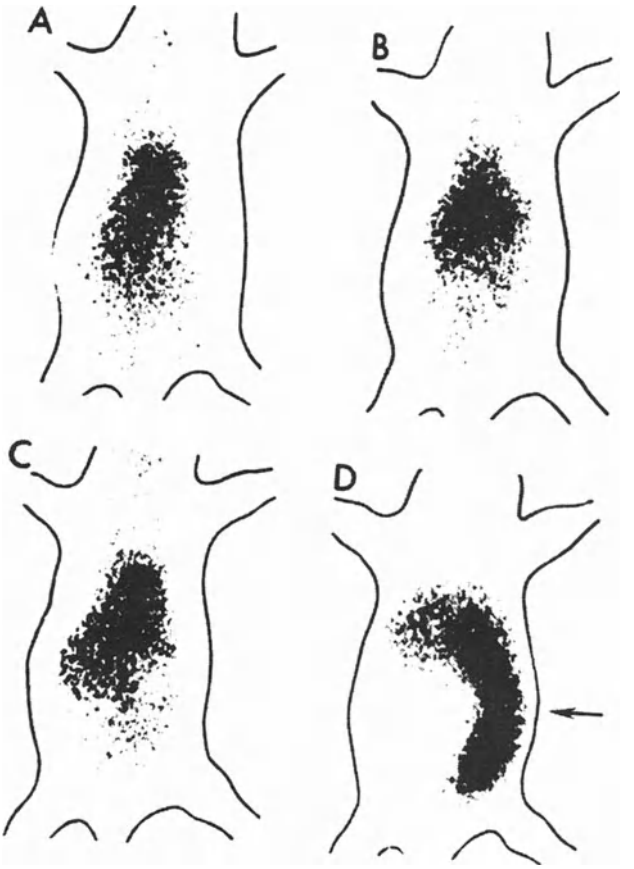

Figure 8. Mice spleens invaded with the Rauscher leukemia virus are easily detected by gamma camera imaging.

energy gamma rays, was used for these studies. Monoclonal antibody B72.3 was produced against a carcinoma metastatis; it binds with high specificity to a tumor-associated glycoprotein (TAG-72) found in human colon and breast cancer.

The carbon-14 labeled SCN-Bz-EDTA and SCN-Bz-DTPA were synthesized by modifying their reported synthesis [23] introducing the carbon-14 with 2-carbon-14- bromoacetic acid. The cyclic dianhydride (CA-DTPA) was synthesized from carbon-14-labeled DTPA (obtained from New England Nuclear), [44]. The labeling of the chelates with carbon-14 was essential for the accurate determination of the chelate to protein ratio.

The B72.3 antibody, typically in a concentration of 10 mg/ml (20 mM HEPES/Cl^-, pH = 8.6) was mixed with excess chelate (4:1 ratio), and the reaction was allowed to proceed for 4 hours at room temperature. Then the chelate-conjugated antibody was isolated from the free chelate by either

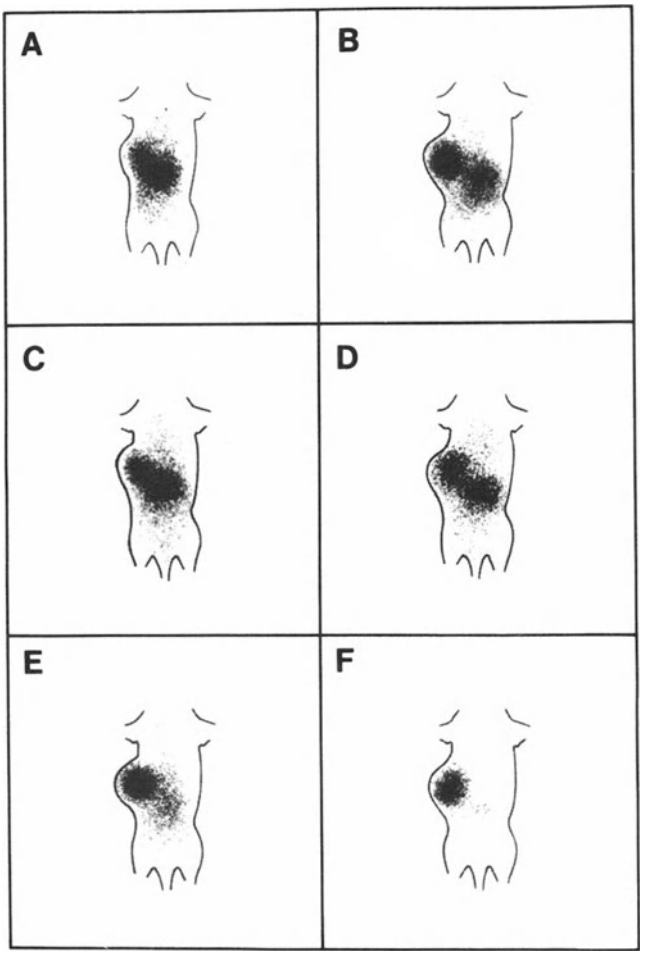

Figure 9. Substantial improvement of solid tumor images may be obtained by using the strongest chelating agent now available.

sequential dialysis or size-exclusion HPLC. Under the above conditions, conjugated protein with 0.5–1.0 moles of chelate per mole of protein was obtained. The immunoreactivity of chelate-conjugated B72.3 was assessed by a competitive binding assay [45]. In all preparations, 1 mg of purified, conjugated protein (10 mg/ml) was labeled with 2 mCi of indium-111 or 0.3 mCi yttrium-88. The radiometals, in acetate form at pH 4.0 in 20–30 μl volumes, were mixed with conjugated protein. After 30 minutes to 2 hours, the reaction was quenched by increasing the pH to 6.0 and making the solution approximately 10^{-4} molar in Na_2EDTA. The immunoprotein was purified by size-exclusion HPLC.

Athymic mice bearing the human colon carcinoma LS-174T were injected

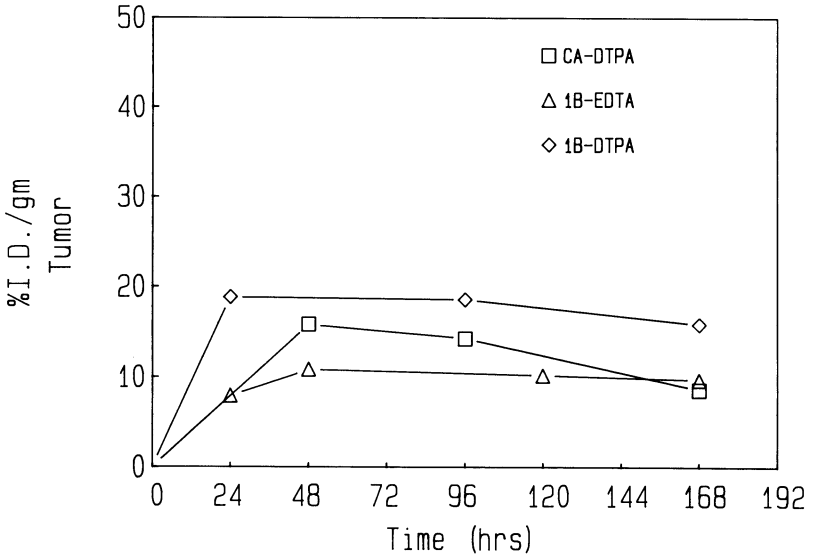

Figure 10. Retention of ^{88}Y-labeled B72.3 antibody by tumor.

IV and sacrificed at various times and the distributions of indium and yttrium labels were compared. The yttrium-88-labeled B72.3 with the CA-DTPA and the EDTA chelates gave 10% ID/g in the tumor at 48 hours compared with 20% ID/g of the DPTA-B72.3 (Figure 10). Major differences were also seen in the femur with 10–18% ID/g of the CA-DTPA- and EDTA-

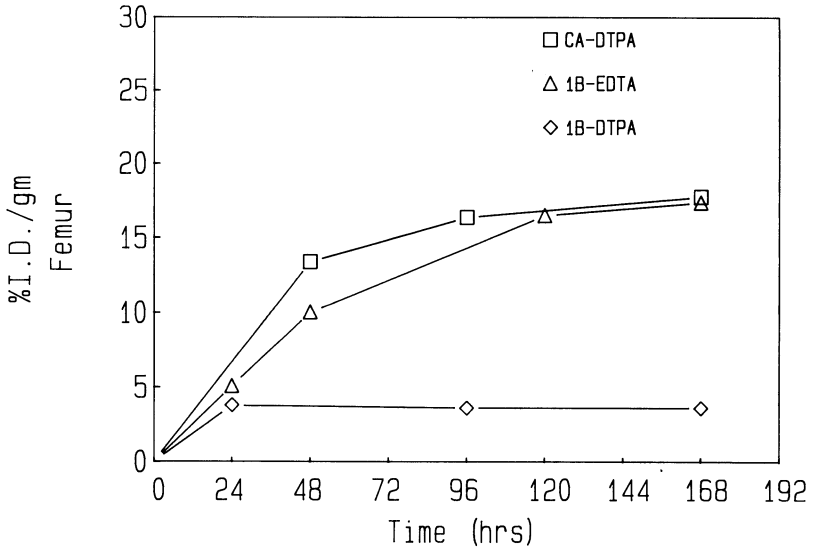

Figure 11. Retention of ^{88}Y-labeled B72.3 antibody by femur.

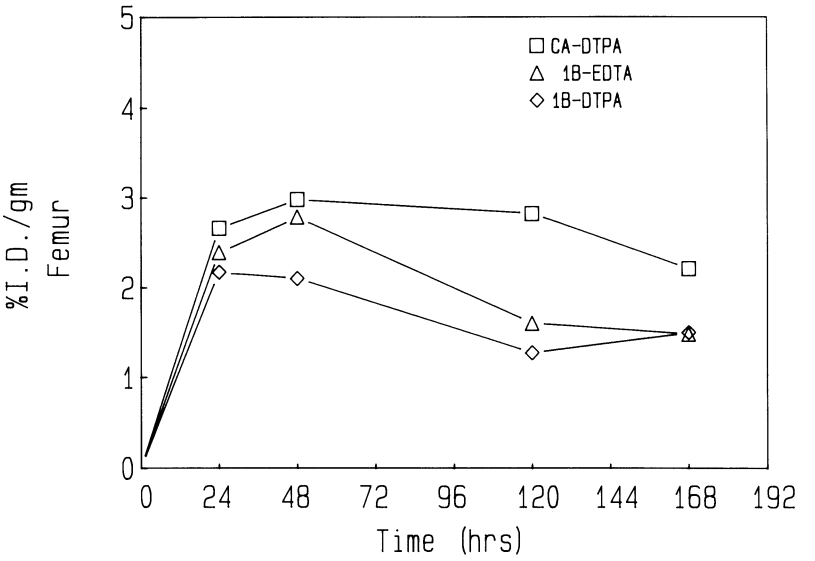

Figure 12. Retention of ^{111}In-labeled B72.3 antibody by femur.

conjugated yttrium-88 versus 2–3% ID/g for the DTPA chelate (Figure 11). Indium-111-labeled Mab using all three chelates yielded only 2–3% ID/g in the bone (Figure 12). The major differences in bone uptake with yttrium-labeled Mab (using CA-DTPA and EDTA) demonstrate the problems in using the biodistribution of indium-labeled Mabs to predict the dosimetry (especially for the bone marrow, the critical organ) of yttrium-90-labeled Mabs.

Thus it would appear that by using DTPA chelates, leakage of yttrium-90 to the bone may be almost entirely eliminated. Now that the proper chemistry is in place, investigations of the efficacy of radioimmunotherapy with yttrium-90 may begin.

References

1. Pressman. D., and Keighley, G.J. (1948) The zone of activity of antibodies as determined by the use of radioactive tracers; the zone of activity of nephrotoxic anti-kidney serum. J. Immunology 59:141.
2. Kohler, G., and Milstein, C. (1975) Continuous cultures of fused cells secreting antibody of predefined specificity. Nature 256:495.
3. Goldenberg, D.M., Preston, D.F., Primus, F.J., and Hansen, J.H. (1974) Photoscan localization of GW-39 tumors in hamsters by radiolabeled heterospecific antibody to carcinoembryonic antigen. Cancer Res. 34:1.
4. Mach, J.-P., Carrel, S., Merenda, C., Sordat, B., and Cerottini, J.C. (1974) In vivo localization of radiolabeled antibodies to carcinoembryonic antigen in human coloncarcinoma grafted into nude mice. Nature 248:704.
5. Capone, P.M., Lawrence, D., Papsidero, L.D., Croghan, G.A., and Ming, Chu T. (1983)

Experimental tumoricidal effects of monoclonal antibody against solid breast tumors. Proc. Natl. Acad. Sci. USA 80:7328.

6. Jones, D.H., Goldman, A., Gordon, I., Pritchard, J., Gregory, B.J. and Kenshead, J.T. (1985) Therapeutic application of a radiolabeled monoclonal antibody in nude mice xenografted with human neuroblastoma. Int. J. Cancer 35:715.
7. Goldenberg, D.M., Gaffar, S.A., Bennet, J., and Beach, L. (1981) Experimental radioimmunotherapy of a xenografted human colonic tumor (GW-39) producing carcinoembryonic antigen. Cancer Res. 41:4354.
8. Epenetos, A.A., Courtenay-Luck, N., Pickering, D., Hooker, G., Lavender, J.P. and McKenzie, C.G. (1985) Antibody guided irradiation of brain glioma by arterial infusion of radioactive monoclonal antibody against epidermal growth factor receptor and blood group. Br. Med. J. 290:1463.
9. Carasquillo, J.A., Krohn, K.A., Beaumier, P., et al. (1984) Diagnosis of and therapy for solid tumors with radiolabeled antibodies and immune fragments. Cancer Treat. Rep. 68: 317.
10. Scheinberg. D.A., and Strand, M. (1982) Leukemia cell targeting and therapy by monoclonal antibody targeting in erythroleukemic mice. Cancer Res. 42:44.
11. Schwarzenbach, G. (1969) *Complexometric Titrations*, 2nd Eng ed. New York: Barnes and Noble.
12. Sillen, L.G., and Martell, A.E., eds. *Stability Constants of Metal Ion Complexes*. London: Chemical Society.
13. For an introduction to coordination chemistry, see Basolo, F. and Johnson, R. (1964) *Coordination Chemistry*. London: Benjamin/Cummings.
14. Kozak, R.W., Atcher, R.W., Gansow, O.A., Freidman, A.M., Hines, J.J., and Waldmann, T.A. (1986) Bismuth-212-labeled anti-Tac monoclonal antibody: alpha-particle-emitting radionuclides as modalities for radioimmunotherapy. Proc. Natl. Acad. Sci. USA 83:474.
15. Kozak, R., Waldmann, T.A. Atcher, R.W., and Gansow, O.A. (1985) Radionuclide-conjugated monoclonal antibodies: A synthesis of immunology, inorganic chemistry and nuclear science. Trends Biotechnol. 259.
16. Welch, M.J., and Kilbourn, M.R. (1986) *Radiolabeled Monoclonal Antibodies for Imaging and Therapy*, NATO ASI Abstract, July 20, 1986, p. 655.
17. Yeh, S.M., Sherman, D.G., and Meares, C.F. (1979) A new route to bifunctional chelating agents: Conversion of aminoacids to analogs to ethylenedinitrilotetraacetic acid. Anal. Biochem. 100:152.
18. Meares, C.F., Goodwin, D.A., Leung, C.S.-H., Girgis, A.Y., Sylvester, D.J., Nunn, A.D. and Lavender, P.J. (1976) Covalent attachment of metal chelates to proteins: The stability in vivo and in vitro of the conjugate of albumin with a chelate of indium-111. Proc. Natl. Acad. Sci. USA 73:3803.
19. DeRiemer, L.H., Meares, C.F., Goodwin, D.A., and Diamanti, C.I. (1981) BLEDTA II: Synthesis of a new tumor-visualizing derivative of Co(III)-Bleomycin. J. Labelled Compd. Radiopharm. 18:1517.
20. Meares, C.F., McCall, M.J., Reardon, D.T., Goodwin, D.A., Diamanti, C.I., and McTigue, M. (1984) Conjugation of antibodies with bifunctional chelating agents: Isothiocyanate and bromoacetamide reagents, methods of analysis and subsequent addition of metal ions. Anal. Biochem. 142:68.
21. Krejcarek, G.E., and Tucker, K.L. (1977) Covalent attachment of chelating groups to macromolecules. Res. Commun. 77:581.
22. Hnatowich, D.J., Layne, M.W., and Childs, R.L. (1982) The preparation and labeling of DTPA-couples albumin. Int. J. Appl. Radiat. Isot. 33:327.
23. Brechbiel, M.W., Gansow, O.A., Atcher, R.W., Schlom, J., Esteban, J., Simpson, D.E., and Colcher, D. (1986) Synthesis of 1-(p-isothiocyanatobenzyl) derivatives of DTPA and EDTA: Antibody labeling and tumor-imaging studies. Inorg. Chem. 25:2772.
24. Fritzberg, A.R. (1987) Advances in 99mTc-labeling of antibodies. Nucl. Med. (Stuttgart) 26:7.

25. Fritzberg, A.R. (ed.) (1986) *Radiopharmaceuticals: Progress and Clinical Perspectives*. Boca Raton, FL:CRC Press.
26. Khaw, B., Strauss, H.W., Carvalko, A., Locke, E., Gold, H.C., and Haber, E. (1982) Technetium-99m labeling of antibodies to cardiac myosin Fab and to human fibrinogen. J. Nucl. Med. 23:1011.
27. Paik, C.H., Phan, L.N.B., Hong, J.J., Sahami, M.S., Herald, S.C., Reba, R.C., Steigman, J., and Eckelman, W.C. (1985) The labeling of high affinity sites of antibodies with ^{99m}Tc. Int. J. Appl. Radiat. Isot. 12:3.
28. Hnatowich, D., Virzi, F., and Doherty, P. (1985) DTPA-coupled antibodies labeled with yttrium-90. J. Nucl. Med. 26:503.
29. Washburn, L.C., Hwa Sun, T.T., Crook, J.E., Byrd, B.L., Carlton, J.E., Hung, Y.-E., and Steplewski, Z.S. (1986) ^{90}Y-labeled monoclonal antibodies for cancer therapy. Nucl. Med. Biol. 13:453.
30. Vaughn, A.T.M., Keeling, A., and Yankuba, S.C.S. (1985) Production and biological distribution of Y-90 labeled antibodies. Int. J. Appl. Rad. Isot. 36:803.
31. Mirzadeh, S., Mausner, L.F., and Srivastaya, S.C. (1986) Production of no-carrier added ^{67}Cu. Appl. Radiat. Isot. 37:29.
32. Franz, J., Freeman, G.M., Barefield, E.K., Volkert, W.A., Ehrhart, G.J., and Holmes, R.A. (1987) Nucl. Med. Biol. 14:479.
33. Cole, W., DeNardo, S.J., Meares, C., DeNardo, G.L., and O'Brien, H. (1983) J. Nucl. Med. 24:30.
34. Cole, D.A., Mercer-Smith, J.A., Taylor, W.A. and Lavalee, D.K. (1986) Lymphatic uptake of Cu-67 *meso*-tetra [4-carboxyphenyl] porphine, an imaging agent for inflamed lymph nodes. Proc. Am. Chem. Soc. September: (Abstr. # 0046).
35. Cole, W.C., DeNardo, S.J., Meares, C.E., McCall, M.J., DeNardo, S.J., Epstein, A.L., O'Brien, H., and Moi, M.K. (1987) Comparative serum stability of radiochelates for antibody radiopharmaceuticals. J. Nucl. Med. 28:83.
36. Doi, J.P., Lavelle, D.K., Srivastava, S.C., Prach, T., Richards, P., and Fawaz, R.A. (1981) Int. J. Appl. Radiat. Isot. Preparation of ^{109}Pd-hematoporphrin for selective lymphatic ablation using n-methylhematoporphyrin. 32:877.
37. Westerberg, D.A., Carney, P.L., Rodgers, P.E., Kline, S.J., and Johnson, D.K. (1989) Synthesis of novel bifunctional chelators and their use in preparing monoclonal antibody conjugates for tumor targeting. J. Med. Chem. 32:236.
38. Stetter, C.C., Franck, W., and Mertens, R. (1981) Darstellung and komplexibildung von polyazacycloalkan-N-essigsauren. Tetrahedron 37:767.
39. Stetter, H., and Franck, W. (1976) Complex formation with tetraazacycloalkane-N, N′, N″, N‴-tetraacetic acids as a function of ring size. Angew. Chem. Int. Ed. (Eng.) 15:686.
40. Desreux, J. (1980) Inorg. Chem. 19:1319.
41. Delgado, R., and Frausto da Silva, J.J.R. (1982) Metal complexes of cyclic tetraazatetraacetic acids. Talanta 29:815.
42. Goodwin, D.A., Meares, C.F., and McCall, M.J. (1985) Chelate conjugates of monoclonal antibodies for imaging lymphoid structures in the mouse. J. Nucl. Med. 26:493.
43. Scheinberg, D.A., Strand, M., and Gansow, O.A. (1982) Tumor imaging with radioactive metal chelates conjugated to monoclonal antibodies. Science 215:1511.
44. Eckelman, W.C., Karesh, S.M., and Reba, R.C. (1975) New compounds: fatty acid and long chain hydrocarbon derivatives containing a strong chelating agent. J. Pharm. Sci. 65:704.
45. Esteban, J.M., Schlom, J., Gansow, O.A., Atcher, R.W., Brechbiel. M.W., Simpson, D.E., and Colcher, O.J. (1987) New methods for the chelation of indium-111 to monoclonal antibodies: biodistribution and imaging of athymic mice bearing human colon carcinoma xenografts.

8. Radiolabeling antibodies via the cyclic anhydride of DTPA — Experiences of 5 years

D.J. Hnatowich

The advantage of the 'bifunctional chelate' as an alternative to radioiodination for the labeling of antibodies and other proteins has been recognized and commented on for several years [1]. This recognition has led to the development of diverse chelators — a process that continues today [2]. Early on, interest focused on diethylenetriaminepentaacetic acid (DTPA) as a suitable chelator for this purpose, since the polyaminopolycarboxylic acids, of which DTPA is an example, form strong chelates with a large number of metallic radionuclides [3]. Prior to 1981, the mixed anhydride of DTPA was the agent of choice for conjugation of DTPA to proteins [4], but in that year this laboratory found that the cyclic anhydride of DTPA (cDTPA) could be used to attach DTPA to proteins by a simpler process, which offers a considerable degree of control over the conjugation [5]. As a result, cDTPA has been used extensively in this and other laboratories for the preparation of DTPA-conjugated antibodies and other proteins. For example, in addition to both polyclonal and monoclonal antibodies, other proteins have been conjugated, such as fibrinogen [6,7], albumin [5], tissue plasminogen activator [8], avidin and streptavidin [9], lysozyme [10], and others [10]. After conjugation these proteins have been labeled primarily with ^{111}In but also with ^{90}Y [11–14], ^{88}Y [15], ^{99m}Tc [10,16], ^{153}Gd [17–19], ^{109}Pd [20], ^{46}Sc, and ^{67}Ga [21]. In the course of performing these investigations, considerable experience was acquired on the behavior of cDTPA during conjugation and on the behavior of the radiolabel while in serum and in vivo. This chapter will provide the reader with a brief overview of these experiences in the use of cDTPA to radiolabel antibodies.

Antibody conjugation

One important advantage of cDTPA over the mixed anhydride is its relative insensitivity towards hydrolysis. As a result, cDTPA may be isolated for characterization and for storage. Because of this property it is no longer necessary for each laboratory to synthesize the anhydride, since cDTPA is now available commercially from several sources. When stored in small lots

Goldenberg, D.M., (ed.), Cancer Imaging with Radiolabeled Antibodies.

at room temperature in a dessicator, the anhydride appears to be stable indefinitely, even when exposed occasionally to air during weighing operations.

Presumably also because of its stability towards hydrolysis, adequate protein conjugation may be achieved at modest anhydride to protein molar ratios. For example, this laboratory prefers to conjugate antibodies at concentrations of about 10 mg/ml using an anhydride/protein molar ratio of about 2:1, although in practice the protein concentration is often closer to 1 mg/ml, and in this case an anhydride/protein molar ratio of about 5:1 is selected [22]. Usually the volume of the protein solution undergoing conjugation is much less than 1 ml and thus quantities of cDTPA are required that are too small to be accurately weighed. As such, this laboratory prefers to disperse the anhydride at a suitable concentration (i.e., 1 mg/ml) in chloroform or ether. The anhydride is not soluble in these solvents, however, after ultrasonication to a fine suspension, the desired weight of cDTPA may be removed accurately [23]. The advantage of chloroform, and especially ether, is their high vapor pressure, which facilitates the evaporation (particularly under a gentle stream of nitrogen) of cDTPA on the bottom of the vessel to be used for conjugation. Dimethylsulfoxide (DMSO) has also been employed for this purpose [7,21,24,25], since cDTPA is more soluble in this solvent. A disadvantage to DMSO is its low vapor pressure, which makes difficult the removal of even a substantial fraction of the solvent from cDTPA prior to conjugation. Thus DMSO is introduced into the protein solution during conjugation. The solvent is effectively removed during purification of the conjugated protein, however, it has been suggested that DMSO may harm sensitive proteins, even at tracer concentrations [21]. It is unclear whether there are advantages to protein conjugation with cDTPA as the solid or in DMSO solution.

Although it remains to be definitely established, it is very likely that cDTPA acylates amines such as those of lysine residues, rather than other nucleophilic species in proteins [26]. Since the pKa of lysine amines is approximately 10 [26], it is not surprising that the coupling efficiency passes through a maximum at about pH 8, since below this value the amines are largely protonated, while above this value the rate of hydrolysis of cDTPA predominates [22]. As such, conjugation is normally performed at pH values of 7–8 and usually in dilute bicarbonate solutions, which act as a buffer in this pH range.

In this laboratory, an antibody to be conjugated is usually dissolved in 0.05 M bicarbonate buffer, pH 8, at the desired concentration and added rapidly to the dried cDTPA while vortexing [23]. Only when a large weight of cDTPA is employed does the pH decrease during conjugation and, in these cases, the molarity of the bicarbonate solution is normally increased to provide effective buffering. Other laboratories have employed 0.25 M phosphate buffer, pH 8.0 [21]; HEPES-HCl buffer, pH 7.0 [20]; 0.05 M HEPES buffer, 0.9% NaCl, pH 7.0 [7]; 0.5 M phosphate buffer, pH 7.5 [19]; 0.1 M HEPES, 0.9% NaCl, pH 7.4 [18]; and 0.1 M borate buffer, pH 8.6 [24] among others, apparently with satisfactory results. In the case of tissue plasminogen activator, a protein that is solubilized in the presence of strong choatropic ions, it was possible to conjugate in 2 M KSCN or urea at pH 8 [8].

An important property of antibody modification with any substituent is the degree of conjugation (i.e., the average number of groups attached to each protein molecule), since antibody integrity suffers with increasing conjugation [24,27,29]. Presumably this is related to the increasing probability of conjugating within the antibody's combining site. Accordingly, if possible, the degree of conjugation should be restricted to an average of approximately one to preserve to the greatest extent the integrity of the antibody. At an average of one group per molecule, only about 25% of the protein molecules posses two or more groups, provided that Poisson statistics apply [23], and this may explain the minimal effects observed at this degree of conjugation.

Radiolabeling

The vast majority of studies with conjugated antibodies have employed ^{111}In as the label because of the favorable physical and chemical properties of this radionuclide. Complicating its use, however, is the tendency of indium to form an insoluble hydroxide in neutral solutions in the absence of complexing ions [30]. It was to avoid the formation of these radiocolloids that investigators first added ^{111}In to the conjugated protein at acid pH, despite the harmful effects of an acidic environment on many proteins. It was soon determined, however, that ^{111}In could be added at near-neutral pH if a weak complexing agent were added that could compete with hydroxyl ions for the metal but yet would not prevent transcomplexation to the DTPA groups [5,31]. Thus this and other laboratories normally add ^{111}In in 0.05 M acetate solution, pH 6, while others prefer 0.03–1.0 M citrate at pH 5–6 for this purpose [24,28]. Being a stronger complexing agent than acetate, citrate is likely to interfere with transcomplexation to a greater degree, although for the same reason the concentration of cirtrate may be reduced below that of acetate to achieve the same result. It has been suggested that, in the presence of trace metal impurities, the effect of this contamination of protein labeling is less serious in the presence of citrate ion [32].

If the labeling efficiency (i.e., the percentage of added radioactivity that is ultimately chelated to the protein) is low, it will be necessary to purify the labeled protein from unbound radioactivity. This has been accomplished in various laboratories by dialysis, open-column G50 Sephadex chromatography, size-exclusion HPLC, and, more recently, by centrifugation using commercially available concentrators. It is preferable, however, that labeling efficiencies be sufficiently high that purification is not required. This is especially true for preparations intended for human use. This laboratory now has clinical experience with three antibodies labeled with ^{111}In and one antibody labeled with ^{90}Y. Using these antibodies conjugated with an average of one group per molecule, it has been possible to label at specific activities of 1–5 mCi/mg with both radioisotopes by 'kit' methods in which, because of 95% or greater labeling efficiency, postlabeling purification was not required or performed [33–35].

Occasionally, investigators will intentionally add a chelating agent such as EDTA or DTPA to an ^{111}In-labeled antibody prior to its use to remove radioactivity bound nonspecifically to the protein at sites other than the attached DTPA groups [36]. Any radioactivity removed from the protein in this manner will be cleared rapidly through the kidneys following administration and thus would not interfere with imaging. This laboratory routinely performs hydrolyzed control studies, which consistently show that under the conditions or radiolabeling and for the antibodies considered, ^{111}In is chelated exclusively to the bound DTPA groups [22]. As such and under these conditions, the use of such a scavenger is probably unwarranted.

To achieve high specific activities of radiolabeled antibodies, particularly accompanied with good labeling efficiencies, it is necessary to observe common sense precautions to avoid introducing trace metals at levels that will interfere. The extent to which trace metals will interfere will depend, in part, on the concentration of DTPA groups. It may be demonstrated, for example, that labeling efficiency will fall with decreasing protein (and therefore DTPA) concentration, even if the specific activity is held constant (i.e., constant millicuries of ^{111}In per milligram of protein) [23]. Thus, even though the ratio of ^{111}In atoms to DTPA groups is unchanged, labeling efficiency will fall with the DTPA concentration to demonstrate that the chelate concentration must be sufficient to complex all of the ^{111}In as well as the trace metals, which are invariably present, if good labeling efficiencies are to be achieved.

Label stability in serum

The stability of a radiolabel on an antibody is difficult to assess in vivo, since normal antibody catabolic processes may result in the release of the radionuclide to confuse the biodistribution. The estimation of the stability of a label in serum is, however, straightforward and meaningful if determined in vitro by incubation in 37°C serum. In the case of DTPA-conjugated antibodies, in-vitro serum incubations have been performed for ^{111}In [22,37,38], ^{90}Y [11], ^{99m}Tc [16], ^{153}Gd [17,19], ^{67}Cu [39], and ^{57}Co [40]. Affinity chromatography of serum samples obtained from animals has been used to assess the serum stability of ^{46}Sc and ^{67}Ga on DTPA-coupled antibodies [21], even though the loss from circulation of the products of label instability in this case would result in an overestimate of serum stability.

The results of these investigators illustrate the extent to which label stability is dependent upon the label. Whereas the serum stability of ^{111}In, ^{90}Y, ^{153}Gd, and ^{57}Co on DTPA-coupled antibodies is probably satisfactory for most in-vivo applications, the instability observed for ^{99m}Tc and ^{67}Cu must be considered unacceptable. In the case of ^{111}In, serum instability is the result of transcomplexation of the label to transferrin, a process that is thermodynamically favored. The extent of transcomplexation is estimated at approximately 9% of the label exposed to transferrin per day and appears to be independent

of the protein [17]. Under the assumption that circulating ^{111}In-labeled transferrin leaves the circulation only slowly, the rate of transcomplexation has been found to occur in patients at approximately the same rate as that observed in vitro [33,34]. Since serum activity levels normally decrease rapidly such that much of the injected activity is no longer exposed to transferrin, the rate of transcomplexation in patients has been estimated for one antibody to be 1–2% of the injected dose per day [33].

Quality assurance

Following conjugation of an antibody with cDTPA, it is often necessary to measure the average number of DTPA groups attached, since too many attached groups may alter the protein, while too few may interfere with antibody labeling. In addition, it is usually important to evaluate the extent of dimer formation and the immunoreactivity of the conjugated antibody.

Various assays have been employed for the determination of the average number of attached DTPA groups following protein conjugation with cDTPA. Liquid scintillation counting of the conjugated protein has provided the answer in cases where ^{14}C- or ^{3}H-labeled cDTPA was employed [21]. An alternative approach is to count the protein after saturation with stable indium containing a known activity of ^{111}In [5,24,27,28]. The simplest method, however, exploits the fact that the formation constant for indium of free DTPA and conjugated DTPA are identical within experimental error [22,27]. Thus a tracer quantity of ^{111}In added to a conjugated protein, still unpurified from free DTPA, will distribute between free and bound DTPA in proportion to the concentrations of each. However, evidence has been presented that at low average numbers of attached DTPA groups (i.e., 0.13), free DTPA competes more effectively than does bound DTPA for indium [28].

Since cDTPA contains two anhydride groups per molecule, the possibility always exists that intramolecular and intermolecular crosslinking will occur. Intramolecule crosslinking is difficult to observe, whereas intermolecular crosslinking leads to dimeric and multimeric protein species, which are usually readily apparent by size-exclusion or gel-filtration chromatography and electrophoresis. The experiences of this laboratory suggest that antibodies differ in their susceptability to crosslinking but that, in the case of one antibody, the presence of 20% dimer had no detectable effect on antibody immunoreactivity or on biodistribution in patients [34]. The extent of dimer formation decreases with decreasing protein concentration at conjugation and increases with an increasing anhydride/protein molar ratio [22].

Related to the degree of conjugation and possibly to dimer formation is the 'immunoreactivity' of the conjugated antibody. Since the process of conjugation can denature sensitive proteins such as antibodies, it is necessary to establish for each conjugated antibody that its ability to bind to its antigen has

not been impaired. This may be accomplished by measuring the immunoreactive fraction and avidity of the antibody before and after conjugation [41]. An alternative approach favored by this laboratory is to measure the ability of the conjugated antibody to compete for its antigen. Using this assay it has been possible to show that antibodies used in clinical trials showed no detectable decrease in competitiveness with the native, unconjugated antibody for their antigens [33,34].

Liver radioactivity levels

An issue that has raised concerns regarding the use of antibodies radiolabeled with ^{111}In via cDTPA is the accumulation of the label in liver. When first observed, it was naturally assumed that this accumulation was the result of antibody denaturation during conjugation and/or radiolabeling. However, the unwanted accumulation of activity in liver and other organs is not the result of antibody denaturation in some, and probably most, cases, since no evidence of radiocolloid formation, nonspecific binding of ^{111}In, or loss of immunoreactivity has been observed in several clinical trials with antibodies labeled via cDTPA [34,35]. It is more likely that the observed liver levels are a result of normal processes occurring in this and other organs of antibody catabolism. If this is the case and, as is likely, accumulation of an antibody in liver is largely independent of its label (when properly attached), then initial liver levels should also be independent of the label. When reduced or decreasing liver levels are then observed, metabolizable linkages may be involved that dissociate upon catabolism, with the release and subsequent diffusion of the label from the organ. This phenomenon certainly occurs in the case of antibodies radioiodinated on tyrosines and may also occur with antibodies radiolabeled with ^{111}In following conjugation with analogues of EDTA [42] and DTPA [43] via an isothiocyanate group. In contrast, the analysis of patient urine collected after administration of antibodies radiolabeled with ^{111}In via cDTPA has shown no evidence for in-vivo dissociation of the amide bond by which DTPA is covalently attached to these proteins [34,35]. The biodistribution of ^{111}In in these cases probably faithfully represents the biodistribution of the antibody. However, since there is little clearance, liver radioactivity levels are elevated and are potentially problematic.

Conclusions

Experiences with cDTPA in this laboratory and others over the past 5 years have demonstrated the usefulness of this anhydride for the attachment of DTPA to antibodies. The anhybride is inexpensive, and because of its stability towards hydrolysis, considerable control over conjugation is possible. As

a result, in many cases it has been possible to choose and then achieve a particular degree of conjugation. When conjugated with an average of approximately one DTPA group per molecule, immunoreactivity is normally preserved. A particular advantage to the use of cDTPA is the fact that conjugation is completed within minutes and an entire labeling in 1–2 hours. This has been particularly useful in those investigations where it was necessary to conjugate and radiolabel many proteins simultaneously. When radiolabeled with ^{111}In, antibodies conjugated with cDTPA have been shown to be unstable in vivo only to transcomplexation and at a rate that is unlikely to be reflected in the quality of the images. Because of the stability of the amide bond, the biodistribution of ^{111}In following administration of antibodies labeled via cDTPA more faithfully reflects the biodistribution of the antibody than do those methods involving metabolizable linkages. Since dissociation and clearance of the label apparently does not occur, liver activity levels may be more pronounced; however, it is possible that a similar increase in tumor levels may result for the same reason. In summary, antibody conjugation via cDTPA is well established, successful, and is at present the simplest conjugation method and is likely to remain so for the foreseeable future.

Acknowledgments

This work was supported in part by Centocor, Inc. and by the National Institutes of Health (CA 33029).

References

1. Sundberg, M., Meares, C.F., Goodwin, D.A., et al. (1974) Selective binding of metal ions to macromolecules using bifunctional analogs of EDTA. J. Med. Chem. 17:1304–1307.
2. Hnatowich, D.J. (1986) Labeled proteins in nuclear medicine — current status. In: Billinghurst, M. (ed.), *Current Applications in Radiopharmacology*. New York: Pergamon Press, pp. 257–270.
3. Meares, C.F. (1986) Chelating agents for the binding of metal ions to antibodies. Nucl. Med. Biol. 13:311–318.
4. Krejcarek, G.E., and Tucker, K.L. (1977) Covalent attachment of chelating groups to macromolecules. Biochem. Biophys. Res. Commun. 77:581–585.
5. Hnatowich, D.J., Layne, W.W., and Childs, R.L. (1982) The preparation and labeling of DTPA-coupled albumin. Int. J. Appl. Radiat. Isot. 33:327–332.
6. Layne, W.W., Hnatowich, D.J., Doherty, P.W., et al. (1982) Evaluation of the viability of ^{111}In-DTPA-coupled fibrinogen. J. Nucl. Med. 23:627–630.
7. Lavie, E., Bitton, M., Ringler, G., et al. (1984) Modified human fibrinogen labeled with ^{111}In. Int. J. Appl. Rad. Isot. 35:69–70.
8. Hnatowich, D.J., Virzi, F., Doherty, P.W., et al. (1987) Functional characterization of indium-111 labeled recombinant tissue plasminogen activator for the imaging of thrombi. Eur. J. Nucl. Med. 13:467–473.
9. Hnatowich, D.J., Virzi, F., and Rusckowski, M. (1987) Investigations of avidin and biotin for imaging applications. J. Nucl. Med. 28:1294–1302.

10. Lanteigne, D., and Hnatowich, D.J. (1984) The labeling of DTPA-coupled proteins with ^{99m}Tc. Int. J. Appl. Radiat. Isot. 7:617–621.
11. Hnatowich, D.J., Virzi, F., and Doherty, P.W. (1985) DTPA-coupled antibodies labeled with yttrium-90. J. Nucl. Med. 26:503–509.
12. Vaughan, A.T.M., Keeling, A., and Yankuba, S.C.S. (1985) The production and biological distribution of yttrium-90 labeled antibodies. Int. J. Appl. Rad. Isot. 36:803–806.
13. Washburn, L.C., Hwa Sun, T.T., Crook, J.E., et al. (1986) ^{90}Y-labeled monoclonal antibodies for cancer therapy. Nucl. Med. Biol. 13:453–456.
14. Chinol, M., and Hnatowich, D.J. (1987) Generator-produced yttrium-90 for radioimmunotherapy. J. Nucl. Med. 28:1465–1470.
15. Buchsbaum, D.J., Hanna, D.E., Randall, B.C., et al. (1986) Radiolabeling of monoclonal antibodies against carcinoembryonic antigen with ^{88}Y and biodistribution studies. Int. J. Nucl. Med. Biol. 12:79–82.
16. Childs, R.L., and Hnatowich, D.J. (1985) Optimum conditions for labeling of DTPA-coupled antibodies with technetium-99m. J. Nucl. Med. 26:293–299.
17. Hnatowich, D.J. (1986) Label stability in serum of four radionuclides on DTPA-coupled antibodies — an evaluation. Nucl. Med. Biol. 13:353–358.
18. Unger, E.C., Totty, W.G., Neufeld, D.M., et al. (1985) Magnetic resonance imaging using gadolinium labeled monoclonal antibody. Invest. Rad. 20:693–700.
19. Anderson-Berg, W.T., Strand, M., Lempert, T.E., et al. (1986) Nuclear magnetic resonance and gamma camera tumor imaging using gadolinium-labeled monoclonal antibodies. J. Nucl. Med. 27:829–833.
20. Fawwaz, R.A., Wang, T.S.T., Srivastava, S.C., et al. (1984) Potential of palladium-109-labeled antimelanoma monoclonal antibody for tumor therapy. J. Nucl. Med. 25:796–799.
21. Anderson, W.T., and Strand, M. (1985) Stability, targeting and biodistribution of scandium-46 and gallium-67 labeled monoclonal antibody in erythroleukemic mice. Cancer Res. 45: 2154–2158.
22. Hnatowich, D.J., Childs, R.L., Lanteigne, D., et al. (1983) The preparation of DTPA-coupled antibodies radiolabeled with metallic radionuclides: An improved method. J. Immunol. Method 65:147–157.
23. Hnatowich, D.J., and McGann, J. (1987) DTPA-coupled proteins — procedures and precautions. Nucl. Med. Biol. 14:563–568.
24. Paik, C.H., Ebbert, M.A., Murphy, P.R., et al. (1983) Factors influencing DTPA conjugation with antibodies by cyclic DTPA anhydride. J. Nucl. Med. 24:1158–1163.
25. Pimm, M.V., Perkins, A.C., and Baldwin, R.W. (1987) Diverse characteristics of ^{111}In labeled anti-CEA monoclonal antibodies for tumor immunoscintigraphy: Radiolabeling, biodistribution and imaging studies in mice with human tumor xenografts. Eur. J. Nucl. Med. 12:515–521.
26. Feeney, R.E., Yamasaki, R.B., and Geoghegan, K.F. (1982) Chemical modification of proteins: An overview. In: Feeney, R.E., and Whitaker, J.R. (eds.), *Modification of Proteins. Food, Nutritional and Pharmacologic Aspects*. Washington, DC: American Chemical Society, pp. 3–55.
27. Sakahara, H., Endo, K., Nakashima, T., et al. (1985) Effect of DTPA conjugation on the antigen binding activity and biodistribution of monoclonal antibodies against alpha-fetoprotein. J. Nucl. Med. 26:750–755.
28. Paik, C.H., Hong, J.J., Ebbert, M.A., et al. (1985) Relative reactivity of DTPA, immunoreactive antibody-DTPA conjugates, and nonimmunoreactive antibody-DTPA conjugates towards indium-111. J. Nucl. Med. 26:482–487.
29. Fawwaz, R.A., Wang, T.S.T., Estabrook, A., et al. (1985) Immunoreactivity and biodistribution of indium-111 labeled monoclonal antibody to a human high molecular weight melanoma associated antigen. J. Nucl. Med. 26:488–492.
30. Welch, M.J., and Welch, T.J. (1975) Solution chemistry of carrier-free indium. In: Subramanian, G., Rhodes, B.A., Cooper, J.F., et al. (eds.), *Radiopharmaceuticals*. New York: The Society of Nuclear Medicine Press, pp. 73–79.

31. Hnatowich, D.J., Friedman, B., Clancy, B., et al. (1981) Labeling of performed liposomes with Ga-67 and Tc-99m by chelation. J. Nucl. Med. 22:810–814.
32. Wu, J.L., Ma, J.M., Look, S.R., et al. (1985) Masking of trace metal contamination with citrate in the In-111 labeling of Mab-DTPA (abstract). J. Nucl. Med. 26:120.
33. Hnatowich, D.J. Griffin, T.W., Kosciuczyk, C., et al. (1985) Pharmacokinetics of an indium-111 labeled monoclonal antibody in cancer patients. J. Nucl. Med. 26:849–858.
34. Hnatowich, D.J., Gionet, M., Rusckowski, M., et al. (1987) Pharmacokinetics of indium-111 labeled OC-125 antibody in cancer patients — a comparison with the 19-9 antibody. Cancer Res. 47:6111–6117.
35. Hnatowich, D.J., Chinol, M., Siebecker, D.A., et al. (1988) Biodistribution in patients of intraperitoneal-administered antibody radiolabeled with yttrium-90. J. Nucl. Med. 29:1428–1434.
36. Carrasquillo, J.A., Bunn, P.A., Jr., Keenan, A.M., et al. (1986) Radioimmunodetection of cutaneous T-cell lymphoma with ^{111}In-labeled T101 monoclonal antibody. N. Engl. J. Med. 315:673–680.
37. Najafi, A., Childs, R.L., and Hnatowich, D.J. (1984) Coupling antibody with DTPA — an alternative to the cyclic anhydride. Int. J. Appl. Rad. Isot. 35:554–557.
38. Halpern, S., Hagan, P.L., Graver, P.R., et al. (1983) Stability, characterization, and kinetics of ^{111}In-labeled monoclonal antitumor antibodies in normal animals and nude mouse-human tumor models. Cancer Res. 43:5347–5355.
39. Moi, M.K., Meares, C.F., McCall, M.J., et al. (1985) Copper chelates as probes of biological systems: Stable copper complexes with a macrocyclic bifunctional chelating agent. Anal. Biochem. 148:249–253.
40. Cole, W.C., DeNardo, S.J., Meares, C.F., et al. (1987) Comparative serum stability of radiochelates for antibody radiopharmaceuticals. J. Nucl. Med. 28:83–90.
41. Badger, C.C., Krohn, K.A., and Bernstein, I.D. (1987) In vitro measurement of acidity of radioiodinated antibodies. Nucl. Med. Biol. 14:605–610.
42. Denardo, S., (1987) Private communication.
43. Estseban, J.M., Schlom, J., Gansow, O.A., et al. (1987) New method for the chelation of indium-111 to monoclonal antibodies: Biodistribution and imaging of athymic mice bearing human colon carcinoma xenografts. J. Nucl. Med. 28:861–870.

9. Bifunctional chelating agents for radiometal-labeled monoclonal antibodies

Ramaswamy Subramanian and Claude F. Meares

Recently there has been a great deal of interest in attaching metal ions to proteins. Since a variety of metal ions possess interesting chemical, physical, nuclear, and magnetic properties, they can be employed to probe the behavior of biologic systems. For example, fluorescent-labeled proteins, proteins containing paramagnetic chelates, and proteins bound to photosensitive metal chelates have been studied [1]. When the metal is radioactive and the protein is an antibody that has high specficity for tumors, the resultant chelate-antibody conjugate can be employed for cancer diagnosis. Monoclonal antibodies that possess a high affinity for tumor-associated antigens can now be prepared due to the technique developed by Kohler and Milstein [2]. By attaching a radionuclide to such a monoclonal antibody of predetermined specificity, one can selectively localize the radioactivity at tumor sites. This principle has been employed in developing new pharmaceuticals for use in radioimmunodiagnosis and, in certain cases, radioimmunotherapy [3,4]. In this review we will briefly examine the chemical aspects of bifunctional chelating agents for linking radiometals to monoclonal antibodies.

Bifunctional chelating agents are compounds that can bind metal ions and at the same time can be covalently linked to a protein such as a monoclonal antibody. Some of the bifunctional chelating agents used previously in nuclear medicine are given in Table 1. A large number of these, such as ethylenediaminetetraacetate (EDTA) [5], diethylenetriaminepentaacetate (DTPA) [6], and iminodiacetate (IDA) [7], contain polyaminocarboxylate groups as the metal-binding moiety (Figure 1). These chelates can bind a variety of metal ions; the literature reveals that more than 70 different elements in the periodic table can bind efficiently to EDTA analogs [8].

Methods of preparation

When designing a BCA several factors must be taken into consideration. The choice of the chelating group depends on the metal ion chosen for binding to the antibody. The metal chelate should be thermodynamically stable. For example, the thermodynamic stability constants for the formation of metal-

Goldenberg, D.M., (ed.), Cancer Imaging with Radiolabeled Antibodies.

Table 1. Some protein-chelate conjugates

Metal	Properties	Chelating Agent	Protein	References
^{111}In	E.C., 2 γ $T_{1/2}$ = 67 hr	1-(p-azophenyl)-EDTA	Albumin	Sundberg et al. [5,20]
		DTPA	Albumin	Krejcarek and Tucker [6]
		1-(p-isothiocyanato-benzyl)EDTA/DTPA	Mabs	Meares et al. [19] Brechbiel et al. [43]
		DTPA	Mab	Hnatowich et al. [22]
		Oxine	Blood cells	McAfee and Thakur [44]
^{90}Y	2.3 MeV β $T_{1/2}$ = 64 hr	DTPA	Human IgG	Hnatowich et al. [45]
^{67}Cu	0.6 MeV β $T_{1/2}$ = 61 hr	TETA	Mab	Meares et al. [42]
		Porphyrins	Polyclonal Ab	Cole et al. [46]
^{99m}Tc	I.T., γ $T_{1/2}$ = 6 hr	DTPA	Mab	Khaw et al. [47]
		Sulfhydryl groups	Albumin	Rhodes and Burchiel [48]
^{212}Bi	6 MeV α $T_{1/2}$ = 60 min	DTPA	Mab	Kozak et al. [49]
^{203}Pb	E.C., γ $T_{1/2}$ = 52 hr	DTPA	Mab	Srivastava et al. [50]

EDTA complexes are usually very high [9]. Note, however, that tabulated stability constants are ideal thermodynamic quantities for reaction between metal ion and chelator *only*; they do not take into account the equilibria involving H^+ binding to the ligand and OH^- binding to the metal that are known to occur in all aqueous solutions (the needed additional equilibrium constants are generally included elsewhere in the same reference, and some calculation is needed in order to understand the effects of pH on metal-chelate equilibria [10]). The *rate* of dissociation of the metal ion from the chelate must be very low under physiologic conditions (pH 7.4, 37°C). It is advantageous to have a BCA that readily combines with metal ions. In particular, if the monoclonal antibody-chelator conjugate is prepared first, and followed by metal ion attachment, one should make sure that the conditions for chelation are mild enough not to affect the properties of the monoclonal antibody. The bifunctional chelating agent must be designed to suit this purpose.

Backbone-substituted EDTA or DTPA molecules bind metal ions such as In^{3+} quite readily at room temperature. Also, the loss of metal from the chelate is very low (< 1% per day for indium) under physiologic conditions [11]. Naturally occurring amino acids can be converted to BCA [12]. The synthetic methodology employed to prepare 1-(p-nitrobenzyl)-EDTA and 1-(p-nitrobenzyl)-DTPA from L-phenylalanine is particularly versatile. First a para nitro group is introduced into the phenyl ring, then the amino acid is

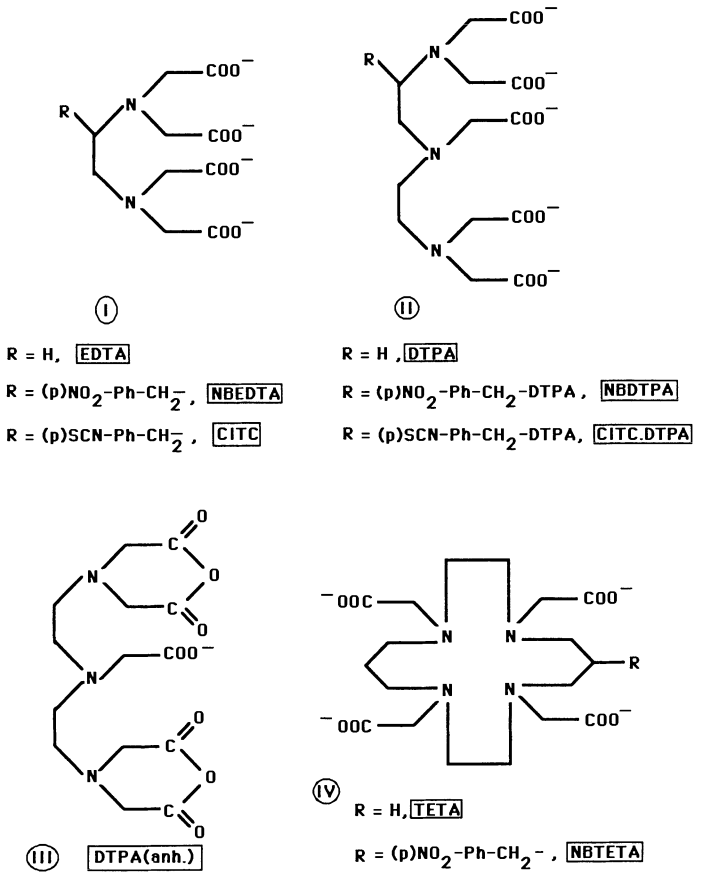

Figure 1. Structures of some bifunctional chelating agents. I: EDTA and analogs of EDTA; II: DTPA and analogs of DTPA; III: DTPA bicyclic anhydride; IV: The macrocycle TETA.

converted to an ester, and then an amide. The amide is reduced to an amine using borane. The product thus obtained is carboxymethylated using bromoacetic acid to give 1-(para-nitrobenzyl)-EDTA [13]. The use of different amines to make the amides leads to the formation of other useful chelating groups such as DTPA, HED3A, etc. [14]. The structures of some of these BCAs are shown in Figure 1 (I, II). Not only can the structure of the chelating group be varied, but the aromatic amino group produced by reduction of the nitrobenzyl side chain may be converted into a number of reagents for attachment to proteins. Also, the use of different amino acids as starting materials provides a variety of different side chains for further chemistry [15].

Methods of attaching chelating agents to antibodies

Let us now look at the various ways in which bifunctional chelating agents can be attached to antibodies. Because an IgG antibody molecule may well

contain 80–90 lysine residues (of which only a small number are likely to be near the antigen combining site), lysine ε-amino groups are usually good targets [16]. There are many target sites on an antibody, and some of them may be essential for biologic activity. It is customary to label only a small fraction (e.g., 1–2 out of 80–90 ε-amino groups) and then assay for immunoreactivity. To a first approximation, it may be expected that chemistry directed toward a particular residue, such as lysine, will produce a statistical mixture of products [17].

As an example, consider the monoclonal antibody MOPC173. This contains 84 lysines [18], of which four are located in complementarity determining regions and thus are important for antigen binding. If all lysines were equally reactive, then modifying one of the 84 lysines present in MOPC173 would involve a lysine in a complementarity determining region with a probability of only 4 in 84, or 4.8%. Assuming that any hit in a complementarity-determining region inactivates the antibody, but any other hit has no effect, this would have a 95% chance of producing an active conjugate.

However, our own experience with antibody conjugation is a reminder that other factors are important. The surroundings of each residue play an important role in determining its chemical reactivity; nearby positively charged groups can lower the pKa of a lysine ε-amino group, densely packed side chains can provide steric hindrance to chemical reactions, and so on. Also, the α-amino groups of the polypeptide chains (four per antibody, near the complementarity-determining regions in the three-dimensional structure) react with the same reagents as lysine ε-amino groups. We have found, using a variety of reagents and conditions, that conjugates with a given monoclonal antibody can be fully active, completely inactive, or anything in between.

If the bifunctional chelating agent contains a primary aromatic amino group on a side chain, it can be linked to a protein in a variety of ways. Some are illustrated in Figure 2. The para-isothiocyanatobenzyl-EDTA in Figure 2 (CITC) can react with the ε-amino groups of lysine residues, or the four α-amino groups in the monoclonal antibody (pH 9, 37°C, 2 hours), to obtain a chelate-antibody conjugate [19]. The para-bromoacetamidobenzyl-EDTA (BABE), when incubated with a monoclonal antibody (pH 9, 37°C, 2 hours) readily forms a chelate-antibody conjugate by alkylating amino groups, imidazole groups, and other nucleophilic sites (such as thiols) in the antibody [19]. The diazonium reagent in Figure 2 can be coupled with a protein [20], reacting with amino, imidazole, and phenol groups. However, the bonds thus formed between protein and chelate are subject to slow hydrolysis under physiologic conditions [21].

Other bifunctional chelating agents containing a reactive group can also be coupled to a Mab. For DTPA anhybride, mixing of anhydride and antibody leads to the formation of an antibody-chelate conjugate by acylation of amino groups [22]. Also, a side-chain carboxylic acid group can be coupled with a protein amino group using a carbodiimide [12].

The various factors to be considered while conjugating a chelating agent to

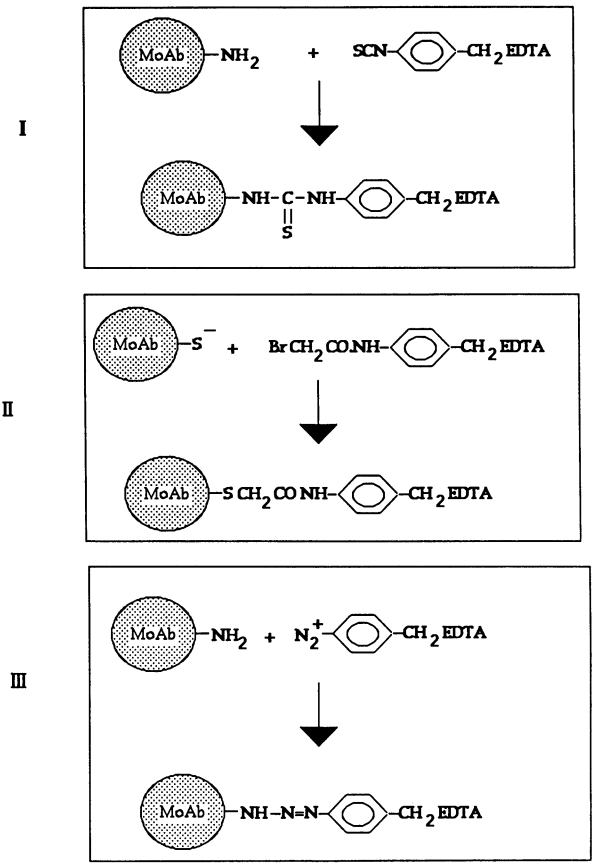

Figure 2. Conjugation of bifunctional chelating agents to monoclonal antibodies (MoAb). I: CITC; II: BABE; III: azophenyl-EDTA.

a monoclonal antibody are that the chelator-antibody conjugate must be stable in vivo, the conjugation should not affect the biologic properties of the antibody, and the process of conjugation should be simple (moderate temperature, pH 4–10, few hours of reaction time). While conjugating a chelating agent to an antibody, one should make sure that this does not lead to cross-linking of protein, aggregation, or other undesirable side reactions.

After the conjugation reaction, the chelator-antibody conjugate must be readily purifiable by a simple technique. The most commonly used methods of purification are gel-filtration column chromatography and high-performance liquid chromatography (HPLC). We use the procedure shown in Figure 3. After conjugation when the reaction mixture is passed through a fel-filtration column (typically, a G50-80 resin), the low molecular weight compounds are retained in the column. Pure chelate-antibody conjugate is collected in the effluent [23]. HPLC with gel-filtration columns (e.g., TSK3000) can be effectively employed to remove aggregates, if any, formed during conjugation.

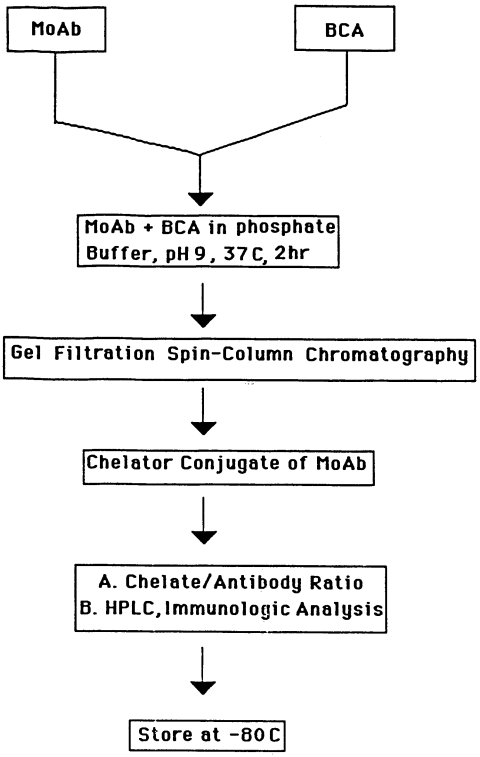

Figure 3. Preparation, purification, and characterization of chelate-antibody conjugates. MoAb, monoclonal antibody; BCA, bifunctional chelating agent; HPLC, high performance liquid chromatography.

Other ion-exchange or affinity-column chromatography techniques (depending on the specificity and nature of the antibody) could also be employed. We use common spectrophotometric methods, gel electrophoretic analysis, and radioimmunoassays to characterize antibody-chelate conjugates.

The number of chelating groups available for binding metal ions can be determined as follows. The chelate-antibody conjugate is treated with an excess of a metal-ion solution of known concentration, containing trace amounts of radioactive metal (typically 10 mM Co^{2+} or In^{3+} solution containing ^{57}Co or ^{111}In, respectively). The mixture is allowed to sit at room temperature for 15–20 minutes at pH 5–6. The unreacted metal ion is converted to its corresponding EDTA chelate by adding excess EDTA to the solution. When this reaction mixture is subjected to thin-layer chromatography or to gel-filtration spin-column chromatography (Sephadex G50-80 resin), the radiometal-chelate-antibody conjugate is separated from the EDTA-metal chelate. A simple calculation provides the desired answer [19].

The ratio of attached chelates to antibody molecule is normally kept around 1–2. Too low a ratio will lead to a lower specific activity of the radiolabeled protein than desirable for radiopharmaceutical purposes. Too high a

ratio could lead to significant loss of immunoreactivity of the protein, though we have seldom found this to be a problem.

Attaching radiometals to monoclonal antibody-chelate conjugates

There are two choices for preparing metal-labeled Mabs. The first method involves the attachment of BCA to Mab, followed by labeling with the radiometal. In the second method, the metal chelate is prepared first and then attached to the Mab. The former is routinely employed for radiolabeling antibodies for clinical use because of the short half-lives of the medically useful radiometals. The details of the methodology employed to bind metals to antibody-chelate conjugates depend on the chemical properties of the metal ion involved. For coupling with ^{111}In, the reaction mixture is kept at room temperature for 0.5–1 hours at pH 5–6 (Figure 5). For ^{67}Cu, the reaction is maintained at pH 7–8. It is not practical to employ a higher pH for ^{111}In, as it readily hydrolyzes at high pH [24] (Figure 4).

Another problem in adding radiometals to protein-chelator conjugates is that, since carrier-free radiometal is employed, the concentration of the metal ion is very low (< 1 μM). Under these conditions extraneous metal ions,

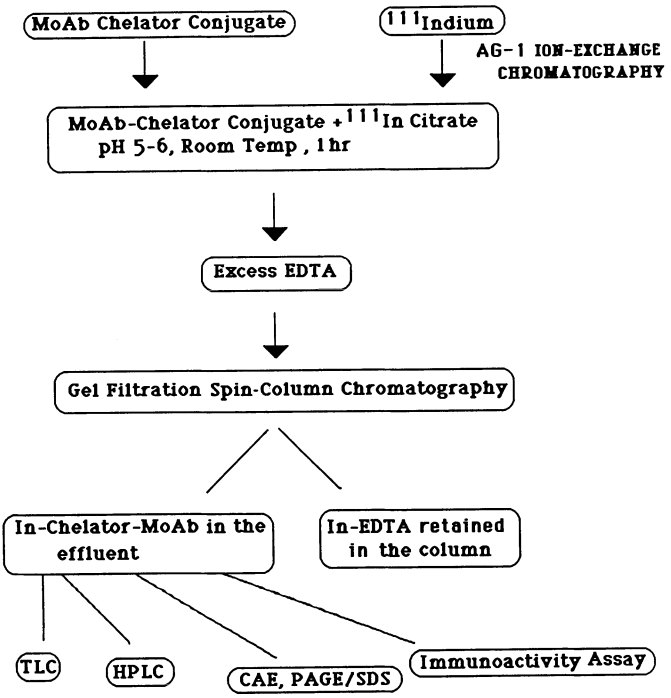

Figure 4. Radiolabeling antibody-chelate conjugates with indium-111. PAGE/SDS = polyocrylamide gel electrophoresis using sodium dodecyl sulfate; TLC = thin-layer chromatography.

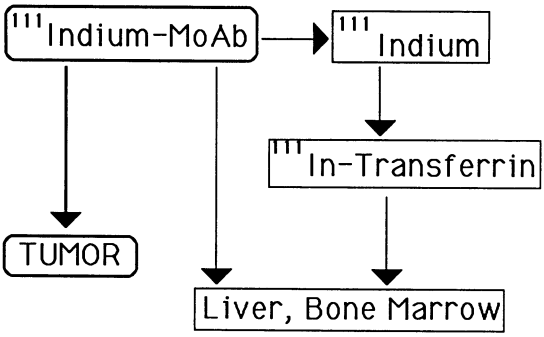

Figure 5. The decomposition of indium-111 radiopharmaceuticals in circulation.

such as Fe^{2+}, Zn^{2+}, or Ca^{2+}, present in buffers and reaction vials as contaminants, can effectively compete with the radiometal for chelation. This will lead to less efficient labeling of the protein and hence lower specific activity than desirable. To avoid this, all reaction vials and other labware should be washed with a mixed acid solution [19]. Ultrapure (18 Mohm) water should be employed for the preparation of buffers. For the labeling reactions the chelator concentration should be at least 10 μM, and preferably 100 μM.

The radiometal employed must not contain significant amounts of metallic impurities. Commercially available radiometals can be purified by a suitable ion-exchange technique (AG-1 column elution for $^{111}InCl_3$). The various stages involved in the preparation of radiometal (^{111}In)-bound monoclonal antibody are shown in Figure 4. As the radiometal undergoes hydrolysis at high pH in water, the chelation is carried out in a buffer with metal-binding properties, such as citrate. The buffer also prevents the metal from binding to the amino acid side chains of the Mab. It is important to remove the unchelated radiometal from the antibody-chelate conjugate, as this would otherwise be deposited in nontarget tissues of the body. This may be accomplished by converting unbound ^{111}In to the In-EDTA chelate by adding excess EDTA and then removing it by gel-filtration. The radiometal-labeled conjugate should then be challenged again with EDTA, under conditions where it has been shown that the EDTA will remove all radiometal from the unmodified antibody, and checked for removable radioactivity by gel-filtration or by thin-layer chromatography. On a silica-gel, thin-layer chromatography plate (employing a 50/50 mixture of 10% ammonium acetate and methanol as the mobile phase), In-EDTA moves to Rf 0.8, whereas Mab-chelate-In conjugates remain at the origin.

The need to verify that all the radiometal in the final preparation is actually in the chelating groups cannot be overemphasized, as there are several published studies of chelate-labeled antibodies in which the uncontrolled presence of unchelated radiometal is obvious. This pervasive problem hinders progress toward development of optimal procedures for the use of radiometal-labeled Mabs.

Table 2. Concentrations of some metal-binding molecules in blood

Substance	Concentration, mM
Transferrin	0.05
Albumin	0.5
Glycine	0.3
Citrate	0.1
Glutamate	0.1

Kinetic considerations

A major consideration in order for a metal chelate to be useful for radiodiagnosis and therapy is its kinetic inertness, that is, the rate of loss of radioactive metal ion from the chelate to other metal-binding molecules in the body must be slow. In general, the radiolabeled Mab is administered intravenously. Blood serum contains substantial concentrations of metal-binding proteins, such as transferrin and albumin, and other metal-binding molecules (Table 2). The concentration of transferrin in serum is at least two orders of magnitude higher than that of the chelate in blood under clinical conditions) [25,26]. When the radiopharmaceutical contains ^{111}In, transferrin, well known for its removal of trivalent ion from chelates, is a dominant factor [27]. For ^{67}Cu, albumin is most important [28].

Radioactive indium ions released from the radiolabeled Mab are bound by transferrin and subsequently deposited in the liver and bone marrow (Figure 5), thus giving undesired background radioactivity in radiologic scans. This is a particular problem with antibodies labeled using the cyclic anhydride of DTPA (Figure 1) [29]. Hence it is important to determine experimentally the rate at which the transfer of the metal from the antibody to transferrin will occur under physiologic conditions and use the most kinetically inert chelate for imaging.

The kinetic inertness of the radiometal-labeled antibody may depend on the nature of the chelating agent. For example, kinetic measurements using sterile serum in vitro have shown that EDTA and DTPA chelates with bulky substituents [e.g., 1-(p-nitrobenzyl) or 1-methyl] on backbone methylene carbons are much more inert than unsubstituted EDTA and DTPA chelates [11,30]. Steric effects often play a dominant role in determining the kinetic inertness of Mab-chelate conjugates. For example, the rate of exchange of ^{111}In from 1-(p-carboxymethoxybenzyl)-EDTA (^{111}In) to transferrin is ten times lower than that of EDTA (^{111}In) in human serum under physiologic conditions [11]. Often macrocyclic ligands form much stabler complexes than other types of chelating agents [31].

Also, some metals can bind the chelating agents much more strongly than others. For example, ^{111}In-labeled Mab is stabler than ^{57}Co-labeled or ^{67}Cu-labeled Mab when a benzyl EDTA bifunctional chelating agent is employed [30]. Cu is lost very readily to albumin from EDTA and DTPA chelates.

Recent in-vivo serum stability measurements conducted in our lab, using

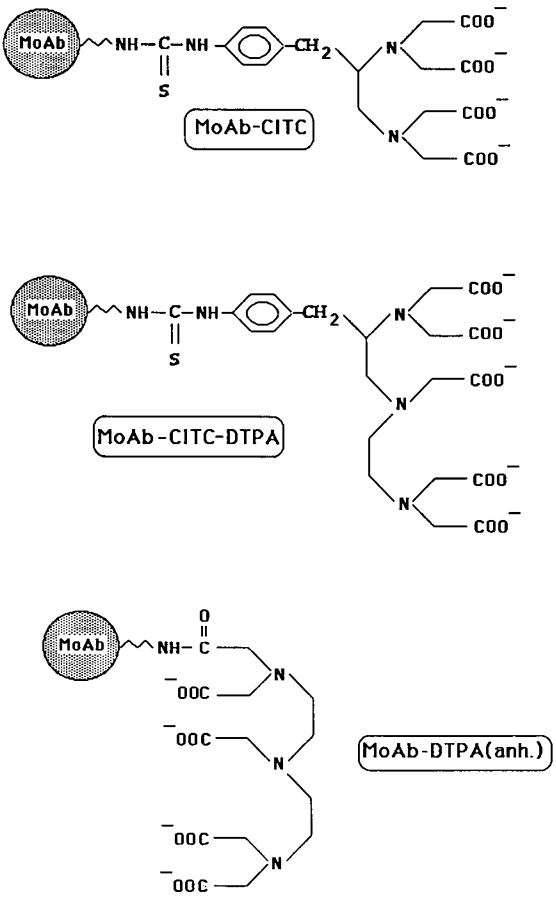

Figure 6. Three antibody-chelate conjugates compared for indium binding in serum.

some ^{111}In complexes of EDTA, DTPA, (1-p-nitrobenzyl)EDTA (NBEDTA), and (1-p-nitrobenzyl)DTPA (NBDTPA), have shown that the inertness decreases in the following order:

$$\text{NBEDTA}(^{111}\text{In}) > \text{NBDTPA}(^{111}\text{In}) \gg \text{EDTA}(^{111}\text{In}) > \text{DTPA}(^{111}\text{In}).$$

For example, NBEDTA(^{111}In) was still 93.5% intact after 6 days under physiologic conditions in human serum, while DTPA(^{111}In) was 76% intact after the same period. These measurements were carried out using HPLC (gel-filtration column) and cellulose acetate electrophoresis.

Similarly, for CITC, CITC-DTPA, and DTPA(anh.) (Figure 1) linked to a monoclonal antibody and labeled with ^{111}In, the inertness decreases in the following order:

$$\text{Mab-CITC}(^{111}\text{In}) > \text{Mab-CITC-DTPA}(^{111}\text{In}) \gg \text{Mab-DTPA}(^{111}\text{In}).$$

For example, Mab-CITC(^{111}In) was still 98.5% intact after 3 days under physiologic conditions in human serum, while Mab-DTPA(^{111}In) was 81.5% intact after the same period. The structures of these conjugates are illustrated in Figure 6; these investigations will be described in detail elsewhere [R. Subramanian et al., manuscript in preparation].

Radiometal-linked antibody for therapy

Radioiodinated monoclonal antibodies have been employed in several institutions for the imaging and treatment of tumors [32]. Although radiometal-linked monoclonal antibodies have been successful in the imaging of tumors (in humans as well as mice), fewer studies of their efficacy for cancer therapy have been performed [33]. A number of radiometals possess radiochemical properties suitable for therapy, e.g., ^{67}Cu, ^{90}Y, and ^{212}Bi [34]. The biologic half-life of radiometal-labeled antibody is long enough for immunotherapy purposes, and it has been found by several investigators that the extent of accumulation in tumors is much higher for radiometal-labeled antibodies than for radioiodinated monoclonal antibodies [35]. The major problem to be overcome before using radiometal-labeled antibodies for therapy purposes is that a significant portion of the radioactivity is distributed in normal tissues — especially in the liver, kidney, and bone marrow. The biologic reasons for this are many. Attempts are currently underway in several laboratories to circumvent this problem.

Reversible equilibrium binding

A novel method for removing the circulating antibody-bound chelates from the circulation is to bind the chelate *reversibly* to an antichelate antibody [36]. The antibody carries the chelate with it until a competing, nonradioactive chelate is injected. At this stage, practically all of the bound chelate remaining in circulation is displaced and rapidly excreted. Since under normal circumstances substantial quantities of radiolabeled antibodies remain in the circulation for many days, this procedure is promising in cases where circulating background radioactivity must be avoided (Figure 7). On the other hand, only a small fraction of the injected dose is retained in the target. The use of metal-chelate-specific monoclonal antibodies as radiopharmaceutical carriers has the additional advantage that monoclonal antichelate antibodies can selectively bind only the desired chelate (e.g., ^{111}In-EDTA) in the presence of a large excess of other molecules (e.g., other EDTA species). These molecules allow rapid selective renal clearance of chelate-labeled radiopharmaceuticals by competitive binding with a nonradioactive chelate chase at the time of imaging. This has been shown to markedly improve both

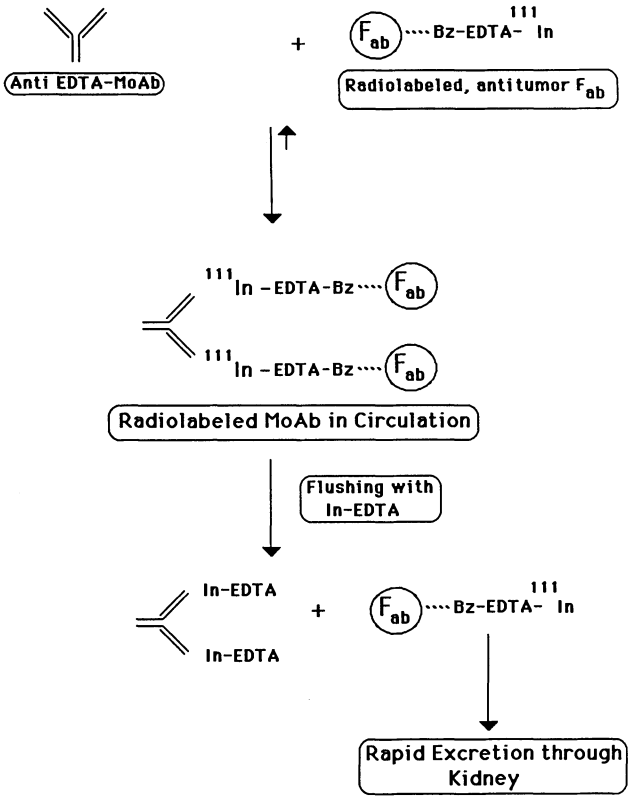

Figure 7. A schematic representation of the various steps involved in the reversible equilibrium binding method.

tumor images and radiation dosimetry in mice and has favorable properties for human use. By properly timing the administration of the flushing dose (Figure 7), one can in effect tune the biologic half-life of the radiolabeled chelate in the circulation.

Another promising approach is the preparation of monoclonal antibodies that are *bispecific* [37], having one arm specific for binding tumor-associated antigens and the other arm for metal-EDTA chelates [8].

Cleavable linkers

When the chelate is attached to the antibody through a spacer group that can be metabolized by the enzymes in the liver, the cleaved products may be returned to the circulation and rapidly excreted through the kidney. This can lead to decreased accumulation in the liver [38]. Further, it has been shown that benzyl-EDTA-^{111}In chelates remain intact from intravenous injection through urinary excretion. A disulfide linkage between antibody and chelate

resulted in a rapid clearance from the liver, compared with several other conjugates containing different linkages, such as a thiourea link, a thioether link, a peptide, and a diester [S.V. Deshpande et al., unpublished].

Monoclonal antibodies fragments

It is thought that sites present in the Fc portion of the monoclonal antibody are responsible for the binding of the antibody to receptors on liver cells. The monoclonal antibody may be digested with either of the enzymes papain or pepsin to get Fab or $F(ab')_2$ fragments. The antibody fragments may be conjugated with a chelating agent, and the resultant radiolabeled antibody fragments should exhibit little accumulation in liver. Clinical studies have shown that this indeed is the case [39]. However, the kidney excretes low molecular weight compounds, including some of the radiolabeled antibody fragments, very efficiently. Therefore, the uptake of radiolabeled antibody fragments in tumors is also lower.

Attachment of the chelate to a sugar moiety

Antibodies contain carbohydrate residues, attached to asparagine-297 or IgG heavy chains [40]. The carbohydrate groups react with oxidizing agents such as periodate, and the resulting aldehyde groups may be linked to chelating agents to produce chelate-antibody conjugates. McKearn and coworkers have reported significant improvements in radioimmunoimaging using such a conjugate [41].

Macrocyclic chelating agents

Recently macrocyclic chelating agents have been developed for use in nuclear medicine [42]. These chelating agents bind a variety of metal ions with useful chemical and physical properties. In addition, these metal chelates containing macrocyclic ligands are kinetically very inert. They do not lost metal easily, even under physiologic conditions, making them suitable for use in nuclear medicine. For example, a 14-membered macrocyclic bifunctional chelating agent containing the TETA structure [6-(p-nitrobenzyl)-1,4,8,11-tetraazacyclo*TE*tradecane-N,N′,N″,N‴-*T*etraacetic *A*cid] (Figure 1, structure IV) binds copper. The resultant Cu(II)-TETA chelate decomposes in the serum at the rate of $\approx$ 1% per day. Because of the potential use of ^{67}Cu (1.3 MeV beta emission) in tumor therapy, this is a promising observation. Furthermore, when ^{67}Cu-TETA is conjugated to a monoclonal antibody, preliminary experiments with tumor-bearing animals have shown good tumor images [S.V. Deshpande et al., unpublished].

The macrocycle TETA binds strongly with Cu^{2+} and Co^{2+}, but gives multiple products with In^{3+}. This may be due to the limited size of the macrocyclic cavity or to other structural features of TETA such as the presence of four amine and four carboxylate groups.

Future prospects

Although several radiometal-labeled monoclonal antibodies have been investigated for radioimmunoimaging and a few for radiotherapy, a number of potentially useful radiometals have not been explored, many amino acids other than lysine are available on Mabs for conjugation, and other approaches such as bispecific Mabs and reversible equilibrium binding using suitable haptenic reagents (and also avidin and biotin) are at very early stages of study in vivo. A great deal of further work is needed in order to discover and develop the best ways for using radiolabeled monoclonal antibodies clinically.

Acknowledgments

The work described here was supported principally by research grant CA 16861 from the National Cancer Institute, National Institutes of Health.

References

1. Meares, C.F., and Goodwin, D.A. (1984) Linking radiometals to proteins with bifunctional chelating agents. J. Protein Chem. 3:215–228.
2. Kohler, G., and Milstein, C. (1975) Continuous cultures of fused cells secreting antibody of predefined specificity. Nature (London) 256:495–497.
3. Goldenberg, D.M., Deland, F., Kim, E., Bennett, S., Primus, F.J., van Nagell, J.R., Jr., Estes, N., DeSimone, P., and Rayburn, P. (1978) Use of radiolabeled antibodies to carcinoembryonic antigen for detection and localization of diverse cancers by external photoscanning. N. Engl. J. Med. 298:1384–1388.
4. Order, S.E., Klein, J.L., Ettinger, D., Adelson, P., Siegelman, S., and Leichner, P. (1980) Use of isotopic immunoglobulin in therapy. Cancer Res. 40:3001–3007.
5. Sundberg, M.W., Meares, C.F., Goodwin, D.A., and Diamanti, C.I. (1974) Chelating agents for the binding of metal ions to macromolecules. Nature (London) 250:587–588.
6. Krejcarek, G.E., and Tucker, K.L. (1977) Covalent attachment of chelating groups to macromolecules. Biochem. Biophys. Res. Commun. 77:581–585.
7. Loberg, M.D., Cooper, M., Harvey, E., Callery, P., and Faith, W. (1976) Development of new radiopharmaceuticals based on N-substitution of iminodiacetic acid. J. Nucl. Med. 17: 633–640.
8. Reardan, D.T., Meares, C.F., Goodwin, D.A., McTigue, M., Davis, G.S., Stone, M.R., Leung, J.P., Bartholomew, R.M., and Frincke, J.M. (1985) Antibodies against metal chelates. Nature (London) 316:265–268.
9. Sillen, L.G., and Martell, A.E., eds. (1964) Stability constants of metal ion complexes. London: Chemical Society.
10. Meares, C.F. (1986) Chelating agents for the binding of metal ions to antibodies. Nucl. Med.

Biol. 13:311–318.
11. Yeh, S.M., Meares, C.F., and Goodwin, D.A. (1979) Decomposition rates of radiopharmaceutical indium chelates in serum. J. Radioanal. Chem. 53:327–336.
12. Yeh, S.M., Sherman, D.G., and Meares, C.F. (1979) A new route to bifunctional chelating agents: Conversion of aminoacids to analogs of ethylenedinitrilotetracetic acid. Anal. Biochem. 100:152–159.
13. DeRiemer, L.H., Meares, C.F., Goodwin, D.A., and Diamanti, C.I. (1981) BLEDTA II: Synthesis of a new tumor-visualizing derivative of Co(III)-bleomycin. J. Labelled Compd. & Radiopharm. 18:1517–1534.
14. Meares, C.F., Anderson, L.D., Yeh, S.M., Sherman, D.G., and Goodwin, D.A. (1981) Synthesis of bifunctional chelating agents from amino acids. J. Labelled Compd. & Radiopharm. 18:160.
15. Abusaleh, A., and Meares, C.F. (1984) Excitation and de-excitation processes in lanthanide chelates bearing aromatic side chains. Photochem. Photobiol. 39:763–769.
16. Benisek, W.F., and Richards, F.M. (1968) Attachment of metal chelating functional groups to macromolecules. J. Biol. Chem. 243:4267–4271.
17. Chang, C.-H., Meares, C.F., and Goodwin, D.A. (1982) Bifunctional chelating agents: Linking radiometals to biological molecules. In: Lambrecht, R.M., and Morcos, C.N. (eds.), *Applications of Nuclear and Radiochemistry*. New York: Pergamon, pp. 103–114.
18. De Préval, C. (1982) Immunoglobulins. In: Bach, J.-F. (ed.), *Immunology*. New York: John Wiley and Sons, p. 177.
19. Meares, C.F., McCall, M.J., Reardan, D.J., Goodwin, D.A., Diamanti, C.I., and McTigue, M. (1984) Conjugation of antibodies with bifunctional chelating agents: Isothiocyanate and bromoacetamide reagents, methods of analysis and subsequent addition of metal ions. Anal. Biochem. 142:68–78.
20. Leung, C.S.H., Meares, C.F., and Goodwin, D.A. (1978) The attachment of metal-chelating groups to proteins: Tagging of albumin in dizaonium coupling and the use of products as radiopharmaceuticals. Int. J. Radiat. Isot. 29:687–692.
21. Meares, C.F., Goodwin, D.A., Leung, C.S.H., Girgis, A.Y., Silvester, D.J., Nunn, A.D., and Lavender, P.J. (1976) Covalent attachment of metal chelates to proteins: The stability in vivo and in vitro of the conjugate of albumin with a chelate of indium-111. Proc. Natl. Acad. Sci. USA 73:3803–3806.
22. Hnatowich, D.J., Layne, W.W., and Childs, R.L. (1983) Radioactive labeling of antibody: A simple and efficient method. Science 220:613–615.
23. Penefsky, H.S. (1979) A centrifuged column procedure for the measurement of ligand binding by beef heart. In: Fleischner, S. (ed.), *Methods in Enzymology*, Vol 56, Part G. New York: Academic Press, pp. 527–530.
24. Welch, M.J., and Welch, T.J. (1975) Solution chemistry of carrier-free indium. In: Subramanian, G., Rhodes, B.A., Cooper, J.F., and Sodd, V.J. (eds.), *Radiopharmaceuticals*. New York: Soc. Nucl. Med., pp. 73–79.
25. White, A., Handler, P., and Smith, E.L. (1968) *Principles of Biochemistry*, 4th ed. New York: McGraw Hill, p. 711.
26. Ritzmann, S.E., and Daniels, J.C. (1982) Serum electrophoresis and total serum proteins. In: Ritzmann, S.E., and Daniels, J.C. (eds.), *Serum Protein Abnormalities: Diagnostic and Clinical Aspects*. New York: Alan R. Liss, pp. 3–26.
27. Hosain, F., McIntyre, P.A., Poulose, K., Stein, R.S., and Wagner, H.N., Jr. (1969) Binding of trace amounts of ionic indium-113m to plasma transferrin. Clin. Chim. Acta 24:69–75.
28. Sarkar, B., Laussac, J.-P., and Lau, S. (1983) Transport forms of copper in human serum. In: Sarkar, B. (ed.), *Biological Aspects of Metals and Metal Related Diseases*. New York: Raven Press, pp. 23–40.
29. Mathias, C.J., and Welch, M.J. (1987) Studies on the entrapment of indium-111 in the liver following the administration of proteins labeled using bifunctional chelates (abstract). J. Nucl. Med. 28:657.
30. Cole, W.C., DeNardo, S.J., Meares, C.F., McCall, M.J., DeNardo, G.L., Epstein, A.L.,

O'Brien, H.A., and Moi, M.K. (1987) Comparative serum stability of radiochelates for antibody radipharmaceuticals. J. Nucl. Med. 28:83–90.
31. Melson, G.A., ed. (1979) *Coordination Chemistry of Macrocyclic Compounds*. New York: Plenum Press.
32. Goldenberg, D.M., Kim, E.E., Deland, F., van Nagell, J.R., Jr., and Javadpour, N. (1980) Clinical radioimmunodetection of cancer with radioactive antibodies to human chorionic gonadotropin. Science 208:1284–1286.
33. Order, S.E., Klein, J.L., Leichner, P.K., Frincke, J., Lollo, C., and Carlo, D.J. (1986) ^{90}Yttrium antiferritin — a new therapeutic radiolabeled cancer. Int. J. Radiat. Oncol. Biol. Phys. 12:277–281.
34. DeNardo, S.J., Jungerman, J.A., DeNardo, G.L., Lagunas-Solar, M.C., Cole, W.C., and Meares, C.F. (1985) The choice of radionuclides for radioimmunotherapy. In: *Developing Role of Short-Lived Radionuclides in Nuclear Medicine Practice*. DOE Symp. Ser. 56, 401–414. DOE Technical Information Center, Conf.820523-NT15.
35. Carrasquillo, J.A., Mulshine, J.L., Bunn, P.A., Jr., Reynolds, J.C., Foon, K.A., Schroff, R.W., Perentesis, P., Steis, R.G., Keenan, A.M., Horowitz, and Larson, S.M. (1987) Indium-111 monoclonal antibody is superior to iodine-131 T101 in imaging of cutaneous T-cell lymphoma. J. Nucl. Med. 28:281–287.
36. Goodwin, D.A., Meares, C.F., David, G.F., McTigue, M., McCall, M.J., Frincke, J.M., Stone, M.R., Bartholomew, R.M., and Leung, J.P. (1986) Monoclonal antibodies as reversible equilibrium carriers of radiopharmaceuticals. Nucl. Med. Biol. 13:383–391.
37. Brennan, M., Davidson, P.F., and Paulus, H. (1985) Preparation of bispecific antibodies by chemical recombination of monoclonal immunoglobulin G1 fragments. Science 229:81–83.
38. Haseman, M.K., Goodwin, D.A., Meares, C.F., Kaminski, M.S., Wensel, T.G., McCall, M.J., and Levy, R. (1986) Metabolizable ^{111}In-chelate conjugated monoclonal antibody for radioimmunodetection of lymphoma in mice. Eur. J. Nucl. Med. 12:455–460.
39. Buraggi, G.L., Callegaro, L., Turrin, A., Cascinelli, N., Attili, A., Emanuelli, H., Gasparini, M., Deleide, G., Plassio, G., Dovis, M., Mariani, G., Natali, P.G., Scassellati, G.A., Rosa, U., and Ferrone, S. (1984) Immunoscintigraphy with ^{123}I, ^{99m}Tc and ^{111}In labeled F(ab')$_2$ fragments of monoclonal antibodies to a human high molecular weight melonoma associated antigen. J. Nucl. Med. All. Sci. 28:283–295.
40. Kabat, E.A. (1976) *Structural Concepts in Immunology and Immunochemistry*, 2nd ed. San Francisco, Holt, Rinehart, & Winston, pp. 270–272.
41. Rodwell, J.D., and McKearn, T.J. (1987) Antibody conjugates for the delivery of compounds to target sites, US Patent No. 4,671,958.
42. Moi, M.K., Meares, C.F., McCall, M.J., Cole, W.C., and DeNardo, S.J. (1985) Copper chelates as probes of biological systems: Stable copper complexes with a macrocyclic bifunctional chelating agent. Anal. Biochem. 148:249–253.
43. Brechbeil, M.W., Gansow, O.A., Atcher, R.W., Schlom, J., Esteban, J., Simpson, D.E., and Colcher, D. (1986) Synthesis of 1-(p-isothiocyanatobenzyl) derivatives of DTPA and EDTA: Antibody labeling and tumor imaging studies. Inorg. Chem. 25:2272–2281.
44. McAfee, J.G., and Thakur, M.L. (1976) Survey of radioactive agents for in vitro labeling of phagocytic leukocytes: I. Soluble agents. J. Nucl. Med. 17:480–487.
45. Hnatowich, D.J., Virzi, F., and Doherty, P.W. (1985) DTPA-coupled antibodies labeled with yttrium-90. J. Nucl. Med. 26:503–509.
46. Cole, D.A., Mercer-Smith, J.A., and Taylor, W.A. (1986) Lymphatic uptake of copper-67 *meso*-tetra(4-carboxyphenyl) porphine, an imaging agent for inflamed lymph nodes. INOR 46, Abstracts of Papers, 192nd National Meeting, Anaheim, CA. Washington, D.C.: American Chemical Society.
47. Khaw, B.A., Strauss, H.W., Carvallio, A., Locke, E., Gold, H.K., and Haber, E. (1982) Technetium-99m labeling of antibodies to cardiac myosin Fab to human fibrinogen. J. Nucl. Med. 23:1011–1019.
48. Rhodes, B.A., and Burchiel, S. (1983) Radiolabeling of antibodies with technetium-99m. In: Burchiel, S.W., and Rhodes, B.A. (eds.), *Radioimmunoimaging and Radioimmunotherapy*.

New York: Elsevier, pp. 207–222.
49. Kozak, R.W., Atcher, R.W., Gansow, O.A., Friedman, A.M., Hines, J.J., and Waldmannn, T.A. (1986) Bismuth-212-labeled anti-Tac monoclonal antibody: α-particle-emitting radionuclides as modalities for radioimmunotherapy. Proc. Natl. Acad. Sci. USA 83:474–478.
50. Srivastava, S.C., Meinken, G.E., and Steplewski, Z. (1987) Preliminary results on labeling antibodies and other radiopharmaceuticals with Pb-203 (abstract). J. Nucl. Med. 28:721.

10. Optimization of biodistribution by introducing different chemical linkages between antibody and an indium-111 chelate

Syed M. Quadri, Chang H. Paik, Richard C. Reba, and Won-Pyo Hong

Radiolabeling of antibody with In-111 requires the use of a bifunctional chelator because antibody by itself does not make a stable complex with In-111. The most common bifunctional chelate reactions to conjugate a DTPA analogue to antibody have been an acylation method using cyclic DTPA dianhydride [1–3], DTPA carboxycarbonic mixed anhydride [4–8], or activated esters of DTPA [9,10]. The acylating agent reacts with the amino group of lysine residues of antibody, which results in formation of an amide bond during the monoacylation reaction. The chelating moiety of the antibody conjugate is, therefore, diethylenetriaminepentaacetic acid monoamide (DTPAA), which contains one less carboxylic group than the native DTPA. The acylation method, especially that using cyclic DTPA dianhydride, has been thoroughly optimized so that it is possible to conjugate one DTPAA to antibody without deactivation and polymerization of antibody [3,11,12]. However, a practical limitation to the use of In-111-labeled antibody for radioimmunoimaging of tumors has been a high background activity in normal organs, especially liver and kidney [13–23]. The mechanism of uptake of the activity in liver was investigated by Sands et al. [24]. They reported that the activity was primarily retained in hepatocytes and hypothesized that a high retention of In-111 activity in hepatocytes as compared with I-125 activity following I-125 antibody injection might be caused by transchelation of In-111 by intracellular protein components such as transferrin and ferritin. Methias et al. [25] investigated the retention of the activities in liver Kupffer cells following the injection of liposome-entrapped I-125 antibody, an In-111 complex of antibody-DTPAA conjugate, and an In-111 complex of C-14-labeled DTPA into rats. They found a higher retention of In-111 activity in the liver compared with I-125 and C-14 activities, and proposed that the retention of In-111 activity might be primarily caused by the transchelation of In-111 to intracellular proteins in Kupffer cells. On the other hand, Shochat et al. [26] prepared liver extract from hamsters following the injection of In-111-labeled antibody-DTPAA prepared by the cyclic DTPA dianhydride method and, using molecular permeation HPLC analysis, found that the major In-111 activity was eluted with small molecular substances and the remaining activity was associated with ferritin and intact antibody.

Goldenberg, D.M., (ed.), Cancer Imaging with Radiolabeled Antibodies.

Three chemical approaches have been proposed to reduce the background activity. The first approach is to conjugate a chelating agent of an improved stability with In-111 to antibody, thereby reducing the transchelation of In-111 to the intracellular proteins. Brechbiel et al. [27] and Esteban et al. [28] synthesized p-(isothiocyanatobenzyl)DTPA, which contains five carboxylic groups, like the native DTPA. The isothiocyanate group was then reacted with the amino group of antibody to conjugate via a thiourea linkage. They reported that the In-111 complex of this antibody-DTPA conjugate produced reduced liver activities compared with the In-111 complex of the corresponding antibody-EDTA conjugate and with the labeled antibodies prepared from the cyclic DTPA dianhydride and the DTPA carboxycarbonic mixed anhydride methods. The authors believed that the reduced liver activity might be the result of a higher stability of the In-111-DTPA complex than of the In-111-EDTA and In-111-DTPAA complexes. However, their study was not designed to quantify how the different chemical linkage (thiourea linkage) reduced the background activity.

The second approach to reduce hepatic uptake is a site-directed conjugation reaction. Rodwell et al. [29] synthesized an amino group containing a DTPAA analogue. The amino group of the bifunctional chelator was conjugated to the carbohydrate moiety in the Fc region of antibody by reacting carbonyl groups derived from the oxidation of the hydroxy groups in the vicinity of the carbohydrate moiety and subsequent reduction of the imine bond to the amine bond. They reported that the In-111 complex of this antibody-DTPAA conjugate produced a reduction of the activity in liver, perhaps because the site-directed conjugation reduced the binding of the labeled antibody to Fc receptors of reticuloendothelial cells. Quadri et al. [30] and Brown et al. [31] also reported the conjugation of DTPAA derivatives containing a primary alkylamine to the carbohydrate moieties. Quadri et al. reported a reduced hepatic uptake.

The third approach is to interpose a readily metabolizable ester bond between antibody and a chelating agent such as DTPAA [30] and EDTA [32]. The preliminary biodistribution studies indicated that a significant reduction of hepatic uptake could be obtained by this strategy. We have extended these studies to maximize the tumor-to-background ratio by placing different chemical bonds between antibody and DTPAA. We report in this paper the synthesis of DTPAA conjugates with six different chemical linkages and the biodistributions of antibody containing these In-111 complexes.

Materials and methods

Synthesis of DTPA-p-(aminoethyl)anilide

Twenty milliliters of 0.1 M citrate buffer at pH 5 in a 50-ml round-bottom flask was stirred rapidly. To this buffer 2-(4-aminophenyl)ethylamine (70 mg,

0.51 mmol) dissolved in 5 ml of the citrate buffer was added dropwise through a 23-gauge needle, and at the same time cyclic DTPA (cDTPAA) dianhydride (700 mg, 1.96 mmol) was added in small portions over a period of 30 minutes. A silica-gel TLC (Macherey-Nagel, Germany) developed with a solvent mixture containing 2 : 2 : 1 10% ammonium formate in water : methanol : 0.2 M citric acid gave a major spot (95%) and a minor spot (5%) at Rfs of 0.7 and 0.55, respectively. These spots were positive on a fluorescamine test, indicating the presence of primary amines [33]. The product solution was negative on an azo coupling test with resorcinol after reaction with nitrous acid [34]. This indicates that the product does not contain an aromatic amine. The product was purified from free DTPA by precipitating DTPA repeatedly at pH 2.0. Although the final product was not completely free of DTPA, the product was used for the following reactions because DTPA does not interfere with the reactions.

Introduction of a disulfide bond

The method of Lomant et al. [35] was used. Twenty microliters of dithiobis (succinimidyl propionate) (7.0×10^{-2} M) in dimethyl sulfoxide was mixed rapidly with 1 ml of DTPA-(p-aminoethyl)anilide (1.4×10^{-3} M) in 0.1 M phosphate buffer at pH 7.2. The reaction mixture was stirred for 10 minutes at room temperature. To this solution 1 ml of rabbit anti-human serum albumin antibody IgG(Ab) solution (7.0×10^{-5} M) in 0.1 M phosphate buffer at pH 7.5 was mixed rapidly. The resulting mixture was stirred continuously for 2 hours at room temperature. The antibody-DTPAA conjugate was purified by affinity column chromatography [6]. The number of DTPAA molecules per antibody was determined to be two by a no-carrier-added In-111 reaction and a titration method with $InCl_3$ using In-111 ion as a tracer [3].

Introduction of diester bonds

The method of Abdella et al. [36] was modified. Ethylene glycolbis(succinimidylsuccinate) was used as a crosslinking agent. For the introduction of two ester bonds, ethylene glycolbis(succinimidylsuccinate) (2.0×10^{-3} mmol) dissolved in 0.1 ml of dimethyl sulfoxide was mixed rapidly with DTPA-p-(aminoethyl)anilide (2.0×10^{-3} mmol) dissolved in 0.9 ml of 0.1 M phosphate buffer at pH 7.0. The solution was stirred gently for 5 minutes at room temperature. To this solution, antibody (1.0×10^{-4} mmol) in 1 ml of the phosphate buffer was added rapidly with stirring. The conjugation reaction was continued for 2 hours at room temperature. The antibody-DTPA conjugate was then affinity purified. The number of DTPAA molecules was 2.0 as determined by a no-carrier-added In-111 reaction and by a titration method with $InCl_3$ using In-111 ion as a tracer.

Introduction of an alkylamine bond to the carbohydrate moiety

The method of Alvarez et al. [37] was used. The vicinal hydroxy groups of the carbohydrate moiety of the antibody were oxidized to carbonyl groups by reacting antibody (1.0×10^{-4} mmol) with sodium periodate (5.0×10^{-4} mmol) in 1 ml of 0.1 M phosphate at pH 6.0 for 1 hour at 0°C. The antibody solution was purified by molecular permeation chromatography using a Bio Gel P-6 DG column (20 × 1 cm) and concentrated using a centricon. The oxidized antibody (1.0×10^{-4} M) was then reacted with DTPA-p-(aminoethyl) anilide (2.0×10^{-2} M) in 0.1 M phosphate buffer at pH 7.0 for 2 hours at room temperature. The resulting imine bond was reduced to amine by reacting with sodium cyanoborohydride (2.0×10^{-2} M) overnight at pH 6 at 4°C. The antibody conjugate was affinity purified and contained an average of 1.4 DTPAA molecules per antibody.

Introduction of the dextran linkage

A modified method of Arnon et al. [38] was followed. The hydroxy vicinal groups of dextran (average MW = 8000, 2.0×10^{-2} mmol) were oxidized to the corresponding carbonyl groups by a reaction with sodium periodate (2.0×10^{-1} mmol) in 1 ml of 0.1 M phosphate buffer at pH 6.0 for 1 hour at 0°C. The reaction solution was placed in a Spectrapor membrane tubing (mol. exclusion = 3500) and dialyzed against three changes of 1 l of distilled water. The oxidized dextran was reacted with DTPA-p-(aminoethyl)anilide (2.0×10^{-1} mmol) in the phosphate buffer at pH 6.0 for 2 hours at room temperature. To this solution antibody (8.0×10^{-5} mmol) was added and the conjugation reaction was continued overnight at pH 7.0 at 4°C. The imine bonds were reduced to amine bonds by reacting with sodium cyanoborohydride (10 mmol) overnight at pH 6 at 4°C. The antibody conjugate was affinity purified and determined to contain an average of six DTPAA molecules per antibody.

Introduction of a thioether bond

The methods of Gitman et al. [39] and Carlson et al. [40] were used. Twenty microliters of succinimidyl-4-(p-maleimidophenyl)butyrate (7.0×10^{-2} M) in dimethyl sulfoxide was reacted with 1 ml of DTPA-(p-aminoethyl)anilide (1.4×10^{-3} M) in the phosphate buffer at pH 7.2 for 1 hour at room temperature to conjugate the amino group of the chelating agent to the crosslinking agent. The maleimido group of the conjugate was then reacted with the sulfhydryl group of antibody at pH 6.2 overnight at room temperature. For the introduction of the sulfhydryl group to the antibody, the method of Carlson et al. was followed. The amino group of the antibody (1.4×10^{-4} M) was reacted with the carbonyl group of N-succinimidyl-3-(2-pyridyldithio)propionate (1.4×10^{-4} M) in the phosphate buffer at pH 7.2 for 1 hour at room temperature. The disulfide bond of the resulting antibody conjugate was reduced to a

sulfhydryl group by reacting with 10 times molar excess dithiothreitol at pH 4.5 for 30 minutes. The unreacted reagents were eliminated by molecular permeation chromatography. The final antibody conjugate was affinity chromatographed and contained an average of 1.7 DTPAA molecules per antibody.

Introduction of a hydrocarbon chain

The reaction procedure for the introduction of the hydrocarbon chain was the same as that for the introduction of the disulfide bond, except that disuccinimidyl suberate was used as a crosslinking agent. The conjugate contained an average of 1.7 DTPAA molecules per antibody.

Introduction of an amide bond

The cyclic DTPA dianhydride method of Paik et al. [3] was used. Briefly, antibody (1.4×10^{-4} M) was reacted with cDTPAA at a cDTPAA/antibody molar ratio of 2 at pH 8.2. The resulting Ab-DTPAA conjugate was affinity purified and contained an average of 1.3 DTPAA molecules per antibody.

HPLC

The molecular weights of the antibody-DTPAA conjugates were determined by HPLC using a Bio-Sil TSK 250 column (600 × 7.5 mm). The column was eluted with 0.02 M sodium phosphate at pH 6.8/0.2 M sodium sulfate at a flow rate of 1 ml/min. The standard samples of IgM, IgG, and human serum albumin gave retention times of 11, 19, and 23 minutes, respectively. All of the antibody-DTPAA conjugates, except the alkylamine-containing conjugate derived from the site-directed carbohydrate reaction, produced a single peak at 19 minutes. HPLC of the alkylamine conjugate resulted in three peaks at 11 (11%), 16 (16%), and 20 (73%) minutes.

Preparation of affinity beads

A procedure provided by Pharmacia Fine Chemicals was used. CNBr activated Sepharose 4B (6 g, 60–180 μ diameter) was washed thoroughly with 0.001 M HCl solution. The beads were added to 30 ml of human serum albumin (HSA, 120 mg) in 0.1 M sodium bicarbonate buffer/0.5 M NaCl at pH 8.2 and gently rotated for 2 hours at room temperature. The solution was filtered and the remaining beads were further reacted with 20 ml of 1 M ethanolamine at pH 8.2 for 2 hours at room temperature. The excess amine was removed by filtration. The remaining Sepharose 4B-HSA was thoroughly washed with 0.1 M sodium acetate/1.0 M NaCl at pH 4.5 and then with 0.1 M sodium borate/1.0 M NaCl at pH 8.0. The affinity beads were stored in 0.02 M phosphate buffer/0.16 M sodium chloride at pH 7.2 at 4°C until used. The Sepharose 4B-HSA beads were used for the affinity chromatographic puri-

fication of antibody-DTPA conjugates and as the antibody binding material used to establish the tumor model.

Biodistribution study

Fifty microliters (about 70,000 beads) of packed beads were diluted with 200 μl of 25% sucrose in saline and injected into the tail vein of rats. Fifteen minutes later 200 μl of In-111-labeled affinity-purified antibody-DTPAA conjugates (30 μg, specific activity of 1 μCi/μg) were injected into another site of the tail vein. The animals were sacrificed 24 hours after the injection of the labeled antibody. Organs were excised, weighed promptly, and counted in a gamma counter.

Results

Syntheses of antibody-DTPAA conjugates

2-(4-aminophenyl)ethylamine was used to synthesize an amino group containing the DTPAA derivative, DTPA-p-(aminoethyl)anilide. The reaction pH was maintained at 5, where the aliphatic amino group (pKa = 10) was completely protonated and protected from the reaction with cDTPAA, while 50% of the aromatic amino group (pKa = 5) was not protonated and reacted with cDTPAA. The amino compound was added dropwise to maintain the concentration of the amino group less than 10^{-4} M throughout the reaction. This condition minimized the formation of diamides of DTPA. The TLC analysis showed that a spot at Rf = 0.55 increased at the expense of a spot at Rf = 0.7 when the concentration of the amino compound was increased.

Most of the crosslinking agents used for the introduction of the different chemical bonds are activated diesters. The crosslinking between the bifunctional chelator and antibody was achieved by stepwise reactions of the activated diesters with the chelator and then with antibody. HPLC analysis indicates that the molecular weights of all of the antibody-DTPAA conjugates, except the carbohydrate-linked conjugate, are similar to monomeric IgG. The carbohydrate conjugate showed two higher molecular weight peaks (27%) in addition to the monomeric IgG peak (73%).

Stability of In-111-labeled antibody-DTPAA conjugates in serum

The In-111-labeled antibody-DTPAA conjugates with different linkages were incubated with rat serum for 24 hours at 37°C under an atmosphere of 95% O_2 and 5% CO_2. The serum samples were spotted on the silica-gel TLC plates and developed with the solvent system described previously. The plates were scanned with a radiochromatogram scanner for the determination of the radioactivity associated with the protein and the metabolites. The protein

remained at the origin as the metabolites moved with Rf values slightly higher than the Rf (0.55) of In-111 DTPA. All of the activity associated with the amide-, hydrocarbon-, and thioether-containing conjugates remained at the origin, whereas the percent activity moving as metabolites was 5% for the disulfide, 12% for the diester, 6% for the alkylamine linked to the carbohydrate moiety, and 10% for the alkylamine linked to dextran. Koizumi et al. [41] also reported that the alkylamine and thioether linkages were stable in serum, whereas the disulfide linkage was slightly unstable.

Biodistribution studies

To investigate the validity of the target model, DTPAA was conjugated to HSA using the cyclic DTPA dianhydride method. HSA-DTPAA was then conjugated to Sepharose 4B. Sepharose 4B-HSA-DTPAA was labeled with In-111, purified, and injected into a tail vein of rats. The biodistribution of the activity determined 30 minutes after the injection showed greater than 95% of the injected activity localized in the lungs, confirming the validity of the model. This model was stable as reported by Otsuka et al. [42]. As a control experiment, Sepharose 4B without HSA conjugation was injected. Fifteen minutes later, In-111-labeled antibody-DTPAA conjugates with either the ester linkage or the amide linkage was injected into two rats, and the animals were sacrificed 24 hours later. The biodistribution (%ID/g) of the diester-linked conjugate was 0.56 ± 0.09 for blood, 0.48 ± 0.19 for lung, 0.79 ± 0.04 for liver, 0.37 ± 0.15 for spleen, 1.35 ± 0.11 for kidney, and 0.11 ± 0.01 for bone. The biodistribution of the amide-linked conjugate was 3.44 ± 0.17 for blood, 1.50 ± 0.08 for lung, 2.40 ± 0.08 for liver, 2.10 ± 0.21 for spleen, and 3.39 ± 0.06 for kidney. The lung activities of the In-111-labeled diester and amide conjugate in the control animals were 7.6 and 2.5 times lower, respectively, than the corresponding activities in the target model with the antigen. This indicates that the localization of the activities in the target model is mainly due to a specific binding of the antibody-DTPAA conjugates to the antigen (Table 1).

Discussion

The purpose of this study was to investigate the effect of different chemical bonds between antibody and the chelator on the biodistribution of In-111-labeled antibody. To achieve this aim, crosslinking agents containing different chemical bonds were conjugated to the same antibody and the same chelating agent. All of the conjugation reactions were directed to the amino group of lysine residues of antibody, except for the carbohydrate-linking reaction. The In-111-labeled antibody-DTPAA conjugates were all affinity purified before injection to avoid a possible problem caused by injection of immunologically impure antibody. All of the antibody-DTPAA conjugates

Table 1. Biodistribution of In-111-labeled antibody-DTPAA conjugates in rats with an antigen target (lung) at 24 hours postinjection

	Blood	Lung	Liver	Spleen	Kidney	Muscle	Bone	Intestine
Ab-disulfide-	0.26 ± 0.06	2.47 ± 0.36	0.84 ± 0.15	0.37 ± 0.19	3.00 ± 0.28	0.08 ± 0.04	0.19 ± 0.08	0.21 ± 0.06
Ab-ester-	0.41 ± 0.19	3.64 ± 0.50	1.81 ± 0.28	0.55 ± 0.15	0.96 ± 0.33	0.04 ± 0.01	0.07 ± 0.01	0.36 ± 0.15
Ab-carbohydrate-	0.71 ± 0.13	3.75 ± 0.75	1.65 ± 0.43	0.94 ± 0.30	2.86 ± 0.66	0.11 ± 0.04	0.20 ± 0.02	0.14 ± 0.01
Ab-dextran-	0.42 ± 0.04	3.83 ± 0.74	2.00 ± 0.40	2.43 ± 0.28	1.49 ± 0.16	0.09 ± 0.03	—	—
Ab-thioether-	1.37 ± 0.25	3.88 ± 0.46	2.38 ± 0.33	1.18 ± 0.51	2.34 ± 0.29	0.11 ± 0.01	0.18 ± 0.05	0.35 ± 0.05
Ab-hydrocarbon-	1.70 ± 0.25	4.29 ± 0.33	2.68 ± 0.40	1.14 ± 0.60	2.34 ± 0.40	0.12 ± 0.02	0.22 ± 0.09	0.32 ± 0.06
Ab-amide-	1.81 ± 0.53	3.70 ±0.29	2.84 ± 0.38	1.04 ± 0.57	2.97 ± 0.45	0.12 ± 0.05	0.23 ± 0.06	—

n = 7 ~ 15.

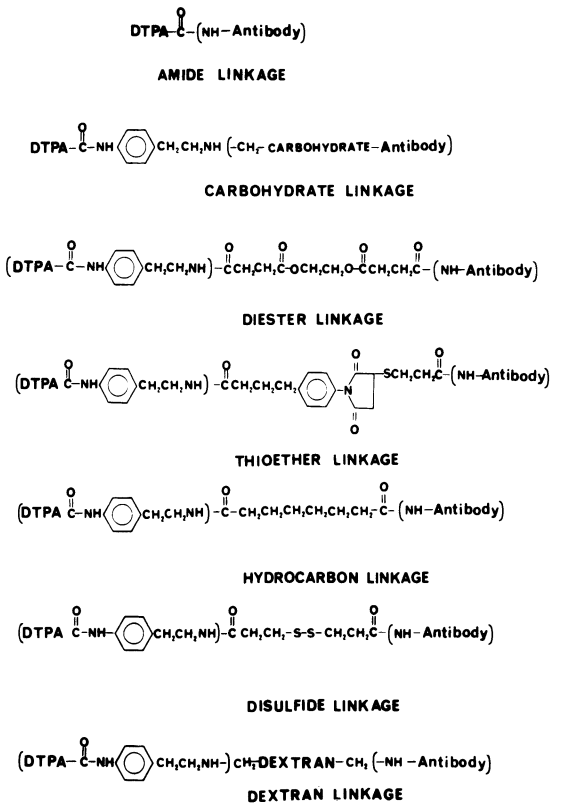

Figure 1. Simplified structures of antibody-DTPAA conjugates.

were monomeric antibodies, except the carbohydrate-linked antibody preparation, which contained 27% high molecular weight species based on UV peak intensities. The number of DTPAA molecules conjugated per antibody was less than two for all of the conjugates except the dextran-linked conjugate.

We have chosen the amide-linked antibody-DTPAA conjugate from the cyclic DTPA dianhydride reaction as a control because it is the most common antibody conjugate reported in the literature. Compared with the In-111-labeled, amide-linked conjugate, all of the newly synthesized conjugates gave similar localizations in the target (lung), except the disulfide-linked conjugate, which gave 50% lower target activity than the control conjugate. This indicates that the chemical bonds are quite stable once the antibody-DTPAA conjugates are bound to the target antigen. Localizations of the thioether and the hydrocarbon-linked conjugates in normal organs such as blood, liver, spleen, and kidney are also very similar to those of the amide-linked conjugate. This indicates that these linkages have a similar stability in vivo and suggests further that they are metabolized similarly in the normal organs. On the other hand, the disulfide, diester, carbohydrate, and dextran-linked conjugates distribute quite differently in the normal organs as compared with

Table 2. Average target-to-normal organ ratios of In-111-labeled Ab-DTPAA conjugates in rats at 24 hours postinjection

	Blood	Liver	Spleen	Kidney	Muscle
Ab-disulfide-	9.5	2.9	6.7	0.8	31
Ab-ester-	8.9	2.0	6.6	3.8	91
Ab-carbohydrate-	5.3	2.3	3.8	1.3	32
Ab-dextran-	9.1	1.9	1.6	2.6	43
Ab-thioether-	2.8	1.6	3.3	1.7	35
Ab-hydrocarbon-	2.5	1.6	3.8	1.8	36
Ab-amide-	2.0	1.3	3.6	1.2	31

the distribution of the control conjugate. The blood activities of these conjugates are especially lower than that of the control amide conjugate. However, the in-vitro serum stability test indicates that the disulfide, diester, carbohydrate, and dextran linkages are quite stable over a period of 24 hours. This, together with the fact that these linkages are stable once the antibody conjugates are bound to the target, indicates that blood is not a major site of metabolism of the linkages. The major site of metabolism might be liver, which contains a high concentration of enzymes, such as carboxyesterases and alkyldeaminases [43]. The readily metabolizable linkages also reduced liver activity, but the effect was not as drastic as that shown in blood. For kidney, a reduced activity was obtained only from the diester and dextran linkages. This indicates that different metabolites are processed differently in kidney. The activity in intestine was low, less than 0.36%, for all of the linkages investigated, whereas urine activity of the ester-linked conjugate was 12% of the total injected dose at 4 hours postinjection. This suggests that the activity is excreted mainly through the kidneys.

In conclusion, a significant amplification of the target-to-blood ratios was achieved by the disulfide (9.5), diester (8.9), carbohydrate (5.3), and dextran (9.1) linkages as compared with the control amide linkage (2.0) (Table 2). The increase in the target-to-liver ratios obtained by the disulfide (2.9), ester (2.0), carbohydrate (2.3), and dextran (1.9) is much less than that achieved for the target-to-blood ratios, but is quite substantial as compared with the target-to-liver ratio (1.3) of the control linkage. For the target-to-kidney ratio, an amplification was obtained only from the ester (2.8) and dextran (2.6) compared with the control (1.2). This study supports the hypothesis that the target-to-nontarget ratio can be optimized by placing a readily metabolizable bond between the antibody and a chelator.

Acknowledgment

The authors would like to thank Dr. K. Yokoyama for his advice regarding the technique for the target model, and K. Paek and H.J. Kim for their technical assistance. This work was supported in part by grant CA 28462 awarded by the National Cancer Institute.

References

1. Hnatowich, D.J., Layne, W.W., and Childs, R.L. (1982) The preparation and labeling of DTPA-coupled albumin. J. Appl. Radiat. Isot. 33:327–332.
2. Paik, C.H., Ebbert, M.A., Murphy, P.R., Lassman, C.R., Reba, R.C., Eckelman, W.C., Pak, K.Y., Powe, J., Steplewski, Z., and Koprowski, H. (1983) Factors influencing DTPA conjugation with antibodies by cyclic DTPA anhydride. J. Nucl. Med. 24:1158–1163.
3. Paik, C.H., Hong, J.J., Ebbert, M.A., Heald, S.C., Reba, R.C., and Eckelman, W.C. (1985) Relative reactivity of DTPA. J. Nucl. Med. 26:482–487.
4. Krejcarek, G.E., and Tucker, K.L. (1977) Covalent attachment of chelating group. Biochem. Biophys. Res. Comm. **000**:581–585.
5. Khaw, B.A., Fallon, J.P., Straus, H.W., and Haber, E. (1980) Myocardial infarct imaging. Science 209:295–297.
6. Paik, C.H., Murphy, P.R., Eckelman, W.C., Volkert, W.A., and Reba, R.C. (1983) Optimization of the DTPA carboxycarbonic mixed anhydride. J. Nucl. Med. 24:930–936.
7. Zogbi, S.S., Neuman, R.D., and Gottschalk, A. (1985) A modified procedure for rapid labeling of low concentrations of bioactive proteins with In-111. Int. J. Nucl. Med. Biol. 12: 159–166.
8. Scheinberg, D.W., Strand, M., and Gansow, O.A. (1982) Tumor imaging. Science 215: 1511–1513.
9. Najafi, A., Childs, R.L., and Hnatowich, D.J. (1984) Coupling antibody with DTPA. Int. J. Appl. Radiat. Isot. 35:554–557.
10. Najafi, A., and Hutchinson, N. (1986) The use of DTPA. Int. J. Appl. Radiat. Isot. 37:548.
11. Hnatowich, D.J., Childs, R.C., Lanteigne, D., and Najafi, A. (1983) The preparation of DTPA-coupled antibodies radiolabeled with metallic radionuclides. Immunol. Methods 65: 147–157.
12. Sakahara, H., Endo, K., Nakashima, T., Koizumi, M., Ohta, H., Torizuka, K., Furukawa, T., Ohmomo, Y., Yokoyama, A., Okada, K., Yoshida, O., and Nishi, S. (1985) Effect of DTPA conjugation. J. Nucl. Med. 26:750–755.
13. Halpern, S.E., Hagan, P.L., Carver, P.R., Kozoil, J.A., Chen, A.W.N., Frinke, J.M., Bartholomew, R.M., David, G.S., and Adams, T.H. (1983) Stability, characterization, and kinetics of In-111 labeled monoclonal anti-tumor antibodies in normal animals and nude mouse-human tumor models. Cancer Res. 43:5347–5355.
14. Powe, J., Pak, K.Y., Paik, C.H., Steplewski, Z., Ebbert, M.A., Herlyn, D., Ernsst, C., Alavi, A., Eckelman, W.C., Reba, R.C., and Koprowski, H. (1984) Labeling monoclonal antibodies and $F(ab')_2$ fragments with In-111 using cyclic DTPA anhydride and their in vivo behavior in mice bearing human tumor xenografts. Cancer Drug Del. 12:125–135.
15. Fawwaz, R.A., Wang, T.S.T., Estabrook, A., Rosen, J.M., Hardy, M.A., Alderson, P.O., Srivastava, S.C., Richards, P., and Ferrone, S. (1985) Immunoreactivity and biodistribution of In-111 labeled monoclonal antibody. J. Nucl. Med. 26:488–492.
16. Khaw, B.A., Straus, H.W., Cahill, S.L., Soule, H.R., Edgington, T., and Cooney, J. (1984) Sequential imaging of In-111 labeled monoclonal antibody in human mammary tumors hosted in nude mice. J. Nucl. Med. 25:592–603.
17. Pimm, M.V., Perkins, A.C., and Baldwin, R.W. (1985) Differences in tumor and normal tissue concentrations of iodine-and indium-labeled monoclonal antibody. II. Biodistribution studies in mice with human tumor xenografts. Eur. J. Nucl. Med. 11:300–304.
18. Perkins, A.C., and Pimm, M.V. (1985) Differences in tumor and normal tissue concentrations of iodine and indium labeled monoclonal antibody. I. The effect on image contrast in clinical studies. Eur. J. Nucl. Med. 11:295–299.
19. Hnatowich, D.J., Griffin, T.W., Kosciuczyk, C., Rusckowski, M., Childs, R.L., Mattis, J.A., Shealy, D., and Doherty, P.W. (1985) Pharmacokinetics in an indium-111 labeled monoclonal-antibody in cancer patients. J. Nucl. Med. 26:849–858.
20. Halpern, S.E., Dillman, R.O., Witztum, K.F., Shega, J.F., Hagan, P.L., Burrows, W.M., Dillman, J.B., Clutter, M.L., Sobol, R.E., Frinke, J.M., Bartholomew, R.M., David, G.S.,

and Carlo, D.J. (1985) Radioimmunodetection of melanoma utilizing In-111 96.5 monoclonal antibody: A preliminary report. Radiology 155:493–499.

21. Murray, J.L., Rosenblum, M.C.T., Sobol, R.E., Bartholomew, R.M., Plager, C.E., Haynie, T.P., Jahns, M.F., Glenn, H.J., Lamki, L., Benjamin, R.S., Papadopoulos, H., Boddie, A.W., Frinke, J.M., David, G.S., Carlo, D.J., and Hersh, E.M. (1985) Radioimmunoimaging in malignant melanoma with In-111 labeled monoclonal antibody 96.5. Cancer Res. 45:2376–2381.
22. Rosenblum, M.G., Murray, J.L., Haynie, T.P., Glenn, H.J., Jahns, M.F., Benjamin, R.S., Frinke, J.M., Carolo, D.J., and Hersh, E.M. (1985) Pharmacokinetics of In-111 labeled anti-p97 monoclonal antibody in patients with metastatic malignant melanoma. Cancer Res. 45: 2382–2386.
23. Sakahara, H., Endo, K., Nakashima, T., Koizumi, M., Kunimatsu, M., Kawamura, Y., Ohta, H., Nakamura, T., Tanaka, H., Kotoura, Y., Yamamura, T., Hosoi, S., Toyama, S., and Torizuka, K. (1987) Localization of human osteogenic sarcoma xenografts in nude mice by a monoclonal antibody labeled with radioiodine and In-111. J. Nucl. Med. 28:342–348.
24. Sands, H., and Jones, P.L. (1987) Methods for the study of the metabolism of radiolabeled monoclonal antibodies by liver and tumor. J. Nucl. Med. 28:390–398.
25. Methias, C.J., and Welch, M.T. (1987) Studies on the entrapment of In-111 in the liver (abstract). J. Nucl. Med. 28:657–658.
26. Shochat, D., Sharkey, R.M., Vattay, A., Primus, F.J., and Goldenberg, D.M. (1986) In-111 chelated by DTPA-antibody is retained in the liver as a small molecular weight moiety (abstract). J. Nucl. Med. 27:943.
27. Brechbiel, M.W., Gansow, O.A., Atcher, R.W., Schlom, J., Esteban, J., Simpson, D.E., and Colcher, D. (1986) Synthesis of 1-p-isothiocyanatobenzyl derivatives of DTPA and EDTA. Antibody labeling and tumor imaging studies. Inorg. Chem. 25:2772–2781.
28. Esteban, J.M., Schlom, J., Gansow, O.A., Atcher, R.W., Brechbiel, M.W., Simpson, D.E., and Colcher, D. (1987) New method for the chelation of In-111 to monoclonal antibodies: Biodistribution and imaging of athymic mice bearing human colon carcinoma xenografts. J. Nucl. Med. 28:861–870.
29. Rodwell, J.D., Alvarez, V.L., Lee, C., Lopes, A.D., Goers, J.W.F., King, H.A., Powsner, H.J., and McKearn, T.J. (1986) Site-specific covalent modification of monoclonal antibodies. Proc. Natl. Acad. Sci. USA 83:2632–2636.
30. Quadri, S.M., Paik, C.H., Yokoyama, K., and Reba, R.C. (1986) Synthesis and in vivo comparison of antibody DTPA conjugates with different chemical bonds (abstract). Proceedings of Sixth International Symposium on Radiopharmaceutical Chemistry, Boston, p. 116.
31. Brown, B.A., Dearborn, C.B., Neacy, W.P., Sands, H., and Gallagher, B.M. (1986) Comparison of carbohydrate directed versus amine directed attachment of DTPA to murine monoclonal antibodies (abstract). Proceedings of Sixth International Symposium on Radiopharmaceutical Chemistry, Boston, p. 115.
32. Haseman, M.K., Goodwin, D.A., Meares, C.F., Kaminski, M.S., Wensel, T.G., McCall, M.J., and Levey, R. (1986) Metabolizable In-111 chelate conjugated anti-idiotype monoclonal antibody for radioimmunodetection of lymphoma in mice. Eur. J. Nucl. Med. 12: 455–460.
33. Udenfriend, S., Stein, S., Bohlen, P., Dairman, W., Leimgruber, W., and Weigele, M. (1972) Applications of fluorescamine, a new reagent for assay of amino acids, peptides, proteins and other primary amines in the picomole range. Science 178:871.
34. Paik, C.H., Eckelman, W.C., and Reba, R.C. (1980) Reactivity of amino acids in the azo coupling reactions. 1. Dependence of their reactivity on pH. Bioorg. Chem. 8:25–34.
35. Lomant, A.J., and Fairbanks, G. (1976) Chemical probes of extended biological structures: Synthesis and properties of cleavable protein cross linking reagent [^{35}S] dithiobis (succinimidyl propionate). J. Mol. Biol. 104:243.
36. Abdella, P.M., Smith, P.K., and Royer, G.P. (1979) A new cleavable reagent for cross-linking and reversible immobilization of proteins. Biochem. Biophys. Res. Commun. 87:

734–742.
37. Alvarez, V.L., Lee, C., Rodwell, J.D., and McKearn, T. (1984) In vivo localization of site-specifically modified monoclonal antibodies. International Symposium on Monoclonal Antibodies, Florence, Italy.
38. Arnon, R., and Sela, M. (1982) In vitro and in vivo efficacy of conjugates of daunomycin with anti-tumor anti-body. Immunol. Rev. 62:5.
39. Gitman, A.G., Kahane, I., and Loyter, A. (1985) Use of virus attached antibodies or insulin molecules to mediate fusion between sendai virus envelopes and neuraminidase-treated cells. Biochem. 24:2762.
40. Carlsson, J., Drevin, H., and Axen, R. (1978) Protein thiolation and reversible protein-protein conjugation. J. Biochem. 173:723.
41. Koizumi, M., Endo, K., Kunimatsu, M., Sakahara, H., Watanabe, Y., Kawamura, Y., Nakashima, T., Arano, Y., Ohmomo, Y., Yamamura, T., Toyama, S., Yokoyama, A., and Torizuka, K. (1987) Tumor imaging with CTA-67 labeled monoclonal antibodies; effect of coupling agents on tumor targeting (abstract). J. Nucl. Med. 28:712.
42. Otsuka, F.L., Welch, M.J., McElvany, K.D., Nicolotti, R.A., and Fleischman, J.B. (1984) Development of a model system to evaluate methods for radiolabeling monoclonal antibodies. J. Nucl. Med. 25:1343–1349.
43. Jakoby, W.B., Bend, J.R., and Caldwell, J., eds. (1982) Metabolic basis of detoxification, metabolism of functional groups. New York: Academic Press.

11. Novel bifunctional linkers for antibody chelation with radiometals

Robert Sundoro Wu

The development of monoclonal antibody technology during the past decade has led to an unprecedented opportunity to develop tissue-specific reagents for in-vivo diagnostic studies. In many instances monoclonal antibodies have progressed from research bioassays to radiopharmaceuticals for radioimmunodetection of cancers and, theoretically, the same antibodies in the form of immunoconjugates could be applied to cancer therapy. The critical consideration when preparing immunoconjugates with other chemical moieties is the preservation of immunoreactivity, and at the same time, sufficient quantities of the agents must be bound to the antibody so that a therapeutic effect can result. Binding must also persist with a long enough half-life to deliver an adequate dose of the agents to the target.

In the case of diagnostic imaging, partial body clearance of the antibody must be accelerated by the label, which may subsequently result in better tumor visualization by increasing the target-to-nontarget ratio. However, much work remains to be done to refine the technology, including the improvement of the formulation of new immunoconjugates and better labeling methodologies. This chapter will discuss the background, strategy, and methods for coupling some of the most effective linkers and chelators to antibodies and other proteins. Finally, methods of antibody conjugation via bifunctional linkers that we have developed in our laboratories will be discussed. For additional information and specific details on the methodology of coupling and preparation of immunoconjugates, the reader is referred to the literature reviewed elsewhere [1–10].

Strategy for the conjugation of ligands to immunoglobulins

The strategy for the coupling of chelators, drugs, and toxins to Mabs involves the identification and selection of the most efficient or 'ideal' conjugation method for the particular compound and for each Mab or protein. After chemical modifications on the antibody, the immunoconjugate product should not have significantly altered the antibody's reactivity, but should have sufficient incorporation of the compounds, drugs, and/or radioisotope-chelates per molecule of antibody to deliver toxic amounts to the tumor. The method

Goldenberg, D.M., (ed.), Cancer Imaging with Radiolabeled Antibodies.

of coupling to antibodies should minimize or avoid polymerization or aggregation of the Mab, and be technically simple and reproducible. Furthermore, the immunoconjugate should be relatively stable upon storage. In the case of tumor visualization by external scintigraphy, the selection of an ideal radionuclide for the labeling of a given Mab is critical.

It is desirable that the radionuclide delivers a sufficiently high photon density for achieving the resolution needed for imaging studies, while contributing as small a radiation dose as possible. The half-life of the photon/gamma emitter should be as short as possible, but must be compatible with the biodistribution pattern of the native monoclonal antibody for sufficient accumulation in the desired target.

Most labeling of Mabs so far has been carried out with one of the radionuclides of either iodine [10–12] or indium [13–16]. Since both these elements possess different half-lives and photon energies, it is theoretically possible to tailor the radionuclide to be chosen for the desired purpose. The use of other radionuclides has also been proposed, such as Ga-67 or Ga-68, Tc-99m, Ru-97, and Cu-67 for diagnostic imaging studies, and Cu-67, Bi-212, Hg-197, Y-90, and Re-186 for therapeutic use. Attachment of these radiometal ions to antibodies requires the use of chelating agents to form 'stable' chelate complexes, in which the chelating agents are previously coupled to antibodies by a variety of coupling procedures. There are a finite number of reactive functional groups available for use in conjugating chelators to antibody. Table 1 shows the reactive functional groups that are widely used for antibody conjugation. On the other hand, functional groups available on the peptide chain of the immunoglobulin include:

1. The C-terminal carboxyl groups, such as aspartic and glutamic acid residues. Theoretically, this carboxyl group can be activated to introduce a good leaving group, which can be displaced (at a later stage) by an amine ligand to form the ligand-antibody conjugate.

   However, the difficulty encountered with this method of coupling is that there are other reactive nucleophiles on the amino acids of the antibody, such as the lysine residues, which are capable of competing to form intramolecular cyclization of the peptide chains of antibodies. This can result in partial or complete loss of antibody activity. Furthermore, intermolecular cross-coupling of the carboxy-activated antibody with the second and third molecule of the same antibody may result in a further polymerization or aggregation of the antibody with concomitant loss of immunoreactivity of the product.
2. The sulfhydryl groups of cysteine residues on proteins are sufficiently reactive to couple to a maleimido ligand or a bromoacetamido ligand [17], as shown in Figure 1 in the preparation of Cu-67-labeled antibody.

   It has been known that haloacetamide reacts readily with sulfhydryl groups on proteins and also with amino groups [17]. At a pH above 9.0, a reaction of bromoacetamide with amines is expected to occur. It is likely that N-terminal amino groups of lysine residues on antibody may be the

Table 1. Potential conjugation methods utilizing reactive functional groups on compounds and proteins

Reactive groups	Bond/linkage
R—CO—X (X: azide, active esters, anhydride & mixed anhydride carbodiimide)	Amide linkage with amines
R—NCS	Thiourea linkage with amines
R—NCO	Urea linkage with amines
R—CHO and R-COR	Schiff base with amines
R—CO—CH_2—X (X: Cl, Br, and I)	Thioether linkage with sulfhydryl groups or alkyl amine bond with amines
R—N or R—NHCO—CH=CH—COOH	Thioether linkage with sulfhydryl groups

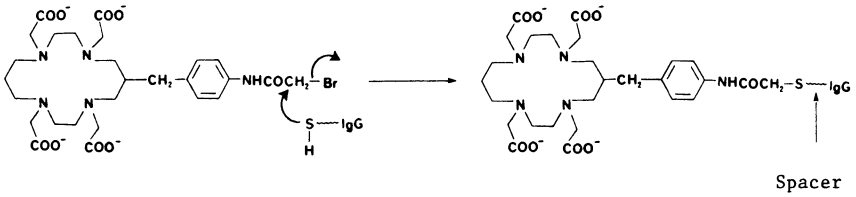

Figure 1. Coupling of IgG-SH to bromoacetamide containing TETA (tetraazacyclotetradecane tetraacetate).

dominant sites of reaction of antibodies with the tetraazacyclotetradecane tetraacetate (TETA) derivatives, in view of the rarity of the available free sulfhydryl groups on antibodies. Theoretically, immunoconjugates can be derived from this direct coupling with bromoacetamido TETA, in considering the simplicity of the method of conjugation, and should be readily labeled with Cu-67. However, a good radiolabeling yield is obtained when this conjugate contains a spacer to increase the separation between protein and TETA, so that by minimizing steric hindrance, the metal ion may reach the chelator easily. Thus, it is necessary to modify the antibody by reacting with 2-iminothiolane (Traut's reagent) to introduce the sulfhydryl groups, which are subsequently coupled to the bromoacetamido TETA to form a thioether linkage [17].

3. The guanidino group of arginine on proteins or immunoglobulins is another reactive functional group capable of forming an addition adduct with 1,2-diketones, such as p-azidophenylglyoxal [19,20] and camphorquinone [21].
4. Phenolic hydroxyl groups on tyrosine residues of antibodies have been utilized successfully for radioiodination of antibodies used in radioimmunodetection and for cancer radioimmunotherapy.
5. Hydroxyl groups on carbohydrate prosthetic groups of the Fc portion of immunoglobulins have been converted into reactive aldehydes for a site-specific linkage [22] with an amine ligand. This method relies on the chemical oxidation of antibody oligosaccharides to aldehydes to yield

unique functional groups on the antibody molecule that can selectively react with compounds containing, for example, amines, hydrazines, and hydrazides. Since the sites of attachment of oligosaccharides of antibodies are specific and distal to the antigen-binding region of antibodies, coupling to aldehydes should yield immunoconjugates with unimpaired antigen-targeting characteristics. In contrast, covalent modification at tyrosines by radioiodine and lysines by radiometal chelate are random attachments, some of which may be located at or near the antigenic sites of antibodies, which, in theory, could weaken the antibody activity of immunoconjugates, especially when the degree to which the binding sites are blocked is chemically oversubstituted. On this basis it appears that antibodies modified on the site-specific oligosaccharides are able to express full immunologic specificity and may provide successful use in diagnosis and therapy.

Methods of conjugation

The approach for conjugation described in this section is based upon identifying reactive functional groups existing on the chelators, followed by the addition of protein through the coupling method to bring the two components together. The method should allow for stoichiometric 'scale up' using gram quantities of antibody containing milligram quantities of chelators. The method should also allow controlled and reproducible incorporation of chelators on the antibodies with optimal preservation of the immunoreactivity of the conjugate. Linkages between the ligands/chelators and immunoglobulins may be either 1) direct covalent coupling or 2) indirect covalent coupling by means of a linker. These approaches will be discussed below.

Direct linkage

One of the most common and naturally occurring bonds is the peptide bond between two amino acids on the polypeptide chain of immunoglobulins. The bond formation is an energy-requiring reaction. For example, carboxylic acids react with amines at elevated temperatures and the amide bond can be produced this way through the loss of one water molecule. The temperatures, however, at which such transformations occur far exceed the limits considered safe for antibody conjugation. In fact, antibody coupling is usually performed at or below room temperature, and coupling methods that involve heating the reaction mixture are regarded as not generally useful. Therefore, in order to form a peptide bond, one of the groups, such as the carboxyl group, must be activated prior to antibody coupling.

Activation and coupling by the anhydride procedure. The activation of a carboxyl group by anhydride formation can be carried out in several ways.

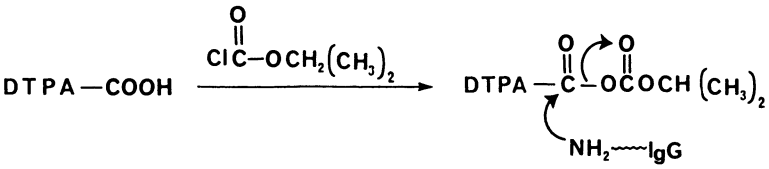

Figure 2. Preparation of DTPA mixed anhydride.

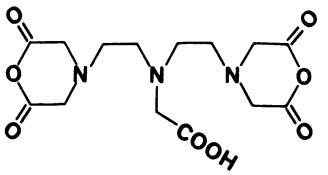

Figure 3. Structure of DTPA cyclic anhydride (CA-DTPA).

One of the most common reagents employed for this activation is acid chloride in solvent, such as benzene and chloroform, under anhydrous conditions. The first example of chelate-protein conjugation through the formation of a peptide bond was described by Krejcarek and Tucker in the preparation of DTPA — albumin conjugate by means of carboxy activation of DTPA using isobutylchloroformate to form the mixed anhydride [15]. The resulting activated DTPA was used without purification. The conjugate binds In-111 stably enough for many applications in vivo and has been used widely since then (Figure 2).

One of the most common feature of mixed anhydrides is the moderate stability of the reactive intermediates, which can be isolated but not stored for long periods of time. Mixed anhydrides are disproportionate to symmetrical anhydrides, and even the latter have a limited shelf life. Thus, reproducibility of one conjugate preparation may be different from the conjugate prepared at a later time. The procedure of antibody coupling by DTPA mixed anhydride was improved by Hnatowich et al. [23], by converting DTPA into a more stable DTPA bicyclic anhydride via heating the starting material in pyridine containing excess acetic anhydride. Immunoconjugates derived by this modification provide better quality control [24,25] (Figure 3).

Activation and coupling by the azide procedure. A number of complications may be encountered by coupling with the azide method. Yet, it is highly regarded among the methods of choice for the synthesis of peptides, mainly because racemization during the coupling reaction has not been observed [26]. The reaction proceeds via several steps: The azide must be prepared via the hydrazide from the carboxy ester by treatment with nitrous acid, and it is

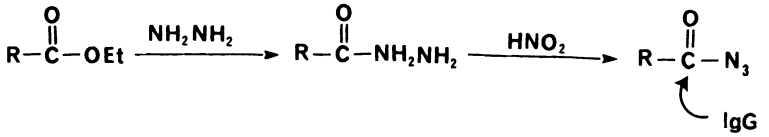

Figure 4. Method of preparation of acid azide.

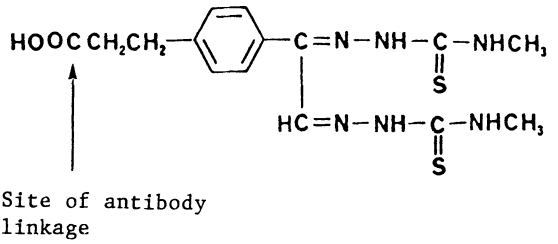

Figure 5. Structure of CE-DTS (carboxyethylphenylglyoxal-di-N-methyl thiosemicarbazone).

then allowed to react with the amino component, as shown in Figure 4.

The azide process offers some unusual advantages. Among these, the carboxyl group can be protected in the form of an alkyl ester (e.g., methyl ester), and the latter can be changed to an acid hydrazide simply by exposure to a solution of hydrazine in an organic solvent such as methanol. The acid hydrazide is often insoluble in organic solvent, from which it separates as it forms. The conversion of acid hydrazide to acid azide in an extremely facile reaction that proceeds rapidly, even in dilute solutions, and requires essentially no excess of nitrites. It is possible, therefore, to use the azide process for the preparation of protein conjugates. Nitrous acid, applied in a calculated amount, reacts preferentially with the hydrazide group and leaves the free amino group at the N-terminus practically intact. Protein modification using this approach seems to be more laborious than conventional carboxy activation.

A relatively recent and popular method has emerged that differs even more from the traditional method of preparation of acid azides. Ligands with a free carboxy group are treated with diphenylphosphorazidate and the desired acid azides are obtained in a smooth reaction and in a good yield. Yokoyama et al. [27] used this reagent to couple CE-DTS, a Tc-chelator, to monoclonal antibodies. The coupling reaction was carried at −5°C using a 1 : 1 molar ratio of chelator/reagent in a pH 9.0 buffer. Conjugation of CE-DTS with IgG under this condition gave a 16.5% coupling yield. The immunoconjugate with one substitution of the compound preserved its full immunoreactivity (Figure 5).

So far, we have avoided the problem of the structure of acid azides. Without going into detail about the chemistry of azides, the Curtius rearrangement has to be mentioned, since it has a direct impact on the coupling process (Figure 6).

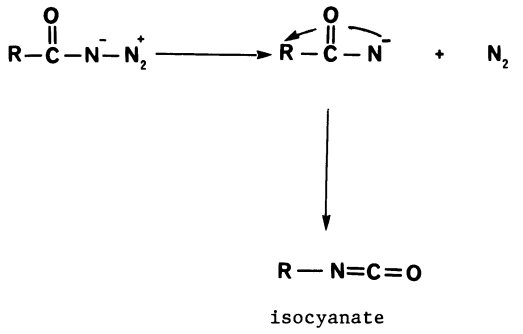

Figure 6. Curtius rearrangement.

This is an unusually noxious side reaction because the resulting isocyanates are very reactive: They produce amines with water. Since most antibody coupling is carried out in an aqueous system, the coupling yield is low. But, most importantly, the acid azides have a limited shelf life. In this respect, active esters are different. Most of them can be secured in crystalline form and kept intact for years if stored in a refrigerator. Thus, simplicity of the execution of coupling reactions, especially in a complex situation such as monoclonal antibody modification, can be controlled with ease. Indeed, this is the coupling method we have selected for modifying monoclonal antibodies with chelators, as described below.

Activation and coupling by the active ester procedure. Even simple alkyl esters, such as methyl or ethyl esters, can be ammonolyzed, but generally the amides form slowly and can be obtained only at elevated temperatures. On the other hand, the ester group is not restricted to methy ether and activation of the ester carbonyl can be accomplished by the selection of hydroxy components in which an electron-withdrawing group is present. This is the underlying idea in the experiments carried out in our laboratories in coupling CE-DTS to monoclonal antibodies. Out of many hydroxy components having a good electron-withdrawing group [8], N-hydroxysuccinimide was selected on the basis that this leaving group is readily soluble in water and can be easily handled at the end of protein coupling. Secondly, most esters of N-hydroxysuccinamide are crystalline and relatively stable. They also have excellent reactivity in the aminolysis reaction, but are somewhat less reactive than pentafluorophenyl esters [28].

In our laboratories, the N-hydroxysuccinamide ester of CE-DTS (Figure 7) is prepared by reacting the chelator with a solution containing a 1 : 1 molar ratio of DCC and N-hydroxysuccinamide.

Anti-CSAp murine monoclonal antibody [60] was reacted with excess CE-DTS-OSu to form the antibody conjugate. The number of CE-DTS molecules coupled to the IgG was determined by UV spectrometry at 280 nm and 320 nm [29]. Experimental results have shown that CE-DTS can be con-

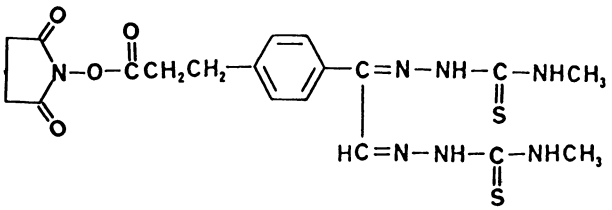

Figure 7. Structure of p-carboxyethylphenylglyoxal di-N-methyl thiosemicarbazone N-hydroxysucinimide ester (CE-DTS-OSu).

Table 2. Conjugation of CE-DTS-OSu with anti-CSAp IgG in 0.1 M borate buffer, pH 8.5, for 30 minutes

Mole of CE-DTS-OSu/IgG	Moles of CE-DTS Coupled	% Coupling
10	5.4	54
6	2.9	48
4	2.6	65
2	1.3	65
1.5	1.0	67

jugated efficiently by the N-hydroxysuccinimide ester coupling procedure. Typically, a 60% coupling yield is obtained under these conditions and immunoreactivity of the conjugate is preserved to a high degree. Table 2 shows that the coupling efficiency is high, even with four ligands per IgG.

In a comparing acid azide with N-hydroxysuccinamide ester coupling, it is obvious that antibody modification by the latter method is far superior, not only in terms of the coupling efficiency, but also the stability and simplicity of the procedure involved in executing the coupling reaction. The need for a practical procedure is understandable, especially in the preparation of laborious immunoconjugates, where a formidable number of steps may be required. We would, nevertheless, like to give some thought to the price paid for simplification.

Activation and coupling by isothiocyanates. Many coupling reagents have been proposed in the literature, yet most of them merely generate well-known intermediates such as anhydrides or active ester. It is certainly justifiable to design a reactive functional group such as isothiocyanate if other known coupling methods described previously may give rise to undesirable intermediates or products, even if such a coupling procedure has been shown to be very efficient. An example of this is highlighted in the preparation of the N-hydroxysuccinimide ester of DTPA [30]. Although this type of pentaester was reported to be more stable than cyclic DTPA dianhydride and consequently gave a higher DTPA coupling yield than coupling by the dianhydride, antibody conjugates derived by this pentaester coupling have been shown to have a higher degree of dimer and polymer formation. In-111-labeled anti-

body conjugate derived from this coupling was reported to be less stable than the one prepared by the dianhydride method [30]. In this case, the advantage of stability is counterbalanced by the poor label. To overcome these problems, Gansow et al. [31] have synthesized ITC-DTPA (p-isothiocyanatobenzyl DTPA) for In-111 labeling of monoclonal antibodies.

ITC-DTPA is very different from and superior to the conventional DTPA (CA-DTPA) cyclic dianhydride, because the one-ligand, carboxylate metal-binding site is occupied by an amide bond to form an antibody-linked diethylene triaminetetracetic acid, in which the acid ligand is known to lose indium faster in vivo than the ligand from DTPA [32]. Furthermore, indium-DTPA was reported to be thermodynamically more stable than the corresponding diethylenetriaminetetraacetic acid [32], and the method of linkage through the isothiocyanate functional group by amine residues on antibody avoids internal or external crosslinkage of the antibody molecule. However, other workers have reported success in preserving the immunoreactivity of the conjugate by the DTPA cyclic anhydride method [33].

Thus far, direct linkages of ligands to proteins and antibodies have been discussed, but there are many other coupling reagents that have been proposed and many of them are commercially available. The next discussion focuses on them of these linkers, including the linker that has been developed in our laboratories.

Coupling by the use of a bifunctional linker

In theory, any compound having two identical reactive functional groups (Table 1) on both ends of the molecule can serve as a crosslinking reagent to join ligands or drugs to other ligands, drugs, or proteins. However, it is more difficult to join ligands to antibodies efficiently and, at the same time, to maintain the integrity of antibody activity, stability of the immunoconjugate, and the ability to bind radioisotopes strongly and efficiently for use in scintigraphy. The following discussion will focus on the various reagents that have been used for monoclonal antibody modification.

Glutaraldehyde (Figure 8) has been widely used to crosslink proteins with the formation of α, ω-Schiff bases. Upon reduction with sodium borohydride or sodium cyanoborohydride, a stable linkage is obtained [34,35]. The reaction of glutaraldehyde with protein proceeds quite rapidly at mild alkaline pH. Eccles et al. [36] used this reagent to couple deferoxamine (DFO) successfully to human IgG and its Fab fragments. A conjugation of 0.9 M DFO per mole IgG was obtained with 40-fold molar excess of DFO at pH 7.4. The immunoconjugate derived from this coupling was shown to be stable. A labeling yield with a specific activity of 80–200 μCi/mg was reported using Ga-67 citrate. However, they also found that the ability of glutaraldehyde to crosslink protein required the concentration of the reagent to be kept as low as possible in order to avoid aggregation and/or oligomer formation [37]. Optimal conditions using a DFO : glut : IgG molar ratio of

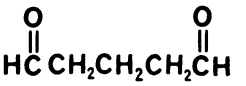

Figure 8. Structure of glutaraldehyde.

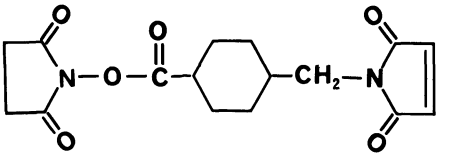

Figure 9. Structure of succinimidyl 4-(N-maleimidomethyl)-cyclohexane-1-carboxylate (SMCC).

500 : 150 : 1 was necessary to yield a conjugate with a high labeling yield and a low amount of aggregates (< 6%).

In view of the nature of this linker, which has two identical reactive aldehyde groups on both termini, it is not surprising that a selective reaction between the chelating agent and proteins cannot be controlled at ease. Furthermore, the quality and molecular integrity of the antibody molecule should be seriously questioned, as glutaraldehyde is capable of intramolecularly crosslinking two adjacent amines within the molecule, since this linker has a remarkable reactivity toward all amines, even under mild condition [34,35,38,39]. There are many such homobifunctional crosslinking reagents available commercially. These are represented by various bisimidates [40], bis-(hydroxysuccinimide) esters [41], diisothiocyanato benzene, bifunctional maleimides, etc. However, these bifunctional linkers have not been reported to be used in conjugating chelating agents to antibodies, perhaps with the expectation that these reagents will behave like glutaraldehyde.

Succinimidyl 4-(N-maleimidomethyl)cyclohexane-1-carboxylate (SMCC, Figure 9), a heterobifunctional crosslinking reagent, has been recently used by the group from duPont [42] in the preparation of metallothionein (MT) conjugation of the B72.3 murine monoclonal antibody. The conjugate was successfully labeled with Tc-99m using transchelation via Tc-99m glucoheptonate, with full immunoreactivity retained. In this procedure, the antibody was initially allowed to react with the active ester to introduce a maleimido group and subsequently thiolated with metalothionein, a polypeptide chelator having sulfhydryl residues known to bind Tc-99m well. There are many bifunctional linkers, such as SMCC, available commercially. These are m-maleimidobenzoyl-N-hydroxysuccinimide ester (MBS), succinimidyl 4-(p-maleimidophenyl) butyrate (SMPB), sulfosuccinimidyl (4-iodoacetyl) aminobenzoate (SIAB), and their water-soluble derivatives. Each one of these reagents is capable of crosslinking chelators to antibodies by the formation of a thioether bond, as described previously in the preparation of

TETA antibody conjugate, whereby the antibody needs to be first modified to introduce sulfhydryl groups prior to coupling to sulfhydryl reacting chelators.

However, one minor inconvenience of this coupling procedure is that it requires an additional step to chemically derivatize antibody in order to introduce the sulfhydryl residues, and the resulting IgG-SH must be used rapidly in the absence of oxygen to effectively react with the chelator to minimize the polymerization of thiolated antibodies.

Another group of coupling reagents that has been used extensively in the preparation of conjugated haptens and throughout peptide synthesis is the carbodiimides. Carbodiimides activate carboxyl groups to bind amines. These reagents form peptide bonds between the agent and protein. The chemistry and utility of carbodiimides have been thoroughly investigated [43,44]. A number of water-soluble carbodiimides [i.e., ECDI, 1-ethyl-3-(3′-dimethyl-aminopropyl)carbodiimide] have been used to link a number of drugs to antibodies and albumins: Conjugation of the amino group of deferoxamine (DFO) to the carboxy groups of human serum albumin [45] in a one-pot preparation. The disadvantage of this method is that the concentration of the amines has to be higher than the concentration of proteins in order to prevent an intermolecular or intramolecular crosslinking between the carboxy and amino residues of the protein. As a result, the coupling yield is very low.

A better coupling reagent that has been widely used to link two amines of different proteins is the heterobifunctional reagent, N-succinimidyl 3-(2-pyridyl-dithio) propionate, commonly known as SPDP [46]. The procedure involves three steps. First, 2-pyridyl disulphide structures are introduced into the proteins ($protein_1$ and $protein_2$) by the reaction of some of its amino groups with the N-hydroxysuccinimide ester side of the reagent (SPDP). Second, the SPDP conjugate of one of the modified proteins ($protein_1$ — S-S-2-pyridyl) is converted into aliphatic thiols ($protein_2$-SH) by reduction with dithiothreitol (DTT). Third, the thiol protein ($protein_1$-SH) thus formed is coupled to the previously prepared $protein_2$-SPDP conjugate by thiodisulphide exchange to make a $protein_1$-S-S-$protein_2$-conjugate.

The disadvantage of this coupling method is that it is a laborious process. In some proteins containing sulfhydryl groups, the N-hydroxysuccinimide ester moiety might also react with thiols, instead leading to an intramolecular crosslinking, although the coupling can be carried out at pH 4–5 since thiol exchange with disulphide groups is usually very much faster. Furthermore, in immunoglobulins, where disulphide groups are present, the effectiveness of this method of coupling is questionable (i.e., Can the newly introduced thiols undergo internal thio-disulphide exchange?). Nevertheless, such a coupling method has been utilized by others in the preparation of Ga-67-labeled monoclonal antibodies [47]. They discovered that the label derived from SPDP coupling (disulphide bond) was unstable in serum, leading to a faster clearance as compared with the labels derived from thioether and alkyl amine linkages and, consequently, resulting in very low tumor uptake of the label.

Antibody conjugate via selective bifunctional sequential linkers

There has been no consensus on the appropriate strategy for the systematic development of immunoconjugates. Some researchers are painstaking in their efforts to custom synthesize the chelators for use in antibody coupling. Others rely on the use of crosslinking reagents to join the agent of interest and the antibody to form a one-to-one conjugate. We shall contrast these methods with the approach we have taken in our laboratories in the preparation of chelate-conjugated monoclonal antibodies.

Unlike other bifunctional linkers that were previously described, we developed a selective, sequential bifunctional linker, p-isothiocyanatobenzoyl chloride (IBC, Figure 10), which had both ends capable of coupling to amino groups, but at different rates [59]. Thus, the more reactive end could be coupled to any chelator containing a free amino group to give a compound already activated for coupling to a second amino group, for instance, amino groups of lysine residues of antibodies. The overall process in the preparation of an immunoconjugate involved two steps:

Step 1: Selective activation of chelator

$$\underset{\text{Chelating agent}}{\text{R-NH}_2} + \underset{\text{Linker}}{\text{ClCOC}_6\text{H}_4\text{NCS}} \rightarrow \underset{\text{Activated chelator}}{\text{R-NHCOC}_6\text{H}_4\text{NCS}}$$

Step 2: Selective conjugation to antibody

$$\underset{\text{Activated chelator}}{\text{R-NHCOC}_6\text{H}_4\text{NCS}} + \underset{\text{Antibody}}{\text{H}_2\text{N-Ab}} \rightarrow \underset{\text{Antibody conjugate}}{\text{R-NHCOC}_6\text{H}_4\text{NHCSNH-Ab}}$$

In the first step, the more reactive acid chloride end of the linker is bound to the aminated chelator as isothiocyanate, then in the second step, it is reacted and bound with an amine on the antibody to form the immunoconjugate.

The advantage of using this linker over conventional reagents, such as glutaraldehyde, diisothiocyanatobenzene, and other imidate esters, is that the coupling avoids crosslinking amines from the same type of molecule, which leads to the preparation of immunoconjugates without aggregation. But, most importantly, the activated intermediate derived from the coupling reaction is clean, simple, and produced in high yield. Lastly, the isolated intermediate provides the structural identity and quality control to permit scrutiny before coupling.

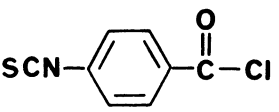

Figure 10. Structure of p-isothiocyanatobenzoyl chloride (IBC).

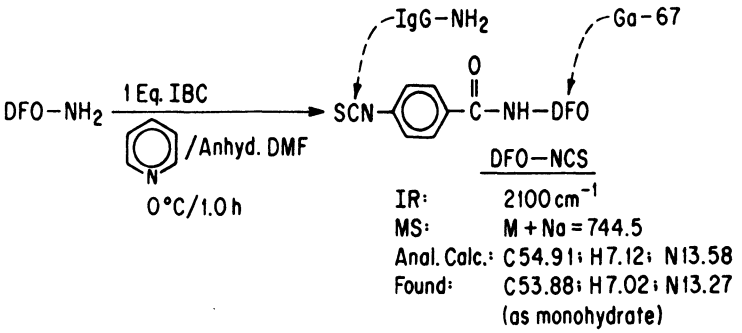

Figure 11. Synthesis of p-deferoxamidophenyl isothiocyanate.

To further illustrate the application of this technology, we selected deferoxamine (DFO), a powerful iron-chelating agent that is known to bind Ga-67 strongly, as a chelator of choice. Thus, deferoxamine is reacted with one equivalent of IBC in anhydrous DMF-containing pyridine as an acid scavenger. The mixture was allowed to react for 1 hour at 0°C. After workup, deferoxamidophenyl isothiocyanate (DFO-NCS) was isolated in a 77% yield as the white solids shown in Figure 11.

Antibody coupling

For antibody conjugation, anti-CEA murine monoclonal antibody was coupled to DFO-NCS. Size-exclusion HPLC analysis of the immunoconjugate revealed one single component with substantially the same retention time as unmodified antibody. There was no aggregation detected. Under this coupling condition, 1.8 M of DFO were substituted per mole of antibody, as determined by a series of carrier-added Ga-67 solutions. The immunoconjugate derived from this preparation was shown to have greater than 95% retention of the original immunoreactivity by CEA affinity column chromatography.

Radiolabeling Ga-67

Radiolabeling of the immunoconjugate with Ga-67 was best achieved at a buffered pH of 8.0 using Ga citrate. A 2-hour incubation time at 37°C with the isotope was necessary to increase the radiolabeling yield while keeping the volume of the mixture as low as possible (8–10 mg/ml). Radiolabeling of the DFO-immunoconjugate with Ga-67 at pH 7.4 by two independent groups [36,45] was reported to yield a specific activity of 50–200 μCi/mg of the label. In contrast, our Ga-67 labeling gave a specific activity in the range of 1–3 mCi/mg (i.e., a 15-fold higher labeling yield). This difference is perhaps reflected in the degree of DFO substitution of 1.8 M per mole of antibody, instead of the 0.9 M DFO per mole of antibody reported [36]. It is not clear

whether the type of linkage used in our experiments reflected any advantage in increasing the Ga-67 incorporation into the conjugate, since no attempts were made to prepare a conjugate with 0.9 M of DFO substituted for a comparison study. However, it is quite clear that Ga-67 labeling at pH 8.0 did improve the isotope incorporation significantly and is currently the method of choice for labeling antibodies with Ga-67 [59].

In summary, the method of coupling one amine to another amine, such as amino residues of lysines in antibodies, is far superior than the commercially available linkers. The reaction with the first amine is selective enough to permit the second amine to be sequentially linked. The procedure is simple and the quality of the intermediate can be monitored. Lastly, the linker can be used not only to link radiolabels, anticancer drugs, and toxins, but also for MRI (magnetic resonance imaging) contrast agents, enzymes, and various other proteins [59].

Conclusions and future directions

There is fairly universal agreement that a major goal in tumor imaging using monoclonal antibodies is to achieve good target concentration and excellent contrast. As we gain more familiarity with the biologic properties of antibodies, such as the use of Fab and $F(ab')_2$ antibody fragments [48] and a second antibody [49–52], it appears that there is a need to further chemically modify antibodies in order to reduce the concentration of radioactivity in nontarget areas such as the liver, the circulatory system, and critical organs. This will be particularly important for radiotherapy applications, where large radiation doses to normal tissue and critical organs need be avoided or reduced. It has been estimated that in order to deliver 6000 rads to a tumor for a favorable tumor response, the concentration in tumor relative to bone marrow, intestinal mucosa, kidneys, and liver must be at least 30, 9, 4, and 2.5 to 1, respectively [53]. It is only by achieving such ratios that toxic consequences of radiation in critical organs can be avoided.

However, such high target-to-nontarget ratios have been difficult to achieve. Two approaches have been recently investigated: a) the use of a metabolizable spacer developed by Paik et al. [54], which is described elsewhere in this book, and b) the use of monoclonal antibodies as reversible carriers [55,56]. The former approach utilizes an enzyme-cleavable linkage, such as an ester group between the metal chelate and the antibody, in order to have a rapid drop in blood levels. The latter involves the use of metal chelate-specific monoclonal antibodies as radiopharmaceutical carriers.

These reagents allow a rapid, selective renal clearance of chelate-labeled radiopharmaceuticals by competitive inhibition with a nonradioactive chelate chase at the time of imaging. This method was reported to have a marked improvement, both for tumor imaging and radiation dosimetry in mice, and may have great potential for human use [56].

Another approach that has not been investigated for radioimmunotherapy that has been extensively explored for chemotherapy is the use of a polymeric carrier linked to antibodies [57,58]. This allows the attachment of numerous toxic radioactive chelates to the polymer carrier backbone, thereby increasing the radiation dose to the target (tumor). These polymer carriers, represented by polycarboxylic acids, polyaminocarboxylic acid, albumins, dextrans, etc., can be effectively coupled to a series of chelating agents by means of bifunctional linkers such as the one we have developed. This also provides a greater versatility in attaching the chelator carrier to the antibody molecule, such that linkage to the carbohydrate portion of the antibody molecule can also be developed, providing a coupled antibody reagent that may have better characteristics (antigen binding, metabolism, etc.) than conjugation based on linkage to free amino groups. However, such a modification is restricted to the use of intact IgG, since antibody fragments do not have the carbohydrate residues to be linked. The use of biodegradable polymers, naturally occurring polymers such as starch, proteins, cellulose, polyamino acids, etc., is also appealing since they have been existing in nature for a length of time sufficient for enzymes to evolve that can degrade them. Principally, such polymers may have the advantage of being rapidly digested in vivo and may help to reduce the radiation dose in the nontarget area when used in antibody imaging or as therapy agents. Many potential applications of this technology are just beginning to be explored.

Acknowledgments

The author gratefully acknowledges the contributions of Marelou Azares and Dr. Frank Fields of Rockefeller University, New York in the MS analysis of synthetic intermediates.

References

1. Lundblad, R.L., and Noyes, C.M. (1984) In: *Chemical Reagents for Protein Modification*, Vol. 2. Boca Raton, FL: CRC Press, p. 123.
2. Ghose, T.I., Blair, A.H., and Kulkarni, P.N. (1983) Preparation of antibody-linked cytotoxic agents. Methods Enzymol. 93:280–333.
3. Erlanger, B. (1980) The preparation of antigenic hapten-carrier conjugates: A survey. Methods Enzymol. 70:85–104.
4. Bauminger, S., and Wilcheck (1980) The use of carbondiimides in the preparation of immunizing conjugates. Methods Enzymol. 70:151–159.
5. Hartman, F.C., and Wold, F. (1987) Cross-linking of bovine pancreatic ribonuclease A with dimethyl adipimidate. Biochemistry 6:2439–2448.
6. Zarling, D.A., Watson, A., and Bach, F.H. (1980) Mapping of lymphocyte surface polypeptide antigens by chemical cross-linking with bsocoes. J. Immunol. 124:913–920.
7. Lewis, R.V., Roberts, M.F., Dennis, E.A., and Allison, W.S. (1977) Photoactivated heterobifunctional cross-linking reagents which demonstrate the aggregation state of phospholipase

A_2. Biochemistry 16:5650–5654.
8. Bodanszky, M. (1984) In: Hafner, K., and Lehn, J. (eds.), *Principles of Peptide Synthesis*. Springer-Verlag, pp. 9–58.
9. Schroder, E., and Lubke, K. (1965) In: *The Peptides*. New York: Academic Press, pp. 76–136.
10. Contreras, M.A., Bale, W.F., and Spar, I.L. (1983) Iodine monochloride (ICI) iodination techniques. Methods Enzymol. 92:277–292.
11. Mather, S.J., and Ward, B.G. (1987) High efficiency iodination of monoclonal antibodies for radiotherapy. J. Nucl. Med. 28:1034–1036.
12. Bhargava, K.K., and Chervu, L.R. (1987) N-hydroxysuccinimide-hippuran ester: Application for radiolabeling of macro-molecules. Biochem. Biophys. Res. Commun. 144:323–328.
13. Halpern, S., and Stern, P. (1983) In: Burchiel, S.W., and Rhodes, B.A. (eds.), *Radioimmunoimaging and Radioimmunotherapy*. Elsevir Science, p. 197.
14. Khaw, B.A., Strauss, H.W., Cahill, S.L., Soule, H.R., Edgington, T., and Cooney, J. (1984) Sequential imaging of indium-111-labeled monoclonal antibody in human mammary tumors hosted in nude mice. J. Nucl. Med. 25:592–603.
15. Krejcarek, G.E., and Tucker, K.L. (1976) Covalent attachment of chelating groups to macromolecules. Biochem. Biophys. Res. Commun. 77:581–591.
16. Meares, C.T., McCall, M.J., Dayton, R.T., Goodwin, D.A., Diamanti, C.I., and McTigue, M. (1984) Conjugation of antibodies with bifunctional chelating agents: Isothiocyanate and bromoacetamide reagents. Methods of analysis and subsequent addition of metal ions. Anal. Biochem. 142:68–78.
17. Moi, M.K., Meares, C.F., McCall, M.J., Cole, W.C., and DeNardo, S.J. (1985) Copper chelates as probes in biological systems: Stable copper complexes with a macrocyclic bifunctional chelating agent. Anal. Biochem. 148:249–253.
18. Means, G.E., and Feeny, R.E. (1971) In: *Chemical Modification of Proteins*. San Francisco: Holdenday, p. 105.
19. Ji, I., Yoo, B.Y., Kaltenbach, C., and Ji, T.H. (1981) Structure of the lutropin receptor on granulosa cells (photoaffinity labeling with the subunit in human choriogonadotropin. J. Biol. Chem. 256:10853–10858.
20. Ngo, T.T., Yam, C.F., Lenhoff, H.M., and Ivy, J. (1981) A heterobifunctional photoactivable cross-linking reagent selective for arginyl residues. J. Biol. Chem. 256:11313–11318.
21. Pande, C.S., Pelzig, M., and Glass, J.D. (1980) Camphorquinone-10-sulfonic acid and derivatives: Convenient reagents for reversible modification of arginine residues. Proc. Natl. Acad. Sci. USA 77:895–899.
22. Rodwell, J.D., Alvarez, V.L., Lee, C., Lopes, A.D., Goers, J.W.F., King, H.D., Powsner, H.J., and McKearn, T.J. (1986) Site-specific covalent modification of monoclonal antibodies: In vitro and in vivo evaluations. Proc. Natl. Acad. Sci. USA 83:2632–2636.
23. Hnatowichs, D.J., Layne, W.W., Childs, R.L., Lanteigne, D., Davis, M.A., Griffins, T.W., and Doherty, P.W. (1983) Radioactive labeling of antibody: A simple and efficient method. Science 220:613–615.
24. Paik, C.H., Ebbert, M.A., Murphy, R.P., Lassman, C.R., Reba, R.C., Eckelman, W.C., Pak, K.Y., Powe, J., Steplewski, Z., Koprowski, H. (1983) Factors influencing DTPA conjugation with antibodies by cyclic DTPA anhydride. J. Nucl. Med. 24:1158–1163.
25. Paik, C.H., Hong, J.J., Elbert, M.A., Herald, S.C., Reba, R.C., and Eckelman, W.C. (1985) Relative reactivity of DTPA, immunoreactive antibody-DTPA conjugates, and nonimmunoreactive antibody-DTPA conjugates toward indium-111. J. Nucl. Med. 26: 482–487.
26. Sieber, P., Riniker, B., Brugger, M., Kamber, B., and Rittel, W. (1970) Menschliches calcitonin. VI[1]. Die synthese non calcitonin M[2]. Helv. Chim. Acta: 53:2135–2150.
27. Arano, Y., Yokoyama, A., Furukawa, T., Horiuchi, K., Yahata, T., Saji, H., Sakahara, H., Nakashima, T., Koizumi, M., Endo, K., and Torizuka, K. (1987) Technetium-99m-labeled monoclonal antibody with preserved immunoreactivity and high in vivo stability. J. Nucl. Med. 28:1027–1033.

28. Gross, E., and Meinhofer, J. (1980) In: *The Peptides*. New York: Academic Press, pp. 510–517.
29. Arano, Y., Yokoyama, A., Magata, Y., Saji, H., Horiuchi, K., and Torizuka, K. (1985) Syntheis and evaluation of a new bifunctional chelating agent for 99mTc labeling proteins: p-carboxyethylphenylglyoxal-di(N-methylthiosemicarbonzone). Int. J. Nucl. Med. Biol. 12: 425–430.
30. Najafi, A., Childs, R.L., and Hnatowich, D.J. (1984) Coupling antibody with DTPA — An alternative to the cyclic anhydride. Int. J. Appl. Rad. Isot. 35:554–557.
31. Brechbiel, M.W., Gansow, O.A., Atcher, K.W., Schlom, J., and Esteban, J. (1986) Synthesis of 1-(p-isothiocyanatobenzyl) derivatives of DTPA and EDTA. Antibody labeling and tumor-imaging studies. Inorg. Chem. 25:2772.
32. Paik, C.H., Herman, D.E., Eckelman, W.C., and Reba, R.C. (1980) J. Radioanal. Chem. 57:553.
33. Anderson, W.T., and Strand, M. (1985) Stability, targeting and biodistribution of scandium-46- and gallium-67-labeled monoclonal antibody in erythroleukemie mice. Cancer Res. 45: 2154–2158.
34. Richards, F.M., and Knowles, J.R. (1968) Glutaraldehyde as a protein cross-linking reagent. J. Mol. Biol. 37:231–233.
35. Jansen, E.F., Tomimatsu, Y., and Olson, A.C. (1971) Cross-linking of chymotrypsin and other proteins by reaction with glutaraldehyde. Arch. Biochem. Biophys. 144:394–400.
36. Motta-Hennessy, C., Eccles, S.A., Dean, and Coghlan, G. (1985) Preparation of Ga-67 labeled IgG and its Fab fragments using desferoxamine as chelating agent. Eur. J. Nucl. Med. 11:240–245.
37. Babich, J.W., Ward, M.C., Roberts, K.R., Bukham, A., Coghlan, G., Weswood, J.H., McCready, V.R., and Ott, R.J. (1986) In: *Sixth International Symposium on Radiopharmaceutical Chemistry*. Boston, p. 287.
38. Quiocho, F.A., and Richards, F.M. (1964) Intermolecular cross linking of a protein in the crystalline state: Carboxypeptidase-A. Proc. Natl. Acad. Sci. USA 52:833–839.
39. Habeeb, A.F., and S.A., (1987) *Schistosoma mansoni*: Chemical stabilization of cercariae by aldehydes. Exp. J. Parasitol. C19 64:111–119.
40. Peters, K., and Richards, F.M. (1977) Chemical cross-linking: Reagents and problems in studies of membrane structure. Ann. Rev. Biochem. 46:523–551.
41. Pilch, P.F., and Czech, M.P. (1979) Interaction of cross-linking agents with the insulin effector system of isolated fat cells (covalent linkage of ^{125}I-insulin to a plasma membrane receptor protein of 140,000). J. Biol. Chem. 254:3375–3381.
42. Hadjan, R.A., Tolman, G.L., Drozynski, C.A., Malone, M.E., Shah, S.A., and Sands, H. (1986) In vivo tumor localization biodistribution, and pharmacokinetic analysis of Tc-99m-metallothionein conjugated mouse monoclonal antibody B72.3. J. Nucl. Med. 27:1015.
43. Shechan, J.C., and Hess, G.P. (1955) A new method of forming peptide bonds. J. Am. Chem. Soc. 77:1067–1068.
44. Avarameas, S., and Ternynck, T. (1977) Conjugation of p-benzoquinone treated enzymes with antibodies and Fab fragments. Immunochemistry 14:767–774.
45. Janoki, G.A., Harwig, J.F., Chanachiai, W., and Wolf, W. (1983) [^{67}Ga] desferrioxamine-HSA: Synthesis of chelon protein conjugates using carbodimide as a coupling agent. Int. J. Appl. Rad. Isot. 34:871–877.
46. Carlsoon, J., Drevin, H., and Axen, R. (1978) Protein thiolation and reversible protein-protein conjugation (N-succinimidyl 3-(2-pyridyldithio) propionate, a new heterobifunctional reagent. Biochem. J. 173:723–737.
47. Koizumi, M., Endo, K., Kunimatsu, M., Sakahara, H., Watanabe, Y., Kawamura, Y., Nakashima, T., Arano, Y., Ohmomo, Y., Yamamuro, T., Toyama, S., Yokoyama, A., and Torizuka, K. (1987) Tumor imaging with Ga-67 labeled monoclonal antibodies: Effect of coupling agents on tumor targeting. J. Nucl. Med. 28:712.
48. Wahl, R., Parker, C.W., and Philpott, G.W. (1983) Improved radioimaging and tumor localization with monoclonal F(ab')$_2$ J. Nucl. Med. 24:316–325.

49. Goodwin, D.A., Meares, C., Diamanti, C., McCall, M., Lai, C., Torti, F., McTigue, M., and Martin, B. (1984) Use of specific antibody for rapid clearance of circulating blood background from radiolabeled tumor imaging proteins. Eur. J. Nucl. Med. 9:209–215.
50. Begent, R.H.H., Green, A.J., Bagshawe, R.D., Jones, B.E., Keep, P.A., Searle, F., Jewhes, R.F., Barratt, G.M., and Ryman, B.E. (1982) Liposomally entrapped second antibody improves tumor imaging with radiolabeled (first) antitumor antibody. Lancet 2: 739–742.
51. Sharkey, R.M., Primus, F.J., and Goldenberg, D.M. (1987) Second antibody clearance of radiolabeled antibody in cancer radioimmunodetection. Proc. Natl. Acad. Sci. USA 81: 2843–2846.
52. Goldenberg, D.M., Sharkey, R.M., and Ford, E. (1987) Anti-antibody enhancement of iodine-131 anti-CEA radioimmunodetection in experimental and clinical studies. J. Nucl. Med. 28:1604–1610.
53. Farwaz, R.A., Wang, T.S.T., Srivastava, S.C., and Hardy, M.A. (1986) The use of radionuclides for tumor therapy. Nucl. Med. Biol. 13:429–436.
54. Paik, C.H., Quadri, S.M., and Reba, R.C. (1987) Enhancement of blood clearance of Tc-99m labeled antibody by placing ester bonds. J. Nucl. Med. 28:602.
55. Goodwin, D.A. (1985) Hapten monoclonal antibody complexes drug carrier systems. American Chemical Society National Meeting, Miami Beach, FL. Nucl. Med. 48: .
56. Goodwin, D.A., Meares, C.F., David, G.F., McTigue, M., McCall, M.J., Frincke, J.M., Stone, M.R., Bartholomew, R.M., and Leung, J.P. (1986) Monoclonal antibodies as reversible equilibrium carriers of radiopharmaceuticals. Nucl. Med. Biol. 13:383–391.
57. Arnon, R., and Hurwitz, E. (1983) In: Goldberg, E.D. (ed.), *Targeted Drugs*. New York: John Wiley & Sons, p. 23.
58. Arnold, L.L., Dugan, A., and Kaplan, N.O. (1983) In: Goldberg, E.D. (ed.), *Targeted Drugs*. New York: John Wiley & Sons, p. 89.
59. Sundoro, B.M. (1987) Bifunctional linked. U.S. Patent 4,680,338, July 14, 1987.
60. Nocera, M., Shochat, D., Primus, J.F., Krupey, J., and Jespersen, D.L. (1987) Representation of epitopes on colon-specific antigen-p defined by monoclonal antibodies. J. Natl. Cancer Inst. 79:943–948.

12. Labeling of anti-tumor antibodies and antibody fragments with Tc-99m

Hans J. Hansen, Anastasia L. Jones, Ruth Grebenau, Arthur Kunz and David M. Goldenberg

The utility of radiolabeled monoclonal antibodies (Mabs) and Mab fragments in the radioimmunodetection (RAID) of cancer has been established with ^{131}I, ^{111}In, and ^{123}I [1–9]. More recently, however, increasing efforts have been expended to label these reagents with ^{99m}Tc. Indeed, successful clinical application of commercial monoclonal antibody imaging products will probably be dependent on the development of simple, inexpensive methods to label antibody or antibody fragments with this radionuclide. When compared with other radionuclides used to label Mabs, ^{99m}Tc has the following advantages: low cost, ready availability, ideal nuclear properties for gamma cameras, and reduced patient radiation exposure per millicurie of radionuclide administered. Strategies employed by different investigators to label antibodies and antibody fragments with ^{99m}Tc fall into two major categories. In one approach, efforts have been made to use a ligand to attach ^{99m}Tc indirectly to the antibody. The second approach has been to bind the radionuclide directly to intrinsic receptor sites or to altered groups of the protein backbone of the antibody molecule.

In this chapter we discuss the following topics: 1) a brief overview of the chemistry of ^{99m}Tc, 2) the biology involved in RAID of neoplastic tissue using intact radiolabeled antibodies and antibody fragments, 3) progress made in development of ^{99m}Tc-labeled antibody and antibody fragments, and 4) recent advances made in our laboratory.

Chemistry of ^{99m}Tc

^{99m}Tc has a 6-hour half-life and upon decay emits a single photon with a gamma energy of 140 keV. It is produced from the parent radionuclide, ^{99}Mo, a fission product with a half-life of 2.78 days. The availability of ^{99m}Tc to most hospitals and research scientists was made possible by the development of a simple ^{99}Mo-^{99m}Tc generator [10]. In this generator, molybdate is adsorbed to a column of alumina and ^{99m}Tc is formed by the decay of the ^{99}Mo. The ^{99m}Tc, in the form of $^{99m}TcO_4^-$, is eluted from the column with saline. The column is enclosed in a lead shield that contains ports for the introduction of

Goldenberg, D.M., (ed.), Cancer Imaging with Radiolabeled Antibodies.

saline onto the top of the column and collection of the ^{99m}Tc-containing eluent from the bottom of the alumina column. Introduction of saline and collection of eluent containing ^{99m}Tc is termed *milking* the generator. These generators have an effective life of 2 weeks before the ^{99}Mo in the column must be replenished.

^{99m}Tc produced by the generator is never carrier free. Fifteen percent of ^{99}MO decays directly to the extremely long-lived isotope, ^{99}Tc, which is also the single decay product of ^{99m}Tc; ^{99m}Tc and ^{99}Tc have identical chemical properties [11]. The specific activity of eluted ^{99m}Tc is dependent upon the time between generator milkings, because the longer the time between milkings, the more ^{99m}Tc that decays to ^{99}Tc. The mole fraction of the metastable isomer (^{99m}Tc) present in the eluted Tc varies from 0.836 at 0.5 hours postelution, to 0.277 at 24 hours postelution, to 0.077 at 72 hours postelution [11].

As discussed above, the products eluted from the generator are the pertechnetate anions, $^{99m}TcO_4^-$ and $^{99}TcO_4^-$, which have a negative valence of one. No effective chemistry exists that can be used to attach the negatively charged pertechnetate ions to small molecules (ligands) or proteins. Reduction of pertechnetate to a lower oxidation state results in the formation of highly reactive forms that complex strongly to many compounds, such as DTPA and albumin. Because of its nearly optimal redox properties, stannous chloride has proven to be the most effective reducing agent, and with few exceptions, most commercial kits employ stannous chloride to reduce pertechnetate [12]. Preparation and use of stannous chloride is not a trivial task. Because conversion of stannous chloride to stannic chloride occurs rapidly, it must be prepared just prior to use, which involves dissolving tin in hydrochloric acid under nonoxidizing conditions. This acid solution can be stored for a period of several hours in an inert atmosphere. Upon adjustment of this solution to physiologic pH, the formation of insoluble tin oxide occurs. This is minimized by the use of a chelating ligand, such as citrate or tartrate. Despite the formidable problems of preparing and stablizing stannous ions, Eckelman and coworkers succeeded in developing stannous-ion-containing kits and stablizing them by lyophilization [13]. This has resulted in the formulation of 'instant-use' pharmaceutical imaging agents that require only the addition of pertechnetate and mixing, prior to injection; in the current vernacular these are termed *shake-and-bake* kits.

Most of the ^{99m}Tc kits now used in nuclear medicine can be classified into one of two types: those in which reduced pertechnetate is complexed to a small ligand and those in which reduced pertechnetate is directly complexed into a macromolecule (protein or colloid). An example of the latter is ^{99m}Tc-human serum albumin, directly labeled by adding the protein to a vial containing stannous chloride and ^{99m}Tc-pertechnetate [14]. Examples of small ligands employed in kits are DTPA and 2,3-mercaptosuccinic acid (used for imaging of kidneys), glucoceptate (used for imaging brain and kidneys), methylene diphosphonate (used for bone imaging), and iminodiacetic acid (used to image the hepatobiliary tree) [12].

As mentioned above, for the past decade attempts have been made to label antibodies with ^{99m}Tc, first by direct labeling of the antibody by the addition of reduced ^{99m}Tc pertechnetate to the antibody, and secondly through the use of a bifunctional chelate of DTPA [15]. More recently, sulfur-containing chelates have been used to bind reduced ^{99m}Tc pertechnetate to antibody and antibody fragments; dimercaptide analogue tetradenenate chelating agents, developed by Fritzberg et al., and bis-thiosemicarbazone analogues, developed by Hosotani et al., are examples of these new chelates [16,17]. Each will be discussed later in this chapter.

Biological considerations

In general, the imaging agents now utilized in nuclear medicine are not biologically active and accumulate in the organ or region of interest because of unique metabolic/catabolic properties of the radionuclide and carrier. In contrast, RAID with radiolabeled antibodies is dependent upon binding of the antibody to antigen localized within the cancer. Goldenberg and his group first demonstrated the potential of RAID to image cancer and defined the major parameter that limited the technology, namely, the problem of background caused by the excess isotope in the blood pool [1,2].

This research was performed using intact antibody (IgG) radioiodinated with ^{131}I. Since ^{131}I has a half-life of 7 days, imaging can be performed several days postinjection, at which time most of the radioiodinated antibody in the blood has been catabolized and the isotope eliminated from the body via urinary excretion. Several methods have been applied to overcome the problem of blood-pool background. In one method a blood-pool marker, human serum albumin labeled with ^{99m}Tc, was administered after the ^{131}I-radioiodinated antibody. Using a gamma camera with multichannel analyzers, the distribution in the body of each isotope was independently determined. Gamma emission of ^{99m}Tc was subtracted from gamma emission of ^{131}I, thus correcting the image for antibody present in the blood pool and revealing accretion of radioactivity in the tumor [1]. In a second approach to overcome the problem of blood-pool background, the excess radioiodinated antibody was rapidly cleared from the blood by injection of a second antibody that was reactive with the primary labeled antibody [18,19]. Both the subtraction method and the second antibody clearance approach have proven to be effective in reducing the time required to image tumor with intact ^{131}I-radiolabeled antibody.

Although the RAID technology described above has proven to be useful to image known and occult cancers, it is too complex to be used by most nuclear medicine departments. In addition, ^{131}I is far from an ideal radionuclide for external imaging due to the high energy of ^{131}I gamma photon emissions (364 keV). The use of ^{123}I-labeled fragments in place of ^{131}I-labeled intact antibodies has brought the use of RAID a step closer to routine hospital applica-

tion [20]. ^{123}I has a low photon gamma energy of 159 keV, an energy almost ideally suited for gamma cameras used by nuclear medicine departments. Use of antibody fragments effectively reduces the time required to obtain positive tumor/blood and positive tumor/normal tissue localization ratios, as compared with localization ratios obtained at comparable times with radiolabeled intact antibody. Brown et al. have published one of the more comprehensive preclinical studies comparing localization of radiolabeled intact IgG, $F(ab')_2$, and Fab′ in a human tumor xenograft in an athymic nude mouse model [21]. Compared with IgG, the time required to obtain positive localization ratios can be reduced one- to two-fold by using $F(ab')_2$, or four-fold by using Fab′; this phenomenon is related to the increased catabolic rate of the fragments compared with the intact antibody. $F(ab')_2$ is primarily metabolized by the spleen and the kidney, while intact IgG is metabolized by the liver and the gastrointestinal tract [22]. Positive tumor/normal tissue ratios are obtained even earlier by using Fab′ as opposed to $F(ab')_2$, because Fab′ is not only catabolized more rapidly than $F(ab')_2$ and IgG, but, due to its low molecular weight of approximately 50,000 daltons, it is also filtered by the kidney [22–24]. The trade-off that must be accepted when using radiolabeled Fab′ for tumor imaging is a decrease in the percent injected dose of the fragment localized in the tumor versus that obtained with intact antibody. This limitation can be minimized by increasing the millicuries of ^{123}I used per imaging dose; the short half-life of 12 hours and a low photon gamma energy of 159 keV permit approximately ten times or more millicuries to be given as compared with ^{131}I. ^{123}I-labeled antibody fragments would represent ideal RAID reagents if ^{123}I were readily available at the low cost of ^{131}I. Unfortunately, the availability is limited and the cost is high. It is therefore necessary to develop techniques for other radionuclides, such as ^{99m}Tc, which are available at a low cost and have desirable properties for RAID.

^{99m}Tc ligand labeling

The use of bifunctional chelates to complex reduced ^{99m}Tc to antibody would appear preferable to direct methods of incorporation of the radionuclide into antibodies/fragments. In theory, the radionuclide should be bound more effectively by a well-defined chemical structure, in contrast with the binding of ^{99m}Tc to heterogeneous receptor groups native to the protein backbone of the antibody molecule. However, the application in practice of the use of chelates to bind reduced ^{99m}Tc to antibodies/fragments has proved to be difficult. Successful labeling of antibodies with ^{111}In, using bifunctional chelates of DTPA, encouraged several investigators to attempt to specifically incorporate reduced ^{99m}Tc into DTPA-antibody chelates. As early as 1982, Khaw et al. claimed specific incorporation of ^{99m}Tc into a DTPA-Fab prepared from an antibody to human cardiac myosin [25]. However, in a study

published in 1985, Childs and Hnatowich performed a more critical evaluation of the incorporation of ^{99m}Tc into a DTPA-antibody conjugate. They concluded that 'it was not possible to reduce to negligible levels nonspecific binding of ^{99m}Tc to the antibody' [26].

With the development of a better understanding of the chemistry of technetium, chelates were designed to complex reduced pertechnetate specifically to antibodies. The chelates that have been evaluated most extensively are dithio, diamino derivatives of N,N's-bis-mercaptoacetyl-diaminocarboxylic, developed by Fritzberg et al. [16]; this class of chelates is commonly referred to as N_2S_2 ligands. These superior chelates have not resolved the problems that prevented the specific incorporation of ^{99m}Tc into DTPA-antibody conjugates, i.e., nonspecific binding of the reduced radionuclide to the antibody.

In an attempt to circumvent these problems, Fritzberg et al. have developed elaborate technology to load the ligand with ^{99m}Tc, purify the ^{99m}Tc-ligand complex from free ^{99m}Tc and impurities, and then covalently couple the ^{99m}Tc-activated ligand to Fab'. NeoRx has developed a kit based on this technology and is presently conducting clinical trials to evaluate a ^{99m}Tc-N_2S_2-Fab' prepared with this kit for melanoma imaging [27,28]. Because of the complexity of the labeling kit, two of the advantages of using ^{99m}Tc have been compromised, i.e., the low cost of the final product and its ease of preparation. Indeed, it is unlikely that this kit can be adapted for use by the hospital nuclear medicine laboratory, and thus its use will be limited to regional radiopharmacies. Clinical performance of this RAID product to detect tumor in the abdomen and pelvis was compromised by liver uptake and hepatobiliary excretion of the radionuclide [27,28]. For reasons that remain to be defined, localization of tumor required preadministration of 40 mg of irrelevent IgG and 7.5 mg of unlabeled specific anti-melanoma IgG. This resulted in induction of high levels of human anti-murine antibody (HAMA) in most of the patients, certainly an undesirable property of a RAID product [28].

We encountered many similar problems in an attempt to develop another second-generation ^{99m}Tc chelate, bis-thiosemicarbazone (unpublished information). When we used antibody coupled with the chelate it was not possible to obtain quantitative incorporation into the chelate. Experiments to preload the chelate with ^{99m}Tc and attach it to the antibody were successful. However, experiments in mice bearing human tumor xenografts demonstrated high uptake of the labeled antibody by normal organs.

We discontinued development of this technology for labeling antibody with ^{99m}Tc for three reasons. First, if successful, the cost of the final product would be excessive. Second, the method was too complex. Finally, the specific activity of the final product was dependent on the frequency of milking of the ^{99m}Tc generator. Although the specific activity of the ^{99m}Tc can be controlled by milking the generator at controlled frequencies, this places significant restraints on the use of the generator for preparing isotope for other diagnostic applications.

Direct antibody labeling with ^{99m}Tc

One of the first reports of successful direct labeling of IgG with ^{99m}Tc was described by Wong et al. in 1978 [29]. They labeled human polyclonal IgG, using trisodium citrate as a chelator, and obtained 95–100% incorporation of reduced ^{99m}Tc into the protein within 30 minutes. They claimed localization of human tumors as determined by scintigraphic scans, putatively due to the presence of tumor-specific antibody in the preparation. The existence of 'tumor-specific antibodies' in normal human polyclonal IgG, in the light of current knowledge, appears highly doubtful. Tumor imaging obtained with this reagent was probably due to nonspecific localization of the labeled antibody in the tumor.

Using this method, Mishkin et al. successfully labeled IgG prepared using antisera from rabbits hyperimmunized with bacterial antigens [30]. They raised high-titer antibody in rabbits to *Staphylococcus aureus*, isolated the IgG, and labeled the IgG with ^{99m}Tc previously reduced by the addition of stannous chloride in 0.05 N HCl. Reduction was performed under acidic conditions to prevent formation of insoluble oxides of both tin and technetium. The pH of the solution was then adjusted to neutral pH using sodium citrate (the citrate ion acts as a weak chelating ligand, stabilizing both the stannous ion and the reduced pertechnetate). These investigators demonstrated that 98% of the radionuclide was incorporated into the IgG. The labeled antibody was administered to rabbits that had aortic valves infected with either staphylococcal or enterococcal bacteria. Impressive localization ratios of aortic valve/normal tissue were demonstrated in animals with staphylococcal infection; the labeled antibody did not localize in enterococcal-infested control aortic values. Despite highly significant localization of the antibody in the bacterial vegetations of the experimental animals, in-vivo imaging failed to detect the infection. Indeed, these investigators rediscovered the 'blood-pool background' problem of using intact IgG for in-vivo imaging, identified by Goldenberg and coworkers several years previously [1].

In the work described above, receptor groups intrinsic to the native polyclonal IgG were effectively labeled without prior activation of the IgG. It has been our experience that these receptor groups are not present in many murine monoclonal antibodies of the IgG subclass and that effective incorporation of reduced ^{99m}Tc-pertechnetate into the intact IgG requires exposure of the IgG to reducing agents such as mercaptoethanol. Apparently other investigators have also failed to label unmodified murine monoclonal antibody IgG. In order to generate receptor sites for incorporation of reduced ^{99m}Tc into murine Mab-IgG, Schwarz and Steinstrasser have pretreated murine monoclonal antibodies with mercaptan reducing agents and have stabilized the partially reduced IgG by lyophilization and storing the vialed Mab under nitrogen [31]. They have then used stannous chloride complexed with phosphonates or pyrophosphate to reduce ^{99m}Tc-pertechnetate prior to incorporation of the radionuclide into the 'activated' antibody.

Utilizing the labeling method of Schwarz and Steinstrasser, Baum et al. have labeled an anti-CEA-Mab (intact IgG) and imaged 40 patients with colorectal carcinoma [32]. Tumor detection was observed 6–24 hours post-injection, with a sensitivity of 92% reported in detecting known lesions. Sensitivity of detecting occult, CEA-producing tumors was 73%. Despite these impressive results, these investigators report several problems that need to be solved. Nonspecific liver uptake was relatively high, varying from patient to patient, and the high blood-pool activity caused problems in early images, especially in patients with questionable lung metastases. Finally, nonspecific accumulation of the isotope in the large bowel presented difficulties in interpretation. Apparently this problem was minimized by the administration of a laxative.

In 1986, Rhodes et al. reported localization of a tumor in a nude mouse with an anti-tumor antibody fragment labeled with ^{99m}Tc [33]. F(ab')$_2$ fragments, prepared from an anti-HCG monoclonal antibody, were incubated with stannous chloride and then lyophilized. ^{99m}Tc was added to the lyophilized vial and incubated for 30 minutes. A molecular sieve column, containing Sephadex-G-25 pretreated with stannous phthalate and gentisate, was used to remove free pertechnetate and isotope bound to low-affinity sites. The purified product was a mixture of labeled F(ab')$_2$ and Fab', with Fab' being the dominant labeled fragment. The yield of ^{99m}Tc in the labeled product was approximately 65% and the immunoreactivity of the antibody was retained. The authors hypothesized that the groups that were labeled with ^{99m}Tc were SH groups that had been reduced by stannous ions [33].

A critical review of the data published by Rhodes et al. suggests that they *did not* obtain specific tumor localization with this ^{99m}Tc-F(ab')$_2$ anti-HCG preparation. The labeled fragment gave similar localization ratios in animals, regardless of whether the tumor was HCG negative or HCG positive. Furthermore, tumor/normal tissue localization ratios, observed in vascularized organs, were barely statistically increased.

Although the preclinical animal studies reported by Rhodes et al. were disappointing, Summa Medical Corp. (Albuquerque, NM) continued to pursue development of the Rhodes' technology. In a recent publication, Zimmer et al. described results obtained in an athymic mouse-human/colonic tumor xenograft with a ^{99m}Tc-labeled anti-CEA-F(ab')$_2$, formulated by Summa [34]. Results of this study were markedly better than those reported by Rhodes et al. using the HCG-labeled fragment. Positive localization ratios were obtained when tumor was compared with several normal organs, and specificity was demonstrated using a control labeled fragment, the one important exception being the liver. The percent injected dose/gram (%ID/g) observed in the liver exceeded the %ID/g in the tumor at 24 hours postinjection of the labeled fragment. In agreement with the findings of Rhodes et al., these investigators observed that the primary labeled product was Fab'; however, the predominant protein in the preparation, prior to addition of the isotope, was F(ab')$_2$. They speculated that the pretinning process caused some reduc-

tion in disulfide bonds, with subsequent generation of monomeric fragments, and that this Fab′ minor component was preferentially labeled with reduced ^{99m}Tc-pertechnetate.

Buraggi et al. have employed a modified 'Rhodes' procedure to label $F(ab')_2$ fragments prepared from anti-melanoma Mabs; the primary modification of the original method was the substitution of an ion-exchange column to remove free ^{99m}Tc, in place of the special gel-filtration–tin column used by Rhodes [35]. Siccardi et al., in a large multicenter study, compared a ^{99m}Tc-labeled fragment to an ^{111}In-labeled fragment [36]. Overall, 74% of antigen-positive lesions were detected with the ^{99m}Tc-labeled fragment and 59% with the ^{111}In-labeled fragment. The optimal imaging time was between 6 and 12 hours for the ^{99m}Tc-labeled fragment and 24–48 hours for the ^{111}In-labeled fragment. Although the size of the ^{99m}Tc fragment was not reported, the optimal imaging time of 6–12 hours could indicate that the predominant labeled fragment was Fab′. As with other studies, the primary site of non-specific accretion of the ^{111}In-labeled fragment was the liver [19]. The ^{99m}Tc fragment accumulated in liver, spleen, and gut. To quote the authors, 'the detection of tumor lesions in these sites is severely limited and could often be achieved only with the aid of subtraction methods or through use of single photon emission computerized tomography' [36].

During the past 2 years we have developed a direct method to label Fab′ fragments with ^{99m}Tc. One of our goals was to obtain a labeled fragment that would give positive tumor/normal liver ratios within 24 hours after injection into athymic mice bearing a xenograft of colonic carcinoma. We considered this a prerequisite to performing phase I RAID studies in patients with colorectal carcinoma, because the liver is the primary organ to which these tumors metastasize. This goal has been achieved. The Fab′ fragment prepared from Immu-4, a Mab that is specific for high molecular weight CEA, has been formulated in a single vial and labeled by simply adding ^{99m}Tc-pertechnetate eluted from the generator. Essentially quantitative incorporation of the isotope into the fragment is complete within 5 minutes after its addition to the vial containing the lyophilized fragment. Table 1 demonstrates the remarkable ability of the fragment to quantitatively complex the added ^{99m}Tc-pertechnetate within 5 minutes of addition of the pertechnetate solution to the vial of lyophilized fragment. Table 2 demonstrates the stability of the complex to DTPA challenge. Clinical studies have demonstrated the effectiveness of the labeled fragment to image colorectal and other carcinomas [37].

Although we expected that it would be possible to incorporate ^{99m}Tc into nonalkylated Fab′, the quantitative incorporation achieved within 5 minutes of adding ^{99m}Tc to the preparation was unexpected. To date, we have labeled Fab′ prepared from anti-CEA, anti-AFP, and other Mabs of the IgG_1 subclass, and have routinely incorporated $> 99\%$ of 20 mCi of ^{99m}Tc into 1 mg of Fab′. It is apparent that the site we have generated and stabilized in the nonalkylated Fab′, prepared from IgG_1 Mabs, has an extremely high affinity

Table 1. Quality assurance results of labeling of lyophilized clinical lot 092888 Immu-4-Fab′ with ^{99m}Tc

Date	% Incorporation		% Immunoreactivity[c]
	HPLC[a]	ITLC[b]	
09/29/88	100	97	84
10/12/88	100	98	87
10/25/88	100	99	78[d]
10/25/88	100	99	76[d]
10/26/88	100	98	86
11/01/88	100	98	80[d]
11/09/88	100	96	71[d]
11/14/88	100	98	72[d]
11/22/88	100	89	77[d]
11/28/88	100	98	87
12/20/88	100	99	76[d]
12/20/88	100	98	72[d]
12/27/88	100	94	75[d]
01/26/89	100	98	81

[a] High-performance liquid chromatography using a sizing-gel column.
[b] Instant thin-layer chromatography.
[c] Determined using an Affi-Gel CEA affinity column.
[d] Performed on CEA affinity column #2, which gives lower values than column #1.

Table 2. DTPA Challenge of ^{99m}Tc-IMMU-4-Fab′

DTPA Challenge Conditions[a]		Distribution of Tc-99m as Determined by HPLC			
Time	Molar Ratio DTPA/Fab′	$F(ab')_2$	Fab′	DTPA	TcO_4^-
0	0	19%	81%	0	0
1 hr	0	10%	90%	0	0
"	910	9%	91%	0	0
"	2600	7%	91%	2%	0
4 hr	0	10%	87%	0	3%
"	910	11%	87%	0	2%
"	2600	11%	89%	0	0

Lyophilized material — lot 102788.
[a] Challenge was done at room temperature.

for reduced ^{99m}Tc-pertechnetate. Our success in generating this receptor site has been accomplished by minimizing damage to the fragment due to prolonged exposure to the agent used to generate the receptor site. Furthermore, the quantity of receptor site in each preparation is controlled, assuring that enough receptor site is present to bind ^{99m}Tc of low specific activity, i.e., eluate from a generator that has not been eluted for 3 days.

Conclusions

From the above discussion it is apparent that significant progress is being made toward the strong binding of reduced ^{99m}Tc to anti-tumor monoclonal antibodies and antibody fragments, while maintaining the immunoreactivity of the antibody. Many of these reagents are now being evaluated in clinical trials. One intriguing difference that has been reported using ^{99m}Tc-labeled intact antibody versus radioiodinated intact antibody is the ability to obtain early tumor imaging (within 24 hours) with ^{99m}Tc-labeled antibody. Preclinical studies using animal models predict that superior imaging results should be obtained with labeled Fab′ versus labeled IgG at time points up to 24 hours postinjection. However, in light of the excellent results reported by Baum et al. [32], carefully controlled clinical studies are needed to compare the effectiveness of imaging with intact IgG versus labeled fragments, with both reagents being prepared from the same monoclonal antibody. Resolution of this issue is of paramount importance. The decision to use intact IgG for tumor imaging is not a trivial matter if therapy with a monoclonal antibody is to be attempted. Intact IgG is much more immunogenic than are similar doses of antibody fragments [22]. Further, it has been documented that preexisting human anti-murine antibodies present in human sera are primarily reactive with determinants on the Fc of Mabs, and it appears that primary sensitization with intact Mab not only results in an increase of Fc-reactive HAMA, but also in sensitization to Fab′ epitopes [38,39]. Obviously, use of fragments for imaging is preferred, assuming at least equal performance of Fab′ to intact IgG reagents.

Acknowledgments

This work was supported in part by N.I.H. contract SBIR CM 87778 from the National Cancer Institute and USPHS grant CA 39841 from the NIH.

References

1. Goldenberg, D.M., DeLand, F., Kim, E.E., et al. (1978) Use of radiolabeled antibodies to carcinoembryonic antigen for the detection and localization of diverse cancers by external photoscanning. N. Engl. J. Med. 298:1384–1388.
2. Goldenberg, D.M., Kim, E.E., DeLand, F.H., et al. (1980) Radioimmunodetection of cancer with radioactive antibodies to carcinoembryonic antigen. Cancer Res. 40:2984–2992.
3. Mach, J.P., Buchegger, F., Forni, M., et al. (1981) Use of radiolabeled monoclonal anti-CEA antibodies for the detection of human carcinomas by external photoscanning and tomoscintigraphy. Immunol. Today 2:239–249.
4. Epenetos, A., Britton, K.E., Mather, S., et al. (1982) Targeting of iodine-I-123 tumor-associated antibodies to ovarian, breast and gastro-intestinal tumors. Lancet 2:999–1005.
5. Goldenberg, D.M., Kim, E.E., Bennett, S., et al. (1983) CEA radioimmunodection in the evaluation of colorectal cancer and in the detection of occult neoplasms. Gastroenterology

84:524–532.
6. Beatty, J.D., Duda, R.B., Williams, L.E., et al. (1986) Preoperative imaging of colorectal carcinoma with ^{111}In-labeled anticarcinoembryonic antigen monoclonal antibody. Cancer Res. 46:6494–6502.
7. Granowska, M., Britton, K.E., Shepherd, J.H., et al. (1986) A prospective study of ^{123}I-labeled monoclonal antibody imaging in ovarian cancer. J. Clin. Oncol. 4:730–736.
8. Epenetos, A.A., Carr, D., Johnson, P.M., et al. (1986) Antibody-guided radiolocalization of tumors in patients with testicular or ovarian cancer using two radioiodinated monoclonal antibodies to placental alkaline phosphatase. Br. J. Radiol. 59:117–125.
9. Colcher, D., Esteban, J.M., Carrasquillo, J.A., et al. (1987) Quantitative analyses of selective radiolabeled monoclonal antibody localization in metastatic lesions of colorectal cancer patients. Cancer Res. 47:1185–1189.
10. Tucker, W.D., Green, M.W., Weiss, A.J., et al. (1958) Methods of preparation of some carrier-free radioisotopes involving adsorption on alumina, BNL 3746. Annual Meeting, American Nuclear Society, Los Angeles, CA, June 1958. Trans. Am. Nucl. Soc. 1:160.
11. Lamson, M., III, Hotte, C.E., and Ice, R.D. (1976) Practical generator kinetics. J. Nucl. Med. Technol. 4:21–27.
12. Kowalsky, R.J., and Perry, J.R. (1987) Chemistry of radiopharmaceuticals. In: *Radiopharmaceuticals in Nuclear Medicine Practice*. Norwalk, CT: Appleton & Lange, pp. 75–95.
13. Eckelman, W.C., and Richards, P. (1970) Instant ^{99m}Tc-DTPA. J. Nucl. Med. 11:761.
14. Kowalsky, R.J., and Perry, J.R. (1987) Heart. In: *Radiopharmaceuticals in Nuclear Medicine Practice*. Norwalk CT: Appleton & Lange, pp. 217–218.
15. Eckelman, W.C., and Paik, C.H. (1986) Comparison of ^{99m}Tc and ^{111}In-labeling of conjugated antibodies. Nucl. Med. Biol. 13:335–343.
16. Fritzberg, A.R., Kasina, S., Reno, J.M., et al. (1986) Radiolabeling of antibodies with Tc-99m using N_2S_2 ligands. J. Nucl. Med. 27:957–958.
17. Hosotani, T., Yokoyama, A., Arano, Y., et al. (1986) In the procurement of a neutral and compact monomeric complex of dithiosemicarbazone (DTS) derivative: ^{99m}Tc-KTS. Int. J. Nucl. Med. Biol. 12:431–437.
18. Goldenberg, D.M. (1987) Advances in cancer; antibody targeting of cancer-prospects for detection and therapy. J. Med. Soc. N.J. 84:195–198.
19. Goldenberg, D.M. (1987) Current status of cancer imaging with radiolabeled antibodies. J. Cancer Res. Clin. Oncol. 113:203–208.
20. Mach, J.P., Forni, M., Ritschard, J., et al. (1980) Use and limitations of radiolabeled anti-CEA antibodies and their fragments for photoscanning detection of human colorectal carcinomas. Oncodevel. Biol. Med. 1:49–69.
21. Brown, B.A., Comeau, R.D., Jones, P.L., et al. (1987) Pharmacokinetics of the monoclonal antibody B72.3 and its fragments labeled with either ^{125}I or ^{111}In. Cancer Res. 47:1149–1154.
22. Covell, D.G., Barbet, J., Holton, O.D., et al. (1986) Pharmacokinetics of monoclonal immunoglobulin G_1, $F(ab')_2$, and Fab′ in mice. Cancer Res. 46:3969–3978.
23. Wochner, R.D., Strober, W., and Waldmann, T.A. (1967) The role of the kidney in the catabolism of Bence-Jones proteins and immunoglobulin fragments. J. Exp. Med. 126: 207–221.
24. Smith, T.W., Lloyd, B.L., Spicer, N., and Haber, E. (1979) Immunogenicity and kinetics of distribution and elimination of sheep digoxin-specific IgG and Fab fragments in rabbit and baboon. Clin. Exp. Immunol. 36:384–396.
25. Khaw, B.A., Strauss, H.W., Carvalho, A., et al. (1982) Technetium-99m labeling of antibodies to cardiac myosin Fab and to human fibrinogen. J. Nucl. Med. 23:1011–1019.
26. Childs, R.L., and Hnatowich, D.J. (1985) Optimum conditions for labeling of DTPA-coupled antibodies with technetium-99m. J. Nucl. Med. 26:293–299.
27. Eary, J.F., Schroff, R.W., Abrams, P.G., et al. (1989) Successful imaging of malignant melanoma with technetium-99m-labeled monoclonal antibodies. J. Nucl. Med. 30:25–32.
28. Salk, D. and the Multicenter Study Group. (1988) Technetium-labeled monoclonal antibodies for imaging metastatic melanoma: Results of a multicenter clinical study. Semin.

Oncol. 15:609–618.
29. Wong, D.W., Mishkin, F.S., and Lee, T. (1978) A rapid chemical method of labeling human plasma proteins with ^{99m}Tc-pertechnetate at pH 7.4. Int. J. Appl. Rad. Isot. 29:251–253.
30. Mishkin, F.S., Wong, D.W., Dhawan, V.K., et al. (1983) Radiolabeled antibody in the detection of infection using endocarditis as a model. In: Burchiel, S.W., and Rhodes, B.A. (eds.), *Radioimmunoimaging and Radioimmunotherapy*. New York: Elsevier Science, pp. 299–369.
31. Schwarz, A., and Steinstrasser, A. (1987) A novel approach to Tc-99m-labeled monoclonal antibodies. J. Nucl. Med. 28:721.
32. Baum, R.P., Hertel, A., Lorenz, M., et al. (1989) Tc-99m labeled intact monoclonal anti-CEA antibody for successful localization of tumor recurrences. In press.
33. Rhodes, B.C., Zamora, P.O., Newell, K.D., et al. (1986) Technetium-99m labeling and murine monoclonal antibody fragments. J. Nucl. Med. 27:685–693.
34. Zimmer, A.M., Kazikiewicz, J.M., Rosen, S.T., and Spies, S.A. (1987) Pharmacokinetics of ^{99m}Tc(Sn)- and ^{131}I-labeled anti-carcinoembryonic antigen monoclonal antibody fragments in nude mice. Cancer Res. 47:1691–1694.
35. Buraggi, G.L., Callegaro, L., Turrin, A., et al. (1984) Immunoscintigraphy with ^{123}I, ^{99m}Tc, and ^{111}In-labeled F(ab′)$_2$ fragments of monoclonal antibodies to human high molecular weight-melanoma associated antigen. J. Nucl. Med. Allied Sci. 28:283–295.
36. Siccardi, A.G., Buraggi, G.L., Callegaro, L., et al. (1986) Multicenter study of immunoscintigraphy with radiolabeled monoclonal antibodies in patients with melanoma. Cancer Res. 46:4817–4822.
37. Goldenberg, D.M., Goldenberg, D.M., Sharkey, R.M., et al. (1990) Clinical studies of cancer radioimmunodetection with carcinoembryonic antigen monoclonal antibody fragments labeled with ^{123}I or ^{99m}Tc. Cancer Res. 50:909–921.
38. Courtenay-Luck, N.S., Epenetos, A.A., Winearls, C.G., and Ritter, M.A. (1987) Pre-existing human anti-murine immunoglobulin reactivity due to polyclonal rheumatoid factors. Cancer Res. 47:4520–4525.
39. Courtenay-Luck, N.S., Epenetos, A.A., Moore, R., et al. (1986) Development of primary and secondary immune responses to mouse monoclonal antibodies used in the diagnosis and therapy of malignant neoplasms. Cancer Res. 46:6489–6493.

IV

Clinical Studies

13. Requirements for the use of radioimmunodetection of cancer in clinical practice

Gianluigi Buraggi

Since its first application in human subjects [1], a wide experience has been acquired by several groups in radioimmunodetection (RAID) of different tumors.

Many biologic and technical problems have been solved by these studies and different evaluations regarding the actual or future clinical usefulness of these methods have been reported.

The problems connected with tumor imaging using radiolabeled antibodies are certainly more complex than would be supposed when considering the conceptual simplicity of this approach.

Nevertheless, despite these difficulties, some radiolabeled antibodies against tumor-associated antigens have been widely tested in patients and in some countries have come to be used as routinely as other radiopharmaceuticals.

The aim of this paper is to analyze and discuss the most relevant requirements for the routine use of the methods for radioimmunodetection of cancer.

The most important factors involved for successful use of these examinations appear to be the following:

1. a good quality tumor image
2. high diagnostic efficacy of examination
3. no risk for the patient
4. a readily available supply of immunoreagents
5. diagnostic usefulness

Quality of tumor image

From a physical point of view, every kind of scintigraphy performed with a gamma-emitting radionuclide and a conventional scintillation camera reveals the same problems, i.e., a tumor can only be imaged if the concentration of radioactivity accumulated in it differs from that reached in the surrounding tissues. A positive value of the ratio between tumor and background (T/B) is more favorable for a suitable representation than is a negative value.

Goldenberg, D.M., (ed.), Cancer Imaging with Radiolabeled Antibodies.

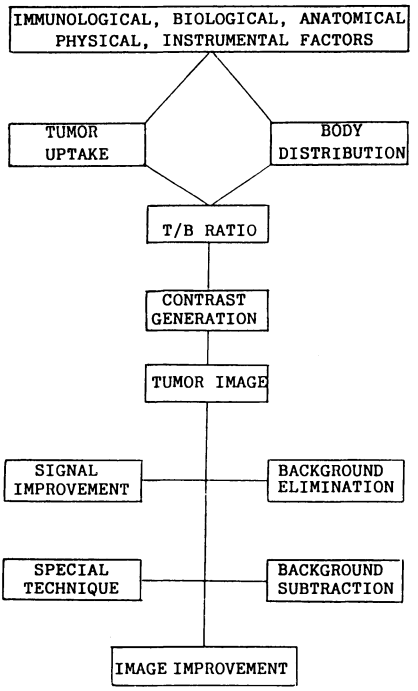

Figure 1. Main factors involved in radioimmunodetection.

Tumor uptake and body distribution of the radiolabeled antibody are the main parameters that are involved in determining the contrast, and therefore the quality, of the tumor image (Figure 1).

A number of biologic and immunologic factors are responsible for the values reached by these parameters, e.g., antigen (Ag) expression by the tumor cells; affinity and avidity of the immunoreaction antibody (Ab) cross-reactions; immunoreactivity variations after Ab radiolabeling; Ag modulation; and characteristics of the Ab used, such as whole IgG, Ab fragments [$F(ab')_2$, Fab, Fab']; monoclonal (Mab), or polyclonal Ab.

As in conventional scintigraphy, physical, instrumental, and anatomic factors may play an important role in determining the quality of the tumor image.

The first step in evaluating whether a given antigen-antibody system may be suitable for immunoscintigraphy is the study of the immunologic characteristics of the system itself.

A more detailed analysis of the influence of these factors on scintigraphic results, derived from personal experience and a survey of the literature, has been reported in a previous paper [2].

We will mention here only some of the relevant conditions that are generally considered indispensable to obtain a suitable immunoscintigraphy [3].

A neoplastic cell should express at least 10^5 sites. The best conditions are

obtained when normal cells do not express the antigen, though a ratio between normal and tumor cells of 0.01 is acceptable. A very high rate (90% or more) of tumors of the same histotype must express the antigen. It should be verified that the selected Ab does not react with blood cells. A suitable Ab shows an affinity constant that is equal to or higher than 10^8 M-1.

The use of fragments instead of the whole antibody modifies the tumor uptake due to the different affinity and avidity shown by the fragments [$F(ab')_2$, Fab], and the body distribution is also usually modified in these conditions.

Important variations in biodistribution can be demonstrated by labeling the same antibody or its fragments with different radionuclides [4,5].

If these evaluations of the antigen-antibody system and the radioimmunoreagents obtained from it seem to be of primary importance, as proven by a wide experience [for an extensive review, see 6–13], it is interesting to discuss how the reported factors can influence other parameters more directly correlated with the scintigraphic image and its quality.

The radioactive concentration reached in the tumor after radiolabeled antibody injection is usually higher in animal models than in humans, where, as a rule, values of 0.1–0.01% of the administered doses per gram of tissue are obtained [14,15].

Table 1 shows an example of this behavior in three patients and allows certain observations. Patients 1 and 2 had the same radioactive concentration in the tumor. If expressed as a percentage of the administered activity, namely, 0.01% per gram of tissue, patient 3 had a concentration that was ten times less than this, e.g. 0.001%.

Nevertheless, the total amounts of radioactivity in the three tumors were very different, due both to the different activities administered to each patient and to the varying tumor masses. This led to a very good scintigraphic image in patient 1, a doubtful result in patient 2, and a negative immunoscintigraphy in patient 3. These results are to be correlated with the different intensities of radiation (signal) emitted by the three tumors and interacting with the instrument.

Table 1. Tumor uptake measured in surgical specimens of melanoma 3 days after administration of 225.28S whole antibody labeled with ^{131}I

Patient			1	2	3
Administered activity	(AA)	MBq	52.5	27.7	25.9
Tumor mass (g)			15	1	4
Radioactive concentration in tumor (AA%/g)			0.01	0.01	0.001
Total radioactivity in tumor	(AA%) kBq		0.15 7950	0.01 277	0.004 103
Immunoscintigraphy			+++	+−	−

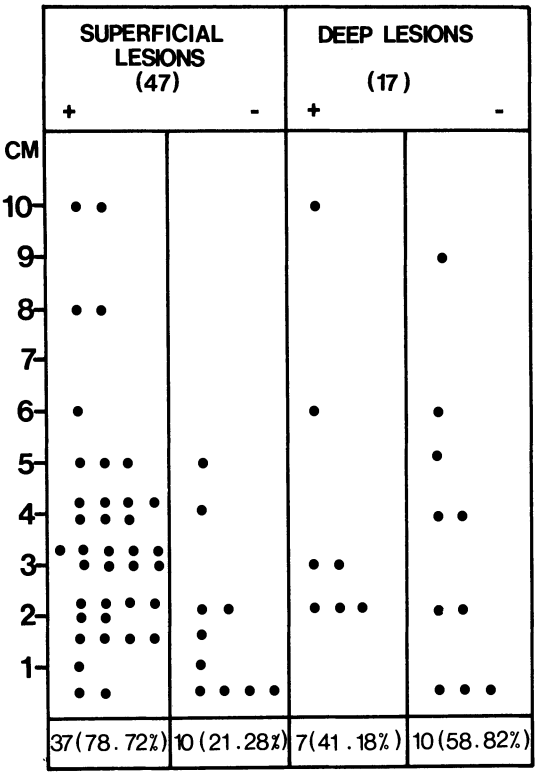

Figure 2. Correlation between immunoscintigraphic results, size, and depth of 64 melanoma localizations.

The intensity of the signal is, in fact, the most important factor for the detection of a radioactive source.

Theoretically, there are no limits to the representation of a radioactive source regarding its size, provided that its radioactivity is high enough. What usually happens in clinical practice is that larger, rather than smaller, lesions are imaged better. This is due to the fact that if both kinds of lesions have the same radioactive concentration, the smaller one may have too low a total activity.

On the other hand, very large lesions are often altered by necrotic areas and, therefore, only representations of poor quality can be achieved.

The geometrical influence of distance (inverse square law) and tissue absorption considerably reduce the detectability of a deep lesion.

These phenomena are well evidenced in Figure 2, which illustrates the scintigraphic results obtained from the study of 64 melanoma localizations. There are certainly other factors that influence these results, but a great difference is seen among the group of 47 superficial lesions, 79% of which were imaged, and a group of 17 deep lesions. In fact, only 41% of the latter were imaged. As can be seen by this distribution, even very large and superficial

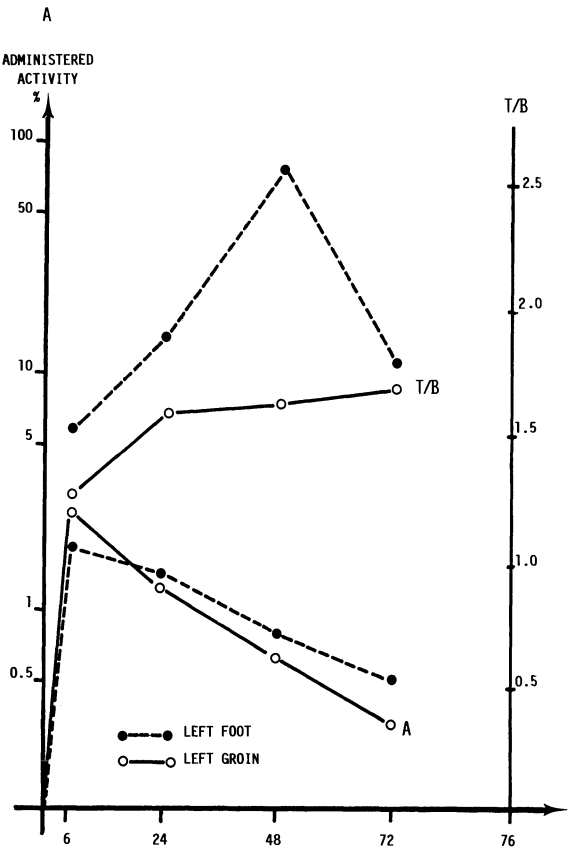

Figure 3. Tumor to background (T/B) ratio variations (top) and effective radioactivity disappearance curves from two different melanoma lesions (A) in the same patient (bottom) after intravenous injection of ^{131}I-F(ab')$_2$ antimelanoma Mab (225.28S).

lesions were not imaged, and this is certainly not due to geometric factors but more probably to anatomic reasons, such as a lack of vascularization or necrosis, which do not allow the antibody to reach the target. Instead, a high incidence of antigen expression was demonstrated in the lesions that had undergone surgical treatment.

If the value of tumor uptake is a determinant factor for immunoscintigraphy, the radioactive distribution in the surrounding tissue is almost as equally important.

As mentioned above, a suitable value of the T/B ratio between tumor and nontumor radioactive concentrations is the condition that permits a scintigraphic representation of the tumor.

Figure 3 shows the radioactivity variations in two different lesions in the same patient. As can be seen, there are no relevant differences between the effective disappearance curves of the radioactivity in the two tumors (A).

However, if we consider the variations in background in the two regions

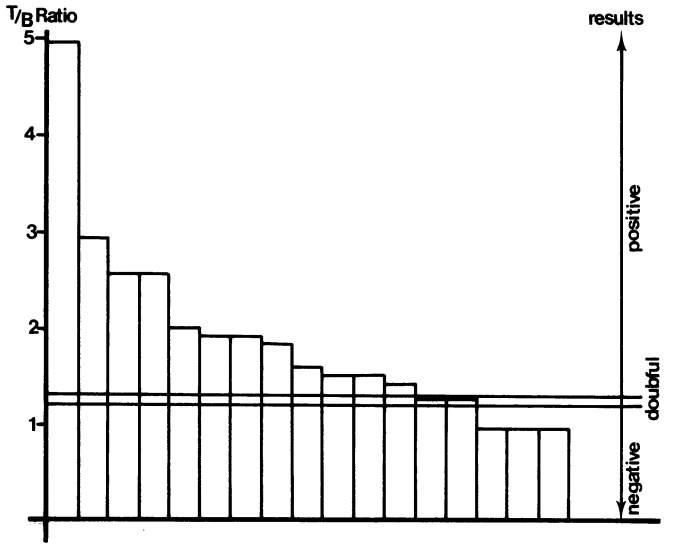

Figure 4. Correlation between immunoscintigraphic results and T/B ratio measured in vivo in 17 patients bearing colorectal tumors of approximately the same size (2–3 cm) injected with the same anti-CEA antibody (F023C5).

(groin and foot) where the tumors are localized, we find an important difference between them, which can be evaluated by the two curves reported on the top (T/B).

Moreover, it is possible to see that the most favorable tumor-to-background ratio does not correspond to the maximum tumor uptake but reaches the maximum values at 48 hours for the foot and at 72 hours for the groin.

The mentioned T/B ratio can be determined in vitro by measuring the radioactivity in tissue samples or in vivo by measuring the content of the regions of interest (ROI) with computerized instruments. It is evident that the two kinds of measurements are not superimposable. The correlation with absolute or relative values of the radioactive concentration in healthy or neoplastic tissues and in biologic fluids is very high when measuring tissue samples. Nevertheless, only a very approximate estimate regarding the scintigraphic results can be obtained with this method.

When the T/B ratio is measured in vivo, even though a number of geometric, physical, and anatomic factors are involved in the evaluation and may result in a higher incidence of errors, the correlation with the quality of the image that can be obtained is very narrow.

Figure 4 demonstrates this behavior. A group of patients bearing colorectal tumors of the same size were examined with the same immunoreagent. The T/B ratio was measured in vivo. In all positive immunoscintigraphies the values of T/B were equal or higher than 1.4. Doubtful results were obtained in two patients where the T/B ratio corresponded to 1.3.

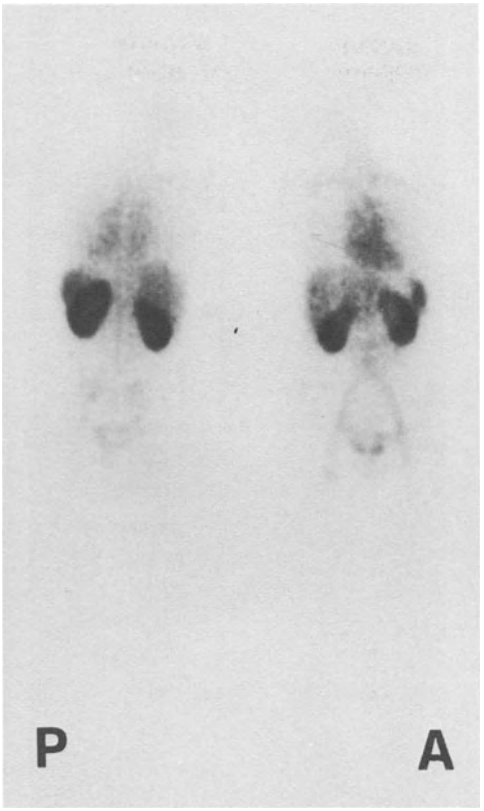

Figure 5. Radioactivity biodistribution 4 hours after injection of technetium-labeled $F(ab')_2$ fragment of 225.28S. Posterior (P) and anterior (A) views. Heart and vessels are still evident; uptake in liver and spleen is increasing. The highest uptake is evident in the kidneys. Arrows show a tumor lesion in the right groin with increasing uptake.

The correlation obtained in vitro, measuring surgical specimens in eight of the same patients, was very low.

As a practical consequence of these observations, it seems possible to conclude that positive immunoscintigraphy can be obtained when the radioactive concentration is almost 1.5–2 times higher in the tumor than in the surrounding tissues and the total activity of the source is high enough to give a signal that is easily detectable by the instrument.

Nevertheless, some other problems should be remembered. First of all, as previously reported, the radioactive concentration in neoplastic and surrounding tissues varies with time, usually in different directions: vascular activity decreases quite quickly during the first few hours, whereas tumor activity increases progressively. The higher the value of the T/B ratio, the better the constrast that can be obtained.

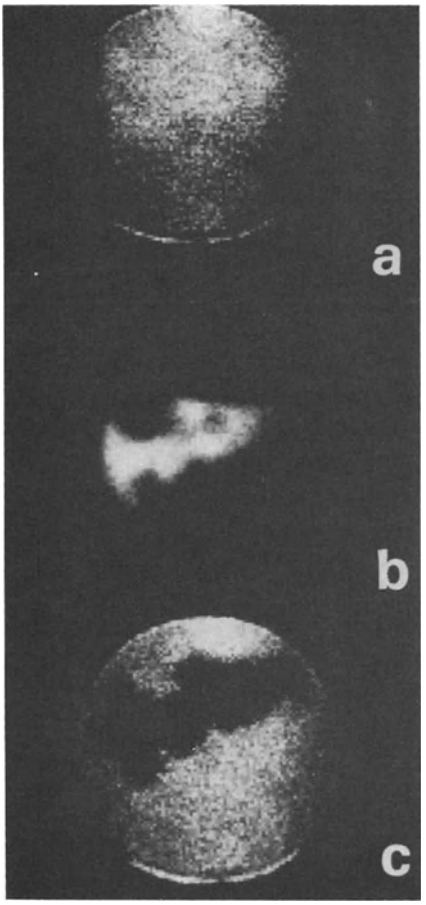

Figure 6. Double-tracer subtraction in liver metastases. A: ^{131}I-anti-CEA liver map; B: ^{99m}Tc sulfur colloid map; C: subtraction map. Liver metastases evident in A are better seen in C. B gives negative images of the localizations.

A high intensity of the signal produced by the source can often result, however, in the same or even better result. This happens, for instance, when short-lived radionuclides are used to label antibodies whose maximum T/B ratio value is reached 3–4 days after injection. In this case, by performing the examination during the first few hours, the favorable effect due to the increment of the signal emitted by the tumor largely exceeds the negative background interference. In fact, the efficacy of a measurement can be evaluated from the ratio S/B between source (tumor = S) and background (B), which clearly indicates the advantage derived from a high tumor radioactive uptake obtained with short-lived radioisotopes relatively soon after injection.

Another important problem concerns the high unspecific radioactive

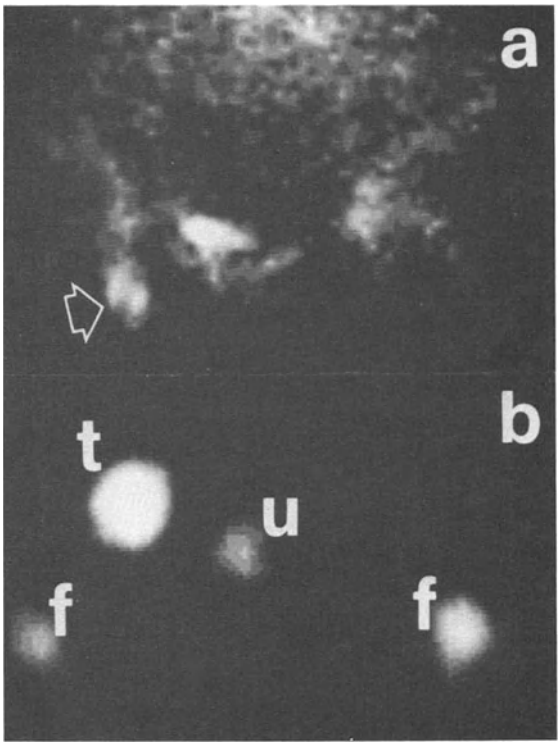

Figure 7. Patient with melanoma localization to the right groin. A: planar map; B: ECT axial reconstruction. The lesion (t) is well isolated for bladder (u) and femural heads (f) without background interference. Immunoscintigraphy performed with ^{123}I-F(ab')$_2$ fragments of 225.28S Mab.

uptake by organs or tissues outside the tumor. This phenomenon could be a great obstacle to detecting tumors localized inside, or very close to, these organs.

Hepatic metastases are a typical example of this situation, since the great majority of antibodies are metabolized in the liver, where high concentrations of activity are reached very soon after administration. Even if a hepatic localization is able to concentrate the immunoreagents, the value of the T/B ratio is very low, often less 1. One of the methods to obtain a visualization of liver metastases in these conditions is the double-tracer subtraction technique. We used a similar technique in the past [16] to better image liver metastases with ^{67}Ga.

De Land et al. [17] elaborated a more extensive technique to be used with radiolabeled antibodies. It is general opinion that these subtraction methods, which can be applied to different organs or regions, can be very helpful if an image of the tumor is evident on the original map. In this case, the subtraction has the aim of representing more clearly the neoplastic area. Its

Figure 8. Primary carcinoma of the transversal colon visualized 72 hours after injection of ^{123}I-F(ab')$_2$ of F023C5 Mab.

limits, as reported [18], consist of the possible creation of artifacts, which can be a dangerous source of errors if the original map does not show enough factors for diagnosis.

In such cases, emission computerized tomography (SPECT) is a more appropriate technique, especially if the antibodies used are labeled with isotopes (^{99m}Tc, ^{123}I, etc.) with emitting energies that are more favorable for conventional tomographic cameras [19,20].

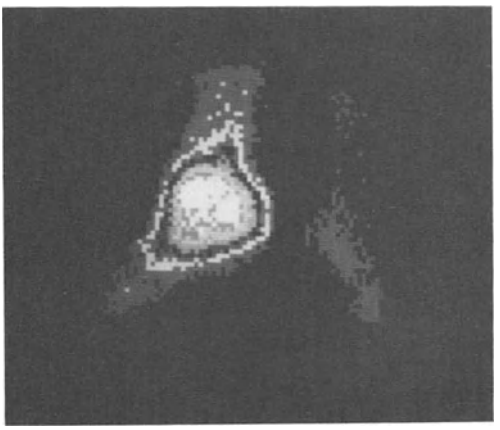

Figure 9. Melanoma metastasis on the right foot. Radioimmunodetection with ^{111}In-F(ab')$_2$ of 225.28S Mab.

Other methods to eliminate background interference have been studied by Granowska et al. [21] and Masi et al. [22]. These methods are based on the fact that when the radioactivity disappears from the blood pool it increases in the tumor. Sequential mapping and differential kinds of elaborations proposed by different researchers have enabled us to obtain an important improvement in the results.

Finally, one of the approaches to lessen background activity has been to use a liposomally entrapped antibody to clear non-tumor-bound antitumor antibodies. Large amounts of immunoglobulins were needed to apply this technique, which is probably why this method, even if the results obtained seem to be very interesting, has thus far received limited application [23].

However, in the great majority of applications, the problem of background reduction does not seem to prevent the possibility of obtaining good, and often excellent, tumor images when monoclonal antibodies, and especially their $F(ab')_2$ or Fab fragments, are used.

Nevertheless, this problem remains the most important one to be solved to further improve the quality of tumor imaging.

At the present time SPECT represents the easiest and most reliable method to analyze uncertain aspects of planar scintigraphy, obtain complementary information, and obtain better results.

It should be stressed, however, that if both the antigen-antibody system and the technical approach fulfil the reported requirements, the quality of tumor images achieved with immunoscintigraphy may be as good as those obtained with current scintigraphic methods.

Diagnostic efficacy of radioimmunodetection methods

Several methods have been proposed and utilized up to now for RAID of cancer. Different antigen-antibodies systems have been utilized to image different tumors. Moreover, the approaches have also been quite different.

It seems, therefore, impossible to discuss the diagnostic efficaey of RAID from a general point of view without taking into account all these situations.

On the contrary, it obviously seems more appropriate to evaluate separately the results obtained with different antigen-antibody systems and with the immunoreagents prepared with a given antibody.

Considerable attention will be given here to the data and results obtained from the personal experience of the author, and they will be reported as an example of what is likely to be obtained with other systems and methods.

The diagnostic efficacy of a RAID technique can be evaluated in two different ways. The first is through the study of a series of patients with well-known tumor localizations (retrospective study). The second is the study of a series of patients with suspected tumors without knowing either the real existence of a neoplastic localization or its eventual localization (prospective study).

Both approaches are, in my opinion, necessary for a correct evaluation of a RAID technique. The first one can give us a large amount of information about the rate of positivity — false-positive and -negative results. If this approach is followed by the examination of surgical samples of the tumor, radioactive measurements and immunohistochemical techniques can reveal further elements of evaluation. It is possible, for instance, to quantify the tumor uptake of the radiolabeled antibody, to evaluate the T/B ratio in vitro, and to compare the RAID results with the rate of antigen expression in the cancer tissue. Theoretically, the rate of the expression of the involved antigen in the neoplastic tissue, as evaluated in the preliminary histochemical studies, should correspond to the positivity rate found in vivo with RAID.

In reality, the interference of several factors, some of which were discussed in the previous paragraph, result in the loss of positive results in this latter condition.

A retrospective study can clarify many of these situations, even if it is difficult, for example, to evaluate the interference of some immunologic or biologic factors, such as the antigen's modulation and the lack of vascularization with or without necrosis in neoplastic lesions.

Systematic studies were performed by us with two monoclonal antibodies, the first of which is 225.28S, an IgG_{2a}, against a high molecular weight, melanoma-associated antigen isolated by Natali and Ferrone [24], extensively studied in a pilot trial [4,5,25,26], and subsequently studied in a multicenter, prospective trial [27,28].

The second antibody is FO23C5, an IgG_1 against CEA that was isolated by Sorin Biomedica and is now being studied with the same protocol, namely, in pilot [29–31], multicenter prospective trials.

Table 2 shows the positivity rate of RAID of melanoma localizations. On the left, the preliminary pilot study shows that by using different radiolabels, the sensitivity increased from iodine (56.5), to indium (76.7), to technetium (85.7), and the mean sensitivity was 73%. In subsequent experimentation performed by a multicenter collaboration, iodine compounds were left out both in whole IgG and ^{131}I-F(ab′)$_2$ due to the poor results obtained and in the case of ^{123}I-F(ab′)$_2$, due to the lack of availability of this compound in our country.

Table 2. Incidence of positivity obtained with radioimmunodetection of melanoma lesions using different radionuclides

Radionuclide	Pilot Study (Positive/Total)	%	Multicenter Study (Positive/Total)	%
Iodine[a]	12/23	56.5	—	—
^{111}In	23/30	76.7	94/159	59.0
^{99m}Tc	18/21	85.7	283/380	74.0
Total	54/74	73.0	377/539	70.0

[a] ^{131}I-Mab, F(ab′)$_2$; ^{123}I-F(ab′)$_2$.

The overall results obtained were similar to those of the first study: a mean sensitivity of 70%. Even if in both cases the sensitivity was higher for technetium than for indium, the positivity rate was lower in the multicenter trial for both radiocompounds.

No false-positive results were observed in the pilot study and only four were observed in the multicenter trial.

Therefore, we could speak of a specificity of nearly 100%. According to current concepts, specificity is defined as the rate of true negative results obtained by examining a healthy population.

Nevertheless, to evaluate RAID's performance it would be interesting to modify the concept of 'healthy patient' to that of 'patient free of cancer.'

In this case, our sample of population 'free of cancer' to be examined should be extended to a large number of non-neoplastic diseases and should give a real evaluation of the 'specificity' of our examinations.

To my knowledge this kind of evaluation has not been systematically performed until now due to the different systems utilized. This is comprehensible if we think that only extensive applications of RAID in cancer patients during the last few years have confirmed the lack of risk due to these techniques. At the moment, we can say that, in our experience, as in a great number of examinations performed by others [32–36], false-negative results are very few. This also happened in the series of patients with colorectal carcinoma examined with the antibody reported and also with other antibodies used by our group in different trials, such as B 72.3, OC 125, UJ13A, and others now under study.

It is important to stress that RAID often permits, even in retrospective studies, the imaging of occult lesions.

For instance, in the reported multicenter study on melanoma, out of 377 radioimaged localizations, 101 were occult lesions and the melanotic origin was only confirmed successfully.

In the study of colorectal carcinoma, performed as a pilot study by our group, 51 patients with 64 localizations were examined using three different immunoreagents (Table 3). No remarkable differences in the positivity obtained are evident among $F(ab')_2$ fragments labeled both with ^{131}I (68%) or ^{111}In (64%). On the contrary, the use of monovalent fragments was less favorable (56%).

Table 3. Positive results of colorectal immunoscintigraphy obtained with F023C5 in 51 patients with 64 localizations

Immunoreagent	Primary Tumor	Local Relapses	Liver	Lymph Nodes	Total	
$F(ab')_2$-^{131}I	3/7	15/16	2/8	3/3	23/34	68%
$F(ab')_2$-^{111}In	6/6	1/2	2/6	—	9/14	64%
Fab-^{131}I	7/12	2/2	0/2	—	9/16	56%
Total	16/25	18/20	4/16	3/3	41/64	64%
	64%	90%	25%			

Table 4. Tumor/background ratios obtained with Mab F023C5 fragments

$F(ab')_2$			Fab		
$\bar{x}$	Range	Time (hr)	$\bar{x}$	Range	Time (hr)
2.4	1.5–3.2	48–96	1.5	1.3–1.9	4–24

Moreover, as shown in Table 4, the imaging conditions obtained with $F(ab')_2$ and with Fab fragments, respectively, are quite different.

The first shows, in fact, a higher maximum value of the T/B ratio, which is correlated with the higher quality of imaging obtained, in spite of the more favorable biodistribution achieved with the monovalent fragments. Moreover, the behavior of the tumor uptake of Fab fragments is also more rapid though less persistent.

From a clinical point of view, we can see from Table 3 that a very high positivity rate was achieved for tumor relapses and lymph nodes, whereas primary tumors showed a poorer imaging rate. Very poor results were obtained from the examination of hepatic metastases. Even with this antibody, no false-positive results were noticed.

Different results obtained by examining tumors localized in different organs can also be observed with other antigen-antibody systems. Figure 10 reports, for example, the different positivity rates obtained in the multicenter trial for different tumors sites using the anti-melanoma antibody, as previously reported. It is worth stressing that the low positive rate obtained here for liver metastases is in agreement with what was discussed earlier in this chapter.

The poor results obtained for lung and skin localizations are probably due to the lack of vascularization of these tumors, thus making it difficult for the antibody to reach its target. As for skin lesions, the use of ^{99m}Tc-$F(ab')_2$ allowed us to achieve better results (70%).

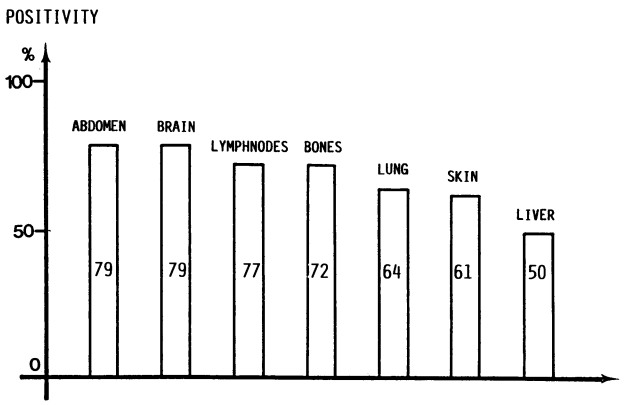

Figure 10. CNR multicenter trial on melanoma. Different positivities obtained by examining 539 lesions localized in different organs.

The examples of the retrospective study reported indicate the possibility of revealing some diagnostically relevant characteristics of the immune system used, such as, sensitivity, which can reach very high values in many cases, and specificity, which in our series was nearly 100%.

Nevertheless, the collection of these and other data reported do not allow a complete evaluation of the diagnostic efficacy. Prospective studies may fulfil this evaluation.

This kind of study has, in fact, the aim of testing the method in a realistic condition, i.e., in the same way as an examination performed on a patient for diagnostic purposes.

Some prospective studies are now in progress in our institute to evaluate the possible diagnostic role of RAID in colorectal carcinoma, ovarian cancer, and melanoma.

The prospective trial on melanoma [28] has now been concluded. The aim of this study was to evaluate the clinical utility of RAID in patients with early-stage melanoma, as a support to clinical findings. Patients bearing primary melanoma of the trunk and arm with axillary or cervical lymph-node enlargement, or who had undergone surgery for this disease, were examined without any previous information after clinical evaluation.

A very simple technique was used. About 700 MBq of ^{99m}Tc-F(ab')$_2$ was injected intravenously, thus allowing us to obtain results that were easier to interprete than those obtainable by intralymphatic injection. Six to 10 hours later, regional and whole-body scintigraphic maps were made. Fifty-four patients with 65 clinically suspect or doubtful lymph-node enlargements were examined.

A sensitivity of 76% and a specificity of nearly 100% were obtained, with an accuracy of 86%. The predictive value was approximately 100% for the positive test and about 75% for the negative test. In comparison, the predictive values for clinical evaluation were 86% for the positive and 84% for the negative test. This indicates that a scintigraphic positivity corresponds, as a rule, to a tumor lymphatic invasion.

Similar results are expected to be obtained from the other abovementioned prospective studies on relapses of reported carcinomas; in these cases, comparisons are made with other diagnostic methods, such as CT, NMR, US, and laparoscopy.

These trials are certainly the best way to complete the study of the diagnostic efficacy of a new antibody, provided that, as we have stated, all the preliminary elements of evaluation of the immune system and antibody preparation and labeling are adequately considered. This method has, in fact, been studied by several researchers [32–36].

Patient safety

Patient safety, in view of the wide clinical use of radioimmunodetection, is a very important aspect to be considered. Fortunately, the results obtained by

different research groups allow one to consider this problem with much less concern.

The use of highly purified monoclonal antibodies or their fragments reduces the risk of allergic reactions. From the data reported in the literature, no adverse reactions have been noted following the first injections of anti-tumor monoclonal antibodies. An important consideration for the clinical use of monoclonal antibodies of murine origin is the possible, immunologic cross-reactivity, other than that desired, of the antibody with human tissue antigens. Such cross-reactions must be avoided because of the possible undesirable damage to healthy tissue or cells, and especially, to blood cells. Every new antibody, therefore, needs to go through appropriate preliminary immunohistochemical screening on human tissues to evaluate the specificity of the reagents.

Monoclonal antibodies must be pure and free from adventitious agents such as microbial contaminations (viral, bacterial, mycotic, or mycoplasmal) and potentially oncogenic macromolecules (nucleic acid chains, DNA fragments). On the other hand, it is well known that gel chromatography and immunoaffinity chromatography can separate substances of different molecular weights; thus, high molecular weight molecules, like viruses, are removed during the purification steps of IgG and the $F(ab')_2$ fragment preparation process. Appropriate tests to demonstrate the absence of viruses and murine polynucleotides are also advisable in order to minimize the potential risk of such contaminations. It should also be considered that allergic reactions may occur as a result of the administration of any foreign protein.

Appropriate precautions must be taken to prevent and treat possible reactions, especially for repeated administration of monoclonal antibodies, which may induce anti-murine antibody production. In our clinical trials, we took the precaution of excluding from the studies patients with an allergic history. However, because this is not an absolute limitation, particular care must be taken in patients affected by allergic diseases before the administration of the radiolabeled monoclonal antibodies.

Among the requirements for the use of radioimmunodetection in clinical practice, special consideration must be given to dosimetric evaluation. In our experience with the radioimmunodetection of melanoma, we calculated the dosimetry for the organs most involved. The results of these evaluations were obtained according to the suggestions of the Medical International Radiation Dose Committee.

We found a great difference (Table 5) between whole immunoglobulins and $F(ab')_2$ fragments, both labeled with ^{131}I. In fact, the longer biologic half-life and the higher uptake in the reticoloendothelial system resulted in the worst dosimetric conditions due to the injection of the whole immunoglobulin.

Among the $F(ab')_2$ fragments (Table 6), compounds labeled with ^{99m}Tc offer the most favorable conditions, followed by ^{123}I and ^{111}In. Distribution of a significant dose to the liver and spleen results from the ^{111}In compound. These data can be taken as an example of the levels of radiation produced by

Table 5. Comparative dosimetric evaluation between whole IgG and bivalent fragment of anti-melanoma Mab 225.28S labeled with ^{131}I (μGy/MBq)

Organ	^{131}I-Mab	^{131}I-F(ab')$_2$
Whole body	189.000	108.000
Bone marrow	207.900	86.400
Kidneys	2103.300	448.200
Spleen	6750.000	2702.700
Liver	545.400	388.800
Ovary	5.400	0.810
Testicle	0.540	0.081

Table 6. Comparative dosimetric evaluation between bivalent fragments of antimelanoma Mab labeled with different radionuclides (μGy/MBq)

Organ	^{131}I-F(ab')$_2$	^{123}I-F(ab')$_2$	^{99m}Tc-F(ab')$_2$	^{111}In-F(ab')$_2$
Whole body	108.000	8.100	1.180	99.900
Bone marrow	86.400	37.800	0.963	72.900
Kidneys	448.200	8.100	32.200	132.300
Spleen	2702.700	162.000	11.000	661.500
Liver	388.800	232.200	2.250	310.500
Ovary	0.810	0.540	0.	0.540
Testicle	0.081	0.003	0.963	0.810

the different kinds of radioistotopes. This risk is, however, of the same order of magnitude as other currently used nuclear medicine examinations.

In conclusion, regarding patient safety, there appears to be no reason why immunoscintigraphic methods should be considered more dangerous than any other examination technique requiring the administration of a radiopharmaceutical, provided that the abovementioned precautions are used.

Supply of radioimmunoreagents

The possibility of having at one's disposal the supply of radioimmunoreagent required to perform a RAID technique is an essential condition for a wide use of these methods in clinical practice. Moreover, in order to guarantee the expected results of the method employed, the technical characteristics of the reagent must always be the same.

It is also difficult, or almost impossible, for a nuclear medicine department to carry out all the quality controls needed before a radiopharmaceutical can be used for clinical purposes, including the specific precautions required for an immunologic product of murine origin, as previously discussed. Thus, the only way to have a ready supply of the reagent required for a clinical application of RAID is through industrial production. For example, strict collab-

oration with the Sorin-Biomedica (Saluggia-Italy) research group allowed us to perform pilot studies with different antibodies and, thereafter, in the cases of anti-melanoma and anti-CEA Mabs, the radiolabeled reagents were routinely prepared in the radiopharmaceutical company's manufacturing facilities and distributed to different nuclear medicine centers. In this way, it was possible to carry out multicenter studies on the clinical efficacy of these methods with the same products.

Similar approaches were followed by other groups, and the possibility of having a readily available supply of reagents for RAID will certainly aid in the rapid development of these methods and permit determining more precise indications for their clinical use.

Diagnostic usefulness of radioimmunodetection

The high diagnostic efficacy of the large number of RAID methods described above encourages us to direct every effort towards verifying their clinical usefulness. Different diagnostic methods are, at present, available in clinical oncology. Nevertheless, there are situations in which new approaches could be useful, and certainly RAID, like other nuclear medicine techniques, has the advantage of simplicity.

A real step forward would be made if it could be demonstrated that immunoscintigraphic methods have the capability to improve the detection of cancer in its very early stages. Unfortunately, at the moment, the probability of obtaining relevant contributions to the diagnosis of early disease seems to be low with the available antigen-antibody systems using either serologic or scintigraphic techniques. Nevertheless, if early diagnosis of cancer is not possible with these techniques, immunoscintigraphy can be very helpful in the early detection of relapse in cancer progression.

Many clinical trials are in progress at present, and in a few years we will certainly obtain more complete knowledge of the diagnostic impact of RAID in clinical oncology. However, at the moment, some evaluations are possible if we consider the large number of examples of useful diagnostic applications in different oncologic situations. We will report here some of these examples.

Immunoscintigraphic sequential images of a patient examined for suspect relapse of an ovarian cancer are shown in Figure 11. The patient had undergone surgery 6 months earlier for a bilateral primary adenocarcinoma. During the follow-up, progressive elevation of the serum marker (Ca-125) was observed. A laparoscopy revealed nodular lesions localized in the right subdiaphragmatic region. Immunoscintigraphy with ^{131}I-OC 125 confirmed a pathologic uptake in the subdiaphragmatic right region and also an unsuspected uptake in the central iliac region. A second surgical look confirmed the presence of two localizations of recurrent tumors. The first was in the peritoneum wall, revealed by laparoscopy, and the second was in the retro-

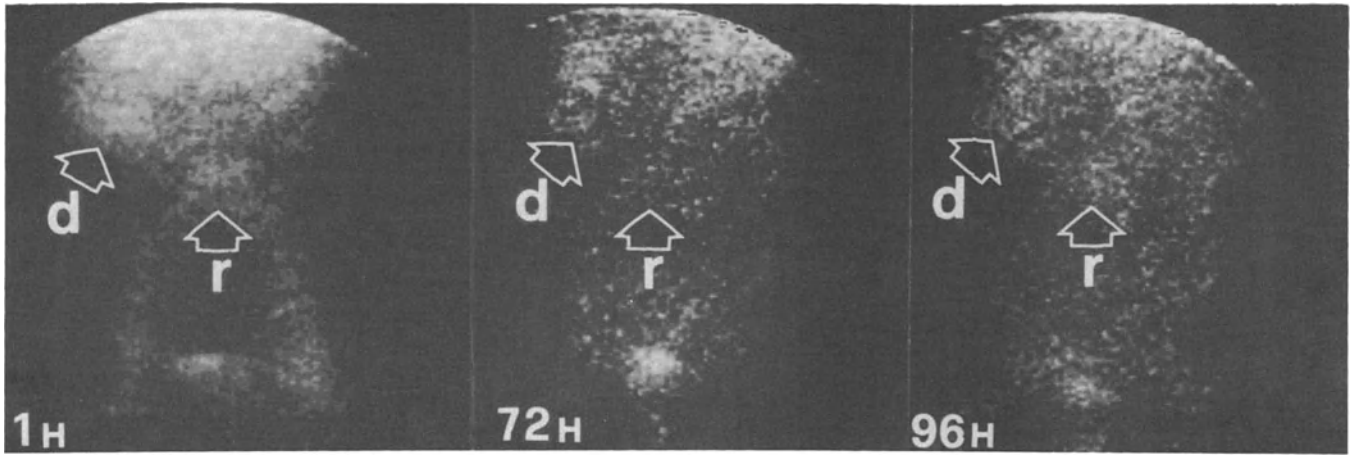

Figure 11. Patient with abdominal recurrencies of an ovarian cancer. Laparoscopy was able to evidentiate the lesions on the right subdiaphragmatic area (3) but not those in the iliac retroperitoneal area, evident in the central region of the scan (r).

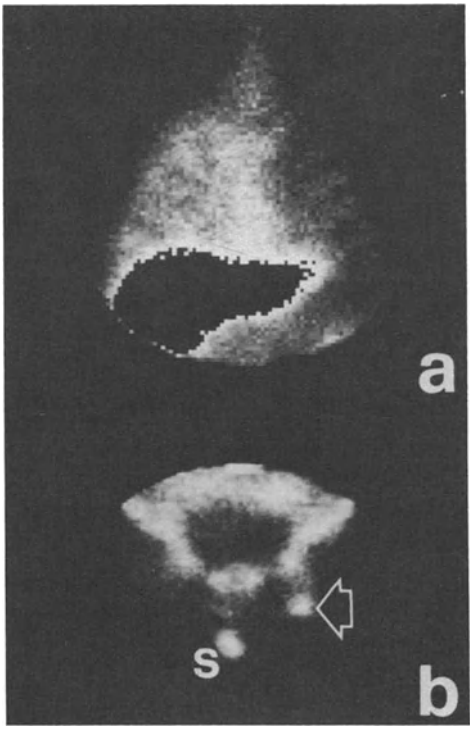

Figure 12. Patient with a melanoma localization (arrow) to the right groin (b) and pleural effusion of unknown origin. Radioimmunodetection confirms the metastatic origin of the pleural lesions (A). s = scrotum.

peritoneal space, due to iliac lymphatic chain invasion, which was not revealed by laparoscopy.

Another patient underwent surgery for a melanoma to the left leg. After 1 year, a lymphatic enlargement of the left groin lymph nodes and right pleural effusion were evident. Even if these data are oriented towards a relapse, very easy verification was obtained with immunoscintigraphy, which showed a high uptake in the groin and in the right thorax (Figure 12).

Figure 13 reports the case of a patient who underwent surgery 2 years earlier for a melanoma of the back. On clinical examination, the patient complained of abdominal pain, and a pelvic mass was revealed by gynecologic examination and by CT scans. An ovarian cancer was suspected. Nevertheless, the correct diagnosis was reached after immunoscintigraphy with anti-melanoma antibody labeled with technetium showed high uptake by the mass.

Figure 14 reports an example of scintigraphic confirmation of a clinically suspected left axillary lymphatic metastasis. A primary melanoma had been

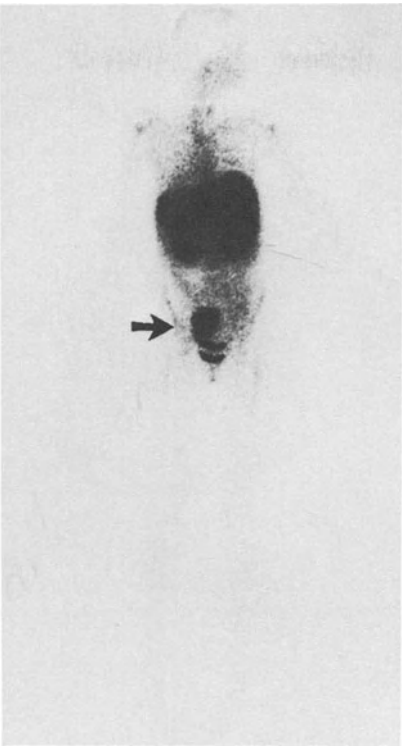

Figure 13. Left pelvic mass of doubtful nature in a patient previously operated on for a melanoma of the back. Immunoscintigraphy allows the correct diagnosis.

removed 9 months before from the left arm. The map was taken 6 hours after intravenous injection of the immunoreagent and shows a high concentration of radioactivity in the suspected lymph nodes. Surgery subsequently confirmed the diagnosis.

In other patients, radioimmunodetection was performed, as a first examination during follow-up, when high levels of circulating tumor markers were revealed. We use this approach in patients operated on for ovarian or colorectal cancer, using the appropriate antibodies, namely OC 125, B 72.3, or MOV 18 for ovarian cancer and FO23C5 and B 72.3 for colorectal carcinoma. Positive images of tumor recurrencies have often been obtained when other imaging methods were negative. An example is shown in Figure 15, which shows the scintigraphic results of a local recurrency of a rectal carcinoma that had been removed 14 months earlier. An increasing level of circulating CEA was noticed during the follow-up. The pictures show very clearly a pathologic uptake, whereas CT was doubtful and US negative.

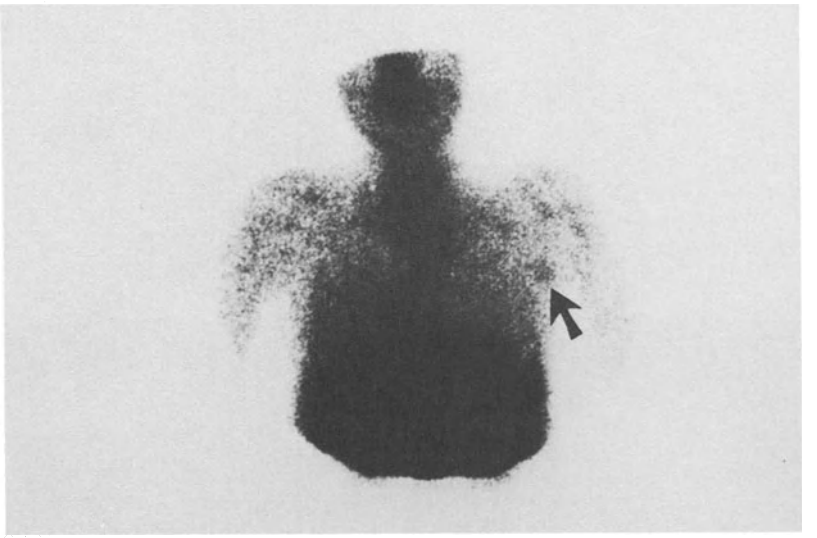

Figure 14. Radioimmunodetection with intravenous injection of ^{99m}Tc-F(ab')$_2$ in a patient operated on 2 years earlier for a primary melanoma. Left axillary invasion with a doubtful clinical finding.

Systematic comparative studies of the diagnostic efficacy of different imaging methods are now in progress. A provisional evaluation of the possible clinical applications of immunoscintigraphy, based on the state of the art to my knowledge and on our personal experience, is summarized as follows.

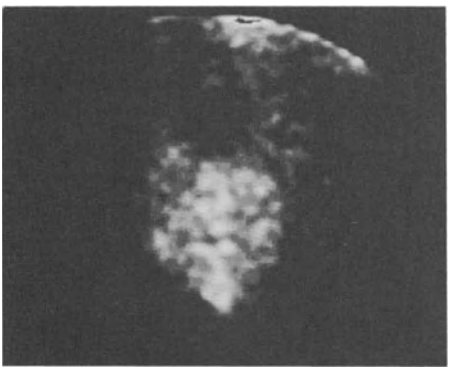

Figure 15. Immunoscintigraphy with ^{131}I-F(ab')$_2$ anti-CEA F023C5 Mab in a patient operated on 7 years earlier for a rectal carcinoma. Circulating CEA levels were increased. A local recurrency is indicated by scintigraphy, whereas ultrasonography was negative and the CT scan was doubtful.

Immunoscintigraphy helps in

- the evaluation of regional or metastatic invasion of a primary tumor
- early detection of tumor relapses and metastatic spread during follow-up
- differentiation between benign and malignant lesions
- detection of new, unsuspected lesions in advanced disease

Other clinical applications are also possible. Two that will certainly be used in the near future are the evaluation of therapy results and the evaluation of tumor uptake and biodistribution of antibodies to be used for immunotherapy [3,37,38].

Acknowledgments

These studies were partially supported by C.N.R. Special Projects on Oncology and on Biomedical and Clinical Engineering.

References

1. Goldenberg, D.M., De Land, F., Kim, E., Bennet, S., Primus, F.J., Van Nagell, J.R., Estes, N., De Simone, P., and Rayburn, P. (1978) Use of radiolabeled antibodies to carcinoembryonic antigen for the detection and localization of diverse cancers by external photoscanning. N. Engl. J. Med. 298:1384–1386.
2. Buraggi, G.L. (1985) Radioimmunodetection of cancer. J. Nucl. Med. Allied Sci. 29: 261–267.
3. Larson, S.M., Carrasquillo, J.A., and Reynolds, J.C. (1984) Radioimmunodetection and radioimmunotherapy. Cancer Invest. 2:363–381.
4. Buraggi, G.L., Callegaro, L., Turrin, A., Cascinelli, N., Attili, A., Emanuelli, H., Gasparini, M., Deleide, G., Plassio, G., Dovis, M., Mariani, G., Natali, P.G., Scassellati, G.A., Rosa, U., and Ferrone, S. (1984) Immunoscintigraphy with ^{123}I, ^{99m}Tc and ^{111}In-labeled $F(ab')_2$ fragments of monoclonal antibodies to a human high molecular weight-melanoma associated antigen. J. Nucl. Med. Allied Sci. 28:283–295.
5. Buraggi, G.L., Callegaro, L., Mariani, G., Turrin, A., Cascinelli, N., Attili, A., Bombardieri, E., Terno, G., Plassio, G., Dovis, M., Mazzucca, N., Natali, P.G., Scassellati, G.A., Rosa, U., and Ferrone, S. (1985) Imaging with ^{131}I-labeled monoclonal antibodies to a high molecular-weight melanoma-associated antigen in patients with melanoma: Efficacy of whole immunoglobulin and its $F(ab')_2$ fragments. Cancer Res. 45:3378–3387.
6. De Land, F., Kim, E., and Goldenberg, D.M. (1982) Radioimmunodetection of cancer by in vivo imaging. In: Burchiel, S.W., Rhodes, B.A., and Friedman, B.E. (eds.), *Tumor Imaging*. Masson, pp. 179–188.
7. Baldwin, R.W., and Pimm, M.V. (1983) Antitumor monoclonal antibodies for radioimmunodetection of tumors and drug targeting. Cancer Metastasis Rev. 2:89–106.
8. Bradwell, A.R., Fairweather, D.S., and Dykes, P.W. (1984) Localization of tumours using radiolabeled antibodies. Med. Lab. Sci. 41:267–278.
9. Larson, S.M. (1985) Radiolabeled monoclonal anti-tumor antibodies in diagnosis and therapy. J. Nucl. Med. 26:538–545.
10. Keenan, A.M., Harbert, J.C., and Larson, S.M. (1985) Monoclonal antibodies in nuclear medicine. J. Nucl. Med. 26:531–537.
11. Bradwell, A.R., Fairweather, D.S., Dykes, P.W., Keeling, A., Vaughan, A., and Taylor, J. (1985) Limiting factors in the localization of tumours with radiolabeled antibodies. Immunol. Today 6:163–170.

12. Primus, F.J., De Land, F.H., and Goldenberg, D.M. (1984) Monoclonal antibodies for radioimmunodetection of cancer. In: Wright, G.L. (ed.), *Monoclonal Antibodies and Cancer*. New York: Marcel Dekker, pp. 305–323.
13. O'Grady, L.F., De Nardo, G., and De Nardo, S. (1986) Radiolabeled monoclonal antibodies for the detection of cancer. Ann. J. Physiol. Imaging 1:44–53.
14. Colcher, D., Zalutsky, M., Kaplan, W., Kufe, D., Austin, F., and Schlom, J. (1983) Radiolocalization of human mammary tumors in athymic mice by a monoclonal antibody. Cancer Res. 43:736–742.
15. Mach, J.P., Chatal, J.F., Lumbroso, J.D., Buchegger, F., Forni, M., Steplewsky, Z., and Koprowski, H. (1983) Tumor localization in patients by radiolabeled monoclonal antibodies against colon carcinoma. Cancer Res. 43:5593–5600.
16. Buraggi, G.L., Laurini, R., Rodari, A., and Bombardieri, E. (1976) Double-tracer scintigraphy with ^{67}Ga-citrate and ^{99m}Tc-sulfur colloid in the diagnosis of hepatic tumors. J. Nucl. Med. 17:369–373.
17. De Land, F.H., Kim, E.E., Simmons, G., and Goldenberg, D.M. (1980) Imaging approach in radioimmunodetection. Cancer Res. 40:3046–3049.
18. Ott, R.J., Grey, L.J., Zivanovic, M.A., Flower, M.A., Trott, N.G., Moshakis, V., Coombes, R.C., Neville, A.M., Ormerod, M.G., Westwood, J.H., and McCready, V.R. (1983) The limitations of the dual radionuclide subtraction technique for the external detection of tumours by radioiodine-labeled antibodies. Br. J. Radiol. 56:101–108.
19. Delaloye, B., Bischof-Delaloye, A., Buchegger, F., von Fliedner, V., Grob, J.P., Volant, J.C., Pettavel, J., and Mach, J.P. (1986) Detection of colorectal carcinoma by emission-computerized tomography after injection of ^{123}I-labeled Fab or F(ab')$_2$ fragments from monoclonal anti-carcinoembryonic antigen antibodies. J. Clin. Invest. 77:301–311.
20. Perkins, A.C., Armitage, N.C., Harrison, R.C., Riley, A.L.M., Wastie, M.L., and Hardcastle, J.D. (1986) Planar and spect imaging of colon cancer using ^{111}In anti-CEA monoclonal antibody (C46). In: Schmidt, H.A.E., Ell, P.J., and Britton, K.E. (eds.), *Nuklearmedizin*. F.K. Schattauer Verlag, pp. 427–429.
21. Granowska, M., Pring, D.W., Nimmon, C.C., Shepherd, J., Ward, B., Singh, P., Mather, S., Bomanji, J., Slevin, M.L., and Britton, K.E. (1986) Kinetic analysis of radioimmunoscintigraphy, RIS, using probability mapping: Comparison with multiple biopsy findings in ovarian cancer. In: Schmidt, H.A.E., Ell, P.J., and Britton, K.E. (eds.), *Nuklearmedizin*. F.K. Schattauer Verlag, pp. 415–417.
22. Masi, R., Pesciullesi, E., Ferri, P., Voegelin, M.R., Paladini, S., Valecchi, C., and Giannotti, B. (1985) Immunodetection of human melanoma metastases by means of F(ab')$_2$ fragments of monoclonal antibodies: The usefulness of digital images. In: Donato, L., and Britton, K.E. (eds.), *Immunoscintigraphy*. Gordon and Breach Science, pp. 267–277.
23. Begent, R.H.J., Keep, P.A., Green, A.J., Searle, F., Bagshawe, K.D., Jewkes, R.F., Jones, B.E., Barratt, G.M., and Ryman, B.E. (1982) Liposomally entrapped antibody improves tumor imaging with radiolabeled (first) antitumor antibody. Lancet 22:739–742.
24. Natali, P.G., Imai, K., Wilson, B.S., Bigotti, A., Cavaliere, R., Pellegrino, M.A., and Ferrone, S. (1981) Structural properties and tissue distribution of the antigen recognized by the monoclonal antibody 635.40S to human melanoma cells. J. Natl. Cancer Inst. 67: 591–601.
25. Buraggi, G.L., Turrin, A., Cascinelli, N., Attili, A., Terno, G., Bombardieri, E., Gasparini, M., and Seregni, E. (1985) Immunoscintigraphy with antimelanoma monoclonal antibodies. In: Donato, L., and Britton, K.E. (eds.), *Immunoscintigraphy*. Gordon and Breach Science, pp. 215–245.
26. Buraggi, G.L., Callegaro, L., Cascinelli, N., Ferrone, S., Turrin, A., Attili, A., Bombardieri, E., Gasparini, M., Deleide, G., Scassellati, G.A., and Seregni, E. (1986) Radioimmunodetection of malignant melanoma with radiolabeled (^{131}I, ^{123}I, ^{111}In, ^{99m}Tc) monoclonal antibodies and F(ab')$_2$ fragments. In: Winkler, C. (ed.), *Nuclear Medicine in Clinical Oncology*. Springer-Verlag, pp. 207–214.
27. Siccardi, A.G., Buraggi, G.L., Callegaro, L., Mariani, G., Natali, P.G., Abbati, A.,

Bestagno, M., Caputo, V., Mansi, L., Masi, R., Paganelli, G., Riva, P., Salvatore, M., Sanguineti, M., Troncone, L., Turco, G.L., Scassellati, G.A., and Ferrone, S. (1986) Multicenter study of immunoscintigraphy with radiolabeled monoclonal antibodies in patients with melanoma. Cancer Res. 46:4817–4822.

28. Buraggi, G.L., Turrin, A., Cascinelli, N., Attili, A., Gasparini, M., Callegaro, L., Ferrone, S., Seregni, E., Bombardieri, E., and Belli, F. (1986) Radioimmunodetection of melanoma: Preliminary results of a prospective study. Int. J. Biol. Markers 1:47–54.
29. Buraggi, G.L., Callegaro, L., Turrin, A., Gennari, L., Bombardieri, E., Gasparini, M., Mariani, G., Doci, R., Regalia, E., and Seregni, E. (1984) Immunoscintigraphy of colorectal carcinoma: Remarks about an ongoing clinical trial. In: Schmidt, H.A.E., and Vauramo, D.E. (eds.), *Nuklearmedizin*. F.K. Schattauer Verlag, pp. 629–632.
30. Buraggi, G.L., Callegaro, L., Turrin, A., Bombardieri, E., Gennari, L., Regalia, E., Doci, R., Gasparini, M., and Seregni, E. (1986) Radioimmunodetection of colo-rectal carcinoma with an anti-CEA antibody. In: Schmidt, H.A.E., Ell, P.J., Britton, K.E. (eds.), *Nuklearmedizin*. F.K. Schattauer Verlag, pp. 430–432.
31. Buraggi, G.L., Turrin, A., Bombardieri, E., Deleide, G., Gasparini, M., Regalia, E., Scassellati, G.A., Callegaro, L., Gennari, E., Mariani, G., Dovis, M., Doci, R., and Seregni, E. (1987) Immunoscintigraphy of colorectal carcinoma with $F(ab')_2$ fragments of anti-CEA monoclonal antibody. Cancer Det. Prev. 10:335–345.
32. Moldofsky, P.J., Powe, J., Mulhern, C.B., Hammond, N., Sears, H.F., Gatenby, R.A., Steplewski, Z., and Koprowski, H. (1983) Metastatic colon carcinoma detected with radiolabeled $F(ab')_2$ monoclonal antibody fragments. Radiology 149:549–555.
33. Smedley, H.M., Finan, P., Lennox, E.S., Ritson, A., Takei, F., Wraight, P., Sikora, K. (1983) Localization of metastatic carcinoma by a radiolabeled monoclonal antibody. Br. J. Cancer 47:253–259.
34. Armitage, N.C., Perkins, A.C., Pimm, M.V., Wastie, M.L., Baldwin, and Hardcastle, J.D. (1985) Imaging of primary and metastatic colorectal cancer using an ^{111}In-labeled antitumor monoclonal antibody (791T/36). Nucl. Med. Comm. 6:623–631.
35. Murray, J.L., Rosenblum, M.G., Sobol, R.E., Bartholomew, R.M., Plager, C.E., Haynie, T.P., Jahns, M.F., Gleen, H.J., Lamki, L., Benjamin, R.S., Papadopulus, N., Boddie, A.W., Frincke, J.M., David, G.S., Carlo, D.J., and Hersh, E.M. (1985) Radioimmunoimaging in malignant melanoma with ^{111}In-labeled monoclonal antibody 96.5. Cancer Res. 45:2376–2381.
36. Chatal, J.F., Herry, J.Y., Lahneche, B., Lapalus, F., Lumbroso, J.D., Pecking, A., Rougier, P., Baum, R.P., Klapdor, R., Maul, F.D., Ruibal, A., and Setoain, J. (1986) Immunoscintigraphic localization of gastrointestinal carcinomas and their recurrences. In: Schmidt, H.A.E., Ell, P.J., and Britton, K.E. (eds.), *Nuklearmedizin*. F.K. Schattauer Verlag, pp. 424–426.
37. De Nardo, G.L., Raventos, A., Hines, H.H., Scheibe, P.O., Macey, D.J., Hays, M.T., and De Nardo, S.J. (1985) Requirements for a treatment planning system for radioimmunotherapy. Int. J. Rad. Oncol. Biol. Phys. 11:335–348.
38. Hooker, G., Snook, D., Courtenay-Luck, N., Dhokia, B., MacGregor, W.G., Halnan, K.E., McKenzie, C.G., Munro, A., Lambert, H.E., Durbin, H., Burchell, J., Taylor-Papadimitriou, J., Bodmer, W.F., and Epenetos, A.A. (1986) Antibody guided irradiation of lesions in advanced ovarian cancer with or without malignant ascites. In: Schmidt, H.A.E., Ell, P.J., and Britton, K.E. (eds.), *Nuklearmedizin*. F.K. Schattauer Verlag, pp. 463–465.

14. In-vivo antibody imaging for the detection of human tumors

David M. Goldenberg, Hildegard Goldenberg, Robert M. Sharkey, Robert E. Lee, Jo Ann Horowitz, Thomas C. Hall, and Hans J. Hansen

Radionuclide imaging has become an important method in the detection and staging of neoplastic diseases. However, most nuclear imaging methods localize lesions by indirectly demonstrating a decrease in the accretion of the radiopharmaceutical (negative image) or by a physiologic attribute of the tissue that permits a positive image of the lesion. For example, to the extent that a tumor lacks organ-specific properties, an organ-imaging agent could be used to show the tumor as a defect, such as with technetium sulfur colloid for imaging the liver and spleen. The development of more selective methods for localizing tumors by means of anti-cancer antibodies labeled with a radionuclide suitable for external imaging has been a recent approach gaining in interest and application for cancer imaging, although it has been pursued for over 30 years [1–3]. Early animal studies in the 1950s showed that radioiodinated antibodies prepared against extracts of rodent tumors could localize in these tumors selectively [1,4,5]. Subsequently, it was found that this preferential tumor accretion of the radioactive antibodies was due mainly to anti-fibrin antibodies [1,6–8]; anti-fibrinogen antibodies were later explored for tumor imaging and therapy [1,9].

The renewed interest in cancer antigens at the end of the 1960s, principally due to the clinical use of carcinoembryonic antigen (CEA) and alpha-fetoprotein (AFP), stimulated our interest in using these and related cancer-associated antigens, or markers, as targets for radioactive antibodies administered parenterally as cancer imaging agents [1,2,10,11]. Initially, these studies employed conventional (goat) antibodies against such cancer markers, and it was found that a high degree of accuracy in imaging known and occult cancer sites could be obtained and that high circulating levels of the target antigen did not sufficiently neutralize the injected radioactive antibody so as to render it ineffective [12,13]. In these early studies, small amounts (0.25 mg) of whole IgG preparations labeled with low doses of I-131 (2.5 mCi) were injected, and images were made shortly after a second radionuclide agent (Tc-99m pertechnetate and serum albumin) was administered as a nontarget background radiopharmaceutical. A computer-assisted method of subtracting nontarget (Tc-99m) from tumor (I-131) radioactivity was used for tumor imaging within 48 hours of injecting the radioantibody

Goldenberg, D.M., (ed.), Cancer Imaging with Radiolabeled Antibodies.

Table 1. CEA radioimmunodetection results by tumor sites

Cancer Type	No. Pts.	No. Pos/Total Primary Site	Secondary Site	Total	%
Colorectal	51	10/12	49/53	51/57	91
Ovarian	19	10/10	11/14	21/24	88
Lung	13	8/12	4/5	12/17	71
Mammary	6	2/5	7/9	9/14	64
Pancreatic	6	3/6	1/2	4/8	50
Cervical	15	6/8	13/13	19/21	90
Other uterine	5	3/3	6/7	9/10	90
Gastric	4	2/3	3/3	5/6	83
Unknown	9	?	8/9	8/9	89
Miscellaneous	26	9/21	8/9	17/30	57
Lymphoma	2	0/2	0/2	0/4	0

[1,12,14]. This permitted detection of tumors as small as 1.5 cm diameter, even in high background radioactivity areas such as the liver. Using this method, we have applied polyclonal and monoclonal antibodies against CEA, AFP, colon-specific antigen-p (CSAp), human chorionic gonadotropin (HCG), and prostatic acid phosphatase (PAP) to over 600 patients [1]. No untoward reactions have occurred, even when repeated studies have been performed with the same antibody preparations. In addition to whole IgG, antibody fragments have been used, as well as monoclonal antibodies against some of these cancer-associated antigens [2,15–19]. The sensitivity (true-positive rate) of affinity-purified goat anti-CEA IgG labeled with I-131 (doses as above) and applied to 156 patients is summarized in Table 1. The results indicate a high level of true positivity in the major cancer types known to produce CEA, approaching 90% when both primary and secondary sites are considered.

The 51 patients with a history of confirmed colorectal cancer were studied in detail retrospectively [20]. On a patient basis, CEA antibody imaging revealed confirmed tumors in 41 of 43 of the cases, representing 95%. Only two putatively false-positive results were found in this series, constituting a rate of less than 4%. A false-negative rate of between 9% and 14% was determined. In 11 of the 51 patients studied, tumor sites were detected that were not found by other clinical measures. These sites of occult tumor were then confirmed by other methods, up to 40 weeks after antibody imaging was done. Circulating CEA levels above 5 μg/ml did not appear to interfere with cancer imaging.

Since antibody imaging appeared to be capable of revealing occult cancer when other diagnostic methods were negative, even when tumors > 2 cm in diameter were present, a correlative study of antibody imaging (radio-immunodetection, or RAID), transmission computed tomography (CT), and magnetic resonance imagine (MRI) was undertaken in a series of 12 con-

secutive patients with metastatic or primary carcinoma of the liver [21]. Eleven patients were imaged with I-131-labeled antibodies to CEA and/or CSAp, and one with antibody to AFP; polyclonal, monoclonal, and $F(ab')_2$ antibodies were used. In eight patients with confirmed liver neoplasms, hepatic tumor was disclosed in all by RAID, whereas MRI revealed tumors in 50% and CT disclosed mass lesions in 37.5% (later, 75%). In the other four patients with suspected, but unconfirmed, liver neoplasms, only RAID was positive, although supportive evidence for liver involvement was present in three of these subjects. These findings suggest that RAID may provide greater accuracy in the detection and location of cancer than other diagnostic modalities in current use. This earlier work and the current literature on cancer RAID have been summarized in other reviews [1–3,22–27].

The current literature has shown that different anticancer antibody preparations have resulted in different rates of sensitivity and specificity in imaging of the appropriate cancers. Some of the factors that may determine the accuracy of antibody imaging are listed in Table 2.

The advent of monoclonal antibodies against human cancer-associated antigens has resulted in an increased enthusiasm for the use of such reagents for the imaging of cancer [1–3,23–27]. However, we have not as yet found any improved imaging results by using monoclonal, as compared with purified, polyclonal, antibodies [26], although monoclonal antibodies are certainly preferred because of convenience and the reduced cost of manufacturing identical reagents. What may prove more important, once suitable tumor-restricted antibodies are identified, are the nature of the radiolabel, the dose of and form of antibody, and the imaging system and method used, as described below.

Antibody

Antibody specificity relates both to the tumor and to the particular antigen being targeted. In the case of the latter, monoclonal antibody technology has revealed that antibodies can recognize different determinants, or epitopes, of an antigen, which can behave quite differently in terms of tumor targeting and specificity. In addition, the nature of the localizing antibody, its isotype, form, epitope specificity, immunoreactivity, avidity, dose, specific activity of the label, etc. all play a role in tumor targeting. The development of monoclonal antibodies has resulted in some confusion in the understanding of monospecificity as compared with monoclonality. Affinity purification of polyclonal antibodies can render them monospecific, with levels of immunoreactivity that are equivalent to those found for monoclonal antibodies. This was achieved with goat anti-CEA antibodies that were purified on CEA immunoadsorbent columns [28]. The monoclonal antibodies, however, are single-epitope restricted and as such are not necessarily more monospecific than an appropriately purified polyclonal antibody. Moreover, the mono-

Table 2. Factors affecting antibody targeting

1. Character of the antibody
   a. Specificity/epitope
   b. Purity
   c. Affinity
   d. Whole or fragment
   e. Isotype
   f. Dose
   g. Species
   h. Clearance and pharmacokinetics
2. Nature of radiolabel
   a. Physical properties; half-life
   b. Chemical properties; conjugate stability
   c. Imaging properties
   d. Specific activity
   e. Dose
   f. Effect on Ab immunoreactivity
   g. Clearance; excretion
3. Tumor target
   a. Size and location of tumor(s)
   b. Location and distribution of antigen in tumor
   c. Antigen/epitope density
   d. Antigen modulation
   e. Target/nontarget ratio
   f. Vascularization and vascular permeability
   g. Distribution of target antigen in other body sites or fluids
4. Imaging system and method of interpretation
   a. Planar
   b. Emission tomography (SPECT)
   c. Computer-assisted subtraction
   d. Second antibody enhancement
   e. Experience and 'blinding' of reader
   f. Time after administration for reading
5. Other factors
   a. Route of administration
   b. Presence or absence of anti-Mab in host
   c. Presence or absence of circulating target antigen and complexes

clonal antibodies are usually of lower affinity constants than corresponding polyclonal antibodies, and since multiple binding sites on an antigen may be more desirable for tumor-cell binding than a single epitope, it is not clear that, in terms of targeting, monoclonal antibodies are preferable to suitable polyclonal antibodies. From the regulatory, supply, and cost perspectives, however, Mabs appear to be the preferred reagents.

The affinity constant of the antibody is believed to be another important attribute, where the higher the constant is, the better is the targeting. This may not be so, since in order to target well the antibody must reach the tumor in high quantities. If circulating or sessile antigen targets are in the path of the localizing antibody prior to encountering the tumor, then the high affinity will result in greater nontarget binding than if a lower affinity antibody were used. Indeed, lower affinity CEA monoclonal antibodies appear to show less

complexation with CEA in the blood than antibodies with higher affinity constants [29]. However, it has not been proved yet that lower affinity antibodies are better targeting agents than those of higher affinity. These issues are raised just so that further thought and experimentation can be stimulated.

The effector functions of an antibody are mediated by structures on the Fc part of the immunoglobulin molecule, which is the portion that is also most immunogenic in foreign hosts. The Fc portion can be deleted by enzymatic digestion of the antibody, resulting in $F(ab')_2$, Fab', or Fab fragments that retain the antigen-binding sites. However, the antibody fragments generally have lower affinity constants than whole IgG, and here again it is not clear whether this is advantageous or not. These reagents, nevertheless, do have more rapid pharmacokinetics (tumor targeting and clearance from nontargeted tissues) than whole IgG, thus affording better target/nontarget (T/NT) ratios at early scanning times (within 48 hours). Unlike Fc fragments, Fab fragments are cleared from the circulation very quickly, accumulate in the kidney [18,19,30–32], and are excreted in the urine [18,32]. $F(ab')_2$ is also cleared rapidly from the body, although not as fast as Fab or Fab' fragments [19,32], and is excreted by the kidneys [19,32].

The dose of the antibody administered has also come to be of importance in tumor targeting. It has been suggested for In-111-labeled antibodies that mixing a high amount of cold antibody (39 mg) with the labeled IgG (1 mg) results in less nonspecific liver accretion [34–37]. This has been explained by the belief that increasing the saturation of antibody binding in the liver and other nonspecific sites by increasing the antibody dose results in better tumor targeting for In-111-labeled antibodies [36,37]. However, others have not found this phenomenon for either In-111- or I-131-labeled antibodies in clinical or experimental studies [38–40]. Thus, the dose may be dependent on a number of issues other than the nature of the label, such as the antibody's target specificity, tumor and antigen burden and site in the body, presence or absence of circulating antigen, antibody affinity, host antibody to the foreign immunoglobulin, etc.

Radiolabel

Several nuclides are available for the labeling of monoclonal antibodies, and the choice is influenced by a number of factors. One, of course, is the nuclide's half-life, which should permit the localization of tumors with low background without long-range radiation exposure to other tissues. Hence, radionuclides with short half-lives are preferred. The energy of the radiation should be suitable for imaging with current instruments, such as between 100 and 250 keV. In imaging circumstances, the absorbed radiation dose should be minimal, while for therapy the intensity of the absorbed dose is very critical. Finally, methodologies need to be available for linking the nuclide to the antibody without affecting the latter's immunoreactivity and targeting

properties. Antibody imaging has been performed, for the most part, with I-131, I-123, In-111, and Tc-99m as labels. I-131 was the first and has been the most frequently used radionuclide in RAID, mostly because of its labeling simplicity, low cost, and ready availability. It has a half-life of 8 days, thus being well suited to the kinetics of antibody uptake by the target tissue. I-131 emits low-energy beta emissions that limit the imaging dose. Although relatively good results have been obtained with this radionuclide, as described above, it has relatively poor imaging attributes, requiring a high-energy collimator for its 364 keV peak. Dehalogenation in vivo has also been listed as a deficiency, although in some circumstances this can be an advantage, such as when rapid clearance from certain normal organs, such as the liver, is desired. Except for dehalogenation, I-123 has ideal imaging characteristics (low energy of 159 keV and a 13-hour half-life), but its limited availability and high cost are prohibitive for its routine use. In-111 also has excellent imaging characteristics (173 and 247 keV and a 68-hour half-life), but it is moderately expensive. Unfortunately, its accretion by normal cells of the RES, particularly liver, make differentiation of tumor from normal organ imaging in the liver very difficult. Thus, the ideal radionuclide from the perspective of favorable radiation characteristics, availability, and very low cost is Tc-99m (no beta emissions, 140 keV, and a 6-hour half-life). Until recently, however, the conjugation methods for linking Tc-99m to antibodies have been deficient.

Tumor target

The first defined human tumor antigens used as a target for radioactive antibodies in animal studies was human chorionic gonadotropin in trophoblastic cancer [41] and CEA in colonic carcinoma [10,11,42]. In patients, CEA antibodies were the first purified antibodies against a known tumor-associated antigen found to locate tumors successfully and specifically [12,13], despite the fact that this antigen is known not to be diagnostic of cancer when used as a serum marker; its principal role is as a monitor of disease activity [43,44]. Although CEA circulates in the blood of cancer patients with various malignant tumor types, and the exogenous antibodies can form complexes with circulating antigen, RAID proved successful with CEA antibodies [47]. As already discussed, the early imaging studies performed by our group, and confirmed subsequently in numerous publications, indicated that improved early imaging could be achieved with dual-isotope image subtraction. However, because of the different pharmacokinetics and isotope distribution and cross-scatter of the radioactivity of the antibody and the subtraction radiopharmaceutical, difficulties in image interpretation can occur. The important observation, however, was that a quantitative difference between CEA in the tumor and in other body sites sufficed for achieving the count ratio needed for producing tumor images [47]. Thus, a true cancer-specific marker, although desirable, has not been essential for RAID, thus providing considerable opportunity for the use of a host of anti-tumor-marker antibodies for cancer

targeting, and suggested that many cancer markers that were only useful for monitoring disease activity could be used for locating, and possibly even treating, tumors when used as vehicles for delivering imaging or therapeutic agents.

Beyond CEA, a number of such markers have been targeted by radiolabeled antibodies in clinical trials (Table 3). The advantage to using a marker

Table 3. Examples of antibodies used in clinical RAID studies

Cancer	Antibody	Radionuclide
Colorectal	CEA (various)	I-131, I-123, Tc-99m
	17-1A	I-131
	PR1A3	In-111, Tc-99m
	ICR2	In-111
	19-9	I-131, In-111
	791T/36	I-131, In-111
B-cell lymphoma	Lym-1	I-131
	IMMU-LL-2	I-131
Cutaneous T-cell lymphoma	T101	In-111
Melanoma	p97	I-131, In-111
	96.5	I-131, In-111
	48.7	I-131
	9.2.27	I-131, In-111
	225.28S	I-131, In-111, Tc-99m
	ZME-018	In-111
Neuroblastoma	3F8	I-131
	BW 575/9	I-131, Tc-99m
Ovarian	CEA	I-131, In-111
	CA 19-9	I-131
	B72.3	I-131, In-111
	HMFG1 and 2	I-131, I-123
	$NDOG_2$	I-123
	791T/36	I-131, In-111
	SM3	I-123, In-111
	OC-125	I-131, In-111
	OV-TL3	In-111
	H317	I-123
Prostate	PAP	I-131, In-111, Tc-99m
	PSA	I-131, In-111
Lung	NR-LU-10	Tc-99m
Breast	B72.3	In-111
	HMFG1 and 2	I-131, I-123, In-111
	MA-5	I-131
	CEA	I-131, In-111
	3E1.2	I-131
	M8	I-131, I-123
	F023C5	I-131, In-111
	B6.2	I-131
	3C6F9	I-123
Liver	AFP	I-131, Tc-99m
Trophoblast and germ cell	AFP/HCG	I-131

that circulates in the patient's blood is that this is an indication, when elevated, for RAID, in order to disclose the site(s) of tumor antigen synthesis. Thus, the marker's high titer in the blood is an indication for a RAID study. However, antibodies against tumor antigens that are not shed offer the advantage of not being complexed in the blood after antibody injection, thus perhaps resulting in improved targeting and prolonged tumor binding, which are desirable for antibody-mediated therapy.

Alpha-fetoprotein (AFP) is an oncofetal marker that is an intracellular secretory product shed into the blood of patients with hepatocellular carcinoma and certain rarer tumors, such as yolk-sac (endodermal sinus) and germ-cell tumors [48–52]. However, modest and transient serum elevations of AFP are also found in about 10% of patients with other liver diseases, most commonly acute and chronic hepatitis, cirrhosis, and metastases to the liver [49,53]. The presence of AFP in tumors and sera of patients with certain cancer types, particularly liver and germ-cell carcinomas, suggested to us that AFP may be a suitable target for radiolabeled antibodies, particularly for RAID, and we proceeded to demonstrate that I-131-labeled anti-AFP antibodies could disclose AFP-producing neoplasms [54–56]. In a study of 13 patients with hepatocellular carcinomas, AFP-RAID identified primary or recurrent liver carcinoma in 10 of 11 patients; in three of these CAT scans failed to disclose the lesions [57]. In the analysis of 49 evaluable sites, 15 true-positive, 7 false-negative, 26 true-negative, and 1 false-positive were found, indicating a sensitivity of 68%, a specificity of 96%, and an accuracy of 84%. The occult lesions found gave a maximum lead time of 9 weeks before confirmation. It was also found that AFP-RAID was positive in patients having normal or only moderately elevated blood AFP titers, as well as in patients with very high circulating levels of AFP. As we have reported for patients with CEA-anti-CEA complexes after injection of radiolabeled anti-CEA antibodies [45,46], AFP-antibody complexes, when formed, do not appear to hinder successful imaging of AFP-containing tumors. These studies with AFP neoplasms, as well as our experience with tumors producing human chorionic gonadotropin [58–60] and prostatic acid phosphatase [61,62], confirm that intracellular markers that are shed into the blood are appropriate markers for RAID, and presumably also for RAIT.

In addition to the specificity of the antigen target for the cancer, the location and density of the antigen associated with the tumor cells is of importance for localizing antibodies. Little is known regarding the optimal location of the target antigen for improved antibody binding. Whereas it was proposed originally that a cell-surface marker that is not shed into the circulation would be ideal, the common tumor markers explored by us were usually cytoplasmic and were released into the tumor milieu and the blood stream. Antibody binding may thus occur in the tumor periphery, thus enlarging the tumor image, or even within the cell. The number of antigen sites in the tumor that is required for optimal antibody binding, either for imaging or for therapy, is yet another poorly defined parameter. This is determined by

a number of other factors, such as tumor size and cellularity, consistency and cell density, vascularization, necrosis, antigen location, variable antigen distribution and expression (heterogeneity), and antibody availability. It is therefore of questionable value to determine the number of antigen sites present on tumor cells growing in cell culture, or to calculate the number of cells and antigen sites in a tumor sphere if only a peripheral zone of viable cells are available for antibody binding. Further, different antibody affinities will affect the binding success of the antibody to the antigen sites. Operationally, nevertheless, it would appear that the larger the number of available antigenic sites, the higher the binding and localization of the antibody to the tumor, thus resulting in improved resolution by imaging or improved cell kill by antibody therapy.

Image processing

Planar imaging within 48 hours of antibody injection shows relatively low T/NT ratios, even less than 2:1 [47]. This is a problem in highly vascular areas, so we introduced blood-pool, dual-isotope subtraction to enhance T/NT ratios and so permit early imaging [12,63]. This usually resulted in a 2.5-fold enhancement of the T/NT ratios within 48 hours [1,63]. However, because the two isotopes used in the subtraction process (I-131 and Tc-99m) have different pharmacokinetics, difficulties were encountered in certain body regions by some investigators [64,65]. It is evident that if imaging is performed at later times, such as after 72 hours, the normal clearance of nontargeted antibody (particularly radioiodine conjugates), tumor imaging without dual-isotope subtraction is feasible.

Whereas relatively high T/NT ratios are required for planar imaging, single-photon emission computed tomography (SPECT) is useful at much lower ratios. SPECT uses mathematical methods that are similar to those of x-ray tomography for reconstructing transverse, coronal, sagittal, or oblique sections of the body using a rotating camera. Clinical results have indicated an improved sensitivity with SPECT as compared with planar imaging. Therefore, SPECT appears to be the preferred method of imaging for RAID. As will be described below, image resolution is improved considerably with SPECT.

Current perspectives

Previous experiences with radiolabeled antibodies indicate that the antibody form of choice is an IgG fragment, either Fab, Fab′, or $F(ab')_2$. The preferred nuclide, as discussed above, is Tc-99m. However, radioiodine conjugation chemistry has been much easier than that of radiometals, so its successful use in RAID preceded Tc-99m as a simple imaging radionuclide. In fact, except

for its having to be shipped from the site of manufacture before use and the resulting high cost, its performance is excellent. For example, we have conjugated I-123 to a CEA monoclonal antibody $F(ab')_2$ by the chloramine-T procedure for evaluating the imaging characteristics of this agent in patients with CEA-producing tumors. An antibody dose of 1 mg having about 10 mCi I-123 was injected IV, and imaging was performed by planar and SPECT methods at 4 and 24 hours, and by planar scanning alone at 48 hours. A total of 44 patient studies have been summarized on a site basis, and it was found that 75 of 78 known tumor sites were detected (96% sensitivity); three false-positives and three false-negatives were recorded, giving an overall specificity of 90%. A total of 66 new lesions were found by RAID that were not known by other methods. Of these, 54 could be followed over 18 months, of which 18, or 33%, have been confirmed as true-positive sites of tumor by CAT scans or surgery; 33 sites are still unconfirmed and are being followed. These results for I-123 CEA-antibody fragment imaging are higher in positivity than those reported by Delaloye et al. [66] in a smaller series of patients, but poorer in terms of new occult lesions confirmed by a multicenter trial involving I-123-labeled Fab′ and $F(ab')_2$ of the same anti-CEA antibody (NP-4) that showed a confirmation rate of new lesions of 73% [67].

Until recently, a simple and reliable method of conjugating Tc-99m to antibodies was not available. Both direct [68,69] and indirect [70] labeling procedures have been attempted, often suffering from poor reproducibility or from being too cumbersome for convenient routine use. Rapid, simple, direct labeling methods have been developed recently [71,72] that appear to have solved the major problems of Tc-99m conjugation chemistry, providing a quantitative incorporation within a 30-minute labeling time. In contrast to the Hoechst method [71], which involves conjugating Tc-99m to intact IgG, the Immunomedics procedure is a one-step, almost instantaneous labeling of Fab′ with Tc-99m. Our initial clinical experience with this new Immunomedics Tc-99m labeling kit for CEA-tumor RAID is worthy of further elaboration.

The Fab′ fragment of the NP-4 CEA monoclonal antibody was labeled with Tc-99m by this method at a dose of 15–20 mCi per mg antibody, and 1 mg was injected IV into a series of 29 patients with a history of tumors of diverse histopathology producing CEA. Imaging was performed at 2–5 hours and again at about 24 hours postinjection. SPECT and planar imaging were performed at the first scanning session, and only planar imaging was performed at 24 hours. The $T_{1/2}$ blood values for the Tc-99m agent were found to be in the range of 3–4 hours, while the total body $T_{1/2}$ elimination time was 5–6 hours. A total-body planar scan made at 5 hours post antibody injection shows minor radioactivity in the major blood organs, such as the heart, as well as activity in the kidneys, presumably because of renal accretion of the Tc-99m-labeled monovalent fragment (Figure 1). However, a focus of increased radioactivity was seen at the lower border of the liver (arrow in Figure 1), which is confirmed by coronal and sagittal SPECT views (Figure 1). The conventional liver scan confirms a filling defect in this site (Figure 1).

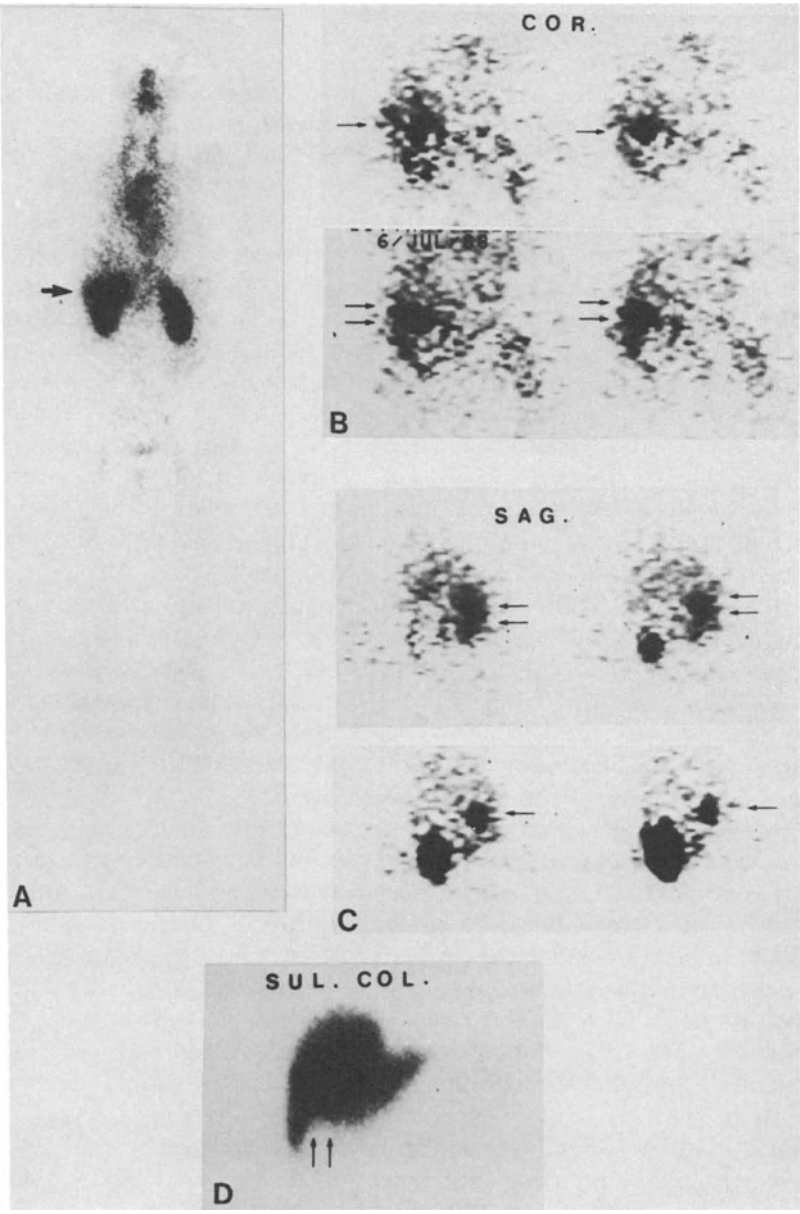

Figure 1. RAID studies of a 62-year-old woman who underwent a hysterectomy for endometrial carcinoma in 1985, followed by external beam irradiation and hormone therapy. From April to November 1988, her plasma CEA titer ranged from 4.0 to 9.2 ng/ml; at this time her chest x-ray and abdominal CT were negative. In July 1988, the patient received 17 mCi of ^{99m}Tc conjugated to the Fab′ fragment of Immu-4 (NP-4) anti-CEA Mab (1 mg). A: A total-body planar RAID scan taken at 4.5 hours after antibody injection indicates a focus of abnormal radioactivity in the right inferior lobe of the liver (arrow), adjacent to the hot right kidney. Except for some blood-pool activity in the chest and neck, only radioactivity in the sinuses of the head and in the kidneys is seen. The same area of increased focal radioactivity is identified in the 5-hour coronal (B) and sagittal (C) SPECT views of the abdomen (arrows). A liver ^{99m}Tc sulfur colloid scan (D) 1 day later confirmed the lesion (arrows). The scan indicates a defect in the lower margin of the right inferior lobe of the liver (arrows). Reprinted with permission from Goldenberg, D.M., Cancer imaging with radiolabeled antibodies. Front. Radiat. Ther. Oncol. 24, 1989, in press.

An analysis of the results of CEA-RAID with Tc-99m-labeled Fab′ shows that 94% of the known tumor sites could be disclosed, including lesions in the lungs and liver, which on CAT scan appear to be less than 0.5 cm in diameter. In fact, RAID revealed some sites that were not seen by CAT scan, basically similar to our findings with I-123-labeled antibody fragments, and to date about 18% of a large number of unknown sites first revealed by RAID have been confirmed by standard detection methods, mostly CAT scans and surgery. These cases are still being followed, and we are assuming that more intensive follow-up over time will increase the confirmation rate. At the present time, we believe that our results support the view that this new RAID method with Fab′ antibody fragments labeled with Tc-99m complements CAT scans, reveals tumors missed by CAT scans and other radiologic methods, and confirms the viability of a lesion revealed by CAT scans and other detection methods. Figure 2 is another example of imaging sites of colorectal cancer metastasis to the liver, showing the disclosure of very small lesions that add to those seen by CAT scan.

A simple, rapid, sensitive method for revealing sites of cancer on a more functional (biochemical) basis, as we have seen for RAID, would appear to have a number of applications in the management of cancer, such as some of the indications listed in Table 4. At the present time, the most frequent applications are to complement CAT scans and other radiologic methods that are less tumor specific and to reveal sites of cancer that are missed by other methods in patients with suspected recurrences.

Our own experiences with RAID have been substantially with CEA antibodies, which may in fact be considered pancarcinoma antibodies, since they have been found to target many cancer types that produce CEA [1,47]. As was shown in Table 3, however, a number of other cancer-associated antibodies have been studied in RAID, some of which may be particularly useful in specific tumor types. Since colorectal cancer has been the major tumor type studied to date with RAID, A brief survey of the antibody imaging studies involving the non-CEA antibodies is appropriate. A comprehensive review of these and CEA antibodies in the imaging of colorectal carcinoma has appeared recently [67].

Aside from CEA-RAID, antibody imaging of colorectal cancer has been pursued with three principal antibodies, 17-1A, 19-9, and B72.3. CA 19-9, recognized by Mab 19-9, and TAG-72, recognized by B72.3 Mab, are mucin antigens [73,74], similar in cellular location to colon-specific antigen-p (CSAp), which was described by us in the late 1970s [75], and to which Mabs have been developed [76]. Whereas 17-1A has not shown good tumor imaging [77,78], 19-9 and B72.3 show somewhat better results [79–81]. Mab 19-9 has been combined with CEA antibodies in several European studies [82,83], and although good imaging was reported, it is not clear whether CEA antibody alone would have given equally good results. B72.3 appears to be another pancarcinoma antibody that has been shown to be useful for imaging a number of carcinoma types [80,84]. In colorectal cancer, however, it does not

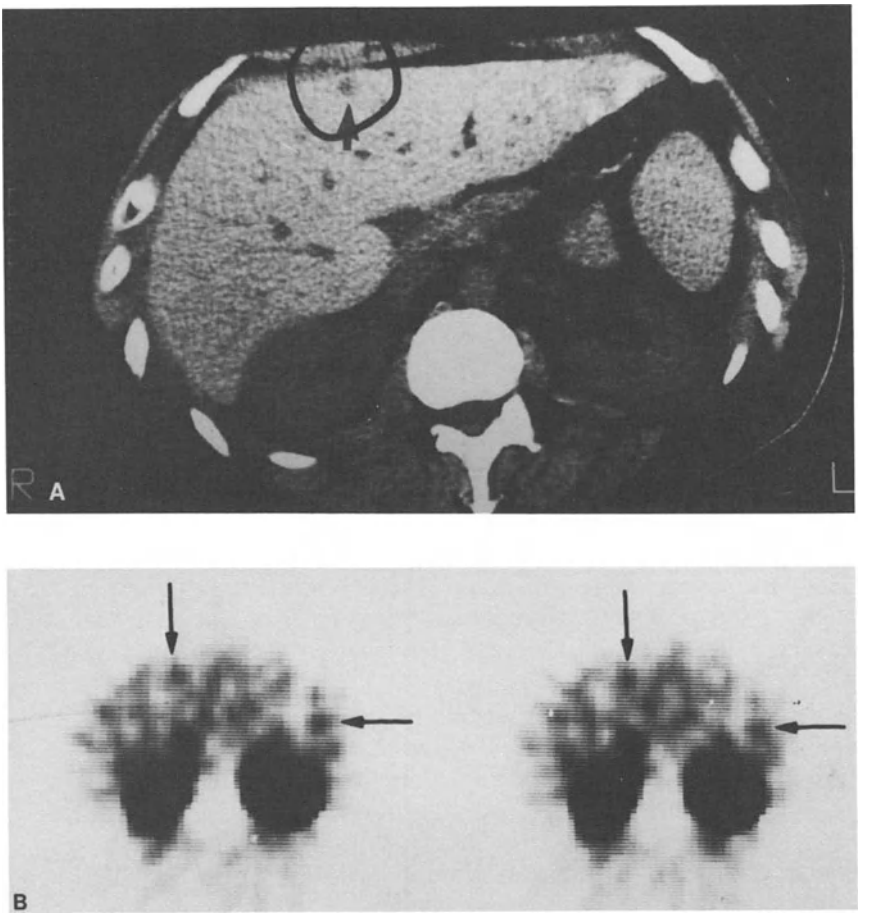

Figure 2. Imaging studies on a 34-year-old male with an unknown primary tumor and a plasma CEA value of 3.0 ng/ml. CT scan (A) shows a pathologic focus in the left lobe (circled, arrow) but was inconclusive in the spleen. The 3-hour CEA-RAID scan made with the Immunomedics Tc-99m-CEA-Fab′ kit reveals a positive focus in the transaxial SPECT images of both the left hepatic lobe and the spleen (arrows). The autopsy 2 weeks later confirmed the tumor sites seen by RAID, including the lesion within the spleen that was missed by x-ray computed tomography.

Table 4. Proposed indications for radioimmunodetection

1. Presurgical staging of extent of disease
2. Postsurgical follow-up to disclose recurrence
3. Disclosure of site(s) of recurrence in patients with rising tumor-marker titers
4. Confirmation of tumor viability when revealed by CT scans or other anatomic radiologic methods
5. Suitability of patient for radioimmunotherapy with the same antibody

Table 5. Common findings of RAID studies

1. Almost no adverse reactions have been reported.
2. Antibody fragments are preferred over whole IgG reagents.
3. Use of antibody fragments permits early imaging with short-lived radionuclides of excellent photon qualities.
4. Circulating antigens against which the imaging antibody is directed can complex with the injected antibody, but such complexes have not hindered successful RAID.
5. Patients with high serum titers of the appropriate antigen target usually have higher rates of positive RAID.
6. Patients who are seronegative for the tumor antigen being studied can have positive RAID findings.
7. SPECT appears to provide better image resolution than planar imaging.
8. Regardless of the sensitivity reported in any single study, most investigators have observed the disclosure of occult neoplasms by RAID.
9. RAID can be complementary to other radiologic methods, such as CAT scans, which are limited to structural information, while RAID is a more functional test of usually high specificity.

appear to show imaging sensitivities equal to the reports for CEA antibodies [67]. This also seems to be the experience with 19-9 and 17-1A antibodies.

Another pancarcinoma antibody (originally developed against osteogenic sarcoma) is 791T/36 [85]. Very high sensitivity percentages have been reported in cancers of the colon and rectum, particularly the former [85,86]. CSAp, which appears to be complementary to CEA in gastrointestinal cancer targeting [1,87], is under clinical study at present by our group.

It appears from a review of the literature that antibodies to CEA have been the most extensively studied immunoglobulins in RAID trials, including all cancer types studied [47,67]. The detection rates of CEA-RAID studies, regardless of antibody form and source and the scanning method, has ranged between 50% and 94%, with lesions as small as 0.3 cm located [67]. Although a number of different anti-cancer antibodies have been used, different antibody forms, different patient populations, different reference points (patient vs. lesion sensitivity), different doses and isotopes, and different scanning procedures, a number of common findings are evident, as summarized in Table 5 [67].

Future perspectives

The previous section has indicated that monoclonal antibodies are gaining a clinical role in the detection of neoplasms by external imaging methods. There is also increasing evidence that antibodies against cancer-associated antigens, when labeled with therapeutic radionuclides, can be used to treat certain cancers [1–3,26,27,88,89]. At the present time, the most ideal cancer RAID method involves the use of 1 mg or less of an antibody fragment labeled with 10–20 mCi of Tc-99m and scanned by SPECT within 2–5 hours

[67]. If frequently repeated studies are desired, human monoclonal antibodies would appear to be desirable to limit host immune reactions to the immunoglobulin, although eventually allotype and idiotype reactions to human or humanized antibodies can occur. Recombinant DNA methods have made it possible to construct antibodies in which the V region of a mouse monoclonal antibody is combined with the C regions of human immunoglobulins in order to generate chimeric molecules [90]. Further, the HV regions of mouse antibodies can be introduced into the framework of human antibodies [91], which could reduce the immunogenicity of the molecule even further. Recent results indicate that mouse/human chimeric antibodies can be used clinically [92], suggesting that such reagents will comprise future RAID, and more likely RAIT, reagents.

Whether single antibodies or antibody mixtures are preferred depends very much on the nature of the antigen targets and their density and distribution in the neoplasms being studied. Our own experience has indicated that mixtures of antibodies made against different epitopes of the same antigen are not as useful for enhancing tumor targeting and accretion as the combination of antibodies developed against distinctly different antigens [93,94]. Whether antibody combinations will be as advantageous in RAID as in therapy applications remains to be proven, but conceptually it would appear to be the case because of the high accretion and binding, required more for therapy than for imaging.

The use of Tc-99m radioconjugation to antibody fragments with human or humanized antibodies should provide the ideal imaging reagent, and it is apparent that this rapidly advancing technology is close to achieving this goal. Therefore, the next major achievement is the increased accretion of monoclonal antibodies or their derivatives in tumors in order to enhance the tumor rad doses needed for successful therapy, particularly of the less radiosensitive solid, and more lethal, tumors. This will require a more fundamental knowledge of tumor physiology, including vascularization and vascular permeability, different antigen targets of the tumor and its stroma, and more extensive use of locoregional applications. Since over the last 5 years of antibody imaging a volume of publications and advances that is a multiple of the previous 25 years has appeared, it is of little risk to predict that the next 5 years will experience similar progress in the area of cancer radioimmunotherapy.

Acknowledgments

Our research has been supported in part by USPHS grants CA39841 and RR05903, contract N44-CM-87778 from the NIH, the New Jersey Commission on Cancer Research, and the New Jersey Commission on Science and Technology.

References

1. DeLand, F.H., and Goldenberg, D.M. (1986) Radiolabeled antibodies: Radiochemistry and clinical applications. In: Freeman, L.M., (ed.), *Freeman and Johnson's Clinical Radionuclide Imaging*, 3rd ed. update, Orlando, FL: Grune & Stratton, pp. 1915–1992.
2. Goldenberg, D.M. (1987) Current status of cancer imaging with radiolabeled antibodies. J. Cancer Res. Clin. Oncol. 113:203–208.
3. Murray, J.L., and Unger, M.W. (1988) Radioimmunodetection of cancer with monoclonal antibodies: Current status, problems, and future directions. CRC Crit. Rev. Oncol./Hematol. 8:227–253.
4. Pressman, D., and Korngold, L. (1953) The in vivo localization of anti-Wagner osteogenic sarcoma antibodies. Cancer (Philadelphia) 6:619–623.
5. Korngold, L., and Pressman, D. (1954) The localization of antilymphosarcoma antibodies in the Murphy lymphosarcoma of the rat. Cancer Res. 14:96–99.
6. Day, E.D., Planinsek, J.A., and Pressman, D. (1959) Loalization in vivo of radioiodinated anti-rat-fibrin antibodies and radioiodinated rat fibrinogen in the Murphy rat lymphosarcoma and in other transplantable rat tumors. J. Natl. Cancer Inst. 22:413–426.
7. Day, E.D., Planinsek, J.A., and Pressman, D. (1959) Localization of radioiodinated rat fibrinogen in transplanted rat tumors. J. Natl. Cancer Inst. 23:799–812.
8. Spar, I.L., Bale, W.F., Goodland, R.L., et al. (1960) Distribution of injected ^{131}I-labeled antibody to dog fibrin in tumor-bearing dogs. Cancer Res. 20:1501–1504.
9. McCardle, R.J., Harper, P.V., Spar, I.L., et al. (1966) Studies with iodine-131-labeled antibody to human fibrinogen for diagnosis and therapy of tumors. J. Nucl. Med. 7:837–847.
10. Primus, F.J., Wang, R.H., Goldenberg, D.M., and Hansen, H.J. (1973) Localization of human GW-39 tumors in hamsters by radiolabeled heterospecific antibody to carcinoembryonic antigen. Cancer Res. 33:2977–2982.
11. Goldenberg, D.M., Preston, D.F., Primus, F.J., and Hansen, H.J. (1974) Photoscan localization of GW-39 tumors in hamsters using radiolabeled anticarcinoembryonic antigen immunoglobulin G. Cancer Res. 34:1–9.
12. Goldenberg, D.M., DeLand, F., Kim, E., et al. (1978) Use of radiolabeled antibodies to carcinoembryonic antigen for the detection and localization of diverse cancers by external photoscanning. N. Engl. J. Med. 298:1384–1388.
13. Goldenberg, D.M. (1978) Carcinoembryonic antigen and other tumor-associated antigens in colon cancer diagnosis and management. In: Grundmann, E. (ed.), *Colon Cancer*. Stuttgart: Gustav Fischer Verlag, pp. 163–178.
14. DeLand, F.H., Kim, E.E., Simmons, G., and Goldenberg, D.M. (1980) Imaging approach in radioimmunodetection. Cancer Res. 40:3046–3049.
15. Ballou, B., Levine, G., Hakala, R.R., and Solter, D. (1979) Tumor location detected with radioactivity labeled monoclonal antibody and external scintigraphy. Science 206:844–847.
16. Mach, J.-P., Buchegger, F., Forni, M., et al. (1981) Use of radiolabeled monoclonal anti-CEA antibodies for the detection of human carcinomas by external photoscanning and tomoscintigraphy. Immunol. Today 2:239–249.
17. Gaffar, S.A., Bennett, S.J., DeLand, F.H., and Goldenberg, D.M. (1982) Carcinoembryonic antigen (CEA) radioactive antibody fragments for cancer localization in vivo. Proc. Am. Assoc. Cancer Res. 23:249.
18. Larson, S.M., Carrasquillo, J.A., Krohn, K.A., et al. (1983) Localization of ^{131}I-labeled p97-specific Fab fragments in human melanoma as a basis for radiotherapy. J. Clin. Invest. 72:2101–2114.
19. Wahl, R.L., Parker, C.W., and Philpott, G.W. (1983) Improved radioimaging and tumor localization with monoclonal $F(ab')_2$ J. Nucl. Med. 24:317–325.
20. Goldenberg, D.M., Kim, E.E., Bennett, S.J., et al. (1983) CEA radioimmunodetection in the evaluation of colorectal cancer and in the detection of occult neoplasms. Gastroenterology 84:524–532.
21. DeLand, F.H., Lieber, A., Ram, M.D., and Goldenberg, D.M. (1986) Preliminary findings

in the evaluation of hepatic malignancies by radioimmunodetection, x-ray computed tomography, and magnetic resonance imaging. Eur. J. Nucl. Med. 12:429–435.
22. Goldenberg, D.M., and DeLand, F.H. (1983) History and status of tumor imaging with radiolabeled antibodies. J. Biol. Response Modif. 1:121–136.
23. Keenan, A.M., Harbert, J.C., and Larson, S.M. (1985) Monoclonal antibodies in nuclear medicine. J. Nucl. Med. 26:531–537.
24. Begent, R.H.J. (1985) Recent advances in tumor imaging; use of radiolabeled antitumor antibodies. Biochim. Biophys. Acta 780:151–166.
25. Larson, S.M. (1987) Lymphoma, melanoma and colon cancer: Diagnosis and treatment with radiolabeled monoclonal antibodies. The 1986 Eugene Pendergrass New Horizons Lecture. Radiology 165:297–304.
26. Goldenberg, D.M. (1988) Targeting of cancer with radiolabeled antibodies. Prospects for imaging and therapy. Arch. Pathol. Lab. Med. 112:580–587.
27. Goldenberg, D.M. (1989) Future role of radiolabeled monoclonal antibodies in oncological diagnosis and therapy. Semin. Nucl. Med. 19:332–339.
28. Primus, F.J., MacDonald, R., Goldenberg, D.M., and Hansen, H.J. (1977) Tumor detection and localization with purified antibodies to carcinoembryonic antigen. Cancer Res. 37:1544–1547.
29. Sharkey, R.M., Ballance, C., Varga, D., et al. (1988) Pharmacological and radiodosimetric analysis of patients given radioiodinated anti-carcinoembryonic antigen (CEA) monoclonal antibody (Mab) for tumor therapy (abstract). Proc. Am. Soc. Clin. Oncol. 7:100.
30. Spiegelberg, H.L., and Weigle, W.O. (1965) The catabolism of homologous and heterologous 7S gamma globulin fragments. J. Exp. Med. 121:323–338.
31. Scheinberg, D.A., and Strand, M. (1983) Kinetic and catabolic considerations of monoclonal antibody targeting in erythroleukemic mice. Cancer Res. 43:265–272.
32. Endo, K., Kamma, H., and Ogata, T. (1988) Radiolabeled monoclonal antibody 15 and its fragments for localization and imaging of xenografts of human lung cancer. J. Natl. Cancer Inst. 80:835–842.
33. Murray, J.L., Rosenblum, M.G., Sobol, R.E., et al. (1985) Radioimmunoimaging in malignant melanoma with ^{111}In-labeled monoclonal antibody 96.5. Cancer Res. 45:2376–2381.
34. Patt, Y.Z., Lamki, L.M., Haynie, T.P., et al. (1988) Improved tumor localization with increasing dose of indium-111-labeled anti-carcinoembryonic antigen monoclonal antibody ZCE-025 in metastatic colorectal cancer. J. Clin. Oncol. 6:1220–1230.
35. Carrisquillo, J.A., Abrams, P.G., Schroff, R.W., et al. (1988) Effect of antibody dose on the imaging and biodistribution of indium-111 9.2.27 anti-melanoma monoclonal antibody. J. Nucl. Med. 29:39–47.
36. Rosenblum, M.G., Murray, J.L., Haynie, T.P., et al. (1985) Pharmacokinetics of ^{111}In-labeled anti-p97 monoclonal antibody in patients with metastatic malignant melanoma. Cancer Res. 45:2382–2386.
37. Lamki, L., Haynie, T.P., Murray, J.L., et al. (1986) The effect of increasing unlabeled monoclonal antibody (MoAb) doses on metastases detection and on body distribution of In-111 MoAbs (abstract). Br. J. Cancer 54:535.
38. Carrasquillo, J.A., Bunn, Jr., P.A., Keenan, A.M., et al. (1986) Radioimmunodetection of cutaneous T-cell lymphomas with ^{111}In-labeled T101 monoclonal antibody. N. Engl. J. Med. 315:673–680.
39. Wahl, R.L., Liebert, M., and Wilson, B.S. (1986) The influence of monoclonal antibody dose on tumor uptake of radiolabeled antibody. Cancer Drug Deliv. 3:243–249.
40. Sharkey, R.M., Primus, F.J., and Goldenberg, D.M. Antibody protein dose and radioimmunodetection of GW-39 human colon tumor xenografts. Int. J. Cancer 39:611–617.
41. Quinones, J., Mizejewski, G., and Beierwaltes, W.H. (1971) Choriocarcinoma scanning using radiolabeled antibody to chorionic gonadotropin. J. Nucl. Med. 12:69–75.
42. Mach, J.-P., Carrel, S., Merenda, C., et al. (1974) In vivo localization of radiolabeled antibodies to carcinoembryonic antigen in human colon carcinoma grafted into nude mice. Nature 248:704–706.

43. Goldenberg, D.M. (1979) Carcinoembryonic antigen in the management of colorectal cancer. Acta Hepatogastroenterol. 26:1–3.
44. Goldenberg, D.M., Neville, A.M., Carter, A.C., et al. (1981) Carcinoembryonic antigen: Its role as a marker in the management of cancer. National Institutes of Health Consensus Development Conference Statement. Cancer Res. 41:2017–2018.
45. Primus, F.J., Bennett, S.J., Kim, E.E., et al. (1980) Circulating immune complexes in cancer patients receiving goat radiolocalizing antibodies to carcinoembryonic antigen. Cancer Res. 40:497–501.
46. Primus, F.J., and Goldenberg, D.M. (1980) Immunological considerations in the use of goat antibodies to carcinoembryonic antigen for the radioimmunodetection of cancer. Cancer Res. 40:2979–2983.
47. Goldenberg, D.M., Kim, E.E., DeLand, F.H., et al. (1980) Radioimmunodetection of cancer with radioactive antibodies to carcinoembryonic antigen. Cancer Res. 40:2984–2992.
48. Abelev, G.I. (1974) α-fetoprotein as a marker of embryo-specific differentiation in normal and tumor tissues. Transplant. 20:3–37.
49. Ruoslahti, E., Salaspuro, M., Pihko, H., et al. (1974) Serum α-fetoprotein: Diagnostic significance in liver disease. Br. Med. J. 2:527–529.
50. Waldmann, T.A., and McIntire, K.R. (1974) The use of a radioimmunoassay for alpha-fetoprotein in the diagnosis of malignancy. Cancer 34:1510–1515.
51. Scardino, P.T., Cox, H.D., Waldmann, T.A., et al. (1977) The value of serum tumor markers in the staging and prognosis of germ cell tumors of the testis. J. Urol. 118:994–999.
52. Norgaard-Pedersen, B., Albrechtesen, R., and Teilum, G. (1975) Serum alpha-fetoprotein as a marker for endodermal sinus tumour (yolk sac tumor) or a vitelline component of 'teratocarcinoma.' Acta Pathol. Microbiol. Scand. 83:573–589.
53. Silver, H.K.B., Deneault, J., Gold, P., et al. (1974) The detection of α_1-fetoprotein in patients with viral hepatitis. Cancer Res. 34:244–247.
54. Goldenberg, D.M., Kim, E.E., DeLand, F.H., et al. (1980) Clinical studies on the radioimmunodetection of tumors containing alpha-fetoprotein. Cancer (Philadelphia) 45:2500–2505.
55. Kim, E.E., DeLand, F.H., Nelson, M.O., et al. (1980) Radioimmunodetection of cancer with radiolabeled antibodies to α-fetoprotein. Cancer Res. 40:3008–3012.
56. Halsall, A.K., Fairweather, D.S., Bradwell, A.R., et al. (1981) Localization of malignant germ cell tumors by external scanning after injection of radiolabeled anti-alpha fetoprotein. Br. Med. J. 283:942–944.
57. Goldenberg, D.M., Goldenberg, H., Higginbotham-Ford, E., et al. (1987) Imaging of primary and metastatic liver cancer with ^{131}I monoclonal and polyclonal antibodies against alphafetoprotein. J. Clin. Oncol. 5:1827–1835.
58. Goldenberg, D.M., Kim, E.E., DeLand, F.H., et al. (1980) Radioimmunodetection of cancer using radioactive antibodies to human chorionic gonadotropin. Science 208:1284–1286.
59. Javadpour, N., Kim, E.E., DeLand, F.H., et al. (1981) The role of radioimmunodetection in the management of testicular cancer. JAMA 246:45–49.
60. Goldenberg, D.M., Kim, E.E., and DeLand, F.H. (1981) HCG radioantibodies in the radioimmunodetection of cancer and for disclosing occult metastases. Proc. Natl. Acad. Sci. USA 78:7754–7758.
61. Goldenberg, D.M., DeLand, F.H., Bennett, S.J., et al. (1983) Radioimmunodetection of prostatic cancer: In vivo use of radioactive antibodies against prostatic acid phosphatase for diagnosis and detection of prostatic cancer by nuclear imaging. JAMA 250:630–635.
62. Goldenberg, D.M., and DeLand, F.H. (1984) Clinical studies of prostatic cancer imaging with radiolabeled antibodies against prostatic acid phosphatase. Urol. Clin. North Am. 11:277–281.
63. DeLand, F.H., Kim, E.E., Simmons, G., and Goldenberg, D.M. (1980) Imaging approach in radioimmunodetection. Cancer Res. 40:3046–3049.
64. Ott, R.J., Grey, L.J., Zivanovic, M.A., et al. (1983) The limitations of the dual radionuclide subtraction technique for the external detection of tumours by radioiodine-labeled anti-

bodies. Br. J. Radiol. 56:101–108.
65. Green, A.J., Begen, R.H.J., Keep, P.A., et al. (1984) Analysis of radioimmunodetection of tumors by the subtraction technique. J. Nucl. Med. 25:96–100.
66. Delaloye, B., Bischof-Delaloye, A., Buchegger, F., et al. (1984) Detection of colorectal carcinoma by emission-computerized tomography after injection of ^{123}I-labeled Fab or $F(ab')_2$ fragments from monoclonal anti-carcinoembryonic antigen antibodies. J. Clin. Invest. 77:301–311.
67. Goldenberg, D.M., Goldenberg, H., Sharkey, R.M., et al. (1989) Imaging of colorectal carcinoma with radiolabeled antibodies. Semin. Nucl. Med. 19:262–281.
68. Pettit, W.A., DeLand, F.H., Bennett, S.J., and Goldenberg, D.M. (1980) Radiolabeling of affinity-purified goat anti-carcinoembryonic antigen immunoglobulin G with technetium-99m. Cancer Res. 40:3043–3045.
69. Rhodes, B.A., Torvestad, D.A., Breslow, K., et al. (1982) ^{99m}Tc-labeling and acceptance testing of radiolabeled antibodies and antibody fragments. In: Burchiel, S.W., and Rhodes, B.A. (eds.), *Tumor Imaging. The Radioimmunochemical Detection of Cancer*. New York: Masson Publishing, pp. 111–123.
70. Fritzberg, A.R., Abrams, P.G., Beaumier, P.L., et al. (1988) Specific and stable labeling of antibodies with technetium-99m with a diamide dithiolate chelating agent. Proc. Natl. Acad. Sci. USA 85:4025–4029.
71. Schwarz, A., and Steinstrasser, A. (1987) A novel approach to Tc99m-labeled monoclonal antibodies (abstract). J. Nucl. Med. 28:721.
72. Hansen, H.J., Jones, A.L., Grebenau, R., et al. (1990) Labeling of anti-tumor antibodies and antibody fragments with ^{99m}Tc. In: Goldenberg, D.M. (ed.), *Cancer Imaging with Radiolabeled Antibodies*. Norwell, MA: Kluwer, pp. 233–244.
73. Magnani, J.L., Steplewski, Z., Koprowski, H., et al. (1983) Identification of the gastrointestinal and pancreatic cancer-associated antigen detected by monoclonal antibody 19-9 in the sera of patients as a mucin. Cancer Res. 43:5489–5492.
74. Johnson, V.G., Schlom, J., Paterson, A.J., et al. (1986) Analysis of a human tumor-associated glycoprotein (TAG-72) identified by a monoclonal antibody B72.3. Cancer Res. 46:850–857.
75. Pant, K.D., Dahlman, H.L., and Goldenberg, D.M. (1977) A putatively new antigen (CSAp) associated with gastrointestinal and ovarian neoplasia. Immunol Commun. 6: 411–421.
76. Nocera, M.A., Shochat, D., Primus, F.J., et al. (1987) Representation of epitopes on colon-specific antigen-p (CSAp) defined by monoclonal antibodies. J. Natl. Cancer Inst. 79: 943–948.
77. Moldofsky, P.J., Powe, J., Mulhern, Jr., C.B., et al. (1983) Metastatic colon carcinoma detected with radiolabeled $F(ab')_2$ monoclonal antibody fragments. Radiology 149:549–555.
78. Mach, J.P., Chatal, J.F., Lumbroso, J.D., et al. (1983) Tumor localization in patients by radiolabeled monoclonal antibodies against colon carcinoma. Cancer Res. 43:5593–5600.
79. Chatal, J.F., Saccavini, J.C., Fumoleau, P., et al. (1984) Immunoscintigraphy of colon carcinoma. J. Nucl. Med. 25:307–314.
80. Colcher, D., Esteban, J.M., Carrasquillo, J.A., et al. (1987) Quantitative analyses of selective radiolabeled monoclonal antibody localization in metastatic lesions of colorectal cancer patients. Cancer Res. 47:1185–1189.
81. Esteban, J.M., Colcher, D., Sugarbaker, D., et al. (1987) Quantitative and qualitative aspects of radiolocalization in colon cancer patients of intravenously administered Mab B72.3. Int. J. Cancer 39:50–59.
82. Baum, R.P., Lorenz, M., and Hor, G. (1987) Radioimmunszintigraphie bei kolorektalen karzinomen — Stellenwert in der rezidivdiagnostik nach 2 jahren klinischer erfahrung. Nuklearmedizin 10:219–234.
83. Baum, R.P., Lorenz, M., Senekowitsch, R., et al. (1988) Clinical experience in cancer diagnosis with radiolabeled monoclonal antibodies in 200 patients and initial attempts at radioimmunotherapy. In: Srivastava, S.C. (ed.), *Radiolabeled Monoclonal Antibodies for Imaging and Therapy*. New York: Plenum, pp. 613–651.

84. Schlom, J. (1989) Innovations in monoclonal antibody tumor targeting. JAMA 261:744–746.
85. Farrands, P.A., Pimm, M.V., Embleton, M.J., et al. (1982) Radioimmunodetection of human colorectal cancers by an anti-tumor monoclonal antibody. Lancet 2:397–400.
86. Armitage, N.C., Perkins, A.C., Pimm, M.V., et al. (1984) The localization of an anti-tumor monoclonal antibody (791T/36) in gastrointestinal tumors. Br. J. Surg. 71:407–412.
87. Nelson, M.O., DeLand, F.H., Shochat, D., et al. (1983) External imaging of gastric cancer metastases with radiolabeled CEA and CSAp antibodies (letter). N. Engl. J. Med. 308:847.
88. Brady, L.W., Woo, D.V., Markoe, A.M., et al. (1987) Monoclonal antibodies in the diagnosis and treatment of cancer. In: Bleehan, N. (ed.), *Radiobiology in Radiotherapy*. New York: Springer-Verlag, pp. 233–241.
89. Order, S.E., Sleeper, A.M., Stillwagon, G.B., et al. (1989) Current status of radioimmunoglobulins in the treatment of human malignancy. Oncology 3:115–120.
90. Morrison, S.L. (1985) Transfectomas provide novel chimeric antibodies. Science 229: 1202–1207.
91. Neuberger, M.S., Williams, G.T., and Fox, R.O. (1984) Recombinant antibodies possessing novel effector functions. Nature 312:604–608.
92. Shar, D.R., Khazaeli, M.B., and LoBuglio, A.F. (1988) Mouse/human chimeric antibodies to a tumor-associated antigen: Biologic activity of the four human IgG subclasses. J. Natl. Cancer Inst. 80:1553–1559.
93. Sharkey, R.M., Primus, F.J., Shochat, D., and Goldenberg, D.M. (1988) Comparison of tumor targeting of mouse monoclonal and goat polyclonal anti-carcinoembryonic antigen antibodies in the GW-39 human tumor-hamster host model. Cancer Res. 48:1823–1828.
94. Gaffar, S.A., Pant, K.D., Shochat, D., et al. (1981) Experimental studies of tumor radioimmunodetection using antibody mixtures against carcinoembryonic antigen (CEA) and colon-specific antigen-p (CSAp). Int. J. Cancer 27:101–105.

15. In-111 monoclonal antibody immunoscintigraphy of colorectal cancer

Lamk M. Lamki, Yehuda Z. Patt, and James L. Murray

Radioimmunoscintigraphy has become an important research tool following the successful production, characterization, and radiolabeling of murine monoclonal antibodies (Mab) [1–4]. Previous investigators have evaluated the clinical utility of radiolabeled monoclonal antibodies for diagnosing the metastatic spread of melanoma [5–8], prostatic cancer [9], colorectal cancer [10–13], and several other malignancies, as well as nonmalignant conditions such as acute myocardial infarction [14] and thromboembolic disorders [15], and for labeling blood cells [16]. At the University of Texas System Cancer Center, M.D. Anderson Hospital, we have studied immunoscintigraphy of melanoma with two different monoclonal antibodies labeled with indium-111 (ZME-018 and 96.5), as well as in In-111-antiprostatic acid phosphatase Mab (PAY 276) for metastatic prostatic adenocarcinoma. These studies, as well as those of other workers, have been reviewed previously [17–19]. In this chapter we will review our experience in colorectal cancer immunoscintigraphy using In-111-labeled intact monoclonal antibody as well as $F(ab')_2$ fragments. We will first discuss advantages and/or disadvantages of the radiolabels used, including iodine-131, iodine-123, indium-111, and technetium-99m, followed by studies of other anti-colorectal antibodies and the antigens targeted. The Mabs to be discussed, both intact antibodies as well as their Fab and $F(ab')_2$ fragments, include anti-CEA, 17-1A, NS19-9, and B72.3. This will be followed by a discussion on the approach to possible solutions to problems encountered in immunoscintigraphy with In-111 Mabs, as well as future prospects for improved imaging of metastatic disease.

The radiolabel

Different radioisotope labels have been used for labeling monoclonal antibodies (Mab) directed against human colorectal cancer. The ideal label has to have a long enough physical half-life to allow imaging of metastatic lesions within a reasonable number of biologic half-lives of the monoclonal antibody used. For the purpose of imaging with conventional gamma cameras, the ideal radiopharmaceutical should have gamma emissions with energies

Goldenberg, D.M., (ed.), Cancer Imaging with Radiolabeled Antibodies.

greater than 100 keV, but less than 300 keV. They should also lack particulate radiation output such as beta and alpha particles, as these may induce an unacceptable level of radiation damage to the recipient. However, the ideal isotope used for both radioimaging and radiotherapy will most likely have a combination of the above characteristics. The radiolabels that have been used to date include radioiodine (both I-123 and I-131) in humans, I-125 predominantly in nude mice bearing human tumor xenografts, and In-111 in both animals and humans. A relative newcomer to the monoclonal antibody fields is Tc-99m, but the ideal labeling procedure is still under experimentation. The choice of the radiolabel partly depends on one's experience and bias. However, there are some general guidelines in choosing the radiolabel, which will be discussed in this chapter. The main thrust of this review will be on In-111-labeled monoclonal antibody scintigraphy of colon cancer.

Iodine-123 can be readily coupled to proteins and has the advantage of good photon flux. Because of a relative lack of beta particles, the radiation dose to the patient is low, and therefore a higher radiopharmaceutical dose may be given to obtain optimal images. Also, the gamma emission is 159 keV, which is close to ideal for the gamma cameras used today for imaging. The disadvantages of I-123 are that it is cyclotron produced (and therefore difficult to obtain), expensive, and has a physical half-life of only 13.5 hours, which means it has to be delivered to the institution either the day it is intended to be used or a maximum of 24 hours prior to use. The short physical half-life is also a disadvantage for labeling intact antibodies, which have plasma half-lives greater than 24 hours. However, I-123 has successfully been used for labeling of Mab fragments [Fab and $F(ab')_2$] due to their shorter biologic half-life.

I-131 is one of the earliest radioisotopes used for labeling Mabs and has an established place in immunoscintigraphy. It has a physical half-life of 8.1 days and thus is suited for labeling intact antibodies. It is also suited for whole IgG antibodies, which accumulate at metastatic sites at a slower rate [20]. An advantage of I-131 is that it is easy to produce, inexpensive, and readily available. The problem with I-131 is that it does have some beta emissions, and therefore the diagnostic dose that can be given to patients has to be limited. Also the gamma emissions are not ideal for our cameras at 364 keV, resulting in relatively poor image quality. A disadvantage that is common among all the isotopes of iodine is that of in-vivo dehalogenation, i.e., when the radioiodinated Mab is injected intravenously, and is localized in the tumor or certain normal organs, a large percentage comes off the Mab and is rapidly excreted in the urine. The immunoglobulin that is detached is metabolized separately from the iodine [21]. This, at least in part, may account for low liver background and good visualization of metastatic lesions in the liver compared with indium-labeled antibodies, which are coupled to Mab via chelation. Iodine dehalogenation in the tumor results in fading of radioactivity in the tumor with time, resulting in a more rapid decrease in the tumor/background ratio compared with In-111-labeled Mab.

Indium-111 has several advantages over iodine-131. It gives better images

because of improved gamma photon flux [22]. It has two gamma photons per disintegration, at 247 keV and 171 keV, with a physical half-life of 2.83 days and relatively no beta rays, thus reducing radiation exposure to the patient. It is chemically stable within cells. The physical half-life is well suited to intact antibody labeling and is also usable for fragments Fab and $F(ab')_2$ of Mab. Indium-111 is readily available, though the cost is still high. The physical properties of In-111 leads to a relatively high radiation exposure, thus limiting the dose to 5 mCi. The other problem with indium-111 is that, unlike iodine, one cannot label immunoglobulins directly with indium, but rather has to use a chelating agent, which may be quite complex to prepare. The stability of the Mab-indium-111 complex is dependent on the relative ratios of indium-111 to Mab. A popular chelating agent is bifunctional diethylenetriaminepentacetic acid (DTPA), but recently other chelate conjugates have been prepared [23], and, indeed, some newer analogues of modified DTPA conjugates are more stable. The DTPA acts as a chemical sandwich between the immunoglobulin and the indium-111 [24,25]. While there is no dehalogenation with In-111, there is a problem with transcomplexation of the indium from the antibody to circulating transferrin. Some indium gets detached from the antibody; and since transferrin has a greater affinity for indium, the indium-transferrin complex may localize in the liver and contributes to the visualization of the bone marrow, too. Patients who are studied with In-111-labeled monoclonal antibodies manifest a high level of activity within the liver, and a variable amount of radioactivity is noted in the bone, kidneys, and spleen, giving a relatively high tissue background, which may interfere with lesion detection. In general, however, tumor uptake improves with time and local tumor activity remains high up to 6 days.

^{99m}Technetium (Tc-99m) has several theoretical advantages over the other radiolabels [26]. Tc-99m has an excellent gamma emission of 140 keV, with practically no beta or alpha particulate emission. This allows the use of large doses (e.g., 30 mCi) with low radiation exposure to the patient compared with the typical 5 mCi of In-111 or I-131 and I-123. The resultant images are of good quality. The major problem is the technical difficulty in getting good labeling as well as a good yield. The two commonly used methods for labeling immunoglobulins with Tc-99m still have to be perfected. The other problems include the short physical half-life of 6 hours, which makes it very difficult to follow the patients for a long time, and some antibodies may take longer to reach peak localization in the tumors. Certainly, it is a problem to use Tc-99m for labeling whole antibodies [27], but more workers are now trying to use ^{99m}Tc for labeling fragments, and there is reason for optimism.

Anti-CEA antibody imaging

Murine Mabs directed against the carcinoembryonic antigen (CEA) have been extensively investigated for imaging colorectal cancer, using both intact antibody [28,29] as well as the fragments Fab and $F(ab')_2$ [30,31]. The earliest

immunoscintigraphy trials were performed using radiolabeled polyclonal antibodies [32,33] directed against carcinoembryonic antigen. Mach used radiolabeled monoclonal anti-CEA and performed imaging with planar views as well as tomoscintigraphy [34]. The in-vivo kinetics of radiolabeled monoclonal anti-CEA antibodies in animal models was studied by several investigators, who showed improved tumor localization using indium-111-labeled anti-CEA antibody compared with the I-131-labeled version of the same antibody [22,28]. The In-111-labeled Mab produced a better signal-to-noise ratio in the scans, thereby facilitating the detection of metastatic lesions with greater certainty.

At the University of Texas M.D. Anderson Hospital, we have used an In-111-labeled murine monoclonal antibody, ZCE-025, which is directed against the CEA antigen. This antibody, which was supplied for study by Hybritech, Incorporated, is a murine immunoglobulin of the IgG_{2a} subclass produced by conventional hybridoma technology [35]. One milligram of the Mab was labeled with 5 mCi of In-111 using the bifunctional DTPA method of Krejcarek and Tucker [36]. The 1 mg labeled antibody was mixed with from 2 mg to 80 mg of unlabeled ZCE-025, diluted in 100 ml of saline, and infused intravenously over 1 hour. Images were acquired at 48–72 hours and then again at 120–144 hours. A regions-of-interest analysis was performed on digital images to evaluate the relative body distribution to different organs. The average activity per pixel over the spleen, bones, and kidneys was compared to that over the liver and heart blood pool. The tumor detection rate (sensitivity) using indium-labeled anti-CEA Mab was evaluated by comparing the number of metastatic lesions detected by this antibody with the number of metastatic lesions diagnosed by other conventional means, i.e., CT scans, physical examination, colonoscopy, biopsy, and surgery [37]. We were able to detect 77% of known metastatic lesions in patients with colorectal cancer at Mab doses greater than 20 mg (Figures 1 and 2). Using a total of 40 mg of Mab (i.e., 1 mg labeled plus 39 mg unlabeled), the loalization of the indium-labeled antibody in normal liver tissue was less than with other doses. Thus, we were able to detect metastatic lesions in the liver as 'hot' lesions, i.e., they accumulated more radiolabeled Mab than normal tissues (Figure 2). However, at other dose levels, for example, 20 mg and 10 mg, the metastatic liver lesions were detected as 'cold' lesions because the normal liver localized a higher concentration of the labeled antibody than did the metastatic lesions. It appeared that when 40 mg of unlabeled Mab was coinfused with 1 mg of labeled antibody, we were able to at least partially block liver localization of the labeled antibody. The exact mechanism(s) underlying this effect is/are not clear. There are several possible explanations for the ability of unlabeled Mab to block the liver uptake of labeled Mab. Nonspecific localization of Mab in the liver is one explanation. However, it is conceivable that we may be blocking specific binding sites. A very low concentration of specific antigens in a very large organ like the liver can amount to significant levels and thus interfere with imaging. Several investigators have demonstrated in nude

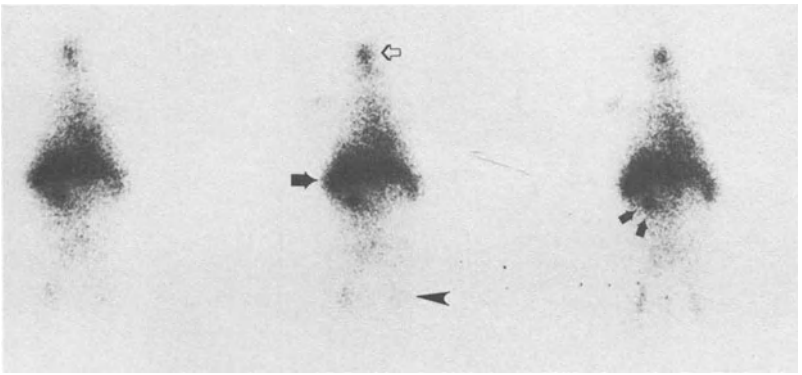

Figure 1. Biodistribution of In-III-labeled anti-CEA Mab ZCE-025 (1 mg labeled with 5 mCi In-111 coinfused with unlabeled ZCE-025). A: Tomographic whole-body slices acquired 24 hours following infusion (5 mg dose): Note distribution is maximum in the liver (arrow) but radioactivity is distributed throughout the body from nasopharynx (open arrow) to femora (arrowhead). A focal metastatic lesion of the transverse colon is noted below the liver (double arrow).

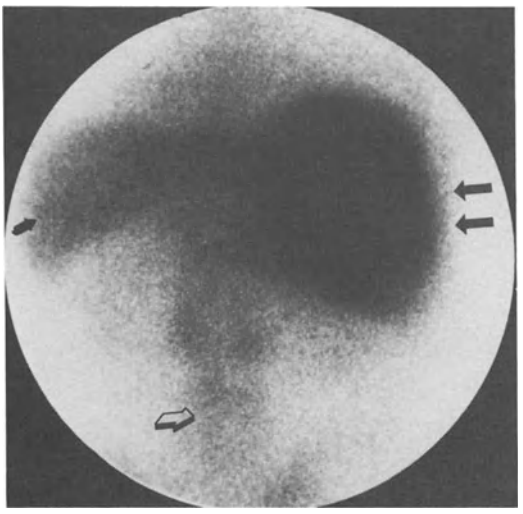

Figure 1B. A gamma camera posterior abdominal view of a patient who received a 20 mg dose. There is intense localization of In-111 ZCE-025 in the liver (double arrow), with the spleen (arrow) showing less activity, followed by the bones (open arrow), and minimal activity in the kidneys.

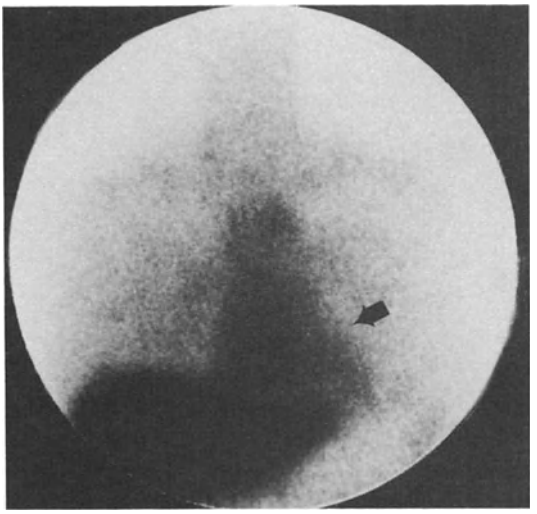

Figure 1C. At a 40 mg dose, blood-pool activity (arrow) remained high, even at 72 hours, as noted in the anterior chest view of this patient.

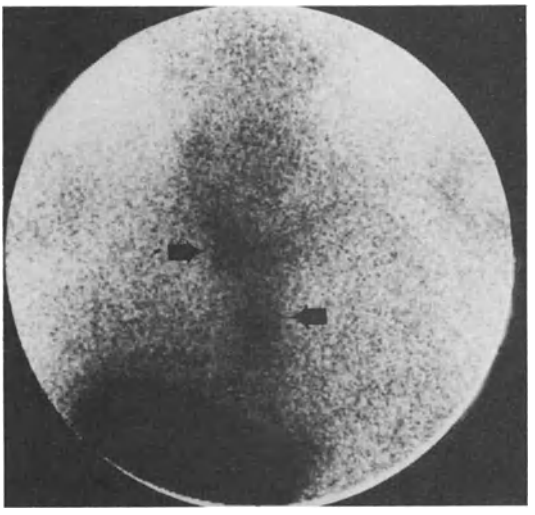

Figure 1D. Anterior chest view of another patient who received 80 mg of ZCE-025. At 168 hours, the blood-pool activity had receded enough in this patient to enable visualization of mediastinal lesions (arrow).

mouse xenograft models that the actual size of liver lesions correlates with whether a 'photon-rich' or 'photon-deficient' image is produced [38,39]. It is believed that shed CEA in the circulation accounts for a high background uptake due to immune complex deposition in liver tissue [39]. We have not seen any correlation between the ability to detect liver lesions as 'hot' or 'cold' based on tumor size or serum CEA levels, however.

Another possible explanation of the high liver uptake is inherent in the In-111 radioisotope itself, as free indium normally localizes in the liver. This will be accelerated as the In-111-Mab is metabolized in the liver, leaving the In-111 bound to hepatocytes and Kupffer cells. The high concentration of indium-labeled anti-CEA within the liver is not only observed in humans, but also was described in animal models [35]. Besides ZCE-025, other indium-111-labeled anti-CEA Mabs have also been shown to localize in human liver [40]. Liver uptake is a common problem with most In-111-labeled Mabs studied to date.

We have also examined the sensitivity and specificity of In-111 ZCE-025 in detecting occult 'CEA-producing' tumors. Patients with a rising serum CEA and no other evidence of disease by conventional CT scans or ultrasound received 40 mg of In-111-labeled ZCE-025. Of the 18 patients evaluated to date, 72% had at least one positive lesion detected by the Mab that was confirmed on follow-up by either surgery or biopsy (Figure 3). The overall specificity of this technique, however, is still uncertain. For example, a total of 45 lesions were actually imaged, yet only 18 (40%) have been confirmed as tumor. However, additional follow-up may yet demonstrate additional areas of occult disease, as has been previously reported by Moldofsky et al. with I-131-labeled anti-171A Mab [41]. In-111-labeled anti-CEA Mab may be useful in guiding the surgeon during 'second-look' exploratory laparotomies.

Fragments [Fab, $F(ab')_2$] of anti-CEA Mab, rather than whole IgG, have been studied by several investigators. Wahl et al. [42] have used a $F(ab')_2$ fragment of a murine monoclonal anti-CEA antibody and compared it with the Fab fragment, as well as with whole antibody labeled with iodine-131 to image human colorectal tumors in nude mice. They showed that the $F(ab')_2$ fragment was superior to Fab and also superior to the intact antibody for imaging. Other workers have used Fab fragments of anti-CEA in human imaging [43] and found these to give slightly higher sensitivity than the intact antibody. Delaloye et al. [13] compared immunoimaging with $F(ab')_2$ to Fab fragments of an anti-CEA Mab labeled with 2.3–8 mCi of I-123. By using emission computerized tomography (SPECT), these investigators found that Fab had an imaging sensitivity of 89% and $F(ab')_2$ 82%. This is in contrast to Wahl's work [42] and that of Khawba [44], who showed that $F(ab')_2$ was better than Fab. Halpern [45] compared anti-CEA Mab Fab versus $F(ab')_2$ fragments for different-size lesions in an animal model and found tumor uptake of Fab > $F(ab')_2$ > intact Mab, respectively. Although the smaller Fab molecule (MW, 50,000) has a better chance of penetrating the tumor capillaries and accumulating in the tumor, they are rapidly cleared by the

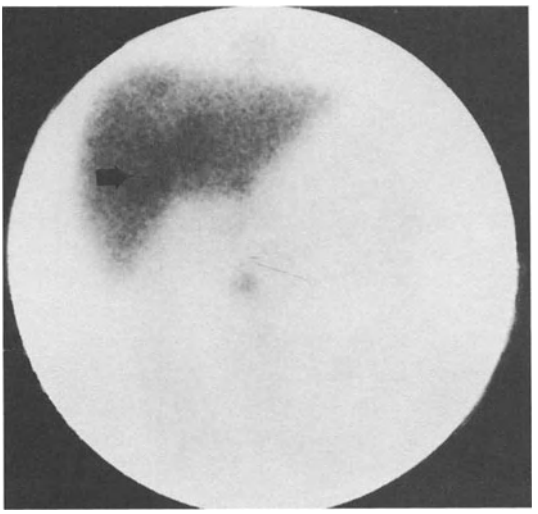

Figure 2. Examples of metastatic lesions of colon cancer detected by In-111 ZCE-025 at the optimal dose of 40 mg. A, B: Liver metastases of this patient appear as 'hot' lesions (arrow) against a background of normal liver tissue. This happened only at the 40 mg dose level. At lower dose levels, the liver blockade was insufficient and the metastatic lesions appeared less active ('cold') relative to normal liver tissue of those patients. A: Anterior planar view of the abdomen;

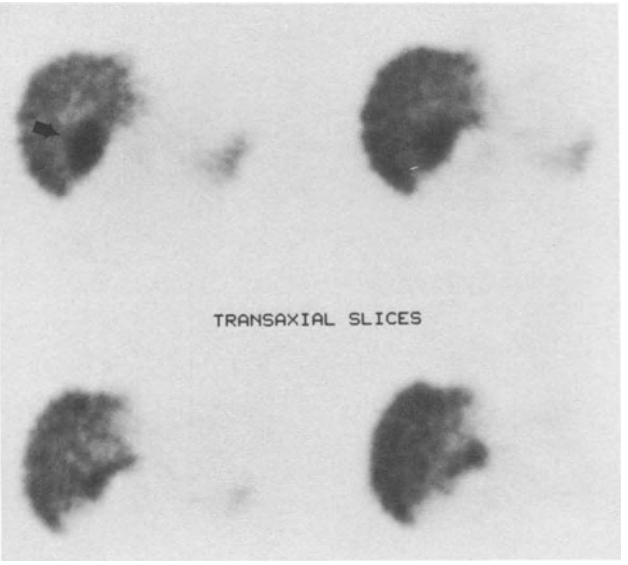

Figure 2B. SPECT slices of the liver. C, D: At this dose all metastatic lesions of soft tissue and bones were detected at a higher rate than other dose levels. In this patient, a metastatic lesion is noted in the left lung (arrow).

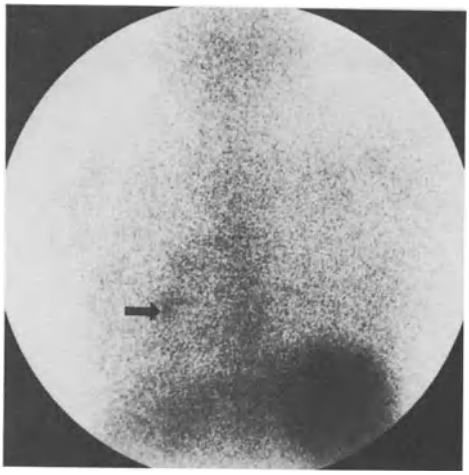

Figure 2C. Posterior gamma camera view of the chest and (d) also in the accompaying chest x-ray.

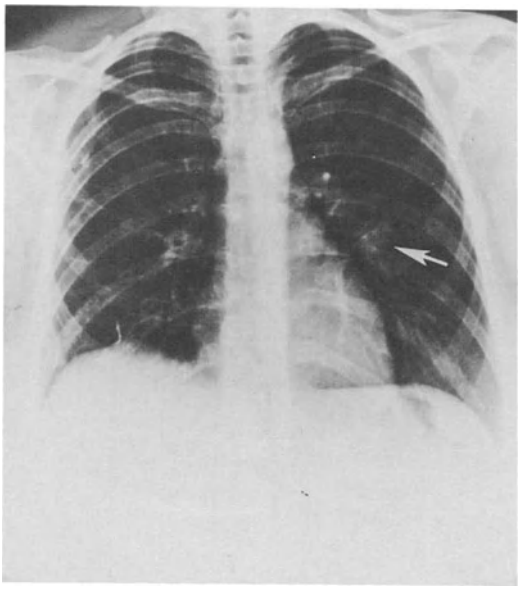

Figure 2D.

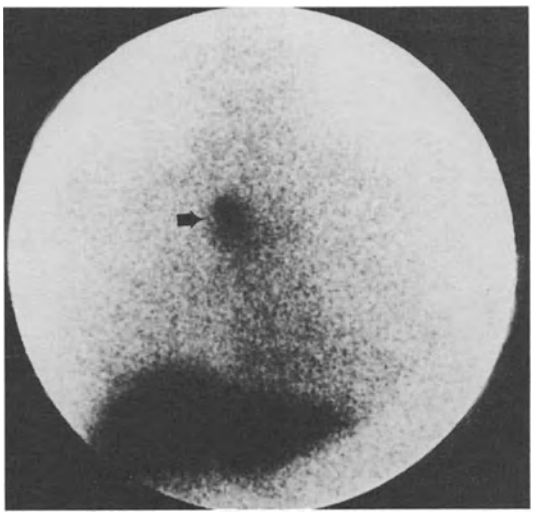

Figure 3. In-111 ZCE-025 for revealing 'occult malignancy' in patients wth rising levels of serum CEA. A: Anterior chest planar image of a patient investigated with 40 mg of the anti-CEA Mab. A metastatic lesion is revealed in the superior mediastinum (arrow).

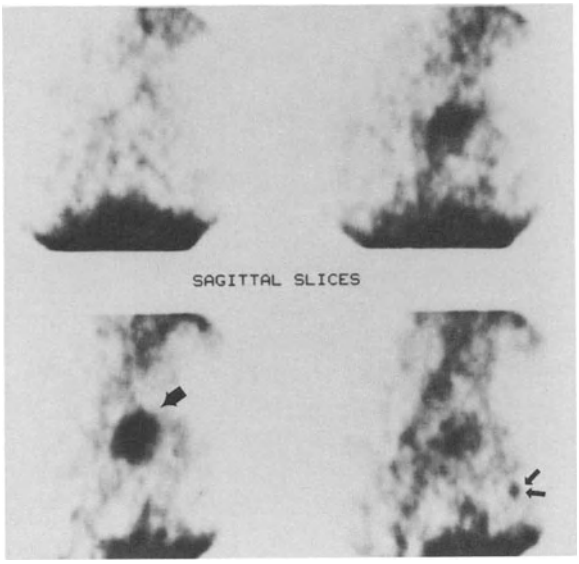

Figure 3B. When SPECT imaging of the patient in Figure 3A was performed, it confirmed the three-dimensional position (arrow) of the lesion, and another smaller lesion was revealed in the anterior chest (double arrow).

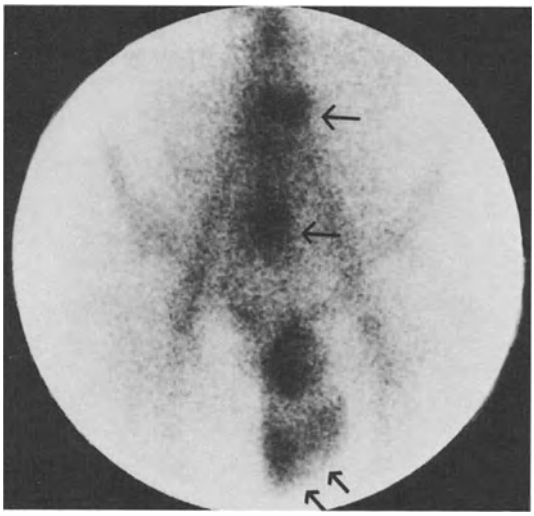

Figure 3C. Complete conventional investigation of another patient with rising serum CEA level failed to uncover a metastatic lesion recurrence. However, immunoscintigraphy using In-111 ZCE-025 detected abnormal uptake in the lower abdomen anteriorly near the midline (arrows) in this planar anterior pelvis view. Note the testicular uptake (double arrow), a normal finding in some patients.

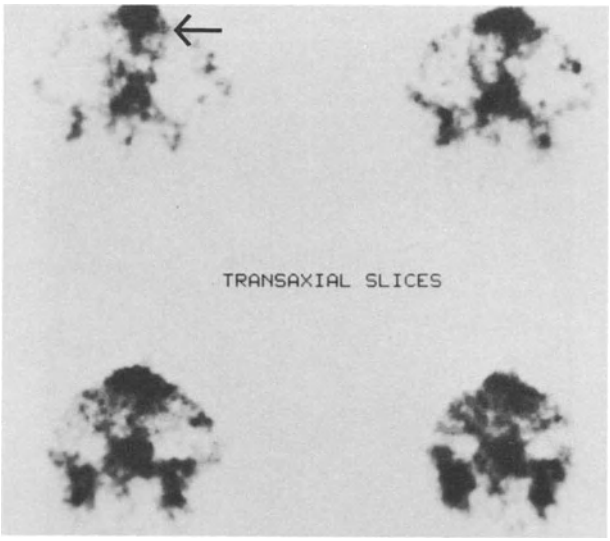

Figure 3D. SPECT transaxial slices of the study in Figure 3C localized the abnormal uptake in the anterior abdominal wall (arrow). This was later confirmed by surgery to be a recurrence of a malignant lesion in the anterior abdominal wall.

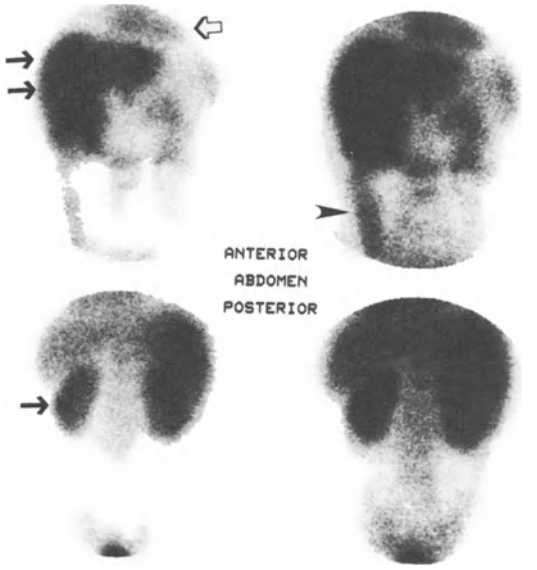

Figure 4. Studies of colon cancer using In-111 $F(ab')_2$ fragments of anti-CEA Mab ZCE-025. A: Biodistribution of the fragments was different from that of the intact anti-CEA Mab ZCE-025. Note the high kidney uptake (arrow) of the In-111 $F(ab')_2$ fragments, even higher than the liver activity (double arrow). Also, colon activity was significant (arrowhead) in this patient, a not uncommon finding. Blood-pool activity (open arrow) was often higher than expected, as noted in this study at 48 hours. A dose of 2 mg of $F(ab')_2$ was used.

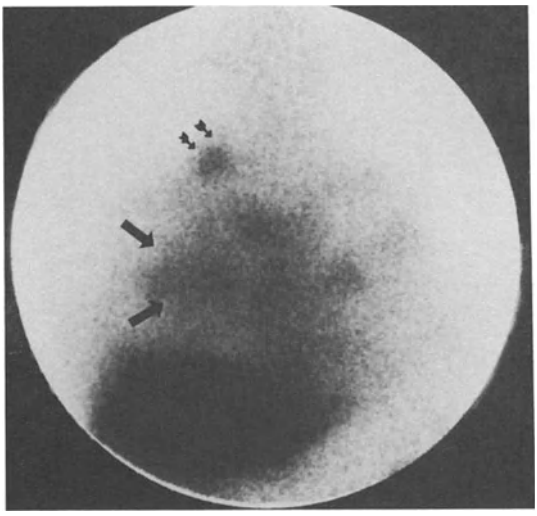

Figure 4B. Metastatic colon cancer was detected by In-111 $F(ab')_2$ in the anterior chest wall (arrows) of this patient, as well as in the right supraclavicular lymph node (double arrow). This anterior chest image was acquired 72 hours following administration.

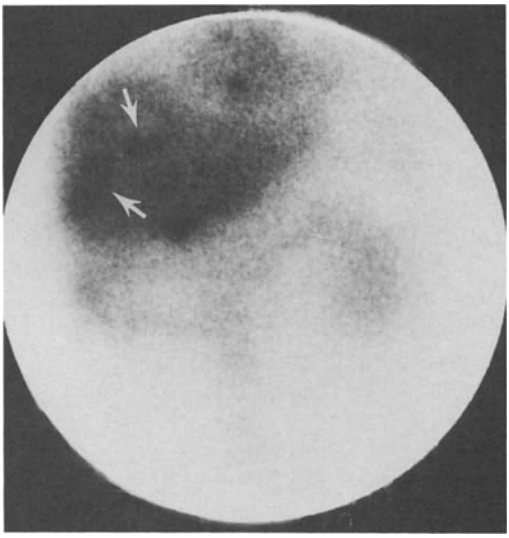

Figure 4C. Anterior planar view of the abdomen of a patient with known liver metastases. Multiple 'hot' lesions (arrows) are seen against a background of relative low radioactivity in the normal liver tissue.

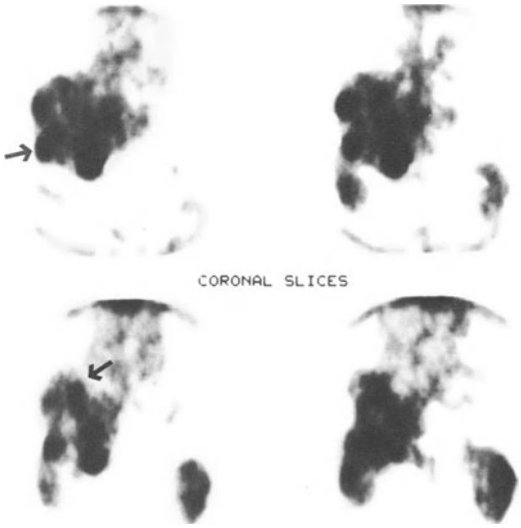

Figure 4D. SPECT tomographic slices of the same patient in Figure 4C, showing that the multiple metastases (arrows) extend to both lobes of the liver, the anterior and posterior aspects.

kidneys, resulting in a short plasma half-life. $F(ab')_2$ has double the molecular weight, but also twice the antigen-binding valency, resulting in equivalent or less tumor uptake over time. Intact IgG Mab is even larger and has a molecular weight of 150,000 daltons.

We are currently performing a clinical trial using $F(ab')_2$ fragments of ZCE-025 in patients with metastatic colorectal cancer. Two milligrams of In-111-labeled $F(ab')_2$ is coinfused with varying doses of unlabeled $F(ab')_2$ up to 18 mg (total 20 mg). Preliminary results so far have suggested that $F(ab')_2$ has a slightly greater lesion detection rate than the intact Mab ZCE-025. These results, however, are still too early for definite conclusions. We have noticed a difference in the biodistribution compared with our previous trial, e.g., there was less liver localization of In-111-labeled $F(ab')_2$ fragments than the intact In-111 Mab. There was more localization of the labeled fragments in the kidneys compared with previous findings with the intact antibody (Figure 4). Pharmacokinetic studies also showed a shortened plasma half-life compared with whole Mab, as expected (data not shown).

We predict there will be more publications regarding the clinical utility of the intact anti-CEA Mabs and their fragments in the near future. Despite their relatively low specificity, anti-CEA intact Mab and fragments have a great potential, particularly for identifying occult abdominal soft-tissue disease in patients with elevated serum CEA values.

Radioimaging with other anti-colorectal cancer antibodies

Mab 17-1A

Mab 17-1A is an IgG_{2a} immunoglobulin directed against a cell-surface antigen associated with human colorectal carcinoma [46,47]. This antibody is produced by murine hybridomas grown intraperitoneally in nude mice and collected from the resulting ascitic fluid after centrifugation and filtration. Chatal et al. [11] studied 17-1A labeled with I-131 and obtained a sensitivity for detection of metastases of about 60%. Mach et al. [3] also used the I-131-labeled 17-1A and demonstrated an imaging sensitivity of 51%. However, their results were a combination of findings from three centers and the exact sensitivity varied from center to center. A significant amount of effort has also gone into the imaging of colorectal cancer with fragments of this antibody. Moldofsky [48] used $F(ab')_2$ fragments of this antibody labeled with I-131 and got a sensitivity of detection of 69% without the use of background subtraction. Lesions ranged from 1.5 to 8 cm. Mach [3] compared the intact antibody with its fragment and showed a higher imaging sensitivity using $F(ab')_2$ fragments than the intact antibody — 61% versus 51%. Chatal [11] also demonstrated a slightly better imaging sensitivity with $F(ab')_2$ fragments compared with the intact antibody. Of the 46 known areas of metastases imaged by either $F(ab')_2$ or whole IgG Mab, 27 were positive (59%). In short,

it is obvious from the above workers' experience that imaging using 17-1A did not prove more sensitive than imaging using anti-CEA antibodies.

Imaging with Mab NS 19-9 and its F(ab')$_2$ fragment

NS 19-9 is a murine Mab directed against a monosialoganglioside that is shed into the circulation [48]. Chatal et al. [11] used both the intact antibody and its F(ab')$_2$ fragment labeled with I-131 to image colorectal cancer. Overall sensitivity was 66% compared with 59% obtained with Mab 17-1A. However, when NS 19-9 was combined with either 17-1A or anti-CEA, the sensitivity of detection rose to 77% (10 of 13 metastatic sites). Hnatowich [49], using In-111-labeled NS 19-9 F(ab')$_2$ fragments, achieved an imaging sensitivity of 67% in 14 patients. In-111 labeling was achieved by the DTPA chelating method, and a ratio of 1.6 DTPA groups per molecule were obtained. The F(ab')$_2$ fragments were routinely found to be 95% pure by high-performance liquid chromatography (HPLC) analysis.

The successful labeling of F(ab')$_2$ fragments with In-111 without significantly changing the immunoreactivity of the preparation was an important achievement. Problems encountered with In-111 still exist, and 9% of In-111 was complexed to circulating transferrin over a 24-hour period. This was about 1–2% of the injected dose and could explain localization of In-111 label in bone marrow. The serum $t_{1/2}$ was biphasic, consisting of alpha and beta phases of 2 and 19 hours, respectively. Whole-body clearance was much slower, with $t_{1/2}$ of 160 hours. This was attributed entirely to urinary excretion of 0.25% of the injected dose per hour. Like intact antibody, In-111 F(ab')$_2$ accumulated significantly in the liver (20% of the injected dose in this case). The potential future use of this antibody or its fragments is probably in combination with other radiolabeled Mabs [11]. Not all colon cancers express the 19-9 antigen [50], and this antibody has failed to produce higher sensitivities than the newer anti-CEA Mabs and other newer colon cancer antibodies.

Imaging with Mab B 72.3 and its fragments

Mab B 72.3 is a murine IgG_1 developed against a human breast tumor metastases as an immunogen [51–53]. It reacts with a glycoprotein complex of high molecular weight (222,000–400,000 daltons) expressed on the surface of approximately 50% of breast tumors and 80% of colon tumors [52]. B 72.3 has the novel feature of not binding to the surface of the noncarcinoma cells tested. Specifically, it has not been found to react with melanoma, sarcoma, leukemia, and a broad range of normal adult human cell types, including red and white blood cells. It also does not react with CEA. The antigen to which it reacts is referred to as *tumor-associated glycoprotein* (TAG-72). This antibody turns out to be better for imaging colorectal cancer than for breast cancer, which was the original immunogen. At least from the studies con-

ducted so far, it has been used in radioimmunoscintigraphy of human colon cancer xenograft in mice with the radioiodinated B 72.3. I-131-labeled B 72.3 has also been studied in colorectal cancer in humans with good results [54]. Biopsies of tumor tissues obtained following infusion of B 72.3 demonstrated tumor/normal tissue ratios of Mab of greater than 3 : 1 in all cases. Effort is underway to label this antibody with In-111 and clinical trials have already begun. A great deal of in-vitro or in-vivo preclinical work with B 72.3 has been published [55].

The ideal antibody for imaging colorectal cancer

While the ideal Mab for immunoscintigraphy of colorectal cancer does not exist, several approaches to dealing with the problems encountered can be formulated. Problems related to the antibody, the antigen, the radiolabel, and imaging instrumentation need to be explored. The above discussion has touched on some of the problems. A search for Mabs with higher affinities and specificities continues. Cross-reactivity of the available Mabs with normal tissues raises the background radioactivity and lowers the sensitivity of immunoscintigraphy. A practical approach currently available to reduce this problem includes administering labeled Mab with unlabeled Mab, as previously discussed. The high background activity may also be approached by the use of liposomally entrapped second antibody [56], which can accelerate the clearance of non-tumor-bound first antibody through the reticuloendothelial system, without affecting the clearance from the tumor.

The use of radiolabeled Fab or $F(ab')_2$ fragments also can increase the sensitivity of imaging. The rapid blood clearance of fragments allows for more convenient imaging times and greater ease of labeling with short-lived radioisotopes such as iodine-123 and technetium-99m. Fragments are also less immunogenic due to removal of the Fc end. This may be of considerable importance with respect to the inevitable development of human anti-mouse antibodies following multiple doses of Mab. Tumor heterogeneity is also a significant problem. Little can be done about the heterogeneity of antigen expression or the size of the tumor [57]; however, studies of combinations of two or more Mabs (cocktails) to image tumors may be more effective [11,51,58,59]. Another approach toward enhancing Mab uptake in colorectal cancer might be to administer other biologic response modifiers such as interferon, which has been shown to improve antibody targeting [60,61].

The choice of the radiolabel depends to some extent on the bias of the investigator, as no radioisotope is ideal. There is enough evidence to support the superiority of In-111 over iodine [21,22], but In-111 still has problems, as discussed above. The future may reside with isotopes of short half-lives such as technetium-99m, especially as Fab and $F(ab')_2$ fragments come into more general usage. Single-photon emission tomography (SPECT) has been used by several investigators [58], and it does detect more lesions than planar imaging alone. We are currently evaluating SPECT; our impressions to date

are that it does produce better results than planar gamma camera images, particularly with respect to detecting disease adjacent to liver. Other innovations of nuclear medicine equipment and techniques, including computer enhancement, will undoubtedly improve the lesion detection rate. We have not used background subtraction techniques, as they often produce more artifacts than true images, but in the future mathematical modeling and manipulation may enhance immunoscintigraphy. It is also not yet clear whether positron emission tomography (PET) will play a major role in immunodetection, but the potential PET has for exploitinig physiologic processes of perfusion and metabolism will undoubtedly open new vistas in the use of radiolabeled Mabs for immunoscintigraphy.

References

1. Kohler, G., and Milstein, C. (1975) Continuous cultures of fused cells secreting antibodies of predefined specificity. Nature (London) 256:495–497.
2. Herlyn, M., Steplewski, Z., Herlyn, D., and Koprowski, H. (1979) Colorectal carcinoma specific antigen: Detection by means of monoclonal antibodies. Proc. Natl. Acad. Sci. USA 76:1438–1442.
3. Mach, J.P., Chatal, J.F., Lumbroso, J.D., et al. (1983) Tumor localization in patients by radiolabeled monoclonal antibodies against colon carcinoma. Cancer Res. 43:5593–5600.
4. Farrands, P.A., Perkins, A.C., Pimm, M.V., et al. (1982) Radioimmunodetection of human colorectal cancers by an anti-tumor monoclonal antibody. Lancet 2:397–400.
5. Murray, J.L., Rosenblum, M.G., Sobol, R.E., et al. (1985) Radioimmunoimaging in malignant melanoma with ^{111}In-labeled monoclonal antibody 96.5. Cancer Res. 45:2376–2381.
6. Larson, S.M., Brown, J.P., Wright, P.W., Carrasquillo, J.A., Hellstrom, L., and Hellstrom, K.E. (1983) Imaging of the melanoma with I-131 labeled monoclonal antibodies. J. Nucl. Med. 24:123–129.
7. Halpern, S.E., Dillman, R.O., Witztum, K.F., et al. (1985) Radioimmunodetection of melanoma utilizing In-111 96.45 monoclonal antibody: A preliminary report. Radiology 155: 493–499.
8. Murray, J.L., Rosenblum, M.G., Lamki, L.M., et al. (1987) Clinical parameters related to optimal tumor localization of indium-111-labeled mouse antimelanoma monoclonal antibody ZME-108. J. Nucl. Med. 28:25–33.
9. Babaian, R.J., Murray, J.L., Lamki, L.M., et al. (1987) Radioimmunological imaging of metastatic prostatic cancer with ^{111}indium labeled monoclonal antibody PAY-276. J. Urol. 137:439–443.
10. Moldofsky, P.J., Powe, J., Mulhern, C.B., et al. (1983) Metastatic colon carcinoma detected with radiolabeled F(ab′)$_2$ monoclonal antibody fragments. Radiology 149:549–555.
11. Chatal, J.F., Saccavini, J.C., Fumoleau, P., et al. (1984) Immunoscintigraphy of colon carcinoma. J. Nucl. Med. 25:307–314.
12. Patt, Y.Z., Lamki, L., Haynie, T.P., et al. (1987) Improved ^{111}In monoclonal anti-CEA ZCE-025 (Mab) localization in colorectal cancer (CRC) liver metastases by the addition of unlabeled ZCE-025 (abstract). Proc. Am. Assoc. Cancer Res. 28:1546.
13. Delaloye, B., Bischof-Delaloye, A., Buchegger, F., et al. (1986) Detection of colorectal carcinoma by emission-computerized tomography after injection of ^{123}I-labeled Fab or F(ab′)$_2$ fragments from monoclonal anti-carcinoembryonic antigen antibodies. J. Clin. Invest. 77:301–311.
14. Khaw, B.A., Fallon, J.T., Strauss, H.W., and Harber, E. (1980) Myocardial infarct imaging of antibodies to canine cardiac myosin with In-111-DTPA. Science 209:295–297.

15. Som, P., Oster, Z.H., Zamora, P.O., et al. (1986) Radioimmunoimaging of experimental thrombi using Tc-99c-labeled monoclonal antibody fragments reactive with human platelets. J. Nucl. Med. 27:1315–1320.
16. Thakur, M.L., White, F., Tricheri, G. (1986) Specific radiolabeling of human neutrophils: Evaluation of In-111 labeled monoclonal antibodies (abstract). J. Nucl. Med. 27:947.
17. Lamki, L.M., Kim, E.E., and Haynie, T.P. (1986) Tumor immunoscintigraphy using monoclonal antibodies. In: Roth, J. (ed.), *Monoclonal Antibodies in Cancer: Advances in Diagnosis and Treatment*. Mount Kisco, NY: Futura Publishing, pp. 259–288.
18. Murray, J.L., Lamki, L.M., and Rosenblum, M.G. (1988) Radioimmunoimaging of malignant melanoma with monoclonal antibodies. In: McGuire, W., and Nathanson, L. (eds.), *Cancer Treatment and Research Series: Malignant Melanoma*. Boston: Kluwer Academic Publishers, in press.
19. Murray, J.L., Rosenblum, M.G., Lamki, L.M., Haynie, T.P., and Hersh, E.M. (1987) Radioimmunoimaging in malignant melanoma patients using ^{111}In-labeled antimelanoma-monoclonal antibody (ZME-018) to a high molecular weight antigen KD 200. NCI Monogr. 3:3–9.
20. Epenetos, A.A., Snook, D., Durbin, H., et al. (1986) Limitations of radiolabeled monoclonal antibodies for localization of human neoplasms. Cancer Res. 46:3183–3191.
21. Khaw, B.A., Cooney, J., Edington, T., and Strauss, H.W. (1986) Difference in experimental tumor localization of dual-labeled monoclonal antibody. J. Nucl. Med. 27:1293–1299.
22. Fairweather, D.S., Bradwell, A.R., Dykes, P.W., et al. (1983) Improved tumour localisation using indium-111 labeled antibodies. Br. Med. J. 287:167–170.
23. Esteban, J.M., Schlom, J., and Gansow, O. (1987) New method of the chelation of indium-111 to monoclonal antibodies: Biodistribution and imaging of athymic mice bearing human colon carcinoma xenografts. J. Nucl. Med. 28:861–870.
24. Goodwin, D.A., Meares, C.F., McCall, M.J., et al. (1985) Chelate conjugates of monoclonal antibodies for imaging lymphoid structure in the mouse. J. Nucl. Med. 26:493–502.
25. Paik, C.H., Hong, J.J., Eggert, M.A., Heald, S.C., Reba, R.C., and Eckelman, W.C. (1985) Relative reactivity of DTPA immunoreactive antibody-DTPA conjugates, and non-immunoreactive antibody-DTPA conjugates toward In-111. J. Nucl. Med. 26:482–487.
26. Fitzberg, A.R. (1986) Radiopharmaceutical chemistry V: Antibodies. J. Nucl. Med. 27: 957–958.
27. Morrison, R.T., Lyster, D.M., Alcorn, L., Rhodes, B.A., Breslow, K., and Burchiel, S.W. (1984) Radioimmunoimaging with Tc-99m monoclonal antibodies: Clinical studies. Int. J. Nucl. Med. Biol. 11:184–188.
28. Hagan, P.L., Halpern, S.E., Chen, A., et al. (1985) In vivo kinetics of radiolabeled monoclonal anti-CEA antibodies in animal models. J. Nucl. Med. 26:1418–1423.
29. Abdel-Nabi, H.H., Schwartz, A.N., Higans, C.S., Sechter, D.G., and Unger, M.W. (1987) Colorectal carcinoma: Detection with In-111 anti-CEA monoclonal antibody ZCE-025. Radiology 164:617–621.
30. Mach, J.P., Buchegger, F., Grob, J., Van Fliedner, V., Bischof-Delaloye, A., and Delaloye, B. (1984) Improved detection of colon carcinoma by using tomoscintigraphy and I-123 labeled F(ab')$_2$ and Fab fragments of anti-CEA monoclonal antibodies. Br. J. Cancer 50:551.
31. Halpern, S.E., Haindl, W., and Dillman, R.O. (1987) Radioimmunoimaging of tumors with indium-111 labeled F(ab')$_2$ anti-carcinoembryonic antigen monoclonal antibody (abstract). J. Nucl. Med. 28:637.
32. Goldenberg, D.M., Deland, F., Kim, E., et al. (1978) Use of radiolabeled antibodies to CEA for the detection and localization of diverse cancers by external photo-scanning. N. Engl. J. Med. 298:1384–1388.
33. Goldenberg, D.M., Kim, E.E., Bennett, S.J., Nelson, M.O., and Deland, F. (1983) Carcinoembryonic antigen radioimmunodetection in the evaluation of colorectal cancer and in the detection of occult neoplasms. Gastroenterology 84:524–532.
34. Mach, J.P., Buchegger, F., Forni, M., et al. (1987) Use of radiolabeled monoclonal anti-CEA antibodies for the detection of human carcinomas by external photoscanning and tomo-

scintigraphy. Immunol. Today 2:239–249.
35. Halpern, S.E., Hagan, P.L., Gomer, P.R., et al. (1983) Stability characterization and kinetics of In-111 labeled monoclonal anti-tumor antibodies in normal animals and nude mouse-human tumor models. Cancer Res. 43:5347–5355.
36. Krejcarek, G.E., and Tucker, K.L. (1987) Covalent attachment of chelating groups to macromolecules. Biochem. Biophys. Res. Commun. 77:581–585.
37. Lamki, L.M., Patt, Y.Z., Murray, J.L., et al. (1986) Scintigraphic findings of colonic cancer using indium-111 labeled anti-CEA monoclonal antibody (ZCE-025) combined with unlabeled antibody (abstract). J. Nucl. Med. 27:1021.
38. Philben, V.J., Jakowatz, J.G., Beatty, B.G., et al. (1986) The effect of tumor CEA content and tumor size on tissue uptake of indium-111-labeled anti-CEA monoclonal antibody. Cancer 57:571–576.
39. Martin, K.W., and Halpern, S.E. (1981) Carcinoembryonic antigen production, secretion, and kinetics in BALB/c mice and a nude mouse-human tumor model. Cancer Res. 44: 5474–5481.
40. Beatty, J.D., Duda, R.B., Williams, L.E., et al. (1986) Preoperative imaging of colorectal carcinoma with ^{111}In-labeled anticarcinoembryonic antigen monoclonal antibody. Cancer Res. 46:6495–6502.
41. Moldofsky, P.J., Sears, H.F., Mulhern, C.B., Jr., et al. (1984) Detection of metastatic tumor in normal-sized retroperitoneal lymph nodes by monoclonal antibody imaging. N. Engl. J. Med. 311:106–107.
42. Wahl, R.L., Parker, C.W., and Phillpot, G.W. (1983) Improved radioimaging and tumor localization with monoclonal $F(ab')_2$. J. Nucl. Med. 24:316–325.
43. Berche, C., Mach, J.P., Lumbroso, J.D., et al. (1982) Tomoscintigraphy for detecting gastrointestinal and medullary thyroid cancers: First clinical results using radiolabeled monoclonal antibodies against carcinoembryonic antigen. Br. Med. J. 285:1447–1451.
44. Khaw, B.A., Strauss, W., Cahill, S.L., Soule, H.R., Edington, T., and Cooney, J. (1984) Sequential imaging of indium-111 labeled monoclonal antibody in human mammary tumors hosted in nude mice. J. Nucl. Med. 25:592–603.
45. Halpern, S.E., and Dillman, R.O. (1987) Problems associated with radioimmunodetection and possibilities for future solutions. J. Biol. Resp. Modif. G:235–262.
46. Moldofsky, J., Powe, J., Mulhern, C.B., Jr., et al. (1983) Metastatic colon carcinoma detected with radiolabeled $F(ab')_2$ monoclonal antibody fragments. Radiology 149:549–555.
47. Herlyn, M., Steplewski, Z., Herlyn, D., and Koprowski, H. (1979) Colorectal carcinoma-specific antigen detection by means of monoclonal antibodies. Proc. Natl. Acad. Sci. USA 76:1438–1442.
48. Mangani, J.L., Brockhaus, M., and Smith, D.F. (1981) A monosialoganglioside is a monoclonal antibody defined antigen of colon carcinoma. Science 212:55–56.
49. Hnatowich, D.J., Griffin, T.W., Kosciuczyk, C., et al. (1985) Pharmacokinetics of an indium-111 labeled monoclonal antibody in cancer patients. J. Nucl. Med. 26:849–858.
50. Fucini, C., Tommasi, S.M., Rosi, S., et al. (1987) Follow-up of colorectal cancer resected for cure: An experience with CEA, TPA, Ca 19-9 analysis and second-look surgery. Dis. Colon Rectum 30:273–277.
51. Jones, P.L., Gallagher, B.M., and Sands, H. (1986) Autoradiographic analysis of monoclonal antibody distribution in human colon and breast tumor xenografts. Cancer Immunol. Immunother. 22:139–143.
52. Shah, S.A., Gallagher, B.M., and Sands, H. (1985) Radioimmunodetection of small human tumor xenografts in spleen of athymic mice by monoclonal antibodies. Cancer Res. 45: 5824–5829.
53. Keenan, A.M., Colcher, D., Larson, S.M., and Schlom, J. (1984) Radioimmunoscintigraphy of human colon cancer xenografts in mice with radioiodinated monoclonal antibody B72.3. J. Nucl. Med. 25:1197–1203.
54. Colcher, D., Esteban, J., Carrasquillo, J.A., Sugarbaker, P., Reynolds, J.C., Bryant, J.C., Larson, S.M., and Schlom, J. (1987) Complementation of intracavitary and intraveous

administration of a monoclonal antibody (B72.3) in patients with carcinoma. Cancer Res. 47:4218–4224.
55. Johnson, V.G., Schlom, J., Paterson, A.J., Bennett, J., Magnani, J.L., and Colcher, D. (1986) Analysis of a human tumor-associated glycoprotein (TAG-72) identified by monoclonal antibody B72.3. Cancer Res 46:850–857.
56. Begent, R.H.J., Green, A.J., Bagshawe, K.D., Jones, B.E., Keep, P.A., Searle, F., Jewkes, R.F., Barratt, G.M., and Ryman, B.E. Liposomally entrapped second antibody improves tumor imaging with radiolabeled (first) antitumor antibody. Lancet 2:739–741.
57. Hagan, P.L., Halpern, S.E., Dillman, R.O., et al. (1986) Tumor size: Effect on monoclonal antibody uptake in tumor models. J. Nucl. Med. 27:422–427.
58. Montz, R., Kilapdon, R., and Rothe, B. (1986) Immunoscintigraphy and radioimmunotherapy in patients with pancreatic carcinoma. Nuklearmedizin 25:239–244.
59. Gaffar, S., Pant, K.D., Sochat, D., Bennett, S.J., and Goldenberg, D.M. (1981) Experimental studies of tumor radioimmunodetection using antibody mixtures against carcinoembryonic antigen (CEA) and colon-specific antigen (CSA). Int. J. Cancer 27:101–105.
60. Greiner, J.W., Hand, P.H., Noguchi, P., Fisher, P.B., Pestka, S., and Schlom, J. (1984) Enhanced expression of surfact tumor-associated antigens on human breast and colon tumor cells after recombinant human leukocyte α-interferon treatment. Cancer Res. 44:3208–3214.
61. Greiner, J.W., Guadagni, F., Noguchi, P., et al. (1987) Recombinant interferon enhances monoclonal antibody-targeting of carcinoma lesions in vivo. Science 235:895–898.

16. Tumor targeting with monoclonal antibody B72.3: Experimental and clinical results

J. Schlom, D. Colcher, K. Siler, A. Thor, G. Bryant, W.W. Johnston, C.A. Szpak, P. Sugarbaker, J.A. Carrasquillo, J.C. Reynolds, A.M. Keenan, and S.M. Larson

Several monoclonal antibodies (Mabs) are currently the subject of active investigation in the diagnostic imaging of human carcinomas [1–11]. While the diagnostic targeting of a primary or metastatic carcinoma lesion with a Mab is an end unto itself, it should also be considered as a first step toward the use of that Mab in tumor therapy. This is particularly true in those studies in which biopsies of tumor and normal tissue are obtained subsequent to radiolabeled Mab administration. Dosimetry calculations can be made by: 1) analysis of these specimens for counts per minute (cpm) of Mab bound per gram of tumor versus cpm of Mab per gram of normal tissues and 2) analysis of the pharmacokinetics of Mab clearance from sera, to estimate the potential therapeutic efficacy of administering higher doses of the same radiolabeled Mab or for administering the same Mab coupled to a more efficient killer isotope. Alternatively, one gains information regarding the use of that Mab in a patient, either coupled to a drug or toxin, or the use of native Mab to elicit effector cell mechanisms.

There are obvious advantages and disadvantages to the various Mab-mediated therapeutic modalities (see Schlom for review [12]). This chapter, however, will consider the use of radiolabeled Mabs as potential therapeutic agents. This modality has two advantages: 1) tumor cell antigenic heterogeneity and phenotypic drift can perhaps be overcome, since many of the radionuclides being considered can kill from 5 to 10 cell diameters. Therefore, one can anticipate killing of an antigen-negative cell if it is adjacent to, or several cell diameters away from, an antigen-positive cell that has bound the radiolabeled Mab; 2) radiolabeled Mabs need not be internalized by tumor cells to kill them.

Mab B72.3 was developed by the immunization of mice with a membrane-enriched fraction of a human carcinoma metastasis [13]. It is a murine IgG_1 and the reactive antigen is a high-molecular-weight glycoprotein, with charac-

Goldenberg, D.M., (ed.), Cancer Imaging with Radiolabeled Antibodies.

teristics of a mucin, that has been termed *TAG-72* (tumor-associated glycoprotein) [14].

TAG-72 antigen

The TAG-72 antigen has been purified from a human colon carcinoma xenograft, designated *LS-174T* [14]. The tumor homogenate was first fractionated by Sepharose CL-4B chromatography. The high-molecular-weight TAG-72 found in the exclusion volume was then subjected to two sequential passages through B72.3-antibody affinity columns. At each step of the procedure, the TAG-72 content was quantitated using a competition radioimmunoassay [15,16], and the degree of purification was expressed as the ratio of antigen in units to total protein. The three-step procedure produced a purification of TAG-72 with minimal contamination by other proteins, as shown by polyacrylamide gel electrophoresis (PAGE), followed by staining with Coomassie blue or periodic acid/Schiff reagent. The density of affinity-purified TAG-72, as determined by cesium chloride gradient ultracentrifugation, was found to be 1.45 g/ml. This density determination, together with the high molecular weight of TAG-72, its resistance to chondroitinase digestion, the presence of blood-group-related oligosaccharides, and its sensitivity to shearing into lower molecular weight forms suggest that TAG-72 is a mucin-like molecule. The apparent molecular weight of TAG-72, as determined by sodium dodecyl sulfate (SDS)-PAGE and Western blotting analyses, is $> 10^6$ daltons [14].

Biologic distribution of the TAG-72 antigen

B72.3 has been reacted with a spectrum of adult and fetal human tissues using avidin-biotin-complex (ABC) immunohistochemical techniques to evaluate

Table 1. Mab B72.3 reactivity with formalin-fixed specimens of human neoplasia[a]

Organ	Histologic Tumor Type	No. Tested/ No. Reactive	> 20% Reactive Malignant Cells[b]
Ovary	Serous cystadenocarcinoma	30/30 (100)	14/30 (40)
	Mucinous cystadenocarcinoma	10/10 (100)	6/10 (60)
Lung	Squamous-cell carcinoma	3/3 (100)	1/3 (33)
	Adenocarcinoma	28/29 (97)	20/29 (69)
	Large-cell carcinoma	1/1 (100)	0/1
Colon	Adenocarcinoma	51/54 (94)	23/54 (43)
Breast	Invasive ductal carcinoma	37/44 (84)	12/44 (27)
Endometrium	Adenocarcinoma	32/32 (100)	

[a] Original data from Thor et al. [17].
[b] Numbers in parentheses show percentage.

the expression of the reactive TAG-72 antigen [17]. TAG-72 is expressed in several epithelial-derived cancers (Table 1), including most colonic adenocarcinomas [18], invasive ductal carcinomas of the breast [19,20], non-small-cell lung carcinomas [21,22], common epithelial ovarian carcinomas [23], as well as the majority of pancreatic, gastric, and esophageal cancers evaluated [17]. TAG-72 expression was not observed, however, in tumors of neural, hematopoietic, or sarcomatous derivation, suggesting that the TAG-72 antigen is 'pancarcinoma' in nature [17]. Appreciable Mab B72.3 reactivity was generally not observed in adult normal tissues (Table 2). This has been reviewed in detail elsewhere [17]. There is one normal adult tissue, however, in which TAG-72 is expressed at levels similar to those seen in carcinomas and that is secretory endometrium. We have shown [24] that while B72.3 is reactive with normal postovulatory endometria, it is nonreactive with proliferative-phase epithelia. TAG-72 expression was detected in all of 32 endometrial carcinomas examined, but was not expressed in resting, postmenopausal endometria. Studies on the biologic relevance of these findings, particularly as they pertain to reproductive physiology, are currently being investigated; at this point, however, no in-vivo binding of radiolabeled Mab B72.3 to normal endometrium has been observed (see below). Limited reactivity of Mab B72.3 has also been observed in some benign lesions of the breast and colon [17]. TAG-72 antigen expression was detected, however, in fetal colon, stomach, and esophagus, thus defining TAG-72 as an oncofetal antigen [17]. TAG-72 has previously been shown to be distinct from carcinoembryonic antigen and other tumor-associated antigens [25,26]. The pancarcinoma distribution and lack of appreciable reactivity with the vast majority of normal adult tissues of Mab B72.3 suggest its potential diagnostic and therapeutic utility for human carcinomas (Table 1).

Patient selection on the basis of immunohistologic data

Mab B72.3 has demonstrated utility as an immunocytochemical adjunct to diagnose carcinoma in cell block and cytocentrifuge preparations of human serous effusions, with selective reactivity for tumor cells (particularly adenocarcinoma) over reactive mesothelium [20,22,27,28]. Using the ABC method of immunoperoxidase staining and formalin-fixed, paraffin-embedded cell suspensions, Mab B72.3 detected tumor cells in effusions from the majority of patients with adenocarcinoma. No reactivity was demonstrated in any cell type in most benign effusions. Moreover, Mab B72.3 showed little or no reactivity to leukemic or lymphomatous effusions or to normal mesothelial cells from malignant effusions [27–29].

Mab B72.3 was also used with fine-needle aspiration biopsies (FNABs) and corresponding surgically excised tumors to determine cellular reactivity [20,28]. Positive staining with Mab B72.3 was observed in needle aspirates of the great majority of 'non-small-cell' carcinomas of the lung, adenocarcinomas

Table 2. Mab reactivity with formalin fixed normal human tissues[a]

Organ	Positive Cell Types (%)[b]
Esophagus	Squamous epithelium (<1)
Stomach	Mucous epithelium (<1)
Lung	Ciliated respiratory epithelium (5)
Kidney	Transitional epithelium (1)
Liver	Bile duct epithelium (1)
Salivary gland ducts	Large striated duct epithelium (15)
Uterus (secretory)	Uterine glandular epithelium (25)
Cervix (endo)	Columnar epithelium (1) (particularly with squamous metaplasia)
All Cell Types Negative: Bone marrow, Lymph node, Spleen, Thymus, Small intestine, Colon, Heart, Brain, Peripheral nerve, Skeletal muscle, Gall bladder, Bladder, Salivary gland, Smooth muscle, Ovary, Fallopian tube, Prostate, Testes, Thyroid, Parathyroid, Adrenal, Pancreas	

[a] Adapted from Thor et al. [17].
[b] Percentage of that particular cell type that is positive.

of the breast, adenocarcinomas of the colon, and carcinomas from other body sites. In contrast, small-cell carcinomas of the lung, malignant melanomas, lymphomas, sarcomas, and glial tumors did not stain with the antibody. Most benign lesions from the breast (with the exception of apocrine metaplasia), lung, pancreas, parotid, and thyroid also showed no staining. In many patients, tumor-bearing tissue had also been resected and was available for comparative examination with Mab B72.3. In more than 90% of these patients, the staining patterns of tumor cells in the aspirates were predictive of the patterns of antibody reactivity in the comparable surgically resected tumors. From these studies, we concluded that Mab B72.3 defines a tumor-associated antigen that is expressed in neo-plastic cells versus most benign cells, is most selectively expressed in carcinomas, and may be used as a novel adjunct for the diagnosis of neoplasms in effusions and in FNABs.

One advantage of the use of Mabs for targeting is the ability to obtain surgical biopsies, FNABs, or cytologic preparations to determine the reactive antigen content of individual patients' primary and/or metastatic lesions. Since Mab B72.3 works equally well in detecting TAG-72 in either formalin-fixed or frozen tissue specimens, patients can potentially be selected for tumor targeting studies (diagnostic and/or therapeutic) on the basis of immunohistologic findings.

TAG-72 in sera of carcinoma patients

Serum assays employing a specific Mab may be useful, not only to detect the presence of occult metastatic carcinoma, but 1) to identify those patients who

Table 3. Serum TAG-72 reference values in patients with cancer, benign diseases, and controls[a]

Group	No.	Mean TAG-72 (U/ml)	Fraction > TAG-72 below (U/ml)		
			> 6	> 10	> 20
Carcinomas	135	54.03	0.61	0.51	0.33
Rectum (NCI)[b]	26	99.76	0.77	0.58	0.38
Colon (NCI)	25	52.21	0.68	0.56	0.36
Pancreatic	19	44.77	0.79	0.74	0.53
Ovarian	19	65.42	0.58	0.52	0.36
Stomach	16	20.71	0.50	0.44	0.31
Lung	15	58.29	0.40	0.27	0.20
Breast	15	6.39	0.13	0.07	0.07
Benign diseases (gastrointestinal)	101	2.61	0.09	0.04	0.00
Controls[c]	1,099	1.83	0.042	0.013	0.002

[a] Taken from Klug et al. [16].
[b] NCI, National Cancer Institute Serum Panel.
[c] Controls include 1060 blood donors plus 39 NCI controls.
Sensitivities are expressed as the fraction of the group with TAG-72 concentrations greater than those specified by the column heading.

may be amenable to therapy using that Mab and 2) to monitor the efficacy of standard therapy. Several serum assays for carcinoma antigens are currently in use, including CEA, CA19-9, and CA125. The levels of TAG-72 in serum have been shown to be independent of the antigens detected by Mabs 19-9, OC125, and anti-CEA Mabs. These results point to the potential of using a TAG-72 assay along with other serum assays to increase the sensitivity and specificity of results.

An immunoradiometric assay has been developed using Mab B72.3 to quantitate TAG-72 in human serum [16] (Table 3). In a simultaneous immunoradiometric assay, the mean TAG-72 concentration in 1099 serum samples from healthy blood donors was 1.83 ± 2.03 U/ml. If the upper limit of normal was set at 10 U/ml of serum, a value including 99% of healthy blood donors, only 4 of 101 (4%) serum samples from patients with benign disease were elevated, whereas 15 of 26 (58%) and 14 of 25 (56%) of rectal and colon carcinoma patient sera, respectively, were positive [16]. Serum samples from 84 benign colorectal disease cases were examined; of these, 0 of 28 (0%) colorectal adenoma, 1 of 39 (3%) ulcerative proctocolitis, 0 of 15 (0%) diverticulosis, and 0 of 2 (0%) irritable bowel disease sera contained more than 10 U/ml TAG-72. At a reference value of 20 U/ml, 0 of 101 (0%) benign disease and 2 of 1060 (0.2%) blood-donor sera had elevated values, whereas 10 of 26 (38%) and 9 of 25 (36%) rectal and colon patient sera, respectively, remained positive. The majority of patients with pancreatic and ovarian cancer and a significant fraction of stomach cancer patient sera also contained elevated levels of TAG-72. The ability of this assay to discriminate between malignant and benign disease suggests its further evaluation for monitoring patients with known or suspected carcinoma [15,16].

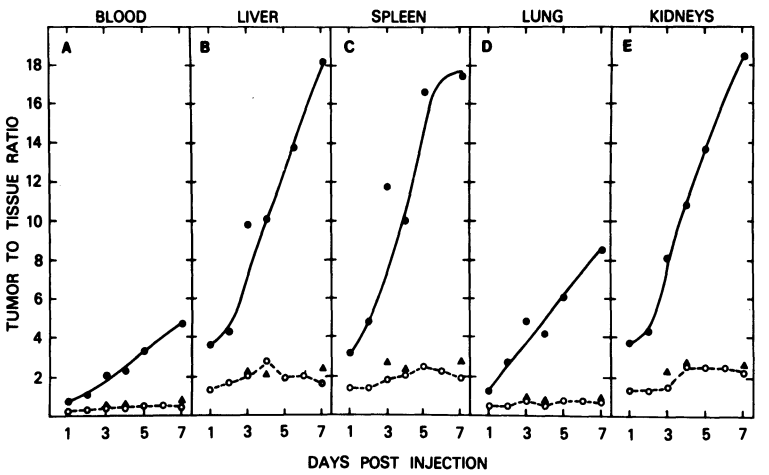

Figure 1. Tissue distribution of ^{125}I-B72.3 IgG in athymic mice bearing human tumors. Athymic mice bearing TAG-72 antigen-positive LS-174T colon carcinomas (closed circles) or antigen-negative A375 melanomas (open circles) were inoculated with approximately 1.5μCi of ^{125}I-B72.3 IgG. The mice were sacrificed over a 7-day period, and radioactivity per milligram of tissue was determined. The ratio of the activity in the tumor as compared with other organs was plotted. Mice bearing LS-174T colon carcinomas were also given isotype-identical control antibody MOPC-21 (closed triangles) [30, 31].

Preclinical model: Radiolocalization of human tumor xenografts in athymic mice

The use of an animal model (i.e., the targeting of a human tumor xenograft) can be criticized as an artificial indicator for tumor targeting in patients. While some criticisms of experimental models are valid, several parameters of tumor targeting can be analyzed in these situations: 1) the ability of a given Mab to remain bound to the tumor in vivo, 2) the ability of the radiolabel to stay bound to the Mab in an in-vivo setting, and 3) penetrance of a Mab through a tumor mass as analyzed via autoradiography.

B72.3 IgG was purified and was shown to be radiolabeled with ^{125}I or ^{131}I without loss of its reactivity to tumor extracts [30,31]. The radiolabeled B72.3 IgG was then shown to efficiently localize human colon carcinoma xenografts in athymic mice [30,31]. Radiolocalization indices rose over the 7-day period studied, with tumor/liver, tumor/spleen, or tumor/kidney ratios of approximately 18:1 at day 7 and a tumor/blood ratio of approximiately 5:1 at day 7 (Figure 1). Tumor/muscle or tumor/brain rose to over 100:1. The amount of radioactivity in the tumor increased for the first 2 days postinoculation of the antibody and stayed constant over a 19-day period of study [30,31]. Thus, there was no appreciable loss of radioiodine from the tumor over the study interval. No localization was seen in mice bearing a B72.3-antigen-negative

Table 4. Binding of ^{125}I-labeled monoclonal antibody B72.3 inoculated into athymic mice bearing LS-174T colon carcinoma xenografts or A375 melanoma xenografts[a]

		% of Injected Dose/Gram					
Tumor	Time (hr)	Tumor	Blood	Kidney	Spleen	Lungs	Liver
Colon carcinoma	18	7.29	9.94	1.82	2.23	5.22	1.89
	48	10.75	9.38	2.17	2.02	4.51	3.44
	72	8.97	4.46	1.07	0.77	1.82	0.93
	96	9.31	4.27	0.84	0.88	2.11	0.85
	120	4.54	1.37	0.33	0.30	0.77	0.34
	144	5.54	1.47	0.34	0.76	1.03	0.61
	166	6.49	1.38	0.34	0.37	0.75	0.37
Melanoma	18	4.77	21.86	3.42	3.40	10.07	3.63
	48	2.77	10.47	1.92	1.98	5.54	1.63
	72	3.91	10.47	2.59	2.35	6.34	1.82
	96	2.28	5.49	0.89	1.11	3.78	0.83
	120	1.06	2.21	0.38	0.43	1.49	0.46
	144	1.64	3.46	0.64	0.71	2.15	0.84
	166	1.92	4.77	0.83	1.06	2.65	1.18

[a] Taken from Colcher et al. [30].
The mean of the percentage of injected dose per gram of two to eight mice per time point is given for various tissues. The mice were given injections of approximately 1.5 μCi of ^{125}I-B72.3.

Table 5. Distribution of ^{125}-I-labeled monoclonal antibody B72.3 in an athymic mouse bearing a human colon carcinoma xenograft[a]

Day	cpm in Tumor	cpm in Total Body	% in Tumor
1	991	14,220	7.04
2	1,294	13,545	9.75
3	1,336	10,984	12.54
4	1,332	10,072	13.92
7	1,127	7,473	16.39
11	1,509	7,975	21.50
14	1,369	4,954	32.52
19	1.037	3,306	39.20

[a] Take from Colcher et al. [30].
Radioactivity was detected by the gamma camera in the region of interest. The counts are corrected for the nonuniformity of the pinhole and for the decay of the radionuclide.

human melanoma xenograft or with an isotype-identical control IgG_1 in mice bearing colon tumor xenografts (Table 4). Gamma-camera imaging with a pinhole collimator confirmed the ability of the radiolabeled antibody to detect the presence of colon carcinoma xenografts < 0.5 cm in diameter over a 19-day period (Table 5). Autoradiographic studies [32] demonstrated a heterogeneous distribution of radioactivity throughout the tumor mass at 11 days post Mab administration.

Radiolabeled Mab B72.3 in the localization of metastatic lesions in colorectal cancer patients

We recently investigated [33,34] the administration of radiolabeled Mab B72.3 in colorectal cancer patients and the quantitative evaluation of its reactivity with tumor lesions versus a wide range of normal tissues. These studies were possible due to a previously ongoing NCI Surgery Branch protocol for the treatment of patients with metastatic colorectal carcinoma that involved the surgical resection of metastatic colorectal cancer lesions plus adjacent 'normal' tissues for staging and therapeutic purposes. Thus, gamma scanning followed by a comprehensive direct examination of tumor and a variety of normal tissues could be achieved.

Approximately 7 days before surgery, patients received ^{131}I-labeled Mab B72.3 IgG. Patients were scanned with a gamma camera at approximately 2 hours post antibody administration and daily until surgery. At surgery, suspected carcinoma lesions and selected normal tissues were removed. Specimens from all biopsies were immediately weighed and placed in a gamma counter to determine cpm per gram. Tissues were then sent to pathology for routine histopathologic processing and examination. All tissues termed *carcinoma* or *normal* in this study were defined so on the basis of histopathologic examination by two pathologists. Fixed biopsy specimens were then analyzed for 1) percentage of tumor cells of total cells present and 2) TAG-72 antigen-positive cells using Mab B72.3 and the ABC immunoperoxidase reaction; the location of the reactive antigen (i.e., intracellular, membrane associated, and/or extracellular) was also noted [33,34].

Twenty-seven patients received ^{131}I-labeled B72.3 IgG and were subsequently scanned via a gamma camera. For medical and/or technical reasons, tissues were not removed at surgery or the tissues were not accessible to us for direct determination of cpm per gram in seven of these patients. Patients received a single dose of between 0.16 mg and 20.0 mg of purified IgG. The amount of ^{131}I coupled to the IgG ranged from 0.8 mCi to 10 mCi, and specific activities (i.e., millicuries ^{131}I per milligram IgG) ranged from 0.30 to 12.58. Positive gamma scans (confirmed at surgery) were observed in 14 of 27 patients and in 10 of 20 patients in which direct examination of tissues were available. There was no effect of IgG dose, millicurie amount, or specific activity on whether a gamma scan was positive or negative. Gamma scans accurately identified tumor lesions in the liver, bone, orbit, rectum, colon, caecum, pelvis, and diffusely in the peritoneal cavity. No anaphylaxis, serum sickness, decrease in white blood cell count or platelets, indication of bone marrow suppression, or other evidence of toxicity was observed in any of the patients administered the various doses and/or specific activities of ^{131}I-labeled Mab B72.3 or the isotype-identical control ^{125}I-labeled Mab BL-3 [34].

The radiolocalization index (RI) value is defined as the ratio of the uptake

Table 6. Radiolocalization index (RI) values of tumor and normal tissue biopsies of patients injected with ^{131}I-labeled B72.3 IgG[a]

	Tumor RI			Tumor Lesions			Normal Tissues		
Name	Min	Max	RI:	< 3	3–10	> 10	< 3	3–10[b]	> 10[c]
JP	8.5	29.6		0[d]	2	2	6	0	2
MP	5.3	45.8		0	5	13	8	0	0
HB	5.1	32.6		0	9	4	4	0	2
HK	10.3	10.3		0	0	1	20	0	0
PH	2.4	17.3		2	18	6	5	0	0
ML	4.8	8.9		0	3	0	20	0	0
BB	4.4	7.4		0	5	0	4	1	0
DF	3.9	7.3		0	5	0	16	0	0
CC	5.5	5.5		0	1	0	13	1	0
ES	2.3	5.3		1	4	0	8	0	0
EL	2.9	4.1		1	1	0	6	0	0
HL	1.1	8.2		10	9	0	3	0	0
TR	2.1	4.2		1	2	0	10	1	0
MS	1.4	4.5		3	5	0	15	2	0
HF	2.2	4.0		1	1	0	15	0	0
RC	2.0	3.4		1	1	0	3	2	0
EP	0.8	5.3		13	2	0	5	0	0
CM	1.7	2.4		5	0	0	7	0	0
JD	1.3	2.4		4	0	0	19	1	0
JR	1.4	1.4		1	0	0	11	0	0

[a] Reprinted from Esteban et al. [33].
[b] The average RI value of all tumor lesions obtained for a given patient.
[c] Spleen (n = 4); lymph nodes (n =2); peritoneum (n = 2); ileum (n = 2); omentum (n = 1); gallbladder (n = 1).
[d] Number of specimens with the indicated RI value.
The uptake of the radionuclide-monoclonal antibody complex in tissues was determined for all specimens removed at surgery. The tissues were examined histologically and classified as tumor or normal. The cpm per gram found in the various tissues was divided by the average cpm per gram found in histologically normal tissue to give the RI.

of ^{131}I-labeled Mab per gram of histologically confirmed tumor to that per gram of histologically confirmed normal tissue; average values (cpm per gram) from biopsy of normal liver and/or intestinal tissue of each patient were normalized to 1.0. RI values of ≥ 3.0 were arbitrarily considered as 'positive' for these studies. As can be seen in Table 6, at least one tumor lesion in 17 of 20 of the patients studied had an RI of ≥ 3.0. In eight of these patients, all 50 tumor lesions biopsied had RI values of ≥ 3.0. Five of the patients studied displayed 26 lesions with RI values of ≥ 10.0. In total, 99 of 142 (70%) carcinoma lesions biopsied displayed RI values of ≥ 3.0 [33,34] (Table 6).

In general, patients could be classified into several categories on the basis of RI values. One category includes those patients in whom all tumor tissues had RI values > 3 and all normal tissues that had RI values < 3. The next category is of patients who showed at least one tumor specimen that displayed an RI ≥ 3. This value appeared to be due to both the antigenic heterogeneity of tumor masses and, perhaps, the inability of IgG to get to particular tumor

Table 7. Mab B72.3 localization in biopsy specimens of patient MP[a]

Biopsy	%ID/g[b] ($\times 10^{-3}$)	RI[c]	Percentage		Immunoperoxidase Reactivity	
			Tumor	Mucin	Cells	Mucin
Carcinomas site						
Liver	6.90	30.5	95	76	15[d]	+++[e]
Serosa, small bowel (n = 4)	4.95	21.8	100	80	20	+++
Omentum, lesser	3.68	16.2	90	72	10	++
Site not specified	3.37	14.9	90	72	20	+++
Spleen	3.07	13.6	70	56	25	++
Colon, distal site	3.11	13.1	80	64	25	++
Lymph nodes, colon	2.65	11.7	80	68	15	+++
Serosa, small bowel	2.51	11.1	60	48	25	+++
Serosa, small bowel	1.56	6.9	90	72	25	+++
Lymph node, small bowel (n = 2)	1.49	6.6	60	51	25	++
Small bowel (necrotic)	1.20	5.3	10	8	15	+
Retroperitoneum (n = 2)	0.74	3.3	20	15	20	+
Normal tissue						
Adipose tissue	0.07	0.3			0	
Colon, distal margin	0.28	1.2			30[f]	
Muscle, abdominal wall	0.53	2.4			0	
Peritoneum, scar tissue abdomen	0.30	1.3			0	
Small bowel (edematous)	0.28	1.3			0	

[a] Reprinted from Esteban et al. [33].
[b] Percentage of injected dose of ^{131}I-labeled Mab B72.3 per kilogram of tissue; surgery was performed 8 days post administration of the antibody.
[c] RI determined by dividing the %ID/kg of the tumors by the average %ID/kg of all normal tissues.
[d] Percentage of carcinoma cells reactive with B72.3.
[e] Scaled from very strong (+++) to negative (−).
[f] Normal colon mucosa adjacent to tumor.

masses or parts of tumor masses. Another category of patients includes those who had one normal tissue with an RI $\geq$ 3.

Table 7 details results of the pattern of Mab biodistributions encountered for one patient as an example. All tumor biopsies removed from various sites demonstrated RI values of > 3, with some higher than 30. RI values of $\leq$ 3 were observed for all five normal tissue biopsies [33].

Tumor biopsies were grouped according to their anatomic site. As shown in Table 8, the percentage of tumor lesions with an RI $\geq$ 3 among the different sites was similar, ranging from 50% to 100%, with the exception of the spleen, where only 1 of 4 tumors was positive; however, this latter observation could very well be due to the small number of biopsy samples available.

Tumor biopsies of all 20 patients were studied by light microscopy on H & E stained slides to determine their type, grade, presence of necrosis, and other histologic characteristics. The tumors represented approximately equivalent numbers of well-differentiated adenocarcinomas, well-differentiated adeno-

Table 8. Localization of IV-administered ^{131}I-labeled B72.3 IgG to carcinoma lesions[a]

Site of Carcinoma	RI[b]			Positive RI/Total[c]
	< 3	3–10	> 10	
Liver	4	24	1	25/29 (86)
Colon	5	10	2	12/17 (71)
Small intestine	3	1	3	4/7 (57)
Lymph node	4	7	2	9/13 (69)
Lung	3	6	2	8/11 (73)
Peritoneum	18	18	8	26/44 (59)
Pelvis	1	1	0	1/2 (50)
Soft tissue	2	3	3	6/8 (75)
Spleen	3	0	1	1/4 (25)
Other[d]	0	5	2	7/7 (100)
Total	43 (30%)	75 (53%)	24 (17%)	99/142 (70)

[a] Reprinted from Esteban et al. [33].
[b] The %ID/kg of every biopsy specimen was divided by the %ID/kg of the normal tissue(s) used as standard to determine the RI.
[c] An RI > 3 is considered positive for Mab localization. Numbers in parentheses are the positive percentages.
[d] Ovaries (n = 3), fallopian tubes (n = 2), pouch of Douglas (n = 1), and vena cava (n = 1).

carcinomas of the mucinous type, and moderately differentiated adenocarcinomas. One tumor was classified as a signet-ring variant of adenocarcinoma. The percentage of lesions with RI values ≥ 3 was very similar for every histologic group, with values of 56%, 75%, 84%, and 47%, respectively. However, there was a striking difference in the histologic characteristics of the tumor when examining those lesions with RI values > 10. Of the mucinous-type tumors, 31% (25 of 81) had an RI > 10, whereas only 0%, 5%, and 0% of the well-differentiated, moderately differentiated, and signet-ring cell adenocarcinomas, respectively, had an RI > 10. Mucinous adenocarcinomas are therefore the histologic type of tumor that had the overall highest uptake of the ^{131}I-labeled B72.3 IgG [33].

Autoradiography was employed to observe the penetration and distribution of the radiolabeled Mab through the tumor mass. The scatter of the radionuclide did not allow the determination of the exact location within the cell (i.e., membrane bound, intracytoplasmic). The distribution of the silver grains was heterogeneous, with foci of intense activity alternating with areas lacking grains, but radioactivity was equally distributed in the medial and peripheral regions of the tumor, indicating a good penetration of the label throughout the tumor mass. Mab localization was predominantly seen within the mucinous pools of tumors, although concentration in the cells was also present.

Of 210 histologically confirmed normal tissues biopsied, 198 showed negative RI values (< 3). In 12 patients, all apparently normal tissue biopsies had a negative RI. Twelve biopsy specimens from eight patients showed RI

values of > 3.0. In all but two cases, these tissues were immediately adjacent to carcinoma or draining carcinoma; in two cases, high RI values were seen in spleen biopsies. These high values may have been due to the presence of antigen-antibody immune complexes in spleen and not direct binding of ^{131}I-labeled Mab to spleen cells, because 1) both patients had high levels of circulating ^{131}I-B72.3/TAG-72 antigen complexes (as analyzed by HPLC size-exclusion chromatography) and 2) spleen biopsy specimens from two other patients who did not have high levels of circulating immune complexes had RI values for spleen of < 3. While immune complexes may also localize in the liver, none were observed either in scans or in biopsies taken from normal liver, although no liver biopsies were obtained from patients with high levels of circulating immune complexes. Thus, of the 210 biopsies of normal tissues, including colon, liver, spleen, lungs, small intestine, peritoneum, etc., no tissue was consistently positive for Mab B72.3 uptake [33].

An isotype-identical Mab (BL-3) was used as a control in four patients to delineate the selective binding of Mab B72.3 for colon carcinoma lesions. Mab BL-3 is a murine IgG_1 antiidiotype Mab that is reactive with a B-cell lymphoma. Mab BL-3 was radiolabeled with ^{125}I, and more than 80% of the activity specifically bound to the idiotype IgM. The same amount (1.5 mg) of ^{125}I-labeled BL-3 as ^{131}I-labeled B72.3 was coinjected into several patients. Mab BL-3 showed no specific localization in tumor tissues, with two to four times less binding than Mab B72.3; however, equivalent amounts of both BL-3 and B72.3 were observed in histologically normal tissues, such as colon, small intestine, liver, peritoneum, omentum, lymph nodes, and gallbladder [34].

TAG-72 antigen levels were evaluated before antibody administration by a radioimmunoassay (RIA) described previously [15,16]. We have shown that approximately 60% of patients with colorectal cancer have elevated TAG-72 levels. In no cases, however, did an elevated TAG-72 level appear to interfere with antibody binding to tumor.

Intracavitary administration of radiolabeled Mab B72.3

Studies were undertaken to 1) determine the feasibility of intraperitoneal administration of radiolabeled B72.3 for tumor localization (via both gamma scanning and direct analyses of biopsy specimens); 2) determine the specificity of tumor localization by the concomitant IP administration of ^{131}I-labeled B72.3 and an isotype-matched, control, ^{125}I-labeled Mab BL-3 (anti-idiotype) IgG; 3) compare tumor localization of IV- versus IP-administered Mab by the simultaneous administration of ^{125}I-B72.3 IgG IV and ^{131}I-B72.3 IgG IP; and 4) define the pharmacokinetics of plasma clearance of both IP- and IV-administered radiolabeled Mab B72.3.

All patients in this study were part of a preexisting NCI Surgery Branch protocol for the surgical resection of metastatic colorectal cancer lesions

followed by IP administration of therapeutic agents. At the time of entry into the protocol, all patients had confirmed or suspected metastatic peritoneal lesions. Four to 7 days before surgery, all patients were administered ^{131}I-labeled B72.3 IgG IP via a catheter.

As mentioned above, previous studies [33,34] using IV-administered ^{131}I-radiolabeled B72.3 IgG have shown that differences in administration of between 0.2 and 20 mg of IgG, or between 0.8 and 10 mCi of ^{131}I (with a specific activity range of 0.3–12 mCi/mg) had little or no effect on the radiolocalization of colon-carcinoma lesions, as determined by gamma scanning or direct analysis of tumor samples (percentage ID of Mab bound per kilogram of tissue, %ID/kg). Therefore, all patients received between 0.76 and 1.2 mg of IgG and between 5.0 and 10.0 mCi ^{131}I, with specific activities of ^{131}I-B72.3 IgG ranging from 6.6 to 11.0 mCi/mg [35].

On the day of, or prior to, surgery, patients were scanned with a gamma camera; all scan results were interpreted before surgery. Gamma scans of 7 of 10 patients showed clearly discernable concentrations of radiolabeled Mab in various distinct regions of the peritoneum. In all such cases, these lesions were identified at surgery as tumor and later confirmed as carcinoma via

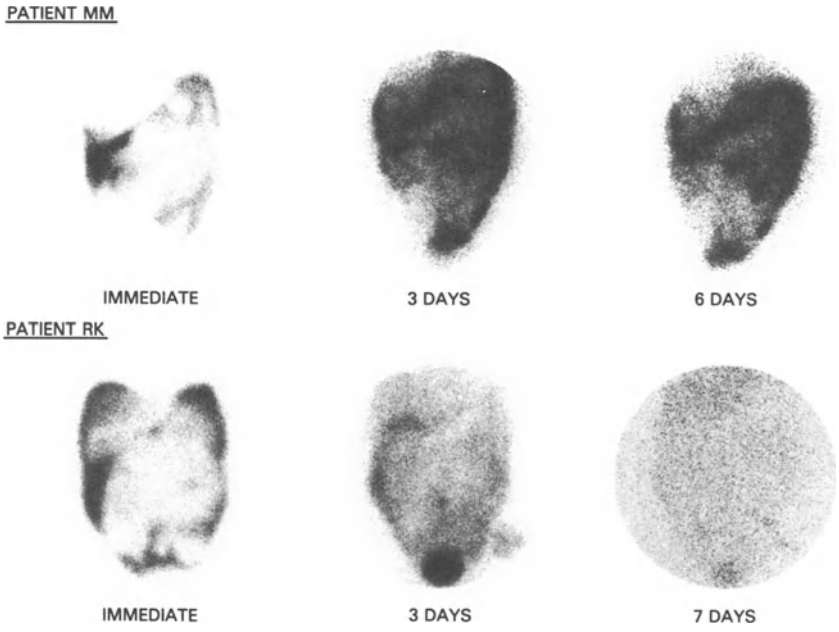

Figure 2. Radioimmunoscintigraphy in patients with metastatic colorectal cancer after IP administration of ^{131}I-B72.3 IgG. Two patients were injected IP with radiolabeled B72.3 IgG. Patients RK and MM were scanned immediately after antibody administration and at various times, as indicated in the figure. Patient RK, with no peritoneal tumor, was negative for B72.3 localization, whereas the peritoneal tumor was visualized by B72.3 in patient MM [35].

histopathologic examination. A representative positive gamma scan is shown in Figure 2 (patient MM). Note the accumulation of radiolabeled Mab in the 'gutters' of the peritoneum immediately after IP Mab administration and at 3 days post Mab administration. The gamma scan at 6 days post ^{131}I-B72.3 administration, however, shows Mab concentration in distinct areas of the peritoneum (confirmed as cancer via surgery and histopathology). These findings can be contrasted with the negative gamma scans of patient RK; patient RK was a patient with no intraperitoneal disease.

Three of the 10 patients studied were positive for Mab localization via gamma scanning (areas confirmed as tumor at surgery) but were negative for

Table 9. IP administration of ^{131}I-B72.3 IgG (patient MM)[a]

Tissue Description	%ID/gm ($\times 10^{-3}$)	RI[b]	% Tumor
Carcinomas			
Peritoneal implants:			
Intraabdominal tumor (n = 4)	16.75	66.5	90
Lesser sac	13.72	54.5	90
Gastrohepatic	13.16	52.3	95
Splenic flexure (n = 2)	11.47	45.6	90
Small-bowel serosa	9.84	39.1	85
Periaortic	7.14	28.4	20
Diaphragm undersurface	6.81	27.1	85
Tail pancreas	6.07	24.1	80
Serosa colon	6.06	24.1	90
Gastric artery	5.88	23.4	70
Omentum	5.03	20.0	80
Pancreas surface	4.49	17.8	80
Ileum lymph node (n = 2)	2.08	8.3	90
Transverse colon serosa (n = 2)	1.66	6.6	90
Falciform ligament	1.52	6.0	25
Sigmoid serosa	1.42	5.6	85
Liver dome	0.94	3.7	70
Nonimplants:			
Cecum and granulation tissue	0.85	3.4	60
Splenic capsule	0.60	2.4	80
Appendix	0.48	1.9	40
Ileum and adipose tissue	0.41	1.6	70
Normal			
Adipose tissue (n = 2)	0.11	0.4	
Colon	0.15	0.6	
Ileum	0.26	1.0	
Lymph node (n = 5)	0.22	0.9	
Skin and fat	0.24	0.9	
Soft-tissue fistula tract	0.36	1.4	

[a] Taken from Colcher et al. [35].
[b] RI was determined by dividing the %ID/kg of the tumors by the averaged %ID/kg of normal ileum and lymph nodes.

tumor via CAT scanning and x-ray studies. Lesions as small as approximately 1.5 cm in diameter were clearly defined via gamma scans.

All specimens removed at surgery were analyzed for counts per minute per kilogram of tissue. Specimens were then fixed, embedded, and analyzed for percentage of carcinoma cells present. Table 9 shows representative data from one patient (patient MM, whose scan is seen in Figure 2); histologically confirmed normal tissues, removed for staging purposes, show between 0.11% and 0.36% injected dose (%ID) of ^{131}I-B72.3 Mab per kilogram (i.e. %ID/g $\times$ 10^{-3}) of tissue. By contrast, the various carcinoma lesions of different sites showed between 0.41 and 16.75% ID/kg. These data can also be expressed as RI values, i.e., the ratio of the %ID/kg in tumor versus the %ID/kg of normal tissue. As seen in Table 9, the RI values of the histologically confirmed normal tissues range from 1.6 to 66.5, and most tumors (23 of 27) have RI values $\geq$ 3 [35].

Table 10 shows the RI values (based on %ID Mab uptake per kilogram of tissue) of the biopsy specimens of tumor and normal tissues from the ten patients receiving IP-administered Mab B72.3. An RI of $\geq$ 3 was arbitrarily chosen as a 'positive' radiolabeled uptake. Eighty-three of 112 (74%) carcinoma lesions showed RI values $\geq$ 3. In some patients with a large tumor burden, as much as 40% of the injected dose was found bound to carcinoma. Note that of the 29 lesions negative for Mab uptake, 11 were from patient MG, the only patient in whom all tumor lesions were negative for TAG-72 antigen expression. Of the 95 histologically confirmed normal tissues biopsied, all but one demonstrated RI values < 3 (Table 10). The one biopsy not in this category had an RI of 3.5 and was a histologically normal spleen from patient JB. Interestingly, this patient had the highest level of circulating antigen/^{131}I-B72.3 IgG immune complex, as determined by HPLC and RIA. The

Table 10. RI values of patients injected IP with ^{131}I-labeled B72.3[a]

	Tumor			Normal		
Name RI:	< 3	3–10	> 10	< 3	3–10	> 10
NJ	0	1	17	12	0	0
MH	2	4	0	10	0	0
RK	5	3	0	8	0	0
MM	4	5	18	11	0	0
MG	11	0	0	7	0	0
WJ	2	7	3	25	0	0
EP	0	7	2	1	0	0
SM	5	6	1	6	0	0
JB	0	0	6	12	1	0
JK	0	0	3	3	0	0
Total lesions	29	33	50	95	1	0
Percentage	26	29	45	99	1	0

[a] Taken from Colcher et al. [35].

other 94 normal tissue biopsies with RI values < 3 were from numerous sites, including colon, spleen, ileum, pancreas, lymph node, fallopian tube, liver, ovary, duodenum, and kidney; the vast majority of RI values ranged from 0.5 to 1.5 [35].

Specificity of Mab B72.3 radiolocalization

To determine if the radiolocalization observed with the IP-administered ^{131}I-B72.3 IgG was specific, four patients received concomitant infusions (administered IP) of ^{131}I-B72.3 IgG and ^{125}I-labeled control Mab BL-3 IgG. B72.3 and BL-3 were administered at the same milligram dose and time for each patient. There were some important observations obtained in these analyses concerning 'nonspecific' Mab uptake. Mab BL-3 uptake was negative (i.e., RI < 3) in 28 carcinoma lesions but showed RI values ≥ 3 in 11 others. When the ratios of %ID/kg of these lesions for B72.3 versus BL-3 were analyzed, in none of the 39 lesions was BL-3 uptake greater than that of B72.3. In eight lesions the ratios were comparable, and in 31 of 39 lesions the B72.3/BL-3 ratios were greater than 2:1, with ratios of greater than 10:1 in the majority of cases; ratios of > 100:1, moreover, were observed for many lesions. Thus, while these results demonstrate the specificity of the B72.3 binding, they do point out that 'nonspecific' binding of irrelevant Mab to carcinoma lesions may and does indeed occur at times.

Simultaneous IP and IV administration of Mab B72.3

Studies were next conducted to determine the relative efficacies of IP- versus IV-administered Mab to localize tumor lesions [35]. To achieve this goal, patients were concomitantly administered ^{131}I-labeled B72.3 IP and ^{125}I-labeled B72.3 IV. Both the IP and IV-administered Mab preparations in each of four patients were identical as far as milligram dose and radiolabeling conditions. In 35 of 55 carcinoma lesion biopsies obtained, the IP-administered B72.3 localized at least two times better in terms of %ID/kg than the IV-administered Mab. In seven lesions, Mab localization was comparable via either route, and in 13 lesions, the IV-administered Mab B72.3 localized at least two times better than the IP-administered Mab. For example, as seen for patient NJ (Table 11), %ID/kg taken up by carcinoma lesions ranged from 11.4 to 45.3 %ID/kg for IP-administered B72.3 (^{131}I) versus values of only 2.8–11.3 %ID/kg for the IV-administered B72.3 (^{125}I). The ratios of uptake of the IP-administered Mab were from 2.8 to 7.6 times greater for individual lesions than the IV-administered Mab. The levels of uptake in the normal tissues of the IV- and IP-administered B72.3 IgG were similar [35].

Table 11. Concomitant administration of ^{131}I-B72.3 IP and ^{125}-B72.3 IV (patient NJ): Advantage of IP route

Tissue Description	%ID/kg		%ID/kg Ratios	RI[b]		
	IP ^{131}I	IV ^{125}I	^{131}I/^{125}I	IP ^{131}I	IV ^{125}I	% Tumor
Carcinoma						
Omentum	44.51	5.85	7.61	32.6	12.2	80
Mesentery, sigmoid colon	40.04	5.42	7.39	29.3	11.3	80
Peritoneal liver capsule (n = 4)	39.62	9.19	5.64	29.0	19.1	66
Peritoneal gastroesophageal junction	39.27	8.45	4.65	28.8	17.6	80
Omentum, greater	11.41	2.75	4.16	8.4	5.7	40
Peritoneal peripancreas	45.27	11.30	4.01	33.2	23.5	85
Omentum, lesser (n = 2)	27.08	7.54	3.68	19.8	15.7	63
Diaphragm (n = 3)	27.23	7.76	3.48	19.9	16.2	68
Peritoneal spleen, capsule (n = 4)	29.30	10.72	2.77	21.5	22.3	69
Normal						
Adipose tissue	0.07	0.05	1.31	0.1	0.1	0
Mesentery, transverse colon	0.52	0.49	1.07	0.4	1.0	0
Peritoneum, right	0.84	0.66	1.26	0.6	1.4	0
Peritoneal adhesions (n = 3)	1.21	0.78	1.56	0.9	1.6	0
Abdominal scar	0.99	0.47	2.09	0.7	1.0	0
Falciform ligament	1.04	0.37	2.82	0.8	0.8	0
Spleen (n = 3)	2.70	3.45	0.78	2.0	7.2	0

[a] Taken from Colcher et al. [35].
[b] RI was determined by dividing the %ID/kg of the tumors by the averaged %ID/kg of all normal biopsies.

In an attempt to define the reason(s) for the divergence in uptake of IP- and IV-administered Mab among different carcinoma lesions, three pathologists independently examined these lesions and characterized them as to various properties (two of the pathologists were not told the reason for this exercise). The most striking correlation with differential Mab uptake was whether a given metastasis was a peritoneal implant or 'nonimplant.' Metastatic lesions were characterized as 1) peritoneal implants or 2) nonimplant metastases, i.e., hematogenously borne metastases, lymph-node metastases, or local recurrences. For those lesions where all three pathologists did not arrive at the identical conclusion, the lesion was listed as 'unclassified.' In all ten nonimplant metastases from three patients, the ratios (%ID Mab/kg) of uptake of the IV-injected B72.3 were at least two times that of the IP-administered Mab, with the ratios ranging up to 38:1. Conversely, in 35 of 40 lesions classified as peritoneal implants, IP-administered B72.3 localized at least two times better than IV-administered Mab, with the ratios obtained for the majority of lesions being greater than 5:1. Five of 40 peritoneal implants bound comparable levels of IP- and IV-administered B72.3.

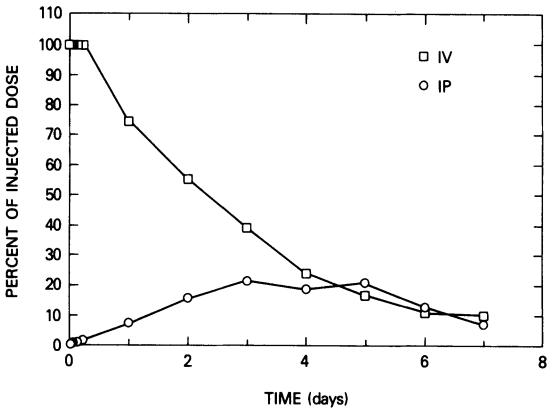

Figure 3. Plasma clearance of B72.3 IgG after administration both IV and IP in patients with colorectal cancer. Patients were injected IV with ^{125}I-B72.3 IgG and IP with ^{131}I-B72.3 IgG. Plasma samples were drawn at various times. The open circles denote the Mab plasma clearance levels for patients receiving IP-administered Mab. The open squares denote the Mab plasma clearance levels for patients receiving IV-administered Mab. [35].

Pharmacokinetics of plasma levels after IP Mab administration

Plasma samples from eight patients studies were obtained before Mab administration and at various time points post Mab administration [35]. The plasma clearance of the IV-administered ^{125}I-B72.3 IgG and the ^{125}I-BL-3 control IgG were similar, with approximately 50% of the injected dose in the plasma at day 2 and approximately 10% of the injected dose in plasma at day 7 post Mab administration (Figure 3). In contrast, no more than 30% of the injected dose of IP-administered B72.3 IgG or BL-3 appeared in the plasma at any point in time, with peak values being obtained at days 2–3.

The appearance of ^{131}I-B72.3 IgG in the plasma was noted to be reduced in 4 of 8 patients studied in that ^{131}I-labeled-Mab levels in plasma did not rise above 10–12% of the injected dose. Pre-Mab administration plasma samples were tested for the B72.3-reactive antigen TAG-72 via RIA, as previously described [15,16], and revealed that sera from these four patients showed the highest levels of circulating TAG-72 antigen.

Several diagnostic implications from the studies can be drawn. Radiolabeled B72.3 may now be considered for use in the localization of suspected colorectal or ovarian carcinoma lesions. Radiolabeled B72.3 can also be used, along with the serum assay for the presence of TAG-72 antigen, to monitor the efficacy of various therapies. The studies reported here demonstrated that carcinoma was detected by IP-administered ^{131}I-labeled B72.3, but could not be detected by CAT scan or other radiographic procedures in 3 of 10 patients studied; lesions as small as 1.5 cm were detected. Furthermore, the efficacy of detection should improve when radionuclides, such as ^{99m}Tc and ^{111}In, with

more favorable imaging characteristics are substituted for ^{131}I.

These studies have also demonstrated the potential of IP-administered B72.3 as a therapeutic agent, whether coupled to drugs, effector cells, or radionuclides. Direct analyses of biopsy and plasma specimens have permitted dosimetry calculations [36] that indicate that if higher doses of ^{131}I-B72.3 IgG are employed, sufficient radiolabeled Mab may be delivered to tumor masses for cell killing with minimal toxicity to normal tissues. Efficiency of killing will increase, moreover, when more efficient cytotoxic radionuclides, such as ^{90}Y, are coupled to B72.3; studies to develop such reagents are currently in progress. The studies reported here have also shown that only a minor component of the IP-administered radiolabeled Mab IgG is found in the plasma, an important point to consider if one wishes to minimize plasma-borne radiolabeled Mab as a potential source of marrow toxicity. Thus, these studies have demonstrated the necessity of considering either the sole use of intracavitary administered Mab or the concomitant use of intracavitary- and IV-administered Mab in protocols aimed at Mab-guided diagnosis or therapy of a wide range of human carcinomas.

Innovations

While successful tumor targeting has been achieved with ^{131}I-B72.3 when administered via the IV or IP route, several innovations in these systems have either recently been accomplished or are being pursued. These include:

Recombinant chimeric B72.3

The development of this reagent [37] makes feasible: 1) the reduction of the human anti-murine IgG response as a result of multiple Mab administrations, since constant regions of the recombinant/chimeric B72.3 are human, 2) alterations in human pharmacokinetics via alterations of Ig domains or glycosylation sites, so that the Mab clears the body faster, 3) the insertion of binding sites for more efficient binding of radionuclide chelate complexes, drugs, or effector cells, 4) changes in Ig isotypes, e.g., human IgG_1 can be substituted for a human IgG_4, and 5) alterations in affinity by modifying the hinge region or via changes in the antigen-binding region.

Chelate chemistry

The studies described above were all conducted with ^{131}I- or ^{125}I-radiolabeled Mabs. Iodine is clearly suboptimal for diagnostic imaging as well as therapeutic purposes. Several studies are ongoing [38] using new chelate chemistries for the more efficient coupling of both diagnostic and therapeutic radionuclides to Mab B72.3.

Mab combinations

We have detailed elsewhere [17] the large degree of heterogeneity of TAG-72 expression within most carcinoma masses. One obvious way of overcoming this heterogeneity is the use of Mab combinations. We have recently demonstrated [39] a great deal of complementarity between the use of B72.3 and an anti-CEA Mab (Mab COL-4) [40] in the reactivity to gastrointestinal malignancies. In a series of 17 gastric carcinomas, B72.3 reacted to greater than 90% of the cells of one tumor, while COL-4 reacted to $\geqslant 90\%$ of the cells in two tumors. When used in combination, however, 13 of 17 carcinomas showed reactivity to $> 90\%$ of cells, with many showing $> 99\%$ of cells with Mab binding.

Enhancement of tumor antigens by recombinant IFN

An alternate approach to overcome tumor cell antigenic heterogeneity and antigenic modulation is the use of recombinant (r)IFN. This has been detailed elsewhere [41–43] and appears to have important implications in the more efficient use of many Mabs for tumor diagnosis and therapy.

Second-generation Mabs and Mabs of predefined specificity

The TAG-72 antigen has been highly purified by a variety of chromatographic techniques, including B72.3 affinity columns [14]. This has led to the use of purified TAG-72 as an immunogen in the development of a 'second generation' of Mabs to B72.3. These Mabs [44] were selected on the basis of their high affinity and their ability to efficiently bind human tumors. Furthermore, as the analysis of the TAG-72 proceeds, amino-acid sequence data may well lead to the development of another generation of Mabs of predefined specificity prepared against synthetic peptides. Thus, the parameters listed here, among others, will determine the ultimate utility of Mab B72.3, or a 'descendent' thereof, in the diagnostic targeting and/or therapy of certain human carcinomas.

References

1. Epenetos, A.A,, Snook, D., Durbin, H., Johnson, P.M., and Taylor-Papadimitriou, (1986) Limitations of radiolabeled monoclonal antibodies for localization of human neoplasms. Cancer Res. 46:3183–3191.
2. Beatty, J.D., Duda, R.B., Williams, L.E., Sheibani, K., Paxton, R.J., Beatty, B.G., Philben, V.J., Werner, J.L., Shively, J.E., Vlahos, W.G., Kokal, W.A., Riihimaki, D.U., Terz, J.J., and Wagman, L.D. (1986) Preoperative imaging of colorectal carcinoma with ^{111}In-labeled anticarcinoembryonic antigen monoclonal antibody. Cancer Res. 46:6494–6502.
3. Allum, W.H., MacDonald, F., Anderson, P., and Fielding, J.W.L. (1986) Localisation of gastrointestinal cancer with a ^{131}I-labeled monoclonal antibody to CEA. Br. J. Cancer 53:

203–210.
4. Pateisky, N., Philipp, K., Skodler, W.D., Czerwenka, K., Hamilton, G., and Burchell, J. (1985) Radioimmunodetection in patients with suspected ovarian cancer. J. Nucl. Med. 26: 1369–1375.
5. Wahl, R.L., Khazaeli, M.B., LoBuglio, A.F., Patillo, R.A., Tuscan, M.J., and Beierwaltes, W.H. (1987) Radioimmunoscintigraphic detection of occult gestational choriocarcinoma. Am. J. Obstet. Gynecol. 156:108–111.
6. Mach, J.-P., Buchegger, F., Forni, M., Ritschard, J., Berchi, C., Lumbroso, J.-D., Schreyer, M., Girardet, C., Accola, R.S., and Carrel, S. (1981) Use of radiolabeled monoclonal anti-CEA antibodies for the detection of human carcinomas by external photoscanning and tomoscintigraphy. Immunol. Today 2:239–249.
7. Moldofsky, P.J., Powe, J., Mulhern, C.B., Jr., Hammond, N., Sears, H.F., Gatenby, R.A., Steplewski, Z., and Koprowski, H. (1983) Metastatic colon carcinoma detected with radiolabeled $F(ab')_2$ monoclonal antibody fragments. Radiology 149:549–555.
8. Mach, J.-P., Chatal, J.-F., Lumbroso, J.-D., Buchegger, F., Forni, M., Ritschard, J., Berche C., Douillard, J.-Y., Carrel, S., Heryln, M., Steplewski, Z., and Koprowski, H. (1983) Tumor localization in patients by radiolabeled monoclonal antibodies against colon carcinoma. Cancer Res. 43:5593–5600.
9. Chatal, J.-F., Saccavini, J.-C., Fumoleau, P., Doulliard, J.-Y., Curtet, C., Kremer, M., LeMevel, B., and Koprowski, H. (1984) Immunoscintigraphy of colon carcinoma. J. Nucl. Med. 25:307–314.
10. Armitage, N.C., Perkins, A.C., Pimm, M.V., Farrands, P.A., Baldwin, R.W., and Hardcastle, J.D. (1984) The localization of an anti-tumour monoclonal antibody (791T/36) in gastrointestinal tumours. J. Surg. 71:407–412.
11. Goldenberg, D.M., Kim, E.E., Bennett, S.J., Nelson, M.O., and DeLand, F.H. (1983) Carcinoembryonic antigen radioimmunodetection in the evaluation of colorectal cancer and in the detection of occult neoplasms. Gastroenterology 84:524–532.
12. Schlom, J. (1986) Basic principles and applications of monoclonal antibodies in the management of carcinomas: The Richard and Hinda Rosenthal Foundation Award Lecture. Cancer Res. 46:3225–3238.
13. Colcher, D., Horan Hand, P., Nuti, M., and Schlom, J. (1981) A spectrum of monoclonal antibodies reactive with human mammary tumor cells. Proc. Natl. Acad. Sci. USA 78: 3199–3203.
14. Johnson, V.G., Schlom, J., Paterson, A.J., Bennett, J., Magnani, J.L., and Colcher, D. (1986) Analysis of a human tumor-associated glycoprotein (TAG-72) using monoclonal antibody B72.3. Cancer Res. 46:850–857.
15. Paterson, A.J., Schlom, J., Sears, H.F., Bennett, J., and Colcher, D. (1986) A radioimmunoassay for the detection of a human tumor-associated glycoprotein (TAG-72) using monoclonal antibody B72.3. Int. J. Cancer 37:659–666.
16. Klug, T.L., Sattler, M.A., Colcher, D., and Schlom, J. (1986) Monoclonal antibody immunoradiometric assay for an antigenic determinant (CA 72) on a novel pancarcinoma antigen (TAG-72). Int. J. Cancer 38:661–669.
17. Thor, A., Ohuchi, N., Szpak, C.A., Johnston, W.W., and Schlom, J. (1986) The distribution of oncofetal antigen TAG-72 defined by monoclonal antibody B72.3. Cancer Res. 46: 3118–3124.
18. Stramignoni, D., Bowen, R., Atkinson, B., and Schlom, J. (1983) Differential reactivity of monoclonal antibodies with human colon adenocarcinomas and adenomas. Int. J. Cancer 31:543–552.
19. Nuti, M., Teramoto, Y.A., Mariani-Costantini, R., Horan Hand, P., Colcher, D., and Schlom, J. (1982) A monoclonal antibody (B72.3) defines patterns of distribution of a novel tumor associated antigen in human mammary carcinoma cell populations. Int. J. Cancer 29: 539–545.
20. Nuti, M., Mottolese, M. Viora, Donnorso, R.P., Schlom, J., and Natali, P.G. (1986) Use of monoclonal antibodies to human breast tumor associated antigens in fine needle aspirate

cytology. Int. J. Cancer 37:493–498.
21. Johnston, W.W., Szpak, C.A., Lottich, S.C., Thor, A., and Schlom, J. (1986) Use of a monoclonal antibody (B72.3) as a novel immunohistochemical adjunct for the diagnosis of carcinomas in fine needle aspiration biopsy specimens. Human Pathol. 17:501–513.
22. Szpak, C.A., Johnston, W.W., Roggli, V., Kolbeck, J., Lottich, S.C., Vollmer, R., Thor, A., and Schlom, J. (1986) The diagnostic distinction between malignant mesothelioma of the pleura and adenocarcinoma of the lung as defined by a monoclonal antibody (B72.3). Am. J. Pathol. 122:252–260.
23. Thor, A., Gorstein, F., Ohuchi, N., Szpak, C.A., Johnston, W.W., and Schlom, J. (1986) Tumor-associated glycoprotein (TAG-72) in ovarian carcinomas defined by monoclonal antibody B72.3. J. Natl. Cancer Inst. 76:995–1006.
24. Thor, A., Viglione, M.J., Muraro, R., Ohuchi, N., Schlom, J., and Gorstein, F. (1987) Monoclonal antibody B72.3 reactivity with human endometrium: A study of normal and malignant tissues. Int. J. Gynecol. Pathol. 6:235–247.
25. Szpak, C.A., Johnston, W.W., Lottich, S.C., Kufe, D., Thor, A., and Schlom, J. (1984) Patterns of reactivity of four novel monoclonal antibodies (B72.3, DF3, B1.1, B6.2) with cells in human malignant and benign effusions: A highly selective recognition of adenocarcinoma over the neoplasms and mesthothelium. Acta Cytol. 28:356–357.
26. Lan, M.S., Bast, R.C., Jr., Colnaghi, M.I., Knapp, R.C., Colcher, D., Schlom, J., and Metzgar, R.S. (1987) Co-expression of human cancer-associated epitopes on mucin molecules. Int. J. Cancer 39:68–72.
27. Johnston, W.W., Szpak, C.A., Lottich, S.C., Thor, A., and Schlom, J. (1985) Use of monoclonal antibody (B72.3) as an immunocytochemical adjunct to diagnosis of adenocarcinoma in human effusions. Cancer Res. 45:1894–1900.
28. Ness, M.J., Pour, P.M., Tempero, M.A., and Linder, J. (1988) Immunohistochemistry with monoclonal antibody B72.3 as an adjunct in the cytologic diagnosis of pancreatic carcinoma. Modern Pathology 1:279–283.
29. Martin, S.E., Moshiri, S., Thor, A., Vilasi, V., Chu, E.W., and Schlom, J. (1986) Identification of adenocarcinoma in cytospin preparations of effusions using monoclonal antibody B72.3. Am. J. Clin. Pathol. 86:10–18.
30. Colcher, D., Keenan, A.M., Larson, S.M., and Schlom, J. (1984) Prolonged binding of a radiolabeled monoclonal antibody (B72.3) used for the in-situ radioimmunodetection of human colon carcinoma xenografts. Cancer Res. 44:5744–5751.
31. Keenan, A.M., Colcher, D., Larson, S.M., and Schlom, J. (1984) Radioimmunoscintigraphy of human colon cancer xenografts in mice with radioiodinated monoclonal antibody B72.3. J. Nucl. Med. 25:1197–1203.
32. Esteban, J.M., Schlom, J., Mornex, F., and Colcher, D. (1987) Radioimmunotherapy of athymic mice bearing human colon carcinoma with monoclonal antibody B72.3: Histological and autoradiographic study of effects on tumors and normal organs. Eur. J. Cancer Clin. Oncol. 23:643–655.
33. Esteban, J.M., Colcher, D., Sugarbaker, P., Carrasquillo, J.A., Bryant, G., Thor, A., Reynolds, J.C., Larson, S.M., and Schlom, J. (1987) Quantitative and qualitative aspects of radiolocalization in colon cancer patients of intravenously administered Mab B72.3. Int. J. Cancer 39:50–59.
34. Colcher, D., Esteban, J.M., Carrasquillo, J.A., Sugarbaker, P., Reynolds, J.C., Bryant, G., Larson, S.M., and Schlom, J. (1987) Quantitative analyses of selective radiolabeled monoclonal antibody localization in metastatic lesions of colorectal cancer patients. Cancer Res. 47:1185–1189.
35. Colcher, D., Esteban, J., Carrasquillo, J.A., Sugarbaker, P., Reynolds, J.C., Bryant, G., Larson, S.M., and Schlom, J. (1987) Complementation of intracavitary and intravenous administration of a monoclonal antibody (B72.3) in patients with carcinoma. Cancer Res. 47: 4218–4224.
36. Larson, S.M., Carrasquillo, J.A., Colcher, D., Reynolds, J.C., Sugarbaker, P., and Schlom, J. (1986) Considerations for radiotherapy of pseudomyxoma peritonei with i.p. I-131 B72.3,

a monoclonal antibody. J. Nucl. Med. 27:1021–1022.
37. Whittle, N., Adair, J., Lloyd, C., Jenkins, L., Schlom, J., Roubitschek, A., Colcher, D., and Bodmer, M. (1987) Expression in COS cells of a mouse-human chimaeric B72.3 antibody. Protein Engineering 1:499–505.
38. Roselli, M., Schlom, J., Gansow, O.A., Raubitschek, A., Mirzadeh, S., Brechbiel, M.W., and Colcher, D. (1989) Comparative biodistributions of Yttrium- and Indium-labeled monoclonal antibody B72.3 in athymic mice bearing human colon carcinoma xenografts. J. Nucl. Med. 30:672–682.
39. Ohuchi, N., Simpson, J., Colcher, D., and Schlom, J. (1987) Complementation of anti-CEA and anti-TAG-72 monoclonal antibodies in reactivity to human gastric adenocarcinomas. Int. J. Cancer 40:726–733.
40. Muraro, R., Wunderlich, D., Thor, A., Lundy, J., Noguchi, P., Cunningham, R., and Schlom, J. (1985) Definition by monoclonal antibodies of a repertoire on carcinoembryonic antigen differentially expressed in human colon carcinomas versus normal adult tissues. Cancer Res. 45:5769–5780.
41. Greiner, J.W., Guadagni, F., Noguchi, P., Pestka, S., Colcher, D., Fisher, P.B., and Schlom, J. (1987) Recombinant interferon enhances monoclonal antibody-targeting of carcinoma lesions in vivo. Science 235:895–898.
42. Greiner, J.W., Horan Hand, P., Colcher, D., Weeks, M., Thor, A., Noguchi, P., Pestka, S., and Schlom, J. (1987) Modulation of human tumor-associated antigen expression. J. Lab. Clin. Med. 109:244–261.
43. Greiner, J.W., Horan Hand, P., Noguchi, P., Fisher, P.B., Pestka, S., and Schlom, J. (1984) Enhanced expression of surface tumor-associated antigens on human breast and colon tumors cells after recombinant human leukocyte alpha-interferon treatment. Cancer Res. 44: 3208–3214.
44. Muraro, R., Kuroki, W., Wunderlich, D., Poole, D.J., Colcher, D., Thor, A., Greiner, J.W., Simpson, J.F., Molinolo, A., Noguchi, P., and Schlom, J. (1988) Generation and characterization of B72.3 second generation monoclonal antibodies reactive with the Tumor-associated Glycoprotein 72 antigen. Cancer Res. 48:4588–4596.

17. Antibody imaging of endocrine tumors

Arthur Bradwell, Peter Dykes, Catherine Chapman, and Gillian Thomas

Accurate localization of relatively slow-growing endocrine tumors, where removal may be curative or at least reduce symptoms from the released hormones, has considerable clinical importance. This applies to parathyroid adenomas, pancreatic tumors (insulinomas and others), adrenal cortical and medullary tumors, and, to some extent, differentiated thyroid and medullary thyroid tumors. By their nature, all these tumors produce one or more unique proteins for antibody targeting and thus radioimmunodetection (RAID). At the moment, experience is limited to locating differentiated [1] and medullary thyroid tumors [2], and insulinomas [3].

Methods

Preparation of radiolabeled antibodies

The three different antigens (thyroglobulin, CEA, and insulin) were purified by established methods [4,5] (except for the insulin antigen, where we used Actrapid-Novo) and sheep were repeatedly immunized until high-titre antisera were obtained. Nonspecific antibodies were adsorbed on glutaraldehyde polymers of human serum and normal tissues until specific reactions to the relevant tissues were obtained using the peroxidase-antiperoxidase technique [6]. Immunoglobulin-G-rich fractions were prepared by ion-exchange chromatography on DEAE 52 cellulose, sterilized by filtration, and tested for pyrogens in rabbits by an independent laboratory. They were then labeled with I-131 (IBS-30 Amersham International) under sterile conditions to a minimum specific activity of 150 MBq/mg [7]. Each was diluted in 1% human serum albumin in physiologic saline, centrifuged at 20,000 g for 12 hours, and refiltered.

Scanning procedure

Thyroidal uptake of I-131 was blocked by a combination of oral potassium iodide and potassium perchlorate. Scans were recorded 24 and 48 hours after

Goldenberg, D.M., (ed.), Cancer Imaging with Radiolabeled Antibodies.

the injection. Data from the I-131-labeled antibody alone was difficult to interpret, because only a small amount (at most 1%) of the antibody attached to the tumor whilst the vast majority was either in the circulation or diffused into other tissues. The antibody that was specifically bound to the tumor was distinguished from the antibody elsewhere using a subtraction technique [8]. Technetium (Tc-99m) pertechnetate (18.5 MBq), which distributes in the extravascular space, and Tc-99m-labeled human albumin (18.5 MBq), which remains in the vascular compartment, were injected 30 minutes and 5 minutes, respectively, before each scan. These substances (which are not specifically bound to the tumor) were distinguished from the I-131 emission by their energy (Tc-99m = 141 keV; I-131 = 364 keV). AP views of the neck, chest, and abdomen were obtained where appropriate (plus PA and lateral scans in some patients) using a Searle LFOV or CGR gammatome gamma camera fitted with a medium-energy, parallel-hole collimator and linked to a DEC PDP 11/40 computer with a dual-isotope facility. Data was stored and displayed in a 64 × 64 matrix and the Tc-99m scan subtracted from the I-131 scan.

The subtraction scan was displayed into two forms: first, as calculated and, secondly, thresholded, to display only significant counts [9]. This threshold was obtained by calculating the variance in the scan due to random fluctuations in the background and subtracting two standard deviations from each pixel. This procedure gives an indication of the relative significance of counts left in the subtraction picture. These counts were regarded as representing possible sites of tumor if they did not correspond to known sites of isotope accumulation. The subtraction picture clearly highlighted the antibody bound to the tumor (Figure 1). Areas in the subtraction scan were graded as definite (++), areas positive in all views on two occasions; probable (+), areas seen in one view on two occasions or two views on one occasion; possible (+/−), areas seen in one view on one occasion; or negative (−). The count density of each area compared with an appropriate background area was also taken into consideration. Patients received between 18.5 and 37 MBq of I-131 antibody, which represented approximately 100 μg of IgG. This gave a whole-body dose and bladder dose of approximately 0.135 and 0.803 mSv, respectively, per MBq administered.

Clinical studies

Differentiated thyroid tumors

Methods and patients. We studied 12 patients (six male, six female), six with follicular tumors, three papillary, and three mixed. They had received a variety of previous treatments; serum thyroglobulin (Tg) varied from < 1 to > 200 ng/ml. Five were on thyroid supplements at the time of the scans. The clinical details are summarized in Table 1.

Figure 1. Chest view of patient 3, 48 hours after scanning with labeled anti-Tg. A: I-131 antibody image; B: after subtraction of nonspecific Tc-99m scan. A — tumor in head of humerus; B — tumor in clavicle.

Table 1. Clinical details of the patients studied

Patient	Age (years)	Sex	Histology	Treatment	Serum Tg < μg/l	Thyroid Supplements
1	69	F	Follicular	DxR Tx	200	Off
2	65	M	Follicular	I-131	135	On
3	42	F	Follicular	Tx I-131x3 DxR	> 200	Off
4	33	M	Papillary	Tx	< 1	On
5	62	F	Follicular/papillary	Tx	62	On
6	68	M	Follicular	None		Euthyroid*
7	72	M	Follicular	I-131x2	89	Off
8	67	M	Follicular/papillary	pTx I-131	72	Off
9	62	M	Papillary	pTx2	48	On
10	55	F	Follicular	pTx x2 I-131x2	10	On
11	66	F	Papillary	Tx I-131 neck exp	56	Off
12	53	F	Follicular/papillary	Tx I-131x2 neck exp	80	Off

Tx = thyroidectomy; pTx = partial thyroidectomy; DxR = deep x-ray therapy; I-131 = ablative dose of I-131; neck exp = second neck exploration (see text).
* Patient scanned preoperatively.

In order to demonstrate that the antibody specifically located thyroid tissue in vivo and to compare the results with conventional I-131 emission scans, the patients were tested on three separate occasions: 1) All patients had a standard scan after oral I-131 (37 MBq). 2) Patients who had positive uptake of I-131 were given thyroid-'blocking' drugs and the scan was repeated. By demonstrating that the I-131 scan could be inhibited, subsequent positive antibody scans carried out during similar 'blockade' (see below) were most unlikely to be due to iodine released from the labeled anti-thyroglobulin. The 'blocking' drugs comprised 420 mg of potassium iodide (KI) 30 minutes before the I-131 and then 120 mg KI 6-hourly plus 400 mg potassium chlorate ($KClO_4$) 8-hourly. 3) All patients had antibody scans whilst on oral KI and six were given additional $KClO_4$.

Results. The results of these scans are presented in Table 2. A total of 40 tumor 'areas' were detected in 11 patients by a variety of clinical and radiologic techniques, and one patient was normal by all criteria. Sixteen areas were detected using conventional I-131 uptake scans, whereas 34 were positive on the antibody scans. However, not all of the 40 areas could be accurately compared.

In patient 3, only 2 of 7 areas showed I-131 uptake, so the second (blocked) I-131 scan was not performed and these two areas were excluded from scan comparisons. Also excluded were four areas in patients 6 and 7, who showed some I-131 uptake while in the supposedly blocked state. Three patients had widespread small pulmonary lesions; those in patient 2 were not detected, whilst patients 3 and 10 had increased antibody uptake in some areas and not in others. Owing to the difficulty in quantitating these three areas, they were also excluded from subsequent analysis. This left 31 areas that could be

Table 2. Comparison of techniques used for localizing the thyroid tumors

Patient	Site	Anti-TG Scan	I-131 Scan	Other Clinical Methods
1	Neck	++	−	+ CE
	Spine	++	−	+ CE
	Mediastinum	++	−	+ XR
	Pelvis	+	−	+ CE
2	Spine	−	−	+ BS
	Sternum	++	−	+ BS
	Pul. diffuse	−	+	+ XR
3	Humerus	++	−	+ XR
	Clavicle	++	−	+ XR
	Pelvis 1	++	+	+ XR
	2	++	+	+ XR
	3	++	−	+ XR
	Knee	++	−	+ XR
	Pul. diffuse	+/−	−	+ XR
4	None	−	−	None
5	Pul. discrete 1	+	−	+ XR
	2	+	−	+ XR
	3	+	−	− XR
	4	−	−	+ XR
6	Neck	++	++	+ OP
	Thyroid	++	++	+ OP
	Mediastinum	++	++	+ OP
7	Scapula	++	++	+ XR
	Neck	+	−	− CE
8	Shoulder	−	−	− XR
	Neck	++	(+)	− CE
9	Neck	−	−	+ CE
10	Neck	++	−	+ XR
	Spine	++	−	+ XR
	Pelvis	−	(+)	− XR
	Pul. discrete	+	(+)	+ XR
	Pul. diffuse	+/−	(+)	+ XR
11	Neck	+	−	− CE
12	Neck	++	−	− CE
	Mediastinum	++	(+)	+ XR
	Pul. discrete 1	++	(+)	+ XR
	2	++	(+)	+ XR
	3	++	(+)	+ XR
	4	++	(+)	+ XR
	5	++	(−)	+ XR
	6	++	−	+ XR

Pul diffuse = diffuse pulmonary micrometastases; pul. discrete = discrete countable lung lesions on CxR anti-Tg scan: ++ = definite, + = probable, − = negative, +/− = some areas positive; I-131 scan: + = positive, (+) = positive but became negative on oral thyroid blocking drugs, ++ = positive and not blocked by oral thyroid blocking drugs, − = negative.
Other clinical methods: + = confirmed; − = unconfirmed; CE = clinical examination; XR = x-ray; BS = isotope bone scan; OP = operation.

compared. Twenty-seven (87%) areas were positive in the anti-Tg scan, whilst nine (29%) were positive on the I-131 scan.

Twenty-four (77%) areas were detected by a combination of clinical and other radiologic criteria. Four of the areas were not detected by the antibody scan. One of these areas was a 2 cm palpable submandibular mass in patient 9. His serum Tg was 48 μg/l at the time of the scan but was undetectable a few weeks later. The site may not have contained tumor. Five sites were positive only on the anti-Tg scan. Three were in the neck; two of these patients had previously proven neck recurrences but had no palpable masses at the time of scanning, whilst the third patient had received an ablative dose of I-131 but not surgery. The other two sites were in the chest and shoulder but were not detectable on x-ray. Biopsy samples of these areas were not available and they have not been further investigated.

Figure 1 shows the 48-hour subtraction chest view of patient 3. Lesions highlighted in the left shoulder and right clavicle by the subtraction process are indicated. This patient also had miliary pulmonary shadows on chest x-ray. The ring shadow and sillhouette are artifacts of the detection and subtraction process.

Discussion. The antibody scans were more sensitive than I-131 scans plus a combination of clinical and the other radiologic techniques that were used in this study. The RAID scans may also have detected subclinical lesions (the excess positive sites). The use of I-131 as a label raised the possibility that positive results might have been obtained merely by the uptake of free I-131 (released from catabolized antibody) into thyroid tumors. The purpose of carrying out the blocked I-131 scan was to demonstrate that adequate blockade of I-131 uptake had been achieved. The first six patients were given oral KI alone and the others $KClO_4$ in addition. Patient 6 showed some uptake of I-131 on the conventional scan; however, his lesions were negative on the subtraction images. We do not think that nonspecific uptake contributed to the results, but to be certain of this comparisons were only made in areas proven to be negative or completely blockable. The serum concentrations of Tg did not appear to influence the success of the technique. Positive localization was obtained in a patient with a Tg of only 10 μg/l (patient 10), although she was taking oral thyroxine at the time. A high circulating antigen concentration did not diminish the quality of the results. This has been the case with scans of other tumors and is presumably accounted for by the great excess of antigen within the tumor available for antibody attachment.

Access of antibody to the Tg must also be relatively unimpeded. A similar situation has been observed with testicular teratomas producing alpha-fetoprotein. This is considered to be an intracellular protein, but antibody scanning again is successful [10]. One might suppose that tumors would be best located by antibodies directed against cell-surface components rather than intracellular proteins, but many surface antigens are removed from the cell surface when combined with antibody and may not be ideal targets.

In general, better count rates and better pictures were obtained with high doses of I-131-labeled antibody (1 mCi). This represents a whole-body radiation dose of about 5 mSv (0.5 rem) using a standard model and taking into account the biologic half-life of sheep IgG. This is acceptable for a routine staging procedure and is comparable with the use of I-131 alone. Views taken at 48 hours gave better contrast (tumor-to-normal tissue ratios) than at 24 hours, and two views were useful in assessing doubtful areas. Lateral views, particularly of the chest, revealed lesions that were not detectable in AP or PA views, presumably because of the effect of the high count rates from vascular structures such as the heart. Normalization over different areas also helped in the assessment of the scans. The smallest lesion detected was 1.7 cm in diameter (on the chest x-ray), but three larger ones were missed. The smallest mass detectable depends mainly on the selective uptake of label and, if high enough, would enable lesions smaller than the resolving power of the gamma camera (probably about 2 cm) to be seen.

The role of this type of scan in the clinical management of thyroid carcinoma is limited at present. Recurrences in the neck are more likely to be detected by other methods, whilst lesions elsewhere rarely require surgery or local radiotherapy. Also, scans are less sensitive than serum levels of Tg for detecting the presence of tumor. Additionally, the scans may not be as sensitive as I-131 scans might be if a much larger dose of radioisotope than conventionally suggested were used. However, the sensitivity of the antibody scans could be increased by using an indium-111 (In-111) label and a more sensitive collimator.

Medullary thyroid tumors

The production of calcitonin by medullary thyroid tumors (MTC) is frequently paralleled by secretion of serum CEA. Although not as sensitive for monitoring small tumors as calcitonin, it is present in the tumor tissue (demonstrated by immunoperoxidase techniques), and serum levels can be as high as those associated with colon carcinomas. We therefore made use of radiolabeled anti-CEA to localize these tumors. Techniques were similar to those described for differentiated thyroid tumors.

Methods and patients. Five patients were studied. Each had raised serum concentrations of calcitonin (1–40 ng/ml) and CEA (13–192 ng/ml) associated with tumor recurrence after total thyroidectomy. All, except one, had symptoms, but only one had a detectable mass. This patient had a 2 cm swelling in the left side of her neck, associated with raised serum markers (CEA, 192 ng/ml; calcitonin, 35 ng/ml). Each patient was given between 25 and 70 MBq of sheep I-131-labeled anti-CEA.

Results. A positive scan coincident with the known mass was obtained in the patient with the neck swelling. The tumor was resected and was shown to be

CEA positive by immunohistochemistry. A postoperative anti-CEA scan was negative. Some months later symptoms recurred in the absence of a detectable swelling. She was then subjected to a third scan, using In-111-labeled antibody, which showed tumor recurrence adjacent to the previous operation site. The scans were normal in the other four patients.

Discussion. The results indicate that the scans were of marginal value, but since the serum markers were quite low in most patients, the tumors could have been very small. Similar results have been reported using a monoclonal anti-CEA and single-photon emission tomography [2]. The three patients studied had positive scans associated with tumor masses of between 4 and 100 g and CEA concentrations of 78–250 ng/ml.

Insulinomas

Methods and patients. Nine patients with suspected insulinoma were scanned with I-131-labeled sheep anti-insulin. These patients were aged from 29 to 79 years, and all had laparotomies as part of their treatment. The scan results were compared with the operative findings.

Thyroidal and gastric uptake of I-131 was blocked by treatment with oral potassium iodide, 180 mg daily for 1 week, and oral potassium perchlorate, 600–800 mg 1 hour before antibody injection and 1 hour before each scan. The anti-insulin scans were recorded and positive areas were graded, as previously described for thyroid tumors.

Results. The results are presented in Table 3. The diagnosis of insulinoma was confirmed histologically in 8 of the 9 patients. In one patient (6) laparotomy failed to reveal an insulinoma but instead revealed a large pelvic sarcoma. Two patients (2 and 4) had malignant insulinomas that had metastasized to the liver.

The primary insulinoma was accurately localized in 4 of the 8 patients. The sizes ranged from 1 to 3 cm in diameter. In one of these patients (8), both CT scanning and pancreatic angiography had given false-negative results. Hepatic metastases were correctly identified in 1 of the 2 patients (4) with liver involvement, and there were no hepatic false-positive reports. Two definite and two probable positive areas were found corresponding to the pancreatic region. These were confirmed as true positives. In three scans, pancreatic areas considered only as possibly positive were not confirmed at laparotomy. All three occurred in the region of the pancreatic body.

There were four false-negative scans. Two of these tumors were found in the pancreatic tail (2 cm and 3 mm in diameter), one in the pancreatic head (1 cm), and one in the pancreatic body (1 cm). A true-negative pancreatic result was obtained in patient 6.

In two patients (1 and 5) samples of both insulinoma and adjacent normal pancreas were obtained for gamma counting. The ratios between insulinoma

Table 3. Results of anti-insulin scans in the patients

Patient Number	Age (yr)	Sex	Serum Insulin mU/l	Scan Report	Laparotomy Findings	Tumor Diameter	Scan Accuracy	Other Methods
1	32	M	18	+ p head − liver	+ p head − liver	1 cm	True +ve True −ve	None
2	58	M	> 130	− pancreas − liver	+ p head + liver + mesenteric node	1 cm	False −ve False −ve False −ve	p angiography attempted but unsuccessful
3	79	M	NK	+/− p body − liver	− p body + p tail − liver	3 mm	False +ve False −ve True −ve	None
4	58	F	200	− pancreas ++ liver	+ p tail + liver	2 cm	False −ve True +ve	None
5	23	M	NK	++ p head +/− p body − liver	+ p head − p body − liver	1.75 cm	True +ve False +ve True −ve	p angiography true positive
6	57	F	6	− pancreas − liver	− pancreas − liver	−	True −ve True −ve	p CT true negative
7	65	F	14	− pancreas − liver	+ p body − liver	1 cm	False −ve True −ve	p CT false negative
8	33	M	NK	+ p head +/− p body − liver	+ p body − p body − liver	1.5 cm	True +ve False +ve True −ve	CT scan and p angiography false negative
9	35	M	NK	++ p tail − liver	+ p tail − liver	3 cm	True +ve True −ve	p angiography true negative

p = pancreatic; +/− = possible positive; + = probable positive; ++ = definite positive; CT = computerized x-ray tomography.

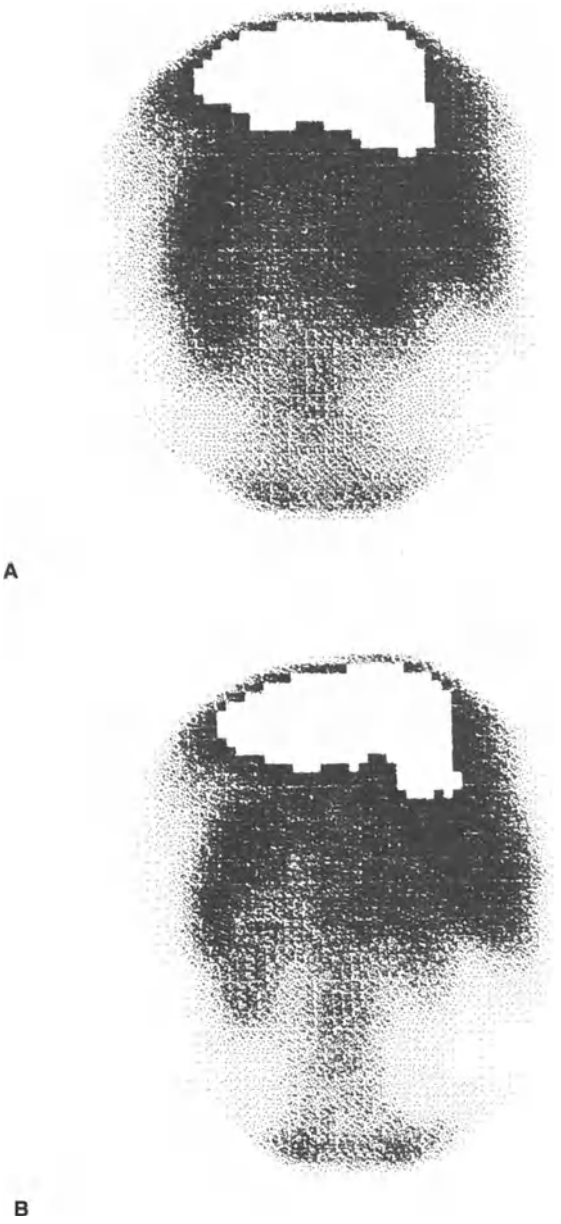

Figure 2. Posterior abdominal scans, patient 4: A: I-131 anti-insulin; B: Tc-99m; C: subtraction image (after normalization over the heart); D: subtraction image thresholded to display only significant counts. The hepatic uptake corresponds with metastases. The blank areas within the liver result from count rates above the display limit. A small hot spot (arrow) is apparent over the tail of the pancreas in D. This corresponded with a 2 cm insulinoma. B = bladder; L = liver.

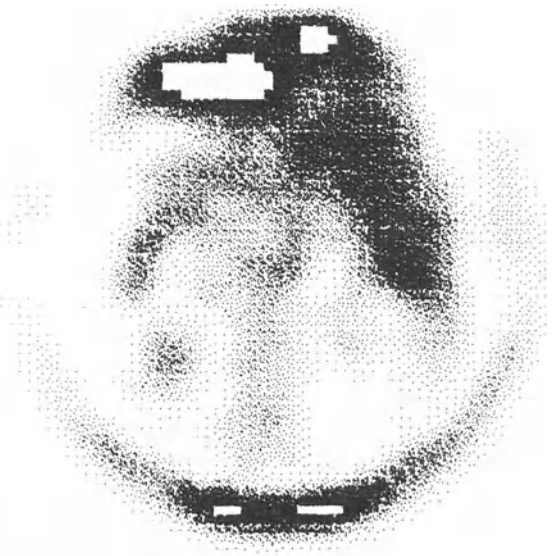

C

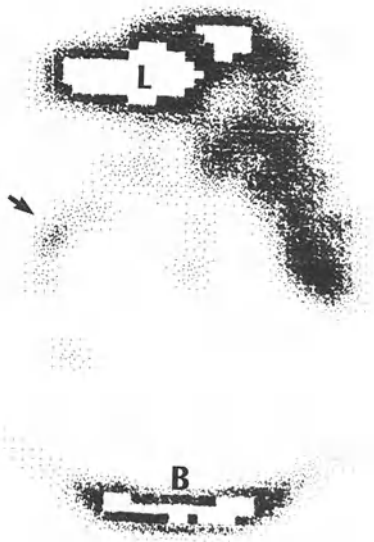

D

counts per gram and normal pancreatic tissue were 1.5:1 and 2.2:1. The scans from two patients are illustrated. Patient 4 provided an example of a positive anti-insulin scan (Figure 2). The patient scanned was a 58-year-old woman who had presented with a history of episodic loss of consciousness and also episodes of weakness and visual disturbance, which had responded to oral glucose. Her serum insulin level whilst fasting was 200 mU/l and her blood glucose was 2.0 m/l. Marked hepatic uptake of I-131 anti-insulin is apparent in both subtraction images (2C and 2D). Subsequent laparotomy revealed metastatic insulinoma in the liver, confirming this as a true-positive scan area. The pancreatic primary was not visible on the scan. The other smaller areas of increased count density were not seen consistently and were not reported as positive.

Patient 6 provided an interesting result. This 57-year-old lady was referred for anti-insulin scanning with a diagnosis of suspected insulinoma following well-documented episodes of hypoglycemia. Her serum insulin during hypoglycemia was as low as 6 mU/l on one occasion, with undetectable C peptide, whilst on another occasion her serum insulin level was unrecordably low. Laparotomy revealed a large pelvic sarcoma and no pancreatic abnormality. The anti-insulin scan showed lower abdominal accumulation of anti-insulin and no pancreatic emission. The anterior abdominal subtraction scans are shown in Figures 3A and 3B. Resection of the tumor provided resolution of her hypoglycemia symptoms. The anti-insulin also reacted, in vitro, with a homogenate of this tumor. This was demonstrated by radioimmunoassay.

Discussion. This technique has the advantage of being simpler and less invasive than pancreatic angiography, but the latter is more sensitive. Antibody scans can also detect extrapancreatic disease. The clarity of anti-insulin scans is, however, inferior to pancreatic angiograms, and interpretation is difficult. In this series, anti-insulin scanning correctly localized 4 of 8 subsequently proven insulinomas. This compares with 90% correctly localized by pancreatic angiography in the best hands [11], although this is rarely achieved. In one patient, a true positive result was obtained by anti-insulin scanning where both pancreatic angiography and CT scanning had given false-negative results. Preferential uptake of antibody in insulinoma compared with the normal pancreas was confirmed by tissue counting.

The accumulation of radioactive anti-insulin in a large pelvic sarcoma may represent a specific interaction between our anti-insulin and an insulinlike molecule expressed by the tumor. The association of hypoglycemia with large mesenchymal tumors is recognized, and immunoreactive insulin or insulinlike sustances have been identified in some, but not all, of these tumors [12]. Nonspecific accumulation of immunoglobulin into the tumor could provide an alternative, but less likely, explanation [13].

Overall anti-insulin scanning was, not surprisingly, more successful for the larger tumors. Small tumors inevitably require more sensitive techniques such as angiography. A considerable increase in the uptake of the radiolabel by the

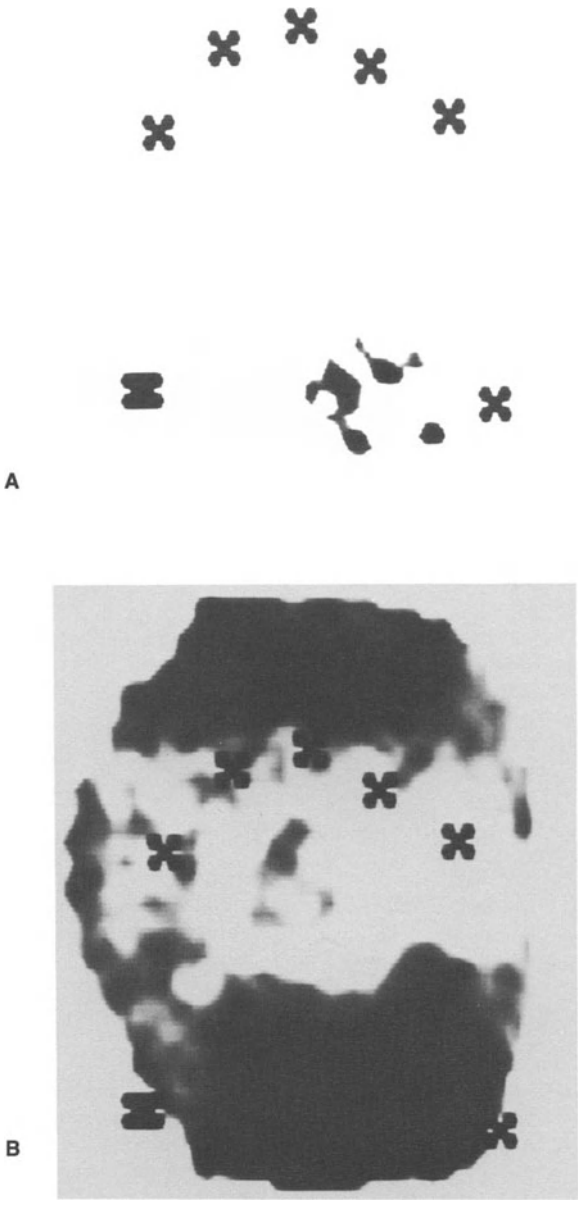

Figure 3. Anterior abdominal scans, patient 6: A: I-131/Tc-99m subtraction image; B: thresholded subtraction image. The pelvic uptake seen on both scans corresponds with a large paraovarian sarcoma. x (upper = costal margins; x (lower) = anterior superior iliac spines.

tumor would be required to markedly improve the antibody scans. How this might be achieved is at present unknown, although there is considerable research in this area. The advantages of the technique are that it is well tolerated and may simultaneously detect metastases.

Conclusion

The ratios achieved in the studies were generally low (1.5:1 and 2.2:1), but uptake ratios of between 2:1 and 5:1 are usual in RAID [14]. This problem remains the dominating limitation of the technique, and until it is solved the results will remain at best little better than other methods.

Acknowledgments

This work was supported by both the Cancer Research Campaign and the Endowment Fund of Central Birmingham Health District. The figures have been reproduced with the kind permission of Pitman Publishing Ltd.

References

1. Fairweather, D.S., Bradwell, A.R., Watson-James, S.F., Dykes, P.W., Chandler, S., and Hoffenberg, R. (1983) Detection of thyroid tumours using radiolabeled anti-thyroglobulin. Clin. Endocrinol. 18:563–570.
2. Berche, C., Mash, J.-P., Lumbroso, J.D., Langlais, C., Aubrey, F., Buchegger, F., Carrel, S., Rougier, P., Parmentier, C., and Tubiana, M. (1982) Tomoscintigraphy for detecting gastrointestinal and medullary thyroid cancers: First clinical results using carcinoembryonic antigen. Br. Med. J. 285:1447–1451.
3. Chapman, C.E., Fairweather, D.S., Keeling, A.A., Chandler, S.T., Anderson, P., Dykes, P.W., and Bradwell, A.R. (1987) An evaluation of anti-insulin scanning in patients with suspected insulinoma. Clin. Endocrinology 26:433–440.
4. Van Herle, A.J., Uller, R.P., Matthews, N.L., and Brown, J. (1973) Radioimmunoassay for measurement of thyroglobulin in human serum. J. Clin. Invest. 52:1320–1327.
5. Pritchard, D.G., and Egan, M.L. (1978) Isolation of carcinoembryonic antigen by an improved procedure. Immunochemistry 15:385–387.
6. Sternberger, L. (1979) The unlabelled antibody peroxidase-antiperoxidase (PAP) method. In: *Immunocytochemistry*, 2nd ed. New York: John Wiley and Sons, pp. 104–169.
7. Watson-James, S.F., Fairweather, D.S., and Bradwell, A.R. (1983) A shielded sterile apparatus for iodinating proteins. Med. Lab. Sci. 40:67–68.
8. Goldenberg, D.M., Kim, E.E., and Deland, F.H. (1981) Human chorionic gonadotrophin radioantibodies in the radioimmunodetection of cancer and for disclosure of occult metastases. Proc. Natl. Acad. Sci. USA 78:7754–7758.
9. Chandler, S.T., and Anderson, P. (1987) A method for thresholding subtracted images in radiolabeled-antibody imaging. Br. J. Radiol. 60:881–886.
10. Halsall, A.K., Fairweather, D.S., Bradwell, A.R., Blackburn, J.C., Dykes, P.W., Howell, A., Reeder, A., and Hine, K.R. (1981) Localisation of malignant germ-cell tumours after injection of radiolabeled anti-alpha-fetoprotein. Br. Med. J. 283:942–944.

11. Edis, A.J., McIlrath, D.C., Van Heerden, J.A., Fulton, R.E., Sheedy, P.F., Service, F.J., and Dale, A.J.D. (1976) Insulinoma — Current diagnosis and surgical management. Curr. Probl. Surg. 13:5–23.
12. Rees, L.H. (1975) The biosynthesis of hormones by non-endocrine tumours — a review, J. Endocrinol. 67:143–175.
13. Goldenberg, D.M., Kim, E.E., Deland, F., Bennett, S., and Primus, F.J. (1980) Radioimmunodetection of cancer with radioactive antibodies to carcinoembryonic antigen. Cancer Res. 40:2984–2992.

18. Diversity of the human immune response to clinically used murine monoclonal antibodies

Nigel S. Courtenay-Luck and Agamemnon A. Epenetos

Murine monoclonal antibodies raised to tumor-associated antigens [1–4] and lymphoid cell receptors [5,6] have been used in clinical trials since 1980. A major complication to their use was thought to be the patient's immune response to these xenogeneic proteins. Such immune responses or hypersensitivity reactions could result in anaphylaxis and abrogation of the antibodies' clinical efficacy.

Since the early clinical trials, both the radiolabeling techniques and means of administration have improved, resulting in a purer and less hazardous therapeutic agent. Where disease is confined to a body cavity, such as the peritoneum, as in ovarian cancer, regional administration has been attempted rather than intravenous administration [7,8]. Regional administration has a number of potential advantages, such as a higher percentage of the radiolabeled monoclonal antibodies being targeted to the lesion.

Although major adverse effects from monoclonal antibody therapy have not been reported, humoral immune responses to them have. It would appear that a large number of people within the population have antibodies capable of binding to mouse immunoglobulin. The presence of these serum antibodies has given rise to the term *preexisting human anti-murine immunoglobulin antibody response*. The etiology of these preexisting antibodies has been the subject of investigation by a large number of research groups, including our own. Apart from this preexisting response, reports have shown that the majority of patients receiving therapeutic doses of monoclonal antibodies develop elevated responses to constant region determinants, and in some cases, variable region determinants, including idiotypic determinants.

The diversity of patients' humoral immune responses to clinically used murine monoclonal antibodies, together with the adverse or potentially beneficial effects of such responses, will be reviewed in this chapter.

Preexisting humoral immune responses to murine monoclonal antibodies

A large number of reports have shown that patients have preexisting human anti-murine immunoglobulin antibody responses [9–12]. The only real

Goldenberg, D.M., (ed.), Cancer Imaging with Radiolabeled Antibodies.

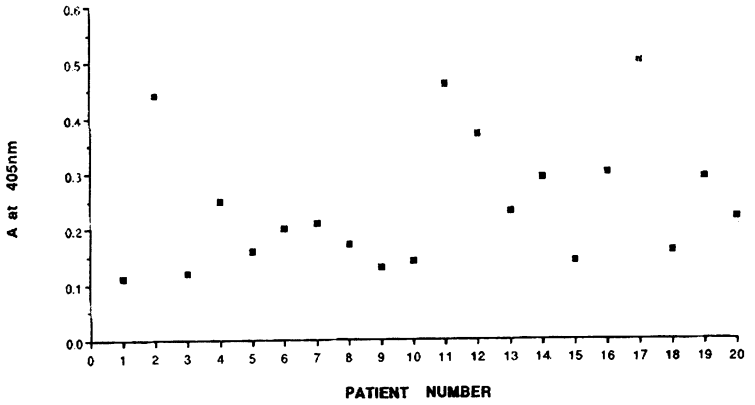

Figure 1. Variation in level of preexisting human antimurine immunoglobulin antibody response for 20 patients prior to monoclonal antibody therapy.

exception to this appears to be patients with certain malignancies of the lymphoid system, such as chronic lymphocytic leukemia (CLL) [10]. Our own experience is that virtually all patients and healthy individuals (blood donors) have preexisting anti-murine Ig responses. The data shown for 20 patients with ovarian cancer, prior to treatment, in Figure 1, demonstrates this phenomenon.

After a number of experiments we realized that the main isotype of these preexisting antibodies to murine Ig was IgM and that the antigenic determinant to which they bound was restricted to the Fc of the murine antibody. Therefore, we tried to determine whether these preexisting antibodies were rheumatoid factors. In order to do this we conducted a number of experiments. We searched for IgM antibodies that bound to both human and mouse IgG. The correlation between the presence of both anti-murine and anti-human IgG could not have been higher. Every patient having one response also had the other.

When the serum from patients with active rheumatoid disease was assessed for anti-murine IgG activity, it was found to be not only higher than ovarian cancer patients' or blood donors' preexisting responses, but often higher than patients receiving therapeutic doses of murine monoclonal antibody. We next assayed a number of purified polyclonal rheumatoid factors from patients with rheumatoid arthritis and monoclonal rheumatoid factor from patients with mixed essential cryoglobulinemia. Our findings showed that polyclonal rheumatoid factors bound to both human and murine IgG, unlike the monoclonal rheumatoid factors, which only bound to human IgG, indicating that a large number, but not all antigenic determinants recognized by rhematoid factors are shared between the two species of IgG.

In order to resolve the question of antigenic sharing between human and murine IgG, purified polyclonal rheumatoid factor was incubated overnight at 4°C with either human or murine IgG. Rheumatoid factor activity was

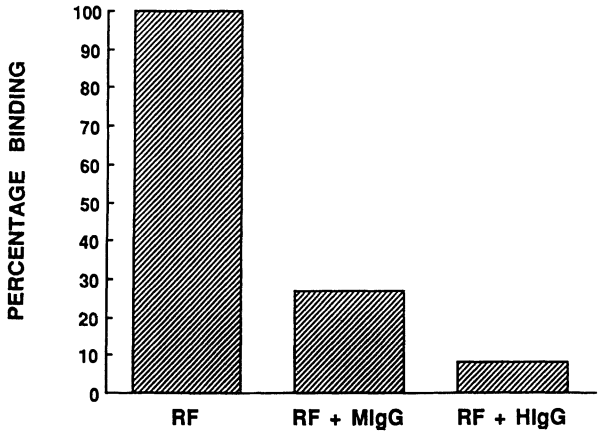

Figure 2. Reduction in human polyclonal rheumatoid factor (RF) binding to human IgG due to preincubation with either murine monoclonal antibody (RF + MIgG) or human immunoglobulin (RF + HIgG).

assayed the following day. It was shown that human IgG could totally block its activity and that incubation with murine IgG blocked the human rheumatoid factor activity by 70% when assayed on human-IgG-coated microtitre plates, as shown in Figure 2. Therefore, we concluded that preexisting human anti-murine IgG responses were due to rheumatoid factors, present in the serum of both patients and healthy controls, that bound to a shared antigenic determinant of human and murine IgG [11].

Diversity of human responses against administered radiolabeled murine antibodies

Determination of the relative contributions in patients' sera of antibodies to Fc and $F(ab')_2$ portions of the injected murine immunoglobulin show the following: After a single therapeutic administration, patients' preexisting responses appear boosted, that is, the majority of antigenic determinants being recognized in the response are located on the Fc portion of the murine immunoglobulin. After repeated administration, a number of studies have detected antibodies binding to both the Fc and $F(ab')_2$ region of the murine immunoglobulin. Furthermore, a number of reports have shown that, within the anti-$F(ab')_2$ antibody pool, these are anti-idiotypic antibodies, that is, antibodies that bind to the idiotopes either inside or outside the murine immunoglobulin-combining site (paratope).

The anti-idiotypic response is probably the most important component of the anti-murine immunoglobulin antibody response to be detected, for a number of reasons. Anti-idiotypic antibodies that bind to idiotopes within the combining site would obviously inhibit the binding of the murine antibody to

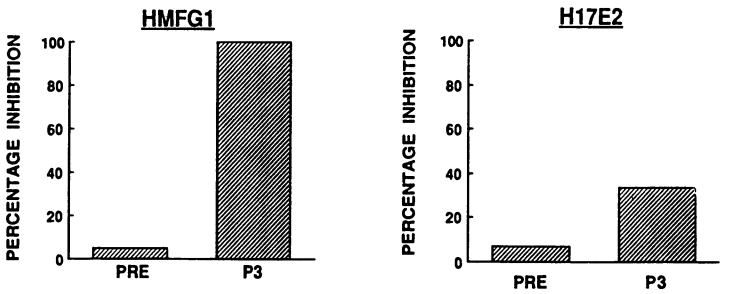

Figure 3. Binding inhibition of administered murine monoclonal antibody (HMFG1) and an idiotypically unrelated, but isotypically related, murine monoclonal antibody (H17E2) to their target antigen by preincubation with the serum of a patient receiving three therapeutic administrations (P3) of monoclonal antibody HMFG1. As control the same patient's pretherapy serum (PRE) was also assayed for its ability to inhibit both antibodies from binding to their target antigens.

its antigen, while those binding to idiotopes outside the combining site could block binding by steric hinderance. Either response would result in reduced therapeutic efficacy of the administered murine monoclonal antibodies [6,13,14].

In our own study of intraperitoneal administration of radiolabeled antibodies for the treatment of ovarian cancer [15], we have observed the emergence of anti-idiotypic antibodies in patients receiving multiple infusions. In Figure 3 the results of an inhibition test are illustrated. For this test, the post third-therapy serum of a patient was diluted 1 in 10 with a 10 μg/ml solution of the administered antibody (HMFG1) or a 10 μg/ml solution of an isotypically related but idiotypically unrelated monoclonal antibody. We then tested for antibody binding to their respective antigens, using an enzyme-linked immunosorbent assay. The administered antibody's binding was totally inhibited, while that of the idiotypically unrelated antibody was inhibited by only about 40%.

These results show that in order to inhibit binding of other murine monoclonal antibodies, anti-idiotypic antibodies alone are not required. Antibodies directed to antigenic determinants other than idiotypic ones can also inhibit binding by mechanisms such as steric hinderance. Although the binding to idiotypically unrelated antibodies is not totally inhibited, it is inhibited to a significant degree. This indicates that once an anti-$F(ab')_2$ response is elicited, reduced therapeutic efficacy could result, even when other unrelated murine monoclonal antibodies are administered.

Positive side of idiotypic responses

In 1974 Jerne postulated a network theory [16], which he stated could account for immune regulation, that is, through idiotopes, receptor-specific regula-

tion of the immune system may be achieved. In a recent study, an anti-idiotypic antibody directed against a monoclonal antibody raised to an epitope on the mammalian reovirus type 3 hemaglobin was shown to have a light chain that had an area of significant amino-acid sequence homology with the hemagglutinin epitope [17]. This study, as well as others, indicate that antigen mimicry by anti-idiotypic antibodies may be achieved by the sharing of primary structure. Therefore, the anti-idiotypic antibody may reflect the internal image of the antigen.

With respect to murine monoclonal antibodies administered to patients, an idiotypic network produced by the following sequence of events could evolve. The administered murine monoclonal antibody (Ab1) stimulates an anti-idiotypic response. Within the set of anti-idiotypic antibodies could be expected to be those that were directly complementary antibodies (Ab2), which would be expected to share the primary structure with the antigen being recognized by Ab1. Therefore, the combining site (paratope) of Ab2 would reflect the internal image of the antigen. According to Jerne's network theory, Ab2 would stimulate the production of a second generation of anti-idiotypic antibodies, among which would be those complementary to the paratope of Ab2. This second-generation anti-idiotypic antibody (Ab3) would therefore be the human counterpart of Ab1, the murine monoclonal antibody.

In one study patients receiving murine monoclonal antibodies for the treatment of gastrointestinal cancer were found to develop antibodies with binding specificities similar to those of the murine monoclonal antibody. These antibodies (Ab3), which could bind to the tumor-associated antigen, were produced by modulation of the patients' immune response. The investigators, therefore, asked the question, 'Is the modulation of patients' immune response to their tumor beneficial?' This question remains to be fully answered.

Our own studies have shown that internal-image antibodies exist within the set of anti-idiotypic (anti-id) antibodies produced to murine monoclonal antibodies administered to patients for the treatment of ovarian cancer. These anti-id antibodies were only found in the sera of patients receiving multiple infusions of murine IG. In some, but not all (Table 1), antibodies with binding specificities similar to those of the administered murine monoclonal antibody could also be detected; any beneficial role these may have had is unclear. Our studies also revealed the in-vivo generation of antibodies that reacted with connective tissue antigens in the host. This autoreactivity was found in four patients developing an anti-idiotypic responses (Table 1). It could have occurred as a result of perturbation of the idiotypic network's regulatory changes in the immune system involving self antigens [18]. In 1 of the 4 patients developing these autoreactive antibodies, further antibody therapy resulted in the loss of autoantibodies, suggesting that such autoimmunity will not present serious clinical problems. We were, however, unable to draw any firm conclusions because of the low number of patients developing such autoantibodies.

Table 1. The existence of anti-idiotypic antibodies in the sera of patients receiving monoclonal antibodies for the treatment of ovarian cancer

Patient	Administered Monoclonal Antibody	Dose Administered	Presence of Anti-Id1 Antibody in Serum	Presence of Anti-Id2 Antibodies in Serum	Presence of Auto-Antibodies in Serum
1	HMFG2	10 mg	–	–	–
2	HMFG2	10 mg	–	–	–
3	HMFG2/H17E2	10 mg	–	–	–
4	HMFG2	10 mg	–	–	–
5	H17E2	10 mg	–	–	–
6	H17E2	10 mg	–	–	–
7	HMFG2	17 mg	–	–	–
8	HMFG1	20 mg	–	–	–
9	AUA1	20 mg	–	–	–
10	HMFG1	10 mg	–	–	–
	HMFG2	10 mg	–	–	–
11	HMFG2	7 mg	–	–	–
	HMFG2	6 mg	+	+	+
12	HMFG1	12 mg	–	–	–
	HMFG1/H17E2	10 mg	+	+	–
13	HMFG1	2 mg	–	–	–
	HMFG1	10 mg	–	–	–
	HMFG1	12 mg	+	+	+
14	HMFG2	2 mg	–	–	–
	HMFG2	10 mg	–	–	–
	HMFG2	10 mg	+	+	+
15	HMFG1	10 mg	–	–	–
	HMFG1	15 mg	+	+	–
	HMFG1	10 mg	+	+	+
	HMFG1	8 mg	+	+	–

From both our own and other studies, in both patients and animals [19–21], it is clear that modulation of the immune response via idiotypic antibodies results in the generation of antibodies with anti-tumor activity. Such anti-idiotypic responses could be enhanced by manipulation of the network, hopefully resulting in clinical benefit to patients.

Future prospects

This chapter outlined the types of human immune responses against murine monoclonal antibodies used in clinical trials. These responses have led to approaches to either suppress the cellular and humoral immune response or to reduce the xenogenic content of the administered therapeutic antibodies. Attempts at immunosuppressing recipients of murine monoclonal antibodies have been made. These include using large initial doses of monoclonal anti-

bodies [22] in order to obtain high zone tolerance or the use of immunosuppressive drugs such as prednisone and azathioprine [00]. High zone tolerance has not been shown to be achievable in most patients. Even the concurrent use of corticosteroids, azathioprine, and anti-T-cell receptor antibodies has not abolished the human anti-murine immunoglobulin antibody response in renal allograft recipients [23].

In a recent study [24] of the anti-Ig response in cynomologus monkeys, it was shown that total lymphoid irradiation (TLI) could reduce but not abolish the anti-Ig response. Cyclophosphamide, a potent immunosuppressive drug, has also failed in preventing anti-Ig responses in patients receiving murine monoclonal antibody therapy [25]. This drug has, however, been shown to be immunosuppressive when administered to cancer patients in low doses [26]. The major determinant of whether cyclophosphamide potentiates or suppresses immunity appears to be related to the time of administration in relationship to the presentation of the antigen [27].

As, on the whole, immunosuppression of the humoral immune response of patients to xenogenic monoclonal antibodies has been unsuccessful, attention has focused on the possibility of reducing the xenogeneic antibody content by either partial substitution of the murine antibodies' constant domains with human domains or by developing human monoclonal antibodies.

Recombinant DNA technology has made it possible to construct human/murine, chimeric antibodies [28]. This method consists of cloning the genomic DNA fragments encoding the heavy- and light-chain variable regions [29] or those encoding just the complementarity-determining regions [30] of a murine monoclonal antibody and inserting them into a mammalian expression vector, containing genomic DNA segments encoding the human constant regions. These expression vectors can then be transferred into mouse myeloma cells [31], resulting in the production of functional mouse-human chimeric immunoglobulin. When chimeric antibodies are eventually used in clinical trials, one would expect them to have at least two possible advantages over existing murine monoclonal antibodies. Firstly, they could be less immunogenic and, secondly, the human constant domains should interact more efficiently with human effector cells, thus enhancing tumor destruction.

The alternative to chimeric monoclonal antibodies is human monoclonals. In the last few years several methods have been developed to generate cell lines producing human monoclonal antibodies. Somatic cell hybridization between specific B lymphocytes and mouse myeloma cells have been hampered by stability problems due to selective loss of human chromosomes [32].

Epstein–Barr virus (EBV) immortalization of sensitized B lymphocytes into B-lymphoblastoid cell lines has been successfully applied to the production of human monoclonal antibodies [32]. However, lymphoblastoid cell lines usually secrete IgM antibodies, which are generally of lower affinity than IgG antibodies. The first true human-human hybridoma secreting human monoclonal antibody of predefined specificity was produced by Kaplan and Olsson [33]. The level of antibody production, however, was too low for

practical applications. Anti-tumor-binding activity of antibodies from hybridoma cells produced by the fusion of lymphocytes from patients with a variety of malignancies and human-myeloma-derived cells has been observed [34]. In this particular study, 12 antibodies with anti-tumor-binding activity were isolated. All, however, showed a low level of specificity and affinity.

It is hoped that both current and future research will result in stable human hybridomas, secreting both IgM and IgG monoclonal antibodies, with predefined specificity for tumor cell-surface antigens. Whether the use of either chimeric or human monoclonal antibodies will result in the development of anti-idiotypic antibodies, which abrogate their therapeutic efficacy, remains to be defined.

Some investigators doubt that the use of human or chimeric monoclonal antibodies will be sufficient to eliminate the antiglobulin response. These doubts are based on the finding that full tolerance is difficult to achieve; that is, even in the presence of tolerance to constant region determinants, cell-binding monoclonal antibodies still elicit strong anti-idiotypic responses [35].

Recently considerable interest has been shown in the possibility of using anti-idiotypic antibodies for modulation of immune responses. Particular interest, of course, has been shown in the use of such antibodies for the treatment of cancer. The concept of idiotype vaccines is based on antigen mimicry. Anti-idiotypes that mimic antigen have been generated in several systems, and their administration in vivo has been shown to either enhance or suppress a relevant immune response [36–38].

In a recent study, rats immunized with a monoclonal anti-idiotypic antibody raised against a tumor-reactive monoclonal antibody showed reduced tumor development following intravenous administration with tumor cells. The serum of these rats was also shown to contain significant levels of antibody indistinguishable in antigen specifity from the original tumor-reactive monoclonal antibody [39]. Other studies have shown that mice vaccinated with anti-idiotypic antibody demonstrated prolonged survival after tumor transfer [40] of SV-40-transformed cells.

It is hoped that these properties of anti-idiotypic antibodies mimicking tumor-associated antigen, by having significant amino-acid sequence homology, will be further exploited for making clinically useful idiotype vaccines against tumors, viruses, bacteria, and parasites [41–48].

References

1. Edwards, P.A.W. (1985) Heterogenous expression of cell-surface antigens in normal epithelia and their tumours, revealed by monoclonal antibodies. Br. J. Cancer 51:149.
2. Burchell, J., Durbin, H., and Taylor-Papadimitriou, J. (1983) Complexity of expression of antigenic determinants, recognised by monoclonal antibodies HMFG-1 and HMFG-2, in normal and malignant human mammary epithelial cells. J. Immunol. 131:508.
3. Mach, J.-P., Carrel, S., et al. (1980) Tumour localisation of radiolabeled antibodies against carcinoembryonic antigen in human colon carcinoma grafted into nude mice. Nature

(London) 248:704.
4. Travers, P., and Bodmer, W.F. (1984) Preparation and characterisation of monoclonal antibodies against placental alkaline phosphatase and other human trophoblast associated determinants. Int. J. Cancer 33:633.
5. Stevenson, G.T., and Stevenson, F.K. (1983) Treatment of lymphoid tumours with anti-idiotype antibodies. Springer Semin. Immunopathol. 6:99.
6. Chatenoud, L., Baudrihaye, M.F., et al. (1986) Restriction of the human in vivo immune response against the mouse monoclonal antibody OKT3. J. Immunol. 137:830.
7. Ashorn, R., Ashorn, P., et al. (1985) The use of radiolabeled monoclonal antibodies to human milk fat globule membrane antigens in antibody-guided tumour imaging, and administration of therapeutic dose of labelled antibody in wide-spread ovarian carcinoma. Ann. Chir. Gynaecol. 74:5.
8. Epenetos, A.A., Courtenay-Luck, N.S., et al. (1984) Antibody-guided irradiation of malignant lesions: Three cases illustrating a new method of treatment. Lancet 1:1441.
9. Davies, A.G., Bourne, S.P., et al. (1986) Pre-existing specific anti-mouse immunoglobulin in a patient receiving 131 I-murine monoclonal antibody for radioimmunolocalisation. Br. J. Cancer 53:289.
10. Schroff, R.W., Foon, K.A., et al. (1985) Human anti-murine immunoglobulin responses in patients receiving monoclonal antibody therapy. Cancer Res. 45:879.
11. Courtenay-Luck, N.S., Epenetos, A.A., et al. (1987) Pre-existing human anti-murine immunoglobulin reactivity due to polyclonal rheumatoid factors. Cancer Res. 47:4520.
12. Pimm, M.V., Perkins, A.C., et al. (1985) The characteristics of blood-bourne radiolabels and the effect of anti-mouse IgG antibodies on localisation of radiolabeled monoclonal antibody in cancer patients. J. Nucl. Med. 26:1011.
14. Dillman, R.O., Shawler, D.L., et al. (1983) Monoclonal antibody therapy of cutaneous T-cell lymphoma (CTCL). Blood 62(suppl 1):212.
15. Epenetos, A.A., Munro, A.J., et al. (1987) Antibody guided therapy of advanced ovarian cancer using intraperitoneally administered radiolabelled monoclonal antibodies. J. Clin. Oncol.
16. Jerne, N.K. (1974) Towards a network theory of the immune system. Ann. Immunol. (Paris) 125C:373.
17. Bruck, C., Sung Co, M., et al. (1986) Nucleic acid sequence of an internal image-bearing monoclonal anti-idiotype and its comparison to the sequence of the external antigen. Proc. Natl. Acad. Sci. USA 83:6578.
18. Zanetti, M., Glotz, D., and Rogers, J. (1986) Perturbation of the autoimmune network. J. Immunol. 137:3140.
19. Koprowski, H., Herlyn, D., et al. (1984) Human anti-idiotype antibodies in cancer patients: Is the modulation of the immune response beneficial for the patient? Proc. Natl. Acad. Sci. USA 81:216.
20. Herlyn, D., Lubeck, M., et al. (1985) Specific detection of anti-idiotypic immune responses in cancer patients treated with murine monoclonal antibody. J. Immunol. Methods 85:27.
22. Sears, H.F., Atkinson, B., et al. (1982) Phase-1 clinical trials of monoclonal antibody in treatment of gastrointestinal tumors. Lancet 1:726.
23. Chatenoud, L., Baudrihaye, M.F., et al. (1986) Restriction of the human *in vivo* immune response against the mouse monoclonal antibody OKT3. J. Immunol. 137:830.
24. Lowder, J.N., Miller, R.A., et al. (1987) Suppression of anti-mouse immunoglobulin antibodies in subhuman primates receiving murine monoclonal antibodies against T cell antigens. J. Immunol. 138:401.
25. Miller, R.A., Oseroff, A.R., et al. (1983) Monoclonal antibody therapeutic trials in seven patients with T-cell lymphoma. Blood 62:988.
26. Berd, D., and Mastrangelo, M.J. (1987) Effects of low dose cyclophosphamide on the immune system of cancer patients: Reduction of T-suppressor function without depletion of the C08+ subset. Cancer Res. 47:3317.
27. Turk, J.L., and Parker, D. (1982) Effects of cyclophosphamide on immunological control

mechanisms. Immunol. Rev. 65:99.
28. Neuberger, M.S., Williams, G.T., and Fox, R.O. (1984) Recombinant antibodies possessing novel effector functions. Nature 312:604.
29. Brown, B.A., Davis, G.L., et al. (1987) Tumor specific genetically engineered murine/human chimeric monoclonal antibody. Cancer Res. 47:3577.
30. Jones, P.T., Dar, P.H., et al. (1986) Replacing the complementarity determining regions in a human antibody with those from a mouse. Nature 321:522.
31. Sun, L.K., Curtis, P., et al. (1987) Chimeric antibody with human constant regions and mouse variable regions directed against carcinoma-associated antigen 17-1A. Proc. Natl. Acad. Sci. USA 84:214.
32. Iris, R.F., Sze, L.L., and Saxton, R.E. (1982) Human antibody to OFA-1, a tumor antigen, produced in vitro by Epstein–Barr virus-transformed human B-lymphoid cell lines. Proc. Natl. Acad. Sci. USA 79:5666.
33. Kaplan, H.S., and Olsson, L. (1980) Human-human hybridomas producing monoclonal antibodies of predefined antigenic specificity. Proc. Natl. Acad. Sci. USA 77:5429.
34. Sikora, K., Alderson, T., et al. (1983) Human hybridomas from patients with malignant disease. Br. J. Cancer 47:135.
35. Benjamin, R.J., Cobbold, S.P., et al. (1986) Tolerance to rat monoclonal antibodies. Implications for serotherapy. J. Exp. Med. 163:1539.
36. Sharpe, A.H., Gaulton, G.N., et al. (1984) Syngeneic monoclonal anti-idiotype can induce cellular immunity to reovirus. J. Exp. Med. 160:1195.
37. Skein, K.E., and Soderstrom, T. (1984) Neonatal administration of idiotype of anti-idiotype primes for protection against *Escherichia coli* K13 infection in mice. J. Exp. Med. 160:1001.
38. Uytdehaag, F.G.C.M., and Osterhaus, A.D.M.E. (1985) Induction of neutralising antibody in mice against polio virus type II with monoclonal anti-idiotypic antibody. J. Immunol. 134: 1225.
39. Dunn, P.L., Johnson, C.A., et al. (1987) Vaccination with syngeneic monoclonal anti-idiotype protects against a tumor challenge. Immunology 60:181.
40. Kennedy, R.C., Dreesman, G.R., et al. (1985) Suppression of in vivo tumor formation induced by simian virus 40-transformed cells in mice receiving anti-idiotypic antibodies. J. Exp. Med. 161:1432.
41. Binz, H., Meier, B., and Wigzell, H. (1982) Induction or elimination of tumor-specific immunity against a chemically induced rat tumor using auto-anti-idiotypic antibodies. Int. J. Cancer 19:417–421.
42. Raychaudhari, S., Saeki, H., et al. (1986) Tumor-specific idiotype vaccines. I. Generation and characterization of internal image tumor antigen. J. Immunol. 137:1743–2000.
43. Raychaudhuri, S., Saeki, H., et al. (1986) Tumor specific idiotype vaccines. II. Analysis of the tumor-related network response induced by the tumor and by internal image antigens (Ab2b). J. Immunol. 139:271–279.
44. Raychaudhuri, S., Saeki, Y., et al. (1987) Tumor-specific idiotype vaccines. III. Induction of T helper cells by anti-idiotype and tumour cells. J. Immunol. 139:2096–2102.
45. Zanetti, M., Sercatz, E., Salu, J. (1987) The immunology of new generation vaccines. Immunol. Today 8:18–25.
46. Nelson, K.A., George, E., et al. (1987) Immunotherapy of murine sarcomas with auto-anti-idiotypic monoclonal antibodies which bind to tumor-specific T cells. J. Immunol. 139: 2110–2117.
47. Herlyn, D., Wettendorff, M., et al. (1987) Anti-idiotype immunization of cancer patients: Modulation of the immune response. Proc. Natl. Acad. Sci. USA 84:8055–8059.
48. Capron, A., Dessaint, J.P., et al. (1987) Immunity to schistosomes: Progress toward vaccine. Science 238:1065–1072.

V

New Approaches

19. Antibody lymphoscintigraphy

John N. Weinstein

The term *antibody lymphoscintigraphy* as used here encompasses two techniques: 1) direct injection into cannulated lymphatic vessels, as was first performed by Order and his coworkers using polyclonal anti-ferritin preparations [1,2], and 2) injection into an interstitial space for uptake by the lymphatic capillaries, as was pioneered by DeLand, Goldenberg, et al. [3,4] using a polyclonal antibody directed against carcinoembryonic antigen. This chapter focuses on animal model studies of antibody lymphoscintigraphy, with only a brief description of the clinical experience. Clinical studies are covered *in extenso* by DeLand elsewhere in this volume.

The rationale for antibody lymphoscintigraphy is clear. Assessment of lymph-node status remains a major part of the staging work-up of most malignancies. The classic example is breast cancer, in which the status of axillary nodes appear to be the single most significant prognostic factor. Unfortunately, palpation of the axillary nodes is notoriously unreliable, as suggested by the 24–29% false-positive and 27–32% false-negative rates reported in various clinical series [5]. Prognosis correlates better with histopathology than with palpation [6]. The hope is that a noninvasive imaging technique might sometime substitute for surgical dissection. But current imaging techniques — standard x-ray, computerized tomography, magnetic resonance — have shown only mixed results for detection of tumors less than 1 cm in diameter. Hence, surgical dissection of the axilla remains a routine part of staging, despite evidence that it does not significantly increase survival rates [7].

The internal mammary chains are even less accessible to clinical evaluation, and they are not routinely dissected. Lymphoscintigraphy with technetium-labeled colloids [8–10] has been used to assess those nodes for breast cancer metastases. However, the technique is not very sensitive, since it depends, like contrast lymphangiography, on nonspecific uptake by macrophages in the nodes.

In principle, antibodies could provide much greater sensitivity, as indicated by the following calculation [11]: Consider a highly antigenic tumor able to bind 500,000 antibody molecules per cell and an antibody labeled with ^{131}I to a specific activity of 10 mCi/mg. Then there would be 2.75 disintegrations per minute per cell at saturation. Conventional gamma cameras can detect ap-

Goldenberg, D.M., (ed.), Cancer Imaging with Radiolabeled Antibodies.

proximately 100,000 disintegrations per minute over spontaneous background in a reasonable imaging time. Accordingly, it would be possible to detect approximately 40,000 antibody-labeled cells, or 0.04 mg of tumor. That represents an improvements of several orders of magnitude over other imaging techniques.

Detection of 40,000 cells may seem an unrealistic goal, but the calculation does indicate that diagnostic imaging with antibodies will not be limited by its intrinsic sensitivity. The practical limits of sensitivity are determined to some extent by geometric factors in imaging, but even more significantly by pharmacologic factors. The idea is to raise the signal-to-noise ratio, and that is where regional delivery in the lymphatics could be helpful. Whereas IV administration delivers only a small fraction of a percent of the dose to the target nodes, the lymphatic route may deliver more than 20% in animals and in humans. That is the basis of *antibody lymphoscintigraphy* (also called *immunolymphoscintigraphy*).

However, it should also be stated at the outset that the future of this approach is not established. Results have been excellent in both animal and clinical studies when the target has been a normal cell type or lymphoma. It remains to be seen whether access is sufficient to permit reliable imaging of solid tumor. A second, obvious limitation of the lymphatic approach is that it will not detect tumor in common sites of metastasis outside of the lymph nodes (except insofar as antibody passes from the lymphatics to the systemic circulation).

Physiology of the lymphatics

In order to understand the dynamics of antibody delivery via the lymph, it is necessary to appreciate certain aspects of lymphatic physiology, as described briefly here.

The lymphatic system functions rather like a recycling plant. It picks up proteins (including immunoglobulins) that have leaked out of the circulation, filters them through lymph nodes (in part, for inspection by the immune apparatus), and returns them to the blood stream. This specialization for protein uptake [12] provides the basis for antibody lymphoscintigraphy.

When small, water-soluble drugs are injected subcutaneously, they are cleared from the site primarily via the blood capillaries. However, molecules the size of immunoglobulins are prevented from entering blood capillaries by the continuous endothelial lining of the vessels and perhaps by the basement membrane. Instead, as indicated in Figure 1, macromolecules may pass into terminal lymphatic capillaries, which have clefts between their endothelial cells [13] and lack a basement membrane [14]. The clefts apparently open and close in response to local muscle activity and hydrostatic pressure differences. They have been reported to remain open in the face of external pressure (such as that of a local injection) because of fibers that pass like guy wires from interstitial collagen fibers to the endothelium.

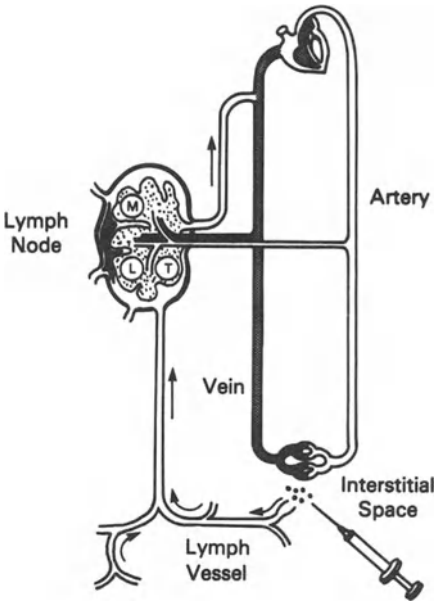

Figure 1. Schematic view of antibody delivery via the lymphatics. In the first node of the chain, or in more distant nodes, antibody may bind to normal cells such as the macrophages (M) and lymphocytes (L), or to tumor cells (T). Antibody not removed from the lymph passes into the blood stream, largely via the thoracic duct. Modified from Weinstein et al. [15].

Whatever the details may be, lymph forms in the capillaries and flows into tributary vessels of progressively increasing caliber. It is propelled by smooth muscle in the vessel walls, by extrinsic skeletal muscles, and by hydrostatic pressure differences (generated, for example, by the volume of injectate). Retrograde flow is prevented by a system of one-way valves. Lymph flows into the marginal sinus of the first lymph node encountered, then through sinusoids in the cortex and medulla and out of the node via an efferent vessel. Immunoglobulin molecules carried in the lymph may bind to target antigen in the node or be removed from the flow nonspecifically. Immunoglobulin remaining in the lymph passes to other nodes in the chain and then to the blood stream, largely via the thoracic duct. Thereafter, it would be expected to distribute to the organs of the body as though injected IV in the first place. However, material draining into the blood stream may not fairly represent that in the injectate. For one thing, bindable immunoglobulin may have been removed selectively by target cells in the nodes.

Monoclonal antibodies against antigens on normal cells

Initial animal studies were done in the mouse with monoclonals directed against normal lymph-node cells [15,16], rather than against tumor. Those

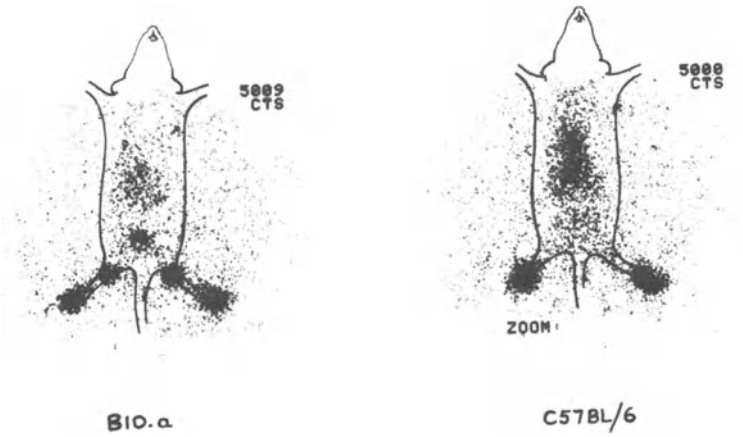

Figure 2. Antibody lymphoscintigraphy in mice. H-2K^k-positive (left) and H-2K^k-negative (right) mice 2 hours after injection in both hind footpads with ^{125}I-labeled anti-H-2K^k IgG (0.25 μCi/foot). The most prominent images are the injection sites. Popliteal nodes (behind the knees) and lumbar nodes (in the lower abdomen) are also prominent in the K^k-positive mouse but not in the K^k-negative animal. Body background is much more pronounced in the negative animal, largely because less antibody has bound in the feet and nodes. Modified from Weinstein et al. [15].

studies delineated the basic pharmacology. They also influenced the design of later clinical studies of patients with lymphoma and suggested ways of modifying regional immune function.

Antigens taken as targets included the class I major histocompatibility molecules H-2K and H-2D, the T-lymphocyte antigens Lyt 2 and Thy 1, and the B-lymphocyte antigen LyB 8. Figure 2 [15] shows gamma scintigraphy of the first pair of mice injected with ^{125}I-labeled monoclonal antibody 36-7-5 [16], a murine IgG_{2a} reactive with a private specificity of H-2K^k. The antigen is expressed on over 90% of the lymphocytes of K^k+ animals and binds 30,000–40,000 IgG per cell at saturation. It is also expressed (usually at lower levels) on almost all other cell types in K^k+ animals. Two hours after injection in the footpads, there were 50 times as many ^{125}I counts in the popliteal nodes of K^k+ mice as in those of K^k− ones. Uptake in the nodes was 10–20% of the injected dose. Since the nodes weighed, on average, 0.8 mg, this corresponded to more than 10,000% of dose per gram in the K^k+ popliteal nodes. High selectivity ratios were also observed for the lumbar and renal nodes, which are farther along the drainage pathway from the foot. Very little ^{125}I appeared in the axillary, cervical, or contralateral popliteal nodes, which are not in the drainage pathway from the footpad [15].

Additional studies showed the importance of antibody dose [17–19]. Above about 0.5 μg, k^k binding sites in the popliteal nodes saturated, and antibody overflowed to the lumbar and renal nodes. At about 1 μg those

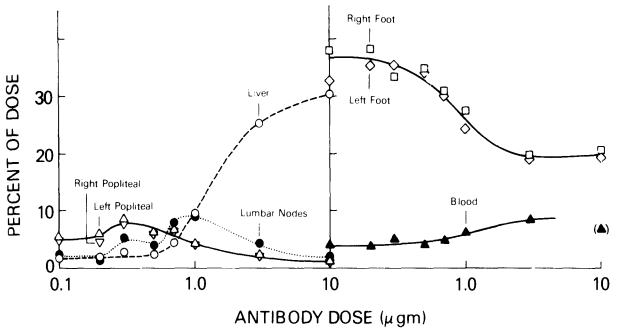

Figure 3. Dose dependence of ^{125}I-anti-K^k distribution 2 hours after injection in the hind footpads of K^k-positive mice. The injection volume was 50 μl/foot, and there were four animals per group. The liver (and other body organs) increase dramatically in uptake at doses above about 0.7 μg, thus reflecting the pattern of 'sequential overflow.' From Weinstein et al. [19].

nodes also saturated. Antibody then overflowed into the blood stream and distributed to the liver, spleen, lungs, kidneys, and other organs. As indicated by Figure 3, a dose of about 0.3 μg optimized the ratio of node image to body background. In antigen-negative mice, however, the kinetics of distribution were linear (i.e., independent of dose). This finding of a dose dependence was reflected in studies of patients with cutaneous T-cell lymphoma [20,21], as will be discussed later.

Kinetic modeling [22,23] of lymphatic delivery in the mouse indicated predominantly a pattern of 'sequential overflow' from one node to the next, and finally to the systemic organs. This pattern applies to antibody directed against antigens on normal lymph-node cells and (in patients) to antibodies against lymphoma. It seems unlikely to hold for antibody directed against isolated solid-tumor metastases in the nodes.

The initial animal experiments with anti-K^k provided information on two extreme cases: an antibody that bound to nothing (in the antigen-negative mouse strain) and one that bound to almost all cells (in the positive strain). Other studies of antibodies against lymphoid cells have used antigens of more restricted distribution. When fluorescein-labeled IgG anti-Lyt 2 was injected in the hind footpads of mice, it labeled all of the Lyt 2+ subpopulation in the popliteal nodes, as assessed by fluorescence microscopy and flow cytometry [15]. However, distribution in a node (even a normal node) is not always uniform. In the mouse, footpad injection drains only slightly and unevenly to the inguinal nodes. In guinea pigs some nodes appear to be segmented functionally and to label unevenly with dye injected in the watershed region [Parker et al., unpublished data].

Extensive pharmacologic studies with an IgG$_{2a}$ anti-LyB 8 (CY34), have shown the basic patterns expected from modeling of the anti-K^k data [Black

et al., manuscript in preparation]. Black et al. [25] have reported the biodistribution 4 hours after footpad injection for several different labels. Similar results were obtained whether the antibody was labeled with 1) ^{125}I by the Iodo-gen method, 2) ^{111}In chelated through 1-(p-phenylisothiocyanatobenzyl) diethylenetriamine pentaacetic acid [26], or 3) ^{212}Bi chelated through the same linker. Unlabeled CY34 effectively competed for binding in the regional nodes, whereas unlabeled irrelevant IgG (MOPC 21) did not.

Wahl et al. [27] have studied the kinetics of clearance from subcutaneous sites of injection in mice and rats. The reagents used were 225.28S, a murine IgG2a, and FT166, a murine IgM. Neither has been found to cross-react with any tissues in the mouse. Hence, these were studies of irrelevant Ig. Clearance appeared to be faster from the footpad than from subcutaneous injection sites on the abdomen, and, as expected, ambulation increased the rate of clearance. IgG and $F(ab')_2$ appeared to clear from the injection site at about the same rate, whereas Fab cleared faster. Pentameric IgM was found to clear at least as fast as the IgG. However, Halpern et al. [24] have reported that an irrelevant IgM clears incompletely and much more slowly than IgG from injection sites on the legs of mice. Further studies will be required to compare IgM and IgG with respect to subcutaneous injection.

Wahl et al. [28,29] have also compared the kinetics of various current and potential lymphoscintigraphy reagents in the rat. Subcutaneous injection resulted in much higher uptake in the regional nodes than did intravenous injection. The ratios of popliteal node/blood radioactivity 1 hour after injection were in the following order: ^{99m}Tc antimony trisulfide colloid > ^{125}I IgM > ^{125}I IgG. Nonbindable immunoglobulins were used in these studies; as noted by the investigators, the results would have been different for immunoglobulins reactive with nodal antigens.

Monoclonal anti-tumor antibodies

Most of the animal studies of *intravenous* antibody delivery to solid tumor have been performed with human tumor xenografts in nude mice. However, few if any implanted xenografts metastasize in a regular way to the regional nodes before becoming widely disseminated. Hence, the only animal model for solid tumor to be investigated extensively for antibody lymphoscintigraphy is the line 10 hepatocarcinoma of guinea pigs.

Line 10 is a methylcholanthrene-induced, transplantable tumor that metastasizes regularly to the regional lymph nodes. If implanted intradermally in the flank of a guinea pig, it metastasizes first to the ipsilateral superficial distal axillary (SDA) node. D3, a murine IgG_1 directed against a 290,000-dalton heterodimer on line 10 cells, selectively accumulates in line 10 tumors after intravenous injection [31,32]. When ^{125}I-labeled D3 was injected subcutaneously in either the front paw or the flank [33], lymph-node metastases were imaged. The resulting scintigrams are shown in Figure 4.

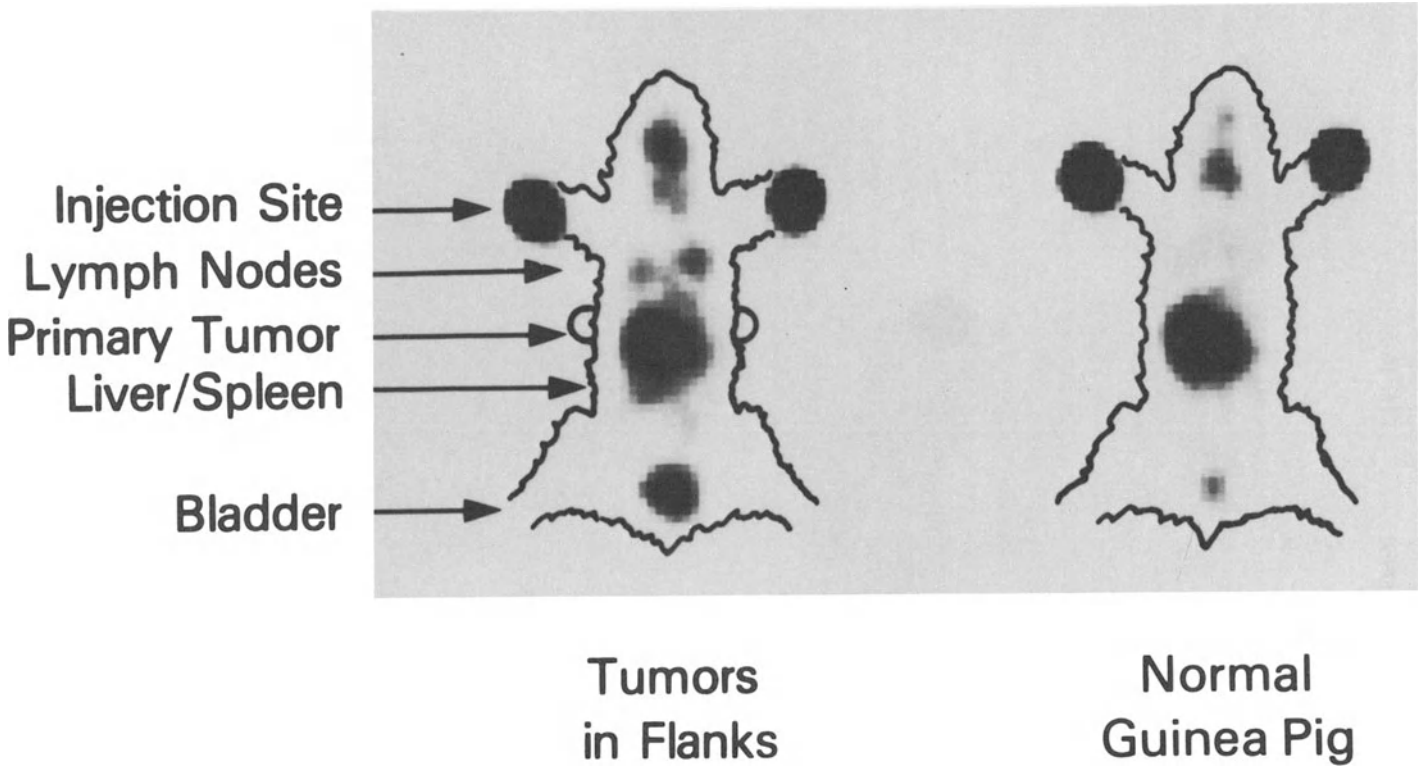

Figure 4. Antibody lymphoscintigraphy. Lymph-node metastases of line 10 hepatocarcinoma implanted intradermally in the flank of a guinea pig. Animals were imaged 27 hours after subcutaneous injection of ^{125}I-labeled D3 (anti-tumor) antibody in the flank. The lefthand panel shows the injection site and an image thought to be a cancerous draining lymph node. Upon excision of the node under anesthesia, the image disappeared. From Weinstein et al. [33].

The specificity of uptake was shown by coinjection of ^{125}I-D3 and ^{131}I-labeled isotype-matched control (MOPC 21). Ratios of 4 : 1 were obtained in the nodes. However, metastatic tumor accounted for only a few percent of node weight, and the ratio within the tumor itself was estimated at 10 : 1 to 100 : 1.

It remained possible that antibody was binding not to tumor cells, but to antigen shed from the primary and deposited in the lymph nodes. That possibility was ruled out by two lines of experiment. In the first [34], guinea pigs were injected with tumor in both flanks, and the primary on one side was excised under anesthesia 9 days later. On day 18, the animals were injected with ^{125}I-D3 and ^{131}I-MOPC. At sacrifice 17 hours later, the ^{131}I-MOPC counts were low and approximately equal on the two sides, showing that surgery had not grossly affected access to the ipsilateral nodes. Likewise, uptake of ^{125}I-D3 was not statistically different on the two sides, indicating that antigen shedding by the primary tumor could not have accounted for the ratios seen (unless the shedding had taken place 9 days earlier). The second line of evidence against binding to shed antigen was provided by autoradiographic studies (Figure 5), which showed localization of counts coincident with tumor. These studies in guinea pigs were done at an early stage of metastatic growth. When a lymph-node metastasis grew larger, to several hundred milligrams, antibody appeared to reach only part of the mass. This finding indicated a major possible limitation of lymphatic delivery, an inability to permeate [35,36], or even reach, bulky metastases.

The line 10 model was also used to test the feasibility of two-antibody techniques for imaging both malignant and normal lymph-node cells [37]. ^{125}I-D3 was injected subcutaneously in the flank of the guinea pig, and the ipsilateral superficial distal axillary node was imaged 24 hours later. ^{125}I-labeled IgG (8BE6) directed against guinea-pig T cells was then injected in the forepaw. The SDA node showed additional uptake. As long as the radioactivity in the second injection was kept high enough, both images could thus be obtained and quantitated using a single isotope. If the two antibodies were labeled with different isotopes, they could instead be coinjected and imaged using different energy windows.

The localization of radiolabeled murine monoclonal IgG (5F9.3) reactive with human choriocarcinoma has been studied in nude mice [30]. Choriocarcinoma xenografts were established in the popliteal regions of mice after repeated injection of cells (BeWo) into the footpad. When antibody was injected in the footpads, somewhat more radiolabel appeared in the tumor than when the antibody was injected intravenously, and there was a slight selectivity of uptake in double-label studies. Since the tumors weighed approximately 200 mg at the time of injection, as compared with a normal node weight of about 0.8 mg, little normal nodal architecture could be seen histologically. These findings suggest that uptake is possible, even when nodes have been essentially replaced by tumor, but 1) there is no information as to whether IgG had penetrated the mass in a uniform way, and 2) the possibility

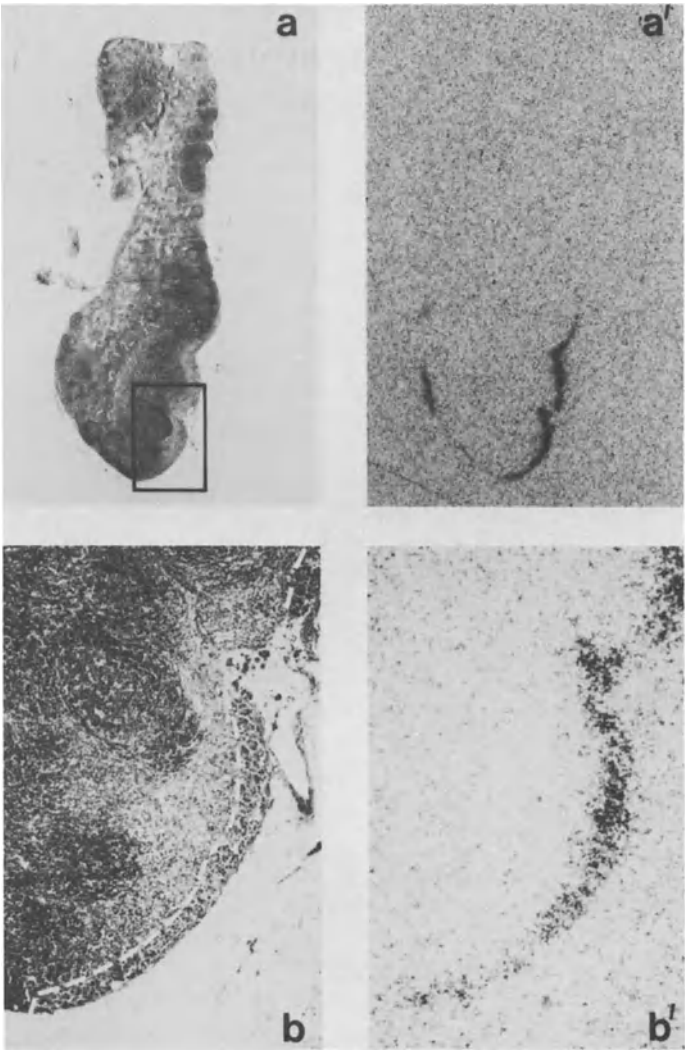

Figure 5. Autoradiographic study of a cancerous superficial distal axillary node 24 hours after ipsilateral subcutaneous injection of ^{125}I-D3 IgG. The guinea pig was injected with 34 μg D3 (3.4 μCi) on day 21 after implantation of 10^6 L10 cells. a) Section showing tumor occupying 2% of the node area. a′) Autoradiogram corresponding to that in a. Grains representing ^{125}I-labeled antibody are seen along the rim of the node at one end. b) Higher magnification corresponding to the inset box in a. Large, pleiomorphic tumor cells occupy the area demarcated by white dashed line. b′) Autoradiogram of section corresponding to that in b. Magnification of a and a′, 14x; of b and b′, 57x. From Weinstein et al. [33].

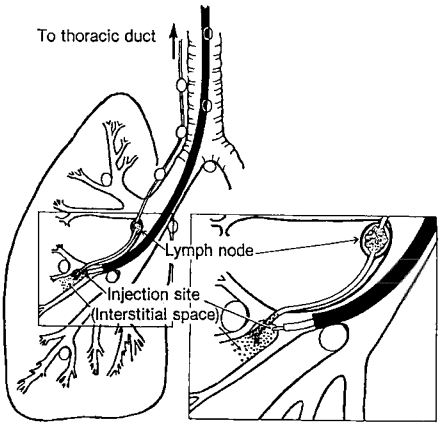

Figure 6. Schematic view of a technique for antibody lymphoscintigraphy in lung cancer. Transbronchial injection of the antibody is obtained via a fiberoptic bronchoscope and cytology needle. Injection is presumed to be in the region of a tumor, and the antibody is expected to follow the lymphatics to nodes in the lung and mediastinum. Analogous techniques might be used to detect lymph-node metastases from other visceral tumors. From Mulshine et al. [38].

of direct extension of radiolabel along tissue planes, rather than along the lymphatic vessels, cannot be ruled out. This proved a very difficult model system, given the low frequency and irreproducibility of tumor establishment, and it required great tenacity on the part of the investigators to work with it at all. A mouse xenograft model that metastasizes regularly and reproducibly to regional nodes would be very useful.

Bronchoscopic antibody lymphoscintigraphy

Subcutaneous injection suffices for most lymph-node groups. However, a different approach is required for nodes draining visceral organs. To reach cancerous hilar and mediastinal nodes, immunoglobulin could, in principle, be injected through the bronchial wall near a primary tumor using a cytology needle and a fiberoptic bronchoscope [38]. The immunoglobulin would then be expected to enter local lymph capillaries and drain, following the same pathway as do metastatic cells, toward nodes of the bronchi, carina, and mediastinum. The bronchoscopic approach is shown schematically in Figure 6.

A feasibility study of this approach has been conducted by Mulshine et al. [38] using ISCR3, an ^{131}I-labeled murine IgG_{2b} reactive with mouse I-E^k. ISCR3 was known to cross-react with determinants on antigen-presenting cells in a number of species, including the dog [39]. Initial experiments in dogs showed uptake in some of the hilar and carinal nodes (Figure 7).

Nodes with little radioactivity appeared not to be in the lymphatic drainage path from the injection sites in that they did not pick up Evans blue dye

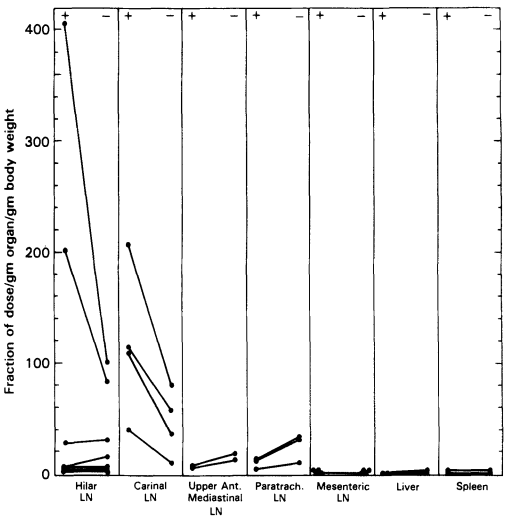

Figure 7. Analysis of radioactivity from pulmonary and mediastinal lymph nodes, liver, spleen, and mesenteric nodes after injection via bronchoscope of specific ^{131}I-labeled and irrelevant ^{125}I-labeled IgG in dogs. The data are expressed as fraction of dose per gram of organ, normalized by the body weight. For each individual organ, a line connects the data points for specific (+) and irrelevant (−) immunoglobulins. The 'specific' antibody was raised against mouse I-E but cross-reacts with antigen-presenting cells in the dog. The individual regional nodes that received large amounts of antibody appeared to be in the lymphatic drainage pathway because they also labeled with Evans blud dye coinjected with the antibody. Nonlabeled nodes may have been outside the drainage path from the lobes injected. From Mulshine et al. [38].

coinjected with the antibody. Uptake of ISCR3 in draining nodes was antigen specific and 15- to 100-fold greater than in distant (i.e., mesenteric) lymph nodes. The uptake in draining nodes was also 10- to 100-fold greater than that in liver, spleen, and kidney (per gram). Visceral organs showed greater uptake of the irrelevant control immunoglobulin than of the ISCR3 (except perhaps in the spleen, which contains cells that express the antigen). The results are shown in Figure 8.

Analogous endoscopic techniques might be useful in other settings. In colorectal carcinoma, for example, the status of regional nodes can sometimes determine whether the anal sphincter is saved at surgery or whether a patient with low rectal carcinoma will require a permanent colostomy. Injection of antibody through the mucosa near the site of a primary tumor might be helpful in that decision, although this possibility remains purely conjectural.

Antibody lymphotherapy

This volume focuses on diagnostic imaging. However, a brief mention of what might be termed *antibody lymphotherapy* seems in order since one motiva-

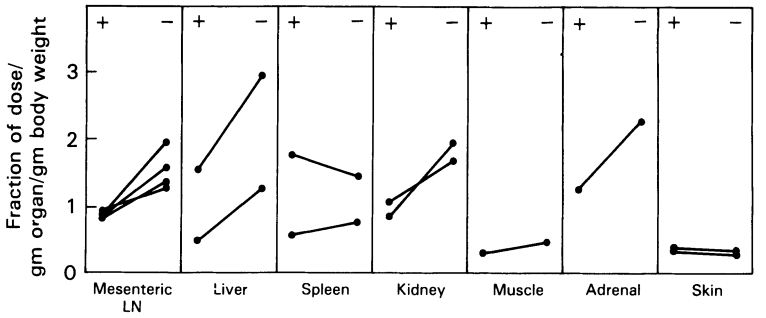

Figure 8. Analysis of radioactivity in organs outside of the regional drainage of transbronchial injection in dogs. ^{131}I (specific monoclonal antibody) and ^{125}I (irrelevant IgG) are indicated by '+' and '−,' respectively, as in Figure 7. The ordinate is greatly expanded from that of Figure 7 to show that the specificity ratios are reversed in distant organs and nodes. From Mulshine et al. [38].

tion for developing diagnostic techniques with antibody is the idea that similar approaches could then be used in treatment.

The potential for therapy via the lymphatics appears more limited than that for diagnostic staging. In breast carcinoma, for example, the regional lymph nodes are considered as indicators of metastatic spread, not as the site at which intervention can prevent dissemination. Surgical excision of the axillary nodes is thought not to influence survival statistics [7], but lymphatic delivery of antibodies might perhaps have advantages over external-beam radiotherapy for the prevention of local recurrences.

Conventional therapy does indicate settings in which antibody lymphotherapy might be useful; external-beam irradiation of regional nodes appears to improve the prognosis for selected patients with tumors that disseminate early via the lymphatics, for example, in Hodgkin's disease, some non-Hodgkin's lymphomas, and seminomatous testicular carcinoma.

The best isotope for therapy in the lymphatics may differ from that for intravenous administration. In particular, shorter lived radionuclides, such as the common alpha emitters, may be practical for direct injection into cannulated lymph vessels. Alpha particles have several advantages [25]: They form dense ionization tracks (high linear energy transfer, LET) with a range in tissues of 40–80 microns, and they are 10–20 times as potent biologically (per emission) as gamma photons or beta particles. Cells are unable to repair the massive damage caused by alpha particles, hence cytotoxicity is independent of dose rate. This could prove an important consideration, given the long period of exposure and low dose rates obtained by administering antibodies. The short range of alpha emissions would minimize radiation dosage to adjacent, nontarget cells.

Black et al. [25] have used conjugates of ^{212}Bi (half-life, 61 minutes) to obtain selective killing of B cells in the lymph nodes of mice. This represented the first antigen-selective use of alpha-emitter/antibody conjugates in

vivo. The antibody, CY-34 anti-Lyb 8.2, was labeled with ^{212}Bi by chelation with 1-(p-phenylisothiocyanatobenzyl) diethylenetriamine pentaacetic acid [26] and injected into the footpads of mice. The conjugate was selectively cytotoxic against B cells in the regional nodes [25]. Although there was no direct proof, this relative selectivity probably required the high spatial resolution of an alpha emitter (range about 70 μm for ^{212}Bi).

Clinical studies of antibody lymphoscintigraphy

Clinical studies of immunolymphoscintigraphy are covered in full elsewhere in this volume. Hence, only a brief summary of results will be given here.

Polyclonal antibodies and solid tumors

In 1975 Order et al. [1,2] reported two case studies in which polyclonal gamma globulin raised against the tumor-associated antigen ferritin was injected directly into cannulated lymph vessels of patients with Hodgkin's disease. Scintigraphic images of the first patient showed radioactivity localized in the area of involved regional lymph nodes. Such images were not seen in a second patient, who also showed no axial disease by ethiodol contrast lymphangiography.

DeLand, Goldenberg, and their colleagues [3,4] reported a series of patients injected subcutaneously with polyclonal ^{131}I-labeled goat IgG directed against carcinoembryonic antigen. Cancerous nodes were imaged. False-positive images also appeared, and the investigators suggested that these might represent binding to antigen shed from the primary tumor and deposited in lymph nodes. They thus pointed to one of the factors that may be important to lymph-node assessment, whether by the lymphatic or the intravenous route: the requirement to avoid antigens that accumulate in the nodes in the absence of viable tumor cells there.

Monoclonal antibodies and solid tumors

Thompson et al. [40] injected ^{131}I-labeled murine monoclonal IgM (3E1.2) into the web spaces between fingers of patients with breast cancer in an attempt to image axillary nodes. The antibody was directed against membrane and cytoplasmic components of breast carcinoma cells and was reactive also with the luminal membranes of normal breast. Nine patients were studied. There was a generally positive correlation between labeling of the axilla at 16–24 hours and the presence of disease. Nonspecific uptake was estimated in some patients by injecting ^{125}I-labeled control IgM. The efficiency of ^{125}I counting in the axillary nodes was determined by comparison with a calibrated ^{125}I source placed in the axilla. Specificity ratios of 2:1 were

estimated, but it was not possible to obtain surgical specimens with which to verify the correlations.

Antibody lymphoscintigraphy has also been tried for malignant melanoma. At the National Institutes of Health (NIH), several different antibody preparations have been studied in patients with stage II melanoma: ^{131}I-labeled Fab fragments of 96.5 (anti-p97) and 48.7 (anti-gp240), as well as IgG 9.2.27 (anti-gp240). The eventual clinical aim was to provide a noninvasive alternative to lymph-node dissection for patients with stage I disease, particularly those with thick and/or level 3 to level 5 primary lesions. Despite controlled, randomized trials that have addressed the question [41], there is still a lively debate [42] about the advisability of prophylactic lymph-node dissection in clinical stage I disease.

Some patients in the NIH study received injections subcutaneously near the site from which the primary tumor had been removed surgically. Others were injected in the finger webs to reach axillary nodes or in the toe webs for access to axial lymph-node groups. Despite sporadic suggestions of selective uptake, no reliable selectivity for cancerous nodes was demonstrated and no clinically useful imaging achieved [43]. Similar studies by Nelp et al. [44] have, likewise, yielded no consistent imaging.

Better antibodies, labels, linkers, and techniques may improve the results significantly. It is clear, for example, that antibodies labeled with ^{111}In by conventional methods deposit far too much ^{111}In in the nodes nonspecifically to permit sensitive imaging of metastases. ^{131}I as a label may underestimate the actual binding. It is also quite possible that lymph-node metastases of melanoma develop in a way that simply precludes effective access to, or percolation into, the nodes, and the same may hold for other tumors.

Monoclonal antibodies in lymphoma

The results are much more positive for lymphoma, as reported by Keenan et al. [20,21]. T101 [45] is a mouse IgG_{2a} directed against a T65 antigen on cells of chronic lymphocytic leukemia and cutaneous T-cell lymphoma (CTCL). Normal T cells also express the antigen. ^{111}In-labeled T101 was injected in the toe webs of CTCL patients. Serial scintigrams showed large accumulations of activity in the inguinal-femoral and iliac lymph nodes within 3 hours after injection. Activity in the regional nodes plateaued within 24 hours and then declined slowly. Figure 9 shows the first two patients imaged [20]. The first had minimal involvement (LN 2) of the regional nodes, which took up 24% of injected ^{111}In. The second had bulky disease in the ndoes, which took up 36%. Additional patients also showed efficient uptake, and injection of an isotype-matched control antibody [20] demonstrated that the uptake of T101 is largely antigen specific, with specificity ratios of 7.7 and 5.9 in the inguinal-femoral and iliac nodes, respectively, at 48 hours [21]. An inguinal-femoral node biopsy of one patient contained more than 2% of ^{111}In dose per gram at 7 days. That number is about two orders of magnitude higher than the local-

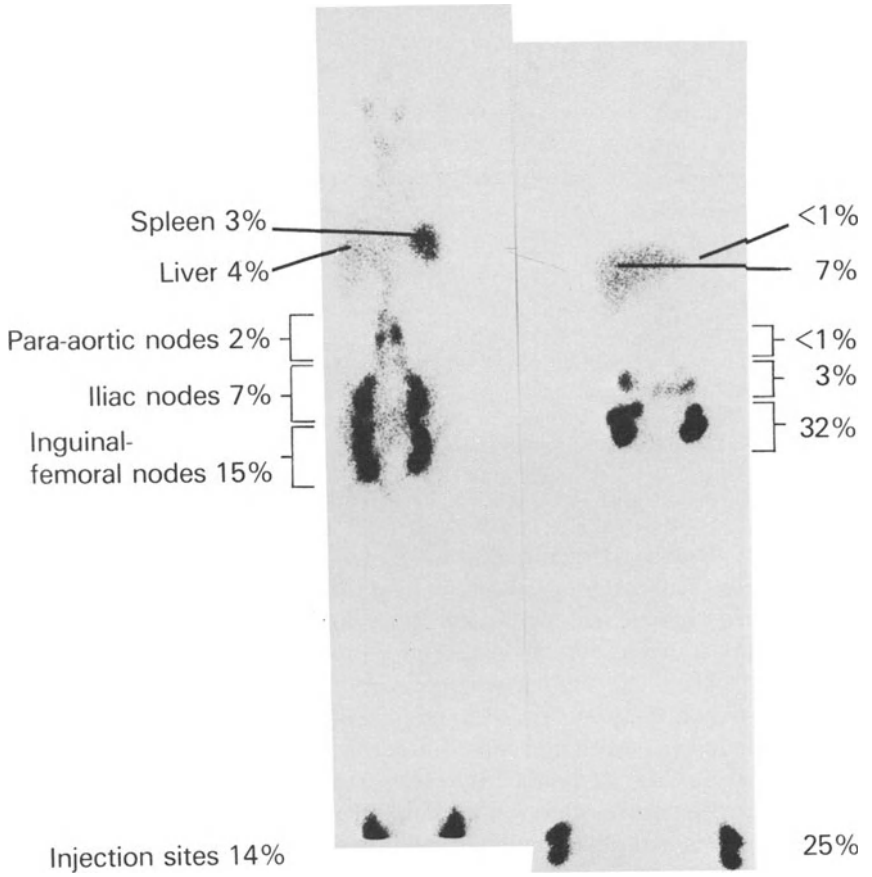

Figure 9. Anterior whole-body scintigraphy 2–3 days after administration of ^{111}In-labeled T101 in the toe webs of both feet. Numbers indicate percentages of injected activity in organs, nodes, and injection sites. Values for iliac and inguinal-femoral nodes represent the means of those obtained separately for the left and right sides. The patient on the left had only minimal disease (LN 2) in the nodes. Percentages given were corrected for decay but not for tissue attenuation. The feet were partly out of the camera view, but percentages were calculated from region-of-interest scans taken at about the same time. The patient on the right had bulky disease. Double foci in the feet of the righthand patient resulted from dorsiflexion and plantar flexion during imaging. The efficiencies of lymph-node imaging were orders of magnitude higher than after IV injection. From Keenan et al. [20].

ization of most antibodies administered IV. It must be remembered, however, that T101 binds to normal T cells as well as malignant cells, hence the uptake cannot be called 'tumor specific.' More selective reagents would be required to detect very small numbers of malignant cells in the nodes.

Figure 9 indicates very efficient imaging of the inguinal-femoral and iliac nodes, but much less labeling of the paraaortic chains, which are more distant from the injection site. Those two patients had been injected with 0.05 mg

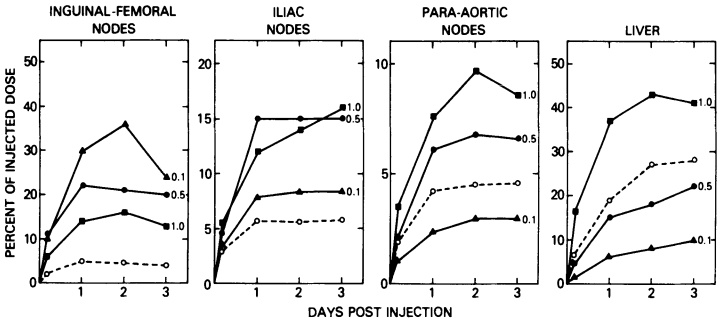

Figure 10. Dose dependence of antibody lymphoscintigraphy with T101 in patients with cutaneous T-cell lymphoma. Doses: 0.1 mg T101 (closed triangles); 0.5 mg T101 (closed circles); 1.0 mg T101 (closed squares); and 0.5 mg 9.2.27 anti-melanoma (open circles). The 9.2.27 served as an isotype-matched negative control, but its accumulation in nodes may have been increased by cross-reactive binding. The pattern suggests 'sequential overflow.' From Keenan et al. [21].

IgG per side. The 'sequential overflow' model [23], based on animal studies such as that in Figure 3, suggested to us that the paraaortics could be imaged if the protein dose were increased severalfold (at the same dose of radiolabel). Figure 10 shows the results when the IgG dose was increased five-fold and ten-fold [21]. All of the subdiaphragmatic nodes then imaged, but the price was a greater overflow into the systemic circulation and therefore a higher uptake in the liver and other organs. Based on these studies, the optimal SC dose of T101 for toe web injection appeared to be about 0.25 mg/foot. However, more extensive data would probably indicate dependence on tumor bulk, variations in lymphatic function, degree of active or passive exercise of the extremity, and other parameters.

Mulshine and coworkers [manuscript in preparation] have compared subcutaneous and direct intralymphatic injection of T101 in patients with cutaneous T-cell lymphoma. Both approaches yielded high percentages of uptake in the nodes. Hence, for imaging of CTCL, there was no clear advantage to direct intralymphatic injection that could offset the logistic difficulty and discomfort of the cannulation procedure. The two techniques have not yet been compared with respect to the detection of metastatic solid tumor or with respect to therapy.

Discussion

Possible advantages and limitations of lymphatic delivery with respect to IV administration have been reviewed previously [46–49] and are summarized in Table 1.

Antibody lymphoscintigraphy is obviously a limited enterprise. It is not intended to detect metastases in sites other than the lymph nodes. Further-

Table 1. Comparison of subcutaneous and intravenous injection of monoclonal antibodies for delivery to tumor in lymph nodes*

Possible Limitations of Subcutaneous Administration	Possible Advantages of Subcutaneous Administration
Restriction to regional nodes	Lower dose
Requirement that lymph vessels be patent and antigens accessible	Detection of smaller masses
Possible toxicity at injection site	Can be faster
Possible immune sensitization to mouse immunoglobulin	Less systemic toxicity
Biologic variability of lymphatics	Less competition by circulating antigen
	Less cross-section with antigen expressed on normal cells

* Modified from Table 1 in Weinstein et al. [11].

more, the lymphatics must be patent and lymph flow patterns not too badly distorted if antibody is to reach its target. The disappointing results in melanoma may reflect an access problem, and the success with lymphoma may reflect easier access and penetration. Lymphatic and intravenous scintigraphy may prove useful in tandem — the former to detect small, early nodal metastases and the latter to detect large ones.

Antitumor antibody may also be useful in combination with an antibody directed against normal lymph-node cells. The latter would be expected to show gross distortion or blockage of the lymphatic chain. The feasibility of that approach was demonstrated in guinea pigs [37], as described earlier.

Toxicity at the injection site appears not to be a major problem for antibody lymphoscintigraphy, even with an unfavorable isotope such as ^{131}I. No local radiation damage has been reported in animal studies or in the clinic. For therapy with armed antibodies, however, local toxicity may be a major issue for subcutaneous injection, and possibly for direct intralymphatic injection as well.

Sequestration of antibody in the lymphatics is expected to reduce cross-reactive binding. Antitumor antibodies unsatisfactory for IV use because of poor selectivity could be useful for delivery via the lymphatics. It might be possible, for example, to use a monoclonal antibody equally reactive with normal cells and cancerous cells of breast or colon. In some cases, cross-reaction may even be an advantage for diagnostic studies. For example, antibody 96.5 (an anti-melanoma IgG) is removed from the circulation by the liver more quickly than are many other antibodies [50], probably because of cross-reactive binding. The liver is sufficiently large that there would presumably be no toxicity at radiation doses used for antibody lymphoscintigraphy. Hence, hepatic accumulation would tend to clear away background radioactivity due to antibody that overflowed the lymphatics into the blood stream.

In conclusion, there are several ways in which either interstitial or direct intralymphatic injection could be applied for 'antibody lymphoscintigraphy':

1. Use of anti-tumor antibodies for detection of lymph-node metastases of solid tumors. There has been only one report of significant clinical success in this context. We do not yet know whether the disappointing results thus far are due to inadequacies of the reagents, labels, and techniques, or to fundamental inaccessibility of the tumor antigens.
2. Use of anti-tumor antibodies for detection of lymphoma in lymph nodes. In this setting, the images obtained (with T101) have been truly striking. The challenge is to develop selective enough antibodies to distinguish normal from abnormal cells.
3. Use of antibodies against normal cells in the node, used analogously to radiolabeled colloids. The ideas is to use the very efficient uptake (> 20% of injected dose) to delineate the architecture of lymph-node chains. Obvious areas of application include the internal mammary and axillary nodes. Antibody could also be used to identify draining nodes in cases of truncal melanoma. Possible advantages vis à vis colloids include the faster and more complete washout of proteins from the injection site and nodes, and the possibility of targeting any of the cell types in the node. It might, for example, be possible to find antigenic correlations with reactive, as opposed to cancerous, nodes. Perhaps the largest single barrier to such nonspecific application is the possibility of immune sensitization to the administered IgG (in immunocompetent individuals). Antibody lymphoscintigraphy will become much more attractive if human-derived antibodies or mouse-human chimeric molecules turn out to be less immunogenic, or else if current attempts to suppress the human anti-mouse response prove successful.

References

1. Order, S.E., Bloomer, W.D., Jones, A.G, Kaplan, W.D., Davis, M.A., Adelstein, S.J., and Hellman, S. (1975) Radionuclide immunoglobulin lymphangiography: A case report. Cancer 35:1487–1492.
2. Order, S.E. (1977) Immunospecific radionuclide immunoglobulin lymphography. In: Clouse, M.E. (ed.), *Clinical Lymphography*, Vol. 7. Baltimore: Williams and Wilkins, pp. 316–322.
3. DeLand, F.H., Kim, E.E., Corgan, R.L., Casper, S., Primus, F.J., Spremulli, E., Estes, N., and Goldenberg, D.M. (1979) Axillary lymphoscintigraphy by radioimmunodetection of carcinoembryonic antigen in breast cancer. J. Nucl. Med. 20:1243–1250.
4. DeLand, F.H., Kim, E.E., and Goldenberg, D.M. (1980) Lymphoscintigraphy with radionuclide-labeled antibodies to carcinoembryonic antigen. Cancer Res. 40:2997–3000.
5. Hellman, S., Harris, J.R., Canellos, G.P., and Fisher, B. (1982) Cancer of the breast. In: De Vita, V.T., Jr., Hellman, S., and Rosenberg, S.A. (eds.), *Cancer, Principles and Practice of Oncology*. Philadelphia: JB Lippincott, pp. 914–970.
6. Haagensen, C.D. (1977) Int. J. Rad. Oncol. Biol. Phys. 2:975–980.
7. Fisher, B., Wolmark, N., Redmond, C., Deutsch, M., and Fisher, E.R. (1981) Cancer 48: 1863–1872.
8. Ege, G.N. (1976) Internal mammary lymphoscintigraphy. Radiology 118:101–107.
9. Ege, G.N. (1983) Lymphoscintigraphy — Techniques and applications in the management

of breast cancer. Semin. Nucl. Med. 13:26–34.
10. Kaplan, W.D. (1983) Iliopelvic lymphoscintigraphy. Semin. Nucl. Med. 13:42–53.
11. Weinstein, J.N., Keenan, A.M., Holton, O.D., III, Covell, D.G., Sieber, S.M., Black, C.D.V., Barbet, J., and Parker, R.J. (1985) Use of monoclonal antibodies to detect metastases of solid tumors in lymph nodes. In: Ceriani, R.L. (ed.), *Monoclonal and Breast Cancer*. Boston: Martinus Nijhoff, pp. 218–232.
12. Yoffey, J.M., and Courtice, F.C. (1970) *Lymphatics, Lymph and the Lymphomyeloid Complex*. London: Academic Press, pp. 1–942.
13. Leak, L.V. (1971) Studies on the permeability of lymphatic capillaries. J. Cell Biol. 50: 300–323.
14. Barsky, S.H., Baker, A., Siegal, G.P., Togo, S., and Liotta, L.A. (1983) Use of anti-basement membrane antibodies to distinguish blood vessel capillaries from lymphatic capillaries. Am. J. Surg. Pathol. 7:667–677.
15. Weinstein, J.N., Parker, R.J., Keenan, A.M., Dower, S.K., Morse, H.C., 3rd, and Sieber, S.M. (1982) Monoclonal antibodies in the lymphatics: Toward the diagnosis and therapy of tumor metastases. Science 218:1334–1337.
16. Sachs, D.H., Mayer, N., and Ozato, K. (1981) In: Hammerling, U., and Kearney, J.F. (eds.), *Monoclonal Antibodies and T-Cell Hybridomas*. Amsterdam: Elsevier/North-Holland Press, pp. 95–101.
17. Steller, M.A., Parker, R.J., Covell, D.G., Holton, O.D., III, Keenan, A.M., Sieber, S.M., and Weinstein, J.N. (1986) Optimization of monoclonal antibody delivery via the lymphatics: The dose-dependence. Cancer Res. 46:1830–1834.
18. Parker, R.J., Weinstein, J.N., Keenan, A.M., Dower, S.K., Steller, M.A., Holton, O.D., and Sieber, S.M. (1987) Targeting of radiolabeled monoclonal antibodies in the lymphatics. Cancer Res. 47:2073–2076.
19. Weinstein, J.N., Steller, M.A., Covell, D.G., Holton, O.D., III, Keenan, A.M., Sieber, S.M., and Parker, R.J. (1984) Monoclonal anti-tumor antibodies in the lymphatics. Cancer Treat. Rep. 68:257–264.
20. Keenan, A.M., Weinstein, J.N., Mulshine, J.L., Carrasquillo, J.A., Bunn, P.A., Jr., Reynolds, J.C., Foon, K.A., Perentesis, P., Ghosh, B., and Larson, S.M. (1987) Evaluation of lymphoma by immunolymphoscintigraphy: Subcutaneous injection of indium-111-labeled T101 monoclonal antibody. J. Nucl. Med. 28:42–46.
21. Keenan, A.M., Weinstein, J.N., Carrasquillo, J.A., Bunn, P.A., Jr., Reynolds, J.C., Foon, K.A., Smarte, N.C., Ghosh, B., Fejka, R.M., Larson, S.M., and Mulshine, J.L. (1987) Immunolymphoscintigraphy and the dose dependence of ^{111}In-labeled T101 monoclonal antibody in patients with cutaneous T-cell lymphoma. Cancer Res. 47:6093–6099.
22. Weinstein, J.N., Steller, M.A., Covell, D.G., Dower, S.K., Segal, D.M., Keenan, A.M., Sieber, S.M., and Parker, R.J. (1983) Use of monoclonal antibodies for diagnosis and therapy of tumor metastases in lymph nodes. In: Chaiken, I.M., Wilchek, M., and Parikh, I. (eds.), *Affinity Chromatography and Biological Recognition*. New York: Academic Press, pp. 337–342.
23. Covell, D.G., Steller, M.A., Parker, R.J., and Weinstein, J.N. (1985) Delivery of monoclonal antibodies through the lymphatics: Characterization by compartmental modeling. Comp. Applica. Med. Care 10:884–888.
24. Halpern, S.E., Hagan, P.L., Bartholomew, R.M., Frincke, J.M., Poggenburg, J.K., Merchant, E.B., and Carlo, D.J. (1986) Kinetics and distribution of subcutaneously administered 111-In IgG and IgM antibodies (A) in a mouse model (abstract). J. Nucl. Med. 27: 902.
25. Black, C.D.V., Atcher, J.B., Brechbiel, M.W., Holton, O.D., III, Hines, J.J., Gansow, O.A., and Weinstein, J.N. (1988) Selective ablation of B lymphocytes in vivo by an alpha emitter, ^{212}Bismuth, chelated to a monoclonal antibody. Antibody, Immunoconju. Radiopharma. 1:43–53.
26. Brechbiel, M.W., Gansow, O.A., Atcher, R.W., Schlom, J., Esteban, J., Simpson, D.E., and Colcher, D. (1986) Inorg. Chem. 25:2772.

27. Wahl, R.L., Geatti, O., Liebert, M., Wilson, B., Shreve, P., and Beers, B.A. (1987) Kinetics of interstitially administered monoclonal antibodies for purposes of lymphoscintigraphy. J. Nucl. Med. 28:1736–1744.
28. Wahl, R.L., Fisher, S., and Petry, N.A. (1986) Antibodies, albumin and antimony: Comparison of three lymphoscintigraphic agents. Radiology 161:322.
29. Wahl, R.L., Liebert, M., Wilson, B.S., and Petry, N.A. (1988) Radiolabeled antibodies, albumin and antimony sulfide colloid: A comparison as lymphoscintigraphic agents. Nucl. Med. Biol. 15:243–250.
30. Wahl, R.L., Laino, L., Fisher, S., Schteingart, M., and Beierwaltes, W.H. (1988) Improved radioimmunolocalization of human tumor xenografts following subcutaneous delivery of monoclonal antibodies. Eur. J. Nucl. Med. 13:530–536.
31. Key, M.E., Bernhard, M.I., Hoyer, L.C., et al. (1983) Guinea pig line 10 hepatocarcinoma model for monoclonal antibody serotherapy II. In vivo localization of a monoclonal antibody in normal and malignant tissues. J. Immunol. 130:1451–1457.
32. Bernhard, M.I., Hwang, K.M., Foon, K.A., et al. (1983) Localization of ^{111}indium and ^{131}iodine labeled monoclonal antibody in guinea pigs bearing line 10 hepatocarcinoma tumors. Cancer Res. 43:4429–4433.
33. Weinstein, J.N., Steller, M.A., Keenan, A.M., Covell, D.G., Key, M.E., Sieber, S.M., Oldham, R.K., Hwang, K.M., and Parker, R.J. (1983) Monoclonal antibodies in the lymphatics: Selective delivery to lymph node metastases of a solid tumor. Science 222: 423–427.
34. Weinstein, J.N., Keenan, A.M., Holton, O.D., III, Covell, D.G., Sieber, S.M., Black, C.D.V., Barbet, J., and Parker, R.J. (1985) Use of monoclonal antibodies to detect metastases of solid tumors in lymph nodes. In: Ceriani, R.L. (ed.), *Monoclonal Antibodies and Breast Cancer*. Boston: Martinus Nijhoff, pp. 218–232.
35. Weinstein, J.N., Black, C.D.V., Barbet, J., Eger, R.R., Parker, R.J., Holton, O.D., III, Mulshine, J.L., Keenan, A.M., Larson, S.M., Carrasquillo, J.A., Sieber, S.M., and Covell, D.G. (1986) Selected issues in the pharmacology of monoclonal antibodies. In: Tomlinson, E., and Davis, S.S. (eds.), *Site-Specific Drug Delivery: Cell Biology, Medicinal and Pharmaceutical Aspects*. New York: John Wiley, pp. 81–91.
36. Covell, D.G., Barbet, J., Holton, O.D., III, Black, C.V.D., Keenan, A.M., Sieber, S.M., and Weinstein, J.N. Global and local factors in the pharmacology of monoclonal antibodies. Ame. Statist. Soc. Sympos., in press.
37. Weinstein, J.N., Black, C.D.V., Keenan, A.M., Holton, O.D., III, Larson, S.M., Sieber, S.M., Covell, D.G., Carrasquillo, J., Barbet, J., and Parker, R.J. (1986) Use of monoclonal antibodies for detection of lymph node metastases. In: Reisfeld, R.A., and Sell, S. (eds.), *Monoclonal Antibodies in Cancer Therapy*. New York: Alan R. Liss, pp. 473–488.
38. Mulshine, J.L., Keenan, A.M., Carrasquillo, J.A., Walsh, T., Linnoila, R.I., Holton, O.D., Harwell, J., Larson, S.M., Bunn, P.A., and Weinstein, J.N. (1987) Immunoscintigraphy of pulmonary and mediastinal lymph nodes: A new approach to lung cancer imaging. Cancer Res. 47:3572–3576.
39. Watanabe, M., Suzuki, T., Taniguchi, M., and Shinohara, N. (1983) Monoclonal anti-Ia murine allo antibodies cross reactive with the Ia-homologies of other mammalian species including humans. Transplantation 36:712–718.
40. Thompson, C.H., Stacker, S.A., Salehi, N., Lichtenstein, M., Leyden, M.J., Andrews, J.T., and McKenzie, I.F.C. (1984) Immunoscintigraphy for detection of lymph node metastases from breast cancer. Lancet 2:1245–1247.
41. Veronesi, U., Adamus, J., Bandiera, D.C., Brennhovd, I.O., Caceres, E., Cascinelli, N., Claudio, F., Ikonopisov, R.L., Javorskj, V.V., Kirov, S., Kulakowski, A., Lacour, J., Lejeune, F., Mechl, Z., Morabito, A., Rode, I., Sergeev, S., van Slooten, E., Szczygiel, K., Trapeznikov, N.N., and Wagner, R.I. (1977) Stage I melanoma of the limbs: Immediate versus delayed node dissection. N. Engl. J. Med. 297:627.
42. Balch, C.M., Cascinelli, N., Milton, G.W., and Sim, F.H. (1985) Elective lymph node dissection. In: Balch, C.M., and Milton, G.W. (eds.), *Cutaneous Melanoma*. Philadelphia:

J.B. Lippincott, pp. 131–157.
43. Lotze, M.T., Carrasquillo, J.A., Weinstein, J.N., Bryant, G.J., Perentesis, P., Reynolds, J.C., Matis, L.A., Eger, R.R., Keenan, A.M., Hellstrom, I., Hellstrom, K.-E., and Larson, S.M. (1986) Monoclonal antibody imaging of human melanoma: Radioimmunodetection by subcutaneous or systemic injection. Ann. Surg. 204:223–235.
44. Nelp, W.B., Eary, J.F., Jones, R.F., Kishore, R., Krohn, K.A., Beaumier, P.L., Hellstrom, K.-E., and Hellstrom, I. (1986) Preliminary studies of radiolabeled monoclonal antibody lymphoscintigraphy in malignant melanoma. J. Nucl. Med. 26:66.
45. Royston, I., Majda, J.A., and Baird, S.M., et al. (1980) Human T cell antigens defined by monoclonal antibodies: The 65,000-dalton antigen of T cells (T65) is also found on chronic lymphocytic leukemia cells bearing surface immunoglobulin. J. Immunol. 125:725–731.
46. Weinstein, J.N., Parker, R.J., Holton, O.D., III, Keenan, A.M., Covell, D.G., Black, C.D.V., and Sieber, S.M. (1985) Lymphatic delivery of monoclonal antibodies: Potential for detection and treatment of lymph node metastases. Cancer Invest. 3:85–95.
47. Weinstein, J.N., Holton, O.D., III, Black, C.D.V., Covell, D.G., Spaulding, G.F., Barbet, J., Steller, M.A., Sieber, S.M., Talley, M.J., and Parker, R.J. (1986) Regional delivery of monoclonal antitumor antibodies: Detection and possible treatment of lymph node metastases. In: Welch, D.R., Bhuyan, B.K., and Liotta, L.A. (eds.), *Cancer Metastasis: Experimental and Clinical Strategies*. New York: Alan R. Liss, pp. 169–180.
48. Weinstein, J.N., Eger, R.R., Covell, D.G., Black, C.D.V., Mulshine, J., Carrasquillo, J.A., Larson, S.M., and Keenan, A.M. (1987) The pharmacology of monoclonal antibodies. Ann. NY Acad. Sci. 507:199–210.
49. Weinstein, J.N., Black, C.D.V., Holton, O.D., III, Covell, D.G., Parker, R.J., Mulshine, J.L., Lotze, M.T., Carrasquillo, J., Eger, R.R., Lewis, A., Larson, S.M., and Keenan, A.M. (1987) Delivery of monoclonal antibodies to lymph nodes via the lymphatics. In: Winkelhake, J.L., and Holcenberg, J.S. (eds.), *The Pharmacology and Toxicology of Proteins*. New York: Alan R. Liss, pp. 75–89.
50. Larson, S.M., Brown, J.P., Wright, P.W., et al. (1983) Localization of ^{131}I-labeled p97-specific Fab fragments in human melanoma as a basis for radiotherapy. J. Nucl. Med. 24: 123–129.

20. Radioimmunoguided surgery: A new intraoperative approach to the detection of tumor

Edward W. Martin, Jr., George Hinkle, Cathy Mojzisik, Marlin O. Thurston

Tumors marked with a radiolabeled antibody may be located by two different techniques. The first is the diagnostic use of a gamma camera to produce an image. The second is the clinical use of a gamma-sensitive probe to 'home in' on tumors intraoperatively. Since the two techniques are quite different, it is not surprising that they differ in advantages, limitations, and design.

The essential elements of the gamma-camera system are the isotope, the collimator, the scintillation crystal, the optical sensor array, and the image-processing electronics. The choice of isotope is dictated primarily by the requirement that the absorption of radiation by intervening tissue be minimized if deep sources are to be seen. High-energy isotopes are therefore preferred.

Since gamma rays cannot be focused to make an image, it is necessary to use a collimator. A practical collimator is complex and only the most basic aspects are described here. The collimator is essentially a bundle of many small tubes made of heavy metal such as lead or tungsten. Each element of the detection crystal is exposed only to the rays entering the tube from a direct source. Only rays that are approximately parallel to the axes of the tubes are used; all other rays are absorbed by the metal between the apertures. Those that strike the metal walls obliquely must be absorbed, and this requires an adequate wall thickness. If a high-energy isotope is selected in order to reduce tissue absorption, the high-energy radiation will also penetrate the walls more readily, and greater wall thickness must be used. The ratio of the open area of the apertures to the cross-sectional area of the metal is consequently reduced. In order to achieve higher image resolution, it is necessary to reduce the area of the collimator apertures at the expense of efficiency. One is usually willing to trade efficiency for resolution, and efficiencies of the order of a small percent are typical.

Another very important factor affecting the performance of a gamma camera is related to the distance between a small source that is to be imaged and the detector crystal. A small source radiates randomly in all directions, but only the fraction of the total radiation that is intercepted by a particular area of the detector crystal can contribute to its part of the image. This fraction is defined by the area of an aperture of the collimator divided by the area of a sphere centered at the source, with a radius equal to the distance from the

Goldenberg, D.M., (ed.), Cancer Imaging with Radiolabeled Antibodies.

source to the crystal. If we call the distance from the source to the crystal r and the area of the aperture A, the fraction will $A/(4\pi r^2)$. Thus, if the distance were increased from 2 cm to 20 cm, the amount of radiation striking the detector element would be reduced by a factor of 10^2, or 100. It might seem that this reduction could be compensated by increasing the imaging time by a factor of 100, but in practice the improvement that can be obtained is limited. The difficulty is that there is always some level of general background radiation from the body, and the intensity of this radiation decreases very slowly with distance from the surface. Thus, at some distance the image from a small source will be lost in background. In addition, as the collimator is moved farther from the source, the radiation spills over into adjacent collimator elements and the image becomes increasingly blurred. It is also true that radiation, as it passes through tissue, may be scattered by interaction with electrons. This so-called Compton scattering causes some of the gamma photons to change direction as well as to lose energy, resulting in further blurring of the image. This difficulty can be reduced to some degree by using energy discrimination to reject Compton-scattered photons.

Another technique for improving image quality is to inject a second labeled carrier that does not go preferentially to the tumor. Radiation counts from this isotope are a measure of background and can be used in a computer subtraction process to increase the tumor-to-background contrast. Nevertheless, it remains difficult to detect small, deep-lying sources with a gamma camera.

The elements of a gamma-detecting probe (GDP) are the isotope, possibly a collimator, the detector crystal, and the signal processing electronics. Since the probe is used intraoperatively, it can be brought close to the source of radiation, and the inverse square law implies that the count rates will be relatively very high. Another result of the proximity of the probe to the source is that loss of radiation by tissue absorption is no longer a serious consideration. Consequently, the use of a low-energy isotope is feasible. In fact, the use of a low-energy isotope has the additional advantage that background radiation from surrounding tissue is attenuated, with a resulting increase in contrast. The isotope that we have found to be particularly useful is ^{125}I. Its use with a handheld probe was first reported by W.G. Myers [1]. We have found it advantageous because its principal gamma rays and x-rays are in the energy range from 25 to 35 keV, where there is fairly strong tissue absorption. Also, the 60-day half-life of this isotope is advantageous for clinical reasons that will be discussed later.

We chose to use a semiconductor gamma detector rather than a crystal because it appeared to offer advantages for compact and rugged design and also because it permitted the use of much lower voltages. It is difficult to use silicon as a gamma detector because of its low stopping power for gamma rays, and germanium is not suitable because it requires refrigeration. We chose, therefore, to use CdTe, which has excellent stopping power and performs well at room temperature. For high-energy gamma rays, the number of counts per second is approximately proportional to the volume of the crystal,

but for the low-energy gamma rays that we use, the absorption is very near the surface, making the number of counts per second more nearly proportional to the area of the surface that the rays strike. A thin-disk geometry is therefore appropriate.

The inverse square law mentioned earlier in connection with the gamma camera applies also to a single detector element in a probe. Since the probe, during the operation, can be brought close to sources of radiation, the count rate is greatly increased. For this reason the probe can be used to detect much weaker sources than can be seen with a gamma camera. It is also especially important to note that the rapid variation of count rate with distance permits accurate location of small sources without the use of a collimator. When the probe is scanned across the location of a source, the count rate peaks sharply at the point of closest approach. It is useful to have the sides and back of the probe shielded from background radiation, but a large angular aperture for the detector often facilitates scanning. The principal value of a collimator is to reduce the background count from tissue and thus to improve the source-to-background ratio.

The design of the electronic signal processing system is dictated by the way in which the probe is used during the operation. The surgeon uses the probe as a homing device and is guided by the sound generated by the control unit. It has been found by experience that clicks or beeps made by individual gamma rays do not enable the hearer to distingush small changes in count rate, particularly when the count rates are low. This is true because gamma-ray emission is a completely random process, and consequently large fluctuations in rate occur when the count rate is low. In order to overcome this difficulty, a synthetic sound based on running averages is generated. It can be adjusted so that no sound is produced when the probe is receiving only the background count from normal tissue and will produce a nearly continuous sound when the count exceeds this level by a small factor. The system continues to provide all of the normal counting functions, regardless of the squelch setting. The system also includes an adjustable energy window to allow discrimination against unwanted radiation.

Historic overiew

Animal studies

Animal studies phase I (Anti-CEA-Mab ^{131}I). The early GDP used in animal studies consisted of a cadmium telluride crystal, a preamplifier, and an amplifier with a digital read-out displaying the radioactive counts (Figure 1). Very shortly after the first probe was developed, the crystal was housed in a 16-mm diameter lead collimator with a 4-mm aperture and then connected in one unit (Figure 2).

Swiss nude mice (supplied by the Animal Production and Genetics Branch

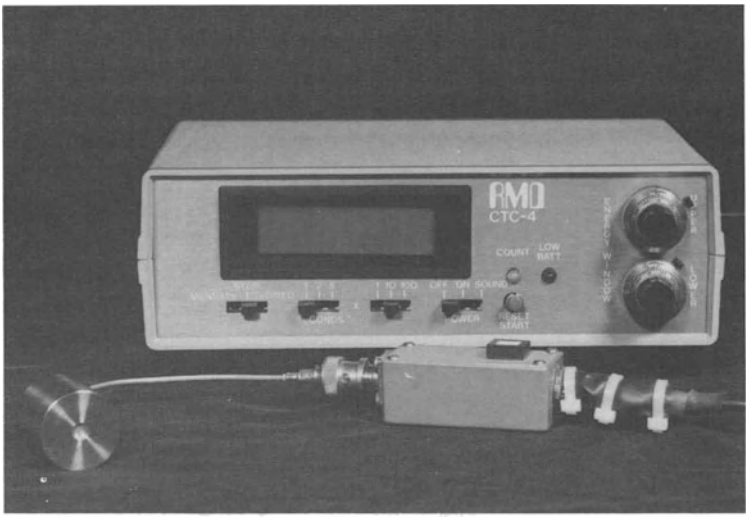

Figure 1. The first gamma detecting probe consisted of a cadmium telluride crystal, preamplifier, and a digital read-out display.

of the National Cancer Institute) had a CX-1 human colon adenocarcinoma implanted in the right flank. The tumor xenograft produced CEA. An affinity-purified baboon antiserum against CEA (CEA-As) was labeled with iodine (^{131}I) using the chloramine-T reaction. The radiolabeled ^{131}I CEA-As (40 μCi)

Figure 2. A later model of the GDP was modified to resemble a surgical instrument.

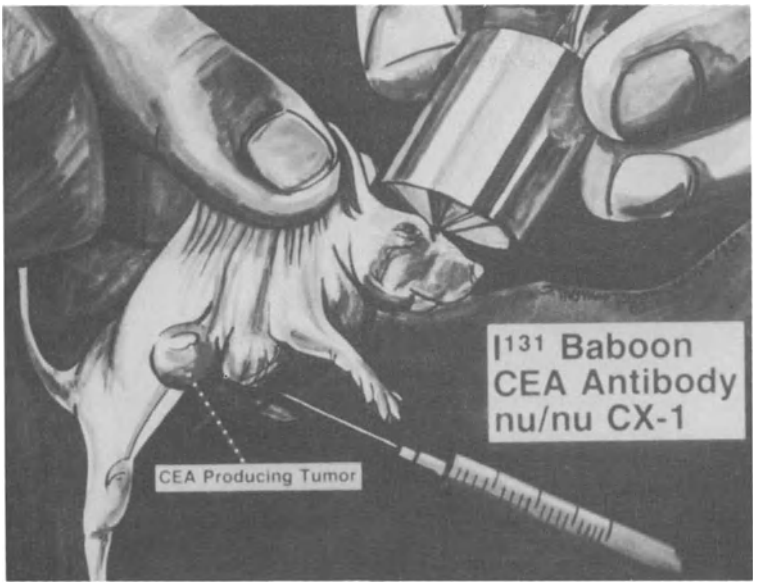

Figure 3. Conceptual representation of CEA-producing tumor growing in the flank of an athymic mouse. Radiolabeled ^{131}I-CEA antisera was injected intraperitoneally and the gamma detecting probe was used to measure radioactivity at various anatomic sites.

was injected intraperitoneally into the mice (Figure 3). The GDP was used to measure activity over the subcutaneous flank tumor, the contralateral flank without tumor (control site), the liver, and the thyroid. Each reading was for a 20-second period and was repeated four times at 12, 24, 48, and 72 hours following injection. The mean and standard deviation of each reading was calculated.

The degree of ^{131}I CEA-As localization in the tumor at each reading was derived from the following ratio of radioactive count activity: tumor-flank counts/non-tumor-flank counts. Following the 72-hour readings, the mice were killed humanely and various tissues were placed in a gamma well counter to determine their activity. Selected mice were imaged each day following the injection of escalating doses of radiolabeled antisera.

Preferential localization of tumor radioactivity was noted as early as 24 hours following intraperitoneal ^{131}I-CEA-As injection (Table 1) [2]. This pattern continued until the death of the animal. Localization was apparent, even though the number of detected counts at the various sites decreased over 3 days. The daily drop in radioactivity was due to both physical decay and biologic elimination. The gamma-well-determined activity in the tumors was increased over that in other tissues, except that the activity in the blood was nearly equal to that in the tumor.

Although preferential radioactivity localization was detected with injection

Table 1. Gamma detecting probe count ratios comparing tumor flank (TF) counts to nontumor flank (NTF) counts

Time After Injection of ^{131}I-CEA-Antisera (hours)	Mean ± SD	Range
12	1.04 ± 0.14	0.88–1.12
24	1.44 ± 0.33	1.10–1.75
48	1.58 ± 0.07	1.50–1.60
72	1.80 ± 0.43	1.26–2.21

Table 2. GDP [^{131}I] CEA-As activity in CX-1 tumor

Hours Post-injection	Tumor Counts (mean)	Opposite Flank Counts (mean)	Tumor: Opposite Flank Counts (ratio)	Log Ratio ± SD
12	814	881	0.936 ± 0.139	−0.076 ± 0.150
24	170	129	1.346 ± 0.313	0.274 ± 0.219
48	115	76	1.560 ± 0.290	0.428 ± 0.182
72	94	56	1.732 ± 0.355	0.530 ± 0.204

of 40 μCi, it was not until the injected dose was increased to 200 μCi that imaging with a scintillation camera was possible.

Animal studies phase II (radiolabeled specific and nonspecific antisera). The use of radiolabeled baboon carcinoembryonic antigen (CEA)-specific antisera produced increased tumor isotope localization in CEA-producing tumors compared with the injection of nonspecific antisera (Table 2) [3]. Tumor isotope-antisera localization was not influenced by the tumor volume or the time since tumor implantation. The GDP probe counts demonstrated a high degree of correlation with gamma-well tissue counts. The probe was able to detect preferential tumor localization of doses lower than could be detected with external scintillation cameras.

Animal studies phase III (preferential localization of antibody combinations). The gamma detecting probe count ratios of tumor-to-nontumor control site (T/NT) for ^{125}I-labeled antibodies consistently exceeded those for ^{131}I-labeled antibodies (Table 3) [4]. No significant difference was observed between the monoclonal and polyclonal antibodies when used as single preparations. However, when the two were used in combination, an increased T/NT ratio was observed (Figure 4).

A comparison of the percent injected dose per gram of tumor was made to that of blood, liver, and muscle for the various ^{125}I-radiolabeled antibodies (Table 4). The polyclonal antibody provided the lowest circulating blood activity at 72 hours postinjection. The blood activity was lowered by the use of the two antibodies in combination. At the same time, the combination of

Table 3. Localization of tumors with antibody combinations: Ratio of the tumor to contralateral flank

Antibody	P-1		M-1		P-1 + M-1	
Hours	^{125}I	^{131}I	^{125}I	^{131}I	^{125}I	^{131}I
24	3.73 ± 1.2	1.51 ± 0.9	3.93 ± 0.9	2.18 ± 0.7	4.04 ± 1.0	2.02 ± 0.9
48	5.33 ± 2.8	1.68 ± 0.8	5.15 ± 2.6	1.89 ± 0.6	5.36 ± 2.7	2.56 ± 1.2
72	7.24 ± 3.9	2.30 ± 0.9	7.48 ± 3.3	2.20 ± 1.0	9.98 ± 3.4	4.27 ± 1.8

antibodies improved tumor localization over that attained by the separate use of the individual antibodies.

This animal study demonstrated that the tumor uptake of both ^{125}I- and ^{131}I-radiolabeled anti-CEA antibodies was accomplished in female Swiss nude mice, each bearing a CEA-producing human colon adenocarcinoma xenografted in one flank. The counts from the tumor and contralateral flank were recorded at 24, 48, and 72 hours following injection. The animals were killed, and the tumors and other organs removed, weighed, and then assessed in an automatic gamma counter. The cadmium telluride GDP counter was more efficient at counting ^{125}I-labeled antibodies than ^{131}I antibodies. The tumor-to-contralateral flank ratios improved with the use of a monoclonal anti-CEA and polyclonal anti-CEA in combination over those attained by the single antibodies. Investigation of the external counting characteristics of the portable gamma detector demonstrated a potential for its adjunctive intraoperative use for the localization of gastrointestinal tumors.

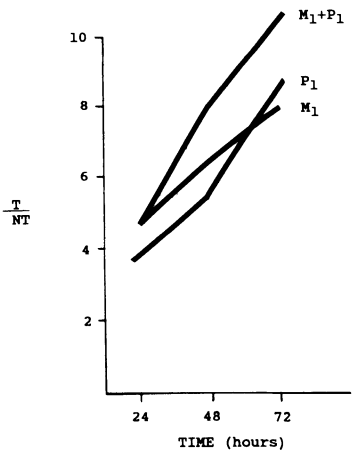

Figure 4. Tumor (T) to nontumor (NT) ratios. Murine anti-CEA monoclonal antibodies (M-1), polyclonal baboon anti-CEA (P-1), and the combination (M-1 + P-1) are expressed by tumor-to-nontumor flank ratios dependent on time.

Table 4. Comparison of tumor to normal tissue distribution of ^{125}I-labeled antibodies 72 hours after injection

Antibodies Tissue	M-1	P-1	M-1 + P-1
Blood	0.45 ± 0.2	1.13 ± 0.4	0.99 ± 0.3
Liver	1.56 ± 0.3	2.62 ± 0.5	2.21 ± 0.5
Muscle	3.24 ± 1.0	5.16 ± 0.8	10.22 ± 1.9

Animal studies phase IV (prolonged binding). The biodistribution and kinetics of seven monoclonal antibodies with known reactivity against CX-1 tumor were examined by a handheld gamma detecting probe (Neoprobe^{TM}) over 21 days. Twenty-eight immunodeprived (athymic) nude mice implanted with human-colon adenocarcinoma CX-1 xenografts were injected intraperitoneally with 50 μCi of ^{125}I-labeled antibodies (four mice/antibody). Of the seven monoclonal antibodies, four were anti-CEA (MA, MB, MC, and MD), two were anti-TAG-72 (B72.3 NCI and B72.3 fermented), and one was anti-colorectal cancer (17.1A IgG) (Table 5) [5]. Daily probe counts were recorded in duplicate over the tumor site and the contralateral nontumor site (background), and tumor-to-background (Tu/Bkg) ratios were calculated (Table 6). Animals were sacrificed on day 21, and blood, heart, liver, spleen, lungs, kidneys, intestine, muscle, and the tumor were removed for gamma-well counting (Table 7).

Even though all antibodies identified the tumor as early as 24 hours post-injection, specific tumor localization continued, and Tu/Bkg ratios improved greatly late in the experiment. Although patterns of prolonged tumor binding varied considerably from one antibody to another, all showed climbing Tu/Bkg ratios, except for MG, which peaked between days 9 and 13. This indicates progressive clearance of the antibodies from the background tissue and a persistence of activity in the tumor. We concluded that most antibodies showed evidence of prolonged binding with tumor antigens, resulting in considerably improved tumor localization with increasing postinjection time.

Table 5. Monoclonal antibodies used for animal trials

Antibody	Radionuclide	Specificity
MA	^{125}I	Anti-CEA
MB	^{125}I	Anti-CEA
MC	^{125}I	Anti-CEA
MD	^{125}I	Anti-CEA
B72.3 NCI	^{125}I	Anti-TAG-72
B72.3 fermented	^{125}I	Anti-TAG-72
17-1A	^{125}I	Anti-colon cancer

Table 6. Mean absolute gamma probe counts tumor to background (T/B) ratios

Days	Anti-CEA MA			Anti-CEA MB			Anti-CEA MC			Anti-CEA MD			Anti-TAG-72 B72.3 (NCI)			B72.3 (Fermented)			Anticolon cancer 17-1A		
	1	2	3	1	2	3	1	2	3	1	2	3	1	2	3	1	2	3	1	2	3
1	7256	3752	1	3566	1836	1	9662	7523	0	5845	4099	0	15991	7126	1	8643	4339	1	1800	872	2
2	9051	4784	3	1648	292	7	10701	6772	1	7828	3962	1	16629	4636	3	9051	2854	2	1796	548	4
3	7903	1511	5	1471	248	7	13795	4296	2	11994	3384	3	17267	3298	5	10444	2846	3	1748	632	3
4	2887	430	10	1522	610	2	13285	2501	5	9274	2192	3	18868	5209	3	5668	1393	3	1540	348	6
5	4628	695	11	977	131	13	11571	2529	5	9802	2718	3	21352	5435	3	10058	2838	3	1408	288	6
6	3501	360	15	*	*	*	10913	2369	4	7107	2204	3	31703	4377	7	11419	2497	4	1324	260	7
7	2975	254	22	814	81	119	11344	2039	6	6747	2098	2	19903	4077	5	11128	2409	5	1184	200	8
8	2591	213	33	776	96	90	6982	1305	9	7211	1904	3	18849	3081	7	11343	2095	6	1104	188	11
9	2775	130	70	*	*	*	11492	1531	10	9545	1680	5	18243	2970	8	13240	1469	11	1184	172	15
10	3202	207	31	557	94	27	11714	1417	10	10268	1378	7	16319	1761	11	13949	1328	12	1000	136	14
11	2924	182	64	587	94	50	12403	1991	6	9927	1994	4	13251	2211	11	14738	1916	7	1000	128	17
12	3095	114	108	504	87	25	8647	788	13	8488	1368	6	18133	3400	8	11758	1607	7	884	148	13
13	2926	111	97	430	57	44	7828	687	16	6854	887	8	15426	2306	10	15235	1604	8	728	120	38
14	4662	85	261	388	51	38	7730	551	24	6464	633	11	16249	1550	18	12777	788	19	732	84	24
15	1949	81	291	*	*	*	6812	605	20	6053	746	8	17777	1647	22	12327	1042	13	616	96	15
16	1767	80	93	325	66	9	4352	457	47	3851	471	12	15982	1039	43	13044	1112	13	656	84	22
17	1786	104	176	309	84	13	7213	523	29	6411	453	15	16661	1310	29	13728	1011	15	544	92	20
18	1680	95	157	291	61	28	7202	384	51	6290	327	23	17311	1214	34	10548	670	19	488	80	15
19	1618	92	107	*	*	*	5505	413	25	5134	399	15	16844	1019	44	13019	670	23	448	68	47
20	1491	76	69	254	42	42	5509	265	89	4483	375	15	15519	1039	38	12775	653	23	444	76	44
21	999	80	197	276	55	21	5833	425	32	4577	301	25	15767	941	49	7151	248	50	404	64	64

1 - Mean tumor counts 2 - Mean background counts 3 - T/B ratios * Probe malfunction

Table 7. Tumor-to-tissue ratios determined by mean organ well counts and tumor well counts — day 21

Tissue	MA		MB		MC		MD		B72.3 (NCI)		B72.3(Ferm)		17-1A	
	■■■	■■■	■■■	■■■	■■■	■■■	■■■	■■■	■■■	■■■	■■■	■■■	■■■	■■■
Blood	10569	(24.0)	1017	(20.0)	290229	(2.3)	155859	(2.2)	329659	(1.7)	925898	(1.0)	27225	(1.65)
Heart	4812	(53.0)	480	(42.9)	128251	(5.3)	47472	(7.1)	182103	(3.1)	212776	(2.5)	8164	(5.5)
Liver	3835	(66.0)	956	(21.5)	81972	(8.3)	43512	(7.8)	178242	(3.1)	191647	(2.8)	6040	(7.4)
Spleen	3926	(65.0)	1324	(15.5)	61420	(11.1)	34221	(9.9)	146910	(3.8)	131793	(4.0)	7236	(6.2)
Lungs	6818	(37.0)	1634	(12.6)	127351	(5.3)	58079	(5.8)	289877	(1.9)	355857	(1.5)	13055	(3.4)
Kidneys	3692	(69.0)	725	(28.4)	82135	(8.2)	35734	(9.5)	132069	(4.2)	139587	(3.8)	10780	(4.1)
Intestines	980	(259.0)	233	(88.4)	15206	(44.6)	29239	(11.6)	28692	(19.5)	76347	(7.1)	2951	(15.2)
Muscle	3462	(73.0)	838	(24.6)	62611	(10.8)	14714	(23.0)	225968	(2.5)	132465	(4.0)	4442	(10.1)
Tumor	254214	-	20617	-	679378	-	338449	-	560253	-	542541	-	45019	-

■■■ - cpm/gm (Counts per minute per gram of tissue)

■■■ - Tu/Tis (Tumor to tissue ratio)

Pathology

Heterogeneity. Murine monoclonal antibody (Mab) 17-1A has been used in radioimmunodetection and immunotherapy trials of intestinal adenocarcinoma in humans. Tumor heterogeneity of antigen expression has been recognized as a potential limiting factor in such studies. We designed a study to evaluate the degree of heterogeneity of 17-1A antigen expression among primary and metastatic human colon carcinomas [6]. In all, 141 specimens, including 74 primary or metastatic colon adenocarcinomas, were evaluated using an avidin-biotin complex immunoperoxidase technique on briefly fixed, frozen-tissue sections. All of these showed at least focal staining with Mab 17-1A. However, well or moderately differentiated tumors generally showed diffuse cytoplasmic immunostaining, whereas poorly differentiated tumors showed minimal immunostaining with no detectable antigen in most areas. In 16 cases that had both primary and metastatic adenocarcinomas or multiple metastatic tumors, 17-1A antigen expression was similar among the tumor sites, except for one case. This case showed variation in tumor differentiation and corresponding variation in 17-1A antigen expression. Of 36 additional malignant tumors that were not of colonic epithelial origin, adenocarcinomas of the stomach, duodenum, endometrium, ovary, and breast showed 17-1A antigen expression.

Heterogeneity of expression of tumor-associated antigens has been previously documented, not only between tumors from different individuals, but among tumors from a single patient. This suggests that tumor-selective monoclonal antibodies may have some limitations in the radioimmunolocalization and immunotherapy of human tumors, and that each Mab needs to be individually evaluated.

Affinity, tumor burden, and tumor size. The study related the in-vitro affinity of Mab 17-1A IgG for human colorectal cancer cells to the limits of detection of the gamma probe. When doubling dilutions were made from SW1116-coated cell pellets and injected subserosally into specimens of human colon, an earlier version of the probe (Figure 2) detected 6.25×10^5 coated cells [7]. The probe count ratios were $< 1\%$ of those obtained by well counter but $20\times$ greater than background. A linear relationship was observed between the number of cells injected and the number of counts obtained with either the probe or the well counter. Improved findings were obtained with a later model (Figure 5) of the probe, 3.9×10^4 cells ($\lll 1$ mm^3). Injected cells, coated with labeled Mabs that had specific activities (< 1 μCi/μg Mab), were counted three times. Replicate counts showed 2–10% variation. Counts obtained with either the probe or well counter increased linearly with increasing numbers of injected cells at various concentrations of the cell-bound ^{125}I Mab 17-1A IgG. Dilutions of cell pellets, which were coated with greater amounts of the labeled antibody, gave higher count rates with both the probe and the well counter. The probe detected as few as 3.9×10^4 antibody-coated

Figure 5. Improvements in the gamma detecting probe included a 1-cm crystal, a modified preamplifier concealed in the handle, and amplified sound.

cells and, at this number of cells, the counts were 10× greater than background but were < 5% of those obtained with the well counter. The counts obtained with either the probe or well counter increased linearly with increasing numbers of injected ^{125}I-17-1A IgG-coated cells. Those cells coated with higher concentrations of ^{125}I-17-1A IgG gave higher probe or well counts.

We have defined the in-vivo minimal numbers of tumor cells detected by a handheld gamma probe that appears to be many times more sensitive than the gamma camera. Assuming that the latter could detect a tumor 1 cm^3 in volume, this would be equivalent to approximately 10^9 cells. As few as 6.25×10^5 ^{125}I-antibody coated cells (< mm^3) could be detected with an earlier version of the probe (Figure 2) and an even smaller number (3.9×10^4 cells) (⋘ 1 mm^3) can be detected by a more recent version (Figure 5). A linear relationship was observed between the number of cells injected and the number of counts obtained with either the probe or well counter. The more recent model of the probe has a larger collimator aperture and detector crystal area. It also has a different preamplifier that permits a more compact design. The reason for redesigning the probe was to increase the counting rate for ^{125}I by a factor of about 15. This improved counting rate results in greater probe sensitivity and extends the limits of detection from 6.25×10^5 cells to 3.9×10^4 ^{125}I-antibody-coated cells. Such small numbers of tumor cells are not discernible by either palpation or external scintigraphy.

Clinical studies

Protocol. Patients with either primary or recurrent gastrointestinal cancer considered candidates for radioimmunoguided surgery came to the Ohio

State University Clinic. The surgeon determined the patient's eligibility to enter study #79H001 approved by Ohio State University Human Subjects Review Committee.

Diagnostic evaluation of patients with primary disease included air-contrast barium enema, computerized axial tomography (CAT scan) of the abdomen and pelvis, serum CEA assay, and colonoscopy. Patients with suspected recurrent disease underwent a CAT scan, hepatic arteriogram, and magnetic resonance imaging (MRI) when indicated. A chest x-ray, bone scan, and CAT scan of the chest were done to exclude patients with extraabdominal metastatic disease. The presence of either pulmonary or bone metastases excluded the patient from the study.

Patients who were accepted for the study received an injection of radiolabeled antibody. Before the injection, they were treated with a saturated solution of potassium iodide (SSKI) to block the uptake of free iodine by the thyroid gland. On the day of the injection, the research protocol nurse reviewed the purpose, risks, and benefits of the study, and the patients signed a consent form.

Subcutaneous hypersensitivity testing to the unlabeled antibody (0.1 mg in 0.1 ml NaCl) was performed on the day of injection. After 15–20 minutes, the area was examined. A positive result was considered to be two times that of the NaCl control, with erythema 20 mm in diameter. If the result was positive, the patient was released from the study. If no reaction occurred, the radiolabeled antibody was given by intravenous injection over 10–15 minutes. The patient remained under observation for 15 minutes following the injection.

Patients were admitted to the hospital 1 day before the operation. During the operation, the handheld gamma probe was used to count obvious tumor and scan the abdomen for areas of increased radioactivity. These areas were biopsied for frozen-section preparation and examination. Probe readings of normal tissue from which the tumor originated were taken to compare tumor-to-tissue counts. Additional counts were routinely obtained from the liver, stomach, kidney, aorta, small bowel, and colon. Each reading was repeated in triplicate.

Fresh specimens obtained at surgical resection were taken to the Division of Surgical Pathology for processing. Ex-vivo probe counts were performed on the gross specimens, and routine and probe-directed samples were obtained for evaluation. Tissue samples were split, and mirror image samples were either formalin fixed and paraffin embedded, or snap frozen in an isopentane-containing vial submersed in liquid nitrogen. Formalin-fixed, paraffin embedded samples were processed for routine hematoxylin and eosin staining. Immunohistochemical localization of colon cancer antigen was accomplished on 6-micron cryostat-prepared frozen sections with an avidin-biotin complex (ABC) immunoperoxidase technique.

Anti-CEA-Mab ^{131}I, 2 mm crystal gamma-detecting probe. We first described intraoperative radioimmunodetection using ^{131}I-labeled, anticarcinoembry-

onic antigen, baboon polyclonal antibody. Tumor/tissue ratios obtained averaged 3.97:1 for primary tumors and 4.18:1 for recurrent tumors, and almost 90% of patients had a tumor/tissue ratio greater than 1.5:1 [8].

Case #1. A 59-year-old man with a 3-month history of rectal tenesmus, occasional diarrhea, and incontinence, who had had hematochezia for 3 days, had an apple-core constricting rectal carcinoma located 6 cm from the anal verge. The serum CEA was 2.7 ng/ml (normal up to 2.5 ng/ml). Three days following the injection of ^{131}I-CEA-As (1.9 mCi), a lateral scintigraphic scan of the rectum showed two small areas of increased radioactive uptake in the midline behind the bladder. Whole-body scans did not demonstrate other tumor 'hot spots.' There was no evidence of metastasis on the chest roentgenogram or the bone and liver-spleen scans.

The GD detected increased radioactivity in the tumor compared with other sites. The tumor invaded the urethra and had been incompletely resected. The GDP indicated increased activity at the site of residual tumor (114 cpm) compared with the immediately adjacent prostate (90 cpm). Gamma-well determinations of tissue activity showed increased tumor counts.

17-1A-Mab ^{125}I, 2 mm crystal gamma-detecting probe. Our next clinical study was designed to test the value of radiolabeled monoclonal antibody (Mab) 17-1A and its fragment 17-1A F(ab')$_2$ in detecting primary and recurrent colorectal cancer using the GDP [9]. The study also addressed the clinical usefulness of the GDP (2 mm cadmium telluride crystal) in assisting the surgeon's intraoperative decision making (Figure 2).

Of the 18 patients who were given injections of radiolabeled antibody, probe counts were obtained in 16. The digital display read-out malfunctioned in two patients. Counts were taken of 20 tumor sites in the 16 patients. Tumor/tissue ratios were 1.5:1 or greater in 15 patients (75%). Tumor/tissue ratios were elevated in all patients with local/regional recurrences, while only 60% of patients with primary tumors and 50% of patients with liver metastases had elevated counts. The mean tumor/tissue ratio obtained with Mab 17-1A whole antibody was 3.4:1 $\pm$ 1.8 at nine sites, while that obtained with F(ab')$_2$ fragments was 2.3:1 at six sites. This difference was not significant. Ratios of less than 1.5:1 were obtained from three Mab 17-1A sites and two F(ab')$_2$ sites.

Of the 20 tumor sites counted in vivo, resected specimens suitable for ex-vivo counts were obtained in ten. Small biopsy specimens from patients with unresectable tumors or small resected specimens, parts of which had been sent for frozen section examination, were considered unsuitable for probe counts. In the ten suitable specimens, the mean ex-vivo tumor/tissue ratio was 8.67 $\pm$ 4.5, significantly higher than the 3.4:1 $\pm$ 1.9 in-vivo ratio ($p = .01$). Probe data contributed to intraoperative decision making in 3 (18%) of the 16 patients in whom probe counts were obtained in vivo.

Case #2. A 48-year-old man had a rising carcinoembryonic antigen level (50 ng/ml) following a small-bowel resection for a perforated small bowel adenocarcinoma. Results of all other investigations were normal. The patient was given an injection of 2.15 mCi of ^{125}I-labeled Mab 17-1A, 4 days preoperatively. At operation, despite an intensive search and examination of multiple biopsy specimens with frozen section diagnosis of suspicious areas, no recurrent tumor could be found. However, a consistent hot spot in the mesentery at the site of previous resection yielded GDP counts 2.5 times those of surrounding mesentery. The mesentery was thickened at this site, but no obvious mass could be palpated. Visceral peritoneum and mesenteric fat were dissected at the site of increased uptake. A 1.5 × 1 × 1 cm mass was discovered deep in the mesentery. Examination of a frozen section confirmed it to be a recurrent adenocarcinoma. A formal wedge resection of this area of the mesentery with its accompanying small bowel was performed. The bowel was reanastomosed in standard fashion. Examination of a permanently fixed section also confirmed recurrent adenocarcinoma, and the patient's carcinoembryonic antigen level returned to 4.2 ng/ml postoperatively.

Case #3. A 59-year-old man had a rising carcinoembryonic antigen level (9.8 ng/ml) following preoperative irradiation and abdominoperineal resection for a Dukes' B rectal adenocarcinoma. Results of all preoperative investigations were normal. Five days preoperatively, the patient was given an injection of 2 mCi of ^{125}I-labeled Mab 17-1A. At operation, no clinical evidence of recurrent tumor was apparent. The GDP counts deep in the pelvis in the presacral area were twice those in surrounding tissue. An obvious mass was not discernible at this site; it is unlikely that specimens from the area would have been removed at biopsy in the absence of such counts. Frozen section diagnosis of GDP directed biopsy specimens at this site were reported as fibrous tissue. Because of high GDP counts, biopsies were repeated and specimens were sent for permanent section and determined to be recurrent adenocarcinoma.

The GDP counts recorded from 20 tumor sites in 16 patients showed tumor/tissue ratios of 1.5:1 or greater (range, 1.5–6.75) in 15 sites (75%). The average tumor/tissue ratio in the patients given injections of radiolabeled whole antibody was 3.4:1, and in those given the injection of radiolabeled $F(ab')_2$ fragment was 2.3:1. Though this difference was not significant, it was in conflict with the dramatic increase associated with the use of fragments in tumor/tissue ratios obtained in our animal data. Counts from renal tissue were 25 times greater with fragments than with whole antibody, while counts from the liver, aorta, and stomach were two to three times those obtained with whole antibody. Ex-vivo tumor/tissue ratios for fragments and whole antibody were 8:1 and 8.5:1, respectively.

This clinical study demonstrated the ability of the GDP to localize disease not clinically evident at operation and to map margins of resection. This made the probe a particularly useful instrument for decision making. In addition,

the GDP was also helpful in a small percent of cases of primary colon cancer in the search for disease outside the normal resection margins. Its use in other cancers with combinations of radiolabeled antibodies and/or more specific antibodies will broaden its application in the future. Compared with other diagnostic techniques, the GDP, a portable instrument that requires little technical expertise to use and gives us an immediate result, will be cost effective.

17-1A-Mab ^{125}I, 1 cm crystal gamma-detecting probe. The third major clinical trial involved 32 patients who were injected with ^{125}I-labeled 17-1A and underwent intraoperative gamma-probe localization of colorectal carcinoma [10]. The following case reports demonstrate how injected radiolabeled antibody was localized and evaluated surgically and pathologically using a larger crystal (1.2 cm) in the probe (Figure 5).

Case #4. A 76-year-old woman sought treatment for rectal bleeding. A barium enema demonstrated a mass in the splenic flexure, and a CAT scan demonstrated a mass in the right lobe of the liver. Her preoperative CEA was 4.5 ng/ml. The hepatic arteriogram demonstrated metastatic disease. The patient received an injection of 17-1A F(ab')$_2$ 1 day before surgical exploration. Intraoperatively, two lesions were identified, a splenic flexure tumor and an isolated, apparently metastatic tumor in the right lobe of the liver. A left colectomy and wedge resection of the liver mass were performed to remove both tumors. The handheld gamma probe counts intraoperatively were 336/2 seconds for normal liver and 204 for the liver tumor. The colon tumor counts were 178, and adjoining normal colon tissue was 192. Ex-vivo counts showed the normal colon count to be 15 and the colon tumor count to be 130, but the liver tumor count was 55 and adjacent normal liver tissue was 202. The ex-vivo counts substantiated that the colon tumor was recognized by the 17-1A F(ab')$_2$-labeled antibody, but the suspected liver metastasis was not.

The tumor resected from the liver measured 10 × 1 × 12 cm and had a lobulated appearance and a pushing border. Histologically, the liver tumor proved to be a primary hepatocellular carcinoma and not an adenocarcinoma metastatic from the colon. Ex-vivo probe counts of the liver tumor showed a 0.3 tumor/normal liver tissue ratio, and immunohistochemical staining of frozen tissue sections of the hepatocellular carcinoma was negative for 17-1A antigen expression. The colon tumor proved to be a moderately differentiated adenocarcinoma that penetrated through the muscularis into the bowel serosa. Ex-vivo probe counts from the colon primary were 9:1 tumor-to-normal colon tissue ratio. Mesentery removed with the specimen showed no evidence of metastatic disease when counted with the gamma probe, and pathologic examination also confirmed no metastatic tumor in any of the eight mesenteric lymph nodes included in the specimen. Immunohistochemical staining of the primary colon tumor for 17-1A antigen showed diffuse positivity of moderate intensity.

Case #5. A 27-year-old woman had a 6 week history of left lower quadrant pain radiating to the left flank and guaiac-positive stools. Physical examination demonstrated an acutely tender left lower quadrant with rebound tenderness and a positive left psoas sign. The echogram demonstrated a left sided abscess in the retroperitoneum. Her temperature was 102°F, and her white blood cell count was 13,500/mm. Barium enema demonstrated a 10–12 cm segment in the mid-distal descending colon suggestive of Crohn's disease or colon cancer. Her CEA was 3.0 ng/ml. An exploratory laparotomy, a left colectomy, and debridement of the left retroperitoneal abscess were performed. An adenocarcinoma of the descending colon that had perforated into the retroperitoneal space and left psoas muscle was present. Pathologic examination disclosed a Dukes' B, moderately differentiated adenocarcinoma with perforation and abscess formation.

Three months after this procedure, the patient was readmitted because of nausea, vomiting, and the acute onset of colicky upper abdominal pain. The upper gastrointestinal series and small bowel follow through demonstrated a small bowel obstruction. At exploratory laparotomy, lysis of adhesions was carried out. There was no evidence of recurrent tumor in the abdomen.

Following the colon resection in June 1984, the patient was followed with serial CEA levels. In August 1985, the serum CEA rose from its previous value of 4.7 ng/ml in July to 11.7 ng/ml. A 7 × 8 cm tumor mass was disclosed in the left gutter, which involved the iliacus muscle on CAT scan. No other masses were visualized or palpated. ^{125}I-labeled monoclonal antibody 17-1A (5 mCi/mg) was injected, and 4 days later a second-look procedure was performed.

Intraoperatively, the tumor was easily found by palpation and localized to the left pelvis. The gamma probe counts were approximately 240/2 seconds in the tumor and 50/2 seconds in the iliacus muscle. The probe helped to guide the surgeon in choosing the margins for resection of the tumor. Following complete removal of the mass, the tumor bed was inspected and considered by the surgeon to be free of tumor. The probe was then used to check the tumor bed for completeness of tumor mass removal. A 'hot' spot was identified, with probe counts of 80/2 seconds to a background count of 40/2 seconds in surrounding soft tissue. This area, which proved to be residual cancer, was surgically removed, and the probe was again used. No further tumor was identified.

The recurrent psoas muscle tumor originally resected measured 5 × 7 × 5 cm. Additional tissue resected at one edge of the recurrent tumor margin because of elevated gamma probe counts was also found to contain moderately differentiated adenocarcinoma. Immunostaining of frozen sections of this recurrent tumor was diffusely positive for 17-1A antigen.

The whole 17-1A antibody data clearly show that the longer the interval between injection and scanning, the better the tumor-to-tissue ratios. However, falling tumor counts obviously limit the length of time one can wait between injection and operation. In our initial investigations using whole 17-1A antibody, 48–72 hours following injection was chosen rather empiri-

cally as the best time to use the gamma probe intraoperatively. With improvements in the probe capabilities, the optimal time for probe use when using whole 17-1A antibody is thought to be 7–10 days.

B72.3 Mab ^{125}I, 1 cm crystal gamma-detecting probe. Our most recent clinical study was performed to assess, 1) the sensitivity of Mab B72.3 to identify colorectal cancer, 2) the GDP's ability to identify radiolabeled Mab B72.3 in colorectal tumors, and c) the ability of radioimmunoguided surgery (the RIGS™ system) to modify the surgical procedure [11]. The Neoprobe™ GDP consists of a 12-mm cadium telluride crystal, a preamplifier, and an amplifier with a digital read-out display, as well as an audio signal. The audible signal has a pitch proportional to the number of radioactive counts per second. Two-second counts were obtained and repeated in triplicate. The GDP shown in Figure 5 was used for this study.

There were seven patients with suspected primary colorectal cancer and 31 patients with recurrent colorectal cancer. All but one of the patients with primary colorectal cancer had tissue diagnoses established by either sigmoidoscopy or colonoscopy. Location of the primary tumors was: right colon (1), transverse colon (1), sigmoid colon (2), and rectum (3). The majority of patients with recurrent colorectal cancers were asymptomatic, and recurrences were suspected because of an elevated CEA level.

After appropriate consents were obtained, all patients were skin tested for allergy to mouse Mab B72.3. Patients were given a saturated solution of potassium iodide to block radioactive uptake of free ^{125}I in the thyroid. The radiolabeled Mab B72.3 was injected intravenously as a bolus 5–34 days (average, 16.4 days) preoperatively.

Routine exploration was performed. The GDP was used to count clinically obvious tumor, suspicious areas, and similar normal tissues for comparison. During explorations, routine counts of liver, spleen, aorta, vena cava, small bowel, mesentery, and abdominal wall were also obtained. Tumor-to-normal tissue ratios were obtained and a ratio of 1.5:1 was arbitrarily taken as a positive result. In addition, the audio signal emitted from the GDP correlated with the amount of radioactivity and aided the surgeon in determining the extent of disease and/or persistence after resection. Tissue that was clinically normal but had elevated GDP counts, a so-called hot spot, was always sent for histologic examination. After completion of tumor resection, margins and tumor bed were reevaluated using the GDP. Tissue was resected when possible until GDP counts were similar to those in normal tissue.

In six patients with primary colorectal cancer, nine possible sites were localized (primary and metastasis). Mab B72.3 was localized by the GDP in 8 of 9 (89% sites with tumor-to-normal tissue ratios ranging from 1.54:1 to 21.8:1 (median, 10.7:1). One patient with a transverse colon lesion was excluded from the study because final pathologic examination of a resected specimen failed to confirm cancer. The patient had false positive localization of Mab B72.3 in an ischemic colonic ulcer. The most probable explanation

Table 8. Results of intraoperative radioimmunodetection of recurrent colorectal cancer

Location of Recurrence	Percent Sites Localized* (no. localized/total no.)	Tumor Tissue Ratios (mean ± SD)
Liver	68.4 (13/19)	6.24 ± 2.99
Pelvis	100 (12/12)	4.94 ± 3.30
Implants	88.9 (8/9)	3.29 ± 1.34
Lymph nodes	80 (8/10)	11.07 ± 6.66
Local recurrence	75 (3/4)	2.84 ± 0.60
Lung	100 (2/2)	39.05 ± 49.85
Second primary	100 (1/1)	3.6

* Indicates a tumor/tissue ratio $\geq 1.5:1$.

for this false positive result is that the lesion caused an obstruction in the gastrointestinal tract and the secretions extracted just proximal to the lesion were where the antibody isotope was collected. Since this case we have had several similar cases of obstruction and the obstructed colon secretions are always 'hot.'

There were 57 possible localization sites in 31 patients with recurrent colorectal cancer [11]. Mab B72.3 was localized by the GDP in 47 (82.4%) of these sites. Localization by site of recurrence is noted in Table 8. There were two false positive localizations of the Mab B72.3 by the GDP in the same patient. A suspicious area on the anterior abdominal wall and an adhesive band obstructing the small bowel were localized by the RIGS™ system, but were histologically free of cancer. In 8 of 31 (25.8%) patients, subclinical tumor deposits unidentified by inspection and palpation were identified by the RIGS™ system. Six patients had recurrent pelvic tumor and all underwent probe-directed biopsies. Two of these patients avoided unnecessary liver resections and two underwent extraabdominal approaches, avoiding major abdominal exploration. One had tumor confirmation through a transsacral approach and the other through a transvaginal approach. The remaining two patients had subclinical lymph node recurrences localized by the RIGS™ system.

Case study #6. A 40-year-old male presented to his physician with the complaint of left lower quadrant pain. Barium enema demonstrated a mass in the sigmoid colon. The biopsy of this mass obtained during a colonoscopy yielded adenocarcinoma. A CAT scan of the abdomen and pelvis and an intravenous pyleogram were interpreted as unremarkable.

This patient received an injection of Mab B72.3 19 days prior to the operation. Following the injection, serial GDP counts over the heart were obtained to assess the rate of clearance of the radiolabeled antibody from the blood. On the day of operation the counts over the heart were $< 20/2$ seconds (Figure 6).

Upon exploration of the abdomen, a large sigmoid tumor was identified.

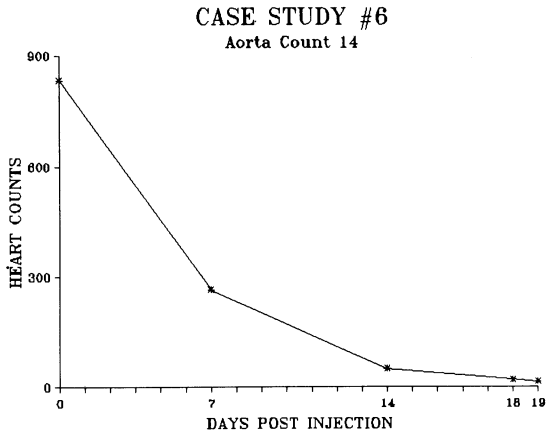

Figure 6. Case study 6: Clearance of Mab B72.3 ^{125}I from the blood over time is reflected in repeated external probe counts over the heart.

Probe counts of the tumor and normal tissue yielded a tumor-to-tissue ratio of 4 : 1. Further exploration disclosed two areas of multiple small nodules on the capsule of the liver near the dome. The GDP counts of these nodules compared to adjacent liver were not significant. Frozen section biopsy of a liver nodule demonstrated granuloma.

Subsequent to the planned sigmoid resection, the GDP was used to survey the abdomen and pelvis, and routine counts were obtained from other organs including the bladder. The counts of the bladder were 50/2 seconds compared with a background count of 14/2 seconds. Because of the difference, the bladder was further palpated and tumor was found. This finding altered the surgical approach. Instead of a surgical resection, which would have necessitated partial cystectomy, a Hartman pouch with end colostomy was performed in preparation for full-dose radiation therapy and then surgical removal of the sigmoid colon tumor.

Case study #7. At another hospital, 69-year-old woman underwent a right colon resection in 1984 for a Duke's C adenocarcinoma. Follow-up included serial CEA determinations. In 1986 an elevated CEA was noted. A CAT scan suggested liver metastases. She underwent an exploratory laparotomy in which retroperitoneal nodes were excised and the liver metastasis was deemed unresectable. She was treated with chemotherapy and followed with serial CEA determinations. Upon completion of the course of chemotherapy, a CAT scan demonstrated no change in the size of the liver metastasis.

She was referred to the Ohio State University for evaluation of metastatic disease. She was deemed a candidate for radioimmunoguided surgery and was injected with B72.3 Mab radiolabeled with ^{125}I. Following the injection, external counts using the GDP were taken over the heart. Operation was cancelled at 20 and 23 days postinjection due to an elevated GDP count of the

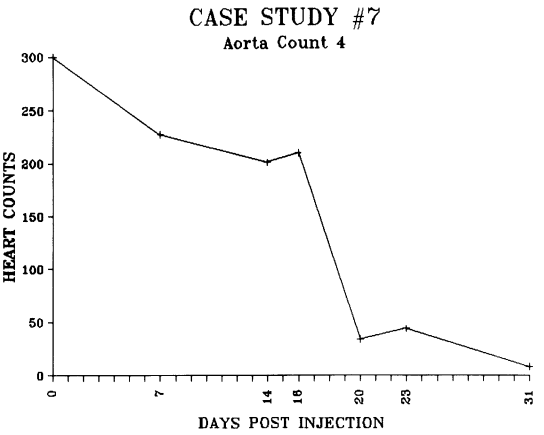

Figure 7. Case study 7: Clearance of Mab B72.3 ^{125}I from the blood over time is reflected in repeated external probe counts over the heart.

heart above 20 counts/second. Finally, on the day of operation, 31 days post-injection, the count over the heart was below 20/2 seconds (Figure 7). No other sites of metastases were noted at the surgical exploration. The GDP count of 150/2 seconds, the liver tumor was 150, and normal adjacent liver tissue was 10/2 seconds. The GDP was used to outline the areas of resection and used continuously during the operation to survey margins for areas of increased radioactivity. Upon completion of the resection, the liver was surveyed using the GDP and the counts of the tumor bed were < 10 counts/2 seconds. The liver tumor specimen was surveyed using the GDP and all margins were < 10. The counts obtained with the GDP following the resection were similar to normal liver tissue. This confirmed the completeness of the resection. The postoperative CEA counts returned to baseline and have remained at baseline.

Discussion

The use of radioimmunoguided surgery (RIGS^{TM}) began in an experimental model consisting of a CX-1 xenograft on the flank of a nude mouse. The early model of the GDP with a 2 mm crystal detected emissions from CX-1 xenografts labeled with ^{131}I-labeled anti-CEA polyclonal antibody [2].

In early clinical studies, colon cancer that would not have been identified by inspection and palpation was identified in 18% of patients [9]. Improvements were made in the GDP, increasing the cadmium telluride crystal size from 2 mm to 1 cm, enhancing its capability to scan the abdomen. The counting interval was improved from 20 seconds/count to 2 seconds/count. This enables the surgeon to scan the abdominal cavity better. Improvements have continued, and the present model (Figure 8) is gas sterilizable. The

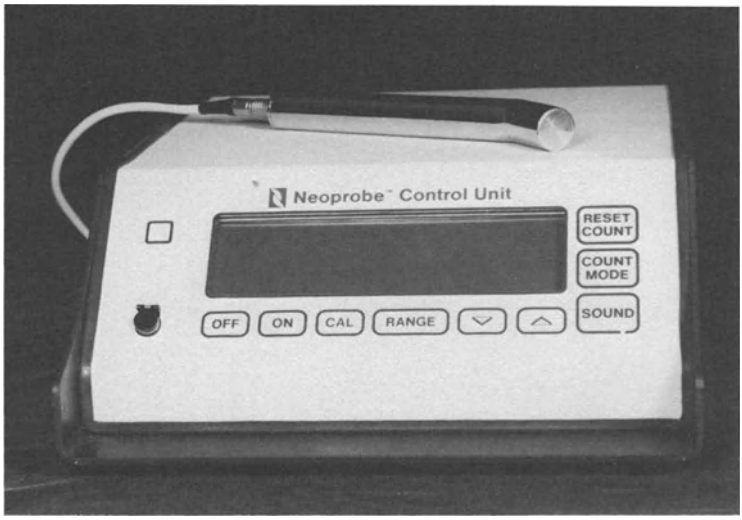

Figure 8. The Neoprobe 1000™ consists of a 1.2-cm CdTe crystal, concealed preamplifier, and computer-generated sound.

abdomen can be completely surveyed in less than 5 minutes, once the adhesions are freed up. Also, tumor superficially located or located near a body cavity orifice can be detected externally, and probe-directed biopsies can be performed.

We have used several whole antibodies (IgG) with varying capabilities to identify colon cancer, primarily several anti-CEA antibodies and 17-1A [IgG, $F(ab')_2$] and B72.3 [9–11]. Anti-CEA and B72.3 antibodies have been shown to detect shed antigen that circulates in the blood stream via in-vitro radioimmunoassay. The 17-1A antibodies (whole and fragments) are specific for membrane bound antigens that do not circulate (nonshed antigens) [10].

Much has been learned about how to deal with the blood-pool radioactivity background. Goldenberg et al. [12], Mach et al. [13], and Colcher et al. [14] attempted to image patients 2 or 3 days after injection of ^{131}I-labeled antibody; in some cases, subtraction techniques were devised in an attempt to distinguish cancer tissue from blood-pool background with limited success [12]. Our early experiments and clinical trials were based on the same time interval after injection, and the blood-pool background, especially in the liver, presented a major problem. It became apparent that 2–3 days after injection was far too early for the radiolabeled whole antibodies to have cleared from the blood. A better understanding of the properties of an isotope with a lower energy level and longer half-life to label the antibody helped to enhance the effectiveness of the radioimmunoguided system. In addition, better labeling techniques may enhance the binding of the antibody to the tumor. We replaced ^{131}I with ^{125}I, which is a less energetic isotope

Table 9. Radiopharmaceuticals

Isotope	Half-Life	Energy (keV)
^{125}I	60 days	27/31/35
^{99m}Tc	6 hours	142
^{111}In	2.8 days	173/247
^{131}I	8 days	365/637
^{123}I	13 hours	159

(365/637 keV vs. 35 keV) and obviated concern about the half-life of the isotope (8 days vs. 60 days — Table 9). ^{125}I continues to be our choice, although the use of other isotopes such as ^{111}In (173/247 keV, half-life 2.8 days) ^{99m}Tc (142 keV, half-life 6 hours), and ^{123}I (159 keV, half-life 13 hours) are still being considered. Further studies in our laboratory concerning the ability of the probe to detect the gamma emissions and detailed pharmacokinetic studies concerning the ability of the body to clear the antibody from the blood make ^{125}I the ideal isotope for the whole antibodies currently being used. Continued phantom studies examining the gamma photon and x-rays are being completed to enhance an understanding of which isotopes might eventually be used for external imaging and intraoperative probing.

With improved understanding of monoclonal antibodies, such as higher affinity whole antibodies or fragments of existing antibodies, a shorter half-life isotope with an optimal energy level that the probe can detect, nearly 100% of the time can be chosen. ^{99m}Tc, ^{123}I, ^{111}In, and other isotopes of similar energy seem to be the best candidates for the RIGS™ system. At this energy level, isotopes are attractive because preoperative external scintillation scans could also be performed, potentially supplying information to the operating surgeon before the patient is explored. Possibly the external scan would demonstrate more accurately the extent of tumor and identify patients with antigen positive tumors before the operative procedure is undertaken. The GDP would then be used intraoperatively to identify both clinically obvious tumor and subclinical tumor not detected by the traditional methods of inspection and palpation.

It is anticipated that improvements will soon be realized with better methods of labeling the antibody in bioengineered antibodies with inserted human constant (Fc) regions, and with the development of human monoclonal antibodies. All may lessen the human associated mouse antibody (HAMA) formation and will likely permit repeated injections of antibodies for immunotherapy or immunotoxin therapy after total or near-total tumor ablation using both the traditional methods and the RIGS™ system in both primary tumor surgery and in recurrent cancer reoperations. The use of monoclonal antibody fragments or other carrier substances with good tumor-binding abilities will also result in radiolabeled antibody or carrier substances clearing more rapidly from the blood, and thus the interval between antibody

or carrier substance administration and operation will be shorter. A double-antibody technique that may help clear the blood-pool background may eventually be employed once multiple antibody injections are safer. Also, improved clinical approaches will be studied using biologic modifiers such as interferon, hyperthermia, and others to increase Mab delivery to the tumor site, or to enhance tumor antigen expression and thus Mab binding to tumor lesions.

Conclusions

The evolution of the radioimmunoguided surgical system has enabled us to identify more than 70% of tumors in the colon, both primary and recurrent. It is also being used to identify malignancies in the stomach, ovary, breast, and skin. In approximately one third of the patients studied with colorectal cancer, additional intraoperative information concerning the presence of subclinical tumor deposits has altered the surgical approach. A routine intra-abdominal survey followed by an intraoperative survey with the current GDP has allowed us to identify tumor deposits that have been previously overlooked. A higher audible signal and an increased count rate emitted by the GDP have enabled the surgeon to more thoroughly explore the liver bed, the suprapancreatic periaortic region, the periportal region, and the thickened mesentery, where lymph nodes involved with tumor have been found. Similarly, higher pitched and more rapid signals in the presence of thickened mesentery and postradiation scar tissue in the pelvic cavity has led to the identification of metastatic tumor previously overlooked. This investigative tool adds an additional sense: The surgeon can now not only see and feel, but can hear the tumor. The fact that monoclonal antibody is being used circumvents the problem of antibody availability. With further improvements in antibody engineering and modification, radioimmunoguided surgery will become even more effective. The use of single antibodies, combinations of antibodies, or high affinity antibodies, along with improved isotope selection and labeling methods, will add significantly to the successful use of this new surgical technique. With antibodies or other carrier substances that clear the blood pool more quickly, the time between the injection of the radiolabeled antibody and surgical intervention will be shortened, ideally from approximately 3 weeks to a matter of days, thus eliminating for patients the anxiety of waiting until an operation can be performed.

References

1. Myers, W.G., and Vanderleeden, J.C. (1980) Radioiodine-125. J. Nucl. Med. 149–164.
2. Aitken, D.R., Hinkle, G.H., Thurston, M.O., Martin, D.T., Olsen, J.O., Haagensen, D.E., Houchens, D.P., and Martin, E.W., Jr. (1984) A gamma detecting probe for radioimmune detection of CEA-producing tumors: Successful experimental use and clinical case

report. Dis. Colon Rectum 27:279–282.
3. Aitken, D.R., Thurston, M.O., Hinkle, G.H., Jr., Martin, D.T., Haagensen, D.E., Jr., Houchens, D., Tuttle, S.E., and Martin, E.W., Jr. (1984) Portable gamma probe for radioimmune localization of experimental colon tumor xenografts. J. Surg. Res. 36:480–489.
4. Hinkle, G., Houchens, D., Miller, E., Nines, R., Nabi, H., Thurston, M., Tuttle, S., Mojzisik, C., and Martin, E., Jr. (1987) Preferential localization of antibody combinations in tumor xenografts in nude mice. IDA Biomed. Res. 248–250.
5. Siddiqi, M.A., Hinkle, G.H., Hill, T.L., Mojziski, C.M., Olsen, J., Rousseau, M., Gersman, M., Houchens, D., Sardi, A., Thurston, M.O., and Martin, E.W., Jr. (1987) An assessment of prolonged reactivity of seven monoclonal antibodies against in situ cx-1 tumor xenografts using a novel hand-held gamma detecting probe. Invest. Surg., in press.
6. Goodwin, R.A., Tuttle, S.E., Bucci, D.M., Jewell, S.D., Martin, E.W., Jr., and Steplewski, Z. (1987) Tumor-associated antigen expression of primary and metastatic colon carcinomas detected by monoclonal antibody 17-1A. Am. J. Path., in press.
7. Oredipe, O.A., Barth, R.F., Tuttle, S.E., Adams, D.M., Sautins, I.E., Bucci, D.M., Mojzisik, C.M., Hinkle, G.H., Jewell, S.M., Steplewski, Z., Thurston, M.O., Martin, Jr., E.W. (1988) Limits of sensitivity for the radioimmunodetection of colon cancer by means of a hand held gamma probe. Nucl. Med. Biol. 15:595–603.
8. Martin, D.T., Hinkle, G.H., Tuttle, S., Olsen, J.O., Nabi, H., Houchens, D., Thurston, M., and Martin, E.W., Jr. (1985) Intraoperative radioimmunodetection of colorectal tumor with a hand-held radiation detector. Am. J. Surg. 150:672–675.
9. O'Dwyer, P.J., Mojzisik, C.M., Hinkle, G.H., Rousseau, M., Olsen, J., Tuttle, S.E., Barth, R.F., Thurston, M.O., McCabe, D.P., Farrar, W.B., and Martin, E.W., Jr. (1986) Intraoperative probe-directed radioimmunodetection using a monoclonal antibody. Arch. Surg. 121:1391–1394.
10. Martin, E.W., Jr., Tuttle, S.E., Rousseau, M., Mojzisik, C.M., O'Dwyer, P.J., Hinkle, G.H., Miller, E.A., Goodwin, R.A., Oredipe, O.A., Barth, R.F., Olsen, J.O., Houchens, D., Jewell, S.D., Bucci, D.M., Adams, D., Steplewski, Z., and Thurston, M.O. (1986) Radioimmunoguided surgery: Intraoperative use of monoclonal antibody 17-1A in colorectal cancer. Hybridoma 5:S97–S108.
11. Sickle-Santanello, B.J., O'Dwyer, P.J., Mojzisik, C.M., Tuttle, S.E., Hinkle, G.H., Rousseau, M., Schlom, J., Colcher, D., Thurston, M.O., Nieroda, C., Sardi, A., Farrar, W.B., Minton, J.P., and Martin, E.W., Jr. (1987) Radioimmunoguided surgery using the monoclonal antibody B72.3 in colorectal tumors. Dis. Colon Rectum 30:761–765.
12. DeLand, F.H., Kim, E.E., Primus, F.J., Dine, M.E., and Goldenberg, D.M. (1982) In vivo radioimmunodetection of occult recurrent colonic carcinoma. Am. J. Radiol. 138:145–148.
13. Mach, J.P., Carrel, S., Forni, M., Ritschard, J., Donath, A., and Alberto, P. (1986) Tumor localization of radiolabeled antibodies against carcinoembryonic antigen in patients with carcinoma: A critical evaluation. N. Engl. J. Med. 303:5–10.
14. Colcher, D., Horan, H.P., Nuti, M., and Schlom, J. (1981) A spectrum of monoclonal antibodies reactive with human mammary tumor cells. Proc. Natl. Acad. Sci. USA 78: 3199–3203.

21. Augmentation of tumor antigen expression by recombinant human interferons: Enhanced targeting of monoclonal antibodies to carcinomas

John W. Greiner, Fiorella Guadagni, Patricia Horan Hand, Sidney Pestka, Philip Noguchi, Paul B. Fisher, and Jeffrey Schlom

The advent of hybridoma technology has provided an unlimited supply of monoclonal, 'monospecific' antibodies (Mab) that has fueled an unprecedented surge in the study of tumor immunology and biology [1]. For the first time, investigators have at their disposal a continuous source of pure antibody that makes possible the identification and extensive characterization of a wide variety of tumor antigens expressed by human carcinomas, melanomas, leukemias, and lymphomas. Subsequent studies have also led to the development of novel assays using Mabs for tumor diagnosis [2–5], as well as a variety of clinical protocols demonstrating radioimmunolocalization of an antibody to occult lesions in a variety of cancer patients [6–15]. In addition to these clinical studies, the use of immunohistochemical techniques, radioimmunoassays (RIA), Western blotting, and other experimental analyses have led to a better understanding of some of the basic principles that characterize tumor antigen expression.

First, unlike the antigens that constitute the major histocompatibility complex (MHC), tumor antigens are, for the most part, integral components of the cell membrane and do not undergo internalization, capping, etc. after antibody binding.

Second, the carcinoma-associated tumor antigens are usually expressed by a variety of different tumor types. An example is the B72.3 Mab that was generated in our laboratory using an enriched membrane extract prepared from a human carcinoma metastasis to the liver [16,17]. B72.3 reacts with a high-molecular-weight glycoprotein antigen, termed *TAG-72* [18]. The range of reactivity of the B72.3 antibody for carcinoma versus normal is very selective, i.e., the only normal adult tissues that show reactivity with the antibody are the proliferative and resting endometrium [19]. In addition, the range of reactivity of B72.3 among different carcinomas is that of a pancarcinoma antigen and includes breast, colorectal, ovarian, stomach, pancreatic, and endometrial cancers [20]. Thus, it has been shown, in this instance, that the generation of a Mab using a metastatic lesion as an immunogen results in an immunologic reagent whose utility extends beyond that of a single type of carcinoma and includes several different types of adenocarcinoma.

Finally, a third characteristic that seems to be shared by all human-

Goldenberg, D.M., (ed.), Cancer Imaging with Radiolabeled Antibodies.

carcinoma-associated antigens is the existence of antigenic heterogeneity among different tumor lesions. This heterogeneity of tumor antigen expression has been documented both in experimental models using established human carcinoma cell lines, as well as in biopsies prepared from in-situ carcinoma lesions [21,22]. Data are available that demonstrate, within primary and metastatic human carcinomas, that not all of the cells express a given tumor antigen. Furthermore, these same studies revealed that, within an antigen-positive tumor cell population, a significant quantitative difference exists with respect to antigen density per cell. Although tumor-cell heterogeneity can be defined according to a large number of cellular criteria (i.e., cell size, metastatic ability), our interests lie in the heterogeneity of antigen expression and its potential impact on Mab use for tumor detection and/or therapy. This review will characterize the extent of antigen heterogeneity in human breast and colorectal tumor cell populations and will briefly outline some intrinsic cellular factors that regulate expression of the surface antigens. Such factors are believed to contribute to the extent of antigenic heterogeneity observed within a tumor cell population. The main focus will present one approach of overcoming antigenic heterogeneity through the administration of a biologic response modifier [i.e., recombinant human interferon (rHu-IFN)]. Initial reports focused on the ability of type I and II rHu-IFNs to induce and/or amplify class I and II MHC antigens, Fc receptors, and tumor antigens on the surface of a wide variety of human cell lines. Data from more recent studies will demonstrate that recombinant human leukocyte (alpha) interferon (rHu-IFN-α) can modulate tumor antigen expression in vivo and results in an enhanced level of Mab targeting to human carcinoma lesions in athymic mice. Finally, the potential clinical usefulness of combining an agent that alters the antigenic phenotype of a human tumor cell population with therapeutically conjugated Mabs will be discussed. Table 1 summarizes the Mabs used in the studies. The antibodies, W6/32 and anti-HLA-DR, that recognize the class I and class II MHC antigens, respectively, are commercially available [23,24], and Mabs B6.2, B72.3, and COL-4 were generated and characterized by this laboratory [16,17,25]. Table 2 lists the relative constitutive level of surface binding of each Mab to the different cell types used in the in vitro and in vivo investigations.

Antigen heterogeneity and intrinsic antigen regulation

As early as 1954, Foulds [26] documented the existence of distinct morphologies in different areas of a single mammary tumor. With the use of immunoperoxidase staining techniques on biopsies of primary and metastatic human breast and colon tumor tissues, as well as live cell RIAs using human carcinoma cell lines, it is quite apparent that an extensive degree of heterogeneity with respect to the cell-surface expression of each of three different tumor antigens (as measured by binding of Mabs B6.2, COL-4, and B72.3)

Table 1. List of Mabs and respective antigens

Antibody	Antigen/M_r	Isotype	Reactivity	References
W6/32	Class I-MHC 43 kD	IgG_{2a}	All human cells, except red blood cells	23, 35
Anti-HLA-DR	Class II-MHC 27 + 36 kD	IgG_{2a}	B lymphocytes, monocytes/ macrophages, activated T cells, thymic epithelium, other lymphoid tissues	24, 40
COL-4	CEA, 180 kD	IgG_{2a}	Colorectal and stomach carcinomas	25, 44, 53
B6.2	90 kD	IgG_1	Breast and colorectal carcinomas; circulating polymorphonuclear leukocytes	16, 39, 51, 54
B72.3	TAG-72, $> 10^6$ daltons	IgG_1	Pancarcinoma — breast, colorectal, stomach, ovarian, etc.; normal adult proliferative endometrium	16, 17, 19, 28

exists within individual human carcinoma masses. Different tumor types exhibit different patterns of staining, ranging from focal, diffuse cytoplasmic, membrane, and apical staining (luminal cell borders) with each given Mab. Heterogeneity in the expression of these distinct tumor antigens was also observed within a given breast tumor cell population. One typical pattern observed was that the tumor cells in one area of the section stained positive for the tumor antigen, while adjacent tumor cells were negative. This type of antigen diversity was termed *patchwork*. In addition, in a given tumor the

Table 2. Relative constitutive level of Mab binding to human tumor and normal cell lines

		Cell-Surface Reactivity (cpm/5 × 10^4 cells)[a]				
		CEA	TAG-72	90 kD	HLA	
Cell Line		COL-4	B72.3	B6.2	W6/32	Anti-HLA-DR
Breast	MCF-7	++	+/−	++	++	NEG
Colon	WiDr	++	NEG	++	+++	NEG
	LS174T	+++	+	++	+	NEG
Melanoma	A375	NEG	NEG	NEG	++	NEG
Normal fibroblasts	MRC-5	NEG	NEG	NEG	++	NEG
	WI-38	NEG	NEG	NEG	+++	NEG

[a] Cells were plated in 96-well microtiter plates (5 × 10^4 cells/well) in complete medium containing Dulbecco's modified Eagle's medium with 5 μg/ml insulin, 1 mM sodium pyruvate, 1x nonessential amino acids, and 10% heat-inactivated fetal bovine serum. After 24 hours, a titration curve for each Mab using 500–0.3 ng/well was determined. The relative levels of maximum binding for each cell line were determined as follows: NEG, < 500 cpm; +/−, 500–999 cpm; +, 1000–2999 cpm; ++, 3000–4999 cpm; +++, > 5000 cpm.

patterns of Mab reactivity varied, so that the same antigen would be cytoplasmic in one portion of the tumor while apical in another portion.

The existence of such heterogeneity in the expression of tumor antigens on the surface of human breast and other carcinoma cells will undoubtedly influence the effectiveness of Mabs that recognize these tumor antigens and are used for the in-situ detection and therapy of primary and metastatic tumor lesions. We believe that an understanding of the nature of this antigenic heterogeneity and the factors that influence the level of tumor antigen expression would be helpful in the prediction and/or control of the expression of these immunologic determinants. Using human breast and colon tumor cell lines, we have found that several 'intrinsic' factors can modulate surface antigen expression. For instance, we and others have reported that the level of constitutive expression of certain cell-surface tumor antigen is cell-cycle dependent [21,27]. In addition, utilizing carcinoma cell lines, it was reported that the antigenic phenotype of certain tumor cell lines changed with extended passage in vitro, a phenomenon termed *antigenic drift*. It was originally thought that such antigenic modulation might be a characteristic of the parental cell type and a more stable phenotype would be observed in a cloned tumor cell population. The human breast-carcinoma cell line (MCF-7) was cloned, and several of the clonally derived cell lines were followed for their surface tumor antigen expression for 4 months. Clearly, the stability of the cell-surface antigen phenotype was a function of each clone — some maintain a stable phenotype, while others continually altered their phenotype until returning to that of the parental line [28]. Of all the intrinsic signals that contribute to the level of constitutive expression of a tumor antigen, the one that presented the most dramatic change in antigen expression was the growth of the human colon-carcinoma cell line LS174T as subcutaneous tumors in athymic mice. The tumor antigen TAG-72 presents an interesting disparity between the expression of a tumor antigen in biopsy material and established carcinoma cell lines from tissue of comparable origin [29]. The level of TAG-72 expression has been shown by RIA and immunohistochemical staining to be substantial in biopsy specimens from breast, colon, ovarian, gastric, and other carcinomas [19,22]. Yet, similar analysis of the expression of this antigen in monolayer cultures of established cell lines has revealed its presence in only 1 of 31 breast and 4 of 35 colon cell lines [29]. In those TAG-72-positive cell lines, moreover, only 5–10% of the cells showed significant B72.3 reactivity. A series of experiments were conducted growing the TAG-72-positive LS174T cells on different substrates or in serum-free, hormone-supplemented media to determine whether any of those in-vitro modifications could augment the expression of the B72.3-reactive TAG-72 antigen. A two-fold increase in TAG-72 levels was measured in LS174T cells after their growth in type I collagen gels. When LS174T cells were grown in agar plugs, RIA analysis of the tissue extracts revealed ten-fold higher levels of the antigen than the monolayer, suggesting that an increased expression of the TAG-72 antigen may result by growing cells in a three-dimensional

matrix. The most dramatic increase in TAG-72 expression was measured in those LS174T cells grown as subcutaneous tumors in athymic mice. RIA analysis of TAG-72 levels in LS174T subcutaneous tumors grown in athymic mice revealed a 100-fold increase in the antigen content when compared with the monolayer cells. This upregulation seemed to be specific for the TAG-72 antigen, since other antigens, such as HLA and CEA, showed no comparable increase in the extracts of the LS174T tumors. These and other studies clearly demonstrate that the antigenic phenotype of a human tumor cell population is the result of dynamic interactions of growth factors, evolution of subpopulations of cells, influences of stromal and other cellular elements, as well as the diverse genotype of the cell population. The result is a cell population that can intrinsically regulate its antigenic phenotype as measured by the binding of Mabs. The remainder of this review will present data that will attempt to demonstrate that the exogenous administration of rHu-IFN can result in the amplification of the cell surface tumor antigen expression, resulting in the increase of the level of Mab binding to the tumor cell population.

Augmentation of tumor antigen expression in vitro

Table 3 lists some approaches that could minimize the overall rate-limiting effect of antigenic heterogeneity during the use of Mabs for immunodetection and/or therapy of occult tumor lesions. For instance, one can envision the administration of a cocktail of Mabs that would take advantage of the expression of multiple tumor antigens within a cell population or the presence of different determinants within the same antigen. Conceivably, a single tumor cell type that could not bind Mab A would bind Mab B due to the expression of the specific tumor antigen, thus increasing the percentage of cells reactive with either or both Mabs. A second approach would be to conjugate a high-energy radionuclide to an appropriate Mab, thus effectively killing an area within the tumor of several cell diameters, which would include those antigen-negative tumor cells. The third approach is the exogenous administration of an agent shown to alter cellular differentiation that includes a selective increase in cellular antigen. This approach would result in an increase in cell-surface tumor antigens that would include an increase in the antigen density per cell as well as an increase in the number of cells that express the antigen.

Table 3. Possible approaches to circumvent the limitations of antigenic heterogeneity in the localization of a conjugated Mab to carcinoma lesions

A. Use of multiple 'cocktail' of Mabs, i.e., complementarity of distinct antigens or separate antigenic determinants
B. Conjugation of Mab with high-energy radionuclides — capable of killing several cell diameters
C. Use of biologic response modifiers (i.e., differentiation agents — alter the antigenic phenotype of the tumor cell population — increase cell-surface tumor antigen expression

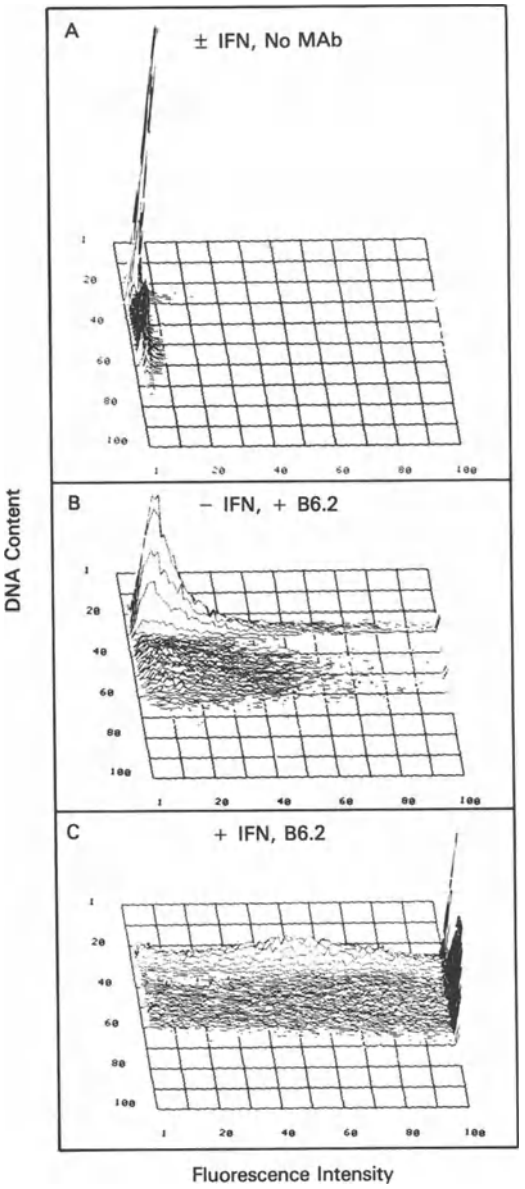

Figure 1. Fluorescence-activated cell sorter (FACS) analysis of Mab B6.2 binding to the surface of human colon carcinoma cells: effect of rHu-IFN-αA. The flow cytometric analysis was done, using an Ortho Cytofluorograf System 50H, with blue laser excitation of 200 mW at 488 nm. WiDr cells were incubated for 24–36 hours in growth medium with or without 850 antiviral units rHu-IFN-αA/ml, harvested, and incubated in culture medium containing 2 μg Mab B6.2/10^6 cells for 30 minutes at 4°C. The cells were then washed thoroughly with Ca^{+2}-Mg^{2+}-free Dulbeccos' PBS and then treated with fluoresceinated goat anti-mouse IgG (heavy and light chains) (1:30 dilution) for 30 minutes at 4°C. The cells were washed, excess antibody was removed, and the cells were resuspended at a concentration of 10^6 cells/ml and stained with propidium iodide

In some cases, this includes the utilization of a cytotoxic compound as an adjuvant for Mab radiolocalization and, possibly, therapy. We have screened retinoids, growth factors, organic solvents, DNA intercalating agents, and vitamin D and its analogs for their respective abilities to increase tumor antigen expression on a variety of human carcinoma cell lines. The most potent group of compounds that elicits an alteration in tumor antigen expression resulting in an augmentation of Mab binding are the type I and type II rHu-IFNs.

The human interferons are known to be potent immunomodulatory compounds capable of altering the cell-surface antigen phenotype of a variety of human cells [26,30–35]. Studies have shown that recombinant human type I and II interferons can amplify the level of expression of class I and II histocompatibility antigens, as well as some specific tumor antigens found on the surface of human melanoma and adenocarcinoma cell populations [35–40]. Considerable work has been done on the molecular events involved in the increase of class I and class II histocompatibility antigens by these biologic response modifiers. Both type I and type II interferon can augment class I HLA expression [36,41]. However, recombinant human interferon gamma (rHu-IFN-γ) is the most potent inducer of HLA-DR mRNAs and is able to induce class II HLA antigens de novo on previously HLA-DR-negative cells [42,43]. The effects of type I and type II rHu-IFNs on tumor antigen expression resemble those on the class I antigens. That is, both rHu-IFN-αA and rHu-IFN-γ can amplify the level of tumor antigen expression on the surface of a variety of human carcinoma cell populations. Shown in Figure 1 is a cytofluorometric analysis of the effects of rHu-IFN-αA treatment on the binding of Mab B6.2, which recognizes a M_r 90,000 tumor antigen expressed primarily by human breast and colorectal carcinomas. Analysis of the untreated colon carcinoma cell line WiDr revealed that approximately 45–55% of the cell population was positive for the surface expression of the B6.2-reactive 90-kD antigen. A 24- to 48-hour treatment with 2000 antiviral units rHu-IFN-αA per milliliter boosted the percentage of antigen-positive cells to > 85% and, in addition, increased the mean fluorescence intensity three- to four-fold (i.e., antigen density per cell). These results were confirmed for this and other tumor antigens in a variety of cell lines (i.e., CEA, TAG-72, etc.) using immunohistochemical staining and measurement of antigen content by RIA [44].

(18 μg/ml) and RNase A (2000 units/ml) for 4 hours at room temperature. The stained cells were analyzed, and under these conditions, propidium iodide bound to nuclear DNA fluoresces red, while surface immunofluorescence bound to the 90 kD tumor antigen fluoresces green [56]. Data from 25,000 cells were stored on an Ortho Model 2150 computer system and used to generate each three-dimensional isometric display of DNA content (y axis), fluorescence intensity, i.e., cell surface expression of the B6.2-reactive 90-kD tumor antigen (x axis), and the number of cells (z axis). A: WIDr cells stained for DNA content but no Mab B6.2. B: WiDr cells stained for nuclear DNA and B6.2 binding. C: WiDr cells treated with 850 antiviral units rHu-IFN-αA for 24–36 hours and stained as in B.

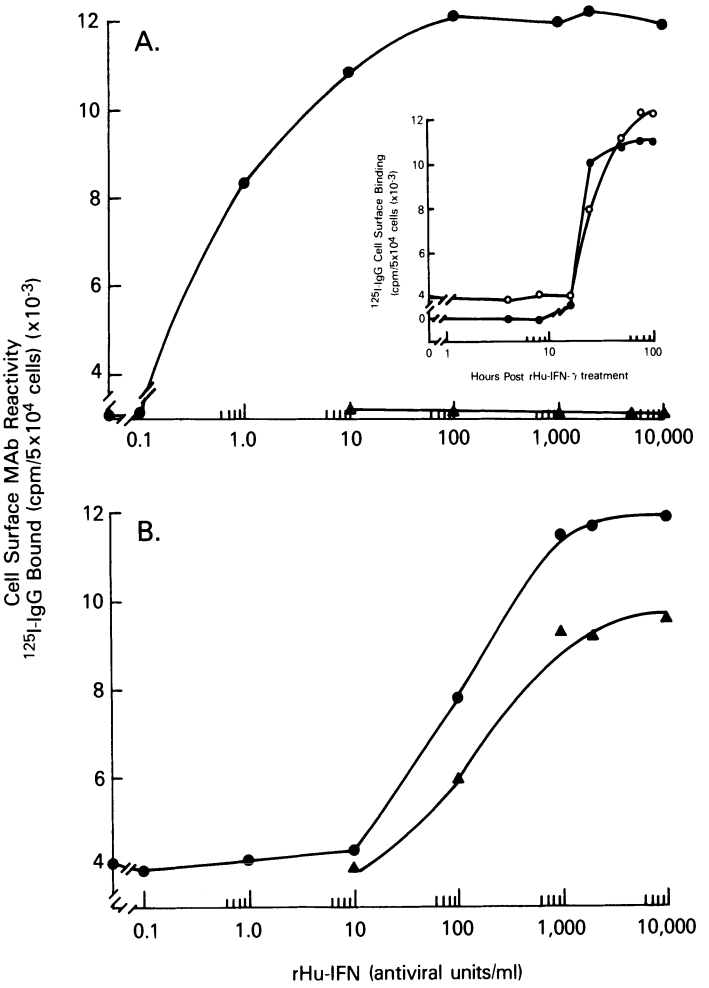

Figure 2. A comparison of the dose-dependent increase in anti-HLA-DR (A) and COL-4 (B) binding to the surface of the WiDr colon carcinoma cells as a result of rHu-IFN-γ and rHu-IFN-αA treatment. A: WiDr cells in complete medium with and without the indicated antiviral concentrations of each rHu-IFN were seeded in 96-well microtiter plates. After 72 hours, the level of expression of the class II MHC antigens were measured using the appropriate Mab and ^{125}I-goat anti-mouse IgG in a live cell RIA. The solid circles (●) represent the level of Mab anti-HLA-DR bound to the surface of the WiDr cells after rHu-IFN-γ treatment. The solid triangles (▲) represent the level of binding of the same Mab after rHu-IFN-αA treatment. An insert is shown in panel A that summarizes the temporal-dependent increase in anti-HLA-DR and COL-4 binding to the surface of the WiDr colon-carcinoma cells. WiDr cells were grown in medium containing 2000 antiviral units of rHu-IFN-γ per milliliter for the indicated time intervals. The solid circles (●) represent the binding of the anti-HLA-DR Mab, and the open circles (○) represent COL-4 binding to the surface CEA of the WiDr cells. B: The level of expression of CEA was measured by the binding of Mab COL-4 to the surface of the WiDr colon-carcinoma cell line as described in panel A. The solid circles (●) represent COL-4 binding to rHu-IFN-γ-treated cells, and the solid triangles (▲) represent COL-4 binding after rHu-IFN-αA treatment.

More recent studies were done to determine whether the type II rHu-IFN-γ could also induce any amplification on the level of tumor antigen expression [24]. The major physiologic role of the type I interferons is related to their antiviral effects. In contrast, investigators have suggested that the major role of the type II interferon-γ may be the regulation of the class I and/or class II histocompatibility antigens [42]. In particular, the class II HLA-DR antigens have been shown to be particularly sensitive to the immunomodulatory properties of interferon-γ. Figure 2 and Table 4 summarize studies in which the effects of rHU-IFN-αA and rHu-IFN-γ on the level of expression of the histocompatibility antigens, as well as certain Mab-defined tumor antigens, were compared. Figure 2 summarizes studies on the dose- and time-dependent increase of HLA-DR and CEA on the surface of the human colon-carcinoma WiDr cell line after rHu-IFN-αA or rHu-IFN-γ treatment. As shown in panel A, the induction of the class II MHC antigens is highly sensitive to rHu-IFN-γ. A 72-hour treatment with as little as 1.0 units rHu-IFN-γ results in a substantial induction of HLA-DR expression on the surface of the WiDr cells. Cytofluorometric analysis revealed that a 72-hour treatment with 1.0 unit rHu-IFN-γ resulted in $> 80\%$ of the WiDr cells expressing the class II antigens. In agreement with previous studies [36], the addition of up to 10,000 antiviral units of rHu-IFN-αA failed to induce HLA-DR expression on the WiDr and other human cell types (Figure 2A). Unlike the class II HLA antigens, the WiDr cells constitutively express CEA, as demonstrated by the surface binding of the anti-CEA Mab COL-4 (Figure 2B). Furthermore, both rHu-IFN-γ and rHu-IFN-αA are effective in eliciting a dose-dependent increase in the level of COL-4 bound to the WiDr cell surface. As also shown in Table 4 with other tumor antigens, treatment with rHu-IFN-γ consistently resulted in a higher level of induction of COL-4 binding than did treatment with similar antiviral titers of rHu-IFN-αA. In both cases, rHu-IFN-γ and rHu-IFN-αA were shown to elicit a measurable increase in the level of COL-4 binding after a 72-hour incubation of approximately 50–100 units/ml. However, rHu-IFN-γ treatment consistently results in a higher increase in COL-4 binding when compared with rHu-IFN-αA at antiviral titers up to 100,000 units/ml. These data suggest that amplification of CEA is much less sensitive than the induction of HLA-DR by rHu-IFN-γ. Yet, the maximum level of HLA-DR induction by rHu-IFN-γ or the maximum level of CEA amplification by either rHu-IFN-γ or rHu-IFN-αA was achieved after a 48- to 72-hour treatment with approximately 2000 antiviral units/ml. The increased expression of CEA or TAG-72, as shown in Table 4, could reflect a selection of subpopulations of carcinoma cells with high tumor antigen levels and/or unspecified membrane changes induced by rHu-IFN-αA or rHu-IFN-γ that permit unmasking of cryptic antigen binding sites [28,45,46]. However, the increase in tumor antigen expression may be caused by an interferon-induced induction and/or amplification of the gene(s) controlling their synthesis. Although previous reports clearly show that type I and type II interferons regulate histocompatibility antigen expression at transcriptional and/or post-

Table 4. Comparison of the effects of rHu-IFN-αA and rHu-IFN-γ on class I MHC and tumor antigen expression on the surface of a variety of human cell lines

		Cell Surface Reactivity (cpm/5 × 10^4 cells)				
		Breast	Colon		Melanoma	Normal Fibroblasts
Mab (Antigen)	Treatment	MCF-7	WiDr	LS174T	A375	WI-38
COL-4 (CEA)	—	5,050	4,020	17,750	NEG[a]	NEG
	rHu-IFN-αA	9,640 (1.91)[b]	9,820 (2.44)	18,410	NEG	NEG
	rHu-IFN-γ	11,210 (2.22)	12,460 (3.10)	17,100	NEG	NEG
B6.2 (90 kD)	—	4,180	5,860	5,330	NEG	NEG
	rHu-IFN-αA	10,440 (2.50)	13,430 (2.30)	5,775	NEG	NEG
	rHu-IFN-γ	13,160 (3.15)	17,660 (3.01)	6,410	NEG	NEG
B72.3 (TAG-72)	—	1,060	NEG	2,470	NEG	NEG
	rHu-IFN-αA	3,320 (3.13)	NEG	2,210	NEG	NEG
	rHu-IFN-γ	3,810 (3.59)	NEG	2,580	NEG	NEG
W6/32 (HLA-A,B,C)	—	4,370	6,100	2,860	4,210	3,660
	rHu-IFN-αA	15,610 (3.57)	14,440 (2.37)	2,910	11,440 (2.72)	6,140 (1.68)
	rHu-IFN-γ	14,770 (3.38)	18,610 (3.05)	3,090	12,680 (3.01)	7,410 (2.02)

The cell lines were initially seeded in 96-well plates at a concentration of 1–3 × 10^4 cells/well in complete medium containing 1000–2000 antiviral units of either rHu-IFN-αA or rHu-IFN-γ per milliliter. After 48–72 hours, the medium was removed and 500–0.03 ng of each Mab was added followed by 75,000 cpm of ^{125}I-goat-mouse IgG. Complete details of the RIA using live intact cells have been published [55].

[a] NEG = negative, i.e., no significant binding (< 1000 cpm per 5 × 10^4 cells).

[b] The numbers in parentheses represent the fold increase in Mab binding as determined by cpm treated cells divided by cpm untreated cells.

transcriptional regulatory sites, little is known of the mechanism of interferon-mediated increase in tumor antigen expression. The development of appropriate molecular probes would facilitate similar studies to determine the site(s) of regulation of tumor antigen expression by rHu-IFN-γ and other interferons. The time lag (16–24 hours) between interferon administration and the observed increases in CEA expression (i.e., COL-4 binding) is consistent with the time required to induce changes in transcriptional and/or post-transcriptional regulatory mechanisms with subsequent phenotypic maturation and transport and insertion in the plasma membrane (Figure 2A, insert).

Table 4 shows that both rHu-IFN-αA and rHu-IFN-γ can also increase CEA expression on a human breast-tumor cell line, MCF-7. However, neither interferon can induce CEA or TAG-72 expression on cell lines (i.e., A375, WI38) that do not constitutively express the respective tumor antigen. Thus, a very important difference is evident between the regulation of the expression of class II HLA-DR antigens and tumor antigens, such as CEA and TAG-72, by rHu-IFN-γ. Whereas type II gamma interferon can induce de novo synthesis of HLA-DR, the augmentation of a tumor antigen by rHu-IFN-γ or rHu-IFN-αA seems to require an actively transcribed gene before augmentation can take place. In those cells that are tumor antigen negative, the administration of as much as 10,000 units of either rHu-IFN- fails to induce expression of the CEA-, TAG-72-, or B6.2-reactive 90-kD antigen. This is not a *sine qua non* requirement for amplification of a tumor antigen. For example, the LS174T human colon-carcinoma cell line is resistant to the antigen-enhancing abilities of either rHu-IFN-αA or rHu-IFN-γ. The administration of either rHu-IFN-αA or rHu-IFN-γ did not alter the level of expression of the three tumor antigens and, moreover, resulted in no substantial change in the class I HLA-A,B,C antigen. Yet, the LS174T cells have a viable receptor for both types of rHu-IFN, as demonstrated in studies showing growth inhibition of the LS174T cells by both rHu-IFN-αA and rHu-IFN-γ. Therefore, the unresponsiveness of this cell type to tumor antigen augmentation by either type I or type II interferon seems to lie at a site(s) distal to receptor occupancy [28]. In any case, given an Mab with a selective range of reactivity, treatment with either rHu-IFN-αA or rHu-IFN-γ could selectively increase tumor antigen expression in the carcinoma cell population while the surrounding normal cells remain tumor antigen negative. This might increase the 'signal-to-noise' ratio by lowering the amount of Mab required for effective radiolocalization and, possibly, radiotherapy by a conjugated Mab.

In-vivo effects of rHu-IFN-αA on antibody targeting

Little was known of the ability of human interferons to alter the expression of cellular antigens in vivo. Reports have shown that type II human gamma

interferon can regulate class II antigen expression on circulating human lymphoid cells [47], as well as on human tumor xenografts grown in athymic mice [48,49]. We chose to determine whether the in vivo administration of rHu-IFN-αA can alter the binding of Mab B6.2 to human breast and colon carcinomas grown as xenografts in athymic mice. Mab B6.2 recognizes a M_r 90,000 antigen expressed in approximately 75% of breast carcinomas and more than 90% of colorectal tumors, but also reacts to circulating polymorphonuclear cells [50]. Nonetheless, this antibody has been extensively used in our laboratory to study the generation of F(ab) and $F(ab')_2$ fragments and their conjugation with radionuclides [51], radioimmunolocalization of occult tumors in athymic mice [51], and the production and characterization of chimeric antibodies [52]. As shown in Table 4, in vitro studies showed that the level of expression of the M_r 90,000 B6.2-reactive antigen was significantly increased in both breast and colorectal cell lines after rHu-IFN-αA treatment, suggesting this antigen may be a good model to pursue the in vivo studies. In our initial studies, the transplantable Clouser human mammary tumor that constitutively expressed the B6.2-reactive antigen was grown in female athymic mice to a size of 0.7–1.2 cm. The animals were then divided into two groups. The rHu-IFN-αA-treated group received daily intramuscular injections of 250,000 antiviral units for 5–7 days, and the control mice received injections of saline. At the time of sacrifice, the mice were bled, the plasma rHu-IFN-αA levels were measured, and the effects of rHu-IFN-αA on the level of expression of the 90-kD tumor antigen were determined by 1) the binding of Mab B6.2 in a solid-phase RIA using Clouser tumor extracts and 2) the determination of the radiolocalization index using as the ratio of cpm of ^{125}I-B6.2-$F(ab')_2$ bound per milligram (cpm/mg) tumor tissue divided by cpm/mg nontumor tissue (i.e., blood, liver, spleen, etc.). The $F(ab')_2$ fragments of Mab B6.2 were used because of their increased blood clearance, which made possible the determination of tumor/blood ratios 24 hours after antibody injection [51]. The analysis of ^{125}I-B6.2 binding to extracts of Clouser tumors isolated from the rHu-IFN-αA-treated group of athymic mice by solid-phase RIA revealed an increase of approximately 200% as a result of interferon treatment (i.e., 7910 cpm vs. 3480 cpm per 20 μg tumor extract). Extracts from the rHu-IFN-αA-treated Clouser tumors and other nontumor tissue (i.e., liver, spleen, etc.) failed to bind MOPC-21, indicating that the increase in the level of Mab B6.2 binding was not a result of induction of Fc receptors. In a subsequent study, untreated and rHu-IFN-αA-treated athymic mice bearing Clouser tumors were sacrificed, and the percentage injected dose of ^{125}I-B6.2-$F(ab')_2$ was determined in tumor and nontumor tissues of each group (Table 5). At the time of sacrifice, the circulating plasma levels of rHu-IFN-αA in the treated group of tumor-bearing mice ranged from 64 to 196 antiviral U/ml. In addition, the average percentage dose of ^{125}I-B6.2-$F(ab')_2$ in the interferon group was approximately two-fold higher than that of the untreated group. No such differences were evident in the blood, liver, or spleen of the mice receiving rHu-IFN-αA. The data

Table 5. Effect of rHu-IFN-αA on ^{125}I-B6.2-F(ab')$_2$ localization to Clouser mammary tumors in athymic mice[a]

Treatment	Mouse No.	Serum rHu-IFN-αA (U/ml)	% Injected Dose per Gram of Tissue			
			Tumor	Blood	Liver	Spleen
Untreated	1	< 30	6.5	2.7	1.2	0.9
	2	< 30	8.0	2.3	1.5	1.0
	3	< 30	3.9	1.8	1.2	0.7
	4	< 30	8.3	1.9	1.5	1.0
	5	< 30	7.9	2.5	1.0	0.9
			x = 6.9 ± 0.7[b]			
rHu-IFN-αA	1	196	12.0	2.1	1.0	1.2
	2	128	16.4	3.1	1.8	1.5
	3	128	14.7	1.9	1.3	1.8
	4	128	11.8	2.4	1.3	1.0
	5	128	11.6	3.0	1.3	1.1
	6	96	11.2	2.4	1.4	0.8
	7	64	8.9	2.1	1.3	0.9
	8	196	18.7	2.0	1.1	1.3
	9	64	9.3	2.6	1.5	1.1
	10	196	13.6	3.1	1.4	1.1
			x = 12.8 ± 0.9[c]			

[a] Athymic mice bearing Clouser tumors were divided into two groups: The untreated mice received intramuscular injections of 0.9% saline, and the rHu-IFN-αA-treated mice received 250,000 antiviral U/day for 7 days. All animals recieved 2 × 10^6 cpm of ^{125}I-B6.2-F(ab')$_2$ on day 6 and were sacrificed 24 hours later.

[b] Values represent the mean ± SE of both groups from a single experiment.

[c] $p < 0.05$ (versus untreated group).

suggest that 1) in vivo administration of rHu-IFN-αA can effectively increase the level of tumor antigen expression in extracts of human mammary xenografts and 2) one component of the increase is the level of cell-surface tumor antigen expression, so that a higher level of radioimmunolocalization of an antibody can be demonstrated. The data also argue against the postulate that rHu-IFN-αA alters the volume distribution of the radiolabeled antibody, thus increasing the localization of the Mab.

The moderately well-differentiated human colon-carcinoma cell line WiDr, which also constitutively expresses the B6.2-reactive 90-kD antigen, and whose level of expression is substantially increased after rHu-IFN-αA or rHu-IFN-γ treatment (Table 4), was also used to determine the in-vivo effect of interferon on Mab localization. Studies were done to determine the effects of rHu-IFN-αA on the localization (i.e., tumor/nontumor tissues) of ^{125}I-B6.2-F(ab')$_2$ at different times post-injection of the antibody. Indeed, as shown in Figure 3, A–C, the tumor/blood ratios for the localization of ^{125}I-B6.2-F(ab')$_2$ to WiDr tumors were 2.5, 4.0, and 6.9, respectively, at 24, 48, and 72 hours post Mab administration. It is believed that the increase in the tumor/blood ratios, as well as the concomitant increase in tumor/liver and tumor/spleen ratios, with time post Mab injection is due to the clearance of

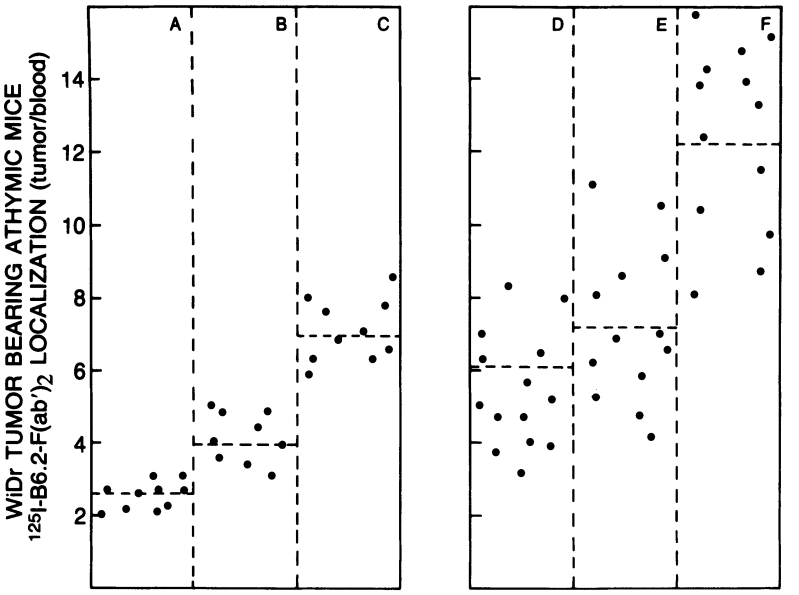

Figure 3. Effect of rHu-IFN-αA on the localization of ^{125}I-B6.2-F(ab')$_2$ to WiDr tumor xenografts in athymic mice. The WiDr tumor-bearing athymic mice were divided into untreated and rHu-IFN-αA-treated groups. The untreated and rHU-IFN-αA mice were implanted with a miniosmotic pump containing approximately 3.0×10^6 antiviral units. After 5 days of interferon treatment, all mice received ^{125}I-labeled B6.2-F(ab')$_2$. The rHu-IFN-αA treated and untreated animals were sacrified 24, 48, and 72 hours later. Panels A–C represent the tumor/blood ratios of ^{125}I-B6.2-F(ab')$_2$ localization from the untreated mice and panels D–F represent tumor/blood ratios of the WiDr tumor-bearing mice that were treated with rHu-IFN-αA and were sacrificed 24(D), 48(E), and 72(F) hours post monoclonal antibody injection. Plasma rHu-IFN-αA levels of the untreated animals were < 30 antiviral U/ml, while those of the treated animals ranged from 200 to 700 antiviral U/ml.

the ^{125}I-labeled antibody from nontumor sites [51]. This same phenomenon was evident in the WiDr-bearing athymic mice implanted with the rHu-IFN-αA containing osmotic pump. In addition, at 24, 48, and 96 hours post ^{125}I-Mab administration, the ratio of antibody localized and measured on the basis of tumor/normal tissues (i.e., blood, liver, and spleen) was approximately two-fold greater than those measured at these same time intervals in the untreated mice. As suggested from previous findings, the increase in Mab localization was primarily due to the increase in the level of 90-kD antigen expression and not to alterations in the blood flow to the tumor site.

Subsequent studies were designed to assess the in-vivo, dose dependent relationship between plasma rHu-IFN-αA levels and the level of ^{125}I-B6.2-F(ab')$_2$ localization (cpm/mg tumor tissue) to WiDr colon carcinomas in athymic mice. A group of WiDr tumor bearing athymic mice were implanted with a miniosmotic pump containing $0.5–2.5 \times 10^6$ antiviral units of rHu-IFN-αA. After a 6-day treatment, the mice were given a single bolus injec-

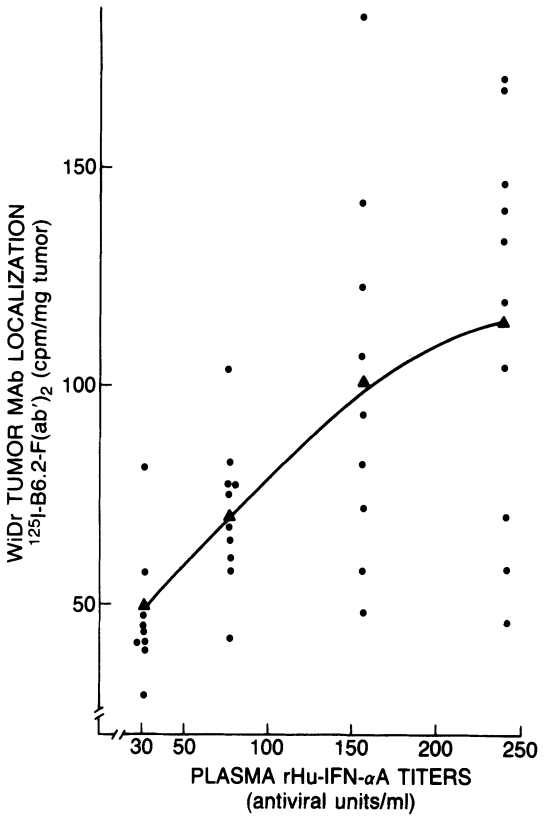

Figure 4. Relationship between plasma levels of rHu-IFN-αA and the level of in-vivo localization of ^{125}I-B6.2-F(ab')$_2$ to WiDr tumors in athymic mice. WiDr tumor-bearing athymic mice were implanted with miniosmotic pumps containing 0.5–2.5 × 10^6 antiviral units of rHu-IFN-αA. Control mice received pumps filled with 0.9% NaCl. After 6 days of interferon treatment, all mice received ^{125}I-B6.2-F(ab')$_2$, as previously described. Twenty-four hours later, all mice were sacrificed, and the localization of ^{125}I-B6.2-F(ab')$_2$ to the human colon-carcinoma xenograft was measured as total counts per minute per milligram tumor wet weight and plasma rHu-IFN-αA antiviral titers, as previously described.

tion of ^{125}I-B6.2-F(ab')$_2$ and sacrificed 24 hours later. The amount of reactivity localized to the WiDr tumors per tumor wet weight, as well as the circulating plasma rHu-IFN-αA levels (i.e., antiviral unitsU/ml) were determined. The results shown in Figure 4 suggest somewhat of a linear relationship between plasma interferon levels and the level of localization of the antibody to the tumor site. The results also indicate that a considerable difference exists among the individual mice as to their ability to localize the ^{125}I-Mab. This is particularly evident in the groups of mice treated with rHu-IFN-αA and exhibiting circulatory plasma rHu-IFN-αA levels of 150 antiviral units or greater. This could be explained by the existence of a wide range of sensitivity among the different WiDr tumors in the athymic mice for the antigen aug-

mentation by rHu-IFN-αA, while other factors, such as tumor vascularization, may play a role in the emergence of this variability.

Summary

The use of Mabs for the detection and treatment of human carcinoma lesions can still be regarded in its infancy. As with other new approaches to cancer therapy, several conceptual as well as real problems exist when designing clinical protocols for Mab-directed immunotherapy. From the Mab standpoint, studies using the intact IgG have shown that, in a majority of patients injected with IgG, human anti-mouse IgG antibodies develop that hamper the effectiveness of subsequent antibody administration. It is believed that the human anti-mouse antibody response is directed against the Fc region of the IgG molecule. The elimination of this region through fractionation of the Mab to obtain the minimum binding site could result in a less immunogenic molecule. Another approach aimed at reducing the immunogenicity of the Mab would be to clone the genes encoding for individual Mabs, reduce them via restriction endonuclease techniques, and insert human immunoglobulin constant regions. The resulting chimeric antibodies are believed to reduce the development of human anti-mouse antibodies.

Effective Mab therapy of human tumor lesions may also be achieved through the recruitment of a portion of the host's immunologic defense system. An example is the use of anti-idiotype Mabs that use as immunogen a Mab to a tumor antigen. The anti-idiotype antibodies are selected for binding to the antigen binding, or idiotype, region of the first Mab. The binding sites of the new anti-idiotype Mabs should reflect the 'internal image' of the original antigen. The anti-idiotype antibodies may be used to immunize patients (i.e., vaccines) in an attempt to mount an active immune response against the antigen-positive tumor cells. Recent studies have shown a synergism between interferon-α and an anti-idiotype Mab for the in-vivo antitumor activity in a murine B-cell lymphoma experimental model [57]. Whether an interferon-mediated increase in the tumor antigen or the Fc receptor was part of the synergism was not investigated. Mabs alone have also been shown to elicit cytotoxic activity in vitro [58] and tumoricidal activity in vivo [59]. Antibodies of the IgG_{2a} isotype can direct macrophage-mediated cytotoxicity. These studies revealed the importance of the number of antibody sites per cell as well as the number of cells that bind the IgG_{2a} Mab, thus suggesting a 'threshold' requirement for the demonstration of effective tumor cell lysis in vitro and in vivo. Such studies underscore the need to know the antigenic phenotype of the tumor cell population in order to explain the response as a result of the administration of a Mab.

Clearly, additional studies are needed to better understand the regulation of antigen expression, including highly complex parameters such as synthesis, processing, membrane insertion, as well as active extrusion into the extra-

cellular spaces. One may predict that the culmination of such investigations, concomitant with the ongoing development of Mabs for immunoscintigraphy and immunotherapy, may be a new combination approach to cancer treatment that includes a biologic response modifier used as an adjuvant for a therapeutically conjugated Mab.

References

1. Kohler, M., and Milstein, C. (1975) Continuous cultures of fused cells secreting antibody of pre-defined specificity. Nature 256:295–297.
2. Bast, R.C., Jr., Klug, T.L., St. John, E., Jenison, E., Niloff, J.M., Lazarus, H., Berkowitz, R.S., Leavitt, T., Griffiths, T., Parker, L., Zurawski, V.R., Jr., and Knapp, R.C. (1983) A radioimmunoassay using a monoclonal antibody to monitor the course of epithelial ovarian cancer. N. Engl. J. Med. 309:883–887.
3. Metzgar, R.A., Rodriguez, N., Finn, O.J., Lan, M.S., Daasch, V.N., Fernsten, P.D., Meyers, W.C., Sindelar, W.F., Sandler, R.S., and Seigler, H.F. (1984) Detection of a pancreatic cancer associated antigen (DU-PAN-2 antigen) in serum and ascites of patients with adenocarcinoma. Proc. Natl. Acad. Sci. USA 81:5242–5246.
4. Ritts, R.E., Del Villano, B.C., Go, W.L.M., Herberman, R.B., Klug, T.L., and Zurawski, V.R., Jr. (1984) Initial clinical evaluation of an immunoradiometric assay for CA 19-9 using the NCI serum bank. Int. J. Cancer 33:339–345.
5. Klug, T.L., Sattler, M.A., Colcher, D., and Schlom, J. (1986) Monoclonal antibody immunoradiometric assay for an antigenic determinant (CA 72) on a novel pancarcinoma antigen (TAG-72). Int. J. Cancer 38:661–669.
6. Mach, J.P., Buchegger, F., Forni, M., Ritschard, J., Berche, C., Lumbroso, J.D., Schreyer, M., Girardet, C., Accolla, R.S., and Carrel, S. (1981) Use of radiolabeled monoclonal anti-CEA antibodies for the detection of human carcinomas by external photoscanning and tomoscintigraphy. Immunol. Today 2:239–249.
7. Moldofsky, P.J., Powe, J., Mulhern, C.B., Jr., Hammond, N., Sears, H.F., Gatenby, R.A., Steplewski, Z., and Koprowski, H. (1983) Metastatic colon carcinoma detected with radiolabeled $F(ab')_2$ monoclonal antibody fragments. Radiology 149:549–555.
8. Mach, J.P., Chatal, J.F., Lumbroso, J.D., Buchegger, F., Forni, M., Ritschard, J., Berche, C., Douillard, J.Y., Carrel, S., Herlyn, M., Steplewski, Z., and Koprowski, H. (1983) Tumor localization in patients by radiolabeled monoclonal antibodies against colon carcinoma. Cancer Res. 43:5593–5600.
9. Hontowich, D.J., Griffin, T.W., Kosciuczyk, C., Rusckowski, M., Childs, R.L., Mattis, J.A., Shealy, D., and Doherty, P.W. (1985) Pharmacokinetics of an indium-111 labeled monoclonal antibody in cancer patient. J. Nucl. Med. 26:849–858.
10. Epenetos, A.A., Britton, K.E., Mather, S., Shepherd, J., Granowska, M., Taylor-Papadimitriou, J., Nimmon, C.C., Durbin, H., Hawkins, L.R., Malpas, J.S., and Bodmer, W.F. (1982) Targeting of iodine-123-labeled tumor-associated monoclonal antibodies to ovarian, breast, and gastrointestinal tumors. Lancet 2:999–1004.
11. Murray, J.L., Rosenblum, M.G., Sobol, R.E., Bartholomew, R.M., Plager, C.E., Haynie, T.P., Jahns, M.F., Glenn, H.J., Lamki, L., Benjamin, R.S., Papadopoulos, N., Boddie, A.W., Frincke, J.M., David, G.S., Carlo, D.J., and Hersh, E.M. (1985) Radioimmunoimaging in malignant melanoma with ^{111}In-labeled monoclonal antibody 96.5. Cancer Res. 45:2376–2381.
12. Larson, S.M. (1985) Radiolabeled monoclonal anti-tumor antibodies in diagnosis and therapy. J. Nucl. Med. 26:538–545.
13. Epenetos, A.A., Hooker, G., Krausz, T., Snook, D., Bodmer, W.F., and Taylor-Papadimitriou, J. (1986) Antibody-guided irradiation of malignant ascites in ovarian cancer:

A new therapeutic method possessing specificity against cancer cells. Obstet. Gynecol. 68: 715–745.
14. Colcher, D., Esteban, J.E., Carrasquillo, J.A., Sugarbaker, P., Reynolds, J.C., Bryant, G., Larson, S.M., and Schlom, J. (1987) Quantitative analysis of selective radiolabeled monoclonal antibody localization in metastatic lesions of colorectal cancer patients. Cancer Res. 47:1185–1189.
15. Colcher, D., Esteban, J.E., Carrasquillo, J.A., Reynolds, J.C., Bryant, G., Larson, S.M., and Schlom, J. (1987) Complementation of intracavitary and intravenous administration of a monoclonal antibody (B72.3) in patients with carcinoma. Cancer Res. 47:4218–4224.
16. Colcher, D., Hand, P., Nuti, M., and Schlom, J. (1981) A spectrum of monoclonal antibodies reactive with human mammary tumor cells. Proc. Natl. Acad. Sci. USA 78:3199–3203.
17. Nuti, M., Teramoto, Y.A., Mariani-Costantini, R., Horan Hand, P., Colcher, D., and Schlom, J. (1982) A monoclonal antibody (B72.3) defines patterns of distribution of a novel tumor-associated antigen in human mammary carcinoma cell population. Int. J. Cancer 29: 539–545.
18. Johnson, V.G., Schlom, J., Paterson, A.J., Bennett, J., Magnani, J.L., and Colcher, D. (1986) Analysis of a human tumor-associated glycoprotein (TAG-72) identified by monoclonal antibody B72.3. Cancer Res. 46:850–857.
19. Thor, A., Viglione, M.J., Muraro, R., Ohuchi, N., Schlom, J., and Gorstein, F. (1987) Monoclonal antibody B72.3 reactivity with human endometrium: A study of normal and malignant tissues. Int. J. Gynecol. Oncol. 6:235–247.
20. Thor, A., Ohuchi, N., Szpak, C.A., Johnston, W.W., and Schlom, J. (1986) The distribution of oncofetal antigen TAG-72 recognized by monoclonal antibody B72.3. Cancer Res. 46: 3118–3124.
21. Horan Hand, P., Nuti, M., Colcher, D., and Schlom, J. (1983) Definition of antigenic heterogeneity and modulation among human mammary carcinoma cell populations using monoclonal antibodies to tumor-associated antigens, Cancer Res. 43:728–735.
22. Schlom, J., Colcher, D., Horan Hand, P., Wunderlich, D., Nuti, M., and Teramoto, Y.A. (1983) Antigenic heterogeneity, modulation and evolution in breast cancer lesions as defined by monoclonal antibodies. In: Rich, M., Hager, J., and Furmanski, P. (eds.), *Understanding Breast Cancer: Clinical and Laboratory Concepts*. New York: Marcel Dekker, pp. 169–213.
23. Barnstable, C.J., Bodmer, W.F., Brown, G., Galfre, G., Milstein, C., Williams, A.F., and Ziegler, A. (1978) Production of monoclonal antibodies to group A erythrocytes, HLA and to the human cell surface antigens — new tools for genetic analysis. Cell 14:9–20.
24. Tran, R., Horan Hand, P., Greiner, J.W., Pestka, S., and Schlom, J. (1988) Enhancement of surface antigen expression on human breast carcinoma cells by recombinant human interferons. J. Interferon Res. 8:75–88.
25. Muraro, R., Wunderlich, P., Thor, A., Lundy, J., Noguchi, P., Cunningham, R., and Schlom, J. (1985) Definition of monoclonal antibodies of a repertoire of epitopes in carcinoembryonic antigen differentially expressed in human colon carcinoma versus normal adult tissues. Cancer Res. 45:5769–5780.
26. Foulds, L. (1954) The experimental study of tumor progression: A review. Cancer Res. 14: 327–329.
27. Kufe, D.W., Nadler, L., Sargent, L., Shapiro, H., Horan Hand, P., Austin, F., Colcher, D., and Schlom, J. (1983) Biological behavior of human breast carcinoma-associated antigens expressed during cellular proliferation. Cancer Res. 43:851–857.
28. Greiner, J.W., Tobi, M., Fisher, P.B., Langer, J.A., and Pestka, S. (1985) Differential responsiveness of cloned mammary carcinoma cell populations to human recombinant leukocyte alpha interferon mediated enhancement of human antigen expression. Int. J. Cancer 36:159–166.
29. Horan Hand, P., Colcher, D., Salomon, D., Ridge, J., Noguchi, P., and Schlom, J. (1985) Spacial configuration of carcinoma cell populations influences the expression of a tumor associated glycoprotein. Cancer Res. 45:833–840.
30. Fellous, M., Kamoun, M., Gresser, I., and Bono, R. (1979) Enhanced expression of HLA

antigens and β_2-microglobulin on interferon-treated human lymphoid cells. Eur. J. Immunol. 9:446–449.

31. Attallah, A.M., Needy, C.F., Noguchi, P.D., and Elisberg, B.L. (1979) Enhancement of carcinoembryonic antigen expression by interferon. Int. J. Cancer 24:49–52.
32. Imai, K., Ng, A.-K., Glassy, M., and Ferrone, S.K. (1981) Differential effect of interferon on the expression of tumor-associated antigens and histocompatibility antigens on human melanoma cells: Relationship to susceptibility to immune lysis mediated by monoclonal antibodies. J. Immunol. 127:505–508.
33. Basham, T.Y., Bourgeade, M.F., Creasey, A.A., and Merigan, T.C. (1982) Interferon increases HLA synthesis in melanoma cells: Interferon-resistant and sensitive cell lines. Proc. Natl. Acad. Sci. USA 79:3265–3269.
34. Ball, E.D., Sorenson, G.D., and Pettengill, O.S. (1986) Expression of myeloid and major histocompatibility antigens on small cell carcinoma of the lung cells analyzed by cytofluorometry: Modulation by interferon. Cancer Res. 46:2335–2339.
35. Greiner, J.W., Horan Hand, P., Noguchi, P., Fisher, P., Pestka, S., and Schlom, J. (1984) Recombinant interferon enhances detection of human breast and colon carcinoma associated antigens by monoclonal antibodies. Cancer Res. 44:3208.
36. Dolei, A., Capobianchi, M.R., and Ameglio, F. (1983) Human interferon-gamma enhances the expression of class I and class II major histocompatibility complex products in neoplastic cells more effectively than interferon-alpha and interferon-beta. Infect. Immunol. 40: 172–176.
37. Schwartz, R., Momberg, F., Moldenbauer, G., Dorken, B., and Schirrmacher, V. (1985) Induction of class II antigen expression on human carcinoma cell lines by IFN-gamma. Int. J. Cancer 35:245–250.
38. Ziai, M.R., Imbesti, L., Tongson, A., and Ferrone, S. (1985) Differential modulation by recombinant immune interferon of the expression and shedding of HLA antigens and melanoma associated antigens by a melanoma cell line resistant to the antiproliferative activity of immune interferon. Cancer Res. 45:5877–5882.
39. Greiner, J.W. (1986) Modulation of antigen expression in human tumor cell populations. Cancer Invest. 4:239.
40. Giacomini, P., Aguzzi, A., and Ferrone, S. (1986) Differential susceptibility to modulation by recombinant immune interferon of HLA-DR and -DQ antigens synthesized by melanoma COLO 38 cells. Hybridoma 5:277–288.
41. Heron, I., Hokland, M., and Berg, K. (1978) Enhanced expression of β_2-microglobulin and HLA antigen on human lymphoid cells by interferon. Proc. Natl. Acadi. Sci. USA 75: 6215–6219.
42. Wallach, D., Fellous, M., and Revel, M. (1982) Preferential effect of gamma-interferon on the synthesis of HLA antigens and their mRNAs. Nature 299:833–836.
43. Collins, T., Karman, A.J., Wake, C.T., Boss, J.M., Kappes, D.J., Fiers, W., Ault, K.A., Gimbrone, M.A., Strominger, J.L., and Pober, J.S. (1984) Immune interferon activates multiple class II major histocompatibility complex genes and the associated invariant chain gene in human endothelial cells and dermal fibroblasts. Proc. Natl. Acad. Sci. USA 81: 4917–4921.
44. Greiner, J.W., Guadagni, F., Pestka, S., and Schlom, J. (1986) Augmentation of antigen expression by recombinant human interferon. In: Friedman, R., Merigan, T., and Sreevalsan, T. (eds.), *UCLA Symposium on Molecular and Cellular Biology*, Vol 50. New York: Alan R. Liss, pp. 17–27.
45. Chandrabase, K., and Cuatrecasas, P. (1981) Changes in fatty acyl chains of phospholipid induced by interferon in mouse sarcoma S-180. Biochem. Biophys. Res. Commun. 98: 661–665.
46. Kuhry, J.G., Poindoin, and Laustriat, G. (1983) Evidence for early fluidity changes in the plasma membranes of interferon treated L-cells, from fluorescence antistropy data. Biochem. Biophys. Res. Commun. 110:88–92.
47. Spear, G.T., Paulnock, D.M., Jordan, R., Hawkins, M.J., and Borden, E.C. (1985)

Modulation of human peripheral blood monocyte HLA-DR expression by recombinant IFN-γ. Proc. Am. Assoc. Cancer Res. 26:277.

48. Rowlinson, G., Balkwill, F., Snook, D., Hooker, G., and Epenetos, A.A. (1986) Enhancement by γ-interferon of in vivo tumor radiolocalization by a monoclonal antibody against HLA-DR antigen. Cancer Res. 46:6413–6417.
49. Balkwill, F.R., Stevens, M.H., Griffin, D.B., Thomas, J.A., and Bodmer, J.G. (1987) Interferon gamma regulates HLA-DR expression on solid tumors in vivo. Eur. J. Clin. Oncol. 23: 101–106.
50. Hayes, D.F., Zalutsky, M.R., Kaplan, W., Noska, M., Thor, A., Colcher, D., and Kufe, D.W. (1986) Pharmacokinetics of radiolabeled monoclonal antibody B6.2 in patients with metastatic breast cancer. Cancer Res. 46:3157–3163.
51. Colcher, D., Zalutsky, M., Kaplan, W., Kufe, D., Austin, F., and Schlom, J. (1983) Radiolocalization of human mammary tumors in athymic mice by a monoclonal antibody. Cancer Res. 43:736–742.
52. Sahagan, B.G., Dorai, H., Saltygaber-Muller, J., Toneguzzo, F., Guidon, C.A., Lilly, S.P., McDonald, K.W., Morrissey, D.V., Stone, B.A., Davis, G.L., McIntosh, P.K., and Moore, G.P. (1986) A genetically engineered murine/human chimeric antibody retains specificity for human tumor-associated antigen. J. Immunol. 137:1066–1074.
53. Thor, A., Muraro, R., Gorstein, F., Ohuchi, N., Viglione, M., Szpak, C.A., Johnston, W.W., and Schlom, J. (1987) Adjunct to the diagnostic distinction between adenocarcinomas of the ovary and the colon utilizing a monoclonal antibody (COL-4) with restricted carcinoembryonic antigen activity. Cancer Res. 47:505–512.
54. Schlom, J., Greiner, J.W., Horan-Hand, P., Colcher, D., Inghirami, G., Weeks, M., Pestka, S., Fisher, P.B., Noguchi, P., and Kufe, D.W. (1985) Human breast cancer markers defined by monoclonal antibodies. In: Sell, S., and Reisfeld, R. (eds.), *Monoclonal Antibodies in Cancer*. Clifton, NJ: Humana Press, pp. 247–277.
55. Greiner, J.W., Horan Hand, P., Wunderlich, D., and Colcher, D. (1986) Radioimmunoassay for detection of changes in cell surface tumor antigen expression induced by interferon. Meth. Enzymol. 119:682–685.
56. Braylan, R.C., Benson, N.A., Nourse, V., and Kruth, H.S. (1982) Correlated analysis of cellular DNA, membrane antigens and light scatter of human lymphoid cells. Cytometry 2: 337–343.
57. Basham, T.Y., Kaminski, M.S., Kitamura, K., Levy, R., and Merigan, T.C. (1986) Synergistic antitumor effect of interferon and anti-idiotype monoclonal antibody in murine lymphoma. J. Immunol. 137:3019–3024.
58. Herlyn, D., Powe, J., Ross, A.H., Herlyn, M., and Koprowski, H. (1985) Inhibition of human tumor growth by IgG_{2a} monoclonal antibodies correlates with antibody density on tumor cells. J. Immunol. 134:1300–1304.
59. Herlyn, D., and Koprowski, H. (1982) IgG_{2a} monoclonal antibodies inhibit human tumor growth through interaction with effector cells. Proc. Natl. Acad. Sci. USA 79:4761–4768.

22. Anti-antibody enhancement of tumor imaging

Robert M. Sharkey, Rosalyn D. Blumenthal, and David M. Goldenberg

Although there are many factors that influence the ability of a radiolabeled antibody to image tumors by external scintigraphy, perhaps the most problematic has been the ability to distinguish specific radioantibody uptake in tumor from the background radioactivity in uninvolved tissues, particularly that due to excessive blood-pool activity. This problem was recognized even as the technology was first developing in the mid-1950s [1], but it was thought that the development of more highly specific anti-tumor antibodies would be a solution. However, even as specificity of the antibodies was improved, tumor imaging was difficult. For example, in animals bearing human tumor xenografts in peripheral sites, such as the cheek pouch in hamsters or subcutaneously in nude mice, tumors were not clearly imaged until 4–7 days after the radioantibody was injected [2–4], because it took several days for the blood-pool radioactivity to clear. Otherwise, the majority of the counts in the images was derived from radioactivity residing in the blood and uninvolved tissues. Excessive background radioactivity also interfered with the detection of tumors in humans [5], but this problem was overcome initially by Goldenberg et al. [6]. They developed a dual-isotope subtraction procedure that used ^{99m}Tc-pertechnetate and labeled albumin to estimate the contribution of interstitial and blood-pool radioactivity in the images produced. With this procedure, they were able to detect a variety of human tumors, even in well-vascularized tissues such as the liver, with a sensitivity exceeding 85% [7]. Although this method has been used successfully by several other investigators [8–10], it has been criticized because the pertechnetate/albumin and the radioantibody do not distribute identically in the tissues, and imaging artifacts caused by the differences in the energies of the two isotopes (^{131}I and ^{99m}Tc) were not corrected [11,12]. Although the computerized subtraction technique has been refined by others [13,14], alternatives to this approach are being investigated.

The most common alternative to the subtraction procedure is the use of antibody fragments. Wahl et al. [15] compared radiolabeled whole IgG, F(ab′)$_2$, and Fab′ fragments of an anti-CEA (carcinoembryonic antigen) mouse monoclonal antibody (Mab) in tumor-bearing animals and found that the radioactivity was cleared more quickly as the antibody was reduced in

Goldenberg, D.M., (ed.), Cancer Imaging with Radiolabeled Antibodies.

Table 1. Comparison of tumor/nontumor ratios for I-131-labeled whole IgG, $F(ab')_2$, and Fab' fragments of goat anti-CEA antibody in hamsters bearing a human colonic tumor xenograft (GW-39)

Time Post-injection	IgG			$F(ab')_2$			Fab'		
	Liver	Kidney	Blood	Liver	Kidney	Blood	Liver	Kidney	Blood
2 hours	ND	ND	ND	0.4	0.3	0.1	1.3	0.1	0.3
8 hours	ND	ND	ND	0.5	0.6	0.2	1.8	0.2	0.5
1 day	4.7	3.6	0.9	3.0	2.5	0.5	2.1	0.5	1.5
3 days	11.0	8.3	2.0	8.9	7.8	1.7	1.8	0.3	1.4
7 days	22.2	18.9	5.8	17.6	15.6	4.2	ND	ND	ND

Adult female hamsters (100–130 g) were transplanted in each cheek pouch with GW-39 tumor suspension 5–7 days prior to the intracardial injection of 100–250 μCi (8–20 μg) of I-131-labeled goat anti-CEA antibody. The whole IgG fraction was affinity purified on a CEA immunoabsorbent. The $F(ab')_2$ and Fab' fragments were prepared by pepsin digestion [$F(ab')_2$] and reduction with beta-mercaptoethanol followed by alkylation with iodoacetamide (Fab'). Immunoreactivity of the iodinated antibodies was between 45% and 55%. Values represent the mean of tumor/nontumor ratios (n = 5–7 animals, 10–14 tumors weighing 0.2–0.5 g).
ND = not determined.

size. $F(ab')_2$ fragments were preferred for tumor imaging, because the Fab' fragments were cleared too rapidly to develop significantly improved tumor/nontumor ratios, and the whole IgG was not cleared as well as the $F(ab')_2$ fragments. Buchegger et al. [16] reported that the monovalent Fab fragment of an anti-CEA Mab was better than the divalent $F(ab')_2$ or whole IgG for tumor localization in nude mice; and in patients, Delaloye et al. [17] have claimed that ^{123}I-labeled Fab fragments improved the quality of tumor imaging in comparison with $F(ab')_2$ using tomography. However, Khaw et al. [18] reported that Fab' fragments of 10-3D2, an anti-human mammary carcinoma antibody, were cleared too rapidly and did not accrete in the tumor as well as $F(ab')_2$ fragments. In our experience with intact versus antibody fragments of goat anti-CEA antibody [19], we agree with the finding of Wahl et al. and Khaw et al. As shown in Table 1, the whole IgG and the $F(ab')_2$ fragments gave similar tumor/nontumor ratios, and the tumor/nontumor ratios for the whole IgG and $F(ab')_2$ generally were higher than the Fab' fragment, except for the very early times postinjection. Thus, at 2 and 8 hours postinjection, tumor/liver and tumor/blood ratios were higher for the Fab' fragment than that observed for the $F(ab')_2$, but this slight advantage was not apparent by 24 hours. Increased uptake of radioactivity in the kidneys was also observed for the Fab' fragments, but not for the $F(ab')_2$. More recently, we have been examining several Mabs against either CEA or colon-specific antigen-p (CSAp; 20) in tumor-bearing nude mice. Fragments gave higher tumor/nontumor ratios at earlier times than the whole IgG for both of these Mabs, with Fab' fragments yielding the highest tumor/nontumor ratios at 24 hours (Table 2). However, using hamsters bearing the same human colonic

Table 2. Comparison of tumor/nontumor ratios for the whole IgG, $F(ab')_2$ and Fab' fragments of an anti-CEA (NP-4) and an anti-CASp (MU-9) mouse monoclonal antibody in nude mice bearing a human colonic tumor xenograft (GW-39)

Time Post-injection	NP-4 IgG			Mu-9 IgG		
	Liver	Kidney	Blood	Liver	Kidney	Blood
24	2.36 ± 0.40	1.99 ± 0.27	0.56 ± 0.05	3.71 ± 1.17	3.52 ± 1.63	1.01 ± 0.46
72	5.53 ± 0.56	4.60 ± 0.47	1.25 ± 0.14	7.62 ± 1.52	8.25 ± 3.20	2.22 ± 0.16
168	10.94 ± 1.43	10.45 ± 1.40	2.85 ± 0.40	34.12 ± 24.16	37.84 ± 34.54	11.43 ± 10.62
336	19.39 ± 2.40	16.33 ± 2.63	5.91 ± 0.93	86.01 ± 41.72	69.38 ± 27.53	21.61 ± 9.98
$F(ab')_2$						
8				11.60 ± 3.00	10.10 ± 5.50	4.60 ± 1.60
24	7.33 ± 0.53	3.57 ± 0.36	1.69 ± 0.15	8.20 ± 1.00	4.50 ± 0.40	3.20 ± 0.75
48	23.60 ± 3.63	12.12 ± 2.12	6.40 ± 0.80			44.70 ± 7.69
72	26.49 ± 2.96	14.19 ± 1.62	9.07 ± 1.35	60.80 ± 3.90	24.50 ± 1.56	
168	38.95 ± 7.33	25.43 ± 4.76	39.82 ± 9.92			
Fab'						
6	2.90 ± 0.70	0.50 ± 0.50	0.90 ± 0.30			
24	13.50 ± 1.20	0.80 ± 0.07	8.00 ± 0.80	11.51 ± 3.31	4.91 ± 0.56	7.88 ± 1.98
30	18.10 ± 2.50	0.90 ± 0.40	13.20 ± 1.50			
48				14.77 ± 3.94	10.07 ± 1.30	20.43 ± 5.14
72				21.72 ± 3.22	16.03 ± 1.98	33.14 ± 5.78

Animals (five animals per time interval) were injected intravenously with 20–50 μCi (2–5 μg Mab protein) of I-131-labeled Mab or its fragments, and were sacrificed at the times indicated. Tumors were 14 days old (approximately 0.2 g) at the time of injection. Values represent means ± SD.

Table 3. Tumor/nontumor ratios for I-131-labeled whole IgG and $F(ab')_2$ fragments of a murine monoclonal antibody against CEA (NP-4) in hamsters bearing GW-39 human colonic tumors in the hind-leg musculature

Time Post-injection (hrs)	IgG			$F(ab')_2$		
	Liver	Kidney	Blood	Liver	Kidney	Blood
24	1.54 ± 1.08	1.17 ± 0.56	0.36 ± 0.17	1.71 ± 0.38	1.71 ± 0.09	0.40 ± 0.09
72	3.31 ± 1.15	2.35 ± 0.88	0.78 ± 0.26	3.99 ± 0.42	2.62 ± 0.24	1.31 ± 0.16
168	6.47 ± 3.16	5.14 ± 2.73	1.65 ± 0.83	ND	ND	ND

Adult female hamsters (100–130 g) were injected intracardially with 150–200 μCi (10–15 μg Mab protein) of I-131-labeled NP-4 IgG or $F(ab')_2$ 11–12 days after tumor transplantation. Values represent means ± SD; n = 10–20 animals, 20–40 tumors per time interval.
ND = not determined.

tumor xenograft in the hind-leg muscle (Table 3), we were unable to show improved tumor/nontumor ratios with the $F(ab')_2$ of the anti-CEA Mab (NP-4) in comparison with whole NP-4. Thus, for very early imaging, Fab′ fragments may have an advantage over $F(ab')_2$ fragments, but our studies suggest that enough differences exist between antibodies that a general prediction cannot be made whether $F(ab')_2$ or Fab′ fragments will be the best molecule to use in all clinical applications. Our studies also indicate that difference may exist in the biodistribution of antibodies in experimental animal models, further indicating that these models may not directly predict the behavior of Mabs in humans. Nevertheless, it can be generally stated that there is more rapid blood clearance, greater kidney uptake, and less tumor uptake with antibody fragments than with whole IgG.

Although antibody fragments provide a means of reducing blood-pool activity by their more rapid clearance from the body, we have no control over the rate at which the fragment is cleared from the body. In addition, antibody fragments frequently have a lower affinity than whole IgG, and fragments may be difficult or costly to prepare. We have been investigating an alternative approach to the problem of reducing elevated blood-pool activities. This procedure uses a second antibody (SA) that is directed against the immunoglobulin of the animal species from which the anti-tumor antibody (primary antibody, PA) was prepared. The specificity of the SA for the PA allows it to complex with the PA without complexing with the tumor-bearing host's immunoglobulin. Our studies have shown that a SA can selectively complex with radioiodinated anti-CEA antibody in either animals or patients [21,22], thereby causing a rapid removal of radioactivity from the body with a significant improvement in tumor/nontumor ratios.

The first trials with SA to improve tumor localization were reported in 1964 by Spar et al. [23]. In their study, normal rats or rats with subcutaneous Murphy–Sturm tumors were first injected with a partially purified, ^{131}I-labeled, rabbit anti-rat fibrinogen antibody (36 μg antibody protein). Twenty-four hours later, some animals were given a second intravenous injection of goat

anti-rabbit IgG antiserum that contained 6 mg of antibody per milliliter. Within 2 hours, the amount of radioactivity in the blood was five times lower in the animals given the SA in comparison with the animals that only received the radiolabeled primary antibody. However, measurements of total body activity showed that it took at least 9 hours after the SA injection to detect a significant change in the total body activity between the two groups, indicating that, despite the rapid removal of radioactivity from the blood, it was not immediately removed from the body. It was found that the radioactivity was first deposited in the liver and spleen, but within 2–3 hours after the SA injection, the radioactivity in the liver began to decline rapidly. However, the radioactivity in the spleen reached its maximum after 12 hours and remained constant for the next 24 hours. Within 24 hours after the injection of the SA, the amount of radioactivity per gram tumor decreased by a factor of two, but tumor/blood ratios were 17 : 1, 2.8 times higher than the tumor/blood ratios found in the control animals. These promising results prompted the investigation of this method in a clinical therapy trial in 1966, where the SA was used to enhance the clearance of the radiolabeled antibody from the body. McCardle et al. [24] reported that total-body activity was reduced by about ten-fold within 48 hours after the administration of a SA that was given 3 days after the injection of the radiolabeled PA.

Despite these encouraging results, SA was not used again for radioimmunodetection until 1981 [25]. Barrett et al. [26] used liposomally entrapped second antibody (LESA) to improve tumor/nontumor ratios in nude mice bearing human colonic-tumor xenografts that were given ^{131}I-labeled goat anti-CEA antibody. In their studies, LESA was given 24 hours after ^{131}I-labeled goat anti-CEA antibody. Tumor/blood ratios were improved by almost four-fold within 6 hours after the administration of LESA, and by almost 11-fold within 24 hours after LESA. Although tumor/blood ratios were markedly improved in a short period of time, there was appreciable uptake in the liver and spleen. In contrast to the rapid removal of radioactivity from the liver that was observed by Spar et al. [23], it took 24 hours before the amount of radioactivity in the liver of animals given LESA was significantly lower than in animals that were only given the radiolabeled PA. In addition, radioactivity in the spleen was almost three times higher in the animals given LESA, even after 24 hours. Although tumor uptake appeared unaffected 6 hours after LESA, reduced tumor uptake was found after 24 hours. Begent et al. [27] subsequently reported that LESA successfully reduced the amount of circulating radioiodinated goat anti-CEA activity, so that tumors could be more clearly imaged in patients.

A major problem with the use of LESA is the poor incorporation of antibody in the liposomes. Indeed, Ryman and Barratt [28] reported that only 50% of the IgG used in the formation of LESA is incorporated into the liposomes, and only 10% of this antibody was available to bind CEA. In addition, it is likely that the antibody may become dissociated at least partially from the liposomal complex after its injection. In a response to the question of whether

Table 4. Comparison of tumor/nontumor ratios in hamsters bearing colonic tumor xenografts in the presence of absence of a second antibody (SA)

Tissue	Time After Injection of SA (hours)	Tumor/Nontumor Ratio*	
		Without SA	With SA
Liver	2	1.7 ± 0.2	0.8 ± 0.2
	6	1.4 ± 0.2	2.4 ± 0.4
	24	2.9 ± 0.3	9.0 ± 2.5
	51	4.3 ± 0.3	15.5 ± 1.6
Spleen	2	2.0 ± 0.3	1.3 ± 0.4
	6	1.5 ± 0.2	2.1 ± 0.5
	24	3.7 ± 0.6	3.7 ± 0.9
	51	4.3 ± 0.3	3.7 ± 0.6
Kidney	2	1.4 ± 0.2	1.8 ± 0.5
	6	0.9 ± 0.1	2.8 ± 0.5
	24	1.8 ± 0.2	4.7 ± 1.0
	51	2.6 ± 0.2	7.4 ± 1.7
Lungs	2	0.7 ± 0.1	1.3 ± 0.5
	6	0.7 ± 0.1	3.0 ± 0.5
	24	1.6 ± 0.2	6.4 ± 1.7
	51	2.1 ± 0.2	12.0 ± 0.5
Blood	2	0.5 ± 0.1	1.4 ± 0.04
	6	0.3 ± 0.04	2.1 ± 0.4
	24	0.8 ± 0.1	3.8 ± 0.7
	51	1.1 ± 0.08	12.4 ± 3.7

* Values are the mean ± SE (n = 6 tumors; n = 3 animals).

LESA was essential for the success of this methodology, Bradwell et al. [29] showed that SA alone could effectively reduce the amount of radioactivity in the blood and whole body of normal rats. Our group [21], as well as Goodwin et al. [30], confirmed that SA alone was as effective as LESA for improving tumor/nontumor ratios. In our first report [21], hamsters bearing a CEA-producing, colonic-tumor xenograft (GW-39) [31] were first injected intraperitoneally with a mixture of ^{131}I-goat anti-CEA antibody and ^{125}I-normal goat IgG (5 μg of each). Twenty-four hours later, affinity-purified donkey anti-goat IgG (250 μg) was given intraperitoneally. We found that, in comparison with animals that were only given the radiolabeled PA, tumor/blood ratios were significantly improved within 2 hours after the injection of SA, and tumor/liver ratios were significantly improved within 6 hours (Table 4).

However, we also observed a two- to threefold reduction in the amount of radioactivity in the tumors within 24 hours after the administration of the SA. The reduction in the amount of radioactivity in the tumor was believed to be due to the rapid loss of radiolabeled antibody from the blood pool rather than an appreciable removal of antibody from the tumor that may have been bound to antigen. Furthermore, the ratio of goat anti-CEA antibody to normal goat IgG in the tumor increased over time in the group of animals given the SA, suggesting that the accumulation of normal IgG in the tumor

was related to its persistance in the blood, whereas the anti-CEA antibody was selectively retained in the tumor.

At least two factors have been recognized for their influence on the removal of radiolabeled PA from the blood. First is the schedule for the administration of the SA after the PA has been injected. Goodwin et al. [30] found that injection of an anti-transferrin antibody 2 hours following the injection of ^{111}In-alkyl-transferrin decreased tumor uptake by about 33% in mice bearing KHJJ tumors and subsequently did not improve tumor/blood ratios. However, injection of the anti-transferrin 18 hours after the injection of the ^{111}In-labeled transferrin led to improved tumor/blood ratios, because there was no effect on tumor uptake measured 2 hours after SA injection. In our experimental animal model, we compared the injection of SA at 6, 24, or 48 hours after the injection of radioiodinated goat anti-CEA antibody [32]. We found that administering the SA at 6 hours improved tumor/blood ratios by four- to eightfold over the ratios observed in animals that were not given the SA (control), but tumor/blood ratios could be improved further if the injection of the SA was delayed until 24 hours after the PA was given (Figure 1). Although tumor/blood ratios could be improved by administering the SA at 6 hours, there was no improvement in the tumor/nontumor ratios for the other major organs. However, when the SA was given at 24 or 48 hours after the PA, tumor/nontumor ratios were significantly improved for all the major organs. As shown in Figure 2, the early administration of the SA resulted in decreased tumor uptake, but when the SA was administered at 24 or 48 hours after the PA, 50–75% of the radioactivity remained in the tumor when compared with the control. These results reinforce the concept that it takes some time for the radiolabeled antibody to reach its maximum concentration in a tumor. Other factors govern how soon, how much, and how long the radiolabeled antibody will bind to the tumor. These factors include the physiology of the tumor (blood flow, volume, and permeability), accessibility of the antigen, and antibody affinity. Thus, in order to achieve the best tumor/nontumor ratios, radioantibody uptake in the tumor must be optimized before the administration of the SA. In this sense, one must be careful in judging the efficacy of the SA method by understanding that both the PA and the SA contribute to the successful application of this method. The SA should be judged according to its ability to remove radiolabeled PA from the blood. If the PA is rapidly removed from the blood by the SA, but tumor/nontumor ratios are not appreciably improved, the problem may be with the ability of the PA to penetrate and tightly bind to antigen within the tumor.

The SA procedure is able to improve tumor/nontumor ratios because maximum tumor accretion occurs before the radioantibody can be removed adequately from the body by metabolic processing mechanisms. The SA complexes with the radiolabeled antibody in the blood, and these complexes are then rapidly deposited predominately in the liver, where the radioiodinated antibody is quickly metabolized, and then the radioiodine is removed from the body.

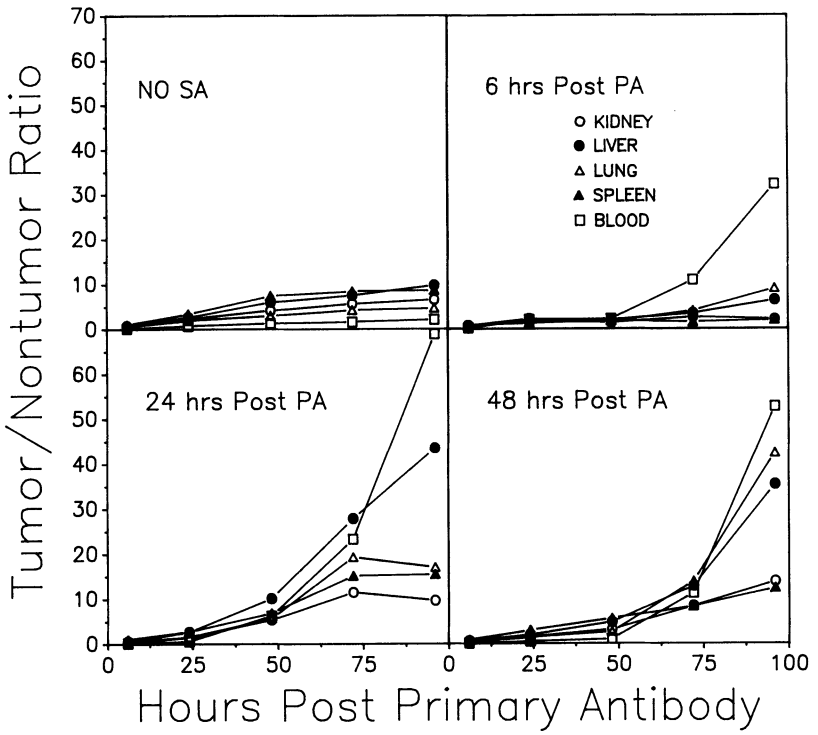

Figure 1. Adult female hamsters bearing GW-39 tumor xenografts (average of 1.0 g at time of injection) in each cheek pouch were injected intracardially with 15 μg of ^{131}I-goat anti-CEA antibody. Separate groups of animals were then administered donkey anti-goat IgG at a 200:1 SA/PA ratio at 6, 24, or 48 hours after the PA. Five to six animals were sacrificed at daily intervals after the PA injection. The values represent means ± SE.

It has been well documented that radioiodinated antibodies are rapidly metabolized with the liberation of small molecular weight radioiodine that is quickly removed from the body. The liver is believed to be the primary organ responsible for the metabolic processing of these complexes. Although the liver appears to be the first and foremost organ where the complexes are deposited, within 2–6 hours most of the radioactivity is cleared from the liver. Soon after the injection of the SA, the radioactivity is also elevated in the stomach mucosa, thyroid (if not blocked by Lugol's solution), kidneys, and bladder. The level of radioactivity in these organs dissipates at different rates over the next 24–48 hours. The progression of radioactive uptake in the tissues supports the view that the liver is the primary site of metabolic activity, with the radioactivity being removed from the body in a similar fashion as that reported for radioiodine [33]. In contrast to the rapid clearance from the liver, radioactivity deposited in the spleen is not rapidly cleared, suggesting that the spleen may be less able to dehalogenate the radioiodinated antibody or that there may be a continuing influx of complexes into the spleen that are not filtered from the blood by the liver.

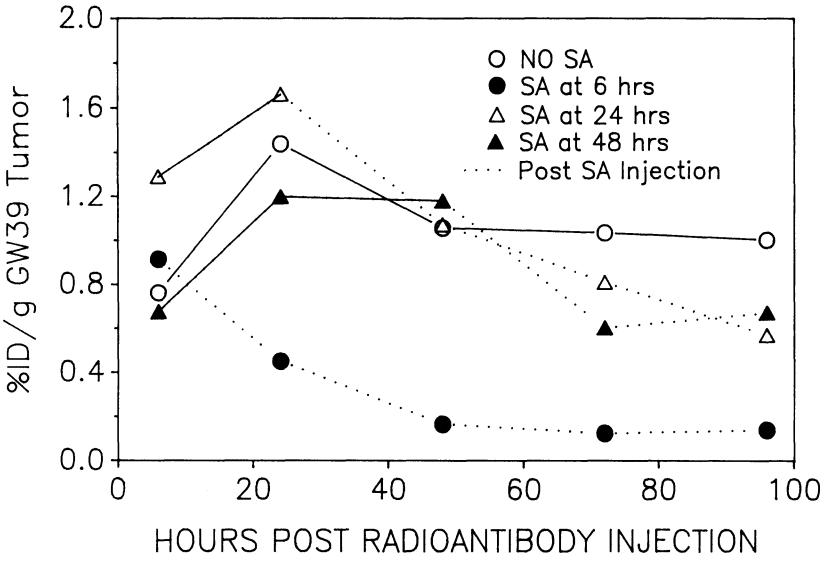

Figure 2. Percent injected dose per gram tumor values taken from the experiment described in Figure 1.

The formation of PA-SA complexes is influenced by the ratio of the SA to the PA. In our experimental animal model, we found that at low SA/PA ratios, there was higher uptake in the spleen than at higher SA/PA ratios [32]. This may indicate that the size or the molecular composition of the complexes plays a role in regulating the deposition of the complexes in the major organs. There is a point, however, where the injection of additional SA does not influence the site of tissue deposition and tumor/nontumor ratios cannot be increased further.

Except for the work of Goodwin et al. [30], the PA has been labeled with radioiodine, either ^{131}I or ^{125}I. A major difference between antibodies labeled with radioiodine or radiometals is the finding that, unlike radioiodine, radiometals concentrate in the liver [34,35]. Since the liver is responsible primarily for the metabolism of the SA-PA complexes, there is a question as to whether the SA method would improve tumor/nontumor ratios if the PA was labeled with radiometals such as ^{111}In. In the study by Goodwin et al. [30], the tissue distribution of ^{111}In-labeled transferrin or alkyl-IgG was reported only for 2 hours after SA injection. At this time, it was noted that the blood activity had been removed by the liver, but whether the liver was able to metabolize the complexes was not reported. However, total-body counting over 18 days of animals with or without SA indicated that the radioactivity had not appreciably left the body, suggesting that the radioactivity deposited in the liver was not cleared as rapidly as that found with radioiodinated antibodies. In our experience with ^{111}In-labeled goat anti-CEA, the amount of radioactivity in the liver after SA injection was higher than if SA was not given, but the radio-

Table 5. Biodistribution of In-111 goat anti-CEA antibody in hamsters

Time Post PA (hours)	Without SA			With SA		
	T/NT			T/NT		
	Blood	Kidney	Liver	Blood	Kidney	Liver
2	0.08 ± 0.03	0.27 ± 0.13	0.16 ± 0.05	ND	ND	ND
24	0.77 ± 0.14	1.35 ± 0.21	0.90 ± 0.12	ND	ND	ND
48	2.14 ± 0.36	3.00 ± 0.68	1.70 ± 0.36	22.53 ± 13.48	2.57 ± 0.79	0.74 ± 0.27
72	3.28 ± 0.92	3.77 ± 1.36	2.14 ± 0.60	21.51 ± 13.87	1.78 ± 0.66	0.42 ± 0.18
	%ID/g			%ID/g		
	GW-39 tumor		Liver	GW-39 tumor		Liver
2	0.20 ± 0.09		1.18 ± 0.38	ND		ND
24	0.96 ± 0.14		1.09 ± 0.25	ND		ND
48	1.27 ± 0.28		0.76 ± 0.10	1.07 ± 0.44		1.42 ± 0.22
72	1.82 ± 0.68		0.85 ± 0.19	0.55 ± 0.22		1.38 ± 0.34

Adult hamsters (five per interval) bearing 0.5–1.5 g GW-39 tumors in each cheek pouch were injected with 15 μg (45 μCi) of In-111-labeled goat anti-CEA antibody. The goat antibody was coupled with DTPA using the derivative. Immunoreactivity was 55% with less than 4% unbound In-111. One group of animals served as a control and was not injected with the SA, while a separate group of animals was injected intracardially with 200 μg of donkey anti-goat IgG 24 hours after the injection of the labeled goat antibody. ND = not determined.

activity in the other major organs also was not markedly reduced (Table 5). The amount of radioactivity in the blood was the only site that was significantly improved in the animals that were given the SA. The amount of radioactivity in the tumor decreased by 30% (not statistically significant when compared with the control group) 24 hours after the SA, and by 70% ($p < 0.01$) 48 hours after the SA. Overall, tumor/blood ratios were 8–10 times higher when the SA was administered than without the SA. Thus, the SA method may not improve the ability of ^{111}In-labeled anti-tumor antibodies to image tumors in the liver, but the higher tumor/blood ratios may assist localization of tumors in other regions of the body.

Although we have shown that tumor/nontumor ratios were improved using the anti-antibody method, and better tumor imaging could be demonstrated in hamsters bearing tumor xenografts in a peripheral site (cheek pouch) [22], we were interested in determining whether the anti-antibody method would improve imaging if the tumor was located in the visceral organs. We had reported that the colonic-tumor xenograft, GW-39, could be transplanted in the liver of unconditioned hamsters and would also result in the growth of tumor in the lungs of approximately 80% of the animals [36]. In this report, we also showed that tumors in the liver could be imaged with ^{131}I-labeled goat anti-CEA antibody after 7 days, but tumors in the lungs could not be detected by external scintigraphy. The failure to image the tumor in the lungs was not due to an inability of the antibody to localize in the tumors, because autoradiographic analysis demonstrated enhanced radioantibody uptake in the

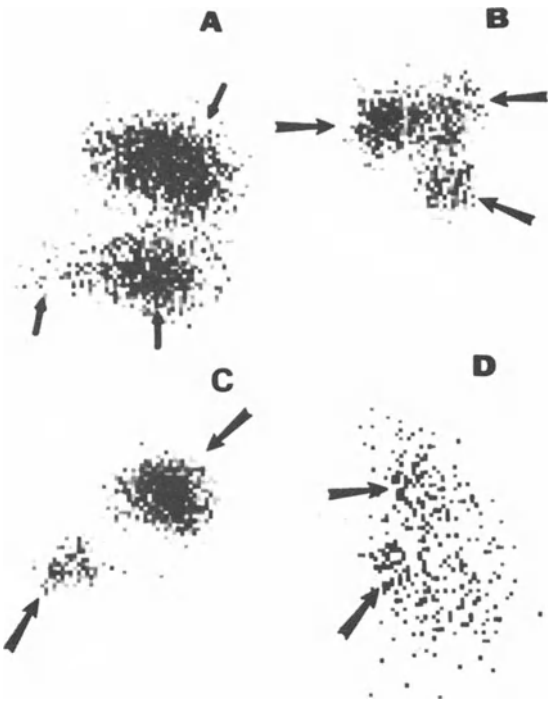

Figure 3. Ten nude rats (10–12 weeks old) were injected with a 50% suspension of GW-39 tumor in the liver in a similar fashion, as described previously [36]. Each rat was given an intravenous injection of 25 μg (0.3 mCi) of ^{131}I-goat anti-CEA antibody. Fourty-eight hours later, six rats were given donkey anti-goat SA (50:1 SA/PA ratio). The rats were imaged using a 5-mm pinhole collimater with a Gemini 700 camera. A: Left lateral view taken 24 hour after injection of the SA of a rat with a 0.131 g tumor in the front portion of the liver (lower left arrow). Top arrow shows activity in the chest on the posterior side, and a high level of activity is also seen in the stomach (lower right arrow). B: Posterior view of rat shown in A taken at 48 hours after the SA. Only activity in the chest (two upper arrows) and the tumor in the liver (lower right arrow) are apparent. C: Left lateral view of rat in A taken at 48 hours after SA, showing only the lung and liver activity. D: Left lateral view of a rat given the radiolabeled PA without the SA taken at 72 hours after the PA injection. A 0.1 g tumor in the liver is barely seen, and, despite the presence of histologically proven tumor in the lungs, the only activity in the chest appeared to be in the anterior area of the chest, suggesting activity residing in the heart.

tumors. In an attempt to increase the spacial resolution of the animal model, we transplanted GW-39 tumors in the liver of athymic (nude) rats. However, even by using these larger animals, and with the aid of a pinhole collimator focusing on the upper torso of the animals, we were unable to detect tumors in the lungs. By injecting the SA 48–72 hours after the PA was given, we found increased radioactivity in the lungs of several animals (Figure 3), which was subsequently confirmed as tumor by histologic evaluation. Thus, improved imaging of tumors in the liver and lungs are found using the anti-antibody method in comparison to PA alone.

It has been necessary to use polyclonal anti-tumor antibodies in order to investigate the SA method in animals bearing human-tumor xenografts, because the SA should complex specifically with the foreign radiolabeled PA without complexing with the host's immunoglobulin. Thus, murine Mabs cannot be tested in nude mice or hamsters because the SA (in this case, an anti-mouse IgG) would also complex with the endogenous mouse or hamster IgG. However, radiolabeled mouse Mabs are more widely used for tumor detection. Thus, before we began a clinical investigation using murine Mabs, we used rabbits to test the efficacy of an anti-mouse SA to remove radiolabeled murine Mab from the circulation. In addition, the anti-mouse IgG SA was tested by double-gel diffusion to ensure that it would not react with human immunoglobulins and other serum proteins and that it passed sterility, pyrogenicity, and general safety testing. The clinical trial was initiated to determine 1) if the SA could be safely administered to patients, 2) if the SA would complex with radioiodinated anti-CEA Mab and cause more rapid blood clearance, and 3) if the anti-antibody method would improve tumor imaging.

In our first series of patients, ^{131}I-labeled anti-CEA Mab, NP-3 [37] was administered to 15 patients with confirmed cancer, but only nine of these patients were evaluable with adequate follow-up data [22]. The patients were administered 225–500 μg of radiolabeled NP-3, followed 24–48 hours later with 1–5 mg of purified goat anti-mouse IgG as the SA, yielding SA/PA ratios of 17–133 at the time of SA injection. As shown in Table 6, tumors were detected in 7 of 9 patients without the aid of computerized, dual-isotope subtraction, and two patients were negative, but these patients were also false negatives with conventional subtraction imaging. In one case, metastatic tumor in the liver was detected by the anti-antibody method when these sites

Table 6. Clinical results with I-131 anti-CEA monoclonal antibody, NP-3, and anti-antibody (SA) RAID[a]

Patient No.	Primary Cancer	Serum CEA (ng/ml)	Time SA (hours)	SA/PA Ratio	Clearance of PA	Imaging Results
708	Stomach	222.0	24	50	ND[b]	Pos.
716	Stomach	2.6	24	100	87%[c]	Pos.
723	Lung	9.9	24	62	94%	Pos.
729	Rectum	326.0	24	133	ND	Pos.
736	Lung	36.0	48	24	21%	Neg.
737	Colon	76.0	48	54	ND	Pos.
739	Colon	5.4	48	17	63%	Pos.
742	Colon	24.0	24	102	ND	Pos.
745	Lung	24.7	48	100	71%	Neg.

[a] The anti-antibody (SA) was administered at 24 or 48 hours post PA injection.
[b] ND = not determined.
[c] Percent reduction in the amount of circulating PA 24 hours after SA injection.

were not appreciated by subtraction antibody imaging (Figure 4). The sites in the liver were later confirmed by CT scans. Blood clearance studies (Figure 5) confirmed that the SA enhanced the removal of circulating NP-3 from the blood, and analysis of the radioactivity in the blood confirmed the SA had complexed with the radiolabeled NP-3 (Table 7). Only one of the patients experienced chills after SA injection, but no other complications were found. Thus, we were encouraged by these initial studies that the anti-antibody method could be used to reduce the amount of circulating PA and provide a useful alternative to conventional dual-isotope subtraction.

Although tumors could be detected with radiolabeled NP-3, another Mab against CEA, designated NP-4 [37], was found to have several advantages over NP-3. Foremost was the finding that NP-4 did not complex significantly with circulating CEA, whereas NP-3 was completely complexed with NP-3 at CEA/NP-3 mole ratios of less than 10 : 1 [38,39]. Thus, our clinical studies shifted to the use of ^{131}I-labeled NP-4 using the goat anti-mouse IgG as the SA. In contrast to the rapid removal of NP-3 with this SA, NP-4 was not cleared rapidly by the goat SA, even when SA/PA ratios were increased, or upon successive injections of the goat SA (Figure 6). In-vitro analysis of the binding kinetics of the goat anti-mouse IgG SA to NP-3 and NP-4 showed that the goat SA was able to bind NP-3 better than NP-4 (Figure 7). We then prepared a specific rabbit anti-NP-4 antibody as a SA for clinical use. As shown in Figure 8, this rabbit SA rapidly cleared radioiodinated NP-4 from the blood, and we were able to detect tumors in several patients without the aid of dual-isotope subtraction (Figure 9). This indicates that not all PAs may be cleared at the same rate by the same SA. However, a specific SA against each PA may not be necessary, because the rabbit anti-NP-4 antibody also effectively reduced the amount of circulating mouse Mab against alpha fetoprotein (Figure 8).

There may be several other factors that influence the anti-antibody method. The animal species used in the preparation of the SA may also influence the ability of the SA to be cleared by the host. If a mechanism of immune recognition rather than just mechanical trapping of macroaggregated proteins is involved in the removal of the SA/PA complexes from the blood, it may be possible that the rabbit SA may have been recognized more readily as a foreign protein than the goat SA, and this led to its more rapid clearance kinetics. Complexing of the PA with circulating antigen may also be important in the clearance of the PA by the SA. In our first series of patients that were injected with NP-3, complexing of NP-3 with CEA may have helped the goat SA clear the PA by adding to the size of the lattice formed by the PA and the antigen. Complexing with antigen should not interfere with SA clearance if the SA binds predominantly to the Fc portion of the PA. However, low titers of human anti-mouse IgG (HAMA) may influence the binding of the SA to the PA, because these antibodies may also bind to the Fc portion of the PA. In the sense, additional studies are necessary to determine how well a SA can clear PA fragments from the blood, or even how well a frag-

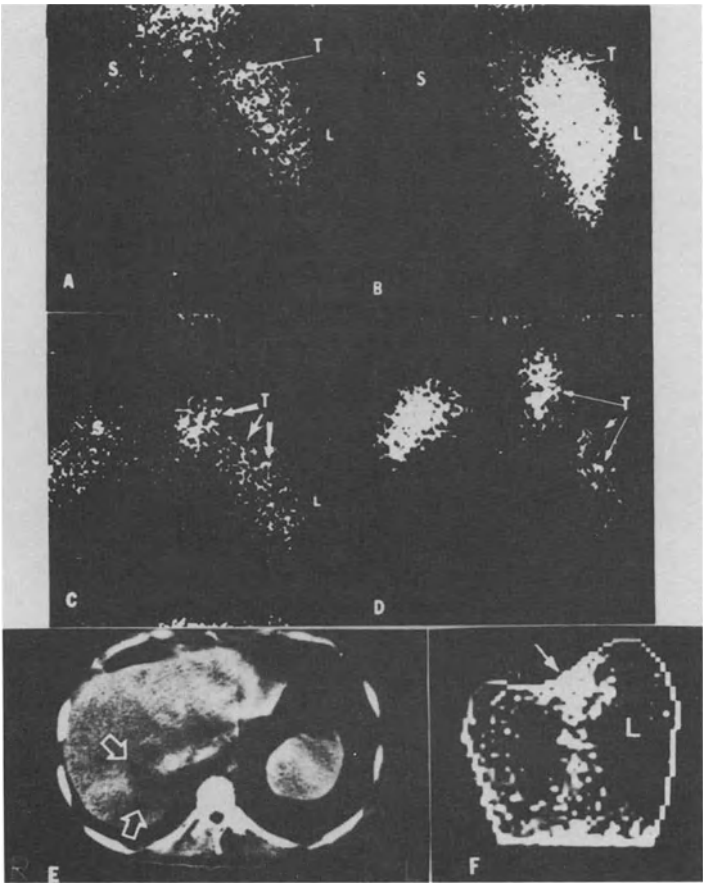

Figure 4. Comparison of the dual-isotope subtraction method and the anti-antibody method for tumor detection. This patient was first studied using the dual-isotope subtraction method with ^{131}I-NP-3 (0.175 mg, 2.8 mCi). In this study, an area of increased activity in the region of the gastroesophageal junction (arrow shown in panel F) was found. This patient had a prior resection of a gastric carcinoma, and this region was believed to be recurrent tumor. In a follow-up study using radioiodinated NP-3 (0.3 mg/3.7 mCi), the posterior abdominal view showed diffuse liver activity (L) before the SA (A; 24 hours post ^{131}I-NP-3). The arrow indicates the area where increased activity in the region of the gastroesophageal junction was shown previously. Two hours after the injection of the SA (B), an increase in radioactivity in the liver is seen, indicating the rapid uptake of PA/SA complexes in the liver, but 24 and 48 hours later (C and D, respectively), most of the activity in the liver decreased. An area of enhanced radioactivity in the gastroesophageal junction was seen again. In addition, two sites of enhanced activity in the liver were found (indicated by the arrows). Tumor in the liver was later confirmed by CT scans (E), but the patient died before the gastroesophageal site could be confirmed by other conventional methods.

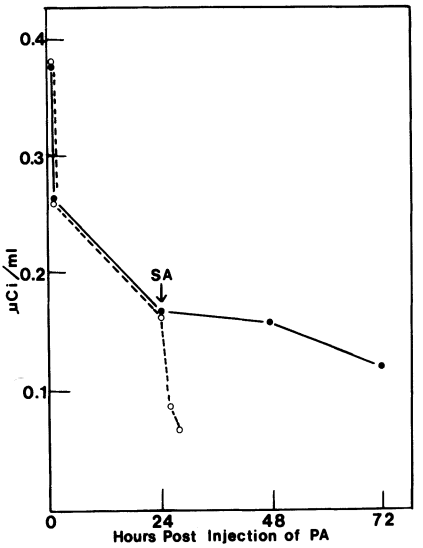

Figure 5. Blood clearance studies from patient shown in Figure 4. Patient was first given ^{131}I-NP-3 alone. One week later, the patient was readministered the same amount of radioiodinated NP-3, but 24 hours later the patient was given 5.0 mg of goat anti-mouse IgG (SA:PA = 61). There was no evidence of a human anti-mouse IgG response in the patient at the onset of both studies, as determined by an immunoassay of a preinjection plasma sample. The closed circles show the blood clearance kinetics from the first study with NP-3 alone, and the open circles (dashed line) show the clearance observed from the second study. The arrow indicates the time of SA administration during the second study.

Table 7. Characterization of radioactivity by gel filtration and immunoaffinity chromatography in patients given I-131 NP-3 followed 24 hours later by second antibody

Patient No.	Time Post-injection	Sephacryl S-200			% Immunoreactivity[b]			
		Void	IgG	Vi	CEA	GAM	GAH	DAG
I-131 NP-3[a]		0.6	98.0	0.4	96	98	0.5	0.7
708	24 hrs	90.0	4.0	6.0	52	72	0.2	0.4
	26 hrs	74.0	4.0	17.0	52	23	2.0	66.0
723	24 hrs	15.0	79.0	3.0	93	80	0.2	0.9
	48 hrs	11.0	0.3	82.0	21	6	ND	3.0

[a] Quality control analysis of typical radioiodinated NP-3 preparation prior to administration to patients.

[b] Immunoabsorbents listed below were prepared by coupling CEA, goat anti-mouse IgG (GAM), goat anti-human Ig (GAH), or donkey anti-goat IgG (DAG) to either affi-gel 10 or Sepharose 4B.

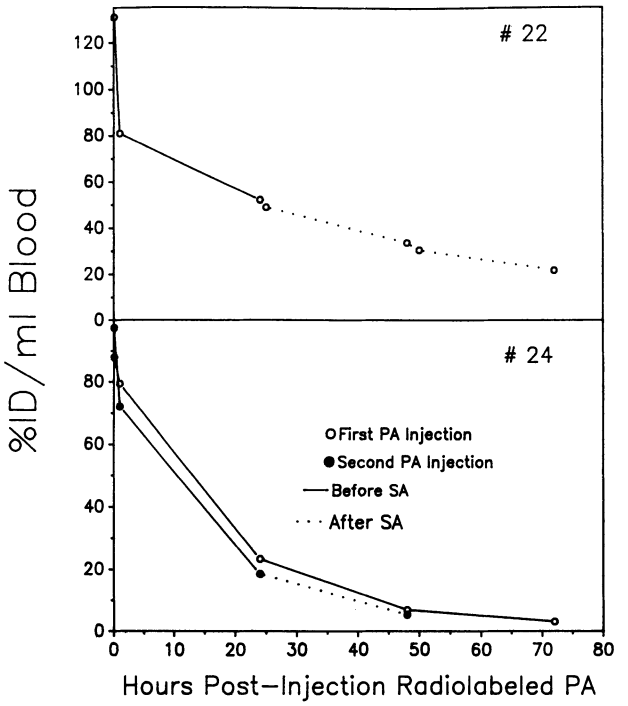

Figure 6. Examples of the clearance kinetics from three patients given ^{131}I-NP-4 followed by goat anti-mouse IgG. In patient #22, goat anti-mouse IgG was given at 24 and 48 hours after the PA (5 mg/injection; SA/PA ratio was 10:1 and 15:1 at 24 and 48 hours, respectively), but there was no significant change in the rate that radiolabeled NP-4 was removed from the blood. Patient #24 was studied twice within 3 weeks. The first week ^{131}I-NP-4 (0.964 mg, 5.3 mCi) was given without SA (open circles). In the next study, the patient was given 0.278 mg of radioiodinated NP-4, and then 24 hours later, 5.2 mg of SA (SA/PA = 100) was given, but there was no change in the rate of NP-4 clearance from the blood.

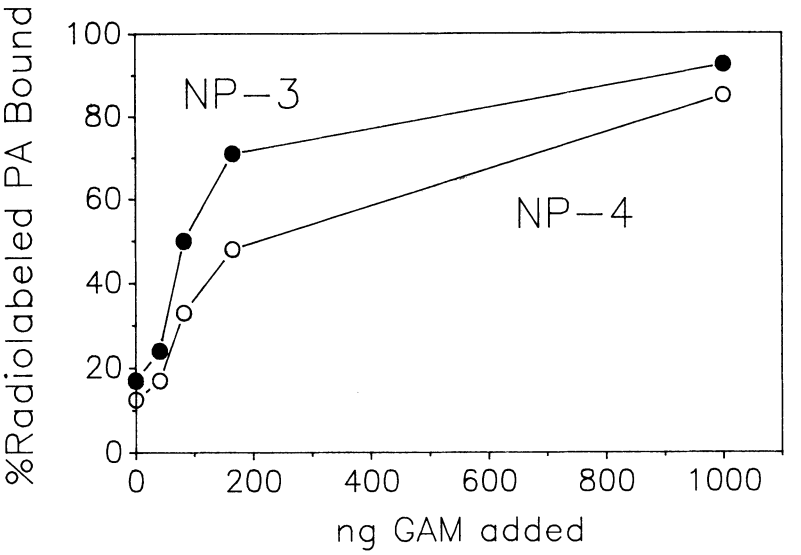

Figure 7. In-vitro studies comparing the ability of goat anti-mouse IgG to bind to radiolabeled NP-3 or NP-4.

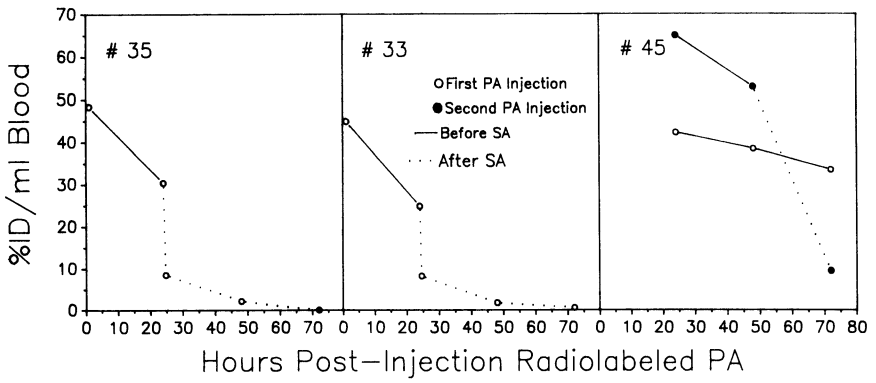

Figure 8. Blood clearance knetics of patients given rabbit anti-NP-4 SA. Patient #35 and patient #33 were given SA at 24 hours after the injection of ^{131}I-NP-4 (100:1 and 66:1 SA/PA ratio, respectively). Patient #45 was given ^{131}I-labeled anti-alpha fetoprotein (AFP) Mab on two separate occasions. In the first study (open circles), a very slow clearance rate from the blood was observed. In a second study, 2 weeks later (closed circles), there was again an indication that the blood clearance rate of the radiolabeled antibody was slow. However, 24 hours after the administration of the rabbit anti-NP-4 SA (dotted line), a substantial amount of the radiolabeled anti-AFP antibody had been removed from the blood.

ment of a SA works. Finally, the clinical status of the patient may also play a role in governing the ability of a SA to clear the PA from the blood. In this case, patients with impaired liver or kidney function may not have the ability to adequately metabolize and remove the radiolabeled antibody from the blood. Thus, these factors, in addition to the time the SA is administered and the SA/PA ratio, must be considered when evaluating the efficacy of the SA method.

Another important feature of the anti-antibody method that is related to its successful application, i.e., rapid clearance of background radioactivity, is the increase in the time required to acquire several views of the body. Without the additional radioactivity in the body that adds to the total counts acquired in each view, it becomes more difficult to image multiple sites in a patient. However, the added contrast afforded by the improved tumor/nontumor ratios may reduce the need for collecting as many counts per view. Similar adjustments have been required when imaging with antibody fragments. Thus, this feature may not be that problematic, especially if sufficient accretion of the radiolabeled PA occurs in the tumor.

Several new applications of the anti-antibody method have recently been reported. Goodwin et al. [40] have used antibody against the chelating agent EDTA to help remove excessive amounts of ^{111}In-labeled, EDTA-conjugated antibodies from the blood, thereby improving localization of lymph nodes in experimental animals. Another novel application is the use of avidin-biotin technology. Hnatowich et al. [41] have explored the possibility of first targeting avidin or biotin-conjugated unlabeled antibody, followed at a later time with labeled biotin or avidin. With biotinylated PA followed by labeled

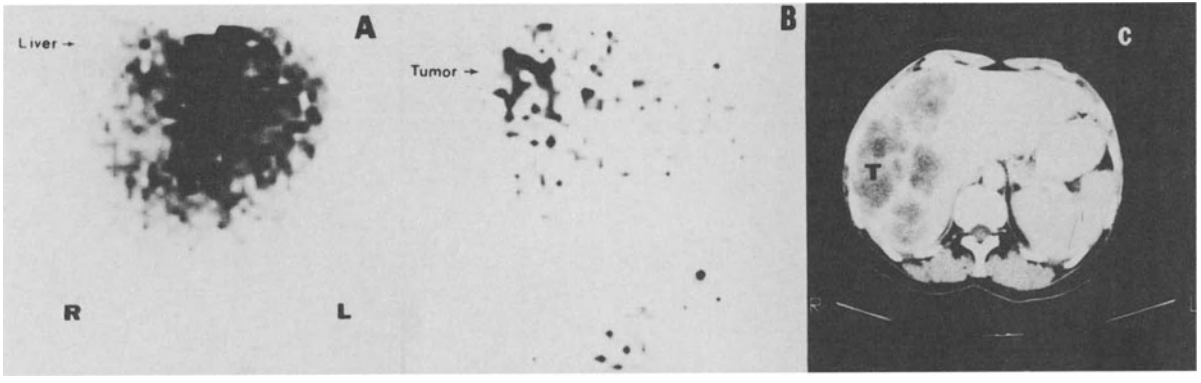

Figure 9. Anterior whole-body scintigraphy 2–3 days after administration of ^{111}In-labeled T101 in the toe webs of both feet. Numbers indicate percentages of injected activity in organs, nodes, and injection sites. Values for iliac and inguinal-femoral nodes represent the means of those obtained separately for the left and right sides. The patient on the left had only minimal disease (LN 2) in the nodes. Percentages given were corrected for decay but not for tissue attenuation. The feet were partly out of the camera view, but percentages were calculated from region-of-interest scans taken at about the same time. The patient on the right had bulky disease. Double foci in the feet of the righthand patient resulted from dorsiflexion and plantar flexion during imaging. The efficiencies of lymph-node imaging were orders of magnitude higher than after IV injection. From Keenan et al. [20].

avidin, the radioactivity was not cleared rapidly from the blood. However, by administering avidin-coupled PA followed later by ^{111}In-labeled biotin, improved target/nontarget ratios were achieved. Goodwin et al. [42] showed that a chase of biotinylated transferrin following the injection of an avidin-conjugated chimeric antibody (one specifically for a mouse B-cell lymphoma, the other specifically for biotinylated p-isothiocyanato benzyl EDTA) could be used to clear the avidin-conjugated antibody from the blood prior to the administration of biotin-conjugated, ^{111}In-labeled EDTA. The chase procedure lowered background activity so that within 1–3 hours after the injection of the radiolabeled EDTA, improved tumor/blood ratios were found. Although further investigation is required, these studies suggest that this modification of the anti-antibody technique may further improve tumor imaging.

Future prospects

The anti-antibody method provides a means for controlled removal of excessive amounts of radiolabeled antibody from the blood, thereby improving tumor/nontumor ratios. However, the major issue of how the SA method compares with antibody fragments remains to be investigated. There are advantages and disadvantages for either procedure. Antibody fragments and the anti-antibody method both improve tumor/nontumor ratios and lower the amount of radiolabeled PA in the tumor when compared with the use of whole radiolabeled antibody alone. However, the SA method may have an advantage over antibody fragments in the sense that by controlling the amount of time the PA is allowed to circulate in the body, higher amounts of PA may be found in the tumor. Further comparisons of the anti-antibody method to antibody fragments need to be made. For example, for whole antibody followed by SA, we have waited 24–48 hours before administering the SA. Improved image quality, at least for tumors in the liver, requires an additional 24–48 hours, or a total of 2–4 days for optimal tumor imaging. Currently, optimal tumor imaging with antibody fragments occurs within 1–2 days. Combinations of the SA with antibody fragments may further reduce the time required for imaging. In addition, SA may be useful in altering the distribution of radiolabeled antibody fragments. For example, whereas antibody fragments have a higher uptake in the kidneys, complexes formed between the SA and radiolabeled antibody fragments may be deposited in the liver, thereby allowing for early and improved images of tumors near the kidneys.

In addition to imaging tumors, the anti-antibody method may provide a distinct advantage for radioimmunotherapy by removing excessive amounts of radiolabeled antibody in the blood pool. In most instances, maximum accretion of radiolabeled antibody in tumors occurs early after the injection of the PA, and the SA method would provide a way of removing excessive

activity from the blood pool that may otherwise add to the toxicity associated with radioimmunotherapy. Indeed, our preliminary studies indicate that higher doses of ^{131}I-labeled antibody can be tolerated in animals given the SA 48 hours after the administration of radiolabeled PA than if the SA was not given [43].

The major disadvantage of the anti-antibody procedure is the need for injecting additional foreign protein into patients. Although our initial studies have shown no untoward effects in patients given as much as 10 mg of SA, caution is required to ensure that the formation of immune complexes by the SA with the PA do not adversely affect the patient. Secondly, there is the question of added host immune stimulation by the administration of another immunoglobulin. The development of an anti-mouse IgG response in patients has been cited as a major complication when considering the need for repeated antibody imaging or therapy studies [44,45]. Although the SA method may act in a similar fashion as the Rho-gam method for reducing the immune response to the Rh factor [46], thereby reducing the host's response to the radiolabeled PA, cross-reactivity between immunoglobulins from different animal species may reduce or negate the potential for this type of benefit.

Thus, there are many issues that remain to be investigated before we can appreciate more fully the potential for improved detection and therapy of cancer by the anti-antibody method.

Acknowledgments

We thank J. Mabus, D. Snyder, R. Aninipot, and C. Ballance for their excellent technical assistance. This work is supported in part by USPHS grants CA 37895 and CA 39841.

References

1. Bale, W.F., and Spar, I.L. (1957) Studies directed toward the use of antibodies as carriers of radioactivity for therapy. Adv. Biol. Med. Phys. 5:285–356.
2. Primus, F.J., Wang, R.H., Goldenberg, D.M., and Hansen, H.J. (1973) Localization of human GW-39 tumors in hamsters by radiolabeled heterospecific antibody to carcinoembryonic antigen. Cancer Res. 33:2977–2982.
3. Goldenberg, D.M., Preston, D.F., Primus, F.J., and Hansen, H.J. (1974) Photoscan localization of GW-39 tumors in hamsters using radiolabeled anticarcinoembryonic antigen immunoglobulin G. Cancer Res. 34:1–9.
4. Mach, J.P., Carrel, S., Merenda, C., Sordat, B., and Cerottini, J.C. (1974) In vivo localization of radiolabeled antibodies to carcinoembryonic antigen in human colon carcinoma grafted into nude mice. Nature 248:704–706.
5. Reif, A.E., Curtis, L.E., Duffield, R., and Shauffer, I.A. (1974) Trial of radiolabeled antibody localization in metastases of a patient with a tumor containing carcinoembryonic antigen (CEA). J. Surg. Oncol. 6:133–150.

6. Goldenberg, D.M., Deland, F., Kim, E., Bennett, S., Primus, F.J., van Nagell, J.R., Jr., Estes, N., DeSimone, P., and Rayburn, P. (1978) Use of radiolabeled antibodies to carcinoembryonic antigen for detection and localization of diverse cancers by external photoscanning. N. Engl. J. Med. 298:1384–1388.
7. Goldenberg, D.M., Kim, E.E., Bennett, S.J., Nelson, M.O., and Deland, F.H. (1983) Carcinoembryonic antigen radioimmunodetection in the evaluation of colorectal cancer and in the detection of occult neoplasms. Gastroenterology 84:524–552.
8. Mach, J.P., Carrel, S., Forni, M., Ritschard, J., Donath, A., and Alberto, P. (1980) Tumor localization of radiolabeled antibodies against carcinoembryonic antigen in patients with carcinoma. N. Engl. J. Med. 303:5–10.
9. Smedley, H.M., Finan, P., Lennox, E.S., Ritson, A., Takei, F., Wraight, P., and Sikora, K. (1983) Localization of metastatic carcinoma by radiolabeled monoclonal antibody. Br. J. Cancer 47:253–259.
10. Sullivan, D.C., Silva, J.S., Cox, C.E., Haagensen, D.E., Jr., Harris, C.C., Briner, W.H., and Wells, S.A., Jr. (1982) Localization of ^{131}I-labeled goat and primate anti-carcinoembryonic antigen (CEA) antibodies in patients with cancer. Invest. Radiol. 17:350–355.
11. Green, A.J., Begent, R.H.J., Keep, P.A., and Bagshawe, K.D. (1984) Analysis of radioimmunodetection of tumors by the subtraction technique. J. Nucl. Med. 25:96–100.
12. Ott, R.J., Grey, L.J.L., Zivaovic, M.A., Flower, M.A., Trott, N.G., Moshaki, V., Combes, R.C., Neville, A.M., Ormerod, M.G., Westwood, J.H., and McCready, V.R. (1983) The limitations of the dual-radionuclide subtraction technique for external detection of tumors by radioiodine labeled antibodies. Br. J. Radiol. 56:101–108.
13. Perkins, A.C., Whalley, D.R., and Hardy, J.G. (1984) Physical approach for the reduction of dual radionucleotide image subtraction artifacts in immunoscintigraphy. Nucl. Med. Commun. 5:501–512.
14. Siegel, J.A., Greenspan, B., Madsen, M.T., Sharkey, R.M., Brennen, K. Lee, R.E., and Goldenberg, D.M. (1987) Improvement of subtraction imaging in radioimmunodetection. Radiology 165:133.
15. Wahl, R.L., Parker, C.W., and Philpott, G.W. (1983) Improved radioimaging and tumor localization with monoclonal F(ab')$_2$. J. Nucl. Med. 24:317–325.
16. Buchegger, F., Haskell, C.M., Schreyer, M., Scazziaga, B.R., Randin, S., Carrel, S., and Mach, J.P. (1983) Radiolabeled fragments of monoclonal antibodies against carcinoembryonic antigen for localization of human colon carcinoma grafted into nude mice. J. Exp. Med. 158:413–427.
17. Delaloye, B., Bischof-Delaloye, A., Buchegger, F., von Fliedner, V., Grob, J.P., Volant, J.C., Pettavel, J., and Mach, J.P. (1986) Detection of colorectal carcinoma by emission-computerized tomography after injection of I-123-labeled Fab or F(ab')$_2$ fragments from monoclonal anti-carcinoembryonic antigen antibodies. J. Clin. Invest. 77:301–311.
18. Khaw, B.A., Strauss, H.W., Cahill, S.L., Soule, H.R., Edgington, T., and Cooney, J. (1984) Sequential imaging of indium-111-labeled monoclonal antibody in human mammary tumors hosted in nude mice. J. Nucl. Med. 25:592–603.
19. Gaffar, S.A., Bennett, S.S., DeLand, F.H., Primus, F.J., and Goldenberg, D.M. (1982) Carcinoembryonic antigen (CEA) radioactive antibody fragments for cancer localization in vivo. Proc. Am. Assoc. Cancer Res. 23:249.
20. Pant, K.D., Dahlman, H.L., and Goldenberg, D.M. (1977) A putatively new antigen (CSAp) associated with gastrointestinal and ovarian neoplasia. Immunol. Commun. 6: 411–421.
21. Sharkey, R.M., Primus, F.J., and Goldenberg, D.M. (1984) Second antibody clearance of radiolabeled antibody in cancer detection. Proc. Natl. Acad. Sci. USA 8:2843–2847.
22. Goldenberg, D.M., Sharkey, R.M., and Ford, E. (1987) Anti-antibody enhancement of iodine-131 anti-CEA radioimmunodetection in experimental and clinical studies. J. Nucl. Med. 28:1604–1610.
23. Spar, I.L., Goodland, R.L., and Desiderio, M.A. (1964) Immunological removal of circulating I-131-labeled rabbit antibody to rat fibrinogen in normal and tumor-bearing rats. J.

Nucl. Med. 5:428–443.
24. McCardle, R.J., Harper, P.V., Spar, I.L., Bale, W.F., Andros, G., and Jiminez, F. (1966) Studies with iodine-131-labeled antibody to human fibrinogen for diagnosis and therapy of tumors. J. Nucl. Med. 7:837–847.
25. Barrett, G.M., Ryman, B.E., Boden, J.A., Keeps, P.A., Searle, F., Begent, R.H., and Bagshawe, K.D. (1981) Liposomal clearance of antibodies to tumour products: Possible improvement of tumour detection. Biochem. Soc. Trans. 9:564–565.
26. Barratt, G.M., Ryman, B.E., Begent, R.H.J., Keep, P.A., Searle, F., Boden, J.A., and Bagshawe, K.D. (1983) Improved radioimmunodetection of tumours using liposome-entrapped antibody. Biochem. Biophys. Acta 762:154–164.
27. Begent, R.H.J., Green, A.J., Bagshawe, K.D., Jones, B.E., Keep, P.A., Searle, F., Jewkes, R.F., Barratt, G.M., and Ryman, B.E. (1982) Liposomally entrapped second antibody improves tumor imaging with radiolabeled (first) antitumor antibody. Lancet 2: 739–742.
28. Ryman, B.E., and Baratt, G.M. (1982) Possible improvement of radioimmunodetection of tumors by liposomal clearance of antibodies to tumor products. In: Akoyunoglou, G., Evangelopopulos, A.E., Georgatsos, J., Palaiologos, G., Trakatelli, A., and Tsiganos, C.P. (eds.), *Progress in Clinical and Biological Research*, Vol 102A. New York: Alan Liss, pp. 299–308.
29. Bradwell, A.R., Vaughan, A., Fairweather, D.S., and Kykes, P.W. (1983) Improved radio-immunodetection of tumors using a second antibody. Lancet 1:247.
30. Goodwin, D., Meares, C., Diamanti, C., McCall, M., Lai, C., Torti, F., McTigue, M., and Martin, B. (1984) Use of specific antibody for rapid clearance of circulating blood pool background from radiolabeled tumor imaging proteins. Eur. J. Nucl. Med. 9:209–215.
31. Goldenberg, D.M., and Hansen, H.J. (1972) Carcinoembryonic antigen present in human colonic neoplasis serially propagated in hamsters. Science 175:1117–1118.
32. Sharkey, R.M., Mabus, J., and Goldenberg, D.M. (1900) Factors influencing anti-antibody enhancement of tumor targeting. Cancer Res., in press.
33. Silver, S., ed. (1968) In: *Radioactive Nuclides in Medicine and Biology*. Philadelphia: Lea and Febiger.
34. Scheinberg, D.A., Strand, M., and Gansow, O.A. (1983) Tumor imaging with radioactive chelates conjugated to monoclonal antibodies. Science 215:1511–1513.
35. Perkins, A.C., and Pimm, M.V. (1985) Differences in tumor and normal tissue concentrations of iodine- and indium-labeled monoclonal antibody. Eur. J. Nucl. Med. 11:295–299.
36. Sharkey, R.M., Filion, D., Primus, F.J., and Goldenberg, D.M. (1986) A human colon cancer metastasis model for radioimmunodetection. Cancer Res. 46:3677–3683.
37. Primus, F.J., Newell, K.S., Blue, A., and Goldenberg, D.M. (1983) Immunological heterogeneity of carcinoembryonic antigen: Antigenic determinants on CEA distinguished by monoclonal antibodies. Cancer Res. 43:686–692.
38. Primus, F.J., Sharkey, R.M., Ballance, C., Kelly, E., Varga, D., and Goldenberg, D.M. (1986) Radiolocalizing monoclonal antibodies against concealed epitopes on carcinoembryonic antigen (CEA). J. Nucl. Med. 27:1016.
39. Sharkey, R.M., Primus, F.J., Shochat, D., and Goldenberg, D.M. (1988) Comparison of tumor targeting of mouse monoclonal and goat polyclonal antibodies to carcinoembryonic antigen in the GW-39 human tumor host model. Cancer Res. 48:1823–1828.
40. Goodwin, D.A., Meares, C.F., McCall, M.J., Haseman, M.K., McTigue, M., Diamanti, C.I., and Chaovapong, W. (1985) Chelate conjugates of monoclonal antibodies for imaging lymphoid structures in the mouse. J. Nucl. Med. 26:493–502.
41. Hnatowich, D., Virzi, F., and Rusckowski, M. (1987) Investigations of avridin and biotin for imaging applications. J. Nucl. Med. 28:1294–1302.
42. Goodwin, D.A., Meares, C.F., McCall, M.J., McTigue, M., Chaovapoong, W., Levy, R., and Starnes, C. (1987) Pre-targeted immunoscintography with chimeric antibodies. J. Nucl. Med. 28(Supplement):561.
43. Blumenthal, R., Sharkey, R.M., Snyder, D., and Goldenberg, D.M. (1989) Reduction by

anti-antibody administration of the radiotoxicity associated with I-131-labeled antibody to carcinoembryonic antigen in cancer radioimmunotherapy. J. Natl. Cancer Inst. 81:194–199.

44. Schroff, R.W., Foon, K.A., Beatty, S.M., Oldham, R.K., and Morgan, A.C., Jr. (1985) Human anti-murine immunoglobulin responses in patients receiving monoclonal antibody therapy. Cancer Res: 45:879–885.
45. Pimm, M.V., Perkins, A.C., Armitage, N.C., and Baldwin, R.W. (1985) The characteristics of blood-borne radiolabels and the effect of anti-mouse IgG antibodies on localization of radiolabeled monoclonal antibody in cancer patients. J. Nucl. Med. 26:1011–1023.
46. Pollack, W., Gorman, J.G., and Freda, V.J. (1969) Prevention of Rh hemolytic disease. Prog. Hematol. 6:121–147.

Index